BIOCHEMICAL AND ANATOMICAL CORRELATES OF CORTICAL PYRAMIDAL NEURONES- IMPLICATIONS FOR THE TREATMENT OF ALZHEIMER'S DISEASE.

Thesis submitted for the degree of Doctor of Philosophy in the Faculty of Science of the University of London

Iain Patrick Chessell

Department of Neurochemistry
Institute of Neurology

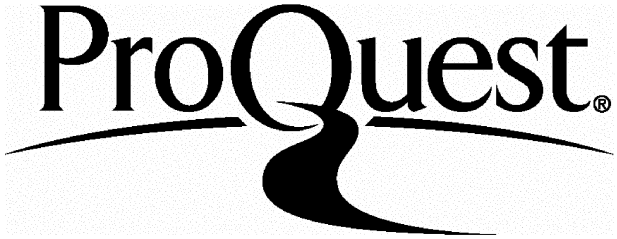

This thesis is dedicated with love to my parents, for their unfailing support and guidance throughout my life.

ABSTRACT.

Dysfunction of the major cell type of the neocortex, the pyramidal neurone, has been implicated in several neuropsychiatric diseases, in particular Alzheimer's Disease. Markers that identify these cells are proposed to provide essential information to enable effective pharmacological targeting of intervention in the treatment of this disease.

The action of a putative partial agonist, D-cycloserine, at the glycine modulatory site of the N-methyl-D-aspartate receptor-ionophore complex (NMDA receptor), known to be present on pyramidal neurones was investigated. In membranes prepared from Alzheimer's brains, D-cycloserine was determined to have partial agonist characteristics consistent with those described in animal studies.

Three lesioning paradigms using the retrogradely transported toxin, volkensin, with appropriate controls, were developed to destroy subpopulations of hippocampal CA3, corticofugal and corticocortical projecting neurones. In each case volkensin injection into the appropriate area produced losses of distant neurones, with preservation of interneurones. Biochemical sequelae following such losses were investigated using the technique of autoradiography.

Unilateral entorhinal injection of volkensin produced significant loss of anterior CA3 hippocampal pyramidal neurones, sparing CA1 and the dentate gyrus. The area of ligand binding to the muscarinic M_1 receptor was reduced to a greater extent than the observed neuronal loss, while binding NMDA, kainate and 5-HT_{1A} receptors was reduced in parallel with the neuronal loss. The rank order of the receptors as effective markers of this subpopulation of pyramidal neurones was M_1 > NMDA, kainate > 5-HT_{1A} > $GABA_A$.

Unilateral intrastriatal injection of volkensin produced significant reductions in the number and size of infragranular pyramidal neurones. In autoradiographic binding studies, significant reductions in ligand binding in deep neocortical layers to the 5-HT_{1A}, muscarinic M_1, nicotinic, adenosine A_1 and kainate receptors were observed compared to control, with sparing of $GABA_A$ and increases in α_1 total and the 1b subtype. The rank order of receptors as effective markers of this subpopulation of pyramidal neurones was nicotinic, 5-HT_{1A} >> kainate, M_1 > adenosine A_1 > $GABA_A$, α_{1total}, α_{1b}.

Cortical injection of volkensin produced significant reductions in the number of both infragranular and supragranular contralateral pyramidal neurones. Autoradiographic investigation of volkensin injected animals revealed significant reductions in binding to M_1 and nicotinic receptors but not adenosine A_1, 5-HT_{1A} or 5-HT_2 compared to ricin and control animals.

These findings are thought to advance the understanding of the biology of pyramidal neurones, and have important implications concerning the treatment of Alzheimer's Disease in the context of symptomatic treatment by correction of hypoactivity of glutamatergic pyramidal neurones; and treatment of the disease progression by influencing production of amyloid, implicated in the formation of senile plaques.

TABLE OF CONTENTS

LIST OF FIGURES

LIST OF TABLES

LIST OF ABBREVIATIONS.

ACh	Acetylcholine
AChE	Acetylcholine esterase
AD	Alzheimer's disease
AMPA	α-amino-3-hydroxy-5-methyl-4-isoxazole propionic acid
ANOVA	Analysis of variance
Apo-E	Apolipoprotein E
APP	Amyloid precursor protein
ATP	Adenosine triphosphate
BA	Brodmann area
BSA	Bovine serum albumin
CA	Cornu Ammon of hippocampus
cAMP	Cyclic adenosine monophosphate
CC	Animal group- intracortical lectin injection
CCD	Charge coupled device
ChAT	Choline acetyltransferase
CNS	Central nervous system
CS	Animal group- intrastriatal lectin injection
CSF	Cerebrospinal fluid
DAG	Diacylglycerol
5,7-DCKA	5,7 dichlorokynurenic acid
DCS	D-cycloserine
DG	Dentate gyrus
DIW	Distilled, de-ionised water
DMSO	Dimethyl sulphoxide
DPCPX	1,3-dipopropyl-8-cyclopentylxanthine
DRN	Dorsal raphe nucleus
EAA	Excitatory amino acid
EDTA	Ethylenediamine tetraacetic acid
ENT	Animal group- intraentorhinal cortex lectin injection
EPSP	Excitatory postsynaptic potential
EXS	Animal group- intrastriatal excitotoxin injection
EXTH	Animal group- intrathalamic excitotoxin injection
GABA	Gamma-amino-butyric acid
GAD	Glutamic acid decarboxylase
GFAP	Glial fibrillary acidic protein
GSK	Glycogen synthase kinase
HRP	Horseradish peroxidase
HPLC	High performance liquid chromatography
5-HT	5-hydroxytryptamine, serotonin
IP_3	Inositol trisphosphate
KRP	Krebs Ringer phosphate
L-689,560	4- trans -2- carboxy- 5, 7- dichloro -4 -phenylamino - carbonylamino- 1,2,3,4-tetrahydroquinoline
LC	Locus coeruleus
LCSF	Lumbar CSF
LTP	Long term potentiation
MAP	Mitogen activated protein kinase

MK-801	(+) -5- methyl-10, 11-dihydro- 5H- dibenzo [a,d] cyclohepten-5, 10-imine, dizocilpine
5-MU	5-methyl-urapidil
NA	Noradrenaline
NBM	Nucleus basalis of Meynert
NMDA	N-methyl-D-aspartate
8-OH-DPAT	8-hydroxy-2-(n-dipropylamino)-tetralin
PBS	Phosphate buffered saline
PDPK	Proline directed protein kinase
PHF	Paired helical filament
PKA	cAMP dependent protein kinase
PKC	Protein kinase C
PLC	Phospholipase C
PNS	Peripheral nervous system
PP-2A	Protein phosphatase 2A
R-PIA	R-phenylisopropyladenosine
SEM	Standard error of mean
SN	Substantia nigra
SSC	Saline sodium citrate
TCP	1-[1-(2-thienyl)cyclohexyl]piperazine
VCSF	Ventricular CSF

Corrigenda

Page 122: All statistical analyses were performed using SPSS V4.0 statistical software
Page 195: Arrows mark infragranular layers in Figure 6.4
Page 360: One rapid *post-mortem* AD brain sample had a terminal coma duration of 168 hr. This brain did not respond to carbachol but results from this sample are included in the data presented.

List of publications arising from the work presented in this thesis

1. Chessell, I.P., Procter, A.W., Francis, P.T., and Bowen, D.M. D-cycloserine, a putative cognitive enhancer, facilitates activation of the NMDA receptor - ionophore complex in Alzheimer brain. *Brain Res.* 565:345-348, 1991.

2. Chessell, I.P., Francis, P.T., and Bowen, D.,M. A cortical pyramidal neurone neurotransmitter receptor that may affect β-amyloid precursor protein (APP). *Biochem.Soc.Trans.* 21:240S-240S, 1993. (Abstract)

3. Chessell, I.P., Francis, P.T., Pangalos, M.N., Pearson, R.C.A., and Bowen, D.M. Localisation of muscarinic (m_1) and other neurotransmitter receptors on corticofugal-projecting pyramidal neurones. *Brain Res.* 632:86-94, 1993.

4. Chessell, I.P., Francis, P.T., Heath, P.R., Pearson, R.C.A., and Bowen, D.M. Effect of entorhinal injection of volkensin on the structure and neurotransmitter receptors of the hippocampus. *Br.J.Pharmacol.* 108:51, 1993. (Absract)

5. Chessell, I.P., Francis, P.T., Pearson, R.C.A., Kirkwood, P., and Bowen, D.M. Receptors on cortical pyramidal cells-implications for amyloid precursor protein (APP) processing. *Soc.Neurosci.Abs.* 19:399-399, 1993. (Abstract)

6. Bowen, D.M., Stratmann, G.C., Webster, M., Chessell, I.P., and Pearson, R.C.A. Amyloid precursor phoshoinositide-regulated "α secretase" leads other membrane proteases as therapeutic target. *Soc.Neurosci.Abs.* 19:1634-1634, 1993. (Abstract)

7. Bowen, D.M., Francis, P.T., Pangalos, M.N., and Chessell, I.P. Neurotransmitter receptors of rat cortical pyramidal neurones: implications for in vivo imaging and therapy. *J.Reprod.Fert.* 46 (Suppl):131-143, 1993.

8. Chessell, I.P., Francis, A.A., Webster, M., Procter, A.W., Heath, P.R., Pearson, R.C.A., and Bowen, D.,M. An aspect of Alzheimer neuropathology after suicide-transport damage. *J. Neural Transm.* 1993. (In Press)

9. Bowen, D.M., Francis, P.T., Chessell, I.P., and Webster, M. Neurotransmission - the link integrating Alzheimer research? *Trends.Neurosci.* 17:149-150, 1994.

10. Chessell, I.P., Alder, J.T., and Bowen, D.M. Unimpaired receptor- stimulated phospholipase C activity in Alzheimer's Disease. Manuscript in preparation, 1994.

CHAPTER 1: Introduction.

1.1 Morphology of the cortex.

1.1.1 Morphology of the mammalian neocortex.

Almost the entire cortex of sub-mammalian vertebrates is olfactory in nature, and contains only three layers of cells. From this allocortex are derived the paleocortex and the archicortex of the mammalian brain, the latter being incorporated in the limbic system and present in the hippocampus and dentate gyrus. The neocortex, which consists of six layers, is a significant feature of the brain in mammals, and is observed to increase in size as higher mammals evolve, mainly due to progressively larger areas of association cortex with corresponding connection complexity (Barr, 1974). Neocortex is also referred to as isocortex, and paleocortex and archicortex are also referred to as allocortex. Early investigations of the morphology of the cortex were invariably microscopic, and the development of staining techniques such as Nissl, Golgi, Cajal and Weigert allowed fibrous and cellular structures within the cortex to be described, expanding on previous 'granular' and 'agranular' demarcations.

The neocortex has the characteristic histological property of having cell bodies and fibres within it arranged in six layers. These laminae are as follows (Warwick and Williams, 1973):

I. **The molecular layer** immediately below the pia, consists of sparsely packed horizontal cells of Cajal, and a dense network of tangential fibres, derived from pyramidal cells (apical dendrites), stellate cells (vertical axons) and other elements, including cortical afferent fibres, both projection and associational. This layer is also known as the **plexiform layer**.

II. **The external granule layer** contains the somata of stellate and small pyramidal cells. Passing through this lamina are vertically arranged dendrites and axons from subjacent layers, and a dense neuropil of local dendrites and axons.

III. **The pyramidal layer** (supragranular) consists of pyramidal cells of medium size, stellate and fusiform cells, whose dendrites and axons extend far beyond the layer itself.

IV. **The internal granule layer** consists mainly of stellate cells, with a number of small pyramidal cells. A prominent band of horizontally arranged fibres is also a feature of this layer, which contains a large number of vertically organised fibres.

V. **The ganglionic layer** (infragranular) contains the largest pyramidal cells in any given area. A small number of stellate cells may also be observed, and there is also a considerable complement of horizontally organised fibres.

VI. **The multiform or fusiform layer** contains a variety of cell types, mostly small in size and thought to be modified pyramidal cells. This lamina is not always well demarcated from the adjacent cortical zone of fibres approaching or departing the cortex itself.

Functional columnar circuitry is one of the fundamental characteristics of the neocortex. This columnar principle essentially states that all neurones in a narrow column, perpendicular to the pia, and approximately 500 μm wide, are functionally coupled (Mountcastle, 1957; Hubel and Wiesel, 1965; Hubel and Wiesel, 1974).

The histological structure of the neocortex is similar in all mammals. Of the neuronal types found in the neocortex, pyramidal cells are most numerous, accounting for almost 70 % of the neuronal count (Winfield et al., 1980), with non-pyramidal (also called stellate) cells accounting for the remainder. Several quantitative studies have shown that the cell density and size may differ between different neocortical laminae and between different areas in the same brain and between species. However, a basic uniformity in the mammalian neocortex has been demonstrated by a number of workers. Sloper et al. (1979) found the absolute number of neurones and the proportions of pyramidal and

stellate cells were similar in two different areas of primate brain that had differing neocortical thickness. Furthermore, an approximately constant number of neurones of the two main types are found in a neocortical strip of constant width in animals ranging from mouse to man, except in visual neocortex (Rockel et al., 1980). The thickness of the neocortex was also reported to increase barely threefold from mouse to man.

Throughout the cortical laminae, there is also a large population of neuroglial cells (astrocytes, oligodendrocytes and microglia) and a close capillary network.

Pyramidal neurones of the neocortex fall into three main categories of the basis of their projections: corticofugal projection neurones project to subcortical targets, association neurones establish ipsilateral connections with other neocortical neurones, and commissural neurones project to other neocortical neurones but in the opposite hemisphere. Projections of neocortical neurones within the cortex are referred to as corticocortical.

1.1.2 Morphology of the mammalian hippocampus.

The characteristic neocortical laminar pattern is derived from the allocortex. However, the allocortex itself is often inconsistent in a patterns of lamination and structure. The archicortical hippocampal formation, while laminar to an extent, is recognised by the densely packed pyramidal neurones which form Ammon's horn (CA fields). This is a U shaped fold of cortex containing a narrow layer of pyramidal cells, extending from the prosubiculum to the hilus of the dentate gyrus (Figure 1.1). The architecture of the hippocampus is labelled longitudinally, with the pyramidal cell layer divided into four areas, CA1 - CA4 (Lorente de No, 1934). Some lack of clarity in the original description has led to confusion about the borders of some of the defined fields, with CA2 areas in the rat hippocampus lacking distinction unless specifically stained with Golgi preparations. Ammon's horn pyramidal cells are characterised by two main groups of dendrites extending from the cell body. The apical dendrite is a single pole extending through the underlying radiatum layer and into the molecular layer. The basal dendrites repeatedly branch in the oriens layer, producing dense tufts.

The dentate gyrus (DG) is a sharply folded trilayered cortex that forms a cap over the free edge of Ammon's horn (Figure 1.1). Its only cell layer contains densely packed granule cells, which send a unipolar dendritic tree into the overlying molecular layer. Apposed between the DG and the CA fields is the polymorph layer, generally considered to be part of the DG, although the original description of CA4 undoubtedly included a proportion of this area (Lorente de No, 1934). This polymorph layer is also referred to as the hilus of the DG, and, as its name suggests, contains a number of different cell types, primarily fusiform and other modified pyramidal neurones. Granule cell axons are designated 'mossy fibres' (Cajal, 1909), the targets of which are discussed below.

The subicular complex is often included in descriptions of the hippocampal formation. In the rat, this is a wedge of cortex which curves anteriorly and laterally to wrap around the posterior extension of the dentate gyrus. Posteromedially, it borders the medial entorhinal cortex, and anterolaterally, field of CA1 of Ammon's horn. There are three distinct cytoarchitechtonic areas in the subicular complex (Figure 1.1). The parasubiculum (PaS) lies dorsal to the medial entorhinal cortex, and is characterised by a superficial layer of moderately packed medium sized cells. The presubiculum (PrS) lies next to the PaS, and dorsomedial to the dorsal subiculum, and is characterised by a superficial lamina of densely packed small cells. Superficial layers of both PaS and PrS overlie a deep layer of small to medium cells similar to those observed in the deep layers of the entorhinal cortex. The subiculum itself has a loosely packed deep layer of pyramidal cells, and a wide superficial molecular layer. Interposed between Ammon's horn and the subiculum is an area known as the prosubiculum (ProS).

1.1.3 Morphology of the mammalian entorhinal cortex.

The term entorhinal cortex is a synonym for Brodmann area 28, and in the rat forms the most posterior ventrolateral forebrain structure. This archicortical region has undergone substantial regional and laminar differentiation in the primate brain relative to the rat brain. In the rat, the entorhinal cortex may be considered to be comprised of three areas, medial (EntM), intermediate (EntI) and lateral (EntL) (Bayer, 1985) (Figure 1.1),

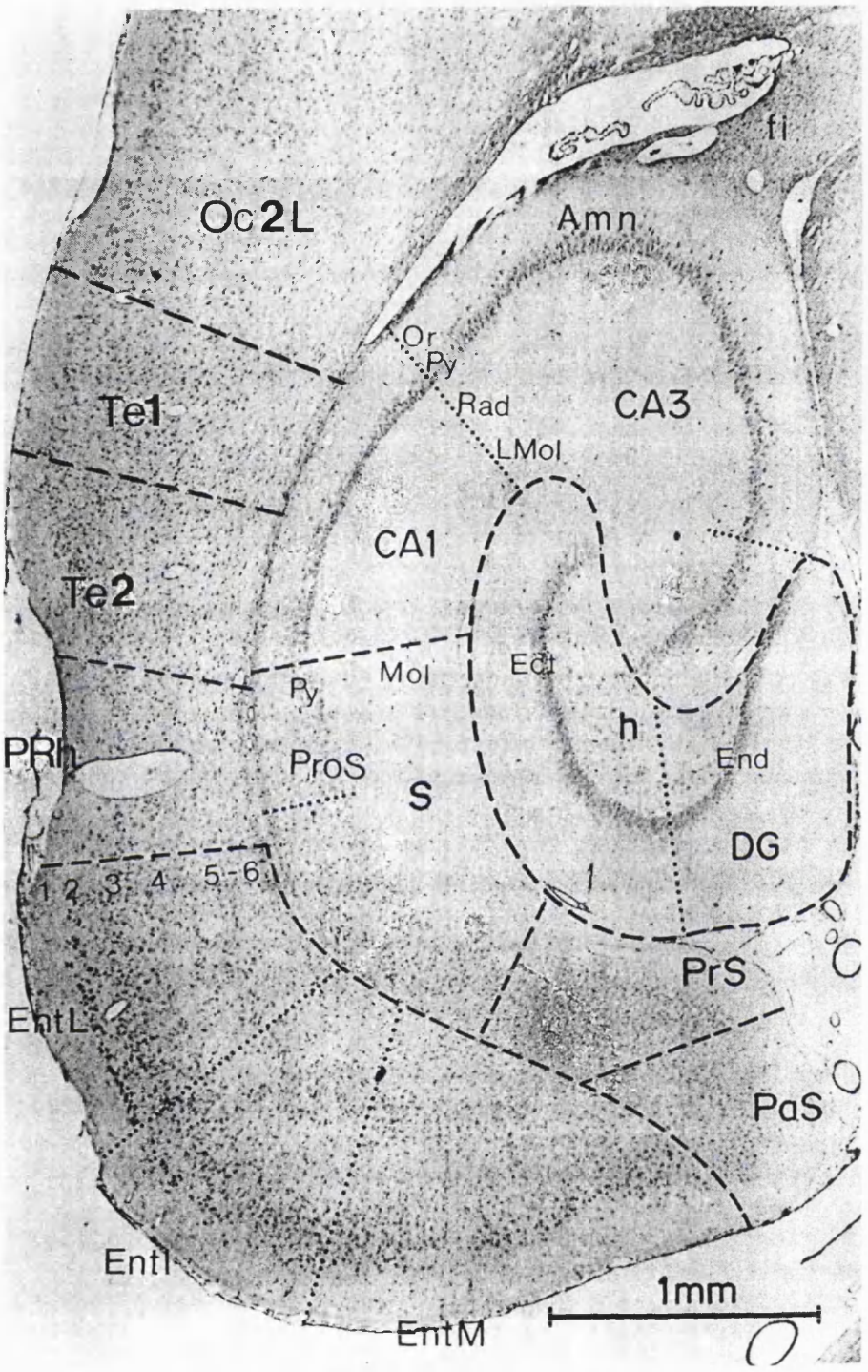

Figure 1.1: PHOTOMICROGRAPH SHOWING MAJOR MORPHOLOGICAL FEATURES OF THE HIPPOCAMPUS AND ENTORHINAL CORTEX.

Abbreviations: Amn, Ammon's horn; CA1, CA1 pyramidal cell field; CA3, CA3 pyramidal cell layer; DG, dentate gyrus; Ect, ectal limb of granular layer, End, endal limb of granular layer; EntI, intermediate subdivision of entorhinal cortex; EntM, medial division of entorhinal cortex; EntL, lateral division of entorhinal cortex; fi, fimbia; h, hilus of denate gyrus (also includes CA4); LMol, molecular layer of CA fields, Mol, molecular layer of subiculum; Oc2L, occipital cortex, area 2 lateral; Or, oriens layer; PaS, parasubiculum; PRh perirhinal area; PrS, presubiculum; Py, pyramidal layer; Rad, radiatum layer; Te1, temporal cortex, area 1; Te2, temporal cortex, area 2. Scale bar 1mm. Figure modified from Bayer (1985).

while in primates, there is a marked gradient of cytoarchitectonic changes from its rostral to caudal extents, which may be differentiated into at least seven different fields (Amaral and Insausti, 1990).

While the allocortical entorhinal cortex is similar to the neocortex as a multilaminate structure, its cellular constituents and laminar organisation are different from other cortical regions. Several numbering schemes have been adopted for indicating its various layers, with Cajal (1909) assigning seven layers, and Lorente de No describing six (1933). The area may be conveniently divided into six layers: Layer I corresponds to neocortical layer I; layer II is a narrow, cellular layer made up of islands of relatively large and darkly stained modified pyramidal (pre-alpha) and stellate cells. This layer is one of the most outstanding and distinguishing features of the entorhinal cortex, and in the human brain, the islands of layer II form small mounds which may be observed on the surface of the brain. These islands, apparent in EntL and EntI of the rat brain, form a continuous layer in EntM. There is usually an acellular gap between layer II and layer III (which corresponds to neocortical layer III, being comprised of medium sized pyramidal neurones). Another characteristic feature of the entorhinal cortex, in all species, is the lack of an internal granular layer (layer IV of neocortex). In its place is an acellular region of dense fibre labelling, the lamina desicans (Rose, 1927), which is inconsistently referred to as layer IV. Layer V corresponds to the neocortical layer V, and consists of large pyramidal cells. Layer VI is not easily distinguished from layer V, with decreasing cell density from this layer into white matter. These layers of the medial entorhinal cortex in the rat consist mainly of small cells.

1.1.4 The areal structure of the rat neocortex.

The rat brain has been the most widely used animal model in neurobiology. Consequentially, studies on the areal and laminar structure of the rat neocortex have been made since the beginning of the century. Brodmann laid down three main postulates for the formulation of neocortical areas: (i) The structure of a given area should be uniform; (ii) The area should be identifiable in related forms of mammalian brain; (iii) the main regions should have a constant structure. Resulting neocortical atlases reveal discrepancies between authors, which may be attributable to differences in rat

weight or strain. Using computer controlled measuring devices, Zilles and Wree (1985) defined topographically defined neocortical areas, which are in close agreement with the commonly used stereotaxic atlas of Paxinos and Watson (1982). The frontal isocortical region is defined by three main regions, Fr1, Fr2 and Fr3, which border medially upon the anterior cingulate cortex, and laterally upon the agranular insular cortex, and may be delineated from parietal areas by the lack of a prominent granular layer IV. The parietal cortex is divided into forelimb area (FL), hindlimb area (HL), Par1 and Par2, with appearance of FL and Par2 at more caudal levels. Par1 is the largest part of the parietal cortex and is bordered ventrocaudally by Par2 and dorsomedially by FL and HL. The occipital cortex is divided into two areas, Oc1 and Oc2, the former appearing at more caudal levels. Oc2 is subdivided into mediomedial (MM), mediolateral (ML) and lateral (L) areas. Oc2MM is bordered medially by the retrosplenial agranular area (RSA), with the granular layer (RSG) closest to the midline. More caudally, Oc1 medial (Oc1M) and binocular (Oc1B) areas interpose between Oc2ML and Oc2L. Primary auditory cortex (temporal) is divided into three areas, Te1, Te2 and Te3. Te1 appears at the ventrocaudal boundary of Par1 and is dorsal to Te3. Te2 replaces Te3 at caudal levels, and is dorsal to the perirhinal area which separates Te3 from the entorhinal cortex, the most ventrocaudal structure of the rat cortex.

1.2 Cell types of the cortex.

1.2.1 Pyramidal neurones.

Pyramidal cells derive their name from the shape of the cell body (Feldman, 1984). Many of these cells fall typically within the range of 10 - 50 μm in cell body length, although a wide diversity of cell area is apparent. The pyramidal cell has a long axon (except for pyramidal cells of layer II), a branching or tufted apical dendrite directed towards the surface of the neocortex (neocortical cells) or toward the "interior" of the hippocampal formation (hippocampal cells). Basal dendrites of hippocampal cells exit from several places along the base of the perikaryon, which repeatedly branch within the oriens layer, producing a dense tuft. The dendrites often bear a large number of spines for synaptic association with other neurones. Many

pyramidal neurones also possess branched axons, with collaterals within their area of origin, which form a large proportion of the presynaptic elements in the neocortex (Peters, 1987). Typically axon collaterals arise both in the vicinity of the parent cell body and also at distances up to several millimetres away (Winfield et al., 1981; Feldman, 1984). Axons of hippocampal pyramidal cells exit either from the perikaryon, or from a proximal segment of a basal dendrite, from where it travels to the alveus (a narrow strip of white matter at the base of the oriens layer) where it may bifurcate. This is especially prevalent in CA1 pyramidal cell axons where one branch travels toward the subicular complex, while the other branch travels toward the fimbria. Within the oriens layer, axons of CA3 pyramidal cells give off recurrent branches (the Shaffer collaterals) which travel up to the molecular layer of CA1. Pyramidal neurones of the neocortex as classified as small, medium or large, their size generally increasing with distance from the neocortical surface. Additionally, there are "giant" pyramidal Betz cells, found in layer V of the motor areas in frontal cortex (Krieg, 1946), or pyramids of Meynert, found in layer V of the visual cortex (Parnavelas et al., 1983), with cell bodies as large as 100 μm in length. Pyramidal cells in layer IV are often ovoid, and are known as fusiform pyramidal cells.

Pyramidal cells are the output cells of the neocortex and hippocampus. Both the neocortex and hippocampus display topographic projections, with cells in different neocortical layers sending axons to different sites (Jones, 1984). Generally, cells in layer II and III project ipsi- and contralaterally to other neocortical areas, while those of layer V project to subcortical sites.

1.2.2 Non-pyramidal neurones.

There are many types of non-pyramidal neurones (Warwick and Williams, 1973; Jones, 1975; Carpenter and Sutin, 1983), which may be subdivided according to staining characteristics and morphology. **Stellate nerve cells**, often called granule cells, encompass a variety of specific cell types. They are generally small in appearance, and appear in variable density of distribution in all the cortical laminae, except the most superficial (layer I), but are concentrated in greater abundance in layers II and IV. The cell layer of the DG is comprised of these granule cells. Granule cells have a rounded soma

drawn out at various angles by their richly branching dendrites, and a single, often relatively short axon. Some cells of the DG have much longer axons which, after collateral branching, run to join efferent fibres in the fornix. The most distinctive axons are known as mossy fibres, which arise from many granule cells in the DG, and pass through the polymorph layer (hilus), to eventually synapse with spines on the initial segments of the apical dendrites of the pyramidal cells of Ammon's horn. Other, scattered cells of the hilus display unique dendritic configurations. Thus a variety of stellate cells may be found in different brain areas. Another type of stellate cell, the **basket cell**, is horizontally extended, and has a short vertical axon which almost immediately divides into a horizontal family of collaterals. These end in pronounced tufts, forming synapses with the somata and proximal parts of the dendrites pyramidal cells. These cells are particularly abundant in the oriens of the hippocampus, where they form GABAergic inhibitory interneurones, receiving axosomatic and axodendritic synapses from some of the afferent fibre collaterals to the hippocampus, and also collaterals from efferent fibres. The basket cells also form numerous, crowded, axosomatic synapses on the cell bodies of the pyramidal neurones. Other stellate cells include **neurogliaform stellate cells**, which are small, with a dense and localised dendritic arborisation, within which the short axon usually ramifies, and **stellate fusiform cells**, most commonly found in layers II, III and VI.

Other non-pyramidal cells include **horizontal cells** (of Cajal), which are confined to layer I of the neocortex, and have bifurcating axons which make synaptic contact with the dendrites of pyramidal neurones (Barr, 1974). The **cells of Martinotti** are present throughout the neocortex, except in the most superficial layers, as are **chandelier cells**. **Pleomorphic cells** are considered to be modified pyramidal cells, with variously shaped soma, whose axons enter the white matter. Their dendrites spread widely in the neocortex. Finally, **double bouquet cells** are made from tightly bundled, unmyelinated, descending and sometimes ascending axon collaterals, giving rise to terminals along the apical dendrites of pyramidal cells caught in the bundle. The soma of these cells are generally found in layers II and III of the neocortex.

1.3 Connections of the rat cortex.

1.3.1 Neocortex.

The neocortex receives and gives rise to a complex connective system, both with other cortical areas and subcortical structures. The neocortex contains primary areas which are the main targets of sensory afferents (primary somatosensory, auditory and visual areas), and the motor and association areas. Because of the extensive connections of the cortex, only those relevant to the present studies will be considered; cortical projections to the striatum are reviewed in section 1.4.2.

The connectivity of frontal neocortical region of the rat brain, Fr1, Fr2 and Fr3 has been studied by many investigators (as reviewed, Zilles and Wree, 1985). All authors agree that these areas are part of the motor cortex in the rat, with Fr1 and Fr3 probably forming the primary motor cortex (Donoghue and Wise, 1982). Fr1-3 receive sparse afferent input from the thalamic nuclei (ventrolateral, ventromedial, parafascicular and intralaminar), geniculate nuclei, locus coeruleus and from almost all homolateral isocortical areas. Fr1 also receives afferents from the ipsilateral and contralateral (via the corpus callosum) Fr2 and Par1, contralateral Fr1, ipsilateral FL and HL, and the basal forebrain nuclei. Contralateral projections of frontal regions are reciprocal. The efferent connections of the frontal areas Fr1 and Fr3 terminate in the spinal cord, pontine nuclei and other subcortical structures. Homolateral and interhemispheric connections of the frontal areas arise from both layers III and V, though the homolateral association fibres are traditionally associated with layer III (MacLean, 1985). Corticocortical fibre projections are better described in primates than in the rodent brain. In primate brain, corticocortical systems have been found to originate in both layers III and V, forming homo- and heterolateral fibres (Zilles, 1990), with the highest density of callosal corticocortical fibres arising from visual (occipital) areas, while association fibres are more widespread throughout all regions of cortex.

The parietal cortex, consisting of Par1, Par2, FL and HL, receives mechanoreceptor (Welker and Sinha, 1972) and gustatory input. FL and HL

areas exhibit characteristics of a sensory and motor cortex, and are often referred to as sensorimotor amalgam (Donoghue et al., 1979). These areas have connectional features of both sensory and motor cortex; HL receives afferents from the ventral posterolateral nucleus, as does Par1, and additionally from the ventrolateral thalamic nucleus, as does the motor cortex (Donoghue et al., 1979). Corticocortical connection features are in common with those described above; the parietal cortex has sparse connections with contralateral Fr1 and Fr3, and to parietal cortex, though parietal contralateral connections are generally "crossed" (i.e. Par1 connects to Par2 and vice-versa). Homolateral connections are extensive within the parietal cortex. Subcortical ipsilateral targets (other than the striatum) include ventral posteromedial and posterolateral, reticular and centrolateral thalamus, pontine nuclei, medulla oblongata and spinal cord.

The temporal region Te1-Te3 consists of primary auditory cortex (Te1) and associational areas (Te2 and Te3) (Zilles and Wree, 1985). Te1 receives intensive thalamocortical projection, and all temporal areas receive afferents from the medial geniculate body and inferior colliculus. Callosal connections in Te1-3 are organised in band-like formations representing places of binaural interaction (Krieg, 1947). Afferent fibres to Te1 and Te2 from the retrosplenial areas have been described by Vogt and Miller (1983). Numerous association fibres also arise from the temporal area, innervating nearby ipsilateral temporal cortex. Subcortical projections include those to the inferior colliculus (which are reciprocal) and to thalamic nuclei.

The occipital cortex comprises two areas, Oc1 and Oc2, subdivided into 2 and 3 subfields, respectively (see section 1.1.4). Oc1 is considered to represent the primary visual cortex, surrounded by the visual areas of Oc2. Connections of these areas are extensive, with afferents to occipital areas from the dorsal lateral geniculate nucleus, locus coeruleus (ipsi- and contralateral), raphe and thalamic nuclei (laterodorsal and lateral posterior), ipsilateral Oc2M, Oc1, Te1, retrosplenial granular and agranular cortices, and contralateral Oc1, Oc2L and Te1. Many of these connections are reciprocal, with additional efferents from occipital areas to superior colliculus, pontine nuclei, reticular thalamic nuclei and pretectal area. The occipital areas give

rise to less homolateral association fibres, although interhemispheric connections via the corpus callosum are extensive.

1.3.2 Hippocampus and entorhinal cortex.

The anatomy and connections of the hippocampus and entorhinal cortex have been extensively studied since Cajal (1909) and Lorente de No (1933) carried out their classical Golgi method studies. More recently connections of the hippocampus have been studied by lesioning and retrograde transport experiments (as reviewed, Bayer, 1985).

The entorhinal cortex is extensively innervated: projections from the brain stem originate in the caudal part of the dorsal raphe nuclei and reticular tegmental nucleus of the pons, the locus coeruleus and the posteromedial ventral tegmental area. Thalamic afferents arise in the reuniens nucleus, and the anterior thalamic nuclei group. There is also diffuse projection from the medial septum, and topographic innervation from the diagonal band. A number of cortical areas project to the entorhinal cortex; these studies are based on cat, monkeys and rabbits. The main olfactory bulb and piriform cortex projects to EntL, and projections from widespread areas of neocortex terminate in EntL and EntM; temporal areas of neocortex are reported to project to the entorhinal cortex in rabbits and cats. Afferents from hippocampal areas also terminate in this area, arising from CA3 (Hjorth-Simonsen, 1971) and CA1 (Beckstead, 1978) and the subiculum (Swanson et al., 1981).

The efferent pathway from the entorhinal cortex known as the perforant path was first described by Cajal (1909). Fibres run from the entorhinal cortex to the deep white matter and "perforate" the subiculum to travel in the molecular layer of the CA fields, and finally terminate in the outer two thirds of the dentate molecular layer. The perforant path is topographically organised: EntL terminates in the superficial molecular layer of CA3 and the superficial third of the DG. EntM terminates in the deep layers of the CA3 molecular layer, and the middle third of DG molecular layer. EntI terminates between the zones innervated by EntL and EntM. These findings were confirmed by Steward (1976), who also demonstrated that these projections arise from layer II cells, and found a sparse topographic projection to CA1,

arising from layer III pyramidal cells. Projection to both CA3, DG and CA1 are bilateral, with the contralateral projections displaying similar topographic organisation.

The subicular complex receives a variety of afferents (Bayer, 1985). The locus coeruleus terminates sparsely in the subiculum, and a dense input from the anterior thalamic nuclei terminate in PaS and PrS. The vertical limb of the diagonal band, and the medial septal nucleus projects to the entire subicular complex. The anterior and posterior cortical areas, basolateral and lateral amygdaloid nuclei project to the ventral parasubiculum and subiculum. CA1 pyramidal cells send a dense projection to the subiculum, which may be more dense than CA1 projections to the septum (see below). CA3 pyramidal neurones are also thought to project to the subiculum (Swanson et al., 1978) via extensions of the Shaffer collateral system, though Hjorth-Simonsen (1971) proposed that all CA3 retrohippocampal projections are destined for the entorhinal cortex.

The subicular complex is an important area of efferent projection from the hippocampal formation to diencephalic structures, with dense projection to the anterior thalamus (mainly from PaS and PrS) and reuniens nucleus. There is a topographic projection from the subiculum to the mammillary body and other hypothalamic structures. The ventral subiculum also projects to the lateral amygdaloid nucleus, olfactory and prefrontal areas. The entire extent of the subiculum projects to nucleus accumbens and the lateral septal nucleus. There may also be projections to the retrosplenial cortex. A number of intrinsic connections are thought to exist within subicular structures, and to ipsilateral CA1 pyramidal cells.

Afferents to the pyramidal cells of Ammon's horn fall into two categories- those which terminate diffusely over the entire dendritic surface, and those that terminate in specific layers and areas of either apical or basal dendrites (laminated afferents) (Bayer, 1985). Diffuse afferents arise from the raphe nuclei, the locus coeruleus, and the medial septum-diagonal band complex. The molecular layer of CA1 receives dense input from the reuniens nucleus of the thalamus, and more diffuse input from the piriform cortex and entorhinal cortex. Topographic laminated afferent input to the molecular layer

of CA3 also arises from the entorhinal cortex. Deep layers of the radiatum of CA3 receive ipsilateral mossy fibre input from the dentate granule cells (see below). The remainder of the dendritic surface of CA1 and CA3 receive extensive commissural and associational input from extensively collateralised CA3 axons. Axons from all CA3 fields project to the radiatum and oriens of ipsilateral CA1 via branched Shaffer collaterals, and another branch of CA3 axons pass through the hippocampal commissure to innervate the radiatum and oriens of contralateral CA1. There are extensive topographic intrinsic connections between CA3 neurones, such that a given segment of CA3 projects both ipsi- and contralaterally to another, equivalent segment.

The lateral septal nucleus is the main target of extrahippocampal projections. Ipsilateral axons from CA1, and bilateral projections from CA3 terminate in a topographic fashion. Branches of CA1 axons also sparsely innervate the olfactory bulb, anterior olfactory nucleus and some areas of prefrontal cortex.

Afferent projections to the dentate gyrus are similar to those of the CA hippocampal fields, being either diffuse or laminated. Diffuse projections arise from the raphe nuclei, where the major postsynaptic targets are GABAergic interneurones (Halasy et al., 1992), locus coeruleus and medial septal nucleus, and terminate throughout the molecular layer. Laminated afferents arise almost exclusively from other hippocampal areas. Entorhinal projections terminate in the outer two thirds of the DG (perforant pathway, see above), where 60 - 70 % of the dendritic field of DG granule cells are taken up with perforant path input (Desmond and Levy, 1982). Adjacent to this terminal zone lies a band which contains commissural and associational afferents, which arise from CA3 and the hilus.

There are two main targets for the dentate granule cell axon- ipsilateral CA3, and the mossy cells distributed throughout the hilus, where mossy fibres descend and collateralise. Some of these collaterals branch within the hilus, and two long branches (infrapyramidal and suprapyramidal) pass toward CA3. The infrapyramidal bundle contacts the spiny basal dendrites of CA3, while the longer suprapyramidal branch forms contact with the apical dendrites of CA3. The interaction between CA3 dendrites and mossy fibres is complex-

electron microscopy demonstrates embedding of these dendritic spines with boutons of mossy fibre projections (Blackstad and Kjaerheim, 1961).

1.4 The rat striatum.

1.4.1 Morphology.

The corpus striatum is one of the main components of the basal ganglia, and consists of the caudate putamen and the globus pallidus (Heimer et al., 1985). The caudate putamen may also be referred to as the striatum, where it forms a large striated mass, dispersed by fibre bundles representing corticofugal and corticopetal projections. The striatum extends ventrally to include a large part of the olfactory tubercle as well as the nucleus accumbens. Therefore the most medioventral parts of the striatum, along with striated olfactory tubercle and nucleus accumbens are referred to as ventral striatum. This term should not evoke the picture of a separate part of the striatum; it simply implies that the striatum reaches the basal surface of the rat brain; the connection pathways of the ventral striatum are basically similar to those of the dorsal striatum.

The striatum contains several morphologically distinct cell types. Most descriptions of cell type are based on the size of the soma and characteristic spiny processes. Greater than 95 % of striatal neurones are medium sized (diameter 20 - 60 μm), whereas small neurones (< 10 μm diameter) are only occasionally seen in Golgi preparations, and constitute a heterogeneous and poorly described group of striatal cells (Chang et al., 1982). Of the medium sized neurones, those most commonly occurring are the "medium spiny neurone" (Chang et al., 1982), of which a proportion form projections to the globus pallidus and substantia nigra (Preston et al., 1980; Chang et al., 1981). Two types of large neurone (30 - 60 μm diameter) are found in the striatum, those which are spine free and have thick, relatively un-branched dendrites, and those which possess somatic and dendritic spines (Heimer et al., 1985). The ventral striatum contains a similar distribution of morphologically distinct cell types.

1.4.2 Connections.

Practically all neocortical and allocortical areas project directly to the dorsal or ventral striatum. Other major afferents come from the intralaminar thalamic nuclei and basolateral amygdaloid body.

Cortical projections to the striatum are mostly direct, which forms a characteristic topographical system with cortical areas projecting to immediately adjacent striatal areas (Webster, 1961). However, despite this direct topographical connectivity, a more complex picture of corticostriatal projections has arisen in more recent years. Goldman and Nauta (1977) reported that the prefrontal cortex of the monkey projects throughout the entire length of the caudate putamen, and similar observations have since been reported for the rat (Beckstead, 1979). Yeterian and Van Hoesen (1978) have shown in monkeys that association areas of the neocortex project to more that one area of the striatum. In addition to the direct topographic projection, secondary projection zones were identified. Moreover, related cortical areas (i.e. those with strong connection between them) seem to project to the same area of striatum.

The cells of origin of the corticostriatal pathway are somewhat controversial. Jones and colleagues (Jones et al., 1977; Wise and Jones, 1977) argued that projections from the somatosensory cortex to the striatum come from small to medium sized pyramidal neurones in the superficial part of layer V, and that these neurones project exclusively to the striatum. However, using intracellular injection of HRP, Donoghue and Kitai (1981) demonstrated that some large pyramidal cells sending projections to other subcortical targets, also send fine collaterals into the striatum, agreeing with the observations of Cajal (Cajal, 1909; DeFelipe and Jones, 1988). In another retrograde study, Royce (1982) reported that corticostriatal projections arising from layers V and VI in the cat may be formed as collaterals of corticothalamic projections. Kemp and Powell (1970) have reported that although all areas of the primate neocortex contribute to corticostriatal projections, there are a greater number of fibres arising from the frontal and parietal lobes than from other neocortical regions.

Amygdalostriatal projections arise mainly from the basolateral amygdaloid complex, and reach almost all areas of the dorsal and ventral

striatum (Heimer et al., 1985). Thalamostriatal projections arise in the intralaminar nuclei of the thalamus, and may also arise in ventral, lateral and posterior thalamic nuclei. Most other connections of the striatum are modifiers of the major connections described, and include reciprocal connection to the substantia nigra (SN), where the medium spiny neurones of the striatum innervate the reticulata (SNr), and receive innervation from the compacta (SNc) neurones.

The principle efferent systems of the striatum are to the globus pallidus, entopeduncular nucleus and SN. Neither striatum, nor ventral striatum are thought to project to the neocortex. The primary efferents of the globus pallidus project to the subthalamic nuclei and the striatum, and also the entopeduncular nucleus and SNr. However, more recently, projections from the globus pallidus to the neocortex have been identified, which appear to be cholinergic in origin (Fisher et al., 1988).

1.5 Transmitter systems of the cortex.

1.5.1 Acetylcholine.

The presence in the brain of acetylcholine (ACh) has long been known (Chang and Gaddum, 1933), and following establishment of its neurotransmitter action in the peripheral nervous system (PNS) by Otto Loewi (1921), Dale (1938) postulated a central neurotransmitter action. The study of cholinergic neurones in the CNS has been the subject of continued reinvestigation and reappraisal for many years. The concentration of ACh, and the activity of choline acetyltransferase (ChAT), which catalyses synthesis of ACh from choline may be measured in tissue samples to determine the relatively density of cholinergic neurones (Fonnum, 1970; Hoover et al., 1978). Additionally, both ChAT and acetylcholinesterase (AChE) may be localised histochemically (Butcher, 1978; Armstrong et al., 1983).

The basal forebrain of the rat contains a large number of projection neurones which stain for ChAT and AChE, suggesting that these magnocellular forebrain nuclei represent the origins of cholinergic projections. These nuclei include the nuclei of the medial septum, diagonal band, medial and lateral preoptic area, the basal nucleus (nucleus basalis magnocellularis or

nucleus basalis of Meynert, NBM), and the entopeduncular nucleus. The borders of individual nuclei are not well demarcated in the rat. Using ChAT immunocytochemistry, neurones were extensively stained in these areas (Armstrong et al., 1983; Houser et al., 1983), and double labelling techniques demonstrated that 80 - 90 % of AChE positive neurones also stained positively for ChAT (Eckenstein and Sofroniew, 1983).

Fibres from the medial septal nucleus and diagonal band have been reported to innervate the oriens and molecular layer of CA2 and CA3 of Ammon's horn, the molecular layer of the dentate gyrus (Wenk et al., 1980), and the entorhinal cortex (Bayer, 1985). Moreover, Houser et al. (1983) reported the presence of ChAT positive neuronal processes in all layers of the hippocampus, but particularly in the oriens of the pyramidal layer, and the molecular layer of the DG adjacent to the granular layer; lower densities were reported in the hilus and granular layer itself. The medial septal nucleus may also innervate the medial limbic cortex (Wenk et al., 1980). Pathways have been demonstrated from the horizontal limb of the diagonal band to olfactory bulbs and the entorhinal cortex (Wenk et al., 1977; Wenk et al., 1980).

Most, if not all areas of the neocortex receive cholinergic input from the NBM (Bigl et al., 1982). However, controversy exists concerning the presence of local cholinergic circuits within the neocortex, as various parameters of cholinergic function remain intact following surgical isolation. In undercut cortical slabs, 17 - 35 % of ChAT activity remains (Green et al., 1970), and Houser et al. (1983) reported the existence of ChAT positive somata throughout cortical layers II to VI. The highest concentration of terminals of NBM projections to the rat neocortex appear to be in upper layer V and layer IV, suggesting that this pathway may modulate neocortical efferent activity (Eckenstein and Baughman, 1984)

1.5.2 Monoamines.

The monoamine neurotransmitters of the cortex include the catecholamines dopamine and noradrenaline (NA), and the indolamine serotonin (5-HT), based on their catechol or indol nucleus respectively. Dopaminergic pathways and receptors are not the subject of the investigations described in this thesis, and thus will not be described.

Monoamines have been neuroanatomically localised using a variety of methods including formaldehyde or glycoxylic acid histoflourescence, immunohistochemistry, high resolution autoradiography using [^{3}H] incorporation into monoamines with light and electron microscopy, anterograde and retrograde tracing techniques coupled with destruction of catecholamine and indolamine pathways using 6-hydroxydopamine and 5,6 or 5,7-dihydroxytrypamine (as reviewed, Sladek and Bjorklund, 1982). Monoaminergic neurones may also be investigated in brain by a number of biochemical techniques, including high performance liquid chromatography (HPLC), and tyrosine hydroxylase activity, involved in the synthesis of monoamines. However, enzymes responsible for the synthesis of catecholamines appear to be unstable *post-mortem*, and are therefore of limited use a markers in *post-mortem*, diseased brain (Palmer et al., 1987a; Francis and Bowen, 1989).

1.5.2.1 Noradrenergic pathways.

The major source of noradrenergic innervation to the cortex arises in the locus coeruleus (LC), which consists of two major segments, the dorsal, or compact LC, and the ventral division (Swanson, 1976). LC innervation of the hippocampus is similar throughout all layers and regions (Loy et al., 1980). The densest innervation is to the hilus of the DG, the subiculum and the molecular layer of CA3. Projections appear to arise in the compact region, and the terminals of these cells synapse on the dendrites and cell bodies of granule cells of the DG and pyramidal cells of the CA fields (Loy et al., 1980). There is also LC innervation of the entorhinal cortex (Bayer, 1985).

LC input to the neocortex exhibits a crude topography; more anterior LC cells project to anterior neocortical regions. Innervation of the neocortex is rather uniform, with LC axons entering at the frontal pole, and running tangentially rostral to caudal in layer VI. Approximately 5 % of the LC projections to the neocortex arise contralaterally (Room et al., 1981). While individual LC cells may not innervate all terminals fields, they do exhibit extensive collateralisation within the neocortex, particularly in an anterior-posterior dimension, with branching of some collaterals to distant targets such as the cerebellum (Loughlin et al., 1982). Noradrenergic axons

may also form varicosities, which release transmitter without forming conventional synaptic contact (Magistretti and Morrison, 1988). There may also exist a sparse innervation from the LC to the striatum, although this has only been demonstrated using retrograde HRP labelling (Mason and Fibiger, 1979).

Adenosine is thought to be co-released with NA from some varicosities present on LC axons (Ossward and Azevedo, 1991), and may act as a regulatory transmitter for NA release, as inhibition of NA release has been demonstrated in hippocampal slices (Fredholm et al., 1983).

1.5.2.2 Serotonergic pathways.

The midline groups of neurones associated with the midsaggital seam of the brain stem, extending from the level of the interpeduncular nucleus to the level of pyramidal decussation form the system of the raphe nuclei, from which the greatest proportion of serotonergic innervation arises. The raphe nuclei are subdivided into seven regions, of which the dorsal raphe nucleus (DRN) is the largest. Serotonergic projections arising outside the raphe complex include those of the hypothalamus, the mesencephalic, pontine and medullary reticular formation and the interpeduncular complex (Tork, 1985). The ascending projections of the raphe nuclei travel via two main routes, which join at the level of the hypothalamus in the medial forebrain bundle, though all of the major fibre bundles of the forebrain may contain axons of raphe origin. The serotonergic innervation of the hippocampal region is highly organised, with the entorhinal cortex containing the densest network of serotonergic axons amongst all cortical areas, arising from dorsal and median raphe nuclei (Kohler et al., 1980). The granule cell layer of the DG is almost completely devoid of 5-HT innervation. A very dense band is present in the molecular layer of CA1 and CA2, and also in the oriens in the region of the basal dendrites of the pyramidal cells. CA3 and the subicular area receive a less dense innervation. Although serotonergic projections to these areas may be crossed, they are not thought to be bilateral, and at least 10 % of the raphe cells project to both hippocampus and entorhinal areas (Kohler and Steinbusch, 1982).

Serotonergic fibres mostly derived from the DRN and median raphe (Fuxe, 1965; Anden et al., 1966; Ungerstedt, 1971) have been shown to innervate the rat neocortex in an extensive and diffuse manner. Cortical projection from DRN cells may also innervate the piriform and cingulate areas as well as the neocortex, although varying proportions of projections to these areas are from the median raphe (Fallon and Moore, 1979). Detailed characterisation of 5-HT innervation in the neocortex (Lidov et al., 1980) reveals that the density of 5-HT axons is highest in the superficial layers of the cortex, although axons are found throughout the depth of the cortex. Serotonergic axons, in common with noradrenergic axons, also form varicosities along their length, which do not make conventional synaptic contact with cellular targets, instead releasing transmitter diffusely, and initiating a neuromodulatory action (Magistretti and Morrison, 1988; Dickenson, 1989). This action may contribute to the regulation of activity of raphe neurones via somatic autoreceptors.

1.5.3 Gamma-aminobutyric acid (GABA).

It has been estimated that 30 - 40 % of synaptic contacts within the CNS utilise GABA as their transmitter (Horton, 1989). The vast majority of GABAergic neurones are short interneurones, mediating local inhibitory control of the innervation targets (Jones, 1986), although there are a number of reports documenting "long" GABAergic pathways, mediating postsynaptic inhibition from one area to another, including the striatonigral pathway, where medium spiny cell bodies of the striatum project to the dopaminergic cells of the SNr, the striato-pallidal pathway and projections from the nucleus accumbens to substantia nigra, ventral tegmentum and globus pallidus (Horton, 1989). GABAergic neurones may be visualised using immunocytochemical markers which reveal large populations of neurones positive for the GABA synthetic enzyme, glutamic acid decarboxylase (GAD) and GABA itself in the hippocampal formation and neocortex of mammals (Hendry and Jones, 1986). Uptake of [^{3}H] GABA *in vitro* or *in vivo* combined with autoradiography has also proved to be a suitable method for the visualisation of GABAergic neurones in the CNS, although a proportion of the observed signal may be attributable to glial uptake (Jones et al., 1984). *In-situ*

hybridisation histochemistry for GAD is also used to visualise GABAergic interneurones (Najlerahim et al., 1990). It should be noted that early neurochemical studies to identify GABAergic neurones measured GAD activity in brain preparations. However, such studies indicated that the integrity of the enzyme was sensitive to the agonal state of the specimen, and thus was not an unequivocal marker of GABAergic nerve terminals in human diseased material (Bowen et al., 1976b; Bowen et al., 1976a). Moreover, measurement of GABA concentration in *post-mortem* tissue appeared to be similarly sensitive (Lowe et al., 1988)

In the hippocampus, the inhibition of the pyramidal cells of the CA fields, and the granule cells of the DG is mediated by local negative feedback circuits via GABAergic basket cells. Basket cells also mediate feedback and feedforward inhibition of pyramidal neurones of the neocortex, activated by recurrent axon collaterals and by extrinsic afferents.

1.5.4 Glutamate.

The determination of the transmitter role of glutamate and the elucidation of pathways utilising transmitter glutamate are commonly confounded by its metabolic role. Glutamate is present in higher concentrations than any other amino acid in the CNS, and in addition to its metabolic role it is incorporated into proteins within the CNS, involved in GABA synthesis and plays an important part in ammonia detoxification by conversion into glutamine. Initial electrophysiological studies (Curtis and Watkins, 1961) demonstrated that glutamate produced strong excitation of spinal cord neurones, and subsequent studies provided additional support for the concept of glutamate as a central neurotransmitter (Fagg and Foster, 1983; Fonnum, 1984).

The mechanism of glutamate release from nerve terminals is the subject of considerable controversy, although recent studies using an enzyme linked flourimetric assay demonstrated Ca^{2+} dependant release from an non-cytosolic pool (Nicholls and Sihra, 1986; Nicholls et al., 1987). More recently, Ca^{2+} dependent release has been shown to occur from a non-cytosolic glutamate pool which exchanges slowly with a cytosolic pool in isolated nerve terminals (McMahon and Nicholls, 1990). Moreover, there is evidence for a vesicular

localisation by visualisation of glutamate immunoreactivity concentrated in apparent synaptic vesicles (Horton, 1989).

Despite intensive research in recent years, a method of unequivocally identifying a transmitter pool of glutamate and thus a marker for glutamatergic neurones remains elusive. The enzymes responsible for the synthesis of both glutamate and aspartate are part of the general metabolic system present in all cells; however, a complex system of compartmentalisation appears to separate the metabolic from the releasable pool. Glutamine has been suggested to be the precursor of the releasable (putatively transmitter) pool of glutamate (Ottersen, 1991), and thus activity (Svennby et al., 1986) or localisation (Donoghue et al., 1985) of the synthetic enzyme glutaminase has been examined as a potential marker of EAA neurones; indeed, glutaminase immunoreactivity has been localised to pyramidal neurones and terminals in both rat and human cortex (Donoghue et al., 1985; Kaneko and Mizuno, 1988). However, although the majority of glutaminase mRNA positive neurones do not co-localise with GABAergic neurones (Najlerahim et al., 1990), the enzyme can also synthesise glutamate in GABAergic nerve terminals, and may display considerable activity in astrocytes (Hertz et al., 1983; McGeer et al., 1990), in common with another enzyme candidate for the production of transmitter glutamate, aspartate amino transferase (Wenthold and Altschuler, 1983).

Immunocytochemical localisation of labelled glutamate has also been proposed as a marker for glutamatergic neurones. However, interpretation is difficult since there is no means to distinguish transmitter glutamate from other pools (Storm-Mathisen and Ottersen, 1983), a problem also encountered when measuring excitatory amino acid concentration (Lowe and Bowen, 1990). *In vivo* administration of [^{3}H] D-aspartate with resulting uptake and retrograde transport is a useful means of identifying glutamatergic neurones (Streit, 1980), although neurones seem to vary in their ability to take up and transport the amino acid.

Many studies rely on glutamate or aspartate uptake and release as a marker for glutamatergic neurones. K^+-stimulated Ca^{2+}-dependent glutamate release is a useful marker of glutamatergic neurones in fresh rat and human tissue (Procter et al., 1988c), synaptosomes (Nicholls and Sihra, 1986) and *in*

vivo dialysis (Young and Bradford, 1986), but could not be demonstrated in *post-mortem* human tissue (Procter et al., 1988c), precluding this technique from being a useful marker in most studies of human disease. Na^+-dependent high affinity D-aspartate uptake is another possible marker of glutamatergic neurones (Procter et al., 1988c; Cowburn et al., 1988), although this technique was sensitive to tissue freezing (Schwarcz, 1980), and some neurones may not possess active transport mechanism for uptake (Garthwaite and Garthwaite, 1988). Glial uptake may also affect this technique, though the uptake mechanism in glia is thought to be of lower affinity (Horton, 1989). Similar drawbacks are applicable to the technique of Na^+-dependent [^{3}H] D-aspartate or [^{3}H] L-glutamate binding. Neocortical ablation reduced both Na^+-dependent glutamate uptake and [^{3}H] glutamate binding in the striatum (Vincent and McGeer, 1980), but striatal lesions reduced [^{3}H] glutamate binding with no effect on glutamate uptake, suggesting the binding sites are associated with intrinsic neurones lacking an uptake site. Autoradiographic studies of Na^+-dependent [^{3}H] D-aspartate binding (Greenamyre et al., 1990) revealed a binding pattern which was not characteristic of an expected presynaptic neuronal uptake site. Additionally, lesions of putative glutamatergic pathways did not result in a decrease in the pathway terminal fields.

While it is obvious that demonstration of a releasable transmitter glutamate pool or demonstration of glutamatergic neurones is difficult, a combination of techniques has provided strong evidence for a transmitter role of glutamate in a number of pathways (Ottersen, 1991). This has been most convincingly demonstrated for corticofugal fibres, especially corticostriatal (Herrling, 1985; Girault et al., 1986) and corticothalamic (Fosse and Fonnum, 1987; Kaneko and Mizuno, 1988). It is reasonable to assume therefore that the infragranular pyramidal neurones in the neocortex which form the corticostriatal pathway are glutamatergic, a proposal supported by retrograde tracing techniques using [^{3}H] D-aspartate (Streit, 1980). Hippocampal pyramidal neurones, as well as DG granule cells also appear to use glutamate as their transmitter (Fonnum and Walaas, 1978), as does the entorhinal-hippocampal perforant path (Kohler, 1986). There is also evidence consistent with glutamate being the major transmitter of corticocortical and

trans-callosal fibres. Hemidecortication is associated with a fall in glutamate concentration in the contralateral cortex (Peinado and Mora, 1986), and the uptake and retrograde transport of [^{3}H] D-aspartate provides further evidence for glutamate as a transmitter of these neurones. Pyramidal cells labelled thus include those of the primary visual (Baughman and Gilbert, 1981), sensorimotor (Fischer et al., 1991) and frontal (Streit, 1980) cortex which give rise to association fibres. Moreover, glutamate immunoreactivity is preferentially localised to corticocortical association fibres in the somatosensory areas (Conti et al., 1988). Labelling of trans-callosal systems has also been observed after [^{3}H] D-aspartate injection in frontal and sensorimotor cortex (Fischer et al., 1991).

1.6 Receptors of the cortex.

1.6.1 Acetylcholine receptors.

1.6.1.1 Acetylcholine and cognitive function.

Acetylcholine receptors, both muscarinic and nicotinic, are widely implicated in cognitive processes and control of neocortical activity. Many studies have documented NBM lesion-associated decline of cholinergic markers in the cortex, which are consistently associated with cognitive deficits (as reviewed, Olton and Wenk, 1987; Pepeu et al., 1990; and Alkon et al., 1991). A number of studies have also demonstrated that these cholinergic deficits may be reversed by administration of cholinomimetic agents, including acetylcholinesterase inhibitors (Haroutanian et al., 1985). Similarly, administration of cholinergic antagonists has been shown to impair cognitive function in rodent and primate models. In humans, nicotine induced improvement of rapid information processing is particularly well documented (Levin, 1992), supported by animal models (Battig, 1970; Haroutanian et al., 1985), and the nicotinic antagonist, mecamylamine was found to impair memory performance (Levin et al., 1987).

The effects of ACh in the neocortex and hippocampus have been extensively investigated; in general, ACh produces excitation; both acute

(mediated by nicotinic receptors) and chronic facilitation of excitatory action of other transmitters is well described (as reviewed, McCormick, 1990).

1.6.1.2 Nicotinic receptors.

Traditionally, nicotinic acetylcholine receptors have been categorised in two classes: muscle type and neuronal type. The irreversible antagonist, α-bungarotoxin is selective for the muscle type, while κ-bungarotoxin has recently been utilised to label neuronal nicotinic receptors (Loring and Zigmond, 1988). Neuronal nicotinic receptors are widely distributed throughout the brain (Clarke et al., 1985), and are thought to be involved in pre- and postsynaptic actions of ACh. The role of nicotinic receptors in cognitive function has been intensively studied (as reviewed, Levin, 1992). Recently, seven genes that encode for neuronal nicotinic receptors have been identified (Heinemann et al., 1991b), and it is likely that these genes code for a number of different receptor subtypes, composed from different gene product combinations, expressed in mammalian brain. This underlies the difference between muscle and neuronal nicotinic receptors; genes encoding for muscle receptors yield six distinct subunits (α1, ß1, γ, δ, and ε), of which five make the pentameric oligomer forming the final receptor. Neuronal receptors, which are also pentamers, are composed from combinations of only two subunit types (α2-5 and ß2-4). It is thought that the α subunit contains the high affinity nicotine binding site. As yet, functional differences between physiologically expressed neuronal types of nicotinic receptor are unknown, although their distribution may be visualised in the brain by *in-situ* hybridisation histochemistry (Wada et al., 1989).

Activation of the neuronal nicotinic receptor opens a cation channel which gates Na^+ and depolarises the associated neurone. The depolarisation may be of short duration and amplitude, giving rise to an excitatory postsynaptic potential (EPSP), which may summate with EPSPs produced from activation of other excitatory receptors, although nicotinic receptor activation alone is capable of producing an action potential.

1.6.1.3 Muscarinic receptors.

Muscarinic receptors are distributed widely throughout the mammalian brain (Yamamura et al., 1974; Yamamura and Snyder, 1974; Levey et al., 1991). In common with nicotinic receptors, they are thought to be involved in a number of central functions, and interest has centred on their role in cognitive function, as small doses of the antagonist, scopolamine, was shown to induce confusion and amnesia (Drachman and Leavitt, 1974).

Early studies which subdivided muscarinic receptors into M_1 and non-M_1 (Hammer et al., 1980) have given way to a wider classification, based on the cloning of m_1 - m_5 genes (Bonner et al., 1987; Bonner et al., 1988) which give rise to M_1 - M_5 receptors. However, the pharmacological distinction between these subtypes is often unclear (Buckley et al., 1988), and only three distinct physiological subtypes have been pharmacologically classified. The precise relationship between muscarinic receptor subtypes and the affinity of pirenzepine, used in the present studies, for the M_1 receptor has been determined from genetically defined subtypes (Buckley et al., 1989; Hulme et al., 1990). Cross-reactivity of this ligand for the M_4 receptor is not considered to be a confounding factor, and is addressed in the discussion of results (see Chapter 5, section 5.3.1).

The muscarinic receptors are structurally classified as part of the family of receptors which, when activated by an agonist, exert their effects by coupling to a G-protein and activating a second messenger signal transduction mechanism (Bonner et al., 1987; Loring and Zigmond, 1988). The action of each of the muscarinic receptor subtypes may be examined by expression of the cloned receptor in a cell system not normally expressing the native form (Felder et al., 1993). Activation of the M_1 receptor stimulates phospholipase C (PLC) activity (Fisher and Agranoff, 1987) via the G-protein G_q (Jope et al., 1994). PLC cleaves inositol-containing phospholipids (phosphoinositides), generating the primary second messengers inositol trisphosphate (IP_3) and diacylgycerol (DAG), which increase internal Ca^{2+} concentration, and activate protein kinase C (PKC), respectively. The M_1 receptor may also be coupled via different G-proteins to a variety of ion channels. The precise mechanism of receptor activation and final effect is unknown; stimulation of the M_1 receptor

undoubtedly mediates slow excitation by reducing a tonic potassium current known as I_M (McCormick, 1990), which has been demonstrated both *in vivo* and *in vitro*. The M_1 receptor may also indirectly stimulate adenylyl cyclase (Baumgold, 1992). By contrast, the M_2 receptor is linked to the G-protein G_i, which inhibits the enzyme adenylyl cylase, reducing the production of cyclic-AMP (cAMP), which may have an excitatory or inhibitory effect (McCormick, 1990). It is thought that the postsynaptic excitation of pyramidal neurones is mediated by the M_1 receptor (McCormick and Prince, 1985; McCormick and Williamson, 1989), while M_2 receptors inhibit transmitter release by a presynaptic mechanism (McCormick, 1990), and may stimulate GABAergic interneurones to reduce pyramidal cell excitability indirectly (McCormick and Prince, 1985; McCormick and Prince, 1986).

1.6.2 Monoamine receptors.

1.6.2.1 Alpha adrenergic receptors.

The α_1 adrenoceptor is widely distributed throughout the neocortex and hippocampus (Blendy et al., 1991; Zilles et al., 1991). Following the cloning of several α receptor subtypes (Strasser et al., 1992), a rational classification system divides α receptors into α_1 and α_2 types, with several subtype of each ($\alpha_{1a\text{ - }1d}$ and $\alpha_{2a\text{ - }2c}$). However, full pharmacological classification of these subtypes awaits the development of selective ligands, though some studies shown regional heterogeneity of α_1 receptor subtypes by autoradiography using [^{3}H] prazosin (Jones et al., 1990), also used in the present study to label both total α_1 receptors and the α_{1b} subtype.

α_1 receptors belong to the G-protein linked superfamily of receptors, and have seven hydrophobic transmembrane spanning regions, in common with the muscarinic receptor family. α_1 receptors are one of the many types of cell surface receptor which produce changes in cellular activity by increasing intracellular levels of Ca^{2+}, by coupling via G_q to PLC, which as described above, yields the second messengers IP_3 and DAG upon activation (Summers and McMartin, 1993). Additionally, α_1 receptors are also coupled directly to a receptor operated Ca^{2+} channel (Han et al., 1987). By contrast, the α_2 receptor subtypes are coupled via G_i to adenylyl cylase. Thus, activation alters cellular

activity by reducing intracellular levels of cAMP, or directly by regulation of ion channel activity (Bylund, 1988). The localisation of the α_1 receptors are thought to be mainly postsynaptic, where activation of the receptor causes inhibition (Mynlieff and Dunwiddie, 1988) or excitation (Madison and Nicoll, 1986). However, the inhibitory responses reported in the rat hippocampus may be attributable to activation of GABAergic interneurones (Andreasen and Lambert, 1991). The α_2 receptor has been traditionally regarded as an autoreceptor (Berlan et al., 1992), negatively regulating release of NA. However, there is now increasing evidence that this receptor may also be localised to postsynaptic targets (Summers and McMartin, 1993) where they mediate an inhibitory action (Curet and De Montigny, 1988).

1.6.2.2 Serotonin receptors.

As with the other receptors described, there are a number of different 5-HT receptor subtypes, first described by Gaddum and Picarelli (1957). The classification into "D" and "M" types has been largely superseded by classification in to 1,2 and 3 (Bradley et al., 1986), although new subtypes of the 5-HT receptor are currently being classified (Beer et al., 1993), and include new subtypes of the 5-HT_1 receptors, and 5-HT_{4-7} (Bockaert et al., 1992; Ruat et al., 1993a; Ruat et al., 1993b). In the CNS, ligand binding as well as molecular biology has been used to classify 5-HT receptors, which, on this basis may be classified into 5-HT_1, 5-HT_2, 5-HT_3 and 5-HT_4 subtypes (Peroutka and Snyder, 1979; Kilpatrick et al., 1987; Radja et al., 1991).

The 5-HT_1 receptor may be further subdivided into 5-HT_{1A}, 5-HT_{1B}, 5-HT_{1C} (now reclassified as 5-HT_{2C}), 5-HT_{1D}, 5-HT_{1E}, and 5-HT_{1F} (Beer et al., 1993). The 5-HT_{1B} is considered to be a species isoform found in rat and mouse, and is equivalent to the 5-HT_{1D} receptor (Radja et al., 1991). The highest affinity ligand for the 5-HT_{1A} receptor in common use remains 8-OH-DPAT (Beer et al., 1993).

The 5-HT_2 receptor has also been cloned, and other than the renamed 5-HT_{1C} receptor, two other subtypes have been identified; the 5-HT_{2A} receptor, which may be preferentially labelled using ketanserin (Branchek et al., 1990), and the incompletely characterised 5-HT_{2B} receptor (Schmuck et al., 1994). Although the pharmacological specificity of ketanserin for this latter receptor

is currently unknown, kinetic analysis of the binding of this ligand reveals conformity with a single high affinity site, and thus in this thesis, the term 5-HT_{2A} will be used to distinguish between the ketanserin high affinity site, and other receptors for which ketanserin has lower affinity (Hoyer et al., 1986).

5-HT_1 and 5-HT_2 receptors are also members of the seven transmembrane spanning region, G-protein linked receptor superfamily. In contrast, the 5-HT_3 receptor is strikingly different in that its properties are typical of a 5-HT gated ion channel (Derkach et al., 1989). Members of the 5-HT_1 family are coupled via G_i to adenylyl cyclase, and thus receptor activation reduces intracellular concentrations of cAMP. The electrophysiological actions of the 5-HT_{1A} receptor have been extensively investigated in both rat (Beck and Choi, 1991; Andrade, 1992) and human brain preparations (McCormick and Williamson, 1989); activation increases potassium conductance and inhibits cell firing. Postsynaptic sites mediate inhibition of pyramidal neurones of the cortex and hippocampus, while 5-HT_{1A} receptors localised on the cell bodies of DRN neurones regulate activity of these cells (Radja et al., 1992; Blier et al., 1993). By contrast, the 5-HT_2 receptor is linked via a G-protein to the PLC signal transduction mechanism. The electrophysiological consequences of 5-HT_2 receptor activation are less clear, although most reports describe an excitatory action (Sheldon and Aghajanian, 1990), particularly associated with activation of inhibitory interneurones.

1.6.3 GABA receptors.

$GABA_A$ and $GABA_B$ receptors are clearly defined receptor subtypes for the inhibitory amino acid transmitter GABA. The distinction between these sites is based on numerous criteria including pharmacological, biochemical and electrophysiological data. Several selective agonists exist for the $GABA_A$ receptor, including muscimol and isoguvacine (Chu et al., 1990). To date, the only known agonist selective for the $GABA_B$ receptor is baclofen (Bowery et al., 1980; Bowery et al., 1987).

Both types of GABA receptors mediate inhibition, but their mechanisms of action and receptor structure are quite different. The $GABA_A$ receptor is

coupled to the benzodiazepine/barbiturate receptor linked chloride channel (Stephenson and Olson, 1983; Mathers, 1987). Activation of the receptor causes opening of the chloride channel with subsequent neuronal inhibition. The $GABA_B$ receptor is G-protein linked to adenylyl cyclase, and also to putative K^+ and Ca^{2+} channels. In hippocampal pyramidal neurones, $GABA_B$ activation is associated with an increased outward potassium conductance (Gahwiler and Brown, 1985), and the K^+ channel involved appears to be the same one as activated by the $5\text{-}HT_{1A}$ receptor (Andrade et al., 1986). Inhibition of cortical pyramidal neurones by $GABA_B$ receptor activation has also been demonstrated in human brain preparations (McCormick and Williamson, 1989).

1.6.4 Adenosine receptors.

Adenosine has effects on many mammalian systems, including the CNS, and while there is not a defined "adenosinergic" pathway, the transmitter may be co-released with NA, and from cells that are metabolically active or stressed (Collis and Hourani, 1993). The first proposal that cell membrane adenosine receptors could be subdivided was made by Van Calker (1979), based on the observation that the purine could activate or inhibit production of cAMP in cultured cells. On the basis of pharmacological and functional studies, the proposed classification of adenosine receptors into A_1 and A_2 subtypes became accepted. Genes encoding A_1 and A_2 receptors have recently been identified (Linden et al., 1991). It has since become apparent that two types of A_2 receptor may be identified, the A_{2A} and A_{2B} subtypes (Daly et al., 1983).

The adenosine A_1 receptor is another member of the G-protein linked receptor superfamily, and stimulates adenylyl cyclase when activated. It is also though that the receptor is linked via different G-proteins to potassium channels, calcium channels and phospholipase A_2 (Collis and Hourani, 1993). Activation of the A_1 receptor has been shown to inhibit transmitter release, and may play a neuroprotective role in ischaemia (Rudolphi et al., 1992).

1.6.5 Excitatory amino acid (EAA) receptors.

Many actions of the neurotransmitter L-glutamate, ranging from fast excitatory transmission to the regulation of developmental processes are

mediated by ionotropic receptors. Historical classification of such receptors has been revised extensively in recent years, following development of selective agonists and antagonists allowing pharmacological classification, and cloning of genes encoding receptor subunits. Currently, ionotropic EAA receptors are subdivided into three main classes on the basis of agonist affinity: N-methyl-D-aspartate (NMDA), kainate and α-amino-3-hydroxy-5-methyl-4-isoxazole propionic acid (AMPA). Additionally, a class of G-protein linked metabotropic glutamate receptors have been demonstrated pharmacologically and by cloning, although at present the relationship between the cloned and endogenous forms is unclear.

1.6.5.1 The N-methyl-D-aspartate receptor ionophore complex (NMDA receptor).

N-methyl-D-aspartate selectively gates a channel with relatively slow kinetics, and high Ca^{2+} permeability. These characteristics, together with a voltage dependent block by Mg^{2+} identify the NMDA receptor, which is a complex of regulatory sites which may be affected by a number of agents. The NMDA receptor is the best characterised EAA receptor in experimental systems, and its involvement is implicated in neurotoxicity and learning and memory (see section 1.6.5.5 and 1.6.5.6). As described above, the NMDA receptor is a key mediator in excitatory transmission; regulation of activity is therefore an important consideration. The transmitter regulation site is the site by which the receptor is defined, and a number of selective ligands, in addition to NMDA, have been described (Fagg and Massieu, 1991). Autoradiographic studies have been interpreted as showing the existence of multiple forms of the NMDA receptor with distinct pharmacological properties; this may reflect a two-state model of high and low affinity agonist binding sites (Fagg and Massieu, 1991), or different combinations of the genetically defined subunits NR1 and NR2A-NR2D (Moriyoshi et al., 1991; Seeburg, 1993; Hollman and Heinemann, 1994).

Patch clamp studies suggested that glycine may have a modulatory role in NMDA receptor regulation (Johnson and Ascher, 1987), as submicromolar concentrations of glycine increased channel opening frequency. Following proposals that glycine acted as an allosteric modulator of the NMDA receptor,

it has become clear that glycine is required for receptor activation, and is now known as a co-agonist (Palfreyman and Baron, 1991; Lodge and Collingridge, 1991). A number of antagonists at this site have been described, which include HA-966, kynurenic acid (and derivatives) and a number of quinoxilinediones (as reviewed, Lodge and Johnson, 1991).

A number of "dissociative anaesthetic" compounds bind to the open channel of the NMDA receptor, including phencyclidine, and its derivative TCP, ketamine and the anticonvulsant dizocilpine (MK-801) (Foster, 1991). Binding of such non-competitive compounds is use dependent, and as such provide a measure of NMDA receptor activation (Foster and Wong, 1987; Huettner and Bean, 1988).

Polyamines increase the binding of [^{3}H] MK-801 induced by glutamate and glycine (Ransom and Stec, 1988; Williams et al., 1991). Spermine and spermidine act as agonists, and putrescine as an antagonist (Williams et al., 1991). New agents active at this site are under development.

In addition to the regulatory sites discussed above, the NMDA receptor may also be blocked by low concentration of Zn^{2+}, a mechanism independent of the voltage dependent Mg^{2+} block (Westbrook and Mayer, 1987). Low concentrations of arachidonic acid have also been recently demonstrated to affect NMDA receptor activation, possibly via an intracellular response (Kwak et al., 1992).

1.6.5.2 Kainate receptors.

It is only recently that the kainate receptor is recognised as being separate from the AMPA receptor, as many early studies were unable to differentiate responses of the two agonists (Patneau and Mayer, 1991; Cai and Erdo, 1992). However, cloning and expression of kainate receptors (Egebjerg et al., 1991; Werner et al., 1991) and examination of their properties in *xenopus* oocytes has led to re-evaluation of these receptor subtypes. Kainate receptors can be generated *in vitro* from expression of the gene products GluR5, GluR6, GluR7 (low affinity kainate receptor) (Hollman and Heinemann, 1994) and KA1 or KA2 (high affinity kainate receptor) (Seeburg, 1993). Importantly, *in-situ* hybridisation histochemistry for these subunits produces a characteristic binding pattern which is very similar to that observed using [^{3}H]

kainate autoradiography. Kainate receptors display regional heterogeneity compared to AMPA receptor, the most striking of which is the lack of expression of the kainate receptor in CA1 of the hippocampus, and its very high level of expression in CA3. However, certain isoforms of both AMPA and kainate receptors may gate Mg^{2+} and Ca^{2+} in addition to monovalent cations when activated. Pharmacological differentiation of kainate and AMPA receptors is being facilitated by the development of more selective ligands (Kwak et al., 1992).

1.6.5.3 AMPA receptors.

AMPA receptors can be reconstituted *in vitro* by expressing one, or co-expressing any two of the four subunits termed GluRA-GluRD, or GluR1-GluR4 (Seeburg, 1993; Hollman and Heinemann, 1994). These subunits occur in two major forms by alternative splicing. The "flip" and "flop" forms display different expression profiles in the developing and mature mammalian brain; prenatal brain expresses flip forms only, whereas a co-expression of both forms appear postnatally. However, although they may be distinguished by electrophysiological methods, pharmacological differentiation of different forms is currently impossible. As described above, it is now accepted that kainate and AMPA receptors are different entities; they may be easily distinguished electrophysiologically. Both kainate and AMPA receptors display different electrophysiological characteristics from that of NMDA receptors; the former receptors activate channels with fast kinetics (onset, offset and desensitisation measured in milliseconds), while NMDA receptors show much slower kinetics.

1.6.5.4 Metabotropic receptors.

Several clones encoding metabotropic glutamate receptors have now been identified (Heinemann et al., 1991a; Hollman and Heinemann, 1994), designated mGluR1-mGluR7. There is virtually no sequence homology between mGluR and other G-protein linked receptors. A number of pharmacological agents show activity at the metabotropic receptors; the actions of quisqualate and trans-ACPD (both agonists) were central to the identification of the metabotropic receptor class.

When expressed in oocytes, both the mGluR1 and mGluR5 metabotropic receptors stimulate the PLC signal transduction mechanism, generating the second messengers IP_3 and DAG. Activation of these receptors produces large, long lasting oscillating currents by Ca^{2+} dependent mechanisms (Hollman and Heinemann, 1994). Membrane depolarisation alone is not sufficient to trigger the mGluR signal transduction pathways. Recently, the mGluR1 receptor has been demonstrated to couple with cAMP and arachidonic acid forming signal transduction mechanisms (Aramori and Nakanishi, 1992); the latter may be implicated in NMDA receptor function.

The mGluR2-mGluR4, mGluR6 and mGluR7 metabotropic glutamate receptors are negatively linked to adenylyl cyclase. In addition, the mGluR2 receptor slightly affects the PLC signal transduction pathway (Tanabe et al., 1992). Activation of these receptors produces an inhibitory response; this finding may suggest a new and expanded role for glutamate receptors, although it may be possible that these receptors are located on inhibitory interneurones and thus are ultimately excitatory. Further investigation of the localisation and physiological properties of all metabotropic receptors await development of selective agonists and antagonists.

1.6.5.5 EAA receptors and neurotoxicity.

Much attention has been paid to the mechanisms by which EAAs may cause excitotoxicity. The mechanism appears to involve two main mechanisms (Rothman and Olney, 1987; Choi, 1991). An acute response is characterised by osmotic cell swelling, which, if left unchecked, spreads to the Golgi apparatus and then the nucleus, resulting in cell lysis. This mechanism is dependent on the continued present of agonist, and may be reversed by agonist removal, or administration of antagonist (Choi, 1991; Westbrook, 1993). Delayed excitotoxicity is dependent on NMDA receptor activity, and may occur up to 24 hr after a 5 min application of glutamate (Westbrook, 1993). The glycine site of the NMDA receptor must be occupied by agonist for this effect; antagonists at the glycine site abolish NMDA receptor associated toxicity, while increased glycine concentrations facilitate (McNamara and Dingledine, 1990). The Ca^{2+}-dependent mechanism of NMDA excitotoxicity leads to activation of proteases and lipases, and mitochondrial dysfunction results in gradual

neuronal disintegration and cell lysis. Both of these mechanisms are mediated by prolonged Ca^{2+} influx with subsequent accumulation (Meldrum and Garthwaite, 1990), although the osmotic features of the acute response may be attributable to Na^+ and Cl^- influx.

Excitotoxicity mediated by AMPA and kainate receptors has also been demonstrated (Meldrum and Garthwaite, 1990), with acute and delayed mechanisms similar to those of the NMDA receptor; it is possible that application of these agents leads to prolonged release of transmitter glutamate, with resulting neurotoxicity mediated by NMDA receptors.

Excitotoxicity may play a role in the cell loss observed in acute and chronic neurodegenerative disease (Rothman and Olney, 1986; Greenamyre et al., 1988; Greenamyre and Young, 1989a). Acute energy deprivation, caused by transient ischaemia produces extensive cell loss in superficial neocortical layers and CA1 of the hippocampus; regions with high densities of EAA receptors (Greenamyre et al., 1985a; Monaghan et al., 1985). Decreased re-uptake (Silverstein et al., 1986), or increased release (Drejer et al., 1985) of EAA may be responsible for overactivation of EAA receptors. A self perpetuating mechanism, whereby the glutamate released from lysed cells affects nearby cells or a change in extracellular K^+ concentration may also contribute to excitotoxicity by facilitation of NMDA responses following removal of the voltage dependent Mg^{2+} channel blockade (Cox et al., 1989). Further support to the involvement of the EAA receptors is provided by evidence that EAA receptor antagonists have a neuroprotective effect in cerebral ischaemia (Rothman and Olney, 1986; Meldrum and Garthwaite, 1990).

1.6.5.6 EAA receptors and learning and memory.

The involvement of long term potentiation (LTP) has been widely implicated in the formation of certain types of memory (Alkon et al., 1991; Staubli and Lynch, 1992). Induction of LTP, which chronically "potentiates" EPSPs induced by EAA receptors, has been most extensively studied in area CA1 of the hippocampus (as reviewed, Collingridge and Singer, 1990). LTP is induced by long lasting tetanic stimulation of the target neurone, mediated by AMPA or kainate receptors, since the EPSPs observed can be blocked with antagonists such as CNQX, but not by NMDA antagonists (Collingridge and

Singer, 1990). However, NMDA receptor activation is an absolute requirement for LTP establishment, since induction can be blocked with NMDA antagonists (Collingridge, 1987), and it has also been demonstrated that the glycine modulatory site must be occupied by an agonist (Bashir et al., 1990).

The sub-cellular processes activated by LTP are unclear, although Ca^{2+} entry and activation of Ca^{2+}-calmodulin dependent enzymes may lead to reorganisation of cytoskeletal elements of the dendritic spines, enhancing transmission of EPSPs to the rest of the dendritic tree (Lynch et al., 1991). A number of other aspects of synaptic plasticity are also dependent on activation of EAA receptors, although these mechanisms may rely on trophic, rather than LTP effects. For example, application of sub-toxic doses of NMDA to cultured neurones promotes survival, while the NMDA antagonist AP5 inhibits survival, neuritic outgrowth, dendritic branching and synapse formation (Mattson, 1988; Mattson et al., 1988; Collingridge and Singer, 1990).

Animal studies implicate the NMDA receptor in learning and memory processes. Administration of NMDA antagonists impairs animal learning, particularly of new information (Staubli and Lynch, 1992). Moreover, drugs which enhance NMDA mediated transmission facilitate such learning behaviour in some species (Handelmann et al., 1989; Monahan et al., 1989). Additionally, it has recently been demonstrated that agents which facilitate transmission via the AMPA receptor also enhance memory function (Staubli et al., 1994).

1.7 Alzheimer's Disease- general overview.

1.7.1 History, incidence and symptoms.

In 1907, Alois Alzheimer published a report describing autopsy findings for a 55 year old woman suffering for 4.5 years from progressive dementia (Alzheimer, 1907). The autopsy revealed many abnormal nerve cells containing tangles of fibres, and a reduction in the number of ganglionic (pyramidal) cells. Prior to this, the clinical condition was described accurately by Esquirol (1838).

In recent years, Alzheimer's disease (AD) is recognised as a problem with staggering medical and social dimensions. Dementia, the global

impairment of cognitive function, affects 5 - 10 % of the population over 65 years of age, and more than 20 % of those over 80 (Katzman, 1976; Plum, 1979; Garland and Cross, 1982). AD is the major cause of dementia, regardless of the age of onset; of dementing disorders, AD accounts for approximately 40 % observed in presenile years (Marsden and Harrison, 1972) and 50 % observed in senile years (Tomlinson, 1977).

Alzheimer's disease is a slowly progressing disorder. Initial symptoms of forgetfulness may be easily dismissed as a benign senile disorder. However, symptomatology becomes clearer as the sufferer enters a phase of confusion, at which point a cognitive deficit may become identifiable in the course of a detailed clinical interview. Individuals in this phase often cannot function as well in employment or social situations, and impairment of language skills, perceptuo-spatial relationships and problem solving become more apparent. The dementia phase can be defined as beginning at the point at which, left on their own, the patient can no longer survive- individuals become severely circumscribed in movements and activities, and travel, even to familiar areas becomes impossible. As the disease advances, the individual cannot walk or talk, and becomes restless and agitated, often displaying aggressive traits. Continuous care must be given at this stage, as the patient is totally incapable of caring for themselves. Dementia symptoms of this sort are associated with a sharp decrease in life expectancy; the disease course lasts on average 6 years, although 10 years is not uncommon (Sulkava et al., 1983).

The aetiology of the disease is, at present, unknown. Currently several hypotheses are favoured as the central event of the disease process (see below and General discussion, section 10.4.2 and 10.6) including: amyloid production, overproduction, aberrant compartmentalisation, or aberrant metabolism of APP; tangle formation by hyperphosphorylation of the microtubule associated protein, tau; or a combination of factors with complex interaction, including that of amyloid or tau with apolipoprotein E4.

1.7.2 Diagnosis.

The only positive means of diagnosis of AD is by neuropathological examination to determine the relative density of the hallmarks of AD; senile plaques and neurofibrillary tangles. Though this may be uncommonly

performed by analysis of biopsy samples, most positive AD diagnoses are performed at autopsy. In life, diagnosis of suspected AD is made by ruling out all other dementing conditions, which include toxic, nutritional, infectious, endocrinological, neoplastic, traumatic and circulatory causes. Most descriptions and operational definitions of AD correctly emphasise cognitive impairment as a key feature of the disease (e.g. Medical Research council, 1987; American Psychiatric Association, 1980), although non-cognitive symptoms (e.g. aggression, wandering, incontinence and depression) are also a major feature.

The two most common tests of mental status are verbal information concentration orientation tests, which assess recent and past memory, and the mini-mental state evaluation test, which assesses drawing, writing and language skills (Blessed et al., 1968).

1.8 Alzheimer's disease- neuropathology.

1.8.1 Overview.

Post-mortem examination of the brains of AD patients reveals characteristic macroscopic and microscopic features (Tomlinson and Corsellis, 1984). The brain is smaller than a normal control, weighing 60 - 80 % of normal, which is attributable to loss of both grey and white matter. As a result the gyri are narrowed and the sulci widened. The affected areas are circumscribed- temporal and parietal areas are particularly affected, with less frontal lobe atrophy. The primary sensory areas are relatively spared (Brun, 1983; Tomlinson and Corsellis, 1984; Esiri et al., 1986; Esiri et al., 1990). The cortical pyramidal neurone is primarily affected in AD; loss of neocortical cells forming association pathways (as reviewed, Hof and Morrison, 1994) in circumscribed (temporal and parietal) cortical and hippocampal (CA1) areas is primarily a disappearance of pyramidal neurones (Terry et al., 1991), and the remaining neocortical pyramidal neurones of layer III and V are sites for tangle formation (Pearson et al., 1985; Lewis et al., 1987). These neurones form the majority of cortical efferents (Jones, 1984). Such neuronal loss is primary to the cognitive deficits observed in AD, a proposal supported by findings of several studies where significant correlations between synapse and

cell loss in these areas and ratings of dementia have been described (Neary et al., 1986; DeKosky and Scheff, 1990; Terry et al., 1991).

Microscopically, AD is characterised by two histopathological hallmarks- senile plaques and neurofibrillary lesions, which constitute extra- and intracellular fibrous deposits, respectively.

1.8.2 Plaques.

The senile, or neuritic plaque is a complex, multicellular lesion, the temporal genesis of which is imperfectly understood. So called "classical" neuritic plaques (also referred to as senile and neuritic plaques), of which Alzheimer himself first described the light microscopic appearance, consist of a compacted spherical deposit of extracellular filaments, composed of ß-amyloid, surrounded by variable numbers of dystrophic neurites, both axonal and dendritic. Such plaques may also contain activated microglial cells intimately surrounding the amyloid core (Wisniewski et al., 1989), as well as reactive astrocytes around the periphery. Amyloid is a generic term used to describe a group of chemically heterogeneous proteins found in a number of different tissues and diseases, which gives rise to the congo red birefringence and proteolysis resistant characteristics of the classical plaque. Amino acid sequencing of senile plaque amyloid (Masters et al., 1985) revealed it to be essentially the same as cerebrovascular amyloid isolated from meningeal blood vessels (Glenner and Wong, 1984), arising from ß-pleating of the 39 - 42 amino acid peptide now commonly referred to as Aß, or ßA4.

Although many classical plaques can be found in the hippocampus, amygdala, entorhinal cortex and neocortical association areas, the advent of highly sensitive antibodies to ßA4 has revealed that they are a minority of all neuronal ßA4 deposits. Far more abundant in most AD brains are amorphous, roughly spherical and less dense deposits of ßA4 referred to as "diffuse" or "pre-amyloid" plaques (as reviewed, Selkoe, 1994). Electron microscopic examination of these deposits reveal few abnormal neurites, astrocytes or microglial cells, and their ßA4 immunoreactivity is not attributable to amyloid filaments, which are sparse or absent. The precise biochemical and structural features of diffuse plaques remains unclear. Diffuse plaques, unassociated with dystrophic neurites, gliosis or tangles are also found in the brains of young

Down's syndrome individuals, and appearance of neuritic plaques progresses with age. It is therefore suggested that diffuse plaques evolve into senile plaques during the disease progression in AD (as reviewed, Selkoe, 1994).

A third type of plaque, referred to as "burnt out" can be identified at the end stages of AD. The dense amyloid core of the classical plaque remains, as do the reactive astrocytes. However, abnormal neurites are not observed, and these plaques may reflect the remaining insoluble material following the death and disappearance of cells whose neuritic processes once infiltrated the plaque.

The origin of the senile plaque remains disputed, although as described above, the best-known hypothesis contends that the neuritic plaque evolves from diffuse forms. However, diffuse plaques are also found in cerebellar cortex and basal ganglia, where the mature neuritic forms are seldom observed. Another hypothesis arises from findings showing clusters of dystrophic neurites in the virtual absence of amyloid, and it has been suggested that these neurites release amyloid from their contained precursor (Terry and Wisniewski, 1970). Alternative hypotheses include cholinergic degeneration giving rise to distant dystrophic neurites which release amyloid (Adrendt et al., 1985), or that plaques develop from amyloid in the blood vessel wall (Glenner, 1979).

1.8.2.1 Structure, processing and functions of amyloid precursor protein (APP) and amyloid.

Following the isolation and purification of ßA4 (Glenner and Wong, 1984), four laboratories independently cloned cDNAs encoding part of or all of the peptide precursor, APP (Goldgaber et al., 1987; Kang et al., 1987; Robakis et al., 1987; Tanzi et al., 1987). The deduced amino acid sequence predicted a polypeptide of 695 amino acids, containing a single hydrophobic stretch at its C-terminal end, having the properties of a membrane spanning domain. Of particular interest was the observation that the 39 - 43 residue ßA4 sequence began 28 residues amino-terminal to the transmembrane domain and extended 11 - 15 residues into that domain (Figure 1.2).

The APP gene undergoes alternative exon splicing to yield several distinct isoforms (Figure 1.2). The 751 residue form (APP_{751}) contains a 56 amino acid insert in the middle of the polypeptide with a 50 % homology to the

Kunitz family of serine protease inhibitors (KPI). A 770 residue form contains the KPI exon and an additional adjacent exon (designated ox-2) of unknown function. These two forms of APP are often categorised together and referred to as $APP_{751/770}$. Additionally, there are at least two distinct mammalian gene products with a high degree of homology to APP, designated APLP1 and APLP2 or APPH, which do not contain an intact ßA4 sequence (Wasco et al., 1992; Wasco et al., 1993). The effects that these molecules may have on APP processing and generation of ßA4 is currently unknown.

APP is expressed at high levels in many different tissues throughout the body. In most tissues, the Kunitz protease containing transcripts $APP_{751/770}$ are the most abundant, but in the CNS, APP_{695} is most predominant. A variety of post-translational modifications of the APP isoforms have been characterised in cultured cells (as reviewed, Selkoe, 1994), including N- and O- glycosylation in the Golgi apparatus, phosphorylation and sulphation.

Mature APP can undergo proteolytic cleavage following glycosylation at residue 16 of ßA4, to release the large, soluble extramembranous portion designated APP_S (Weidemann et al., 1989; Esch et al., 1990; Sisodia et al., 1990). Such constitutive secretion precludes the formation of intact ßA4, and this secretory pathway is now often referred to as the **α-secretase** pathway (Figure 1.2). However, the percentage of precursor processed by this pathway varies between cell types, but seems not to exceed about one third of newly synthesised APP (Weidemann et al., 1989). Following identification of this pathway as the first secretory mechanism for APP, it was rightly assumed that other pathways must be responsible for the production of intact ßA4. The lysosomal pathway produces several low molecular weight C-terminal fragments, some of which show ßA4 immunoreactivity, suggesting that they contain intact ßA4 (Golde et al., 1992). APP processing via this pathway is supported by findings of mature APP in lysosomal vesicles, as well as a number of low molecular weight C-terminal fragments containing ßA4 (Haass et al., 1992a).

A third processing pathway for APP has recently been described following identification of two APP_S derivatives that do not end at residue 16 of ßA4. One of these soluble forms extends at least to residue 28 of ßA4 and

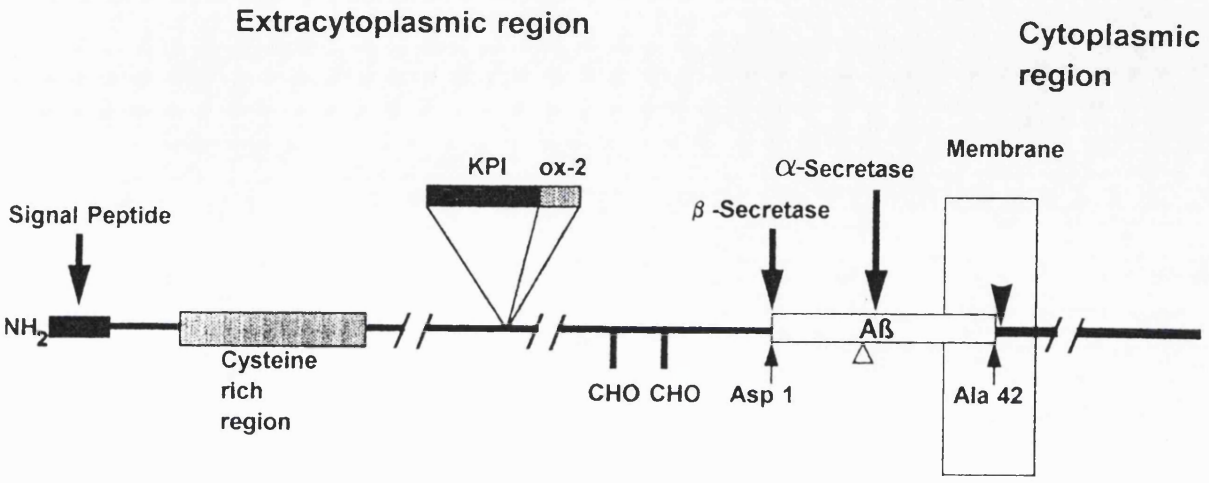

Figure 1.2: SCHEMATIC REPRESENTATION OF THE STRUCTURE OF APP. The molecule depicted corresponds to APP_{695}. Splicing of the KPI encoding region in the indicated position yields APP_{751}, while inclusion of both KPI and ox-2 exons yields APP_{770}. The molecule may undergo glycosylation at two sites (marked -CHO). α-secretase cleaves APP in the ßA4 encoding region between residues 16 and 17, and precludes intact ßA4 formation; ß-secretase cleaves at the N-terminal of ßA4. Putative transmembrane cleavage is performed by an unidentified enzyme. A number of mutations at three main sites have been described in APP; at the residues immediately N-terminal to the ßA4 region (Swedish mutation; one and two residues N-terminal to the ß-secretase cleavage point); within the ßA4 region (residue 21 from N-terminal; open triangle); and within the membrane spanning region, two residues C-terminal of ßA4 (717 mutation; unmarked arrowhead).
Figure modified from Selkoe (1994).

probably beyond, and may contain intact ßA4. A substantial proportion of APP secreted by human mixed brain cell cultures, as well as present in CSF, is a shorter form precisely cleaved at the amino terminus of the ßA4 sequence by "**ß-secretase**" (Figure 1.2) (Seubert et al., 1993), demonstrating that the amyloid fragment may arise in part from secretory processing at or near the cell surface.

Although it was widely assumed that the membrane associated ßA4 sequence would not be found as a free peptide, it appears that ßA4 is produced and secreted as a normal cellular process. Examination of the media of a variety of primary or APP transfected cells revealed secretion of soluble ßA4 (Haass et al., 1992b; Seubert et al., 1992) under normal metabolic conditions. ßA4 has also been detected in normal CSF of humans and lower mammals (Seubert et al., 1992; Shoji et al., 1992). It remains unclear by what cellular processing pathway ßA4 is generated- lysosomal or ß-secretase pathways may both play a part.

Hypotheses regarding the normal function of APP are many (as reviewed, Selkoe, 1994). The presence of a KPI domain in $APP_{751/770}$ led some to assume that an important function of APP might be to inhibit certain serine proteases (Nakamura et al., 1992). Another function based on cell culture studies is as a growth promoter- treatment of fibroblasts with antisense APP oligonucleotides inhibited proliferation, which could be restored by the addition of APP. In another study, APP_S was found to have a neuroprotective role, downregulating Ca^{2+} concentrations, and suggesting that an APP_S receptor may exist (Mattson et al., 1993). APP_S may also play a part in cell-cell or cell-matrix interactions (Schubert et al., 1989).

Several studies imply that ßA4 itself may have a neurotoxic role. Two hypotheses are currently favoured. First, ßA4 may directly injure cells (Yankner et al., 1990), independent of other factors. The second hypothesis proposes that ßA4 may increase susceptibility to neurotoxic factors such as EAA (Koh et al., 1990; Mattson et al., 1992) by a calcium dependent mechanism. Credibility to the hypothesis that decreased 'normal' α-secretase APP processing resulting in less APP_S production, with overproduction of ßA4 is central to the pathogenesis of AD is lent by the latter finding- decreased

APP_S may result in impaired Ca^{2+} homeostasis, synergising with the effects of ßA4's calcium dependent toxicity.

1.8.2.2 Regulation of APP processing.

The role of phosphorylation in APP processing has been the subject of intensive research following the observation that application of phorbol esters to several cell types increased APP_S production, presumably by stimulation of the α-secretase pathway (Caporaso et al., 1992). Direct phosphorylation of APP by PKC may account for this observation, as phosphorylation of a synthetic APP, and APP found in PC12 appears to be at the same site (Suzuki et al., 1992). Furthermore, Nitsch et al. (1992) described regulation of APP processing by stimulation of M_1 receptors in PC12 cells transfected with the receptor, an effect blocked by the PKC inhibitor, staurosporine. APP secretion stimulated by PKC activity has been confirmed in a number of laboratories, including our own (Webster et al., 1993). This is supported by *in vivo* studies: treatment of depressed patients with lithium and antidepressants, thought to interfere with PLC linked signal transduction mechanisms, significantly reduced $APP_{751/770}$ secretion (Clarke et al., 1993a) in CSF. It appears that APP_S and ßA4 secretion may be reciprocally regulated: stimulation of PKC has also been demonstrated to reduce ßA4 secretion (Buxbaum et al., 1993; Fukushima et al., 1993; Gabuzda et al., 1993). Regulation of the α-secretase pathway may also be regulated by neuronal activity. Nitsch et al. (1993) demonstrated increased release of APP fragments following electrical stimulation, and increased APP secretion has been observed *in vivo* in push-pull canula perfusates of rat striatum following potassium evoked depolarisation (Dijk et al., 1994b), although full characterisation of these secreted fragments is not yet complete. It is also possible that phosphorylation regulation of APP secretion may occur by phosphorylation not of APP, but of α-secretase itself (Hung et al., 1994).

1.8.3 Neurofibrillary lesions.

The intraneuronal deposits found in the brains of AD patients are commonly described as neurofibrillary lesions (as reviewed Goedert, 1993). There are a number of types of these lesions: neurofibrillary tangles (NFT) are

found in predominately large, pyramidal neurones and apical dendrites. Neuropil threads are found in distal dendrites. Intraneuronal fibrillary lesions are also found in the abnormal neurites associated with neuritic plaques. Ultrastructurally, all three lesions contain abnormal paired helical filaments (PHF) as their major components, and a number of straight filaments (SF) as a minor fibrous component. Neurofibrillary lesions develop in cells which undergo degeneration in AD, and their relative insolubility enables them to survive after the death of the associated neurone, which give rise to the characteristic, extracellular "ghost" tangles which accumulate in the neuropil. As with senile plaques, the temporal mechanisms leading to the formation of neurofibrillary lesions are poorly understood, however, unlike plaques, these lesions seem to be much more closely associated with neurones which undergo degeneration in AD, and correlations have been described between tangle count, dementia and neocortical synapse number (Terry et al., 1991).

Paired helical filaments are a common feature of the intraneuronal neurofibrillary lesions. Current evidence suggests that PHFs are made entirely of the microtubule associated protein, tau, in an abnormally phosphorylated state. The PHF, as its name suggests is comprised of two strands of subunits which twist around one another in a helical fashion. PHF can be isolated from tangle fragments or dispersed filaments (Wischik et al., 1988; Greenberg and Davies, 1990); these two types of PHF have tau epitopes in common, but differ in their solubility in strong denaturing agents, and sensitivity to proteases (Goedert et al., 1992; Goedert, 1993). Straight filaments also contain PHF, which also share tau epitopes with the former types (Goedert, 1993). Tau containing PHF are therefore a common feature of neurofibrillary lesions.

1.8.3.1 Tau protein- structure, function and PHF formation.

Multiple tau isoforms are produced from a single gene by alternative mRNA splicing. In adult human brain, six isoforms can be identified, which range from 352 to 441 amino acids, and differ from one another by the presence, absence and combinations of three different inserts (Goedert et al., 1992). The microtubule binding domain is localised to a number of tandem repeats of 31 or 32 amino acids found in the C-terminal half. In immature brain, only the transcript encoding the shortest form with three tandem

repeats is expressed (Goedert et al., 1992). Immature brain tau is phosphorylated on six to eight sites, whereas the tau of normal mature brain is only phosphorylated at two or three sites, which demonstrates that tau phosphorylation may be developmentally regulated (Brion et al., 1993).

Tau is known to be a potent promoter of tubulin polymerisation *in vitro* (Cleveland et al., 1977); binding of tau to microtubules reduces their dynamic instability. Tau appears to have a similar function *in vivo*- microinjection into fibroblasts increases microtubule mass and resistance to depolymerising agents. Tau function appears to be necessary for normal neuronal function and maintenance of transport in neurites (Kosik and Greenberg, 1994), as well as stabilisation of axonal morphology (Goedert, 1993).

Phosphorylation of tau by a number of kinases shifts its apparent mobility when run on polyacrylamide gels (Goedert et al., 1992). Moreover comparison of recombinant tau isoform mobility with that of tau extracted from dispersed filaments (which is much more soluble than that extracted from tangles) revealed a similar shift in mobility of all six isoforms of tau, implying that the tau found in PHF (PHF-tau) is phosphorylated at a number of sites. In normal adult brain, tau is phosphorylated at few (1-3) sites, whereas PHF tau is additionally phosphorylated at an as yet unknown number of different sites. Currently, it is proposed that there are eight possible phosphorylation sites on the molecule (Kosik and Greenberg, 1994). Phosphorylation of tau negatively regulates its ability to bind to microtubules, although little is known about the relative contributions made by individual phosphorylation sites (Goedert et al., 1992). This reduction of the affinity of tau for microtubules may account for self-aggregation into PHF, together with destabilisation of microtubules and resultant disruption of cell function. These data lend support to the hypothesis that in AD, abnormal phosphorylation of tau gives rise to PHF and tangle formation, with consequent disruption of organelle trafficking in neuronal processes leading to cell death.

1.8.3.2 Regulation of tau phosphorylation.

Little is known of the processes which lead to the hyperphosphorylation of tau. Although activation of PKC may lead to phosphorylation of tau, this does not give rise to the characteristic mobility shift associated with PHF-tau

(personal communication, B.H. Anderton). Additionally, one kinase that is implicated in the production of PHF-tau, glycogen synthase kinase 3ß (GSK-3ß) (Brion et al., 1993), may be downregulated and inactivated by PKC activation (Goode et al., 1992). A number of other kinase candidates have also been suggested, which include serine directed mitogen activated (MAP) kinase (Drewes et al., 1992), proline directed protein kinase (PDPK) (Vulliet et al., 1992; Paudel et al., 1993), and cAMP dependent protein kinase (PKA) (Robertson et al., 1993).

To date, there have been very few reports concerning mechanisms of tau dephosphorylation (Goedert, 1993). However, one candidate, phosphatase 2-A (PP-2A) appears to be particularly active in the dephosphorylation of tau hyperphosphorylated by kinases shown to produce PHF-tau (Paudel et al., 1993). Treatment of PHF-tau extracted from AD brain dispersed filaments reverted the mobility characteristics to that of normal tau isoforms. Mechanisms of modulating the activity of this phosphatase are currently under investigation.

1.8.4 Risk factors.

1.8.4.1 Genetic mutations.

Since the discovery that the gene encoding for APP is localised to chromosome 21, intensive research has identified a number of genetic mutations (Figure 1.2) that are associated with the incidence of AD in a small population of sufferers. At least six missense mutations have been detected within or immediately flanking the amyloid encoding region of the APP gene (Goate et al., 1991; Hardy and Higgins, 1992). Although most of the known missense mutations in exons 16 and 17 of APP are strongly linked to AD, the mechanisms by which they produce the phenotype remain unresolved. However, this evidence led many investigators to assume that dysfunctional APP or amyloid regulatory mechanisms were directly linked to the disease, giving rise to the "amyloid cascade hypothesis" of AD, and moving attention away from the highly implicated tangle hypothesis of cell death. However, it should be noted that that individuals with these mutations are rare- the incidence of sporadic AD far outweighs early-onset familial forms. Moreover,

there is now evidence that an APP missense mutation alone may not be sufficient to cause the disease- a recent report describes an individual with such a mutation, who, at the time of writing remains asymptomatic at 2 standard deviations beyond the mean age of onset of the disease in other members of the pedigree (St.George-Hyslop et al., 1994). However, this individual, in contrast to other, symptomatic members of the same pedigree, lacks an apolipoprotein E4 (apo-E4) allele (see below).

It had been known for some time that a number of large pedigrees with early-onset AD did not link to the APP gene or any other locus on chromosome 21. Most of these families have now been linked to an as yet unknown gene on the long arm of chromosome 14 (as reviewed, Mullan and Crawford, 1993). In common with individuals with the chromosome 21 mutation, subjects undergo a very early and severe ßA4 deposition. Again, the proportion of AD suffers with these mutations is a small fraction of those with sporadic AD.

1.8.4.2 Apolipoprotein E.

There are three common forms or alleles of the apolipoprotein-E gene, designated apo-E2, apo-E3 and apo-E4. The role of apo-E4 in AD was first discovered in studies which showed apparent linkage with a site on chromosome 19 (Pericak-Vance et al., 1991). Strittmatter et al. (1993) reported an allele frequency of apo-E4 of 50 % in 30 affected familial AD patients. A study of 95 affected late onset familial AD individuals revealed 80 % who had the E4 allele, with an apparent gene dosage effect (Corder et al., 1993). Since then, several studies have examined sporadic AD cases, and between 45 and 65 % of individuals carry at least one apo-E4 allele (as reviewed, Katzman, 1994). It may be calculated that between 25 and 40 % of all AD cases can be attributed to apo-E4, making this the most common risk factor for AD.

The mechanism by which the dosage effect of the apo-E4 allele predisposes AD is currently unclear. However, Strittmatter et al. (1993) have shown high avidity binding of apo-E4 to soluble ßA4 with formation of amyloid *in vitro*. This is in keeping with findings that brains of patients homozygous for the E4 allele contain increased amounts of vascular amyloid, and increased numbers of neuritic plaques compared to those homozygous for the E3 allele

(Schmechel et al., 1993). It is also proposed that the E3 form stabilises tau, preventing hyperphosphorylation (personal communication, B.H. Anderton).

1.9 Alzheimer's disease- neurochemistry.

1.9.1 Acetylcholine.

One of the most consistently described deficits in AD brains is that of the cholinergic system, first described by Bowen et al. (1976b), closely followed and corroborated by other groups (Davies and Maloney, 1976; Perry et al., 1977a; Perry et al., 1977b; Davies, 1979).

Neuropathological studies confirm that there is usually a considerable loss of cholinergic neurones of the NBM (Whitehouse et al., 1982; Nagai et al., 1983), and assay of cholinergic terminals by ChAT activity revealed *post-mortem* reductions in all neocortical areas studied (Bowen et al., 1976b; Davies and Maloney, 1976; Perry et al., 1977a; Perry et al., 1977b). Determination of the integrity of the cholinergic system at earlier stages of the disease by biopsy (Bowen et al., 1982a; Sims et al., 1983a) also revealed deficits. Furthermore, the loss of this activity has been correlated both with the severity of dementia (Francis et al., 1985; Neary et al., 1986), and neuropathological changes (Mountjoy et al., 1984).

Studies of cholinoceptor populations are discrepant, with reports of decreased, increased or unchanged numbers of muscarinic receptors (Hardy et al., 1985; Whitehouse, 1987; Giacobini, 1990; Perry et al., 1990; Flynn et al., 1991), although the M_2 receptor, thought to represent a presynaptic autoreceptor, is more consistently reduced (Mash et al., 1985; Nordberg et al., 1992a; Svensson et al., 1992). *In-situ* hybridisation histochemistry for m_1 mRNA also revealed both increases (Harrison et al., 1991) and decreases (Wang et al., 1992). The nicotinic receptor is reported to be reduced in most studies (Giacobini, 1990), and this may reflect loss of both pre- and postsynaptic sites.

There is little doubt that the cholinergic system is involved in cognitive processes, learning and memory (as reviewed, Hasselmo and Bower, 1993; see also section 1.6.1.1, section 1.10.1, and Discussion, section 10.4.1). Attempts to ameliorate AD symptoms with drugs aimed at facilitating cholinergic

transmission have produced only modest improvements (Collerton, 1986; Francis and Bowen, 1989; Byrne and Arie, 1994); some demented patients with AD have been reported to have normal numbers of NBM cholinergic neurones (Perry et al., 1982; Pearson et al., 1983). Additionally, degeneration of the NBM appears to be topographic in that more severe degeneration is observed in parts which project to the most severely affected neocortical areas (Adrendt et al., 1985). These findings suggest that cholinergic pathology may not precede neocortical pathology, a theory supported by the work of Sofroniew and Pearson (Sofroniew and Pearson, 1985), who demonstrated retrograde NBM degeneration following topical cortical application of EAA.

1.9.2 Monoamines.

1.9.2.1 Noradrenaline.

A number of studies describe loss of locus coeruleus cell bodies in AD (Mann et al., 1980; Bondareff et al., 1981), with concurrent tangle occurrence and NA markers in neuritic plaques (Fowler et al., 1992b). There is also a corresponding loss of NA in some neocortical areas (Cross et al., 1981; Francis et al., 1985; Palmer et al., 1987b), although the concentration of the NA metabolite MHPG has been reported to be elevated (Gottfries et al., 1983; Palmer, 1987), unaltered (Palmer, 1987) or reduced (Cross et al., 1983), which may arise as a result of the preterminal state of AD patients. Analysis of NA content, uptake and release revealed reduced concentration and uptake of NA in the temporal lobe, although release in the frontal lobe was unaffected (Palmer, 1987). Deficits in NA do not appear to correlated with dementia, although they may contribute to the non-cognitive deficits (Fowler et al., 1992b).

Postsynaptic α and ß adrenoceptors are unaffected in most studies of autopsy AD material (Cowburn et al., 1989; Francis et al., 1992a), although there is some evidence of regional increases in binding to ß receptors in hippocampus and cortex (as reviewed, Young and Penney, 1994). α_2 adrenergic receptors are thought to exist presynaptically on the terminals of noradrenergic neurones projecting from the locus coeruleus. Loss of high

affinity α_2 receptor binding has been reported in *post-mortem* tissue from frontal cortex and hippocampus of AD brain (Pascual et al., 1992).

1.9.2.2 Serotonin.

Cell loss and morphological changes in the dorsal raphe are well established in AD (Iishi, 1966; Mann and Yates, 1983; Yamamoto and Hirano, 1985; Chen et al., 1994). Presynaptic markers of the serotonergic system are often reduced in AD brain, although the metabolite 5-HIAA is generally unaltered (Bowen et al., 1983; Cross et al., 1983; Palmer et al., 1987a; Francis et al., 1993). In neocortical biopsy samples, concentrations of 5-HT and 5-HIAA, 5-HT uptake and release were all reduced (Palmer et al., 1987a), and 5-HIAA concentration inversely correlated with tangle count.

Most studies support a decrease in forebrain serotonin receptors, with reductions in binding to 5-HT_1 (Cross et al., 1984a; Cross et al., 1984b) and 5-HT_{1A} receptors (Middlemiss et al., 1986b; Bowen et al., 1989) commonly described, although [^{3}H] 5-HT binding in *ante-mortem* biopsy samples was unchanged compared to control (Bowen et al., 1983). Autoradiography using [^{3}H] ketanserin binding to the 5-HT_{2A} receptor demonstrated no change in frontal cortex and hippocampus (Dewar et al., 1990a). However, subsequent studies have shown changes in all cortical layers, CA1, CA3 and DG of the hippocampus and the entorhinal cortex (Reynolds et al., 1984; Cross et al., 1988; Jansen et al., 1990; Cheng et al., 1991). These reductions in [^{3}H] ketanserin binding may reflect loss of neocortical interneurones that have been found to be reduced in a number of neocortical brain areas (Procter et al., 1988a; Bowen et al., 1989).

1.9.3 GABA.

Although the assessment of the activity and integrity of GABA containing neurones in *post-mortem* tissue may be affected by agonal state (see section 1.5.3), several reports indicate loss of these neurones from the cortex of AD patients (Rossor et al., 1982; Ellison et al., 1986). However, study of *ante-mortem* biopsy tissue did not show as great a loss of these cells (Lowe et al., 1988), which suggests that the clinical features and pathological changes in AD brain are not dependent on the loss of GABAergic neurones.

In AD brain, $GABA_A$ receptor binding is decreased by a modest amount in frontal cortex when assessed by membrane binding, and also in posterior cingulate when assessed by autoradiographic analysis (Lloyd et al., 1991; Vogt et al., 1991). Benzodiazepine binding in the hippocampus was slightly reduced in CA1, subiculum and entorhinal cortex (Jansen et al., 1990). In another study, binding to the $GABA_B$ receptor was reduced to 50 - 60 % in frontal cortex, although no changes were described for $GABA_A$ binding (Chu et al., 1987).

1.9.4 Adenosine.

A method for detection of adenosinergic neurones which can separate transmitter from metabolic pools has not yet been developed. An autoradiographic study of adenosine A_1 receptors in *post-mortem* AD brain revealed a significant reduction in the perforant pathway terminal zone of the hippocampus, which was thought to reflect degeneration of this pathway- the innervated targets (dentate granule cells) were relatively spared in this study, and the number of NMDA receptors, which represent postsynaptic elements, was not reduced (Jaarsma et al., 1991).

1.9.5 Excitatory amino acids.

Loss of cortical pyramidal neurones with resultant hypoactivity of remaining neurones (which may be exacerbated by the cholinergic deficit) is implicated in the primary cognitive impairment of AD (as reviewed, Francis et al., 1993; also see section 1.8.1), which is supported by the implication of glutamatergic function in learning and memory (see sections 1.6.5.6 and 1.10.1).

As described previously, many presumed markers of glutamatergic neurones are rather non-specific (see section 1.5.4). Nevertheless, a number of studies have reported reduced glutamate concentrations in AD brain (Arai et al., 1985; Ellison et al., 1986; Sasaki et al., 1986). Moreover, the glutamate content of temporal lobe biopsy samples from AD patients was also reduced, and the value from individual subjects related to the density of pyramidal neurones in layer III of the neocortex (Lowe et al., 1990). Additionally, Hyman et al. (1987) reported an 80% reduction in glutamate concentration in the

terminal zone of the perforant pathway. Consistent with this, decreased glutamate staining was observed in the molecular layer of the DG (Kowall and Beal, 1991), and the same study also reported reduced numbers of glutamate and glutaminase immunoreactive pyramidal neurones in the CA fields of the hippocampus.

A 40 - 50 % decrease in Na^+-dependent D-aspartate uptake into synaptosomes prepared from prompt autopsy AD material was reported by Procter et al. (1988c), although it is unclear whether this represents a reduction of glutamatergic neurones (the most likely interpretation), or a *perimortem* effect, as non-demented control tissue with short autopsy was not available.

Other studies have examined a number of putative markers of glutamatergic neurones (see section 1.5.4), such as high affinity [^{3}H] D-aspartate uptake in frozen material (Hardy et al., 1987), Na^+-dependent [^{3}H] D-aspartate binding (Cowburn et al., 1988), K^+-stimulated Ca^{2+}-dependent EAA release (Procter et al., 1988c), with varied findings. Immunocytochemical localisation of glutaminase immunoreactive neurones may be a more reliable method; loss of glutaminase positive neurones has been noted in the cortex of AD brains (Akiyama et al., 1989; Kowall and Beal, 1991), although glutaminase activity was unaffected in temporal and frontal cortex.

Evidence of deficits in postsynaptic EAA receptors is conflicting. Some investigators have observed that areas of control brain with the highest density of EAA receptors are those which undergo the most severe degeneration in AD (Young and Penney, 1994). The binding of [^{3}H] glutamate has often been used to assess EAA receptors; Greenamyre et al. (1985b) reported reductions in neocortical areas of AD brain compared to control and Huntington's material, that appeared to be primarily attributable to loss of NMDA receptors; similar deficits in NMDA receptors were reported in autoradiographic studies of hippocampal AD tissue, particularly in CA1 pyramidal cell and molecular layers (Greenamyre et al., 1987), although other investigators have reported more widespread loss of NMDA receptors in the hippocampus (Maragos et al., 1987a). However, no loss of binding of [^{3}H] TCP or [^{3}H] MK-801 (Mouradian et al., 1988) binding to the NMDA receptor ion

channel was reported for homogenate binding, although reductions were noted in the frontal cortex (Simpson et al., 1988), in agreement with Ninomyia et al. (1990), but in contrast to Steele et al. (1992). Therefore, although little change has been identified in homogenate studies, autoradiographic studies have more consistently described abnormalities in NMDA receptors in AD (Young and Penney, 1994). Moreover, several studies have reported reduced sensitivity of the NMDA receptor to glycine in AD (Steele et al., 1989; Procter et al., 1989; Procter et al., 1991), which may reflect differential loss of a glycine sensitive NMDA receptor subtype, or selective alteration of glycine site coupling to the receptor.

Studies of non-NMDA receptor subtypes are also conflicting; [^{3}H] kainate binding was significantly increased in deep layers of frontal cortex, which correlated with plaque number in the same area (Chalmers et al., 1990), but no change in [^{3}H] AMPA binding was found. However, decreases in both kainate (Geddes and Cotman, 1986; Penney et al., 1990), AMPA (Penney et al., 1990), and metabotropic (Dewar et al., 1991) receptors were found in AD hippocampus, in agreement with Greenamyre et al. (1987), who used [^{3}H] quisqualate to label both kainate and AMPA receptors, but in contrast to *in-situ* hybridisation histochemistry studies for kainate/AMPA receptors, which described modest increases of mRNA in CA4 and subiculum (Harrison et al., 1990).

Discrepancies in the study of postsynaptic EAA receptor density in AD may be caused by several factors; differences in experimental technique (e.g. autoradiographic or homogenate binding study); severity of the disease; or inadequate control for epiphenomena such as *post-mortem* delay, age match of AD and control tissue or agonal state. However, taken together, data indicate a substantial deficit in the glutamatergic system of AD brain.

1.10 Lesioning techniques of the brain.

1.10.1 Traditional techniques.

The technique of lesioning specific areas of the brain are fundamental in gathering information regarding their functions and connections . A vast number of studies have used various lesioning techniques to study the

interaction of one brain area with another, with consequential behavioural and cognitive changes. Techniques developed to lesion different regions in animal brain fall into two main categories:

(i) Mechanical lesions, which include knife cuts, often using a thin wire to isolate one region of the brain from the rest; aspiration, where a part of the brain may be removed using a pipette; and electrolytic lesions, in which specific brain areas can be damaged by electric current passed between two fine electrodes.

(ii) Chemical lesions. Mechanical lesions are often rather non-specific, and are generally dependent upon the skill of the operator to produce consistent results. A number of neurotoxic compounds offer a greater degree of specificity. In 1967, the first transmitter specific neurotoxin, 6-hydroxydopamine was introduced, which was observed to accumulate in, and selectively destroy catecholaminergic neurones (Tranzer and Thoenen, 1967). Other transmitter selective toxins have since developed, including 5,7-dihydroxytryptamine, which selectively destroys serotonergic neurones (Baumgarten and Lachenmayer, 1972), N-2-chloroethyl-N-ethylbromobenzylamine, which selectively destroys noradrenergic terminals (Jaim-Etcheverry and Zieher, 1980), and 1-methyl-4-phenyl-1, 2, 3, 6-tetrahydropyridine (MPTP) which is thought to selectively destroy dopaminergic neurones (Davis et al., 1979).

Excitotoxins are now routinely used to destroy certain neuronal populations, and rely on the ubiquitous nature of EAA receptors. Excitotoxins destroy neuronal dendrites and perikarya, but spare axons of passage. Commonly used excitotoxins include kainate (Olney et al., 1971), quinolinic acid (Fuxe et al., 1984), ibotenic acid (Jonsson, 1980) and NMDA (Sofroniew and Pearson, 1985).

Lesions produced by these methods are commonly used to investigate memory and learning, a paradigm pioneered by Franz and Lashley (1929; as reviewed, Dudai (1989)). These lesions also allow workers to investigate the effects drugs which are proposed to enhance learning and memory ("cognitive

enhancers"). One of the most widely studied paradigms is that of cholinergic system lesioning, where destruction of the NBM and/or the septal nuclei disrupt memory formation and learning (e.g. see Hagan et al., 1988; Dekker et al., 1990; Dunnett et al., 1991; and review by Hagan and Morris, 1988). The specific effect of ACh on learning and memory can be determined using these lesion types; administration of cholinomimetics, such as anticholinesterase inhibitors and muscarinic agonists often reverses the memory impairment (as reviewed, Dawson et al., 1992). There is also evidence of interaction between the cholinergic and serotonergic systems in cognitive function- depletion of the serotonin system enhanced some aspects of cognition, an effect completely abolished by NBM lesioning (Normile et al., 1990). Many aspects of memory and learning deficits induced by lesioning the cholinergic system can be mimicked by administration of NMDA antagonists (Staubli and Lynch, 1992), which indicates that the common result- impairment of cortical pyramidal neurone activity (McCormick, 1990) is responsible. This proposal is supported by findings of hippocampal lesioned animals, in which cognitive deficits are commonly reported (e.g. Jarrard, 1986; Kesslak et al., 1991), which may be reversed using agents which facilitate NMDA receptor function (e.g. Schuster and Schmidt, 1992).

1.10.2 Suicide transport and immunolesioning.

Specific, restricted lesions enable precise interpretation of results. However, traditional techniques (above) have achieved only limited neuronal population selectivity. To produces lesions with greater selectivity, two techniques have been developed: suicide transport and immunolesioning. In both cases, cytotoxins are targeted to restricted groups of neurones, allowing biochemical sequelae to be ascribed with greater confidence than those following traditional lesioning techniques.

Suicide transport (Wiley et al., 1982), the anatomically selective destruction of neurones by injection of cytotoxin with subsequent retrograde transport, has proved to be useful for the study of neurones in the PNS (Wiley et al., 1982; Yamamoto et al., 1985; Wiley and Stirpe, 1988). Currently ricin, a toxic lectin extracted from castor beans, is the toxin of choice for ablating peripheral nerves in rats. Studies have shown that this toxin, following

injection or dipping of nerves, binds to oligosaccharides on the cell membrane, and is probably internalised by receptor mediated endocytosis. The toxin is then axonally transported to the cell body, where it catalytically inactivates ribosomes, thereby inhibiting protein synthesis, resulting in cell death (Wiley and Stirpe, 1988). However, ricin is not an effective suicide transport agent in the CNS, where injection causes local necrosis, but no cell death at distal sites which are known to project to the injected site (Wiley et al., 1983).

Other toxic lectins, including volkensin and modeccin are effective suicide transport agents in the CNS. Although they seem to act in a similar manner as ricin in the PNS, they appear to have different oligosaccharide binding specificity (Contestabile and Stirpe, 1993).

Volkensin (MW 62K) is isolated from the roots of the kilyambiti plant, *Adenia Volkensii*, and is a galactose specific glycoprotein consisting of two subunits linked by disulphide and non-covalent bonds (Stirpe et al., 1985). In rats, volkensin has been demonstrated to selectively destroy subpopulations of neurones in the substantia nigra following striatal injection, in the striatum following nigral injection, in the cortex following striatal injection, in the medial septum and contralateral CA3 hippocampal region following injection into the hippocampus, in the posterior pituitary following hypothalamic injection and in the inferior colliculus following injection into the auditory system (as reviewed, Contestabile and Stirpe, 1993).

Immunolesioning is performed by injection of monoclonal antibody conjugated to various toxin moieties. Two ribosome inactivating proteins are often used; the A chain of ricin, and saporin. Saporin has the advantage of a lack of a binding subunit. The first effective immunotoxin described was OX7-saporin. OX7 recognises Thy-1, and abundant surface molecule present on all neurones (as reviewed, Wiley, 1992), and the immunotoxin is an effective suicide transport agent in both the PNS and CNS. OX7-saporin has been used to investigate cortical pyramidal neurone biology following intrathalamic injection. The first subtype specific anti-neuronal immunotoxin was comprised of 192 IgG coupled to the ricin A chain; 192 IgG is a monoclonal antibody to the low affinity rat nerve growth factor receptor which is found on cholinergic nerves; lateral ventricle injection of this immunotoxin destroys cholinergic

neurones of the basal forebrain; immunolesioning of the basal forebrain in this way has been shown to impair learning tasks in the rat (Nilsson et al., 1992).

1.11 Rationale and aims of the studies.

From the preceding discussion, it is clear that there are several reasons for the study of the biochemistry of cortical pyramidal neurones with respect to Alzheimer's disease: (i) The cerebral neocortex and hippocampus are major sites of pathological changes in AD. (ii) The principle cell type affected is the pyramidal neurone, both in neocortical and hippocampal areas, which give rise to corticocortical, corticofugal, corticopetal and subcortical pathways. Pyramidal cells of the cortex are thought to use glutamate as their transmitter. (iii) Glutamatergic hypoactivity of cortical pyramidal neurones has been implicated as contributing to the primary cognitive deficit in AD, and glutamate has been independently implicated in mechanisms of memory formation and neurotoxicity. (iv) Transmitter based manipulation of the activity and biochemical processes of these cells may affect the processing of amyloid precursor protein and (speculatively) tau hyperphosphorylation, both hypothesised to contribute to the progression of the disease.

Despite the evidence that these pyramidal cells are glutamatergic, the neurones are difficult to study, since, as yet, no definitive marker has been ascribed. EAA receptors are probably located on pyramidal neurones to facilitate transmission between this cell type; however, these receptors are inadequate markers, as they are present ubiquitously on a number of neuronal types; moreover, excessive activation is associated with neurotoxicity. Pharmacological manipulation of the activity of these cells is therefore difficult to target and control. This thesis addresses the problems associated with identification of such cells by establishing markers, which in some cases may be used for manipulation.

(1) The antituberculosis compound, D-cycloserine (DCS) has been described as a cognitive enhancer in a number of animal and human models of impaired cognition, and has been classified pharmacologically as a partial agonist at the glycine site of the NMDA receptor. It was hypothesised that this compound may be useful in AD, as facilitation of NMDA receptor activation could be

achieved without the associated problem of excitotoxicity. Since the integrity of the glycine site of the NMDA receptor in AD may be impaired, it was unknown whether the partial agonist characteristics of the compound would be maintained in AD brain. Therefore, the action of the compound in rapid autopsy AD material was investigated using a marker for NMDA receptor activation, [^{3}H] MK-801.

(2) A novel method for selective destruction of hippocampal pyramidal neurones, using volkensin, was developed. Injection of volkensin into the entorhinal area was proposed to destroy hippocampal-entorhinal projections. The validity of the pyramidal cell loss caused by volkensin injection was determined using several techniques. Biochemical sequelae following such a cell loss were investigated using autoradiography to try to establish a marker for these neurones. Receptors investigated were: 5-HT_{1A}, 5-HT_2, muscarinic M_1, kainate and NMDA glutamate and $GABA_A$.

(3) A method for selective destruction of neocortical pyramidal neurones of the corticostriatal pathway had been previously established, and one marker identified (5-HT_{1A} receptor). In the current study, two groups of animals selectively deficient in this neuronal population were prepared by intrastriatal injection of volkensin. Findings of the previous study were confirmed, and a number of other receptor types investigated for their suitability as markers, including several which were proposed to affect processing of APP by activation. Receptors investigated were: 5-HT_{1A}, muscarinic M_1, nicotinic, kainate glutamate, $GABA_A$, α_1 adrenergic, and adenosine A_1.

(4) Since the loss of corticocortical projecting neurones in AD is proposed to be a primary deficit, an attempt was made to selectively destroy a subpopulation of corticocortical projection neurones in rat brain, by intracortical injection of volkensin. Again, various techniques were employed to determine the validity of such a pyramidal neurone loss. Receptor autoradiography was used to investigate the biochemical sequelae of cell loss. Receptors investigated were: 5-HT_{1A}, 5-HT_2, muscarinic M_1, nicotinic and adenosine A_1.

The findings from these studies are discussed in the context of (i) establishing a marker for cortical pyramidal neurones, (ii) improving glutamatergic transmission between remaining pyramidal neurones in AD, (iii) consequences of pharmacological manipulation in terms of disease progression and (iv) developing techniques to visualise pyramidal neurones to aid diagnosis and monitor progression of the disease.

CHAPTER 2: Materials and methods.

2.1 Chemicals

The radiochemicals [^{3}H] 8-hydroxy-2-(n-dipropylamino)-tetralin ([^{3}H] 8-OH-DPAT, 135.5-228 Ci/mmol), [^{3}H] ketanserin (60-64 Ci/mmol), [^{3}H] (+)-5-methyl-10,11-dihydro-5H-dibenzo[a,d]cyclohepten-5,10-imine maleate ([^{3}H] MK-801, dizocilpine, 28.8 Ci/mmol), [^{3}H] pirenzepine (84.2 Ci/mmol), [^{3}H] 1,3-dipropyl-8-cyclopentylxanthine ([^{3}H] DPCPX, 88.2 Ci/mmol), [^{3}H] nicotine (75.7 Ci/mmol) and [^{3}H] kainate (58.0 Ci/mmol) were purchased from New England Nuclear (NEN, Stevenage, Hertfordshire, UK). [^{3}H] prazosin (79 Ci/mmol), [^{3}H] gamma-amino-butyric acid ([^{3}H] GABA, 91.7 Ci/mmol) were purchased from Amersham International plc, Little Chalfont, Buckinghamshire, UK. Unlabelled MK-801 and [^{3}H] L-689,560 (28 Ci/mmol) was a gift from Merck, Sharp and Dohme (MSD Ltd., Harlow, Essex, UK) as was the unlabelled compound. Amino acids (all L-forms unless otherwise stated) and other chemicals glutamate, glycine, kainate, NMDA, quinolinic acid, ibotenic acid, 5-hydroxytryptamine creatinine sulphate (5-HT), mianserin, atropine sulphate, R-phenylisopropyladenosine (R-PIA), adenosine 5'-triphosphate (ATP), carbamyl choline, phosphate buffered saline (PBS) tablets, paraformaldehyde, ethylenediamine tetraacetic acid (EDTA), adenosine deaminase (ADA), baclofen, D-cycloserine, L-cycloserine, cresyl violet, bovine serum albumin (BSA), maleic acid, sodium formate and ammonium formate were purchased from Sigma Chemical Co. (Poole, Dorset, UK). Guanylyl-imidodiphosphate (Gpp(NH)p) was purchased from Boehringer Mannheim (Lewis, East Sussex, UK). 7-chlorokynurenic acid, phentolamine mesylate, 5-methyl-urapidil and chloroethyl clonidine were purchased from Research Biochemicals Inc., via Semat (St. Albans, Hertfordshire, UK). 5,7-dichlorokynurenic acid was a gift from Merrell Dow. Analar grade sodium dihydrogen orthophosphate (NaH_2PO_4), disodium hydrogen phosphate (Na_2HPO_4), gelatine, absolute ethanol, acetone, isopentane, xylene, OCT compound, chromic potassium sulphate, DPX- mountant, Tris buffer, hydrochloric acid (HCl), citric acid, and acetic acid were all purchased from BDH Ltd. (Poole, Dorset, UK). Emulsifier safe scintillant was purchased from

Packard (Pangbourne, UK) and Lipshaw M1- embedding matrix from Lipshaw (Detroit, U.S.A.). Halothane and pentobarbitone sodium (Sagatal) were purchased from May and Baker Ltd. (UK), and gaseous oxygen, nitrous oxide, and dry ice from BOC Ltd. (London, UK) and Distillers MG Ltd. (Reigate, Surrey, UK) respectively. All other chemicals were of the highest grade purity available.

2.2 Human Tissue Samples.

The three conventional *post-mortem* control brains were obtained from the Radcliffe infirmary, Oxford (Dr. M.M. Esiri), and from the Manchester Royal Infirmary, Manchester (Dr. D. Neary). Prompt autopsy material was obtained from Manchester Royal Infirmary, or from Bexley Hospital, London (Dr. A.W. Procter).

Conventional *post-mortem* material (with a *post-mortem* delay of 24 hr or more) was used for preliminary investigation of the characteristics of the glycine modulatory site of the NMDA receptor. *Post-mortem* examinations of undemented control subjects were made between 24 and 48 hours after death. Brains were bisected sagitally, one hemisphere was fixed in 10% formalin and used for histological examination and the other frozen at -70°C. The hemisphere used for biochemistry was chosen at random for these cases. The frozen hemispheres were subsequently warmed to -10°C and cut into 0.5 cm coronal slices.

The full study of the partial agonist characteristics of DCS, dose-response curves to glycine and action of 5,7-dichlorokynurenic acid was performed using prompt *post-mortem* human brain tissue. *Post-mortem* examinations were made within 3 h of death, of patients who had a clinical diagnosis fulfilling DSM-III criteria for Dementia (American Psychiatric Association). Brains were removed and bisected sagitally. One hemisphere was preserved for histopathological confirmation of diagnosis, and the other sliced coronally into 1 cm thick slices which were placed in ice-cold KRP-A buffer and transferred to the neurochemistry laboratory in an insulated box, as previously described (Bowen et al., 1982b). Two control brains, confirmed to be AD free by histopathological examination were also obtained with short *post-mortem*

times. Membranes prepared from these brains were included in some experiments for comparison.

Details of patient sex, age, *ante-mortem* state, *post-mortem* time and laterality are given in the results section, for both conventional and short *post-mortem* material. Brain slices were removed from storage at -70°C and placed at -20 °C for a few hours. Samples from Brodmann areas 39/40 (inferior parietal, a severely affected area (Najlerahim and Bowen, 1988)-prompt *post-mortem* material), and Brodmann area 9 (frontal cortex-conventional *post-mortem* material) were subsequently removed, making sure that all neocortical layers were being sampled. The tissue was then allowed to thaw at 4°C and the meninges and any underlying white matter were separated from grey matter, before total membrane preparations were performed.

2.3 Radioligand binding experiments using [^{3}H] MK-801 to assay activation of the NMDA receptor-ionophore.

2.3.1 Total membrane preparations.

Total membranes were prepared using modifications to previous methods (Steele et al., 1989; Procter et al., 1991). A 500 mg aliquot of grey matter was weighed and homogenised in 9 volumes of ice cold 50 mM Tris-HCl, pH 7.4 using a glass teflon homogeniser (model Tri-R; Stir-R Instruments, New York, U.S.A.) with 8 up and down strokes. The homogenate was transferred to centrifuge tubes and spun at 18,000 *g* (12,000 rpm) for 25 minutes, using a JA-20 rotor on a Beckman model J2-21 centrifuge (Beckman, High Wycombe, UK). The resulting supernatant was then carefully removed and the pellet re-suspended in 75 volumes of ice cold 50 mM Tris-HCl, pH 7.4 using an Ultra-Turex T25 homogeniser (IKA Laboratory, Hamburg, Germany) set at 13,500 rpm and centrifuged at 30,000 *g* (20,000 rpm) for 25 min. This washing procedure was repeated once with ice cold 5 mM Tris-HCl, pH 7.4 buffer and then three further times with ice cold de-ionised water. The final pellet was stored at -70°C for at least 18 hours and not more than a week.

On the day of the assay, membrane pellets were thawed on ice, re-suspended in 75 volumes of ice cold 5 mM Tris-HCl, pH 7.4 and centrifuged at 30,000 *g* (20,000 rpm) for 25 min, and then subjected to a further three cycles of this washing, before final re-suspension in 5 mM Tris-HCl, pH 7.4 to give a total membrane preparation containing approximately 300 μg protein/ 750 μl.

2.3.2 Binding assays.

Binding conditions were initially based on previously published methods (Hood et al., 1989), although modifications were introduced as experimental data was gathered. Initially, the partial agonist characteristics of DCS were investigated using DCS alone, followed by comparison with glycine and glutamate responses. Finally, the action of 5,7 dichlorokynurenic acid as a glycine site antagonist was investigated. Incubations were carried out in triplicate at 25°C, in a final volume of 1 ml 5 mM Tris-HCl, pH 7.4, which contained 750μl tissue membranes, 5 nM [^{3}H] MK-801, 30μM glutamate, and various concentrations of glycine (0 to 3 mM), DCS (0 to 0.1 mM), L-cycloserine (0 to 0.1 mM), and 5,7-dichlorokynurenic acid (0 or 30μM). Non-specific binding was defined with 100μM MK-801, and was typically 30% of the total binding. Incubations were terminated after 35 min by rapid filtration over acrylic/glass (1.5μm pore size) fibre filters (Skatron Instruments Ltd., Newmarket, Suffolk), which had been previously soaked in a 0.05% solution of polyethylenemine and dried, under reduced pressure using a Skatron cell harvester. The filters were washed with ice cold 5 mM Tris-HCl, pH 7.4 buffer for 5 seconds, and then transferred using a Harvesting Press (Skatron) to Pico-Pro scintillation vials (Packard). The radioactivity was determined by liquid scintillation spectrometry 24 hr after addition of 2 ml Emulsifier-Safe (Packard) to the scintillation vials.

Before comparison of [^{3}H] MK-801 binding between Alzheimer's disease and control tissue, various optimal parameters for the assay were determined. Equilibrium time for [^{3}H] MK-801 binding had already been previously demonstrated (2 hr; Steele et al., 1991), so a suitable non-equilibrium incubation time was chosen to investigate the functional aspects of putative

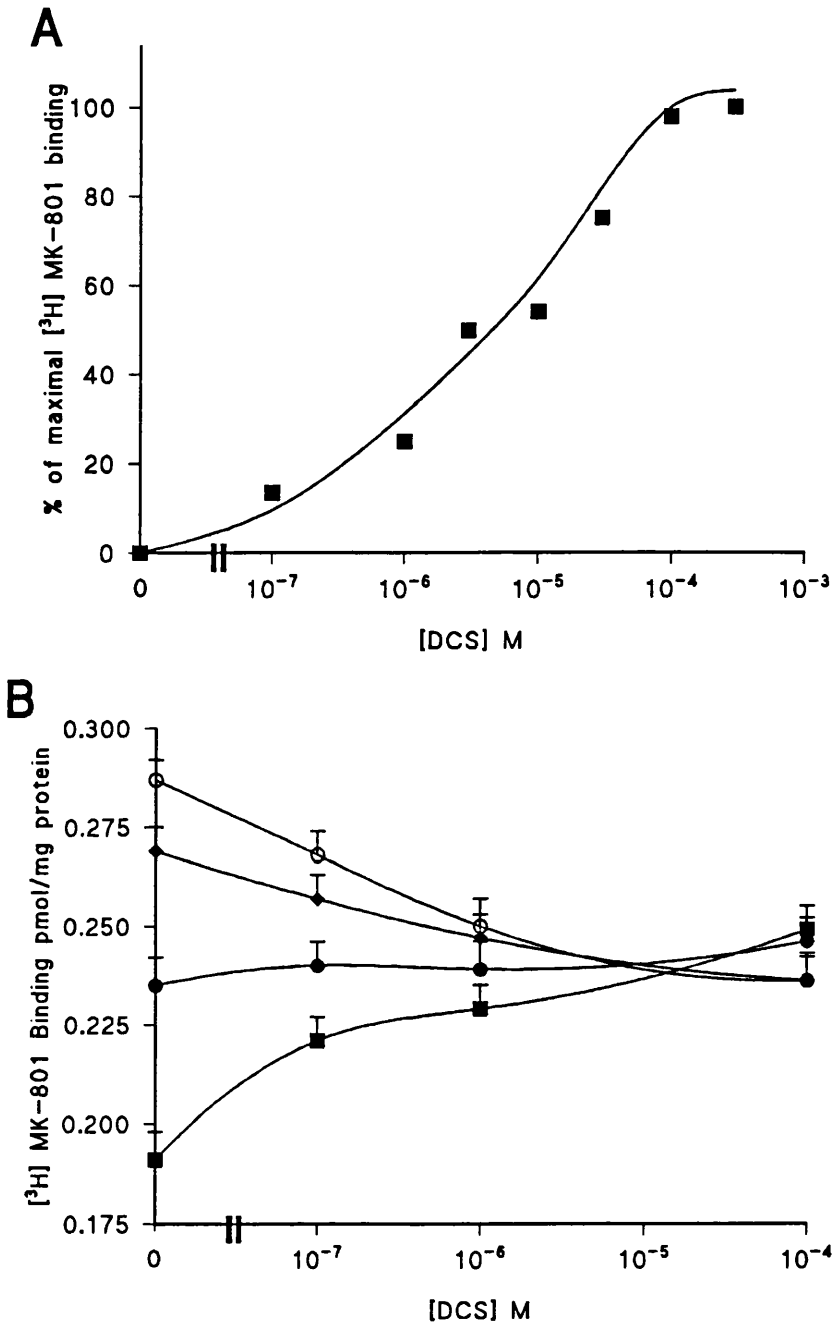

Figure. 2.1: A: REPRESENTATIVE DOSE-RESPONSE CURVE OF DCS DEPENDENT [^{3}H] MK-801 BINDING. Experiments (n=2) were performed using conventional *post-mortem* control human frontal cortex. Maximal binding of [^{3}H] MK-801 was achieved using 100μM DCS. Results are expressed as % of maximal stimulation over basal. B: PRELIMINARY PARTIAL AGONIST CHARACTERISTICS OF DCS. Studies (n=3) of [^{3}H] MK-801 binding was examined using four concentrations of DCS with different concentrations of glycine: (■) 0 μM, (●) 0.1 μM, (◆) 0.3 μM, (O) 0.6 μM. DCS competes with glycine at the strychnine insensitive modulatory site of the NMDA receptor to reduce the binding of [^{3}H] MK-801 (concentrations of glycine above 0.1μM), and potentiates binding at lower glycine concentrations thus fulfilling the criteria for classification as a partial agonist. Results are expressed as pmol/mg protein bound ± SEM.

partial agonist characteristics of DCS (45 min). To determine effective concentrations of DCS, a dose-response curve was generated, using concentrations ranging from 0 to 0.5 mM DCS, although only two conventional *post-mortem* brains were investigated. The dose- response curve produced from this experiment (Figure 2.1A) showed that a maximal response to DCS could be obtained at a concentration of 100μM. Preliminary investigation of the partial agonist characteristics of DCS were investigated by co- incubation of 0 to 100μM DCS with 0 to 0.6 μM glycine. Partial agonism curves produced from these experiments are shown in Figure 2.1B.

Demonstration of partial agonist characteristics of DCS was then performed on rapid autopsy AD brains (n = 4 - 11), and DCS and glycine dose-response curves were generated for the same series of AD brains. Total membrane protein content was determined as described in the following section.

2.4 Protein assay

The assay was adapted from the method of Lowry et al. (1951). 200μl aliquots (approximately 100μg of protein) of the tissue homogenate used in the binding experiments were incubated in triplicate in 1 ml 0.5 M sodium hydroxide solution, vortexed and incubated in a water bath at 37°C for 60 min. A standard curve was constructed from a bovine serum albumin standard (fraction V; dissolved in 0.5 M NaOH to give 1 mg/ml), with a 7.5 to 250μg range. Standards, protein samples and blanks were treated simultaneously with 5 ml of a solution containing sodium carbonate (2% w/v), copper sulphate (0.01% w/v) and sodium potassium tartrate (0.02% w/v). Colour development was initiated by addition of 0.5 ml Folin-Ciocalteu's reagent (diluted 1:1 v/v with distilled water). The tubes were vortexed and allowed to stand at room temperature for 45 min before reading the optical density of each tube at 660 nm using a Gilford Spectrophotometer (Model 300N; Cambridge, UK).

2.5 Purification and preparation of toxic lectins.

2.5.1 Volkensin purification and preparation.

Purified volkensin was obtained from Prof. F. Stirpe in powdered form. It was dissolved in 0.1 M phosphate buffered saline to a concentration of 100 ng/ml and stored in 500 μl aliquots at -70°C until required.

Purification of volkensin as performed by Prof. Stirpe is described (Barbieri et al., 1984). Briefly, roots of *A. volkensii* were peeled, minced and homogenised with 0.14 M NaCl containing 0.005 M sodium phosphate buffer (pH 7.2) and 0.1 M cystamine (to prevent HCN release). The homogenate was stored overnight at 2-4°C and then centrifuged twice to give a clear supernatant. Solid ammonium sulphate was added, with constant stirring, to 100% saturation and the precipitate collected by centrifugation and redissolved in the same phosphate buffered solution as described above. After extensive dialysis, any precipitate was removed and the clear extract applied to a column of acid-treated Sepharose 6B, previously equilibrated with PBS at 4°C. A sharp peak of protein, volkensin, was eluted with 0.2 M galactose in PBS. Volkensin was dialysed against water, freeze dried and stored at -25°C.

Volkensin showed one major band of MW 62 K and two smaller bands with MW 36 K and 29 K as judged by polyacrylamide gel electrophoresis (PAGE). The toxin inhibited protein synthesis in rabbit reticulocytes and this effect was abolished after heating the protein for 25 min at 75°C.

2.5.2 Ricin purification and preparation.

Ricin was kindly provided by Dr. P. Thorpe in 10 μg/ml sterile solution. It was diluted to a 100 ng/ml stock and stored in 250 μl aliquots at -70°C.

Ricin was purified from African castor beans, *R.communis* (Croda Premier Oils Ltd., Hull, UK), based on the methods of Fulton et al. (1986). Briefly, beans were blended in 0.02 M NaCl, 0.005 M sodium phosphate buffer, pH 7.2. After 3 hr the extract was filtered, centrifuged and the solution adjusted to 0.6 saturation using ammonium sulphate before being left overnight at 5°C. After further centrifugation, the pellet was washed with more buffer and applied to an agarose column. The ricin agglutinins were eluted

using either 0.2 M galactose or 0.01-0.5 M lactose in NaCl- sodium phosphate buffer. Two agglutinins were found to be separated, one of MW 120 K and one of MW 60 K as determined by PAGE. The 60 K agglutinin was always used and was free of contaminating 120 K agglutinin.

2.6 Lesioning procedures.

2.6.1 Entorhinal/posterior hippocampal injections (ENT).

54 male hooded lister rats (200-270g) were anaesthetised using halothane/ nitrous oxide/ oxygen gaseous anaesthesia (induction: 1 l/min N_2O, 1 l/min O_2, 2.5-3% Halothane; maintenance: 0.8 l/min N_2O, 0.9 l/min O_2, 1.5-2% halothane- typical values, adjusted according to animal response, respiration rate, weight and reflex response). Following induction in a gas box, the animals were transferred to a stereotaxic frame (David Kopf instruments, U.S.A.), and the scalp reflected to expose the skull. Lignocaine hydrochloride (1:5 dilution with saline, Pheonix Pharmaceuticals, Gloucester, UK) was pipetted onto the skull surface and wiped away after one minute, prior to scraping of the skull periosteum. The dura overlying the caudal neocortex and rostral cerebellum was exposed by drilling and removal of a bone flap. All injections were made using a 1μl Hamilton syringe, with a glass micropipette (gift from R.C.A. Pearson, University of Sheffield, UK) of approximately 1 cm in length attached to the needle tip. Initial positioning experiments were carried out by injection of Evans blue (Sigma) dye (1:100 w/v dissolved in saline). All subsequent injections were then made with the injection apparatus angled at 30° to the vertical, 6.1 mm left of the midline, with the micropipette entry point just anterior to the transverse sinus, at two depths of 4.3 and 3.2 mm from the cortical surface (Figure 2.2). Toxin injections were made commencing not less than one minute after tip placement, over a period of 5 min, preceding a 5 min equilibration time. The micropipette tip was adjusted to the second placement coordinates, the injection procedure repeated, and then withdrawn over a period of 5 min. Initially, using volkensin, various doses, injection volumes and survival times were employed, and entorhinal damage and toxin transport assessed qualitatively. Animals injected with 1 ng volkensin showed very little entorhinal damage. In animals injected with 4 ng

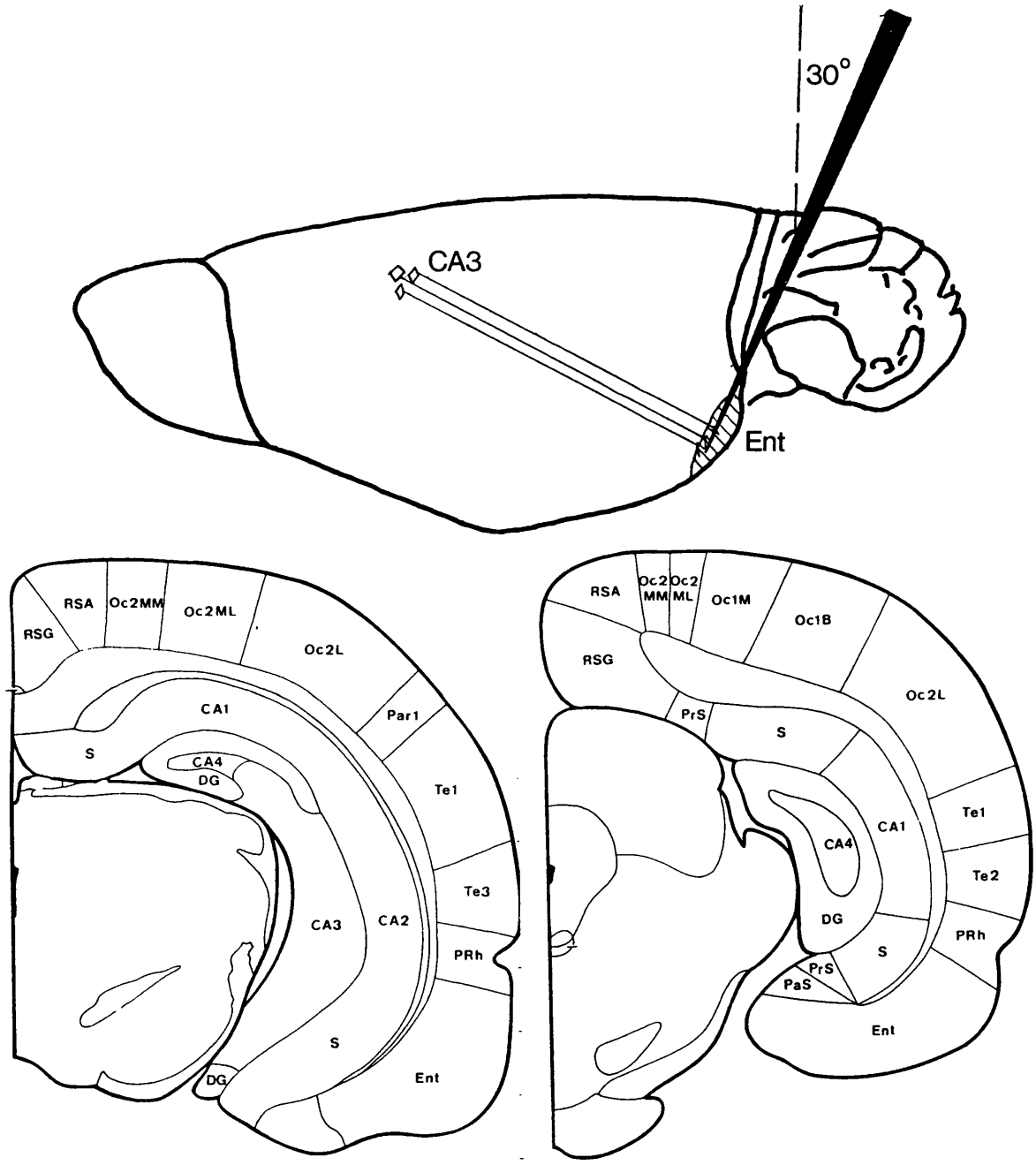

Figure 2.2: SCHEMATIC REPRESENTATION OF THE STEREOTAXIC INJECTION OF TOXIN INTO THE ENTORHINAL CORTEX. When volkensin is injected into the entorhinal cortex (hatched area; ENT), it is retrogradely transported by neurones which project to the injection site, for example anterior hippocampal CA3 neurones (CA3). Note that the injection apparatus must be angled to achieve correct placement.

The lower panel shows the location of the entorhinal cortex in schematic coronal sections of rat brain at two rostro-caudal levels, with associated areas.

Abbreviations: CA1, CA2, CA3, CA4 subfields of hippocampal Ammon's horn; DG, dentate gyrus; Ent, entorhinal cortex; Oc1 and Oc2 occipital cortex, areas 1 and 2 (L, lateral; M, medial; MM, mediomedial; ML, mediolateral); Par1, parietal cortex area 1; PaS, parasubiculum; PRh, perirhinal area; PrS, presubiculum; RSA and RSG, retrosplenial area, agranular and granular; S, subiculum; Te1, Te2, Te3, temporal cortex, areas 1 - 3.

volkensin, subcortical structures adjacent to the entorhinal cortex and hippocampus became involved, so the optimal dose of volkensin was judged to be 2 ng, where evidence of cell degeneration at sites distal to the injection were observed. For the 2 ng dose of volkensin or the 10 ng dose of ricin, two 0.2μl injections (PBS containing 5 ng volkensin/ μl or 25 ng ricin/ μl) were made into the left entorhinal cortex.

Post operative survival times, following volkensin injection, of 7, 14, 21, and 28 days (n=6 for each group) were used to determine the optimum duration for subsequent histological analysis. In the 7 day group, there was no evidence of cell degeneration in the anterior hippocampus due to retrograde transport of the toxin. At 28 day survival times, there was no consistent pattern of degeneration, with little conformity between animals. At both 14 and 21 day survival times, cell loss or hippocampal shrinkage was observed, and though the action of volkensin was not highly consistent between animals, these survival times gave the most reproducible results. In all animals where degeneration of anterior hippocampal pyramidal cells was observed, there was involvement of posterior hippocampus at the injection site. Exclusive lesioning of entorhinal pre-alpha cells was not possible to acheive with volkensin. Two groups of 10 ng ricin injected animals were prepared as controls at the above survival times (each n=4).

After the corresponding postoperative survival period, animals were rendered temporarily unconscious by immersion in CO_2, and anaesthetised with a lethal intraperitoneal dose of Sagatal, and perfused transcardially with PBS (approx. 200 ml), followed by PBS containing 30 (14 day volkensin group) or 20 (all other groups) % sucrose (approx. 300 ml). The lower concentration of sucrose produced less brain shrinkage, and made sectioning easier. The brains (minus cerebella) were carefully removed, rapidly ("snap") frozen (isopentane/ dry ice at -40°C) and mounted on cork disks using OCT embedding compound. The brains were then coated in a thin layer of Lipshaw M1-embedding matrix, wrapped in aluminium foil, and stored in airtight containers at -70°C.

2.6.2 Striatal injection (CS).

18 male Sprague-Dawley rats (200-250g) were anaesthetised using halothane / nitrous oxide / oxygen gaseous anaesthesia (as above). Lesioning

procedures were performed as described (Pangalos et al., 1991a; Pangalos et al., 1991b); Figure 2.3. Two groups (groups 2 and 3) of six animals were injected with 2 ng volkensin using a 2μl Hamilton syringe (two 1μl injections each containing 1 ng volkensin) and one group (n=6) with 10 ng ricin (two 1μl injections each containing 5 ng ricin), at the following coordinates with respect to bregma: Site 1; anterior 0.2 mm, lateral 2.7 mm, ventral to the cortical surface 6 mm; site 2; posterior 0.2 mm, lateral 3.0 mm, ventral to the cortical surface 6 mm.

After a 28 day postoperative survival time, animals were rendered unconscious by immersion in CO_2, and anaesthetised with a lethal intraperitoneal dose of Sagatal, and perfused transcardially with PBS followed by 20% sucrose in PBS. The brains, minus cerebella were then removed and "snap" frozen, mounted on cork disks and coated with a thin layer of M1 embedding matrix, before storage at -70°C.

2.6.2.1 Control excitotoxic thalamic injection (EXTH).

12 Male Sprague-Dawley rats (200-250g) were anaesthetised as above and mounted in a stereotaxic frame. Following removal of a bone flap, two injections, each of 0.2 μl of 0.12 M ibotenic acid dissolved in PBS were made unilaterally into the reticular thalamic nucleus (RT) and the ventrolateral thalamic nucleus, at the following coordinates with respect to bregma: site 1; posterior 1.4 mm, lateral 1.8 mm, ventral to the cortical surface 6.1 mm; site 2; posterior 1.8 mm, lateral 2.2 mm, ventral to the cortical surface 5.9 mm. Injections were made using a 2μl Hamilton syringe with a glass micropipette bonded to the needle, over a 5 minute period. After a 5 min equilibration, the micropipette tip was slowly withdrawn over a further 5 min. The cortical surface was irrigated with PBS, and the incision sewn up using sterile surgical thread. The animal was then removed from the stereotaxic frame, injected with Temgesic (Reckitt and Coleman, Hull, UK; buprenorphine hydrochloride 0.3 mg/kg, i.p.) and allowed to recover.

After a postoperative survival period of 6 (n=6) or 12 (n=6) days, animals were terminally anaesthetised with Sagatal, and perfused and processed as above.

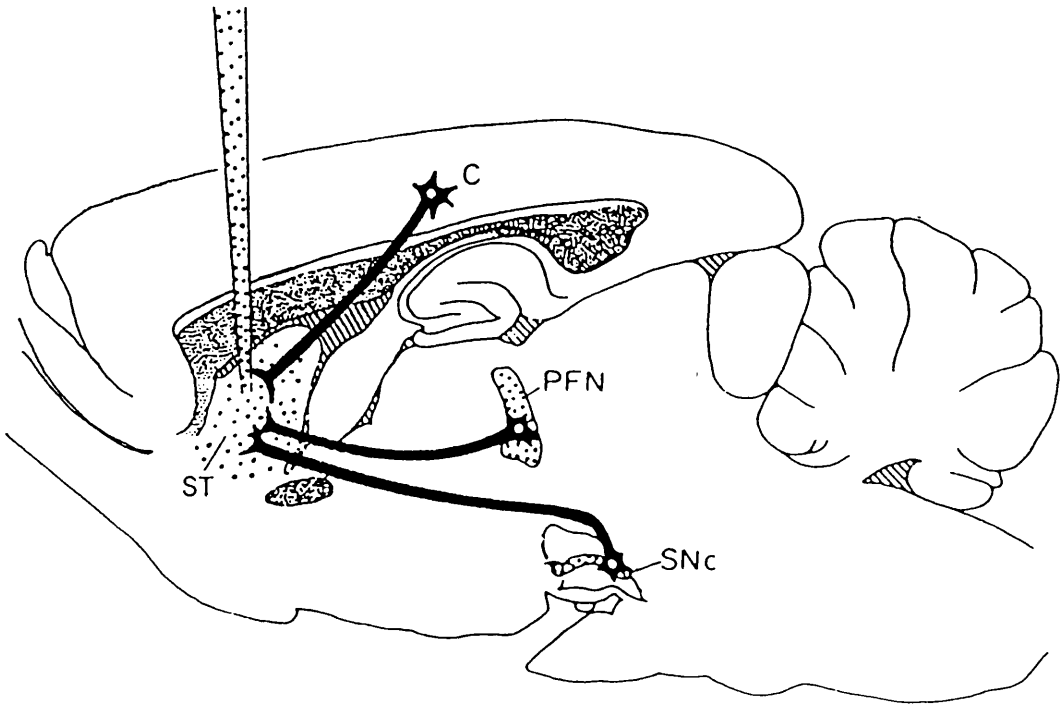

Figure 2.3: SCHEMATIC ILLUSTRATION OF THE STEREOTAXIC INJECTION OF TOXIN INTO THE STRIATUM. When volkensin (dots) is unilaterally injected into the striatum (ST), it is retrogradely transported by neurones which project to the injection site (solid black). Examples of such neuronal projections include those from layer V of the cortex (C), the intralaminar thalamus (parafascicular nucleus (PFN)) and the substantia nigra pars compacta (SNc).
Figure modified from Wiley and Stirpe, (1988).

2.6.2.2 Control excitotoxic striatal injection (EXS)

Surgical procedures were carried out at the Department of Pharmacology at Bristol University, UK, by G.A. Hicks. 6 male Sprague-Dawley rats were anaesthetised using Hypnorm (Jannsen Pharmaceuticals, Oxford, UK; fentanylcitrate and fluanisone 0.16 and 5.0 mg/kg, respectively, i.p.), and diazepam (25 mg/kg). Surgical procedures were as described in section 2.6.2 with the following exceptions: Unilateral injections of 1μl PBS containing 10μg quinolinic acid were made into the right striatum at the following coordinates relative to lambda: anterior 8.4 mm, lateral 2.2 mm, ventral to cortical surface 6 mm. After a postoperative survival time of 7 days, animals were perfused with PBS (200 ml) only, and brains were "snap" frozen and stored at -70°C.

2.6.3 Cortical injection (CC).

All lesioning procedures were performed at the Department of Biomedical Science, University of Sheffield, UK, by Prof. R.C.A. Pearson, according to the general procedures above. Briefly, male Wistar rats (200-250g) were anaesthetised with Hypnorm (as above) and Hypnovel (Roche, Welwyn Garden City, UK; midazolam hydrochloride 1.0 mg/kg, i.m.), and placed in a stereotaxic frame. The scalp was then reflected, and following periosteal scraping, a bone flap was removed from the calvarium (anterior line over coronal suture, posterior line 5 mm from coronal suture, medial line 1-2 mm from sagital suture, lateral line 3 mm from medial line). Five injections were made into the cortex (Figure 2.4), each of 1μl containing either 0.5 ng volkensin (n=7), or 2.5 ng ricin (n=5) in PBS, using a 5μl Hamilton syringe with a sharp tip. Injections were made over a period of 5 minutes, left to equilibrate for 5 min, before slowly withdrawing the needle tip. The area was thoroughly irrigated with PBS before the incision was sewn up with sterile surgical thread. Two animals had their left neocortex ablated with a sterile needle in the area under the craniotomy, and five rats of the same age and weight were used as un-operated controls.

Following a postoperative survival period of 28 days, animals were anaesthetised with a lethal dose of Sagatal, perfused transcardially with

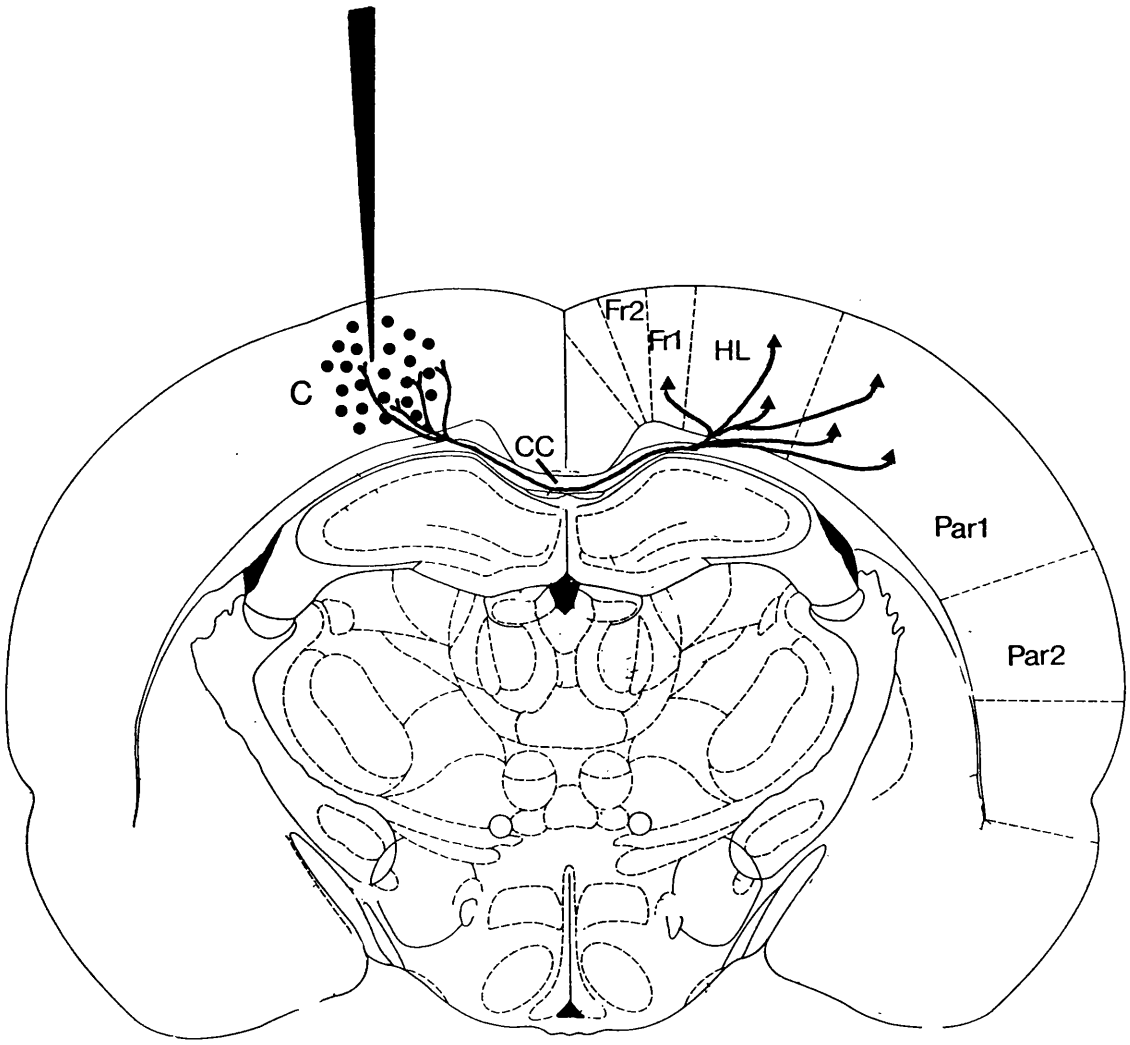

Figure 2.4: SCHEMATIC ILLUSTRATION OF THE STEREOTAXIC INJECTION OF TOXIN INTO THE CORTEX. When volkensin (dots) is injected into the neocortex (C), it is retrogradely transported by neurones which project to the injection site. Examples of such neurones (triangles with solid black lines) are those in superficial and deep layers of contralateral cortical areas, such as frontal (motor) cortical areas Fr1/Fr2 and HL (hindlimb area), and parietal (sensory and sensorimotor) cortical areas Par1/Par2. These neurones project via the corpus callosum (CC) to the injection site.
Figure modified from Paxinos and Watson (1986).

sodium phosphate buffer (pH 7.4) followed by 30% sucrose in phosphate buffer. Brains were then processed as above.

As additional confirmation that the action of volkensin targetted contralateral cell bodies which projected to the injection site, 3 animals were injected with 1 μl deionised water containing 20 % HRP, 2 % Triticum Vulgaris and 1% DMSO, at one site. Following a 24 hr survival time, animals were perfused transcardially with 200 mls of phosphate buffer containing 2 % paraformaldehye and 1.5 % glutaraldehyde. Brains were brains carefully removed, soaked in phosphate buffer containing 30 % sucrose for 24 hr, frozen, and sectioned (50 μm) in a free floating system. Labelled cells were visualised using a tetramethylbenzedine (TMB) chromogen (Olucha et al., 1985), and the regional and laminar distribution compared with cells destroyed by the retrograde action of volkensin.

2.7 Techniques of the histological studies.

2.7.1 Slide preparation.

Microscopic slides were always subbed prior to use. Subbing solution was prepared by complete dissolution of 2.5 g gelatine in 500 ml of DIW at 70°C and then adding 0.25 g of chromic potassium sulphate. Approximately 250 ml was poured into a polyacetyl slide box, and racked, prewashed microscope slides (76 x 26 mm, 1.0-1.2 mm thick, twin frosted; R.A. Lamb, London, UK) were briefly dipped into the hot solution. Slides were then dried in a drying oven for a few hours, and cooled before use. Unused subbing solution was stored in a fridge (for not more than 1 month) and reheated when required.

2.7.2 Brain sectioning.

Prior to sectioning, brains were stored at -20°C for a few hours. The cork mounted brain was mounted onto a ball chuck which allows complete control over the alignment and positioning of the brain, and then firmly fixed onto the cutting arm of the cryostat (Model OTF/AS; Bright instruments Ltd., Huntingdon, UK). The brain was trimmed and centred, and coronal sections of 12μm thickness were cut at -16°C from approximately; bregma +2.7 mm to

-8.8 mm (entorhinal injections), bregma +3.0 mm to -5.8 mm (striatal and thalamic injections), or bregma +2.7 mm to -6.3 mm (cortical injections) (Paxinos and Watson, 1982). Sections were then thaw- mounted onto subbed slides (2 sections per slide except those processed for *in-situ* hybridisation, where 1 section was collected per slide). Sections processed for *in-situ* hybridisation were kept below 0°C at all times after thaw mounting until processing. All other slides were air dried for 15 min before being stored in sealed boxes at -70°C until required for histology or autoradiography.

2.7.3 Cresyl violet staining of Nissl substance in frozen sections.

To study cell loss and morphological changes following lesioning procedures, sections were stained using acidic cresyl violet. Prior to staining, all sections were fixed in buffered formalin solution for 5 min at room temperature and rinsed thoroughly in PBS.

Cresyl violet stain was prepared by adding 0.408 g of sodium acetate to 270 ml of DIW to which 40.25 μl of 90% formic acid had been added. 0.2 g of cresyl violet was dissolved in 40 ml DIW, heated to 60 °C, stirred continuously, and filtered. 30 ml of the filtrate was added to the above solution, and the final pH of the stain was checked and adjusted with acetic acid (to pH 4.2). Washed, fixed sections were dipped into the stain for 1-5 min, rinsed in PBS to remove excess stain, and transferred through a series of 70, 80, 95, 100 and 100 % alcohol solutions for approximately 2 min per wash, dried, immersed in xylene, and mounted with coverslips using DPX mountant.

2.7.4 *In-situ* hybridisation histochemistry for glutamic acid decarboxylase.

In-situ detection of the mRNA encoding the enzyme glutamic acid decarboxylase (GAD) was performed using a previously described method (Najlerahim et al., 1990).

Sections were thawed to room temperature, and pre-treated as follows: sections were fixed in freshly prepared 4% paraformaldehyde in DIW for 5 min, rinsed thoroughly in PBS, and treated for 10 min in 0.1 M triethanolamine HCl / 0.9% NaCl (corrected to pH 8.0 with sodium hydroxide),

containing 0.25% acetic anhydride (acetylation step to reduce non-specific binding). After a further wash in PBS, sections were dehydrated using 70, 80, 90 and 100% ethanol / water (v/v) solutions, for 2 min per wash, followed by delipidation for 10 min in chloroform, then partially rehydrated by 1 min dips in 100 and 95% alcohol solutions. Sections were then air dried, re-boxed and stored at -20°C until required.

An HPLC purified synthetic oligonucleotide probe, directed against bases 1621 to 1650 of GAD mRNA was made by Oswell DNA services (Edinburgh, UK). The region of the target gene sequence had an approximate 43 % base content of cytosine and guanine, and the existence of any other gene containing a sequence within 6 bases of the proposed probe in either the sense or the antisense orientations determined (checked against the European Molecular Biology Laboratory gene database). This reduced the likelihood of the probe binding to another mRNA species. The probe was diluted to 2 pmol/μl and stored at -40°C until use.

On the day of the experiment, the probe was labelled using a 3' end labelling kit (NEN Dupont, Boston, USA). In a microfuge tube, 10 pmol of probe was incubated with 5 pmol of [^{35}S] deoxyadenosine 5' thiotriphosphate ([^{35}S]dATP; specific activity 1200 mCi/ml; NEN Dupont) in the presence of $CoCl_2$, 36 U terminal deoxynucleotidyl transferase, and reaction buffer for 1 hr at 37°C. This adds a homopolymeric tail to the probe of approximately 10 [^{35}S]dATP molecules. A Nensorb column (NEN Dupont) was primed with 2 ml methanol and 2 ml reagent A, before the labelled probe was added to the column. Initially, reagent A (2 ml) was added as the eluent, and two fractions (1 and 2) were collected. 2 ml of 50% ethanol was then used as the eluent, and fractions 3, 4, 5 and 6 were collected (10 drops each). The radioactivity in a 5μl sample of each fraction was determined by adding 5 ml scintillant, and counting on the ^{14}C channel of a liquid scintillation counter. Fraction 4 was expected to contain the most probe, and indeed showed the highest level of radioactivity.

Pre-treated sections were thawed to room temperature, and 100μl of hybridisation buffer containing 1-2 x 10^6 cpm was carefully pipetted onto each section to avoid air bubbles. The hybridisation buffer comprised of 50%

deionised formamide, 10% dextran sulphate, 20 mM phosphate buffer (pH 7.4), 4 x SSC (saline sodium citrate; 1 x SSC is 150 mM NaCl and 15 mM Na-citrate), 1 x Denhardt's solution (0.02% (w/v) Ficoll, 0.02% (w/v) polyvinyl pyrrolidine and 0.02% (w/v) BSA), 0.1% dithiothreitol, and 100 μg/ml of poly (A), denatured salmon sperm and total yeast tRNA. The sections and the incubation buffer were then covered by a square of parafilm cut to the appropriate size. Slides were placed on moistened filter paper in trays, which were then sealed and placed in an incubator at 24°C for 18 hr. The hybridisation temperature was set at 15°C below the melt temperature (T_m) for the probe.

Following hybridisation, cover slips were removed in a large volume of 1 x SSC (500 ml) and the sections were washed in 1 x SSC at 50°C (4 changes, 15 min each) followed by a further two hours at room temperature. Following a brief dip in distilled water to remove excess salt, the slides were air dried and dipped in photographic emulsion for 5 sec (Ilford K5 1:1 with 2% glycerol at 43°C). Once dry, sections were placed in light- tight boxes, and left at 4°C for 21 days, before developing by immersion in Ilford Phenisol (1:4 with water; 2.5 min), stop bath (30 sec), and 30% sodium thiosulphate (5 min), all at 18°C. Developed sections were then washed with water, air dried, fixed and counter stained with cresyl violet to enable visualisation of cell bodies.

Previous examination of this oligonucleotide probe has demonstrated it's specificity for rat GAD mRNA by northern analysis and appropriate histochemical controls (Najlerahim et al., 1990). Concurrent hybridisation of the adjacent sections using a separate oligonucleotide probe with the same sequence as the selected area of GAD mRNA (sense strand) confirmed the specificity of these experiments.

GAD-mRNA positive cells were viewed using a Zeiss Jenaval microscope (Zeiss, East Germany), and transferred to an image analysis system (Seescan, Cambridge, UK). For all volkensin and ricin injected animals (ENT, CC), the distribution of GAD mRNA positive cells was carefully examined. For the entorhinal injection, the number of positive cells in the anterior hippocampus both ipsilateral and contralateral to the injection were compared. A group of animals receiving intrastriatal volkensin and ricin had

been previously examined as described (Pangalos et al., 1991b; Francis et al., 1992b). For the cortical injection, GAD mRNA positive cells were counted contralateral to the lesioned area of the cortex at two depths comprising layers I-III and IV-VI. The data obtained for the volkensin animals was compared with the number of GAD-mRNA positive cells in ricin injected and control animals.

2.7.5 Immunocytochemistry for glial fibrillary acidic protein (GFAP).

Immunocytochemical staining to visualise glial cells and hence the extent of neocortical gliosis in CC animals (volkensin, ricin and control groups), was performed using an avidin biotin peroxidase technique. Soluble fraction GFAP was isolated from normal human spinal cord by Dr. J. Newcombe using the method of Ruutiainen et al. (1981) and shown to consist of highly purified GFAP polypeptides by PAGE and immunoblotting with two rabbit antisera against GFAP. Monoclonal antibodies were prepared using mice, and antibody specificity was examined by immunoblotting on human, rabbit, guinea pig, rat and mouse CNS samples (Newcombe et al., 1986).

Sections were ringed using a glass cutter to minimise solution spreading and stained with the avidin biotin peroxidase complex method (Vector Laboratories, Peterborough, UK). All incubations were performed at room temperature in a humidified box to prevent drying. Following fixation in acetone at 4 °C for 10 min, sections were incubated for 20 min with 50 μl normal horse serum (0.2 %), diluted in PBS, to block nonspecific binding of biotin conjugated horse immunoglobulins to human anitgens. The excess serum was drained from each section and repaced with 50 μl of the monoclonal anti-GFAP (clone 5.2E4, 1:750 dilution of ascites fluid in PBS) for 1 hr. Slides were then washed by immersion for 3 x 5 min in PBS agitated with a magnetic stirrer. The slides were blotted to remove excess PBS and 50 μl of biotin conjugated anti-mouse IgG (diluted 1:200) was applied to each section. Following a 30 min incubation, slides were again washed and blotted. The avidin biotin peroxidase complex solution was mixed according to the manufacturers instructions 30 min prior to use to allow complex formation. 50 μl of the complex solution was applied to each section for 1 hr. Peroxidase substrate was prepared by dissolving a 250 mg aliquot of 3'3-diaminobenzedine

(DAB) in 250 ml PBS and mixing this with 250 ml of freshly prepared 0.02 % hydrogen peroxide. Sections were washed and incubated in the substrate solution for 2-5 min, and washed with tap water. Sections were then dehydrated and counterstained with cresyl violet according to the method described in section 2.7.3.

2.7.6 Image processing and quantification of cresyl violet stained sections.

For all the lesions performed cresyl violet stained sections were viewed using a Leitz Diaplan microscope (magnification x 10; Leica, Cambridge, UK), and a live image produced on a Quantimet 570 image analysis system (Leica Cambridge) using a 3-CCD colour camera (Model KY-F30; JVC, Tokyo, Japan). The colour image was viewed by selection of the green channel, which produced a high contrast monochrome image (**grey image**). Contrast was enhanced using an image analysis algorithm, and grey images were captured and stored in memory for analysis.

In order to make geometric measurements of a multitonal grey image (256 possible grey levels), it has to be converted into a **binary image**. Instead of grey tones being represented by the 256 grey levels, only 2 levels are used to represent objects of interest, 0 (black) and 1 (white). The process of defining the binary image from the grey image was achieved by using the "detection" facility of the system. This allows the zones of interest, in this case the cells, to be picked out by adjustment of a "threshold" control. Objects were detected by adjusting the threshold to a value between 0 (no cells detected) and 255 (objects and background detected). At the correct threshold level all cells in the grey image were detected, the threshold level was stored and a binary image produced. The binary image was then processed in a standard manner: (i) spots of size 1 pixel were removed, (ii) objects (cells) close together but unseparated were split into individual components by the image analysis system, (iii) the binary image was compared to the grey image and any further editions required were made manually.

2.7.6.1 Entorhinal injection.

The affected cell type in the entorhinal injected animals was the anterior hippocampal pyramidal cell. Initial investigation of morphological changes indicated that the CA3 field of the hippocampus was most affected, with apparent sparing of CA1 and CA2. Initially, the cell number and size of each of the hippocampal fields were counted, with a view to making a side to side comparison, but further investigation revealed that the values obtained were dependent upon the exact orientation at which the brain had been cut in the cryostat. To circumvent these problems, it was decided to measure the overall area of each of the hippocampal fields CA1, CA3 (including CA2, but not CA4) and the dentate gyrus (DG) from the beginning of the hippocampus, to the point at which the dorsal and ventral hippocampi joined, on sides ipsilateral and contralateral to the injection site. To achieve this, the length of each of the fields was measured using the Quantimet. To achieve accuracy in determining the extent of each field, sections were initially viewed though a microscope with an attached drawing tube, and simultaneously viewing a schematic of the hippocampus. As histological sections had been taken every 200μm, multiplying the above measurement by 200μm gave the area of that segment of the hippocampal field. By adding the areas of each hippocampal segment, an overall area of the hippocampal field for each side of the brain was obtained (Figure 2.5). The area of each field ipsilateral to the injected side was then compared to the corresponding contralateral area.

2.7.6.2 Striatal injection.

The objects in the final binary image were sized and counted as described (Pangalos et al., 1991b; Francis et al., 1992b). An exclusion criteria was set to 70 μm^2 for counting supragranular (layer III) pyramidal cells, and to 80 μm^2 for counting infragranular (layer V) pyramidal cells. In all cases, the frame size was noted. Cells were counted in medial areas (Fr1/Fr2 and part of HL, see Zilles, 1985) and more laterally in Par1/Par2 (Zilles, 1985). The mean number of cell profiles per field (cell number) and mean size of profiles per field (mean cell size) $\pm$ SEM from at least 6 section per rat were calculated. Comparisons were then made between measurements obtained for sides ipsilateral and contralateral to the injection site.

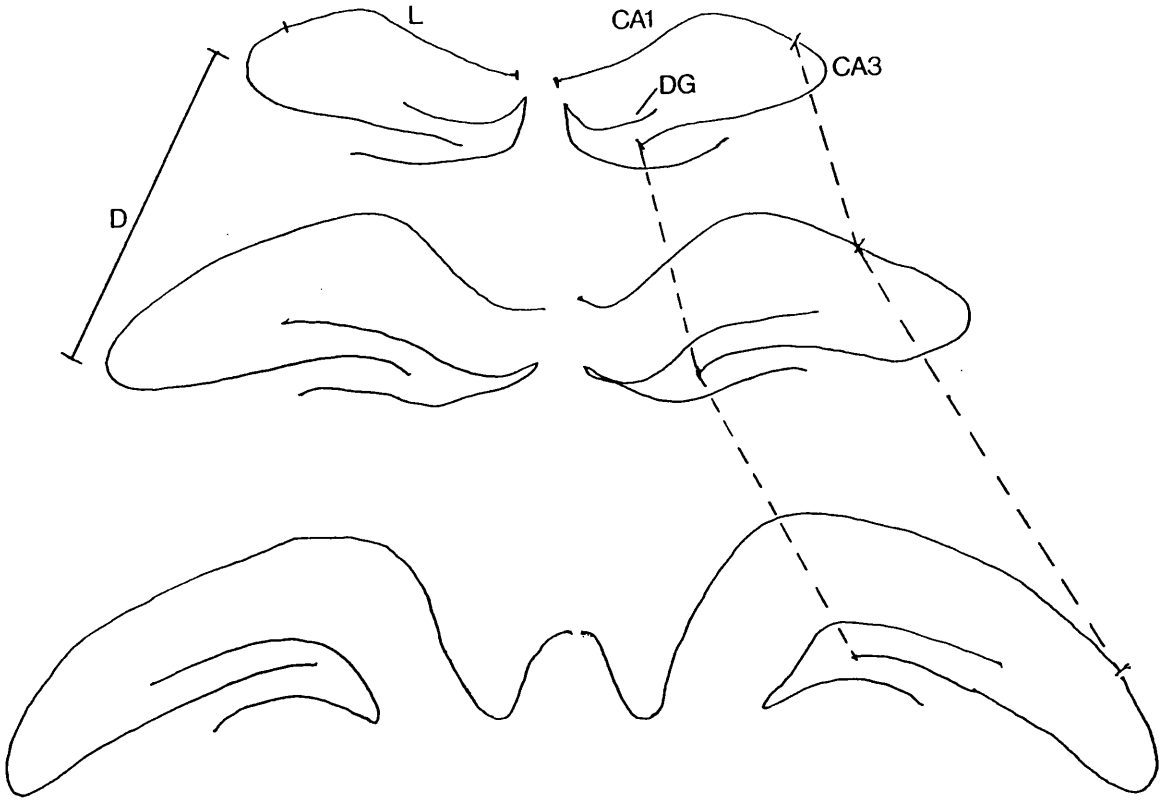

Figure 2.5: SCHEMATIC ILLUSTRATION OF METHOD OF HIPPOCAMPAL AREA CALCULATION. The diagram shows schematic representations of hippocampi in coronal rat brain sections at three different rostro-caudal levels. After measuring the length (L) of hippocampal fields (Ammon's horn pyramidal cell layers CA1 and CA3 (including CA2) and dentate gyrus (DG) granule cell layer), area calculations were performed by multiplying (L) by the distance between each stained, measured section (D). Dotted lines indicate examples of corresponding points (start and end of CA3) in rostro-caudal sections.

2.7.6.3 Cortical injection.

The objects in the final binary image were examined by eye. Exclusion criteria were carefully assessed and set following the measurement of several, identified, supragranular and infragranular pyramidal cells. On the basis of this, exclusion criteria of 50 μm^2 (supragranular layers) and 70 μm^2 (infragranular layers) were set. Cells were counted on the side contralateral but corresponding to the lesion, spanning two levels, approximately corresponding to layers I-III and IV-VI, in neocortical areas Fr1 and HL rostrally, and more caudally in Oc2 MM, ML and L, and Oc1 M and B (Zilles, 1985). Data obtained from volkensin injected animals were compared to that obtained from ricin and control animals. At least six section were examined per animal.

HRP labelled cells were counted by eye in four contiguous fields throughout the contralateral cortex correponding to the area injected in the ipsilateral cortex (R.C.A. Pearson, University of Sheffield).

2.8 Autoradiographic techniques.

Changes in receptor density, affinity and anatomical distribution following lesioning experiments was performed using the technique of autoradiography. The methods described below were applied to sections from lesioned animals, to obtain data concerning the neurobiology of the pyramidal cells affected by a lesion. Not all of the receptors described below were applied to all of the lesioned animal groups- the suitability of investigation of a receptor in a lesion type was carefully assessed. Table 2.1 summarises the methods used for the autoradiographic techniques, and Table 2.2 describes which receptors were studied in each lesion group.

2.8.1 Autoradiography of the 5-HT_{1A} receptor using [^{3}H] 8-OH-DPAT.

Anatomical distribution of the 5-HT_{1A} receptor in lesioned animals was visualised by autoradiography, using [^{3}H] 8-OH-DPAT. Autoradiography using this ligand was performed on all lesion groups (ENT, CS (all groups), CC and control excitotoxin lesioned animals). Incubation conditions were based on those according to previously published procedures (Pazos and Palacios, 1985;

Ligand	Displacer	Incubation Buffer	Preincubation	Incubation	Wash
[^{3}H] 8-OH-DPAT [1 nM] (5-HT_{1A})	1 μM 5-HT	0.17 M Tris-Hcl, 4 mM $CaCl_2$, 0.01% ascorbate, pH 7.6	30 min, 25°C	60 min, 25°C	2 x 5 min, 4°C
[^{3}H] ketanserin [2 nM] (5-HT_{2A})	1 μM mianserin	0.17 M Tris-HCl, pH 7.7	15 min, 25°C	120 min, 25°C	2 x 10 min, 4°C
[^{3}H] pirenzepine [2.5 nM] (muscarinic M_1)	10 μM atropine	PBS	20 min, 25°C	90 min, 25°C	1 x 5 min, 4°C
[^{3}H] nicotine [6 nM] (nicotinic)	100 μM carbachol	50 mM Tris-HCl, 8 mM $CaCl_2$	30 min, 25°C	90 min, 25°C	2 x 10 sec, 4°C
[^{3}H] kainate [30 nM] (kainate glutamate)	10 μM kainate	50 mM Tris-citrate, pH 7.0	45 min, 4°C	45 min, 4°C	2 x 20 sec, 4°C
[^{3}H] L-689,560 [5 nM] (NMDA glutamate)	1 mM glycine	50 mM Tris-acetate, pH 7.0	60 min, 4°C	120 min, 4°C	4 x 1 min, 4°C
[^{3}H] GABA [20 nM] ($GABA_A$)	100 μM isoguvacine	50 mM Tris-HCl, 100 μM baclofen, pH 7.4	25 min, 25°C	45 min, 25°C	2 x 25 sec, 4°C
[^{3}H] prazosin [0.4 nM] (alpha$_1$ adrenoceptors)	10 μM phentolamine	50 mM Tris-HCl, pH 7.4, with 30 nM 5-MU for 1b component	30 min, 30°C	45 min, 30°C	2 x 5 min, 4°C
[^{3}H] DPCPX [2 nM] (adenosine A_1)	100 μM R-PIA	0.17 M Tris-HCl, 1 mM EDTA, 10 μM Gpp(NH)p, pH 7.4	30 min, 37°C, with 2 U/ml ADA	80 min, 37°C	2 x 5 min, 4°C

Table 2.1: SUMMARY OF AUTORADIOGRAPHIC EXPERIMENTAL CONDITIONS. All preincubations and incubations were performed in modified coplin jars (25 ml) except for [^{3}H] kainate binding. All washes were 250 ml buffer per wash. Typical ligand concentration shown in square brackets; receptor subtype shown in parentheses.

Ligand	ENT	CS	EXS	EXTH	CC
[^{3}H] 8-OH-DPAT	X	(1),2,3	X	X	X
[^{3}H] ketanserin	X	(1)	-	-	X
[^{3}H] pirenzepine	X	(1),3	X	X	X
[^{3}H] nicotine	-	3	X	X	X
[^{3}H] kainate	X	1,2	X	X	-
[^{3}H] L-689,560	X	(1)	-	-	-
[^{3}H] GABA	X	2	-	-	-
[^{3}H] prazosin	-	2	-	-	-
[^{3}H] DPCPX	-	3	-	-	X

Table 2.2: SUMMARY OF AUTORADIOGRAPHIC EXPERIMENTS PERFORMED ON LESION TYPES. ENT- entorhinal injection (volkensin and ricin); CS- striatal injection (volkensin and ricin); EXS- excitotoxic striatal injection (quinolinic acid); EXTH- excitotoxic thalamic injection (ibotenic acid); CC- cortical injection (volkensin, ricin and uninjected controls). Experiments were performed on one group of animals (X) except for CS animals, where the experiments were performed on one or more groups of animals (animal group number is indicated). Group number in parentheses indicates previous investigation in CS animals reported elsewhere.

Francis et al., 1992b). Sections were sorted at -70°C, and thawed to room temperature when required. After drying under an air stream, sections were preincubated in buffer (0.17 M Tris-HCl, 4 mM $CaCl_2$, 0.01% ascorbic acid, pH 7.6) for 30 min at 25°C, and incubated for 60 min at 25°C in the presence of 1-2.5 nM [^{3}H] 8-OH-DPAT. Non-specific binding was generated using a parallel series of sections incubated as above, but also in the presence of 10 μM 5-HT creatinine sulphate. Preincubations and incubations were carried out in modified coplin jars, total volume 25 ml, which contained a maximum of 10 slides. Following the incubation, slides were transferred to racks, and washed in ice cold buffer for 2 x 5 min. Slides were then laid out on the bench and dried with a stream of cold air. Autoradiograms were then generated as described in section 2.8.10.

Optimum binding conditions had already been established by generating association and dissociation curves using control coronal rat brain sections (Francis et al., 1992b). Non-specific binding was similar to that described (5-15 % of total binding).

2.8.2 Autoradiography of the 5-HT_{2A} receptor using [^{3}H] ketanserin.

Autoradiography of the 5-HT_{2A} site was based on conditions previously described (Pazos et al., 1985; Francis et al., 1992b), and was performed on ENT and CC animals. Sections were thawed as described in section 2.8.1. and preincubated in buffer (0.17 M Tris-HCl pH 7.7) for 15 min at 25°C. Incubations were performed for 120 min in the above buffer but also containing 2 nM [^{3}H] ketanserin. Non-specific binding was determined by the addition of 10μM mianserin. Following incubations, sections were washed for 2 x 10 min in ice cold buffer. Sections were then air dried, and autoradiograms generated as described in section 2.8.10.

2.8.3 Autoradiography of the M_1 receptor using [^{3}H] pirenzepine.

[^{3}H] pirenzepine binding was performed using a method modified from previously published conditions (Spencer et al., 1986; Buckley and Burnstock, 1986; Vogt et al., 1990), on all groups of lesioned animals (CS groups 1 and 3). Sections were thawed and dried, preincubated in PBS for 20 min at 25°C,

incubated in PBS containing 2.5 nM [^{3}H] pirenzepine for 90 min at 25°C, and washed in ice cold PBS for 1 x 5 min. Non-specific binding was determined in the presence of 10μM atropine sulphate prepared on the day of the assay. Sections were then air dried, and autoradiograms generated as described in section 2.8.10.

Optimal binding conditions were previously established by performing association and dissociation experiments on control rat brain sections. Equilibrium was reached by 90 min ($t_{1/2}$ of 10 min), and the dissociation curve produced a $t_{1/2}$ of 60 sec. A 5 min wash produced 88% specific binding (Pangalos, 1992).

2.8.4 Autoradiography of the nicotinic receptor using [^{3}H] nicotine.

Anatomical distribution of nicotinic receptors was visualised by autoradiography using [^{3}H] nicotine. The distribution of this receptor was investigated in lesion groups CS, group 3, excitotoxin controls and CC animals. Incubations were modified from published methods (Clarke et al., 1985; Perry et al., 1992). Sections were thawed and dried, preincubated for 30 min at 25°C in buffer (50 mM Tris-HCl pH 7.4, 8 mM $CaCl_2$), and incubated for 90 min at 25°C in the presence of (typically) 6 nM [^{3}H] nicotine. Non-specific binding was defined using 100 μM carbamyl choline chloride (carbachol). Sections were then washed for 2 x 10 sec in ice cold buffer, dipped briefly in ice cold DIW to remove buffer salts and dried. Autoradiograms were generated as described in section 2.8.10.

Before incubations were performed on the valuable lesioned animal sections, standard binding conditions described above were determined by performing association and dissociation experiments with control rat brain sections. The association curve (Figure 2.6A) was generated using incubation times ranging from 1 min to 120 min. Dissociation (washout, Figure 2.6B) curves were generated using wash times from 2 sec to 10 min. Binding to sections in these experiments were determined by "scratch and count" methods (transferring the sections from the slides onto Whatman GF/A filter discs using a single sided razor blade, with subsequent liquid scintillation counting after immersion of the filter disc in 10 ml Packard emulsifier safe scintillant).

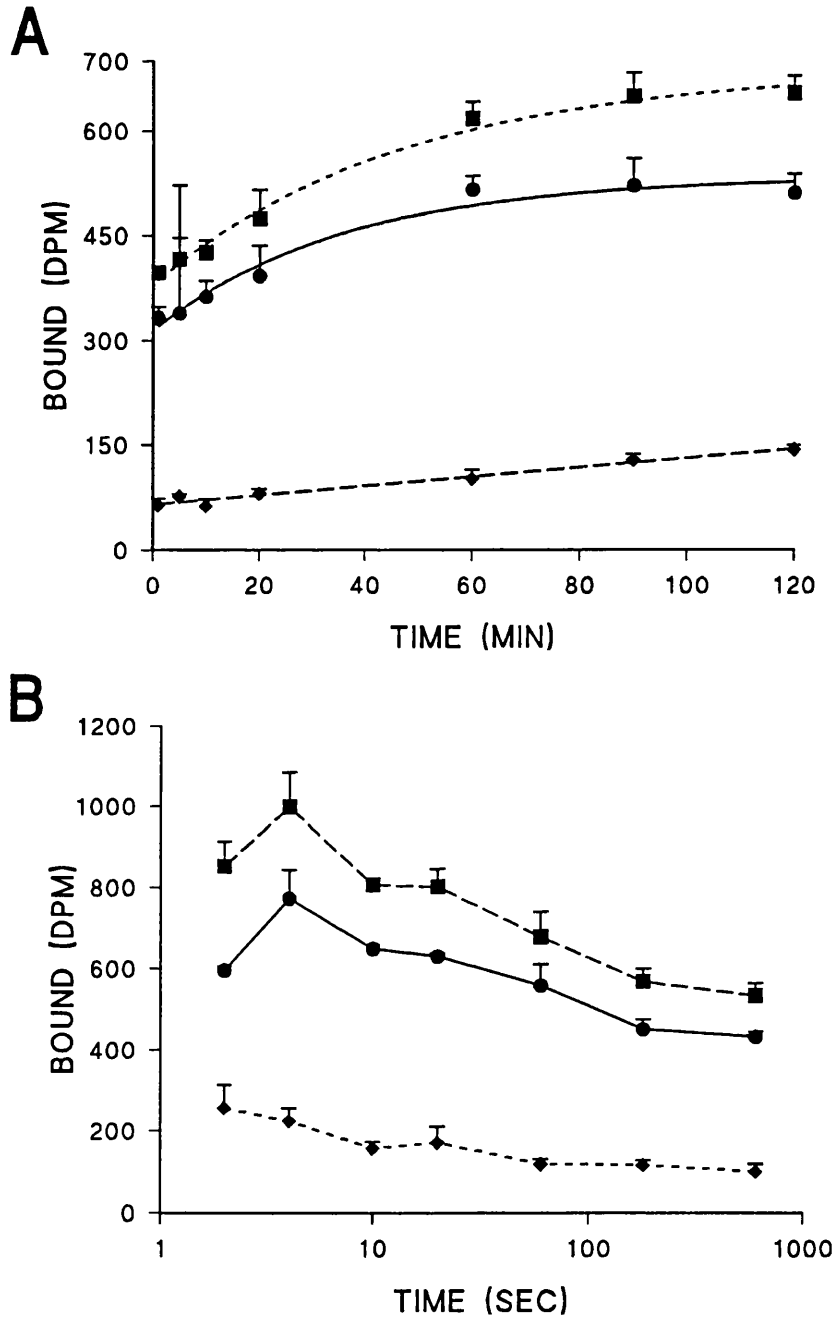

Figure 2.6: TIME DEPENDENCY AND REVERSIBILITY OF [^{3}H] NICOTINE BINDING. Experiments performed using control rat brain sections, incubated in 50 mM Tris-HCl and 8 mM $CaCl_2$ with a final concentration of 6 nM [^{3}H] nicotine. Non-specific binding was determined using 100 μM carbachol. Binding was determined using liquid scintillation spectrometry. Graph A shows ligand association, and graph B the washout characteristics.
Values are mean ± SEM, n=3. Data points represent; mean specific binding (●), total binding (■) and non-specific binding (◆).

Figure 2.6A shows that equilibrium had been achieved after 90 min ($t_{1/2}$=25.2 min). The dissociation curve gave a $t_{1/2}$ of 13 sec, and a wash time of 2 x 10 sec provided a good total to non-specific ratio (approx. 75 % specific binding).

For saturation analysis (CS animals only, group 3), sections were incubated under standard conditions with varying concentrations of [^{3}H] nicotine (0.5 nM - 50 nM). The binding characteristics were assessed by "scratch and count" methods for one volkensin injected animal, and by autoradiography in specific brain areas to compare binding parameters on the ipsilateral and contralateral sides in sections from four volkensin injected animals.

2.8.5 Autoradiography of the kainate receptor using [^{3}H] kainate.

Anatomical distribution of the kainate sensitive glutamate receptor in lesioned animals (CS (group 1), EXS, EXTH and ENT) was visualised by autoradiography using [^{3}H] kainate. Incubation conditions were based upon those previously described (Cross et al., 1987; Ulas et al., 1990; Penney et al., 1990; Dewar et al., 1991). Sections were thawed as previously described.

It had been previously reported that the addition of Ca^{2+} ions in the incubation media of [^{3}H] kainate binding experiments selectively inhibits high affinity kainate binding (Greenamyre et al., 1985a; Monaghan et al., 1985); therefore the effect of Ca^{2+} was investigated in control rat brain sections. Various incubation and wash conditions have also been reported for optimal [^{3}H] kainate binding; association and dissociation experiments were performed by "scratch and count" methods. The addition of calcium did indeed reduce the binding of [^{3}H] kainate (Table 2.3), so all subsequent experiments were performed in the absence of calcium.

Incubations based on previous methods require high concentrations of [^{3}H] kainate (15 nM - 50 nM) to achieve adequate binding, thus the methods described for autoradiography in the preceding sections were modified. Sections were preincubated for 45 min at 2°C in 50 mM Tris-citrate buffer (pH 7.0), using modified coplin jars (25 ml) containing not more than ten slides. The sections were then washed briefly with two changes of ice cold DIW. Incubations were performed by pipetting 100μl of buffer containing 30 nM [^{3}H]

Binding (dpm)	**0 mM Ca^{2+}**	**10 mM Ca^{2+}**
Total	2282 ± 83	1864 ± 105
Non-specific	353 ± 24	283 ± 38
Specific	1929 ± 67	1581 ± 99

Table 2.3 EFFECT OF INCLUSION OF Ca^{2+} ON [^{3}H] KAINATE BINDING. Experiments were performed using control rat sections from 2 animals, which were incubated for 45 min in 100 μl of 50 mM Tris-citrate buffer containing 30 nM [^{3}H] kainate in the presence or absence of exogenously added Ca^{2+}. Non-specific binding was defined using 10 μM cold kainate. Values are mean dpm ± SEM, n = 10 (5 values from each animal, 2 animals).

kainate onto each section, at 2°C for 45 min. Each incubation consisted of not more than 20 slides. Non-specific binding was defined using 10μM unlabelled kainate. Following the incubation, the buffer was carefully removed and slides were racked and washed for 2 x 20 sec in ice cold buffer (250 ml per wash). Slides were then dipped briefly into a solution of 2.5% glutaraldehyde in acetone. Drying was performed as usual. All procedures were performed in a cold room at 4°C, with ice cold solutions. This was to prevent the generation of endogenous glutamate, which displaces the binding of [^{3}H] kainate.

Association and dissociation experiments were performed on control sections by varying the incubation time from 30 sec to 90 min, and the wash time from 2 sec to 2 min. The association curve (Figure 2.7A) shows that equilibrium was reached by 15 min ($t_{1/2}$ = 2.9 min). Two 20 sec washes (Figure 2.7B; $t_{1/2}$ = 19 sec) produced 94% specific binding.

At the time at which the experiments were performed, it was unclear whether the kainate and AMPA receptor were distinct subtypes of glutamate receptors, equally sensitive to the two ligands (Miller, 1991; Patneau and Mayer, 1991). The effects of kainate and AMPA were not separable by some investigators in rat neocortical cultures (Cai and Erdo, 1992). It has subsequently become clear that the kainate and AMPA receptors are separate, with varying subunit composition from alternative splice and gene products (Werner et al., 1991; Egebjerg et al., 1991). However, the "selective agonists" kainate and AMPA have been shown to overlap in their binding characteristics. As it was considered important to establish which receptor would be labelled by [^{3}H] kainate, a competition curve was generated using increasing concentrations of AMPA (1 nM to 10 μM) in the presence of 50 nM [^{3}H] kainate. Control rat brain sections (12 μm) from three animals were incubated and washed as above. Calcium was not present in the incubation buffer. Autoradiograms were generated (section 2.8.10) and cortical areas Fr1/Fr2 (upper and lower layers) and Par1/Par2 (upper and lower layers) along with hippocampal areas CA3 and DG were examined and the binding levels determined (see Chapter 5, Figure 5.3).

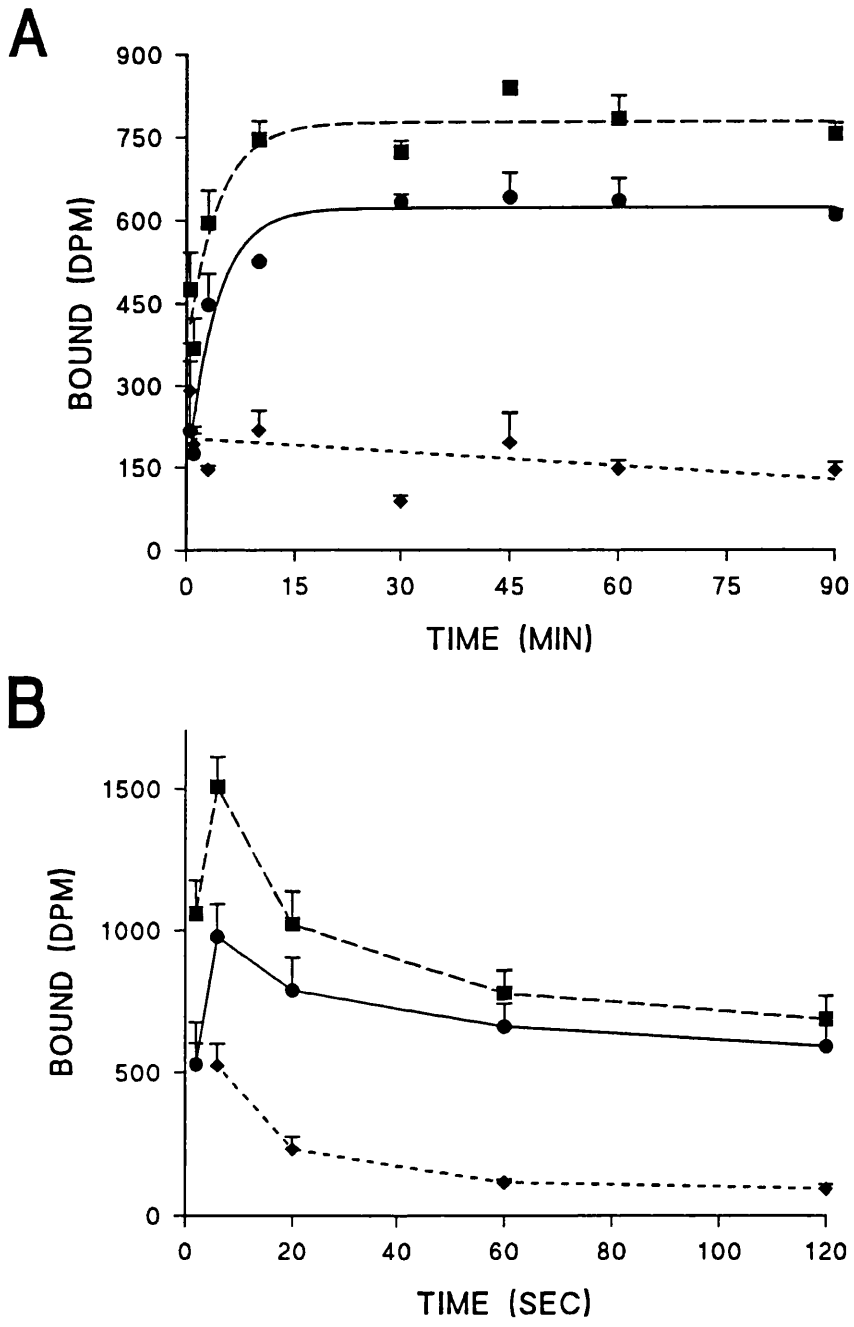

Figure 2.7: TIME DEPENDENCY AND REVERSIBILITY OF [^{3}H] KAINATE BINDING. Experiments performed using control rat brain sections, incubated in 100 μl of 50 mM Tris-HCl with a final concentration of 30 nM [^{3}H] kainate. Non-specific binding was determined using 10 μM unlabelled kainate. Binding was determined using liquid scintillation spectrometry. Graph A shows ligand association, and graph B the washout characteristics. Values are mean $\pm$ SEM, n=3. Data points represent; mean specific binding (●), total binding (■) and non-specific binding (◆).

2.8.6 Autoradiography of the strychnine- insensitive glycine site on the NMDA receptor complex using the novel antagonist [^{3}H] L-689,560.

[^{3}H] L-689,560 binding was initially based on membrane binding conditions (Grimwood et al., 1992), and modified to achieve optimal binding conditions for autoradiography (Pangalos et al., 1992). [^{3}H] L-689,560 was synthesised at Merck, Sharp and Dohme research laboratories (Harlow, UK). Sections were thawed and dried as described in section 2.8.1.

Sections from entorhinal injected animals were preincubated in buffer (50 mM Tris-acetate, pH 7.0) for 1 hr at 4°C, and incubated for 120 min in a similar buffer but in the presence of 5 nM [^{3}H] L-689,560. Preincubations and incubations were performed in box containers (250 ml). Non-specific binding was determined using a parallel series of sections by incubation in the presence of 1 mM glycine which was prepared on the day of the assay. Following incubations, sections were washed for 4 x 1 min (250 ml of ice cold buffer / wash) and air dried. Autoradiograms were generated as described in section 2.8.10.

2.8.7 Autoradiography of the $GABA_A$ receptor using [^{3}H] GABA.

[^{3}H] GABA binding was performed on sections from ENT and CS (group 2) animals, based on a modified method of previously published conditions (Bowery et al., 1987; Chu et al., 1990).

Sections were thawed and dried, preincubated for 25 min in 50 mM Tris-HCl, pH 7.4 buffer at 25°C, and incubated for 45 min in buffer also containing 20 nM [^{3}H] GABA, with 100 μM baclofen to exclude the $GABA_B$ site. Non-specific binding was defined using 100 μM isoguvacine. Following incubation, sections were washed for 2 x 25 sec (250 ml ice cold buffer / wash), and dried. Autoradiograms were generated as described in section 2.8.10.

To determine the optimal binding conditions, association and dissociation experiments were performed on sections from control sections by "scratch and count" methods. The association curve incubation times were varied from 5 to 60 min, and the dissociation curve wash times varied from 2 sec to 8 min. The association curve (Figure 2.8A) shows that equilibrium was

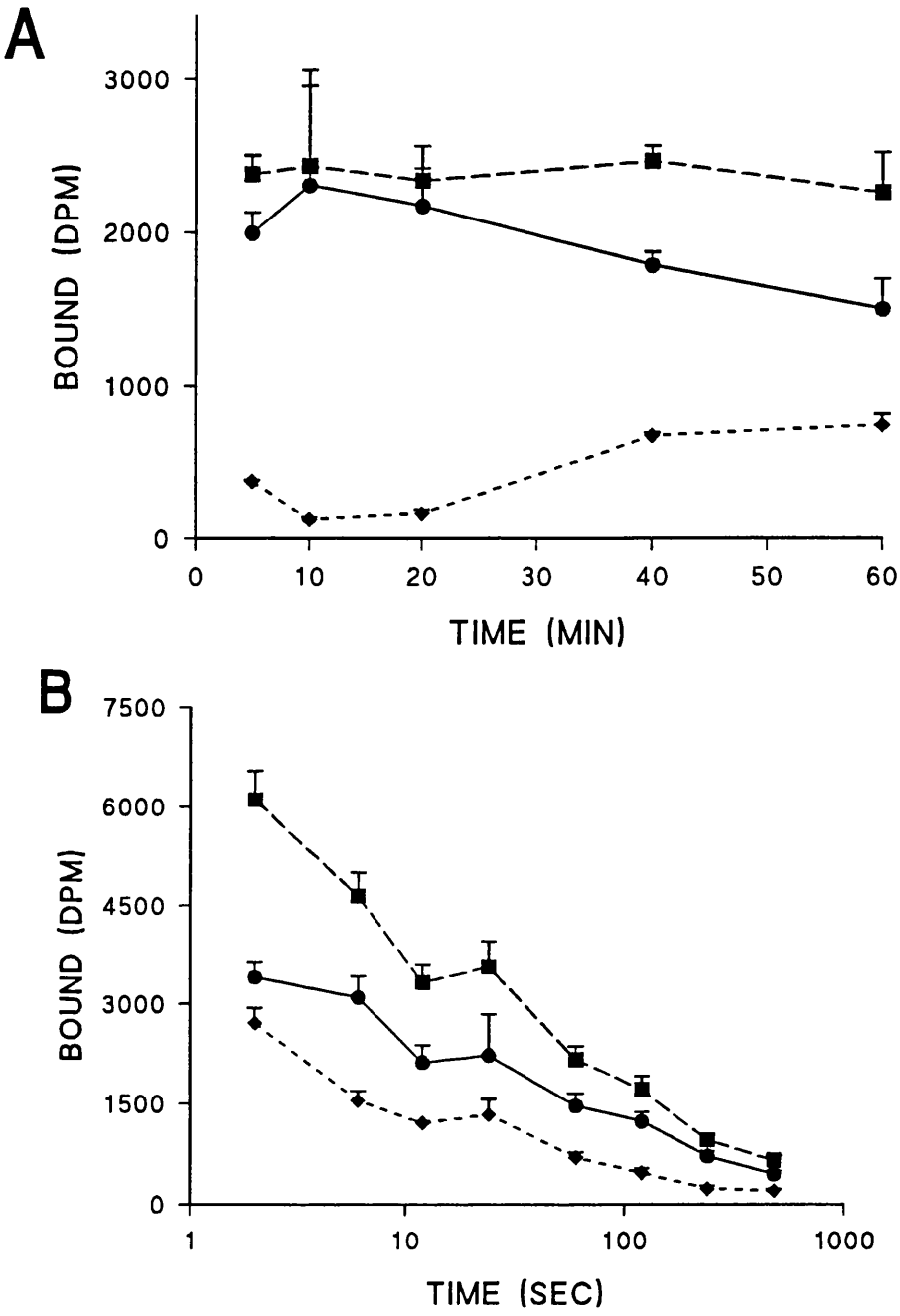

Figure 2.8: TIME DEPENDENCY AND REVERSIBILITY OF [^{3}H] GABA BINDING. Experiments performed using control rat brain sections, incubated in 50 mM Tris-HCl containing 100 μM baclofen with a final concentration of 20 nM [^{3}H] GABA. Non-specific binding was determined using 100 μM isoguvacine. Binding was determined using liquid scintillation spectrometry. Graph A shows ligand association, and graph B the washout characteristics. Values are mean $\pm$ SEM, n=3. Data points represent; mean specific binding (●), total binding (■) and non-specific binding (◆).

reached very quickly, apparently by 5 min, which is in agreement with personal communications from P. Britton (N.G. Bowery's group). The dissociation curve (Figure 2.8B) produced a $t_{1/2}$ of 31 sec. Two 25 sec washes produced 85% specific binding.

2.8.8 Autoradiography of α_1 adrenoceptors using [^{3}H] prazosin.

[^{3}H] prazosin binding was utilised to visualise total α adrenoceptors (α_{1total}), and the 1b subtype (α_{1b}), in group 2 CS animals only, using a method based on a previously published method (Zilles et al., 1991).

For both total and 1b binding, sections were preincubated for 30 min in 50 mM Tris-HCl (pH 7.4) buffer at 30°C. Incubations were performed in the presence of 0.4 nM [^{3}H] prazosin for 45 min at 30°C. To determine the 1b component, 30 nM 5-methyl-urapidil (5-MU) was also present in the incubation medium. Non-specific binding was defined using 10 μM phentolamine mesylate. Sections were then washed for 2 x 5 min in ice cold buffer (250 ml / wash). Autoradiograms were generated as described in section 2.8.10.

Optimal binding conditions were determined by association and dissociation experiments, performed on control rat sections, without 5-MU. The association curve incubation times were varied from 1 min to 120 min, and for the dissociation curve wash times varied from 1 min to 60 min. The association curve (Figure 2.9A) showed that equilibrium was reached by 40 min ($t_{1/2}$ value of 7.3 min), and the dissociation curve (Figure 2.9B) produced a $t_{1/2}$ of 10.1 min. Two 5 min washes produced 82% specific binding.

2.8.9 Autoradiography of the adenosine A_1 receptor using [^{3}H] DPCPX.

Autoradiography of the high affinity adenosine receptor was based on a modified method from previously published conditions (Parkinson and Fredholm, 1992; Lohse et al., 1987).

Sections were thawed and dried as previously described. Sections were preincubated for 30 min in 170 mM Tris-HCl pH 7.4, containing 1 mM EDTA and 2 U/ml of adenosine deaminase (ADA), to remove endogenous adenosine,

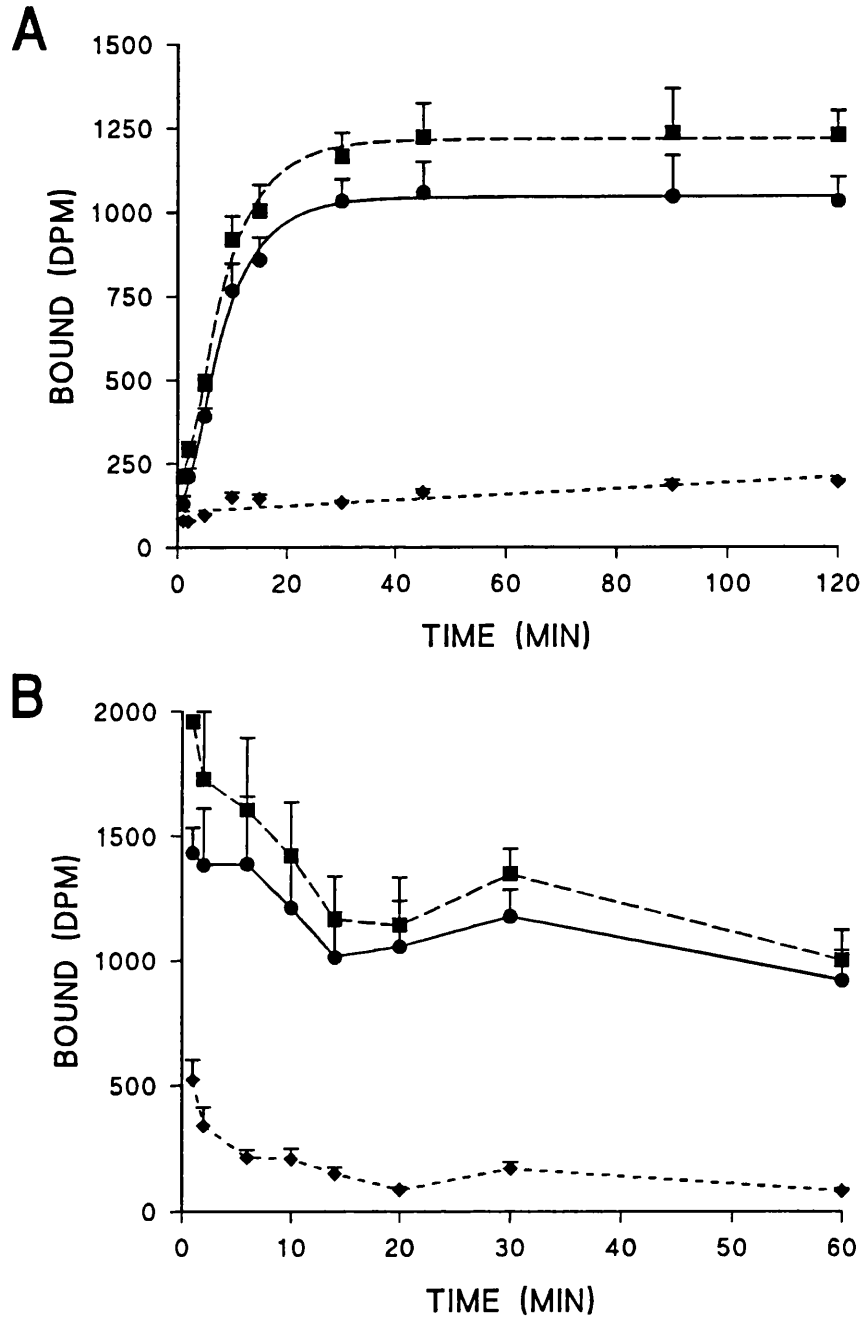

Figure 2.9: TIME DEPENDENCY AND REVERSIBILITY OF [^{3}H] PRAZOSIN BINDING. Experiments performed using control rat brain sections, incubated in 50 mM Tris-HCl with a final concentration of 0.4 nM [^{3}H] prazosin. Non-specific binding was determined using 10 μM phentolamine. Binding was determined using liquid scintillation spectrometry. Graph A shows ligand association, and graph B the washout characteristics. Values are mean $\pm$ SEM, n=3. Data points represent; mean specific binding (●), total binding (■) and non-specific binding (◆).

at 37°C. Incubations were performed in a similar buffer (without ADA) for 80 min with 2 nM [^{3}H] DPCPX in the presence of 10 μM Gpp(NH)p (Boehringer Mannheim), at 37°C. No Mg^{2+} was present in the incubation medium (see below). Non-specific binding was defined using 100 μM R-phenylisopropyladenosine (R-PIA). Following incubation, sections were washed for 2 x 5 min in ice cold buffer, dipped briefly in ice cold water and dried. Autoradiograms were generated as described in section 2.8.10.

The effect of the addition of Mg^{2+} to the incubation medium was investigated, as various reports have indicated increases (Goodman et al., 1982) or decreases (Fastbom and Fredholm, 1990) in agonist or antagonist binding with the addition of this cation. "Scratch and count" experiments were performed using control rat brain sections with and without 10 mM $CaCl_2$ in the incubation medium. Table 2.4 summarises the results obtained.

2.8.10 Autoradiogram generation.

Following incubation with a particular [^{3}H] ligand sections, together with [^{3}H] Micro-scales (Amersham International, Amersham, UK) were co-exposed to [^{3}H] Hyperfilm (Amersham International) for an appropriate time, depending upon the amount of radioactivity bound, which was assessed in all autoradiography experiments by the inclusion of several sections for "scratch and count". Based on the exposure times defined (Kuhar, 1985) and those subsequently determined from these experiments, [^{3}H] 8-OH-DPAT sections were exposed for approximately 30 days (1500 - 6000 dpm), [^{3}H] ketanserin for 40 days (1000 - 3000 dpm), [^{3}H] pirenzepine for 24 days (3500 - 4000 dpm), [^{3}H] nicotine for 65 days (400 - 1000 dpm), [^{3}H] kainate for 28 days (1500 - 3500 dpm), [^{3}H] L-689,560 for 14 days (5000 - 7000 dpm), [^{3}H] GABA for 25 days (1500 - 3000 dpm), [^{3}H] prazosin for 28 days (1000 - 3500 dpm) and [^{3}H] DPCPX for 6 days (18000 - 22000 dpm).

Films were developed using Kodak LX-24 X-Ray developer (1 part developer + 3 parts water) for 2 min, dipped briefly in stop bath (Ilford 1+40), and fixed with Kodak FX-40 X-Ray liquid fixer (1+4) for 2-3 min. Each set of films was developed with the same chemicals on the same day. Films were

Binding (DPM)	0 mM Mg^{2+}	10 mM Mg^{2+}
Total	15054 ± 1664	7014 ± 1009
Non-specific	1274 ± 214	1170 ± 134
Specific	13779 ± 1860	6165 ± 1285
% specific	91.6	83.3

Table 2.4 EFFECT OF INCLUSION OF Mg^{2+} ON [^{3}H] DPCPX BINDING. Experiments were performed using control rat brain sections which were incubated for 80 min in 170 mM Tris-HCl containing 2 nM [^{3}H] DPCPX in the presence or absence of exogenously added Mg^{2+}. Non-specific binding was defined using 100 μM R-PIA. Values are mean ± SEM, n=3.

hardened using Ilford liquid hardener, and washed thoroughly before drying in a vertical heated drying cabinet.

2.8.11 Analysis of autoradiograms.

2.8.11.1 Densitometric analysis (CS and CC).

For both CS and CC lesions, autoradiograms images were transferred to a Quantimet 570 image analyser (Leica, Cambridge, UK) using a binocular macroscope (Model M3Z; Wild Leitz, Heerburg, Switzerland), and a monochrome high resolution CCD camera. A macroscope was used in preference to a macroviewer because the light source is more constant, and the object to camera distance is less, reducing the effects of ambient light. Corrections for variance of illumination over the examination area were made using the shade correction facility of the image analyser, where a correction factor is applied to the incoming signal so that a grey image of uniform tone is observed over the whole field of view. This process was observed for each autoradiographic film before quantification. Autoradiograms were quantified using receptor autoradiography software designed for the Quantimet 570. A non-linear calibration curve was generated from [^{3}H] Micro Scale standards, hence allowing receptor binding for each ligand to be expressed as fmol/mg tissue wet weight, using tissue equivalents and specific activity of the ligand (Geary and Wooten, 1983).

To determine the receptor density in the neocortex the mode grey level within a representative area from each region in a total binding autoradiogram was measured and the specific binding determined by subtraction of binding in the same area of the non-specific autoradiogram. For each rat, 4-12 autoradiograms were examined. In CS and excitotoxin control sections, specific binding close to the midline (neocortical areas Fr1/Fr2 and HL (Zilles, 1985)), as well as more laterally (Par1/Par2) was determined on the sides ipsilateral and contralateral to the injection site, corresponding to sections from bregma 2.70 mm to -3.30 mm (mid-hippocampus) (Paxinos and Watson, 1982). In CC sections, specific binding was determined in the equivalent area contralateral to the injection site, Fr1 and HL rostrally, and more caudally in Oc2 MM, ML and L, and Oc1 M (see Introduction, section 1.1.4), corresponding to sections

from bregma -1.40 mm to -7.50 mm. Binding densities on the side ipsilateral and contralateral in CS animals were compared using paired analysis, which has the advantage that each animal is its own control. Side to side comparison in this manner was not appropriate in CC animals, as the injection affected the ipsilateral cortex, and thus comparisons were made between animals groups, and in most cases, control values were augmented with values from contralateral cortex of animals receiving intrastriatal ricin injections, which increased the n for statistical analysis.

In the case of saturation analysis the micro scales were calibrated according to dpm/mg tissue. Mode grey values were determined (and hence dpm/mg tissue) within similar representative areas (as before) from sections incubated with different concentrations of [^{3}H] ligand. Scatchard analysis of the data was performed using the EDBA binding program (Biosoft).

2.8.11.2 Two dimensional spatial analysis (ENT).

Autoradiograms were transferred to a Quantimet 570 image analyser as described in section 2.6.11.1. After experimentation, the software used to analyse the other lesion types was deemed unsuitable to make an assessment of the changes observed in the ENT animals, mainly because the area of change was very discreet, and where shrinkage of a hippocampal field had occurred, there was no equivalent area on the side contralateral to the injection site. The hippocampal area expands rapidly toward the caudal end of the brain, and thus small errors of orientation when cutting the brain lead to large side to side discrepancies in hippocampal appearance. It was therefore necessary to devise another method for localisation of receptor populations on the affected cells. To acheive this, binding length (length of labelling of hippocampal field), or in some cases, area was measured using the Quantimet. Similarly, the equivalent length or area (as appropriate) measured in the closest cresyl violet stained section was obtained. A ratio was then calculated by division of autoradiographic binding length/area by the equivalent Nissl stained measurement. Ratios calcuated for sides ipsilateral and contralateral to the lesion were then compared. Thus where binding is reduced in parallel with histological cell loss, it is possible to deduce that the receptors under study are localised upon the affected cells. The mean grey level of the hippocampal area

remaining after lesioning was also calculated, to determine whether the remaining neurones carried the same proportion of a receptor compared to those neurones on the contralateral side, and thus may be considered as an indication of the heterogeneity of receptor distributions.

2.9 Statistics.

For comparisons between groups with similar population variance (Bartlett's Box, homogeneity of variance test), parametric statistics were used; single comparisons were by the Students *t*-test or the paired Student's *t*-test and multiple comparisons by one way analysis of variance (ANOVA) followed by least significant difference test.

For variables where the population variance of groups were significantly different, non-parametric tests were employed. For multiple comparisons, the Kruskal-Wallis ANOVA was used, followed by Mann-Whitney U test for groups with a significant ANOVA result.

Correlation coefficients were calculated using Pearson's correlations. Data which did not conform to normal distribution models was correlated using Spearman's rank tests. Correlations of data subject to influence by dependent related data were correlated by multiple regression analysis.

All probabilities refer to two-tailed tests and were considered significant when $p < 0.05$.

CHAPTER 3: Radioligand binding to the NMDA receptor ionophore complex in control and Alzheimer brain.

3.1 Introduction.

Membrane preparations from diseased and control brain were subjected to minimal fractionation, to avoid the possibility that the disease state may alter the constitution of tissue fractions (White et al., 1978; Procter et al., 1991) and thus produce misleading results. Thus workers have avoided the use of P_2 fractions when performing radioligand binding (Kornhuber et al., 1988; Kornhuber et al., 1989). For these reasons, crude membrane preparations were prepared as described in section 2.3.1.

The binding of [^{3}H] MK-801 to the cation channel of the NMDA receptor- ionophore complex has been extensively described in both human and rat brain tissue (Wong et al., 1986; Foster and Wong, 1987; Mouradian et al., 1988; Hubbard et al., 1989; Procter et al., 1989), as have the effects of the co-agonist glycine upon the activation and subsequent binding of MK-801 to the complex (Wong et al., 1987; Mayer, 1991; Procter et al., 1991). Studies in Alzheimer brains have identified a functional receptor- ionophore complex, although there may be a degree of coupling impairment (see section 3.3.2 and Introduction, section 1.9.5). The aim of the present study was to determine if, given this impairment, the compound D-cycloserine (DCS) exhibited partial agonist characteristics at the glycine site of the NMDA receptor- ionophore complex in a manner consistent with those described in animal studies and cell culture (Hood et al., 1989; Henderson et al., 1990; Watson et al., 1990).

Previous analyses of [^{3}H] MK-801 binding kinetics have demonstrated a linear relationship with protein concentration. Scatchard analysis of the binding of [^{3}H] MK-801 to preparations of rat and human tissue showed that binding was compatible with a single saturable site. Hill analysis of binding in all preparations showed Hill coefficients close to unity (Procter et al., 1991). The potency of unlabelled MK-801 displacing [^{3}H] MK-801 was stereospecific, and addition of glycine in AD preparations produced predictable but reduced increases in the level of [^{3}H] MK-801 binding when compared to control tissue (Steele et al., 1989; Procter et al., 1991). These data suggest that the NMDA receptor- ionophore complex in AD is a viable target for study, provided that

the possibility of reduced coupling between the glycine modulatory site and the complex is considered. The action of 5,7-dichlorokynurenic acid (5,7-DCKA) at the glycine site of the NMDA receptor has also been fully investigated and full antagonist properties described (Baron et al., 1990).

3.2 Results

3.2.1 Preliminary investigations of DCS characteristics using conventional *post-mortem* material.

Total membranes were prepared from the frontal cortex of conventional *post-mortem* brains. The demographic features of the material is shown in Tables 3.1 and 3.2. Samples were matched for age and *post-mortem* delay.

Figure 2.1 in the methods section summarises the findings using conventional *post-mortem* material. Preliminary investigation demonstrated that maximal [^{3}H] MK-801 binding was achieved at DCS concentrations of 0.1 mM. Addition of glycine in the incubation medium stimulated [^{3}H] MK-801 binding in a dose dependent manner. Radioligand binding stimulated by higher concentrations of glycine were antagonised by DCS in a dose dependent manner. Glycine stimulation over basal binding were 123, 141 and 151 % at concentrations of 0.1, 0.3 and 0.6 μM glycine respectively.

Addition of increasing concentrations of DCS either stimulated or inhibited [^{3}H] MK-801 binding, depending upon the concentration of exogenously added glycine present, resulting in mean [^{3}H] MK-801 binding of 242 $\pm$ 3 fmol/mg protein at the highest (0.1 mM) DCS concentrations. Variation in binding at 0.1 mM DCS concentrations was less than 4 %, indicating that this concentration of DCS was effective in displacing all glycine binding and normalising the binding to the maximum achievable with DCS alone. Thus the preliminary findings in this investigation indicated that AD brain is a suitable material for the partial agonist characteristics of DCS to be observed.

Case	Sex	Diagnosis	Age (y)	PM delay (h)	Agonal State	Hemisphere
1	M	NC	86	24	Sudden	Right
2	M	NC	85	48	Protracted	Right
3	F	NC	84	48	Sudden	Right

Table 3.1: SUMMARY OF THE PARAMETERS OF THREE NORMAL CONTROL (NC) BRAINS USED IN PRELIMINARY DCS STUDY. Confirmation of the absence of AD hallmarks was made by histopathological examination. All brains had conventional *post-mortem* delay.

Case	Sex	Diagnosis	Age (y)	PM delay (h)	Terminal Coma (h)	Drug Treatment
AP2	F	AD	83	3	0	Free
AP3	F	AD	58	2	72	Treated
AP8	F	AD	80	2	0	Treated
AP9	F	AD	78	1.8	336	Treated
AP12	F	AD	67	3.5	?	?
AP13	F	AD	78	2	24	Free
AP14	F	AD	64	2.5	12	Treated
AP15	F	AD	65	3	?	Free
AP18	F	AD	62	3.5	?	?
AP21	F	AD	88	1.5	12	Free
AP26	F	AD	73	2	10	?
SB34	M	NC	67	1	0	Free
SB37	F	NC	68	1	0	Free

Table 3.2: SUMMARY OF PARAMETERS OF RAPID *POST-MORTEM* BRAIN MATERIAL USED FOR INVESTIGATION OF DCS CHARACTERISTICS. All brains except SB34 and SB37 met DSM-III criteria for dementia in life and diagnoses were confirmed by histopathological examination. NC; normal control; free from histopathological hallmarks of AD when examined *post-mortem*.

3.2.2 [^{3}H] MK-801 binding in prompt *post-mortem* brain tissue.

3.2.2.1 Glycine and DCS dose- response curves.

The effect of glycine and DCS on [^{3}H] MK-801 binding is shown in Figure 3.1. Linear transformation showed straight lines with correlation coefficients of 0.99 and 0.98 for DCS (Figure 3.2A) and glycine (Figure 3.2B), respectively. L-cycloserine, at the same concentrations, did not cause any stimulation. DCS, in the absence of exogenously added glycine had agonist properties, and stimulated [^{3}H] MK-801 binding to a maximum of 64 $\pm$ 3 % of the maximal stimulation produced by glycine alone. At concentrations of DCS greater than 100 μM, binding of [^{3}H] MK-801 decreased, and was comparable with that in the presence of L-cycloserine.

The paucity of control tissue meant that although normal controls were included in the dose response experiments, statistical analysis could not be performed on the resulting data. However, glycine and DCS stimulation of [^{3}H] MK-801 binding in the AD samples were considerable smaller than those observed in control tissue (glycine maximal stimulation 66 % of control value, DCS maximal stimulation 75 % of control value). This finding is in agreement with previous findings that coupling of glycine site of the NMDA receptor-ionophore complex may be functionally impaired (Procter et al., 1989; Procter et al., 1991).

3.2.2.2 Partial agonist characteristics of DCS in AD brain.

Figure 3.3 shows that in the presence of the highest concentration of glycine (100 μM), DCS had a significant antagonist action on the glycine stimulated binding of [^{3}H] MK-801. Statistical significance of this effect was achieved at DCS concentrations of 1 μM and above ($p < 0.05$, Student's paired *t*- test). Addition of increasing concentrations of the L isomer had no significant effect on the stimulation produced by this concentration of glycine alone. At lower concentrations of glycine, the binding of [^{3}H] MK-801 was not reduced. Binding of [^{3}H] MK-801 at the highest concentration of DCS was more variable (43 to 64 % of maximal glycine stimulation) than that observed using conventional *post-mortem* tissue. However, the results do conform to a

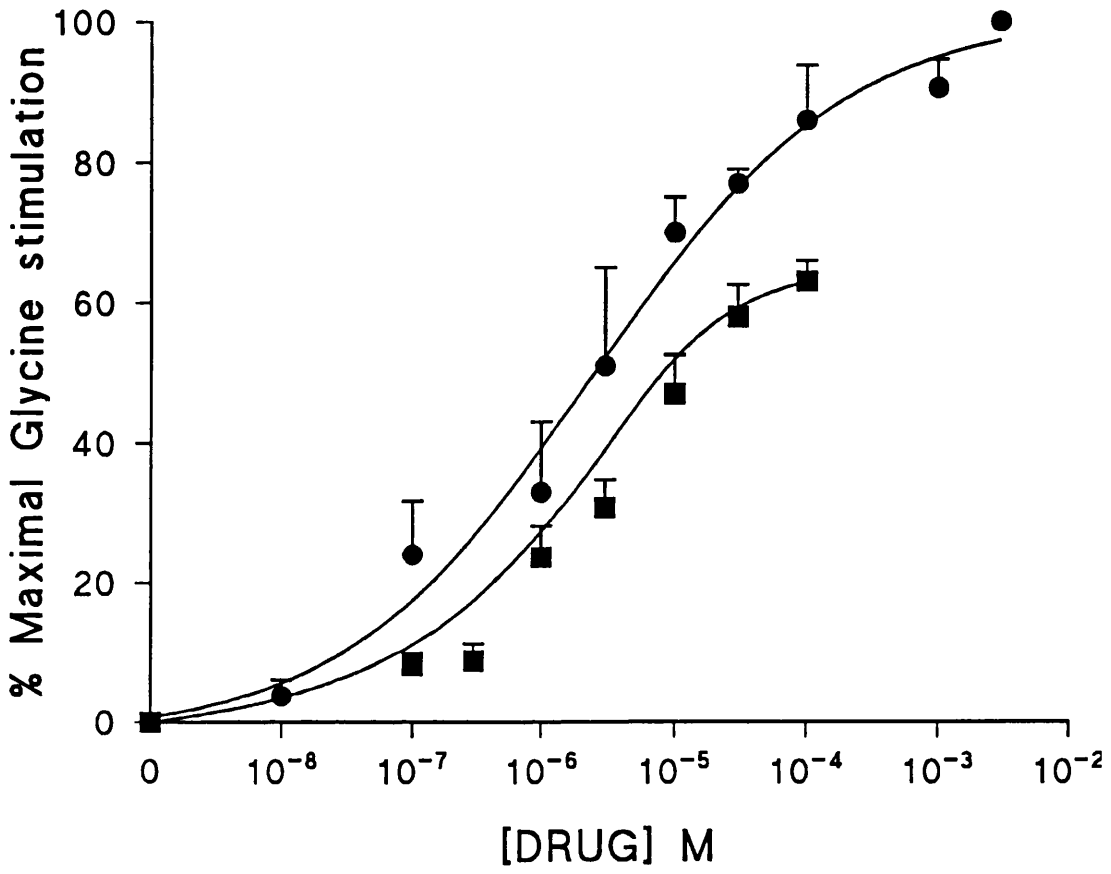

Figure 3.1: DOSE RESPONSE CURVES FOR DCS AND GLYCINE DEPENDENT [^{3}H] MK-801 BINDING. Stimulation of specific binding of 5 nM [^{3}H] MK-801 by glycine (●, n=4) and DCS (■, n=9) in inferior parietal cortex of rapid *post-mortem* AD brain.
Maximal response to DCS is 64 ± 3 % of that of maximal glycine response. Values are mean ± SEM.

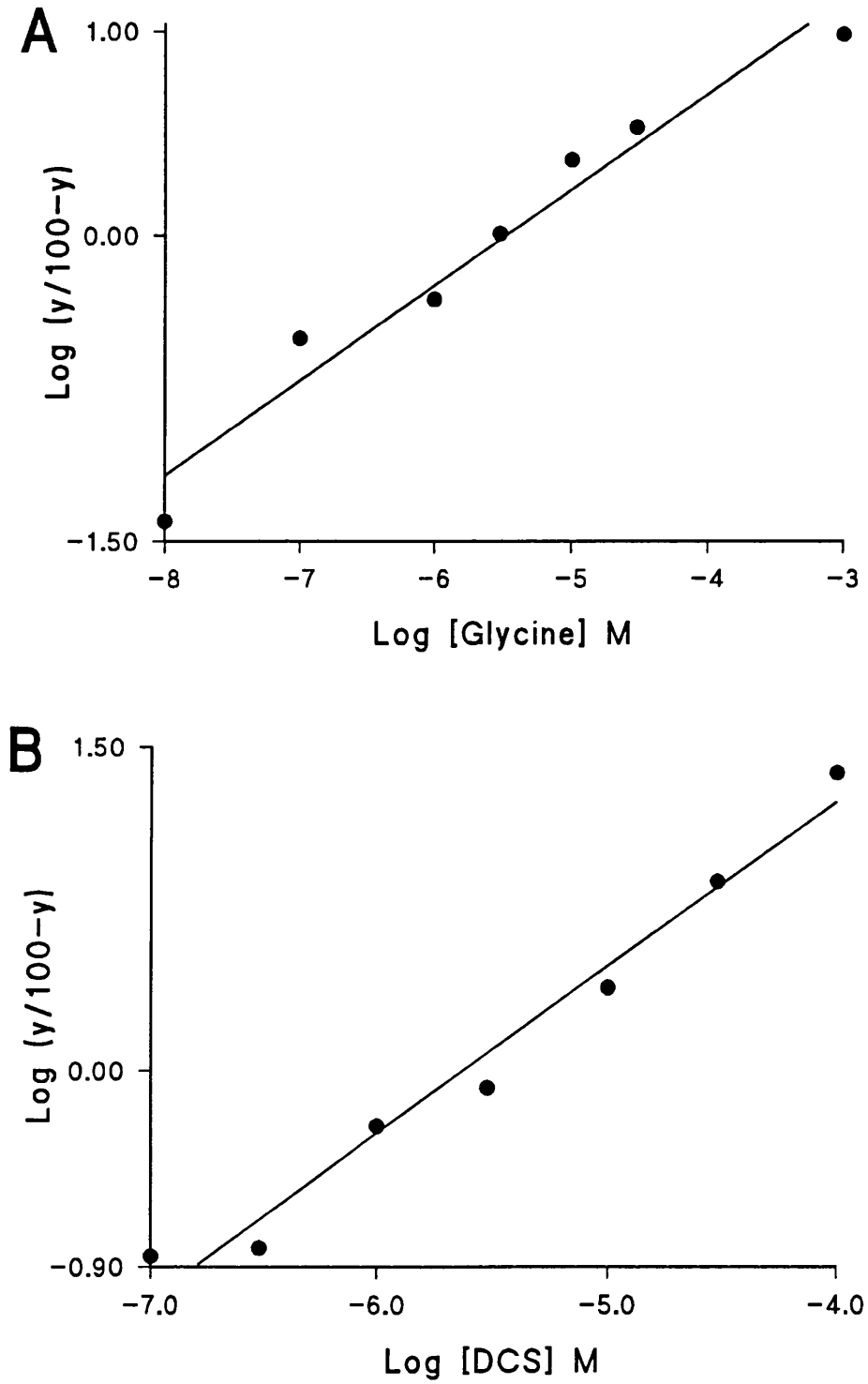

Figure 3.2: LINEAR TRANSFORMATION OF GLYCINE (A) AND DCS (B) DEPENDENT [^{3}H] MK-801 BINDING. Transformations were performed on data presented in Figure 3.1, obtained from inferior parietal samples of rapid *post-mortem* material, for glycine stimulation (upper panel, n=4) and DCS stimulation (lower panel, n=9). Correlation coefficients of 0.99 and 0.98 were determined for glycine and DCS dose response curves respectively. Hill transformation was not applicable to this binding paradigm as experiments were not performed at equilibrium. However, correlation coefficients not significantly different from unity are indicitive of single site binding kinetics.

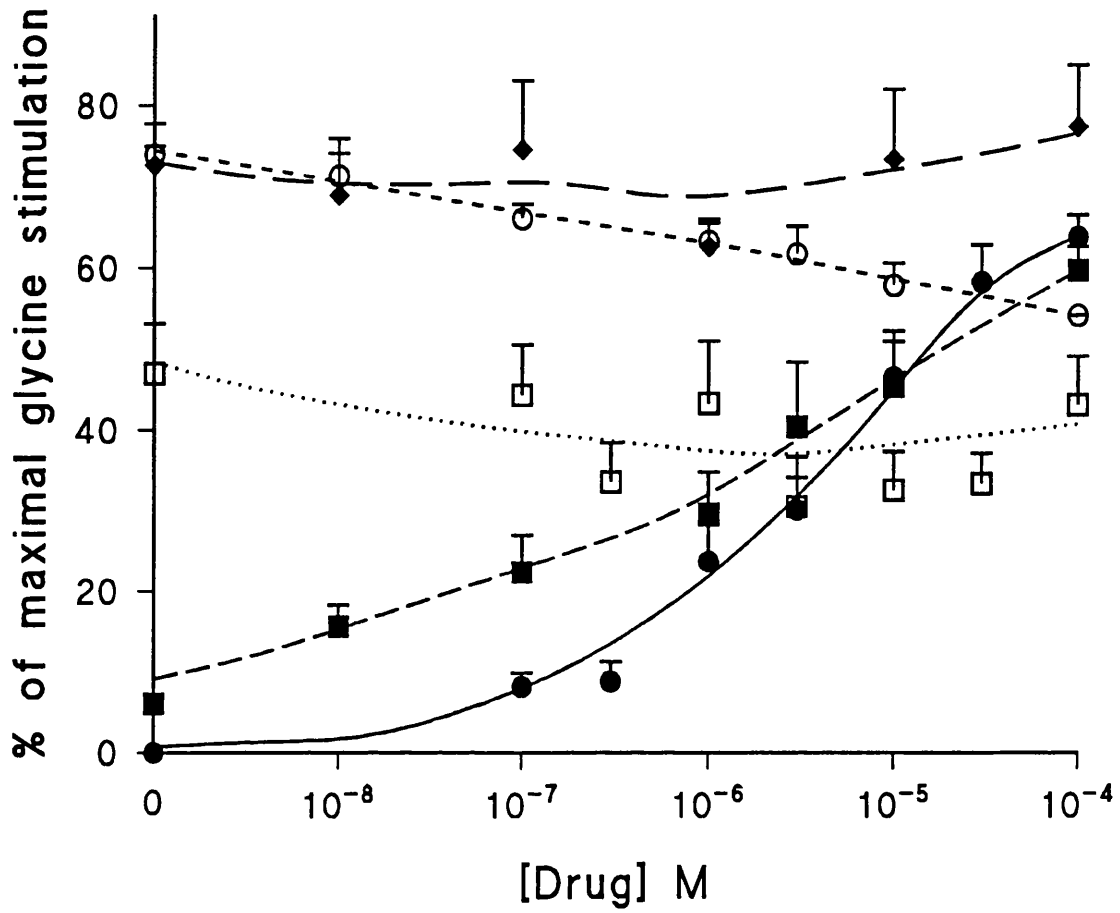

Figure 3.3: EFFECTS OF CYCLOSERINE ON THE BINDING OF [^{3}H] MK-801 IN THE PRESENCE OF VARIOUS CONCENTRATIONS OF GLYCINE. The antagonist property of DCS increased in the presence of increasing glycine concentrations (●, no glycine, n=9; ■, 0.3 μM, n=4; □, 0.6 μM, n=9; O, 0.1 mM, n=7).
At the highest concentration of glycine, significant antagonist property was observed in all subjects at the 4 highest concentrations of DCS ($p < 0.05$ at 3 and 6μM DCS, $p < 0.01$ at 10 and 100 μM DCS, Student's paired *t*-test significantly different from 0.1 mM glycine signal). L-cycloserine with 0.1 mM glycine had no antagonist effect at any concentration (♦, n=3).

pattern consistent with DCS having partial agonist characteristics at the glycine site of the NMDA receptor- ionophore complex in these tissue samples.

The results are qualitatively consistent to those described in rodent and oocyte preparations (Hood et al., 1989; Henderson et al., 1990; Watson et al., 1990), and clearly demonstrate that DCS has a modulatory property at the glycine site. Also consistent with previous findings and with the dose- response profile of DCS improving learning and memory in animals (Monahan et al., 1989; Manallack et al., 1990) and humans (Wesnes et al., 1991) is the finding that at higher concentrations of DCS, the stimulation of [^{3}H] MK-801 binding is dramatically reduced, which suggest that therapeutically effective doses of DCS may lie within a narrow range. The characteristics of specific binding of 5 nM [^{3}H] MK-801 in AD brain are summarised in Table 3.3.

3.2.2.3 Action of 5,7-dichlorokynurenic acid on [^{3}H] MK-801 binding.

5,7-DCKA is one of the most potent excitatory amino acid receptor antagonists, binding to the strychnine insensitive glycine site of the NMDA receptor- ionophore complex (Baron et al., 1990). The action of this compound was studied in four of the short *post-mortem* delay AD brains. In three of the four brains, basal binding could be reduced to 41, 42 and 54 % of that observed with no additions of glycine. This suggests that under basal conditions, in this well washed membrane preparation, the receptor complex is subject to a positive modulatory influence by endogenous compound(s), so the apparent EC_{50} values in Table 3.3 may be somewhat higher than the true values.

The action of 5,7-DCKA was not studied in the conventional *post-mortem* tissue, but it was noted that this material was more sensitive to glycine stimulation, and that lower concentrations of glycine were antagonised by DCS. This indicates that the level of endogenous ligand for the glycine site of the receptor complex may be higher in the rapid *post-mortem* tissue, possibly due to enhanced metabolic viability of the tissue, which produced endogenous ligand during the experimental procedures.

Basal Binding (fmol/mg protein)		104 ± 37 (8)
Maximal response (fmol/mg protein)		
	DCS (0.1 mM)	176 ± 26 (9)*
	Glycine (1 mM)	213 ± 30 (4)*
EC_{50} (μM)		
	DCS	3.84 ± 2.78 (7)
	Glycine	4.41 ± 3.97 (4)

Table 3.3: CHARACTERISTICS OF SPECIFIC BINDING OF 5 nM [^{3}H] MK-801 IN AD BRAIN.
* Significantly different from basal binding (ANOVA, $p < 0.001$; LSD, $p < 0.01$). Values are mean ± SEM.

3.2.2.4 Possible confounding factors affecting [^{3}H] MK-801 binding- effects of age, coma time and post-mortem delay.

Rapid *post-mortem* tissue samples in this study were matched for age, gender and *post-mortem* delay. They were not matched for agonal state, since rapid *post-mortem* delay tissue is rare.

Drug treatment had no significant effect on the degree of glycine or DCS stimulation of [^{3}H] MK-801 binding in patients where data was available (Table 3.4, Student's *t*-test). Correlations of age, coma time, and *post-mortem* delay against basal [^{3}H] MK-801 binding, degree of maximal stimulation of binding by DCS, and stimulation at one concentration of glycine (0.6 μM) were made. Results are summarised in Table 3.5, and outlined below.

No significant correlation of age against any variable was found. Distribution of *post-mortem* delay in these samples was normal, and closely matched (range 1.5 - 3.5 h) but a positive correlation between DCS stimulation and *post-mortem* delay was found for both unranked and ranked data ($p=0.018$ and $p=0.023$ respectively).

No correlation was found between duration of storage time at -70°C and any variable examined. The range of storage time were between 15 and 72 months (data not shown).

Duration of terminal coma did have an effect on the binding of [^{3}H] MK-801 in AD tissue. Terminal coma times were not normally distributed, so the data was ranked before performing Spearman's correlations and multiple regression analysis. A negative relationship was found between coma time and basal binding of [^{3}H] MK-801 ($r_s=-0.731$, $p=0.039$, Spearman's rank correlation), which may reflect endogenous ligand production during the assay. As data for maximal DCS stimulation and glycine stimulation were both calculated with respect to basal binding, Spearman's rank correlations were not appropriate for this data given the correlation above. Therefore, multiple regression analysis was performed to provide relationships independent of basal binding. No correlations were observed between duration of terminal coma and maximal DCS stimulation of [^{3}H] MK-801 binding. A negative correlation ($p=0.026$) was found between coma time and degree of glycine

stimulated (at 0.6 μM glycine concentration) [^{3}H] MK-801 binding. This is in agreement with previous findings (Procter et al., 1991).

	Maximal specific binding (fmol/mg protein)	
	DCS	**Glycine**
Receiving Drugs	64.3 ± 4.5 (n=3)	100.5 (n=2)
Drug Free	71.0 ± 14.4 (n=3)	108.7 (n=2)

Table 3.4: DRUG EFFECTS ON THE SPECIFIC BINDING OF [^{3}H] MK-801 IN AD BRAIN. Experiments were performed using total membrane preparations incubated in the presence of 5 nM [^{3}H] MK-801.
No significant effects on maximal DCS stimulated binding were observed (Student's *t*-test). Significance of maximal glycine stimulated binding could not be tested (paucity of data). Values are mean ± SEM.

Correlations	Age	*post-mortem* delay	Storage time at -70°C	Duration of terminal coma
Basal binding	-0.675 (11) p=0.844	0.582 (11) p=0.061	0.251 (11) p=0.525	(a) -0.731 (8) **p=0.039**
Maximal DCS stimulation	0.264 (9) p=0.499	-0.757 (9) **p=0.018**	-0.066 (9) p=0.864	(b) 0.102 (9) p=0.823
Glycine stimulation	0.474 (10) p=0.167	-0.226 (10) p=0.531	0.300 (10) p=0.400	(b) -1.218 (10) **p=0.026**
Correlation type	Unranked, Pearson's	Unranked, Pearson's	Unranked, Pearson's	(a) Ranked, Spearman's (b) Ranked, multiple regression analysis

Table 3.5: CORRELATIONS BETWEEN ON SPECIFIC [^{3}H] MK-801 BINDING AND *POST-MORTEM,* STORAGE, AND TERMINAL COMA TIMES. Experiments were performed using total membrane preparations, incubated in the presence of 5 nM [^{3}H] MK-801. Values in parentheses are n's for each correlation analysis. Maximal DCS stimulation in the presence of 0.1 mM DCS. Glycine stimulations in the presence of 0.6 μM glycine. Bold values where $p < 0.05$.

3.3 Discussion.

3.3.1 The NMDA receptor- ionophore complex in Alzheimer's Disease.

Studies of the NMDA receptor- ionophore complex in AD brain have employed both [^{3}H] MK-801 and a phencyclidine derivative, [^{3}H] N-[1-(2-thienyl) cyclohexyl] piperidine ([^{3}H] TCP) as markers for the cation channel of the complex. Whilst both compounds have been characterised as non- competitive antagonists at the channel of the complex (Fagg, 1987; Foster and Wong, 1987; Stirling et al., 1989), differential properties of the two ligands have been noted in AD brain (Steele et al., 1991). In assessing the putative changes in AD, it must be borne in mind that the NMDA receptor- ionophore complex is subject to regulation by several different compounds, many of which affect activation of the cation channel and subsequent binding of the above ligands.

Given these *caveats*, glutamate receptor abnormalities have been reported in patients with AD, especially in outer cortical layers and in CA1 and CA2 regions of the hippocampus (Greenamyre et al., 1985b; Maragos et al., 1987a; Maragos et al., 1987b). The changes reported in levels of the NMDA receptor are, however, varied, with some affecting only a subgroup of AD patients (Monaghan et al., 1987), and others reporting no change (Geddes et al., 1986). Previous reports of [^{3}H] MK-801 binding on the rapid autopsy material used in the present study concluded that under both basal and glutamate stimulated conditions there were no significant differences in [^{3}H] MK-801 binding between control and AD samples. This data suggests that levels of the NMDA receptor- ionophore complex in these samples, and possibly in AD tissue generally, are sufficient to perform a feasible study of the glycine modulatory site of the receptor.

3.3.2 The glycine site of the NMDA receptor in AD brain.

There is evidence to suggest that the glycine site of the NMDA receptor-ionophore complex is selectively altered in Alzheimer's Disease. Procter et al. (1989) observed significantly reduced [^{3}H] MK-801 binding to the frontal cortex of patients with AD under maximally stimulated conditions, a feature

not observed using glutamate alone, and thus attributable to reduced glycine stimulation. In preparations of semi-purified membranes from frontal cortex, a significant reduction in B_{max} was found for [^{3}H] glycine binding in AD tissue compared with control (Procter et al., 1991). Studies using the novel glycine site antagonist [^{3}H] L-689,560 revealed significant reductions in binding in the frontal cortex, and in parietal cortex at lower ligand concentrations (Pangalos, 1992).

Reductions in markers for the glycine site of the NMDA receptor were most consistently found in frontal cortex. Variation in reductions observed in temporal and parietal lobes may be affected by atrophy and thus results expressed as binding per milligram protein are subject to variability because of loss of structures organised in a columnar manner (Pearson et al., 1985). However, in proposing an effective rationale for treatment of glutamatergic hypoactivity using a partial agonist such as DCS, it is important to study areas which are severely affected in the disease, including inferior parietal areas employed in the present study.

3.3.3 The action of DCS in AD brain, and possible confounding factors.

DCS has been characterised as a partial agonist in many paradigms (Hood et al., 1989; Watson et al., 1990) and its behavioural actions in rat and human studies implicate the compound as a cognitive enhancer (Monahan et al., 1989; Wesnes et al., 1991; Thompson et al., 1992). The results obtained in this study are qualitatively similar to those described in rodent and oocyte preparations, and clearly demonstrate that DCS is a partial agonist in AD affected tissue. The ability of DCS to facilitate activation of the NMDA receptor- ionophore complex in living AD brain is dependent upon physiological levels of endogenous ligand at the glycine site of the receptor. Although this is difficult to assess in human brain, studies in rat brain suggest that the modulatory site is not saturated with endogenous ligand (Baron et al., 1990; Thiels et al., 1992). Based on the action of 5,7-DCKA in this study, DCS may have a greater agonist effect *in-vivo*, as levels of endogenous glycine in the present study appear to be anomalously high. The most probable explanation

for this is that prompt *post-mortem* tissue remains metabolically active after membrane preparation, and glycine is produced during the incubation which produces artificially high basal levels of [^{3}H] MK-801 binding.

Patients immediate pre-terminal state seemed to affect both basal and glycine stimulated binding. This is in agreement with previous studies (Procter et al., 1989). It is possible that the duration of terminal coma affected the ability of the tissue to produce glycine, or that increased coma time leads to loss of coupling between the glycine site and the remainder of the receptor, although the duration of terminal coma had no affect upon the degree of stimulation of [^{3}H] MK-801 binding by DCS. Reduced sensitivity to glycine appears to reduce the maximal receptor activation, without producing a parallel shift in any dose- response relationship, so it is not unexpected that no correlation was found between terminal coma and degree of maximal DCS stimulation, a feature dependent on the partial agonist characteristic of DCS.

Correlations between *post-mortem* delay and maximal DCS stimulation of [^{3}H] MK-801 binding are less relevant to this study, as the range of *post-mortem* delay is small. However, this finding is in agreement with previously described characteristics (Procter et al., 1989).

The findings of the present and previous studies on the action of DCS at the glycine modulatory site of the NMDA receptor- ionophore complex are in good agreement. It is apparent that in AD, the agonist site and cation channel of the NMDA receptor complex are unaltered, but the apparent number of glycine sites are reduced. It is possible that subtypes of the NMDA receptor complex may exist that are differentially sensitive to glycine, and that in AD a subtype of the complex with a greater number of glycine sites is located on neuronal structures that are selectively affected by the disease process. It therefore seems that the glycine site of the NMDA receptor- ionophore complex is a particularly pertinent site for therapy, and that the partial agonist characteristics of DCS are preserved in diseased brain.

CHAPTER 4: Histological investigation of a subpopulation of hippocampal pyramidal neurones following unilateral entorhinal cortex injections of neurotoxic lectins.

4.1 Introduction.

The major cell type of the hippocampus is the pyramidal neurone, which accounts for some 70% of all neurones. Early degeneration in the CA1 area of the hippocampus in AD is difficult to selectively mimic in animal models of the disease, as experiments which cause ischaemia tend to induce a non-selective loss of cells in this area (Pulsinelli et al., 1982). The present study has investigated the use of volkensin, a retrogradely transported suicide transport agent (see Introduction, section 1.10.2) to produce loss of a subpopulation of hippocampal pyramidal neurones. The target of the injection was the pre-alpha (layer II islands of pyramidal cells; see Introduction, section 1.1.3) cells of the entorhinal cortex, though technical difficulties meant that in most cases posterior hippocampal structures were also involved (see methods, section 2.6.1). With this novel approach, it may be possible to investigate biochemical sequelae following loss of anatomically defined subpopulations of neurones which project to the entorhinal cortex, another early target for degeneration in AD (Braak and Braak, 1991), and to compare and contrast the biochemical properties of these pyramidal neurones with other, neocortical, pyramidal neurones. The immediate objective therefore, was to determine whether unilateral injection of volkensin into the entorhinal cortex induced selective loss of hippocampal pyramidal cells, and to determine which pyramidal neurones were affected.

4.2 Results.

4.2.1 Determination of volkensin dosage.

Previous studies where volkensin has been used to destroy pyramidal neurones projecting from cortical lamina V to the striatum have used doses of 2 and 6 ng of volkensin (Pangalos et al., 1991b). These doses were determined by quantitative and qualitative study of the effects of volkensin injection, and these experiments were used as a guide to determine optimal dosage in the

paradigm described here. Section 2.6.1 describes preliminary results obtained using various doses of volkensin.

Initially lesions of the entorhinal cortex were attempted using volkensin doses ranging from 2 to 6 ng, in a vehicle volume ranging from 0.5 to 4 μl, at either 2 or 4 sites. Qualitative investigation of small numbers (typically n=2) of animals receiving combinations of the above parameters were made after a 28 day survival period. The optimal target for these investigations was predetermined to be a discrete lesion, centred on the entorhinal cortex, with minimal spread of damage to the surrounding structures. Unsurprisingly, larger vehicle volumes produced more generalised damage, and initial conclusions were that the smallest volume possible was most appropriate. At doses of greater than 2 ng volkensin, damage extended to areas beyond the boundaries of the entorhinal/ transentorhinal cortex, posterior sections of the hippocampus, and pre- and para-subiculum, and often involved brainstem structures and piriform cortex. 1 ng volkensin produced local damage but no apparent changes in areas distant to the injection site. A dose of 2 ng volkensin, in a volume of 0.4 μl at two sites (0.2 μl per site) produced local damage with limited spread, with qualitative morphological changes at areas distant to the injection site. It was not possible to determine an injection dose and volume which produced exclusive entorhinal damage without limited spread to surrounding structures, and in most cases there was a component of posterior hippocampal involvement.

4.2.2 Determination of survival time following volkensin injection.

Post operative survival times following volkensin injection of 7, 14, 21 and 28 days were used to determine the optimal post operative period for histological and subsequent autoradiographic analysis. At a survival time of 7 days (n=6) there were no morphological changes in pyramidal neurones or overall shape of the hippocampus.

At survival times greater than 7 days, evidence of cell degeneration at anterior hippocampal sites were observed, along with enlargement of the lateral ventricle on the lesioned side at the level of the anterior hippocampus. Subsequent histological investigation of the anterior hippocampus confirmed these changes; however, animals left for 28 days post operatively displayed

inconsistent patterns of cell loss, with increasing involvement of the posterior hippocampus and collapse of cortical structures proximal to the injection site. As the aim of these studies was to produce animals consistently deficient in a subpopulation of hippocampal pyramidal neurones, animals with a post operative time of 14 (n=5) and 21 (n=6) days were used for the histological and autoradiographic studies. Animals injected with 10 ng ricin (n=4 for both survival times) and left for the same time post operatively were used as controls.

4.2.3 Cell loss as a result of spread of volkensin and ricin directly from the injection site.

Volkensin and ricin injections were centred on the pre-alpha neurones of the entorhinal cortex. In all cases in volkensin and ricin injected animals, this area was markedly affected, with all but three animals having an estimated destruction of three quarters or more of these neurones. The estimated proportion of the destruction of these cells in the other two volkensin injected animals were one third and one half, and one third in one ricin injected animal.

In all volkensin injected animals, a substantial proportion of the entorhinal cortex was destroyed, with direct extension of the lesion more dorsally and rostrally (Figure 4.1). All animals displayed evidence of destruction of ventral subicular and dorsal endopiriform structures, with spread dorso-rostrally into temporal cortex area 3 (see Introduction, Figure 1.1 and Methods, Figure 2.2). Of the 11 animals injected with volkensin, 2 also had substantial involvement of temporal cortex area 2, with 1 of these animals also displaying slight involvement of posteroventral occipital structures (area 2L, see Figure 2.2). The parasubicular area was involved in some animals, with spread into the subiculum in only the most severely affected animals, and spread of the toxin rostrally involved the amygdalopiriform transition and perirhinal cortex in all but one animal. Slight (2 animals) to moderate (2 animals) involvement of the posterior piriform cortex was evident in some cases. More medially, areas of the amygdaloid nuclei were involved in the lesion- the posteromedial amygdalohippocampal area is closely apposed to the

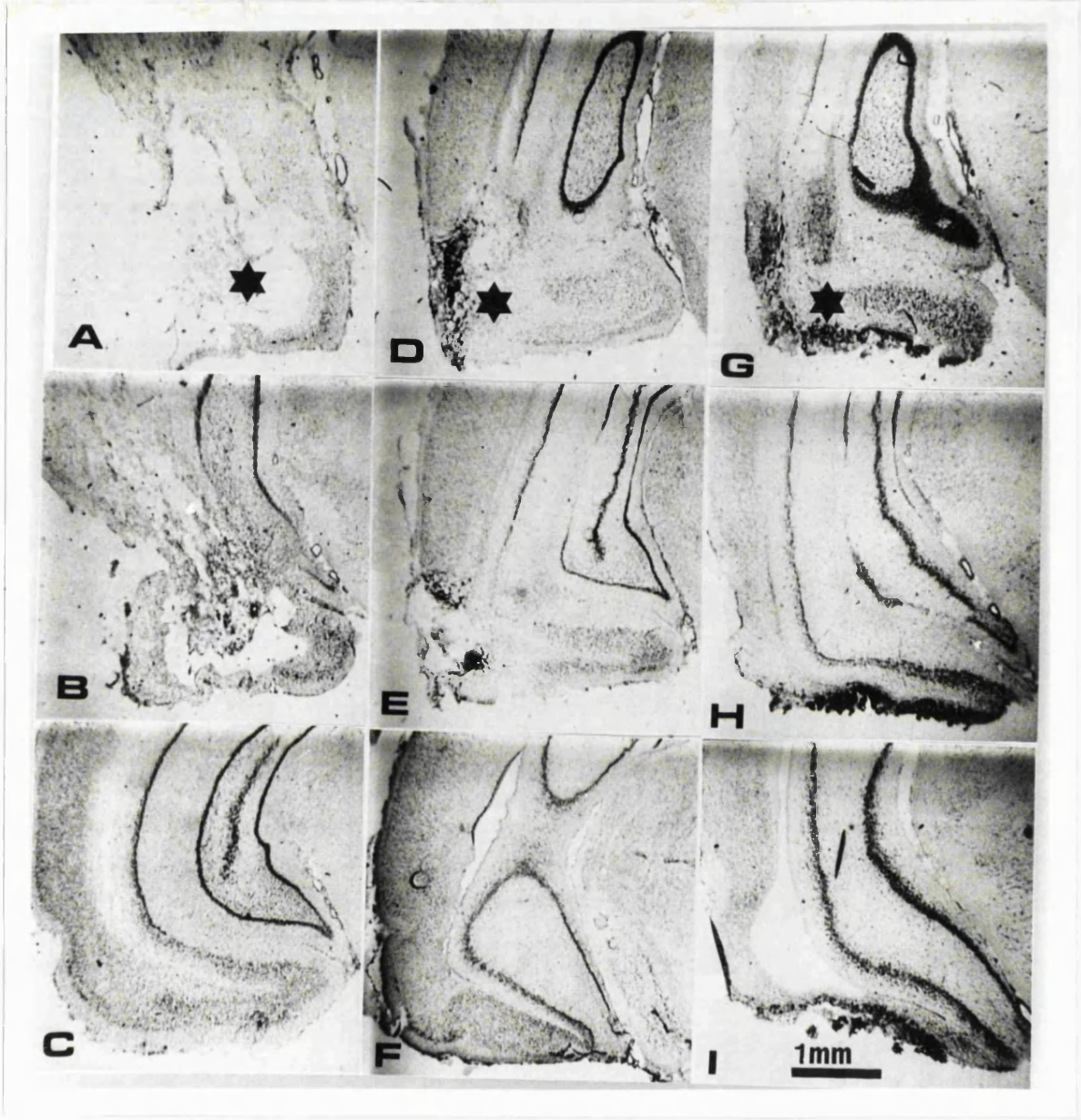

Figure 4.1: PHOTOMICROGRAPHS OF APPEARANCE OF ENTORHINAL CORTEX AFTER INJECTION OF 2 ng VOLKENSIN OR 10 ng RICIN, AT DIFFERENT ROSTRO-CAUDAL LEVELS. Two injections of 0.2 μl, each containing 1 ng volkensin or 5 ng ricin were made unilaterally, centering on the left entorhinal cortex. Extent of damage was variable between animals. A (caudal) - C (rostral): Largest lesion observed in any volkensin injected animal. D - F: Smallest lesion observed in any volkensin injected animal. G - I: Representative appearance following injection of 10 ng ricin. * target and stereotaxic centre of lesion.
Sections counterstained with cresyl violet. Scale bar 1.0 mm.

entorhinal cortex, as are the posteromedial cortical amygdala nuclei. Both of these regions were involved in all animals. The basolateral posterior amygdaloid nucleus was involved in 3 animals. Moving dorso-medially into the posterior hippocampus, area CA1 is closest to the entorhinal cortex, and the lower third of CA1 showed varying levels of disruption in all animals. CA2 was affected in 5 animals, but CA3 was only mildly affected in 1 animal. The dentate gyrus and posterior dorsal CA3 regions were not directly affected in any animal. In no animal examined was there any evidence of direct spread to structures underlying or in the vicinity of the anterior hippocampus.

Injection of 10 ng ricin caused extensive necrosis in the entorhinal cortex (Figure 4.1), with approximately the same area of spread as volkensin injections. Rostrally, the extent of direct cell damage did not extend beyond the perirhinal area in any animal. Temporal cortex area 3 was involved in most animals, with spread into area 2 in only 2 animals. Posterior ventral CA1 was affected in all animals, but CA2 was affected in only 4 animals. CA3 and the dentate gyrus were preserved in all animals.

4.2.4 Quantification of hippocampal morphological changes after volkensin and ricin injections.

Qualitatively, alterations of the appearance of the anterior portion of the hippocampus was clearly visible in animals injected with 2 ng volkensin, at postoperative intervals of 14 and 21 days. No changes were apparent in animals injected with ricin. Hippocampi (and overall brain size) of 14 day animals were dramatically smaller than those of 21 day animals (see below, but for example ipsilateral CA1; 4.13 and 7.12 mm^2 in area, 14 and 21 day animals respectively), which was wholly attributable to the different concentrations of sucrose used for the perfusion of the two animal groups. Two apparent effects on the appearance of the anterior hippocampus ipsilateral to the injection were observed- thinning of the CA3 area (Figure 4.2A) with varying degrees of collapse of the surrounding structures or substantial topographic cell loss, with a resultant gap in the CA3 area (Figure 4.2B). In all cases there was substantial ventricular enlargement. Histologically, the appearance of the affected cells was rather shrunken, with obvious

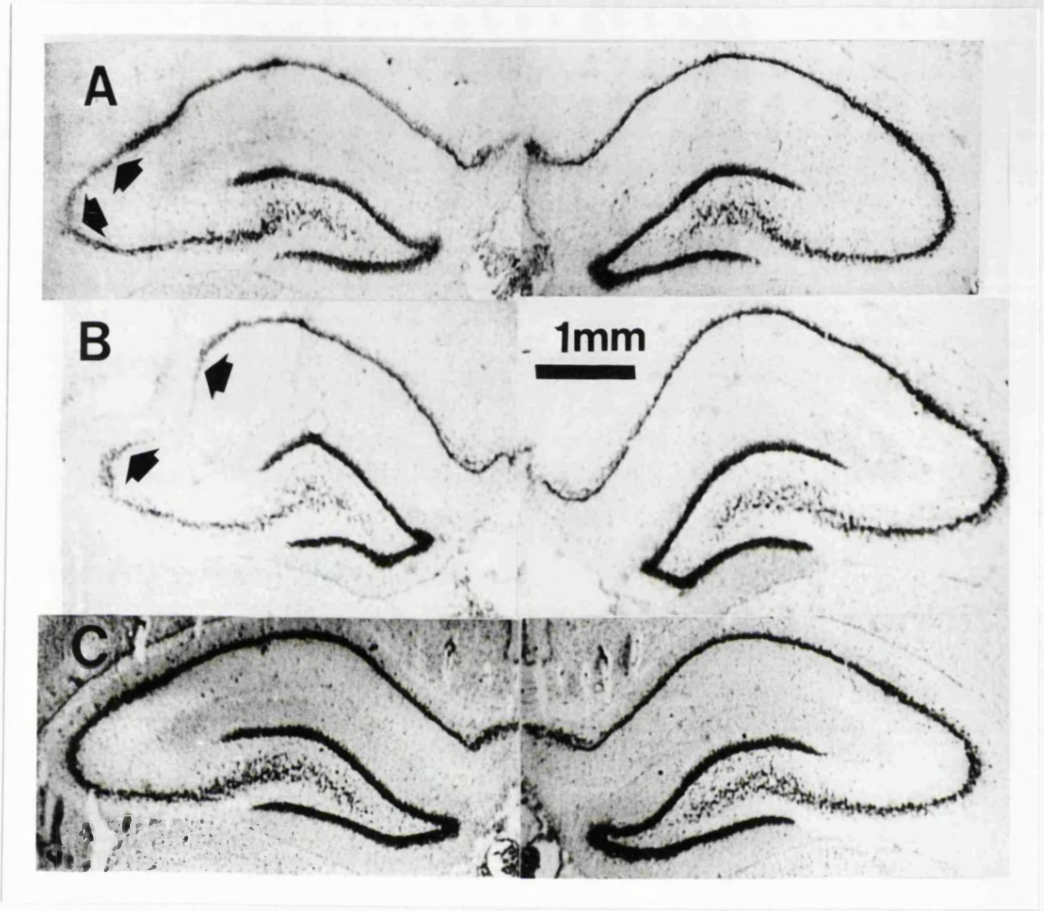

Figure 4.2: PHOTOMICROGRAPHS OF APPEARANCE OF ANTERIOR HIPPOCAMPI IN VOLKENSIN INJECTED AND CONTROL ANIMALS. Following entorhinal injection of 2 ng volkensin into the left entorhinal cortex, two effects were observed in the ipsilateral anterior hippocampal CA3 field. A: Thinning of the cell layer with discrete areas of cell loss, or B: substantial topographic cell loss with subsequent collapse of the surrounding structures. Arrows indicate margins of morphological changes. Both animals had a 21 day survival period following surgery. The appearance of a control hippocampus is shown in C.
Scale bar 1 mm. All micrographs taken at the same magnification. Sections counterstained with cresyl violet.

degeneration. The cell profiles were rather indistinct, with varying degrees of apparent cell lysis.

As described in the methods section (section 2.7.6.1), direct measurements of cell number and size in the hippocampal fields was subject to erroneous interpretation because of the possibility of uneven sectioning of the brain. Measurements of the each hippocampal field area, from the anterior margin of the hippocampus to the level at which dorsal and ventral hippocampi join (bregma -4.52 mm (Paxinos and Watson, 1982)), were made using the image analysis system as described in section 2.7.6.1. Where a gap appeared in the hippocampus, measurements excluded this area. No measurements or estimates of hippocampal cell layer depth were made, as side to side comparison of these measurements would also have been subject to uneven sectioning artefact.

At a survival time of 14 days, the overall area of the CA1 hippocampal field was unchanged (4.13 and 4.37 mm^2, ipsilateral and contralateral to lesion side respectively). The area of the CA3 field was significantly reduced on the side ipsilateral to the injection site to 76 % of that of the side contralateral to the injection (3.72 and 4.87 mm^2, $p=0.018$; Student's paired *t*-test). The area of the dentate gyrus was not significantly affected (3.78 and 4.07 mm^2). There were no significant changes in any hippocampal field measured in ricin control animals (n=4) with the same postoperative survival time. These results are summarised in Figure 4.3.

At a postoperative survival time of 21 days, the morphological changes observed in the hippocampus were similar to those observed at a survival time of 14 days. No significant changes were measured in the area of CA1 (7.12 and 7.02 mm^2, ipsilateral and contralateral side respectively). The area of CA3 was reduced on the side ipsilateral to the injection to 83 % (6.07 mm^2) of the contralateral value (7.28 mm^2). The area of the dentate gyrus was not significantly affected (6.48 and 6.42 mm^2). There were no significant changes in the area of any hippocampal field in ricin control animals (n=4) with the same postoperative survival time. These results are summarised in Figure 4.3.

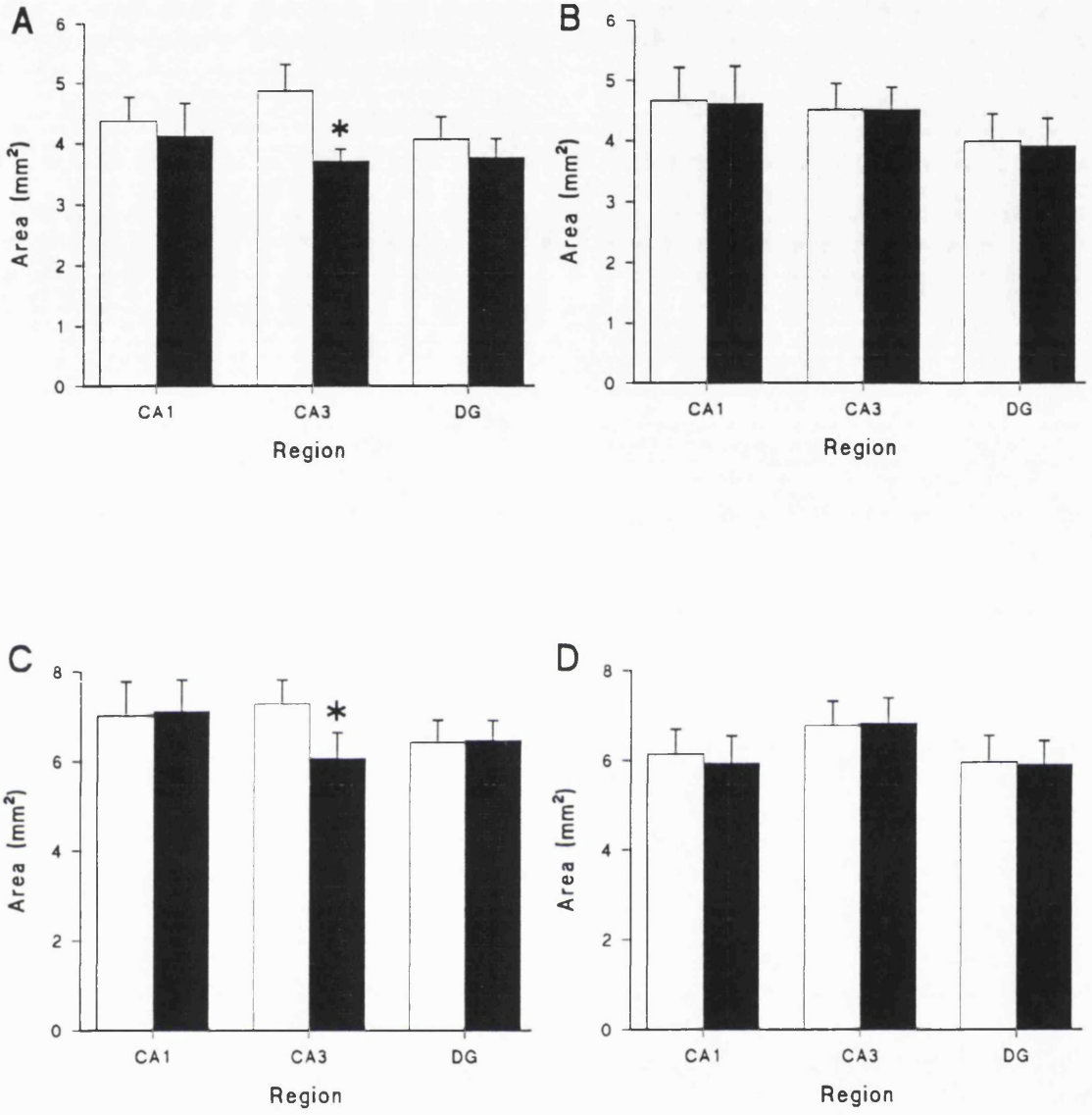

Figure 4.3: CHANGES IN HIPPOCAMPAL FIELD AREA FOLLOWING INJECTION OF TOXIC LECTINS INTO THE ENTORHINAL CORTEX. Histograms showing the mean anterior hippocampal field area (mm^2) after injection of 2 ng volkensin with survival times of 14 (A; n=5) and 21 (C; n=6) days or 10 ng ricin with survival times of 14 (B; n=4) and 21 (D; n=4) days on the side contralateral (open bars) and ipsilateral (filled bars) to the injection site.
Error bars are SEM; * $p < 0.02$, significantly different to contralateral side (Student's paired *t*-test).

4.2.5 Quantification of glutamic acid decarboxylase (GAD) mRNA positive cells in volkensin treated animals.

To confirm that the observed actions of volkensin at sites distant to the injection were wholly attributable to its retrograde action, *in-situ* hybridisation histochemistry for GAD mRNA was carried out. This enzyme is involved in the synthesis of GABA, and is a well established marker of interneurones (see Introduction, section 1.5.3). Thus preservation of GAD mRNA positive cells indicates specific retrograde action of the toxin, rather that direct spread from the site of the injection. GAD mRNA positive cells (Figure 4.4) were counted from the same areas as those showing loss of cresyl violet stained cells. No significant differences were observed in the number of GAD mRNA positive cells per field between ipsilateral and contralateral sides (Table 4.1) where counts were performed in areas of a gap or thinning of the cell layer in CA3.

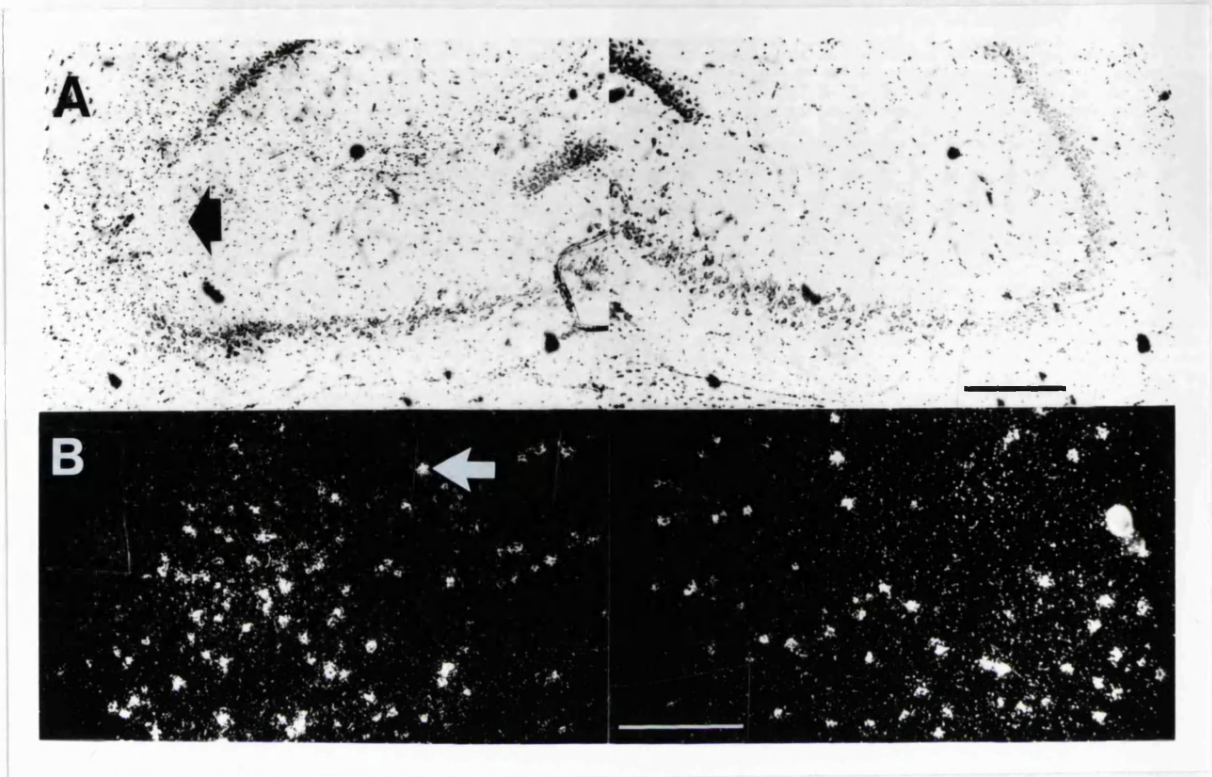

Figure 4.4: PHOTOMICROGRAPH OF RAT HIPPOCAMPUS SHOWING CELL LOSS AND *IN-SITU* HYBRIDISATION WITH GAD mRNA. Upper panel (A) shows ipsilateral (left) and contralateral (right) anterior hippocampus from a volkensin injected rat. Black arrow shows area of loss of CA3 pyramidal cells. Lower panel (B) shows photomicrograph of emulsion dipped section on sides ipsilateral (left) and contralateral (right) to the injection, from the area in which cell loss was observed in the panel above, and an equivalent area on the contralateral side. GAD mRNA positive cells are heavily labelled with silver grains (white; example shown by white arrow). Sections counterstained with cresyl violet. Scale bars: top panel, 500 μm; lower panel; 300 μm.

	14 Day survival time (n=5)		21 Day survival time (n=5)	
	Ipsilateral	Contralateral	Ipsilateral	Contralateral
Number	18.9 ± 1.8	15.8 ± 1.2	24.7 ± 5.4	21.7 ± 3.1
Mean size (μm^2)	88.2 ± 3.8	90.7 ± 7.8	99.7 ± 6.6	107.3 ± 9.3

Table 4.1: NUMBER OF GAD mRNA POSITIVE CELLS/FIELD AND MEAN CELL PROFILE AREA IN VOLKENSIN INJECTED ANIMALS. Experiments were performed using coronal rat brain sections (12 μm) incubated with a previously prepared ^{35}S labelled probe specific for glutamic acid decarboxylase (GAD) mRNA for 16 hr at 24°C. After development of emulsion, sections were counterstained with cresyl violet.
Data is mean ± SEM. No significant differences in the number or mean size of GAD mRNA positive cells per field between ipsilateral and contralateral sides was found.

4.3 Discussion.

4.3.1 Interpretations of the histological findings following volkensin injection.

The present study employs doses and post operative survival times based on the previous studies investigating the effect of intrastriatal volkensin injection (Pangalos et al., 1991b). These conditions are different from those used by other workers (as reviewed, Contestabile and Stirpe, 1993). Wiley and Stirpe (1988) used volkensin concentrations ranging from 1 - 8 ng, with a postoperative survival time of 2.5 - 12 days to lesion neurones projecting from the substantia nigra to the striatum. Contestibile et al. (1990) used a dose of 1.2 ng volkensin with a postoperative delay of 3 - 10 days to observe loss of septum and CA3 of contralateral hippocampus following unilateral injection into the dorsal hippocampus. At higher doses of volkensin (1.5 - 3 ng), most animals died after 3 - 5 days. Moreover, Harrison et al. (1992) determined that most D_1 receptor density reductions in the striatum occurred after a postoperative survival delay of 10 days. The differences observed in the relative toxicity may be dependent on the pathway being studied, with factors such as axonal transport speed and metabolic activity having a significant bearing. Volkensin is also very difficult to dissolve- this may explain the variability in the extent of the lesion from one animal to another, and also making it likely that the doses quoted above are approximations.

Postoperative survival times required to obtain suitable loss of the subpopulation of neurones under study differ considerably. Cell death in layer V of the cortex following intrastriatal volkensin injection is first observed after 21 days. Cell death in the substantia nigra following the same injection occurs more quickly (2.5 - 12 days (Wiley and Stirpe, 1988)), while degeneration of contralateral hippocampal CA3 neurones occurs after 5 days following hippocampal injection of volkensin (Contestabile et al., 1990).

The present study demonstrates that injection of volkensin into the entorhinal/posterior CA1 region produces a significant loss of anterior CA3 hippocampal neurones. The connections of the entorhinal cortex and hippocampus are rather complex (see Introduction, section 1.3.2); however, the

original hypothesis was that the CA1 region of the hippocampus would be primarily affected by entorhinal volkensin injection. The targets of injection were the pre-alpha cells of the medial and lateral entorhinal areas. It was not possible to lesion this area exclusively and, as outlined above, there was involvement of posterior CA1 regions. Efferents from anterior hippocampal areas arise from CA1 and CA3, and also in the subiculum (Hjorth-Simonsen, 1971; Beckstead, 1978) and terminate in the entorhinal cortex. The lack of involvement of the CA1 area of the entorhinal cortex may be for several reasons; (i) projections from CA1 to the entorhinal cortex may be topographically distinct and discrete, and in most cases the lesion did not involve the corresponding entorhinal areas; (ii) projections from CA1 are more posterior and thus there was only involvement of posterior CA1, which was not investigated in this study because of the possibility of direct involvement; (iii) the subpopulations of CA1 neurones projecting to the entorhinal cortex are less sensitive to volkensin, or that the binding sites required for internalisation of the toxin are more sparse on CA1 projections; (iv) projections from the CA1 layer are not from the pyramidal cells themselves, but rather from cells present in the molecular layer of CA1; (v) projections arising in CA1 are far more collateralised than those arising in CA3, with projections from CA1 to the subiculular complex, septum, fornix, contralateral CA1 and the entorhinal cortex. Thus, assuming constant axon diameter and standard rate of axonal transport, CA1 pyramidal neurones would receive a reduced dose of volkensin compared to CA3 neurones, whose main projections are to the entorhinal cortex and via Schaffer collaterals. Alternatively, a higher proportion of CA3 pyramidal cells may project to the entorhinal cortex (assuming little collateralisation), namely 1 in 2 neurones, rather than 1 in 5 for the CA1 region. Less likely explanations for the lack of change in CA1 are; (i) the speed of axonal transport of CA1 neurones is slower than that of CA3, and the postoperative delay was not sufficient to observe CA1 changes; (ii) loss of CA3 neurones was a result of destruction of perforant pathway neurones projecting from the entorhinal area with resulting adaptive changes in CA3- this is unlikely as similar changes would be observed with ricin injection; (iii) contralateral changes in CA1 masked the cell loss on the side ipsilateral to the

injection- again this is unlikely as the contralateral CA1 area had a normal appearance and size when compared to controls- there was no thinning of the cell layer, no ventricular enlargement and no collapse of overlying cortical structures; (iv) projections from the septal nuclei to the entorhinal cortex and posterior CA1 degenerated and were followed by re-uptake of the toxin by axons projecting from CA3 to the septum. It is also possible that the direct involvement of posterior CA1 made primary contributions to morphological changes observed in anterior CA3- there are extensive collateralised projections from CA3 to both radiatum and oriens layers in ipsilateral CA1 via branches extending from the Shaffer collaterals (Gottleib and Cowan, 1973; Swanson, 1981; Bayer, 1985).

It is not possible in these experiments to exclude the possibility of loss of anterior CA3 pyramidal cells which send projections to other cortical areas, passing through the entorhinal cortex and posterior CA1 without synapsing. However given the knowledge of the topographic connections of anterior CA3, it is certain that the population of cells lost includes those projecting from anterior CA3 to the entorhinal cortex/posterior CA1.

The possibility that volkensin may spread from the injection site to directly affect anterior CA3 cells, or that volkensin is re-released from neurones initially transporting the lectin and then releasing it into the surrounding neuropil upon cell lysis (from where it may be taken up by adjacent neurones) has been carefully considered. If direct spread were responsible, it would be expected to observe similar morphological changes using ricin, a lectin very similar in nature to volkensin, but transported only in the PNS, which was not a feature of this study. Ricin produced local lesions around the injection site, but no observable cell loss in other areas or nuclei distant from the site of injection. However, the diffusion rates of volkensin and ricin through the neuropil may be quite different. Morphological changes in the hippocampus attributable to adaptive changes following the lesion are also excluded by the lack of change in ricin injected animals, and the findings that orthograde transneuronal changes visible in Nissl stained sections is confined to primary sensory systems. Several other findings support the interpretation that only cells undergoing retrograde suicide transport of volkensin are

destroyed. Firstly, *in-situ* hybridisation for GAD mRNA, a marker of interneurones was investigated. Any loss of GAD mRNA positive cells following injection of volkensin may be a consequence of either (i) passive diffusion or (ii) secondary spread from cells that retrogradely transported the toxin and were subsequently lysed. No significant differences were observed between the number of GAD mRNA positive cells between ipsilateral and contralateral sides (Table 4.1). Secondly, histological analysis confirmed that the cell loss distant to the injection site conformed to known afferent projections to the injection site, and was not seen in nuclei or areas closer to the injection site but without afferent axons to the entorhinal cortex. Finally, as outlined above, injection of ricin did not mimic the action of volkensin.

CHAPTER 5: Autoradiographic analysis of ligands binding to hippocampal neurones in animals injected with toxic lectins.

5.1 Introduction

The regional and laminar distribution of various receptor subtypes in the rat and human hippocampus and neocortex have been extensively studied. Differences in the laminar distribution of receptors may indicate localisation of the receptor to certain cell types or structures. The excitability of the major cell type of the cortex, the pyramidal neurone, is affected by many neurotransmitters, based on *in vitro* electrophysiological studies (McCormick and Williamson, 1989). However, such studies have consistently reported that only a proportion of neurones may respond to a particular transmitter, which suggests that there is a substantial degree of heterogeneity with respect to the neurotransmitter receptors of pyramidal neurones. Francis and colleagues (Pangalos et al., 1991b; Francis et al., 1992b; Pangalos et al., 1992) used receptor autoradiography on sections of rat brain from volkensin-injected animals to establish whether a subpopulation of cortical pyramidal cells are enriched with a particular receptor type. The present study extends these techniques to investigate the receptors of the hippocampus. The hippocampal formation is the origin and target of extensive innervation to and from many areas of the brain (see Introduction, section 1.3.2), and excitatory amino acid receptors appear to be particularly abundant. The aim of this study was to discover, using quantitative autoradiography with [^{3}H] L-689,560, [^{3}H] kainate, [^{3}H] GABA, [^{3}H] 8-OH-DPAT, [^{3}H] ketanserin, and [^{3}H] pirenzepine, if certain receptors were selectively enriched on a subpopulation of CA3 hippocampal pyramidal neurones destroyed following entorhinal injection of volkensin (see Chapter 4). It is considered to be important to discover and describe the relative abundance of receptors which have a modulatory role, and thus in addition to "fast" transmitter receptors (NMDA, kainate and GABA), the localisation of several second messenger linked receptors have also been investigated (serotonin 5-HT_{1A}, 5-HT_{2A}, and muscarinic M_1), using, respectively, the ligands above. The techniques described here can be used to compare and contrast receptor populations on CA3 hippocampal pyramidal cells with the populations of receptors on other, neocortical, pyramidal cells,

including those which project sub-cortically and within the neocortex (this thesis). Investigation of ricin injected animals was also performed, though only where significant differences were observed between ipsilateral and contralateral sides in volkensin injected animals.

5.2 Results

5.2.1 The binding of [^{3}H] L-689,560 to the glycine modulatory site of the NMDA receptor- ionophore complex.

Using the binding conditions previously described (Pangalos et al., 1992), an incubation time of 2 hr, with a wash time of 4 x 1 min gave approximately 46% specific binding. The highest level of binding was observed in the ventral blade of DG, followed by CA1 radiatum, with a relatively high level of binding in the oriens of CA1 and CA3. The binding pattern followed the appearance of the lesion, with little binding of [^{3}H] L-689,560 was apparent in areas of "gapped" CA3. Binding was apparently reduced in areas of cell thinning, and reductions in binding appeared to follow patterns of cell loss seen in cresyl violet stained sections (Figure 5.1).

Quantification of the autoradiographic binding characteristics of [^{3}H] L-689,560 was performed as described in the methods section (section 2.8.11.2). When autoradiograms and Nissl stained sections were superimposed, it was apparent that a component of the binding of [^{3}H] L-689,560 was localised to an area corresponding to the pyramidal cell layer in the CA fields and the granular layer of the DG. Measurements of the lengths of binding to these areas were made (see Chapter 2, Section 2.8.11.2), and a ratio calculated between autoradiographic binding length and histologically stained length. No significant differences were found between the ratios calculated or the mean grey levels measured for the sides ipsilateral and contralateral to the injection in CA1, CA3 or DG in animals left for 14 or 21 days postoperatively after injection of 2 ng volkensin (Figure 5.2).

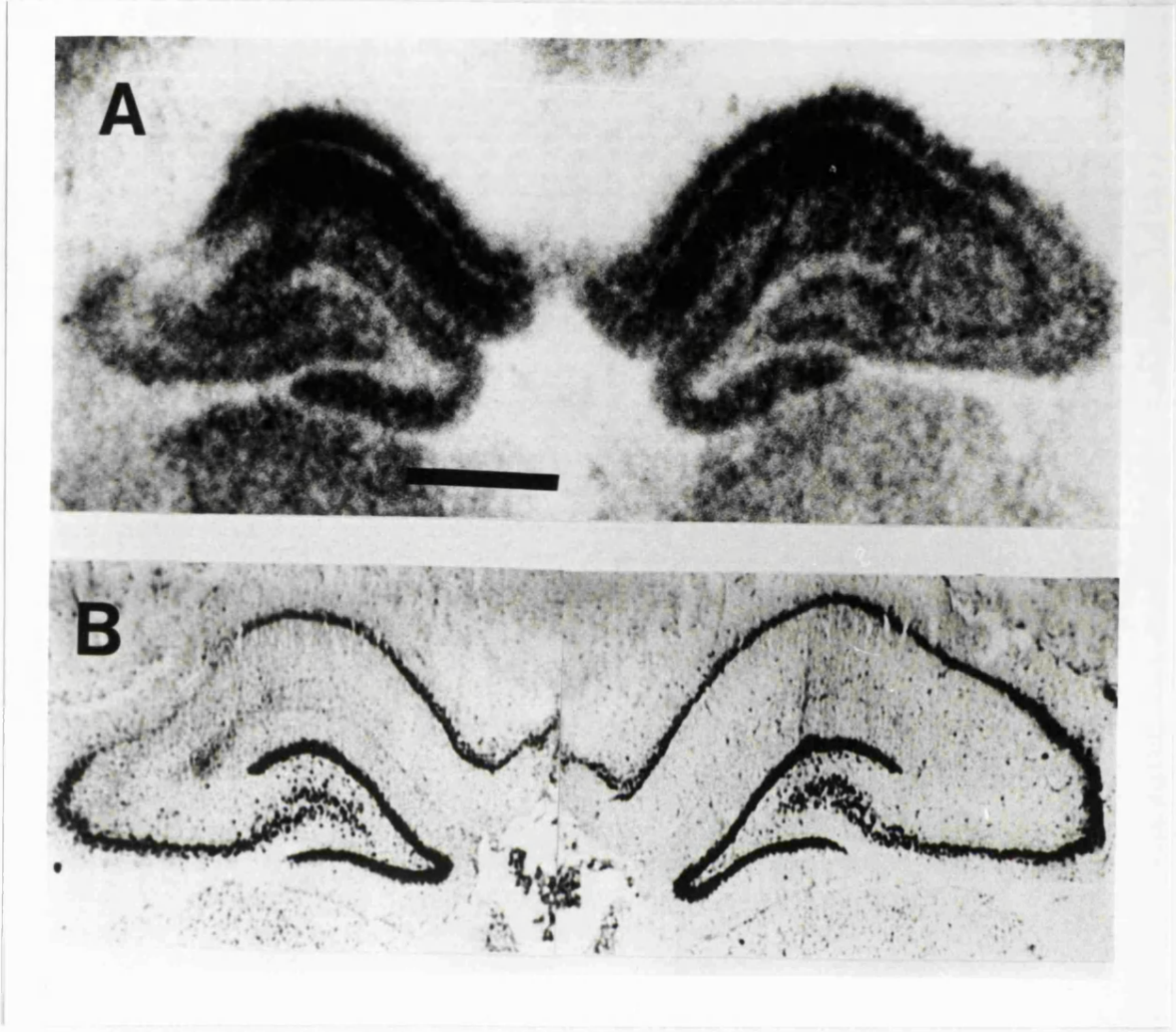

Figure 5.1: A: REPRESENTATIVE AUTORADIOGRAM OF [^{3}H] L-689,560 BINDING IN THE HIPPOCAMPUS OF A VOLKENSIN INJECTED ANIMAL WITH B: CORRESPONDING NISSL STAINED SECTION. Experiments were performed using coronal rat brain sections (12 μm) incubated in 50 mM Tris-acetate (pH 7.0) containing 5 nM [^{3}H] L-689,560 for 120 min at 4 °C. Non-specific binding was generated using 1 mM glycine. Nissl staining of the closest corresponding section was performed as described in section 2.7.3. Injection site on left side. Scale bar (A) 1 mm.

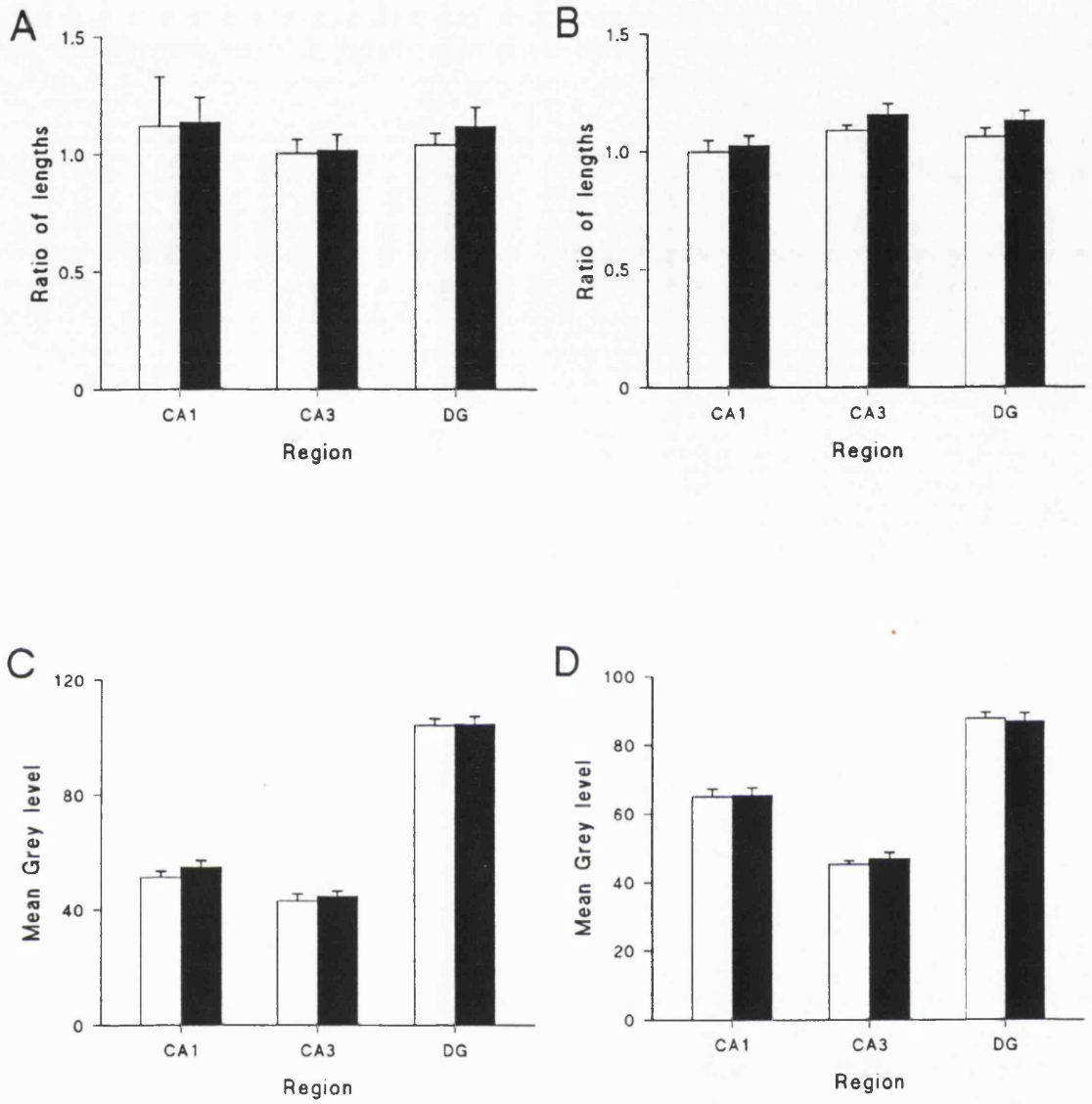

Figure 5.2: [^{3}H] L-689,560 BINDING IN VOLKENSIN INJECTED ANIMALS. Experimental conditions were as described in Figure 5.1. Figures A and B show ratios calculated between length of autoradiographic binding and Nissl staining in hippocampal fields in animals injected with 2 ng volkensin with survival times of 14 (n=5) or 21 (n=6) days respectively. Figures C and D show corresponding grey levels measured in the same animals and sections. Error bars are SEM. Contralateral side- open bars; ipsilateral side- filled bars. No significant differences.

5.2.2 The binding of [^{3}H] kainate to kainate sensitive glutamate receptors.

5.2.2.1 Effects of incubation and wash time.

Using the conditions described in the methods section (2.8.5), an incubation time of 45 min with a wash time of 2 x 20 sec gave 90% or greater specific binding. Addition of calcium to the incubation medium significantly reduced the binding of [^{3}H] kainate (Chapter 2, Table 2.3, (Monaghan et al., 1985)), so all incubations were performed in the absence of exogenously added calcium. Association and dissociation experiments were performed to achieve optimal binding (Chapter 2, section 2.8.5).

5.2.2.2 Displacement of [^{3}H] kainate using AMPA.

The effects of co-incubation of [^{3}H] kainate with increasing concentration of unlabelled AMPA (1 nM - 10 μM) were examined to investigate the characteristics of the kainate sensitive glutamate receptor (see methods section 2.8.5). Autoradiograms were examined and quantified in cortical areas Fr1/Fr2 and Par1/Par2 (upper and lower layers) and hippocampal areas CA3 and DG. Increasing concentrations of AMPA caused slight reductions in binding of [^{3}H] kainate, though at no concentration of AMPA did the reduction of [^{3}H] kainate binding become significantly different from the binding observed in the absence of exogenously added AMPA in any area examined (Figure 5.3)

5.2.2.3 Characteristics of [^{3}H] kainate binding in lesioned rat brain sections.

The laminar and regional distribution of [^{3}H] kainate binding in the hippocampus of a volkensin treated animal is shown in Figure 5.4, with closest adjacent cresyl violet stained section for comparison. The highest level of binding was observed in areas which closely corresponded to the CA3 pyramidal cell layer, with very little binding in CA1. In DG, the highest binding was observed in the inner one third of the molecular layer. Detailed examination of the autoradiograms by superimposing the closest corresponding Nissl stained section revealed a clear lamination of binding confined to the immediate vicinity of the pyramidal cell perikarya in CA3 and the granule cell

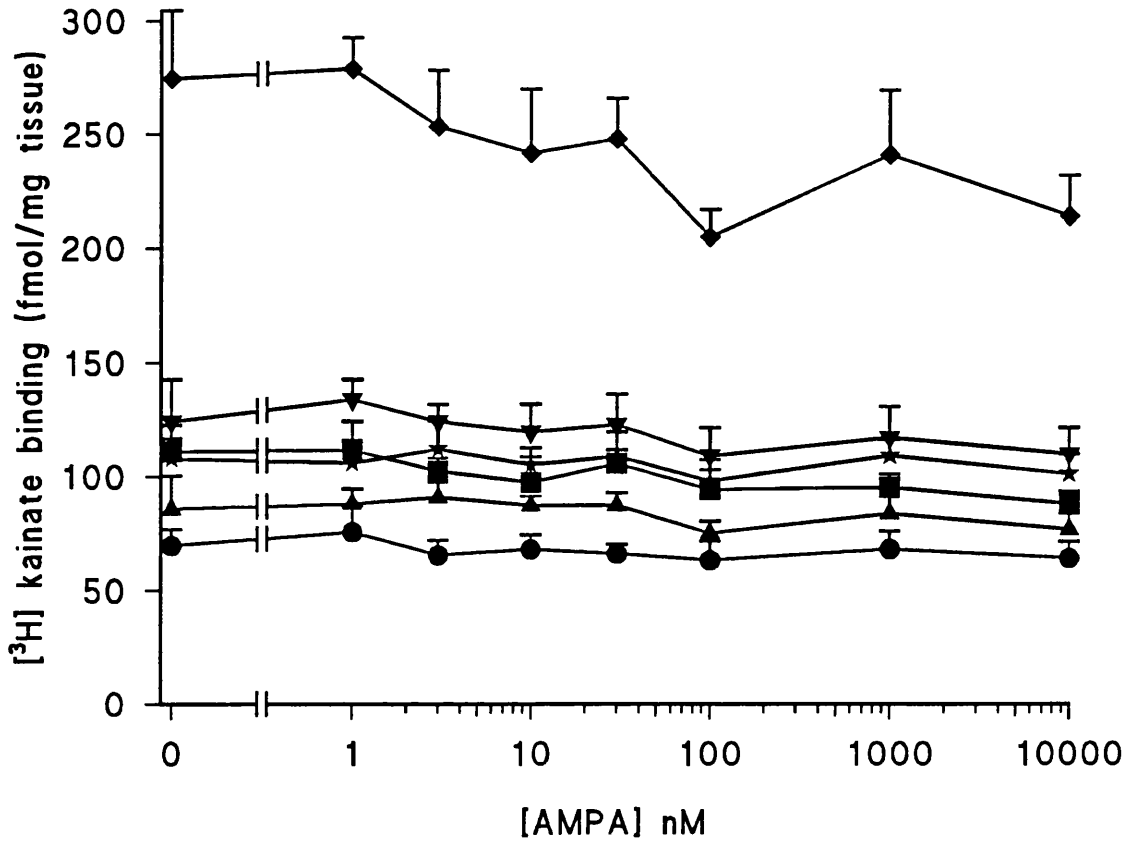

Figure 5.3: DISPLACEMENT OF [^{3}H] KAINATE BINDING BY AMPA IN CONTROL SECTIONS. Quantitative autoradiography was performed using coronal control rat brain sections (12 μm) incubated at 4°C in Tris-citrate (pH 7.0) containing 50 nM [^{3}H] kainate with increasing concentrations of AMPA (1 nM - 10 μM), and quantification of binding performed in medial cortex upper (●) and lower (■) layers, lateral cortex upper (▲) and lower (▼) layers, and hippocampal CA3 (◆) and dentate gyrus (★).
Error bars are SEM. Each value is mean of two sections from each animal, 3 animals. No significant differences in binding of [^{3}H] kainate in any area at any concentration of AMPA compared with binding in the absence of AMPA (Student's paired *t*-test).

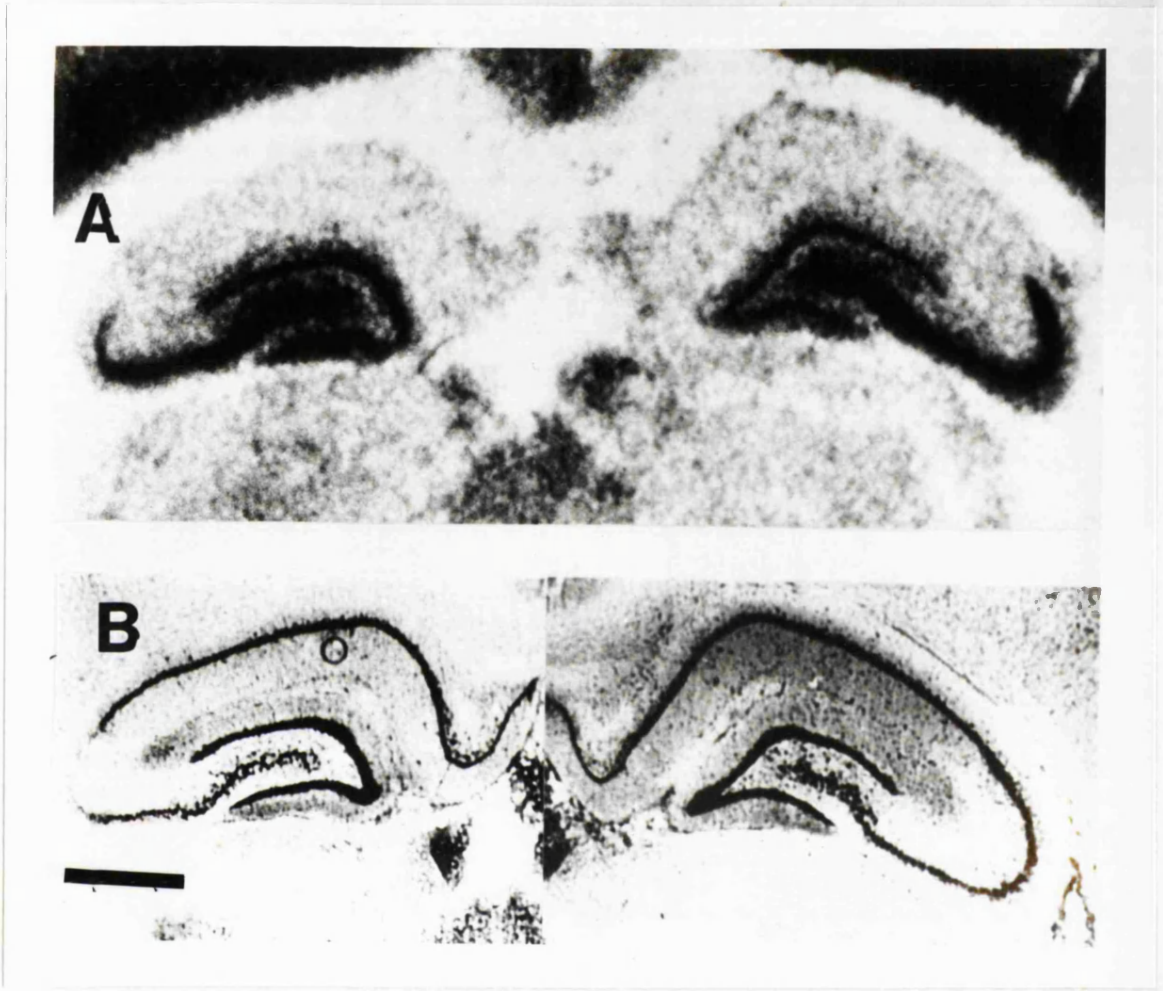

Figure 5.4: A: REPRESENTATIVE AUTORADIOGRAM OF THE BINDING OF [^{3}H] KAINATE IN THE HIPPOCAMPUS OF A VOLKENSIN INJECTED ANIMAL WITH B: CORRESPONDING NISSL STAINED SECTION. Experiments were performed using coronal rat brain sections (12 μm), incubated in Tris-citrate buffer (pH 7.0) containing 30 nM [^{3}H] kainate for 45 min at 4 °C. Non-specific binding was generated using 10 μM unlabelled kainate. Nissl staining of closest corresponding section was performed as described in section 2.7.3. Injection site on left side. Scale bar (B) 1 mm.

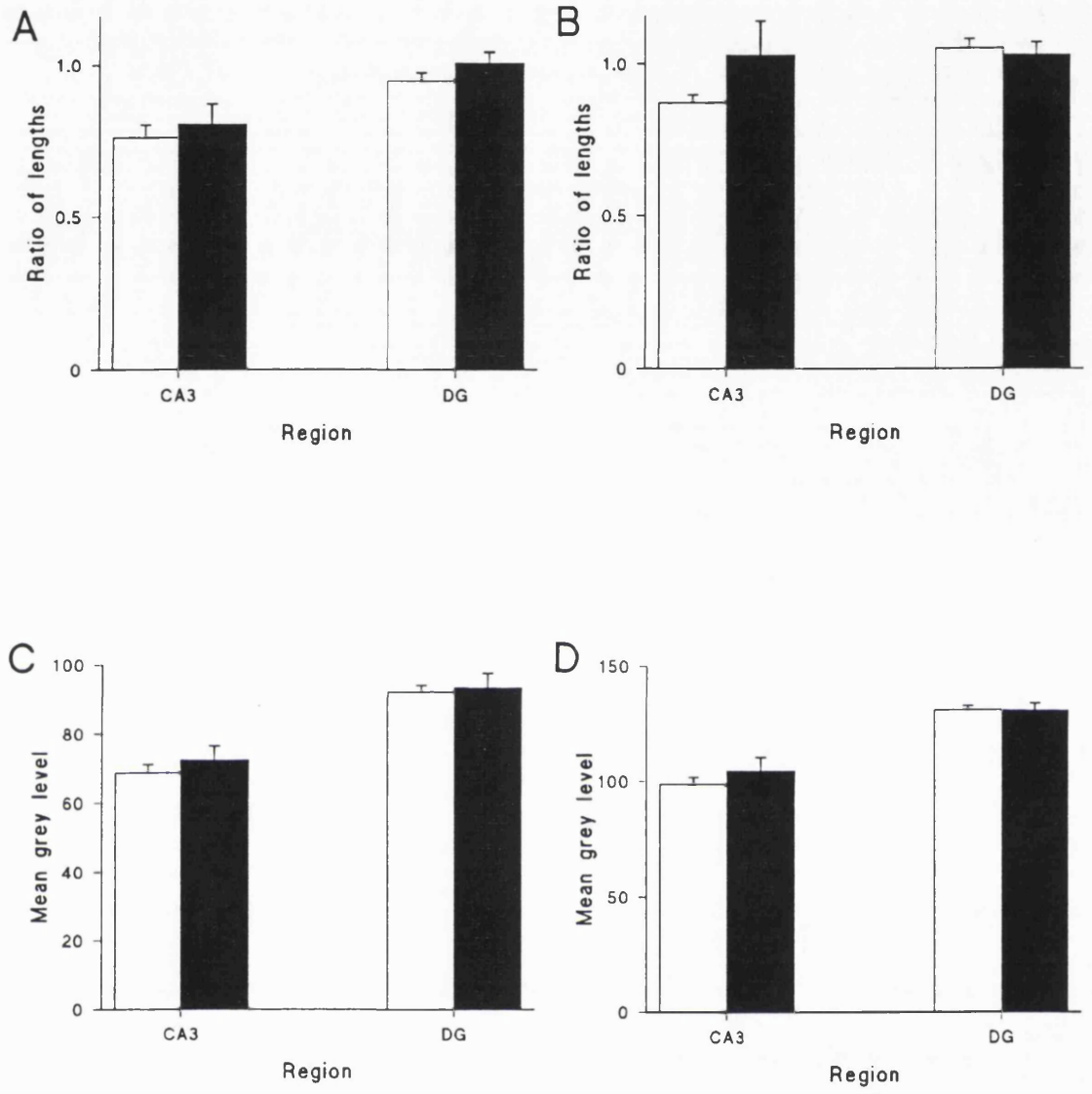

Figure 5.5: [^{3}H] KAINATE BINDING IN VOLKENSIN INJECTED ANIMALS. Experimental conditions were as described in Figure 5.4. Figures A and B show ratios calculated between length of autoradiographic binding and Nissl staining in animals injected with 2 ng volkensin with survival times of 14 (n=5) or 21 (n=5) days respectively. Figures C and D show the corresponding mean grey levels measured in the same animals and sections.
Error bars are SEM. Contralateral side- open bars; ipsilateral side- filled bars. No significant differences.

perikarya in the DG so the length of binding in these areas were measured in the autoradiograms, and a ratio calculated as before (see section 5.2.1). Binding in CA1 was low and not possible to reliably quantify.

No significant differences were found between ratios calculated for ipsilateral and contralateral sides in volkensin injected animals with a survival time of 14 (n=5) or 21 (n=6) days. No significant differences were observed in grey levels between sides ipsilateral and contralateral to the lesion at either survival time. These results are summarised in Figure 5.5.

5.2.3 The binding of [^{3}H] GABA to $GABA_A$ receptors.

5.2.3.1 Effects of incubation and wash time.

As described in Chapter 2, section 2.8.7, an incubation time of 45 min was considered to be at equilibrium, and produced approximately 85% specific binding. Dissociation of [^{3}H] GABA was very rapid. All incubations were performed in the presence of 100 μM baclofen to exclude binding to the $GABA_B$ receptor.

5.2.3.2 Characteristics of [^{3}H] GABA binding in lesioned rat brain sections.

The laminar and regional distribution of [^{3}H] GABA binding to the $GABA_A$ receptor is shown in Figure 5.6, with the closest Nissl stained section shown for comparison. Highest binding was observed in the DG. Binding in the CA fields was not localised to the pyramidal cell layer, and was abundant in the most superficial layer of CA1, and lower in the CA3 region. Qualitative examination of the autoradiograms showed an apparent preservation of binding in areas where cell loss was apparent in Nissl stained sections. Detailed examination of the correspondence between the autoradiograms and corresponding Nissl stained sections (by superimposition using a microscope with drawing tube) revealed that binding was not confined to the immediate vicinity of the pyramidal cell perikarya, but extended into the radiatum and oriens, with no apparent demarcation between binding in CA1 and CA3. In these circumstances the area of binding in CA1 + CA3 and DG was measured, to include all the regions of receptor binding. The ipsilateral CA1 + CA3 area ratio was increased (19%, p = 0.05, Student's paired *t*-test) compared to that

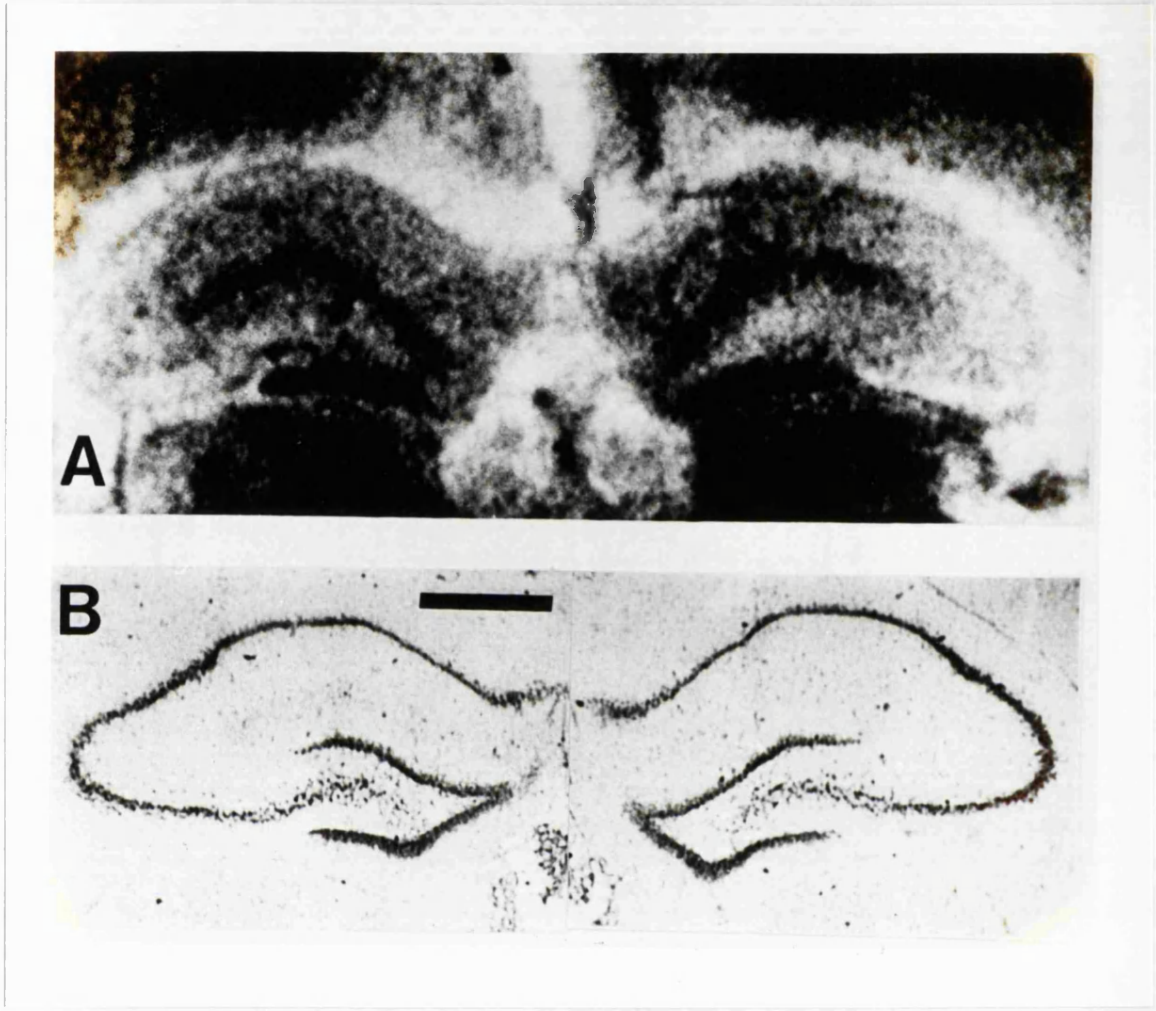

Figure 5.6: A: REPRESENTATIVE AUTORADIOGRAM OF THE BINDING OF [^{3}H] GABA IN THE PRESENCE OF BACLOFEN IN THE HIPPOCAMPUS OF A VOLKENSIN INJECTED ANIMAL WITH B: CORRESPONDING NISSL STAINED SECTION. Experiments were performed using coronal rat brain sections (12 μm), incubated in Tris-HCl buffer (pH 7.4) containing typically 30 nM [^{3}H] GABA in the presence of 100 μM baclofen for 45 min at 25°C. Non-specific binding was generated using 100 μM unlabelled isoguvacine. Nissl staining of closest corresponding section was performed as described in section 2.7.3. Injection site on left side. Scale bar (B) 1 mm.

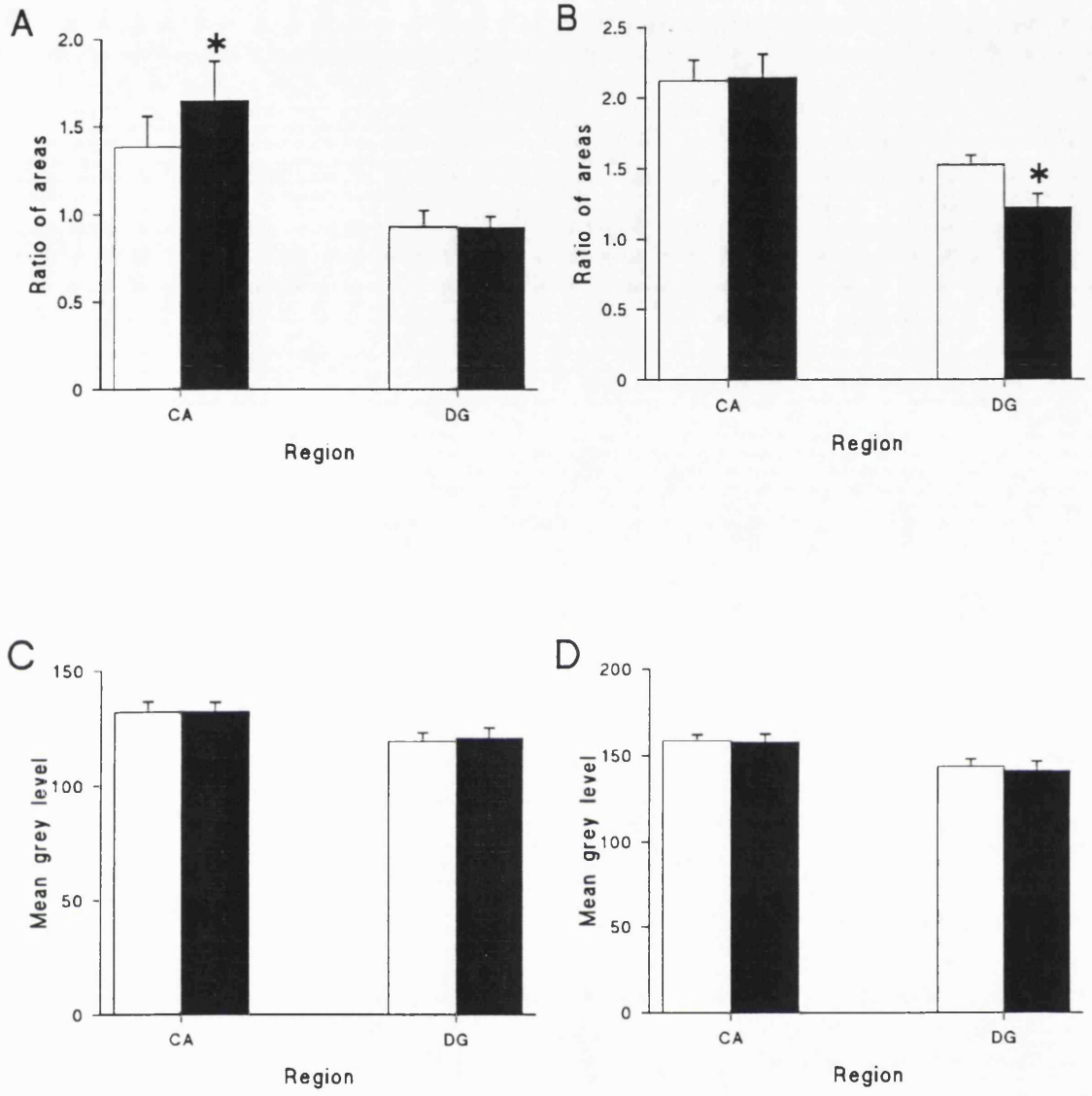

Figure 5.7: [^{3}H] GABA BINDING IN VOLKENSIN INJECTED ANIMALS. Experimental conditions were as described in Figure 5.6. Figures A and B show ratios calculated between area of autoradiographic binding and Nissl staining in animals injected with 2 ng volkensin with survival times of 14 (n=5) or 21 (n=6) days respectively. Figures C and D show the corresponding mean grey levels measured in the same animals and sections.
Error bars are SEM. Contralateral side- open bars; ipsilateral side- filled bars.
* $p < 0.05$ (Student's paired *t*-test).

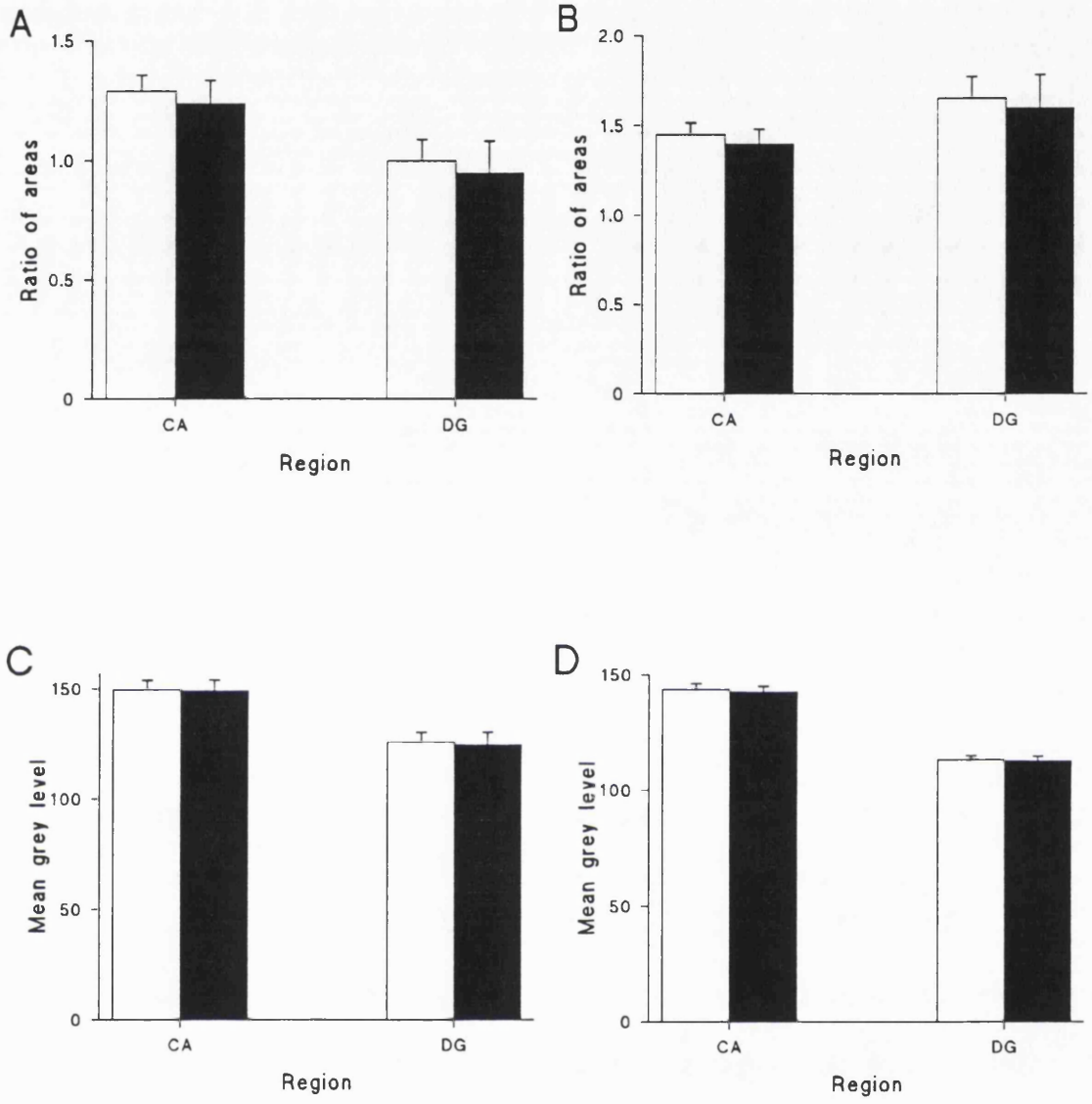

Figure 5.8: [^{3}H] GABA BINDING IN RICIN INJECTED ANIMALS. Experimental conditions were as described in Figure 5.6. Figures A and B show ratios calculated between area of autoradiographic binding and Nissl staining in animals injected with 10 ng ricin with survival times of 14 (n=4) or 21 (n=4) days respectively. Figures C and D show the corresponding mean grey levels measured in the same animals and sections.
Error bars are SEM. Contralateral side- open bars; ipsilateral side- filled bars. No significant differences.

contralaterally, but only in animals with a 14 day (n=5) survival time (Figure 5.7A). Although there was no apparent dentate atrophy, at 21 day survival times (n=6) there was reduced binding (19%, p = 0.011, Student's paired *t*-test) to $GABA_A$ receptors on the side ipsilateral to the injection compared to the corresponding contralateral region (Figure 5.7B). There were no significant differences between grey levels in ipsilateral and contralateral sides in any area at either survival time (Figure 5.7). Ratios were also calculated for animals injected unilaterally with 10 ng ricin. No significant changes were found for any ratio or grey level at survival times of 14 (n=4) or 21 (n=4) days. These results are summarised in Figure 5.8.

5.2.4 The binding of [^{3}H] 8-OH-DPAT to 5-HT_{1A} receptors.

Using the binding conditions previously described (Pazos and Palacios, 1985; Francis et al., 1992b), an incubation time of 60 min, with a wash time of 2 x 5 min gave approximately 85 % specific binding. The laminar and regional distribution of binding in the hippocampus is shown in Figure 5.9. Highest binding to the 5-HT_{1A} receptor was observed in CA1, DG and sections of CA3 subfields. The most lateral part of CA3 however, exhibited low binding, and coincidentally coincided with the area affected by volkensin injection. Detailed examination of the correspondence between the autoradiograms and corresponding Nissl stained sections (by superimposition using a microscope with drawing tube) revealed that binding was not confined to the immediate vicinity of the pyramidal cell perikarya, but extended into the radiatum and oriens. In these circumstances the area of binding in CA1, CA3 and DG was measured, to include all the regions of receptor binding. Ratios were then calculated as described in the preceding sections.

No significant differences were found between the ratios calculated for any area in animals with a survival time of 14 days (n=4) or in CA1 or CA3 areas in animals with a 21 day (n=6) survival time for sides ipsilateral and contralateral to the lesion. Although there was no apparent dentate atrophy, at 21 days there was reduced binding to the 5-HT_{1A} receptor (13% difference in ratios, p=0.02, Student's paired *t*-test) on the side ipsilateral to the lesion. There were no significant changes in grey levels for any area or survival time. These results are summarised in Figure 5.10. In animals injected with 10 ng

Figure 5.9: A: REPRESENTATIVE AUTORADIOGRAM OF THE BINDING OF [^{3}H] 8-OH-DPAT IN THE HIPPOCAMPUS OF A VOLKENSIN INJECTED ANIMAL WITH B: CORRESPONDING NISSL STAINED SECTION. Experiments were performed using coronal rat brain sections (12 μm), incubated in Tris-HCl buffer (pH 7.6) containing 4 mM $CaCl_2$, 0.01% ascorbate and 1 - 2 nM [^{3}H] 8-OH-DPAT for 60 min at 25 °C. Non-specific binding was generated using 10 μM unlabelled 5-HT. Nissl staining of closest corresponding section was performed as described in section 2.7.3.
Injection site on left side. Scale bar (A) 1 mm.

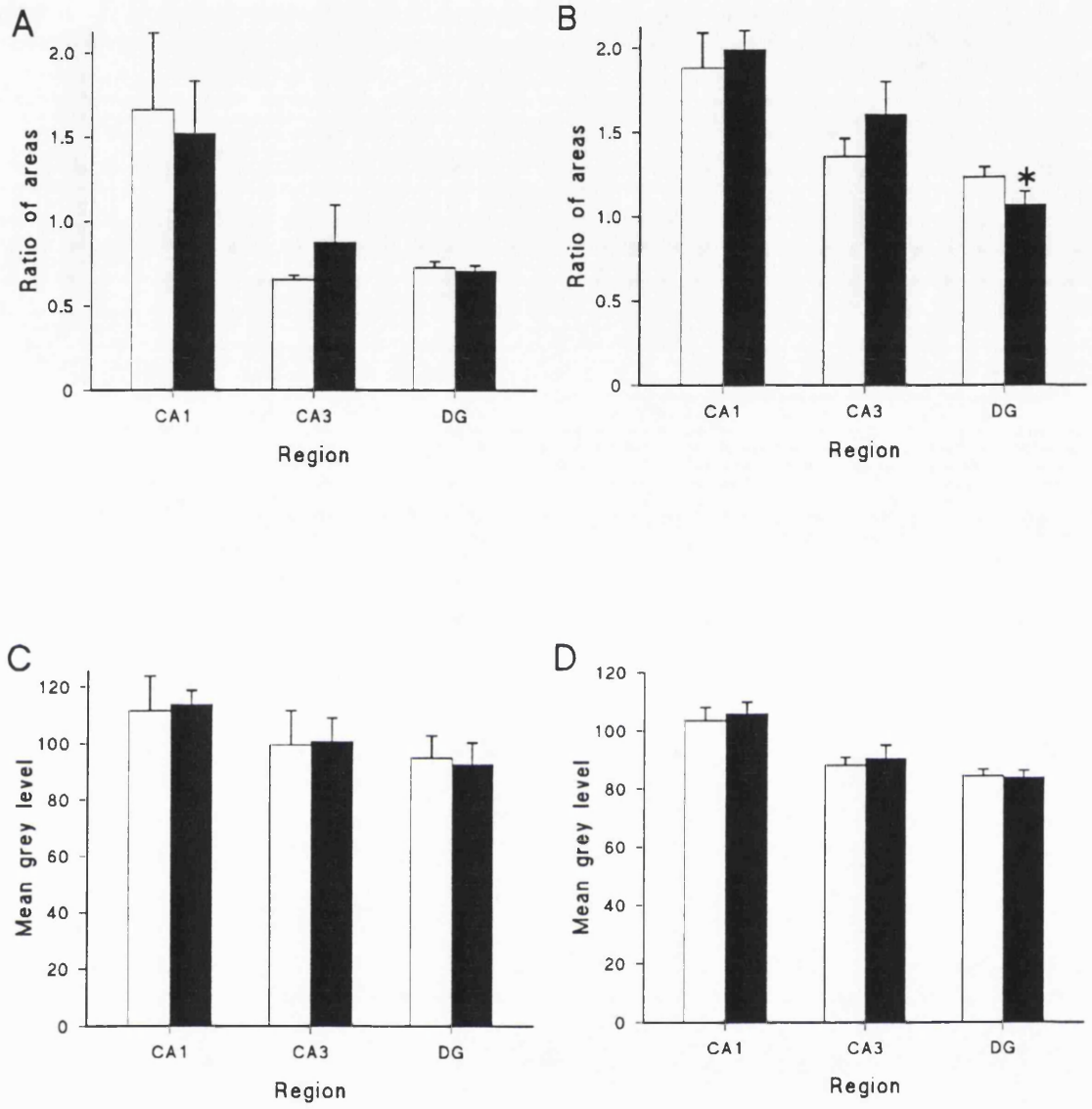

Figure 5.10: [^{3}H] 8-OH-DPAT BINDING IN VOLKENSIN INJECTED ANIMALS. Experimental conditions were as described in Figure 5.9. Figures A and B show ratios calculated between area of autoradiographic binding and Nissl staining in animals injected with 2 ng volkensin with survival times of 14 (n=4) or 21 (n=6) days respectively. Figures C and D show the corresponding mean grey levels measured in the same animals and sections.
Error bars are SEM. Contralateral side- open bars; ipsilateral side- filled bars.
* $p < 0.05$ (Student's paired *t*-test).

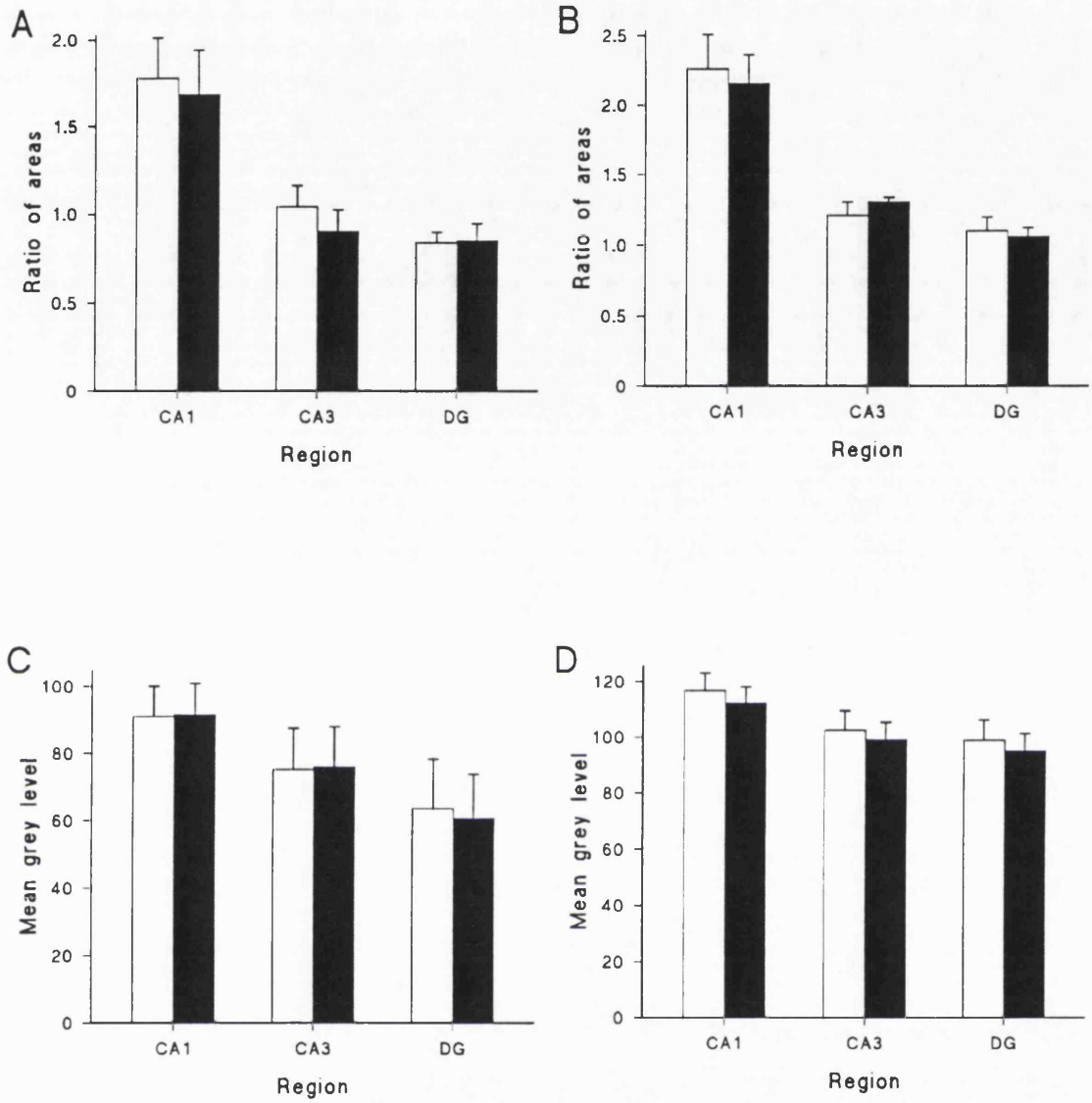

Figure 5.11: [^{3}H] 8-OH-DPAT BINDING IN RICIN INJECTED ANIMALS. Experimental conditions were as described in Figure 5.9. Figures A and B show ratios calculated between area of autoradiographic binding and Nissl staining in animals injected with 10 ng ricin with survival times of 14 (n=4) or 21 (n=4) days respectively. Figures C and D show the corresponding mean grey levels measured in the same animals and sections.
Error bars are SEM. Contralateral side- open bars; ipsilateral side- filled bars. No significant differences.

ricin, no significant changes in ratios or grey levels were found in any area at survival times of 14 (n=3) or 21 (n=4) days. These results are summarised in Figure 5.11.

5.2.5 The binding of [^{3}H] ketanserin to 5-HT$_{2A}$ receptors.

Using the binding conditions previously described (Pazos et al., 1985; Francis et al., 1992b), an incubation time of 120 min, with a wash time of 2 x 10 min gave approximately 60% specific binding. Though relatively high binding of [^{3}H] ketanserin was observed in cortex, binding in the hippocampal regions were extremely low, even with long film exposure times. Exposure times sufficient to allow visualisation of the hippocampal areas were such that non-linearity of the grey levels on the film could not be excluded. Therefore, quantification of the binding of [^{3}H] ketanserin to the 5-HT$_{2A}$ receptor in the hippocampi of animals injected with 2 ng volkensin was not performed. The appearance of a representative autoradiogram is shown in Figure 5.12, with the closest adjacent Nissl stained section for comparison.

5.2.6 The binding of [^{3}H] pirenzepine to muscarinic M$_1$ receptors.

Using the conditions previously described (Pangalos, 1992), an incubation time of 90 min, with a wash time of 1 x 5 min produced approximately 88 % specific binding. The regional and laminar distribution of binding in the anterior hippocampus is shown in Figure 5.13, with the closest Nissl stained section for comparison. Highest binding was observed in the oriens of CA1, followed by DG and CA3. Detailed examination of the correspondence between the autoradiograms and corresponding Nissl stained sections (by superimposition using a microscope with drawing tube) revealed that binding was not confined to the immediate vicinity of the pyramidal cell perikarya, but extended into the stratum radiatum. In these circumstances the area of binding in CA1, CA3 and DG was measured, to include all the regions of receptor binding. Ratios were then calculated as described in the preceding section.

No significant differences were found between the ratios calculated for CA1 and DG in animals with a survival time of 14 days (n=5) or in any area in animals with a survival time of 21 days (n=5) for sides ipsilateral and

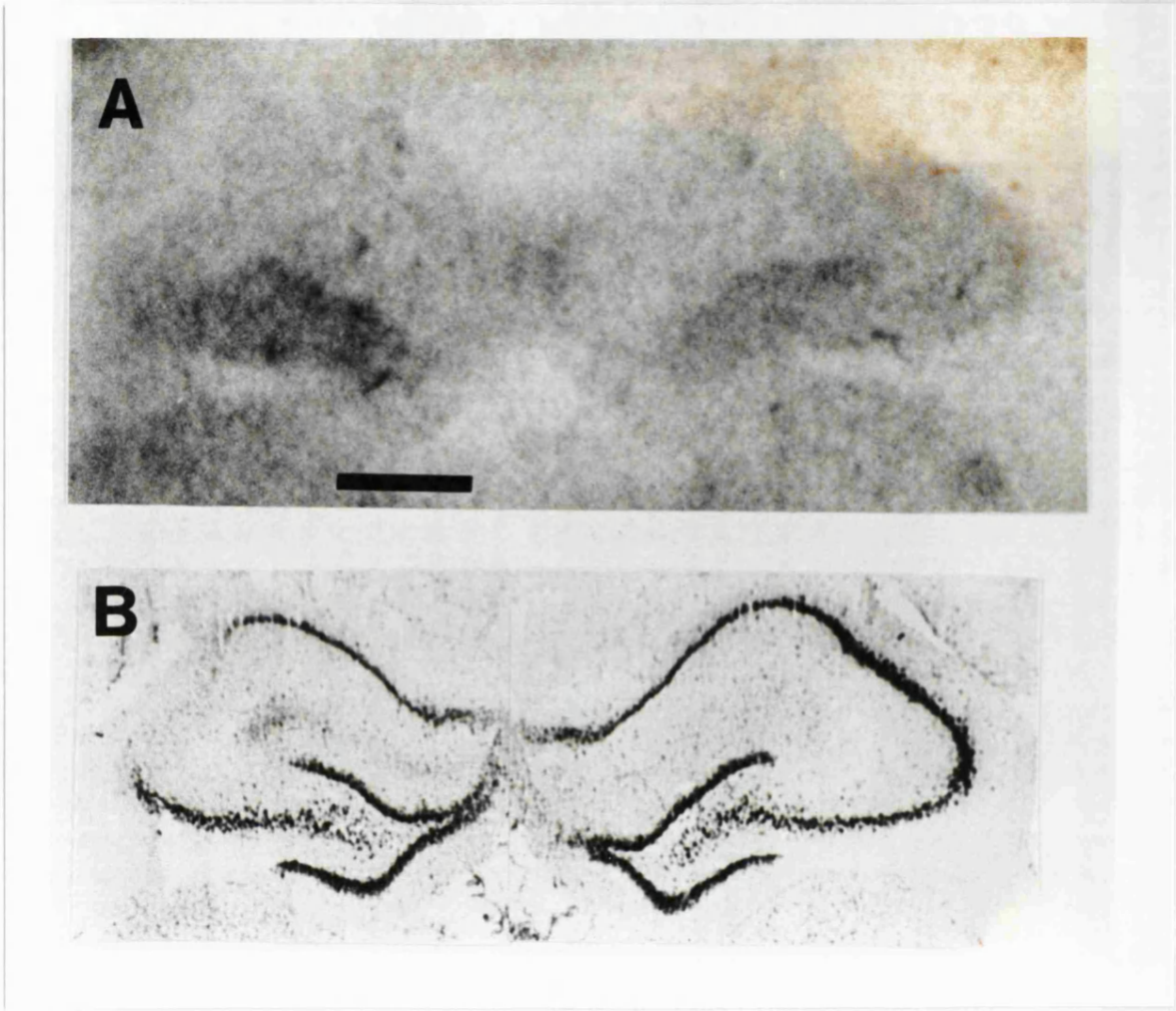

Figure 5.12: A: REPRESENTATIVE AUTORADIOGRAM OF THE BINDING OF [^{3}H] KETANSERIN IN THE HIPPOCAMPUS OF A VOLKENSIN INJECTED ANIMAL WITH B: CORRESPONDING NISSL STAINED SECTION. Experiments were performed using coronal rat brain sections (12 μm), incubated in Tris-HCl buffer (pH 7.7) containing 2 nM [^{3}H] ketanserin for 120 min at 25 °C. Non-specific binding was generated using 10 μM unlabelled mianserin. Nissl staining of closest corresponding section was performed as described in section 2.7.3. Binding was very low in the hippocampus and not reliably quantifiable.
Injection site on left side. Scale bar (A) 1 mm.

contralateral to the lesion. At 14 days, a significant decrease in the ratio calculated for CA3 on the side ipsilateral to the injection was found (12%, $p = 0.009$, Student's paired *t*-test) compared to that contralaterally, reflecting reduced binding. There were no significant changes in grey levels between sides ipsilateral and contralateral to the injection for any area or survival time. These results are summarised in Figure 5.14. In animals injected with 10 ng ricin, no significant differences in ratio or grey level were measured between sides ipsilateral and contralateral to the lesion in animals with a survival time of either 14 (n=3) or 21 (n=4) days (Figure 5.15).

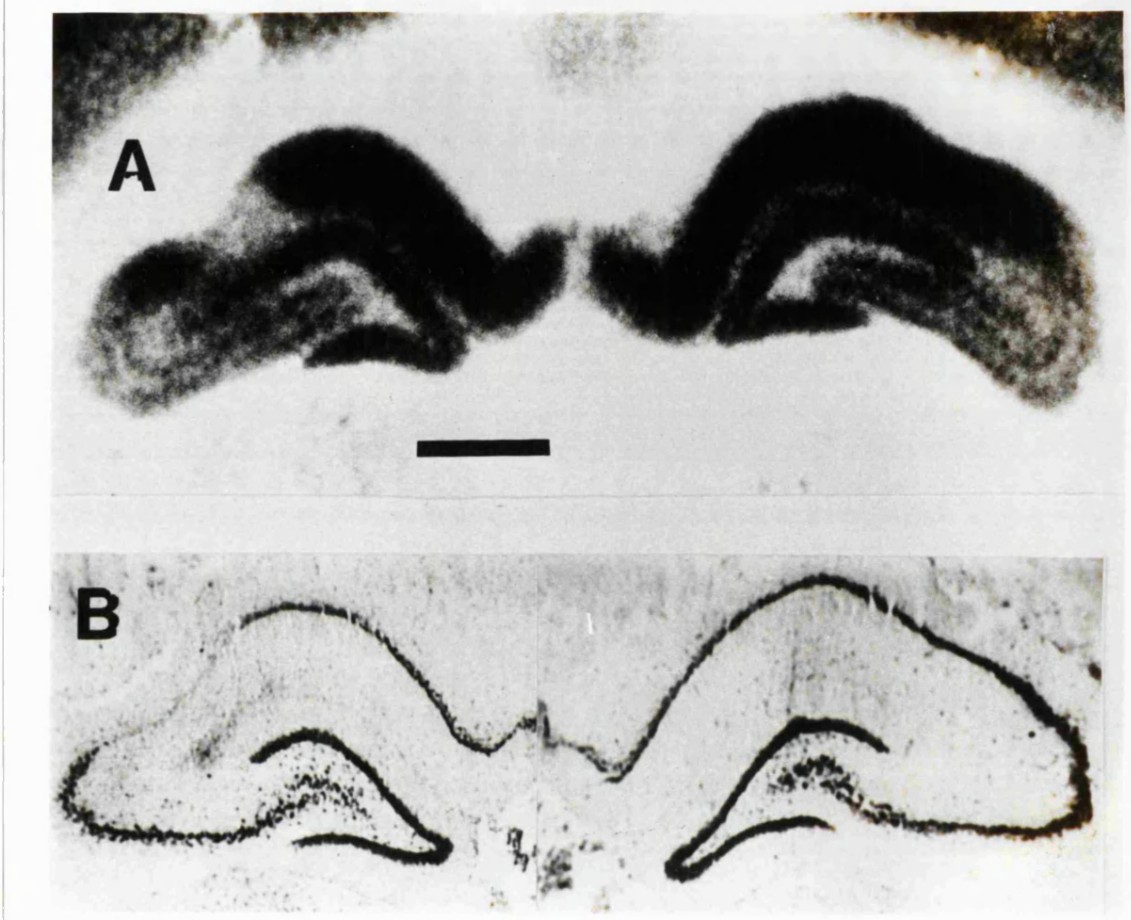

Figure 5.13: A: REPRESENTATIVE AUTORADIOGRAM OF THE BINDING OF [^{3}H] PIRENZEPINE IN THE HIPPOCAMPUS OF A VOLKENSIN INJECTED ANIMAL WITH B: CORRESPONDING NISSL STAINED SECTION. Experiments were performed using coronal rat brain sections (12 μm), incubated in PBS containing 2.5 nM [^{3}H] pirenzepine for 90 min at 25°C. Non-specific binding was generated using 10 μM unlabelled atropine. Nissl staining of closest corresponding section was performed as described in section 2.7.3.
Injection site on left side. Scale bar (A) 1mm.

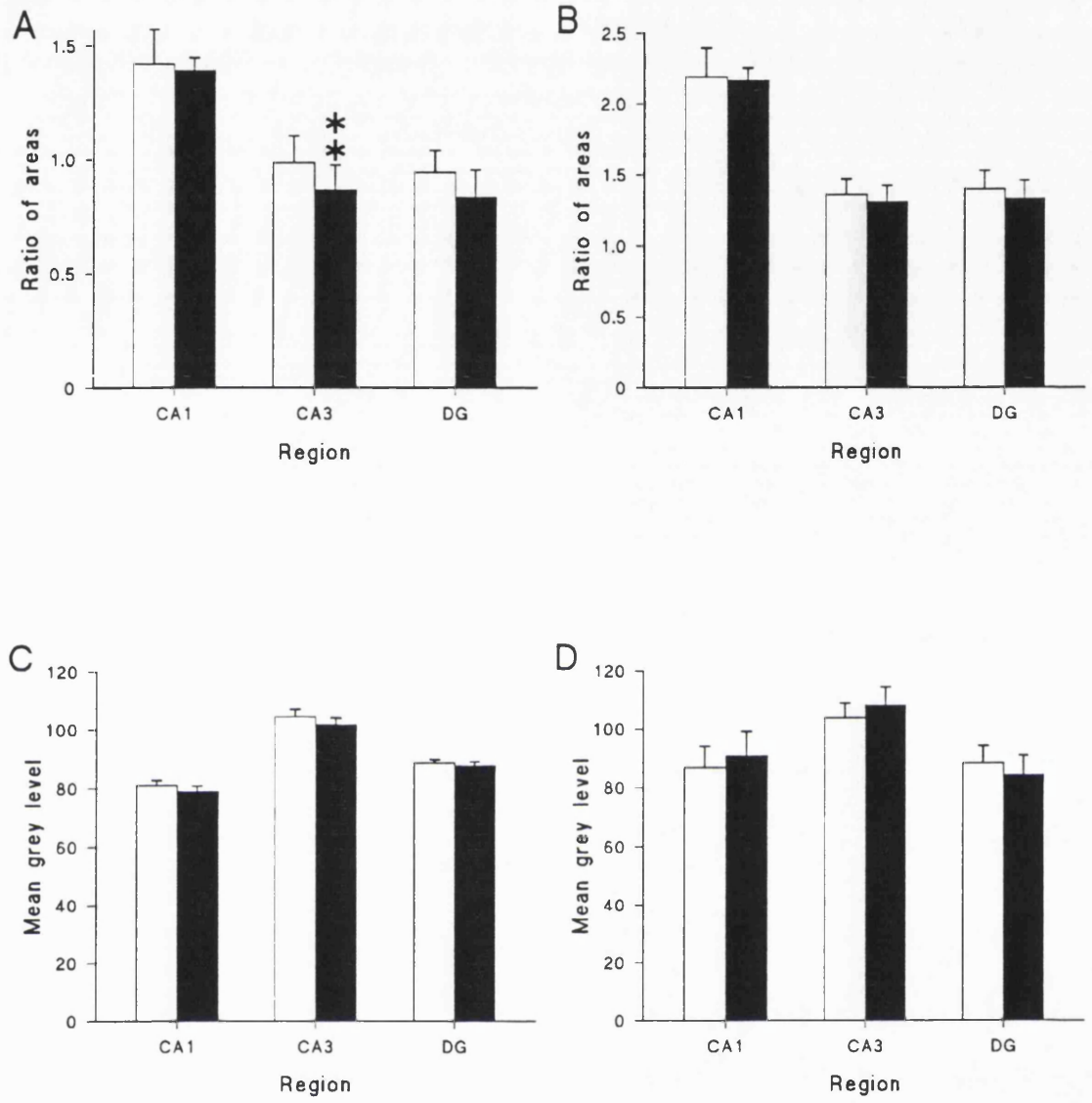

Figure 5.14: [^{3}H] PIRENZEPINE BINDING IN VOLKENSIN INJECTED ANIMALS. Experimental conditions were as described in Figure 5.13. Figures A and B show ratios calculated between area of autoradiographic binding and Nissl staining in animals injected with 2 ng volkensin with survival times of 14 (n=5) or 21 (n=5) days respectively. Figures C and D show the corresponding mean grey levels measured in the same animals and sections.
Error bars are SEM. Contralateral side- open bars; ipsilateral side- filled bars.
** $p < 0.01$ (Student's paired *t*-test).

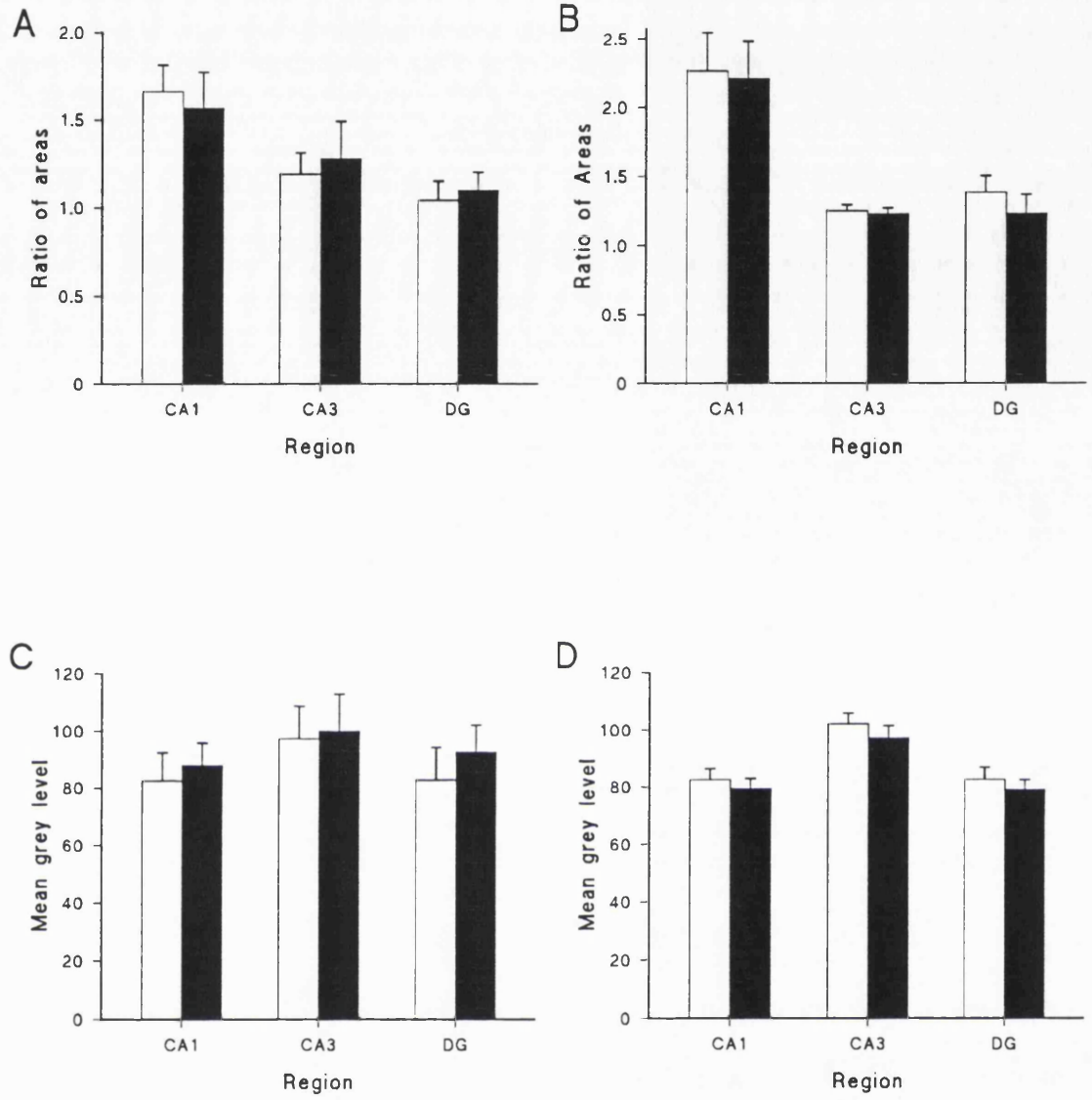

Figure 5.15: [^{3}H] PIRENZEPINE BINDING IN RICIN INJECTED ANIMALS. Experimental conditions were as described in Figure 5.13. Figures A and B show ratios calculated between area of autoradiographic binding and Nissl staining in animals injected with 10 ng ricin with survival times of 14 (n=3) or 21 (n=4) days respectively. Figures C and D show the corresponding mean grey levels measured in the same animals and sections.
Error bars are SEM. Contralateral side- open bars; ipsilateral side- filled bars. No significant differences.

5.3 Discussion.

5.3.1 Experimental considerations.

The distribution of the NMDA receptor- ionophore complex in the hippocampus as visualised using [^{3}H] L-689,560 was similar to that observed by other workers using various ligands. Monaghan and co-workers (1985) used [^{3}H] glutamate and reported that binding sites in the stratum radiatum of the hippocampus exhibited pharmacological profiles characteristic of the NMDA receptor. Other workers have used [^{3}H] CGP-39653 (Cimino et al., 1992) or [^{3}H] MK-801 (Subramanium and Mcgonigle, 1990) and report a similar pattern of binding in the hippocampus as that observed in the present study. The pharmacological specificity of [^{3}H] L-689,560 has been investigated in a report using rat brain membranes (Grimwood et al., 1992), and a comparison of the IC_{50} values of 21 compounds for [^{3}H] glycine and [^{3}H] L-689,560 indicated a 1:1 correlation with a coefficient of 0.97. It can therefore be confidently assumed that [^{3}H] L-689,560 binds to the glycine modulatory site of the NMDA receptor- ionophore complex. The non-specific signal using [^{3}H] L-689,560 was lower than that reported using [^{3}H] amino acids (Pangalos, 1992).

The distribution of the kainate sensitive glutamate receptor visualised using [^{3}H] kainate was similar to that observed by other workers (Monaghan and Cotman, 1982; Ulas et al., 1990), with preferential labelling of sites corresponding to the pyramidal cell layer of CA3. At the time that these experiments were performed, it was not clear whether the kainate and AMPA sensitive glutamate receptors were identical (Miller, 1991; Patneau and Mayer, 1991; Cai and Erdo, 1992), so displacement experiments using unlabelled AMPA were performed. No significant displacement of [^{3}H] kainate by AMPA was observed. Cloning and *in-situ* hybridisation for the KA1 gene product has demonstrated predominate expression in hippocampal CA3 pyramidal cells (Werner et al., 1991), which is in good agreement with autoradiographic findings. The effects of the addition of Ca^{2+} in the incubation medium were investigated, following reports that Ca^{2+} selectively inhibits high affinity kainate binding (Greenamyre et al., 1985a), and [^{3}H] glutamate binding to a kainate sensitive site (Monaghan et al., 1985). Addition of this ion significantly

reduced [^{3}H] kainate binding, and subsequent experiments were performed in the absence of Ca^{2+}.

The distribution of the $GABA_A$ receptor complex visualised using [^{3}H] GABA in the presence of baclofen was similar to that observed by other workers. Chu et al. (1990) and Bowery et al. (1987) described homogeneous binding in oriens, radiatum and pyramidal cell layers of the hippocampus, with higher levels of binding in the molecular layer of DG. This is in good agreement with *in-situ* hybridisation studies for $GABA_A$ receptor subunit expression levels (Wisden et al., 1992), which also hypothesised that hippocampal $GABA_A$ receptors lack a functional benzodiazepine binding site. It was noted that in animals injected with 2 ng volkensin, with a 14 day survival time, binding was less distinct than that observed in the other groups. This may be attributable to two factors: the 14 day volkensin group of animals were perfused with 30 % sucrose in PBS; all other groups were perfused with 20 % sucrose in PBS. Brains from animals perfused with the higher concentrations of sucrose were dramatically shrunken when compared with the remaining groups, and this may have contributed to the lack of resolution. Additionally, volkensin injected animals with a 14 day survival time were the first group to be prepared, and thus sections from these animals had the longest duration of storage, although comparison of the binding of [^{3}H] GABA to these sections with binding to control sections with a longer storage time revealed no apparent relationship between storage time and binding resolution.

The distribution of the 5-HT_{1A} receptor visualised using [^{3}H] 8-OH-DPAT was similar to that described by other workers (Pazos and Palacios, 1985; Chalmers and Watson, 1991). Tanaka et al. (1991) found a similar distribution of 5-HT_{1A} receptors using [^{3}H] tandospirone, a high affinity ligand for the receptor. Correlation of receptor binding with *in-situ* hybridisation for mRNA encoding for the 5-HT_{1A} receptor revealed differences in distribution (Pompeiano et al., 1992) which may be accounted for by a preferential location of 5-HT_{1A} receptors on the dendrites of the pyramidal cells of the CA fields and granule cells of the DG. This finding may also explain the lack of confinement of binding of [^{3}H] 8-OH-DPAT to distinct laminae of the hippocampal fields. Electrophysiological studies confirm the presence of

receptors on the dendrites of hippocampal pyramidal cells consistent with a pharmacological profile of 5-HT_{1A} receptors (Andrade and Nicoll, 1987a; Beck and Choi, 1991; Andrade, 1992).

The distribution of muscarinic M_1 receptors, visualised using [^{3}H] pirenzepine, is similar to that described by other workers (Tonnaer et al., 1988), as are binding patterns observed using other ligands (Atack et al., 1989; Messer et al., 1989; Frey and Howland, 1992). *In-situ* hybridisation histochemistry revealed a high level of mRNA encoding for the m_1 receptor in the pyramidal cell layer of the hippocampus and the granule cell layer of the DG (Brann et al., 1988; Buckley et al., 1988). The pharmacological specificity of pirenzepine has been previously established by both ligand binding (Buckley and Burnstock, 1986; Frey and Howland, 1992) and by comparison with data obtained by cloning and transfection of receptors into cell lines (Buckley et al., 1989; Hulme et al., 1990). However, a component of pirenzepine binding can be attributed to affinity for the M_4 receptor, a factor which has been carefully considered in the context of this study. The relative K_d values for pirenzepine binding to M_1 and M_4 receptors respectively are 16 and 87 nM (N.R. Buckley, personal communication), and on the basis of this it is possible to calculate the proportional occupancies of each receptor subtype. At the concentration of [^{3}H] pirenzepine used in these studies, the highest theoretical proportion of binding attributable to the M_4 receptor is approximately 15 %. It is unlikely that the actual percentage of [^{3}H] pirenzepine binding to the M_4 receptor will be this high, as *in-situ* hybridisation histochemistry revealed a low level of m_4 mRNA in the hippocampal formation (Buckley et al., 1988).

5.3.2 Inferences and limitations of ratio calculations.

As described in chapter 4, the main histological finding of these studies was loss of a discrete subpopulation of CA3 hippocampal pyramidal neurones. Due to the nature of the morphological changes observed, previous methods of ascribing biochemical changes to the affected neurones (Francis et al., 1992b) were considered to be inappropriate. Therefore, comparisons between change observed in Nissl stained sections and corresponding autoradiograms were performed by calculation of a ratio, though as previously, the mean grey level

in each of the areas measured was determined, and was considered to reflect the receptor density. It is likely that this additional iteration in analysis, rather than direct comparison, would reduce the sensitivity of this technique to identify small changes in the receptor binding associated with autoradiograms. Therefore, in some cases, qualitative differences in ratios where statistical differences were not attained are considered, along with those that have reached or exceeded the normal value for rejection of the null hypothesis.

There are three possible outcomes for comparison of ratios calculated for sides ipsilateral and contralateral to the injection, each with its own interpretation:

(1) No difference in ratio:
Interpretation: The loss of binding in the autoradiogram corresponds directly to the neuronal loss observed in Nissl stained sections; the receptors under investigation are present on the neurones affected by volkensin but are equally abundant upon the remaining neurones.

(2) Ratio increased on ipsilateral side compared to contralateral:
Interpretation: Binding is maintained where neuronal loss has occurred in the corresponding Nissl stained sections; the receptors under investigation are not present on the neurones affected by volkensin.

(3) Ratio decreased on ipsilateral side compared to contralateral:
Interpretation: Loss of binding exceeds neuronal loss in corresponding Nissl stained sections; the neurones affected by volkensin carry a disproportionately high number of the receptors compared to the remaining neurones and the receptor can be considered to be "enriched" on the affected neurones.

There are several possible confounding factors to these interpretations: (i) that the length or area measured in the autoradiogram does not correspond to the area of cell loss observed in Nissl stained sections; this is unlikely, as the

pattern of binding observed in the autoradiogram was very carefully matched to the area of neuronal loss observed in the corresponding Nissl stained sections, by superimposing one image onto the other, so that measurements made from autoradiograms were in areas of cell loss observed in Nissl stained sections. (ii) Adaptive changes in receptor number occurred following volkensin injection and neuronal loss; though this is possible, only upregulation of the receptor type under investigation would effectively mask any changes observed, and the lack of change of mean grey level measured in the autoradiograms predominately excludes this possibility. (iii) Changes observed are due to the loss of receptors present on terminals of neurones projecting from the entorhinal cortex to the area of neuronal loss; this is unlikely, as no differences in ratios between sides ipsilateral and contralateral to the lesion were found in animals injected with 10 ng ricin. (iv) Changes observed are due to the diffusion of volkensin from the injection site; this possibility is described in Chapter 4, section 4.3.1, and is excluded by investigation of animals injected with 10 ng ricin, and by performing *in-situ* hybridisation for GAD mRNA. No changes were observed for either of these parameters between sides ipsilateral and contralateral to the injection.

5.3.3 Receptor distribution and localisation in lesioned animals.

The ratios calculated for the binding of [^{3}H] L-689,560 were unchanged between sides ipsilateral and contralateral to the lesion. This data suggests that binding to the NMDA receptor- ionophore complex is reduced in parallel with the loss of hippocampal pyramidal neurones, consistent with the hypothesis that these receptors are present on the affected neurones, but are equally abundant upon the remaining neurones. As the binding of [^{3}H] L-689,560 extends beyond the boundaries of the pyramidal cell perikarya, it may be assumed that the receptors are also present on the dendrites of the pyramidal neurones. The localisation of the NMDA receptor- ionophore complex to hippocampal pyramidal neurones suggests that these receptors have a role in the regulation of the activity of the hippocampal formation, in accordance with electrophysiological data (Gibb and Colquhoun, 1991). Indices of the NMDA receptor- ionophore complex can also be obtained from studies of arachidonic acid release (Pellerin and Wolfe, 1991) and investigation of the

effects of nitric oxide synthase inhibitors (Kato and Zorumski, 1993); both studies support the presence of NMDA receptors on the pyramidal cells of the hippocampus. Preservation of GAD-mRNA positive cells in this study suggests that the receptors are not localised on interneurones. It is unlikely that the receptors are presynaptic autoreceptors on terminals of axons projecting from the entorhinal cortex, as volkensin injection would destroy these projections, and no changes consistent with this hypothesis were observed. Electrolytic lesions of the entorhinal cortex (Bekenstein et al., 1990) or knife cuts of efferents from the entorhinal cortex (Maragos et al., 1991) had no effect of the number of NMDA receptors in CA1 and CA3 pyramidal cell layers which is additional confirmation that the receptors are located postsynaptically. The lack of change in grey levels between hippocampal areas, measured ipsilateral and contralateral to the lesion suggests that no adaptive upregulation of receptor number occurred subsequent to the lesioning procedure.

The ratios calculated for the binding of [^{3}H] kainate were unchanged between sides ipsilateral and contralateral to the lesion. This data suggests that binding to the kainate sensitive glutamate is reduced in parallel with the loss of hippocampal pyramidal neurones, consistent with the hypothesis that these receptors are present on the affected neurones, but are equally abundant upon the remaining neurones. Though autoradiograms suggest a heterogeneous distribution of [^{3}H] L-689,560 and [^{3}H] kainate, the present study suggests that both NMDA and kainate sensitive glutamate receptors are localised to the pyramidal neurones of CA3. Electrophysiological (Jonas and Sakmann, 1992) and *in-situ* hybridisation (Werner et al., 1991) studies confirm the presence of kainate sensitive receptors on these neurones. Unilateral lesions of the entorhinal cortex increased the number of kainate binding sites in the DG (Ulas et al., 1990), but only at postoperative survival times of more than 21 days. In the present study, no significant increases in binding on the lesioned side were observed, though the ratio calculated for the lesioned side at 14 days was slightly increased, and it is possible that animals with a survival time of longer than 21 days would have exhibited more profound changes in the DG. Preservation of GAD-mRNA positive cells in this study suggests that the receptors are not localised on interneurones. It is unlikely that the

receptors are presynaptic autoreceptors on terminals of axons projecting from the entorhinal cortex, as volkensin injection would destroy these projections, and no changes consistent with this hypothesis were observed. The present study, therefore, indicates that the excitatory amino acid receptors sensitive to NMDA and kainate are present on CA3 hippocampal pyramidal neurones.

Studies of autoradiograms of the binding of [^{3}H] GABA to the $GABA_A$ receptor revealed that in volkensin injected animals with a survival time of 14 days, the ratio calculated for the side ipsilateral to the lesion was increased compared to that of the contralateral side. These data suggest that binding to the $GABA_A$ receptor was maintained in areas where neuronal loss had occurred, and that these $GABA_A$ receptors are not associated with the affected neurones. However, $GABA_A$ receptors have been reported to be present on cultured hippocampal pyramidal neurones (Kristiansen et al., 1991), and the difference in ratios observed in the present study was not observed in animals with a 21 day survival time, so other interpretations must also be considered. In animals receiving unilateral intrastriatal injection of volkensin, marked reactive gliosis occurred in the area of cell loss, and in preliminary investigations of gliosis in these animals, a similar phenomenon was observed. Paucity of sections meant that a full immunocytochemical study using antibodies to glial fibrillary acidic protein could not be performed. However, the available evidence does suggest that some degree of gliosis occurred, and it is possible that this gliosis accounts for increase in the binding of [^{3}H] GABA to the $GABA_A$ receptor, as these receptors have been reported to be present on glia (Von Blankenfeld and Kettenmann, 1992). However, it is unlikely that the gliosis would recede after a further 7 day survival time. A more likely interpretation for the persistence of binding observed ipsilaterally at a 14 day survival time is that a proportion of $GABA_A$ receptors are localised on neurones remaining after volkensin injection, which are in close apposition to CA3 pyramidal neurones. Destruction of the entorhinal cortex reduces the perforant path input to the DG, which in turn reduces excitatory mossy fibre innervation to CA3. At a survival time of greater than 14 days, an adaptive change in the number of $GABA_A$ receptors may occur, as a compensatory effect following loss of excitatory or inhibitory input. Additional support for adaptive

change in the inhibitory control of mossy fibres is provided by the observation that $GABA_A$ binding is reduced in the DG in areas corresponding to the cells of origin of these fibres on the side ipsilateral to the injection at a 21 day survival time (reduction in ipsilateral ratio compared to contralateral in the DG). Alternatively, the increases observed in [^{3}H] GABA binding may be attributable to re-innervation of the hippocampus following loss of entorhinal-hippocampal projections (Parent et al., 1993), although this hypothesis is not supported by data from ricin injected animals. However, the lack of change of grey levels in any area measured supports a topographical loss in perforant pathway innervation.

The ratios calculated for the binding of [^{3}H] 8-OH-DPAT were unchanged between sides ipsilateral and contralateral to the lesion. This data suggests that binding to the 5-HT_{1A} receptor is reduced in parallel with the loss of hippocampal pyramidal neurones, consistent with the hypothesis that a proportion of these receptors are present on the affected neurones. Though statistical significance was not attained, the ratio calculated for the side ipsilateral to the lesion was higher in CA3 compared to that calculated for the contralateral side in both 14 and 21 day survival animal groups (0.88 vs. 0.66 and 1.61 vs. 1.35 respectively). This indicates that a small component of binding was preserved in areas where neuronal loss had occurred. There are two possible interpretations of this data. Firstly, it has been reported that 5-HT_{1A} receptors are present on glial cells (Whitaker-Azmitia and Azmitia, 1989; Whitaker-Azmitia et al., 1990), which may account for the increase in binding observed. Secondly, a small proportion of 5-HT_{1A} receptors may be present on the neurones remaining after volkensin injection and, in the context of determination of the degree of localisation of receptor types on the affected neurones, it is possible that 5-HT_{1A} receptors are less enriched than those of the excitatory amino acid transmitters. However, this data does indicate that some localisation of the receptor to CA3 pyramidal cells, which is in agreement with electrophysiological data (Beck and Choi, 1991). At the 21 day survival time, the ratio calculated for the DG ipsilateral to the injection was reduced compared to the contralateral value, reflecting reduced binding in this area. As 5-HT_{1A} receptor activation is inhibitory (McCormick and Williamson, 1989), it

is probable that an adaptive change occurred in this area to compensate for the loss of excitatory perforant pathway innervation. Again, the lack of change of grey levels between sides ipsilateral and contralateral to the lesion is indicative of topographical changes in the DG.

Studies of autoradiograms of the binding of [^{3}H] pirenzepine to the muscarinic M_1 receptor revealed that in volkensin injected animals with a survival time of 14 days, the ratio calculated for the side ipsilateral to the lesion in the CA3 area was significantly decreased compared to that of the contralateral side. This data suggests that the number of M_1 receptors in the area affected by volkensin injection was reduced over and above that of the magnitude of the cell loss. The most likely interpretation of this data is that muscarinic M_1 receptors are significantly enriched upon the affected pyramidal neurones, which is supported by data from *in-situ* hybridisation studies, where high levels of m_1 mRNA was observed in the pyramidal cell layer of the hippocampus (Buckley et al., 1988). No significant differences in ratios between ipsilateral and contralateral sides were observed for CA1 or DG at either survival time. It is interesting to note that the difference in ratio observed in CA3 at a 14 day survival time is not maintained at a 21 day survival time, where no significant differences were observed. The reason for this is unclear, though Monaghan et al. (1982) observed plasticity of muscarinic receptors following entorhinal ablation with a subsequent upregulation of receptor number in the DG, though the ligand utilised ([^{3}H] quinuclidinyl benzilate) labels all muscarinic receptor subtypes. Thus, the apparent increase in receptor number on CA3 pyramidal neurones may reflect an adaptive upregulation of M_1 receptors upon the remaining neurones, though no differences in ratios in any area were observed in animals injected with 10 ng ricin. An alternative explanation is that the M_1 receptor is rather labile, and is lost at a rate which exceeds that of neuronal loss, and thus a disproportionate receptor loss is observed at a 14 day survival time.

In the context of this study, it is not possible to provide a <u>direct</u> quantitative comparison of the degree of receptor enrichment on CA3 hippocampal pyramidal neurones. However, this study does demonstrate the

presence of muscarinic M_1, NMDA and kainate sensitive glutamate, and 5-HT_{1A} receptors upon these cells with some certainty. The neurones affected by volkensin appear to carry a disproportionately high number of muscarinic M_1 receptors compared to the remaining neurones and the receptor can be considered to be enriched on the affected neurones. By contrast, little localisation of the $GABA_A$ receptor was observed, and the remaining structures carry a higher proportion of this receptor. Enrichment of NMDA, kainate and 5-HT_{1A} receptors appears to be intermediate, and this study indicates a similar proportion of these receptors upon the affected neurones and the remaining neurones.

CHAPTER 6: Histological investigations of a subpopulation of pyramidal neurones following unilateral striatal injections of neurotoxic agents.

6.1 Introduction.

The major cell type of the neocortex is the pyramidal cell, which accounts for some 70 % of all neurones. It has proved difficult to lesion selectively these neurones using traditional techniques, and to subsequently ascribe biochemical changes observed in some neurodegenerative diseases to loss of specific cell structures (Sofroniew and Pearson, 1985; Middlemiss et al., 1986a). Previous studies have developed the use of the retrogradely transported toxic lectin, volkensin, to produce a loss of a subpopulation of neocortical neurones (Pangalos et al., 1991b; Pangalos, 1992), and to investigate a number of biochemical sequelae following the loss of this anatomically defined subpopulation of cells (Pangalos et al., 1991b; Francis et al., 1992a; Pangalos et al., 1992). In the present study, these investigations have been extended to include the study of additional receptor subtypes (Chapter 7), with biochemical and histological examination of additional groups of volkensin and ricin injected animals. The initial objective, therefore, was to prepare groups of animals and to investigate the consistency of volkensin induced selective loss of pyramidal cells of origin of the corticostriatal pathway located in neocortical lamina V.

6.2 Results.

6.2.1 Determination of injection placement, volkensin dosage, and survival time.

Experiments investigating volkensin dosage and survival time were based on the findings of Pangalos et al. (1991b), where doses of 2 ng volkensin, with a 28 day postoperative survival time were used. Initial stereotaxic placements were modified following injection of Evans Blue, to allow optimal targeting of the striatum. All subsequent injections were performed as described in section 2.6.2.

6.2.2 Determination of excitotoxin injection placement, dosage and survival time.

All experiments pertaining to the injection placement, dosage and survival time for the excitotoxic striatal injection (EXS) were performed elsewhere (G.A. Hicks, Dept. Pharmacology, University of Bristol). Preliminary experiments to determine the optimal placement of the injection apparatus for the excitotoxic thalamic injection (EXTH) were performed using Evans Blue dye. Initial estimates of dosage and survival time were provided by other workers (T.W. Robbins and M. Snape, personal communications). Lesions of the thalamic nucleus by other workers confirmed that the doses and survival times used in this study were sufficient to cause neurochemical (Price et al., 1993) and behavioural changes (McAlonan et al., 1993). Lesions utilising excitotoxins rather that agents which inhibit protein synthesis are considerably more difficult to assess histologically, as gross anatomical and morphological changes are often masked by extensive gliosis and the lack of clear histological cellular markers in the thalamic and striatal regions precludes quantitative cell number analysis. However, qualitative examination of sections from EXTH and EXS animals confirmed that some degree of disruption had occurred in the target areas, and it must be inferred that loss of terminals projecting to sites distal to the injection had occurred.

6.2.3 Cell loss as a result of spread of toxins directly from the injection site.

Injections of 2 ng volkensin and 10 ng ricin centred on the left striatum, and 10 μg quinolinate injections centred on the right striatum. The thalamic injection of 7.5 μg ibotenate centred on the (left) reticular thalamic nucleus (RTN), ventral posterolateral (VPL) and the ventrolateral thalamic nucleus (VLTN).

Damage caused by injection of 2 ng volkensin (Figure 6.1) was compared with that observed in a previously prepared group of animals (group 1). In the second group of 6 animals (group 2), the volume of the striatum destroyed was similar to that observed in group 1 animals. The third group of animals (group 3) exhibited slightly more damage than the other two groups, which may be

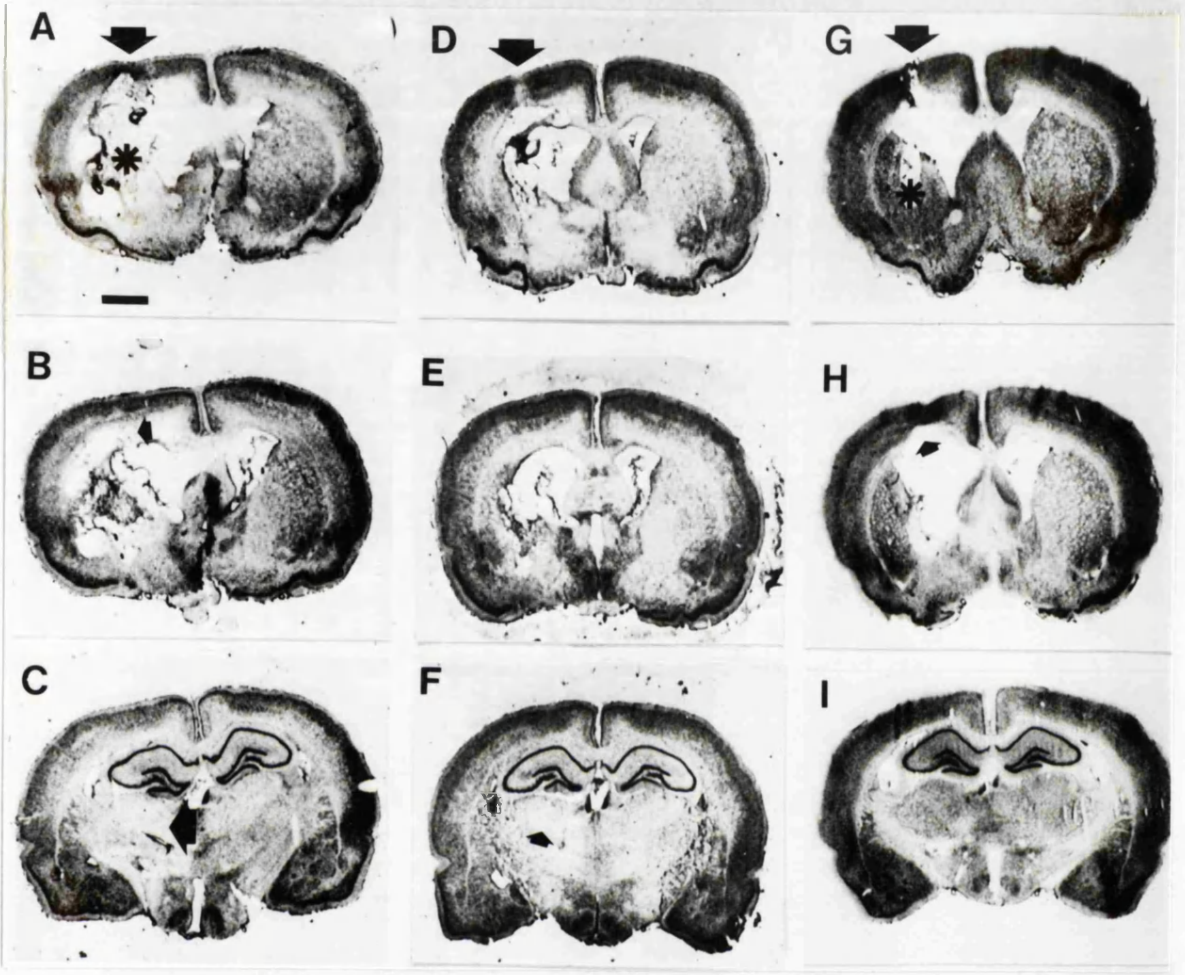

Figure 6.1: PHOTOMICROGRAPHS OF CORONAL SECTIONS OF THE BRAIN AT DIFFERENT ROSTRO-CAUDAL LEVELS FOLLOWING UNILATERAL INTRASTRIATAL INJECTION OF VOLKENSIN OR RICIN. A-C; rat brain from group 3 following 2 ng volkensin injection. Large arrow and asterisk on A mark areas of neocortical damage caused by the needle, and the centre of the injection, respectievly. Small arrow in B shows damage caused by limited spread of the toxin to deep layers of the cortex. Direct involvement of the thalamic nuclei is marked in C (arrow). D - F; rat brain from group 2 following 2 ng volkensin injection, showing needle damage to the cortex (arrow in D), and direct thalamic damage (arrow in F). G - I; appearance of rat brain following intrastriatal injection of 10 ng ricin. Arrow and asterisk in G mark needle damage and centre of injection, respectively. Arrow in H shows limited cortical damage caused by direct spread of ricin from the injection site.
All micrographs taken at the same magnification. Injection on left side. Sections counterstained with cresyl violet. Scale bar (in A) 2 mm.

attributable to the use of a different batch of volkensin. In both groups, more than 70 % of the volume of the striatum was destroyed with limited collapse of the structure of the hemisphere. Cell loss in the septal nucleus was observed in one animal, though damage to other basal forebrain structures was observed in 5 of the 12 animals; there was damage of thalamic areas (mainly anterolateral, anteroventral and ventrolateral poles, group 3) due to spread of the toxin. Damage to the dorsal endopiriform nucleus, which is in very close apposition to the striatum, was observed in the majority of animals. The neocortex overlying the striatum showed evidence of direct damage due to the passage of the needle, though there was limited evidence of damage due to spread of the toxin around the needle tract in some animals. In volkensin injected animals, all showed no more damage to the overlying cortex than was seen in ricin injected animals. Subsequent histological and biochemical investigation in all animals was performed at least 1.5 mm posterior to the needle tract. At this level, the lamina structure of the neocortex was intact, and there was no evidence of cell loss in the underlying hippocampus (except in one group 3 animal, where limited damage to the CA1 anterior hippocampal areas was observed) or damage to the corpus callosum, indicating that changes in these areas were not due to spread of the toxin from the injection site.

Injection of 10 ng ricin caused extensive necrosis in the striatum, producing a lesion similar in volume to that following 2 ng volkensin (Figure 6.1). No damage was observed in any surrounding structures. Only one group of 6 animals was prepared using 10 ng ricin, as a number of sections were available from a previously prepared group.

Injection of 10 μg quinolinate into the striatum caused qualitative changes in the appearance of the striatum in freshly cut sections, with visible areas of necrosis in Nissl stained sections (Figure 6.2). As described above, excitotoxins cause necrosis at the needle tip, though the exact area of spread becomes more subtle at the outer margins of the affected area. However, in all animals studied, the toxin diffused throughout the striatum. In one of the six animals, there was also apparent involvement of more posteromedial structures, including ventrolateral and anteroventral thalamic nuclei and the mamillothalamic tract. Confirmation of the loss of terminals of neurones

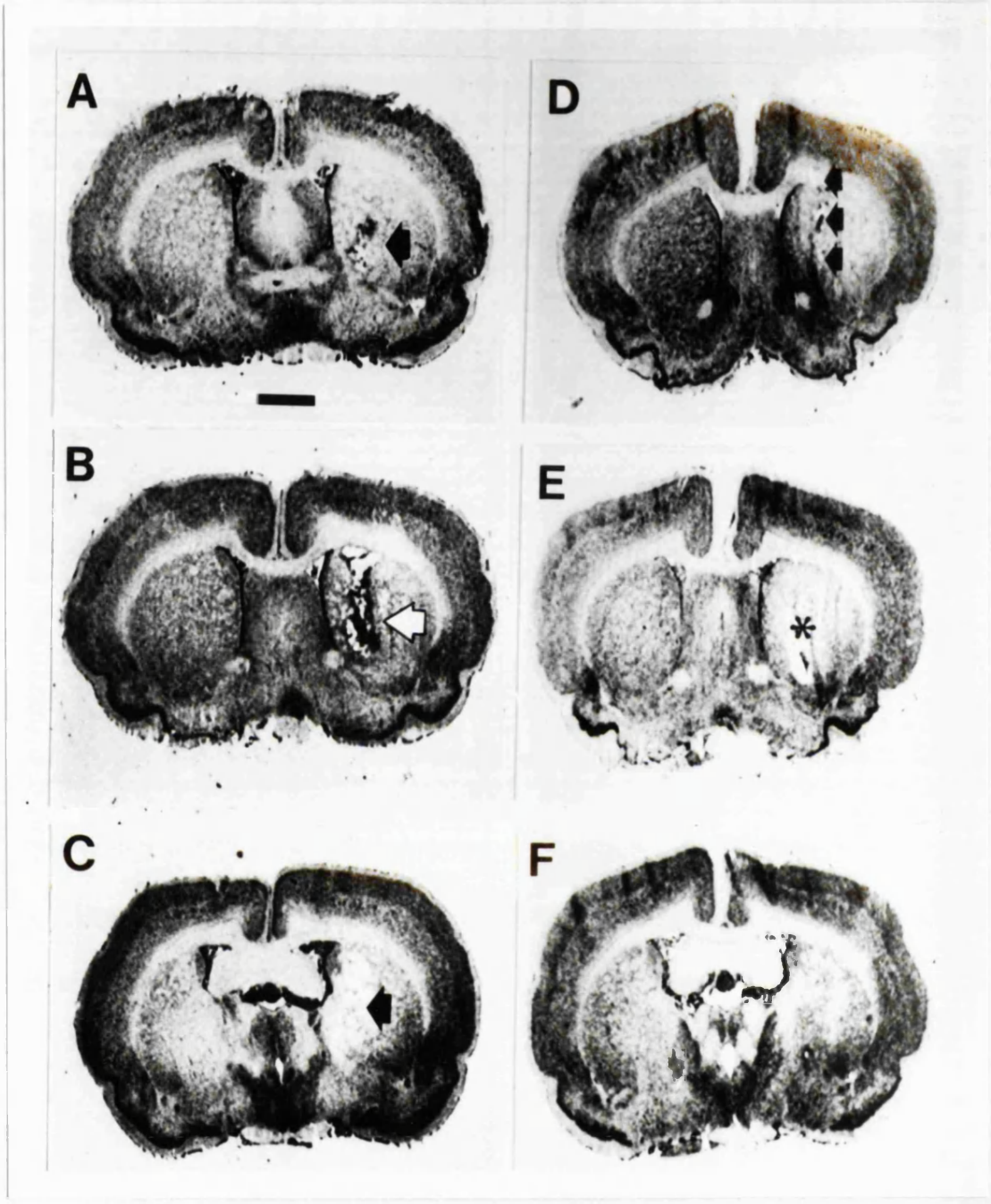

Figure 6.2: PHOTOMICROGRAPHS OF CORONAL SECTIONS OF THE BRAIN AT DIFFERENT ROSTRO-CAUDAL LEVELS FOLLOWING UNILATERAL INTRASTRIAL INJECTION OF 10 μg QUINOLINATE. A-C; rat 1 showing typical lesion; necrosis and gliosis in the striatum is marked by arrows in A, B and C. D-F; rat 2 showing more limited lesion; arrowheads in D show needle tract, and asterisk in E shows stereotaxic centre of injection.
All micrographs taken at the same magnification. Injection on right side. Sections counterstained with cresyl violet. Scale bar (in A) 2 mm.

projecting from the striatum was provided by the finding of a 40 % reduction in the binding of [^{3}H] SCH-23390 to D_1 receptors in the substantia nigra pars reticulata, a marker for terminals of projections from the striatum (Harrison et al., 1990; Cameron and Williams, 1993).

Injection of 7.5 μg ibotenate caused a degree of local necrosis and gliosis at the site of injection (Figure 6.3), which was more marked in the 12 day survival time group. Careful microscopic examination of sections from animals with both survival times revealed that in all cases, anterior (anterodorsal and anteromedial), ventral (ventrolateral and posterolateral) and reticular nuclei groups were affected (Faull and Mehler, 1985). Mediodorsal and paratenial nuclei groups were also affected, though to a lesser extent. In 4 animals, there was evidence of involvement of the basal nucleus of Meynert, and in 2 animals the entopeduncular nucleus was also affected.

6.2.4 Cell loss in sites distal to the injection site (other than in the neocortex) following intrastriatal volkensin and ricin injection.

Several neuronal populations known to project to the injection site were examined qualitatively for neuronal loss and compared with the corresponding contralateral side. There was substantial cell loss in the substantia nigra zona compacta in volkensin injected animals with subsequent collapse of the pars reticulata. Estimations of the extent of cell loss on the basis of Nissl stained area were 70 - 90 % (G.A. Hicks, personal communication), which is a little higher than that previously reported (Wiley and Stirpe, 1988), and may be attributed to a longer survival time. Interestingly, a loss of zona compacta neurones (30 - 40 %) was also observed in animals injected with 10 ng ricin. The most likely interpretation of this is that ricin destroys terminals of the striatonigral pathway, which terminate in the reticulata and compacta, and use GABA as their transmitter, release of which is regulated by dopamine D_1 receptors (Harrison et al., 1990; Cameron and Williams, 1993). Removal of tonic inhibition by GABA may give rise to excitotoxicity in the target neurones of the zona compacta, leading to cell death. Cell loss in the SN zona compacta was not observed following intrastriatal injection of quinolinate, where animals had a survival time of only 7 days, and it is likely that the

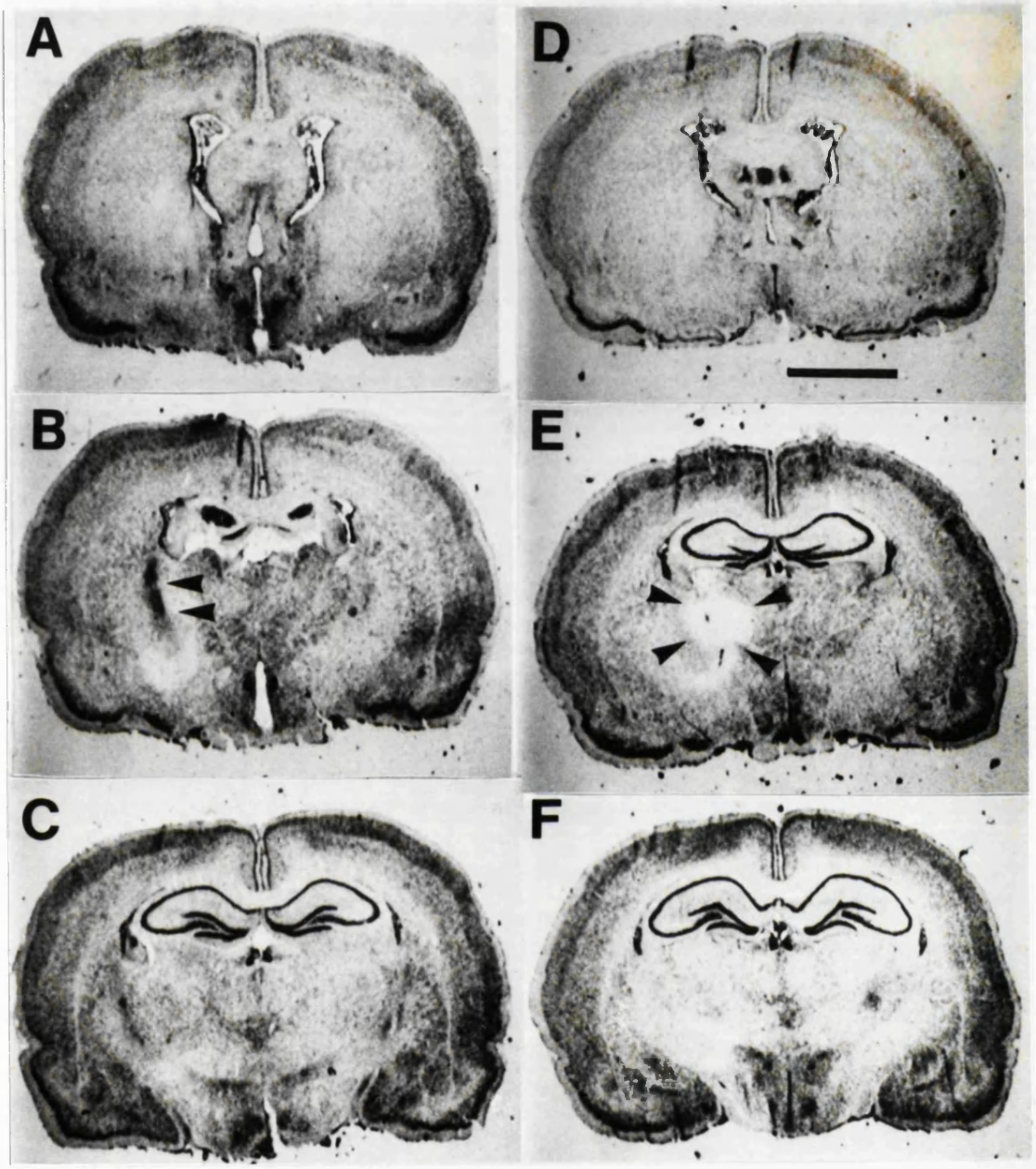

Figure 6.3: PHOTOMICROGRAPHS OF CORONAL SECTIONS OF THE BRAIN AT DIFFERENT ROSTRO-CAUDAL LEVELS FOLLOWING UNILATERAL INTRATHALAMIC INJECTION OF 7.5 μg IBOTENATE. A-C; representative appearance of lesion in 6 day postoperative survival time animal; arrowheads in B show area of marked gliosis at the centre of the injection, with damage visible to the reticular, ventrolateral and ventromedial thalamic nuclei, with more limited damage in the basal nucleus of Meynert. D-E; representative appearance of lesion in 12 day postoperative survival time animal; arrowheads (E) mark area of necrosis and cell loss, involving ventrolateral, ventral posteromedial, ventral posterolateral, laterodorsal and reticular thalamic nuclei.
All micrographs taken at the same magnification. Injection on left side. Sections counterstained with cresyl violet. Scale bar (in D) 3 mm.

trans-synaptic degeneration of zona compacta neurones is dependant on postoperative survival time. Studies using Abrin, another toxic lectin which is not transported in the CNS also reported inconsistent changes in the SN (Wiley and Stirpe, 1988). Assessment of cell loss in the thalamic centromedial nucleus following toxic lectin injection was not performed, as changes observed here could have been caused by diffusion of the toxins. There was evidence of cell loss in the ipsilateral dorsal raphe nucleus in volkensin injected animals, which was not apparent in animals injected with ricin.

6.2.5 Cell loss in sites distal to the injection site following injection of excitotoxins.

Qualitative examination of areas surrounding the injection site in Nissl stained sections for both thalamic and striatal lesions. At the level of the injection, no cell loss or apparent morphological changes were observed in any cortical lamina, except for slight damage caused by the passage of the needle. Examination of known areas of efferent connection of the thalamic regions (cingulate cortex, posterior hippocampus, substantia nigra, and areas of cortex distant from the injection site (Faull and Mehler, 1985)) revealed no apparent cellular changes. Examination of areas of known efferent projection of the striatum (substantia nigra and ventral tegmental areas, as well as several thalamic regions and cortical regions distant from the injection site (Heimer et al., 1985)) in animals receiving intrastriatal injection of quinolinate revealed no apparent cellular changes.

6.2.6 Assessment of neuronal loss in the neocortex following intrastriatal volkensin and ricin injections.

Loss of layer V neocortical pyramidal cells was clearly visible in animals injected with 2 ng volkensin, on the side ipsilateral to the injection (Figure 6.4), and occurred both anterior and posterior to the injection site. Cell loss posterior to the injection site was apparent in a broad area of cortex, from the medial margin to the rhinal fissure. Quantification of cell number and size was performed posterior to the injection site near to the medial margin (cortical areas Fr1/Fr2 and part of HL; groups 2, 3 and ricin) and more laterally

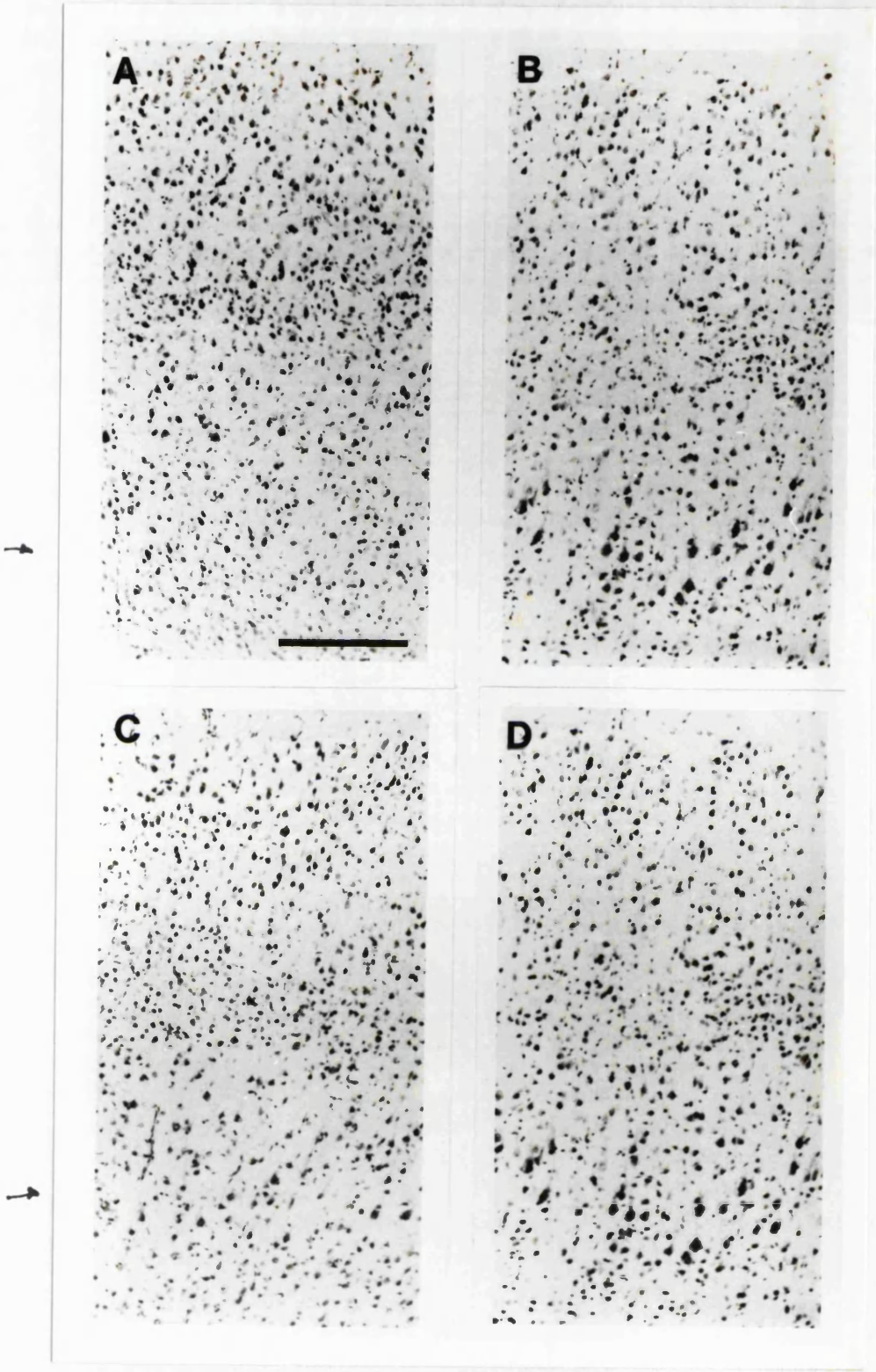

Figure 6.4: PHOTOMICROGRAPHS OF NEOCORTICAL CELL LOSS FOLLOWING UNILATERAL INTRASTRIATAL VOLKENSIN INJECTION. Photomicrographs show 12 μm coronal sections through the rat neocortex, counterstained with cresyl violet, 28 days after injection of volkensin into the left striatum (group 3 animal). A and B show ipsilateral and contralateral sides of medial neocortical areas (Fr1/Fr2), and C and D show more lateral areas (Par1/Par2) of the same case. Note the loss of large infragranular pyramidal neurones on the ipsilateral (left) side in both medial and lateral areas.
Scale bar 400 μm.

(cortical areas Par1/Par2; group 3 and ricin). Counts were performed only in sections where all six of the cortical laminae were apparent.

As described in the methods section (section 2.7.6.2), constraints were set on the image analysis system so that only cells of 70 μm^2 (supragranular cell counts) or 80 μm^2 (infragranular cell counts) or greater would be counted. These constraints excluded all glia and most smaller neurones. A loss of neocortical neurones on the side ipsilateral to the injection was clearly seen compared to the contralateral side (values are mean ± SEM, contralateral values in parentheses). Attention should be given to the percentage reductions, as the absolute cell number was a function of the frame size, which was varied between animal groups.

In a previously prepared group of animals (group 1; Pangalos et al., 1991b), in areas Fr1/Fr2, injection of 2 ng volkensin produced a significant reduction on the ipsilateral side to 71 % of the contralateral side in the infragranular layers, 107.5 ± 16.4 (151.6 ± 10.7), ($p < 0.01$, Student's paired *t*-test), and also a significant reduction to 84 % of the contralateral side in the supragranular layers, 125.2 ± 28.1 (149.8 ± 31.6), ($p < 0.05$, Student's paired *t*-test). These results are presented for comparison with animal groups prepared in this study (Table 6.1).

In group 2 animals (n=6), counts in Fr1/Fr2 yielded similar results. Injection of 2 ng volkensin produced a significant reduction on the ipsilateral side to 78 % of the contralateral side in the infragranular layers, 45.2 ± 5.5 (57.6 ± 7.3), ($p = 0.002$, Student's paired *t*-test). However, a reduction in the number of cells counted on the ipsilateral side in supragranular layers was not observed compared to contralateral in this group of animals, 57.8 ± 6.2 (56.4 ± 8.2). These results are summarised in Table 6.1, and Figure 6.5.

In group 3 animals (n=6), in areas Fr1/Fr2, injection of 2 ng volkensin produced a significant reduction on the ipsilateral side to 59 % of the contralateral side in the infragranular layers, 82.3 ± 11.2 (138.6 ± 16.8), ($p \approx 0.001$, Student's paired *t*-test). No significant reduction of cell number was observed in supragranular layers ipsilateral to the injection site compared to contralateral in this group of animals, 114.9 ± 12.8 (122.2 ± 9.7). In this group of animals, counts were also performed for Par1/Par2 areas, in both

Group	Fr1/Fr2		Par1/Par2	
	Infragranular	Supragranular	Infragranular	Supragranular
1	71*	84**	nd	nd
2	78†	102	nd	nd
3	59‡	94	72‡	94
Ricin	100	102	102	99

TABLE 6.1: NEOCORTICAL CELL LOSS FOLLOWING UNILATERAL INTRASTRIATAL INJECTION OF TOXIC LECTINS. Values are number of cell profiles of area > 80 μm^2 (infragranular) or > 70 μm^2 (supragranular) on ipsilateral side as % of contralateral side, following injection of 2 ng volkensin (groups 1,2 and 3, all n=6) or 10 ng ricin (n=6). Group 1 animals were prepared in a previous study.
* $p < 0.05$, ** $p < 0.01$, † $p < 0.005$, ‡ $p < 0.001$, significantly different to contralateral side, Student's paired *t*-test. nd; not determined.

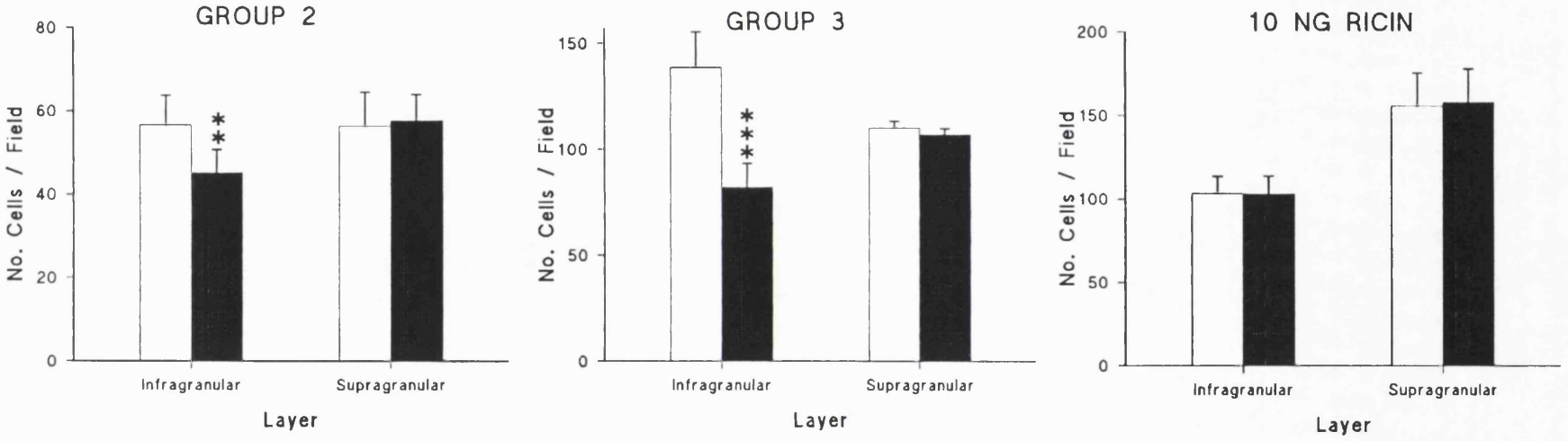

Figure 6.5: NEOCORTICAL CELL LOSS IN MEDIAL Fr1/Fr2 AREAS FOLLOWING INTRASTRIATAL INJECTION OF TOXIC LECTINS. Histograms show the mean number of cell profiles / field > 80 μm^2 (infragranular) or > 70 μm^2 in cross sectional area in the neocortex following intrastriatal injection of 2 ng volkensin (groups 2 and 3) or 10 ng ricin. All groups are n=6. Open bars; contralateral side; filled bars- ipsilateral side.
Error bars are SEM; ** $p < 0.005$; *** $p < 0.001$, significantly different to corresponding contralateral side (Student's paired *t*-test).

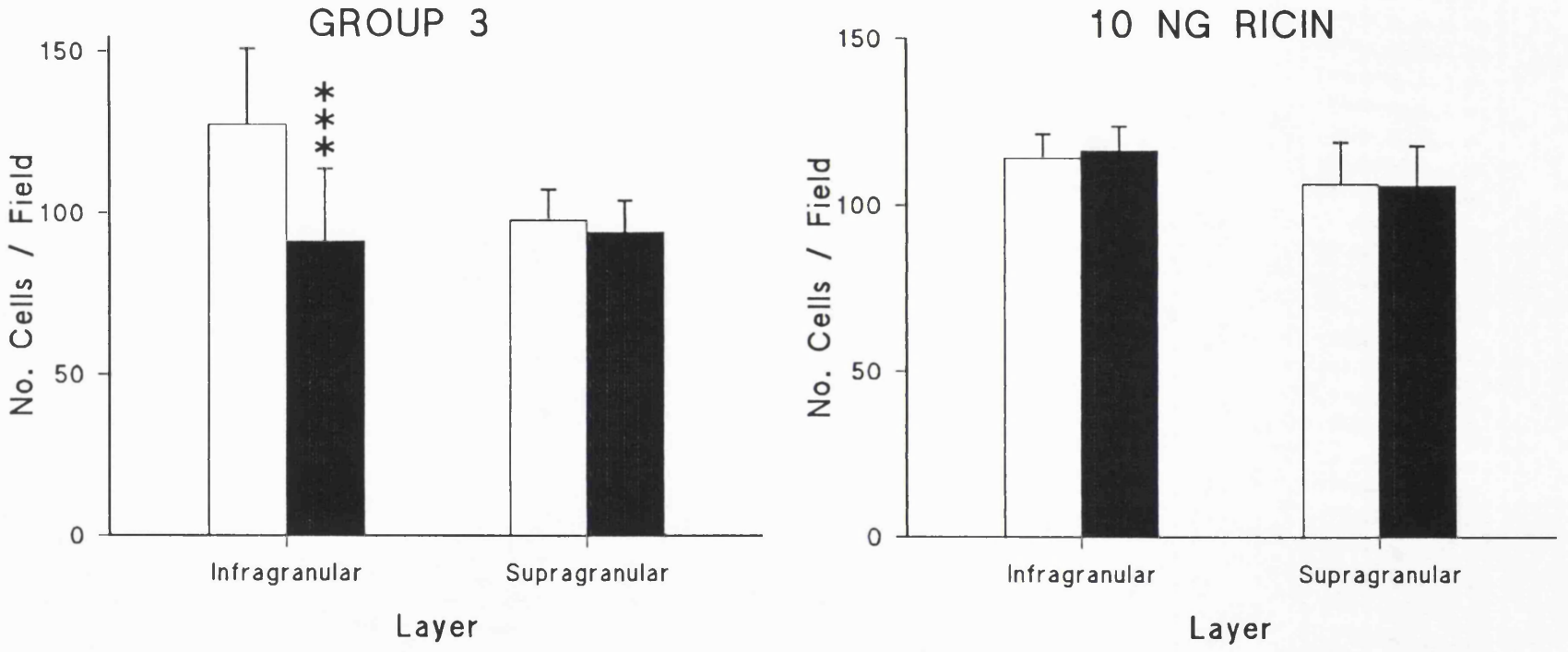

Figure 6.6: NEOCORTICAL CELL LOSS IN LATERAL Par1/Par2 AREAS FOLLOWING INTRASTRIATAL INJECTION OF TOXIC LECTINS. Histograms show the mean number of cell profiles / field > 80 μm^2 (infragranular) or > 70 μm^2 (supragranular) in cross sectional area in the neocortex following intrastriatal injection of 2 ng volkensin (group 3) or 10 ng ricin. All groups are n=6. Open bars; contralateral side; filled bars- ipsilateral side.
Error bars are SEM; *** $p < 0.001$, significantly different to corresponding contralateral side (Student's paired *t*-test)

infragranular and supragranular layers. Injection of 2 ng volkensin produced a significant reduction on the ipsilateral side to 71.9 % of the contralateral side in infragranular layers, 91.6 ± 22.2 (127.4 ± 23.5), ($p = 0.001$, Student's paired *t*-test). No significant reduction of cell number was observed in supragranular layers ipsilateral to the injection site compared to contralateral in this group of animals, 114.9 ± 12.8 (122.2 ± 9.7). These results are summarised in Table 6.1, and Figure 6.6.

In a group of animals injected with 10 ng ricin (n=6), no significant differences were observed in the number of cells counted ipsilateral to the injection compared with contralateral, in Fr1/Fr2 infragranular layers, 103.2 ± 10.5 (103.1 ± 10.3) and supragranular layers, 158.3 ± 22.6 (155.8 ± 19.8); Figure 6.5, or in Par1/Par2 infragranular layers, 116.5 ± 7.3 (114.1 ± 6.3) and supragranular layers, 106.2 ± 11.9 (106.5 ± 12.6); Figure 6.6. These results are summarised in Table 6.1.

6.2.7 Assessment of cell size in the neocortex following intrastriatal volkensin and ricin injections.

Previous studies indicated that cell loss in all volkensin injected animals was accompanied by a significant reduction of 20 - 25 % in mean cell size above 80 μm^2 (group 1; Pangalos et al., 1991b), values are mean cell size, μm^2 ± SEM, contralateral values in parentheses), 125.2 ± 5.6 (155.0 ± 6.6), ($p < 0.001$, Student's paired *t*-test, Table 6.2). No reduction in mean cell size between ipsilateral and contralateral sides was observed in the supragranular layers in this group of animals.

In group 2 animals (n=6), measurements of cell size in Fr1/Fr2 gave similar results. Injection of 2 ng volkensin produced a significant reduction in mean cell size on the ipsilateral side to 89 % of the contralateral value in the infragranular layers, 117.9 ± 3.9 (131.4 ± 2.3), ($p = 0.042$, Student's paired *t*-test, Table 6.2). A reduction in the mean size of cells above 70 μm^2 on the ipsilateral side in supragranular layers was not observed compared to contralateral in this group of animals, 114.2 ± 0.9 (115.2 ± 0.9). These results are summarised in Figure 6.7.

Group	Fr1/Fr2		Par1/Par2	
	Infragranular	Supragranular	Infragranular	Supragranular
1	**80**†	97	nd	nd
2	**90***	99	nd	nd
3	**85****	97	**97***	**93**†
Ricin	100	100	100	102

TABLE 6.2: CHANGES IN NEOCORTICAL CELL SIZE FOLLOWING UNILATERAL INTRASTRIATAL INJECTION OF TOXIC LECTINS. Values are mean size of cell profiles of area > 80 μm^2 (infragranular) or > 70 μm^2 (supragranular) on ipsilateral side as % of contralateral side, following injection of 2 ng volkensin (groups 1,2 and 3, all n=6) or 10 ng ricin (n=6). Group 1 animals were prepared in a previous study.
* $p < 0.05$, ** $p < 0.005$, † $p < 0.001$; significantly different to contralateral side, Student's paired *t*-test. nd; not determined.

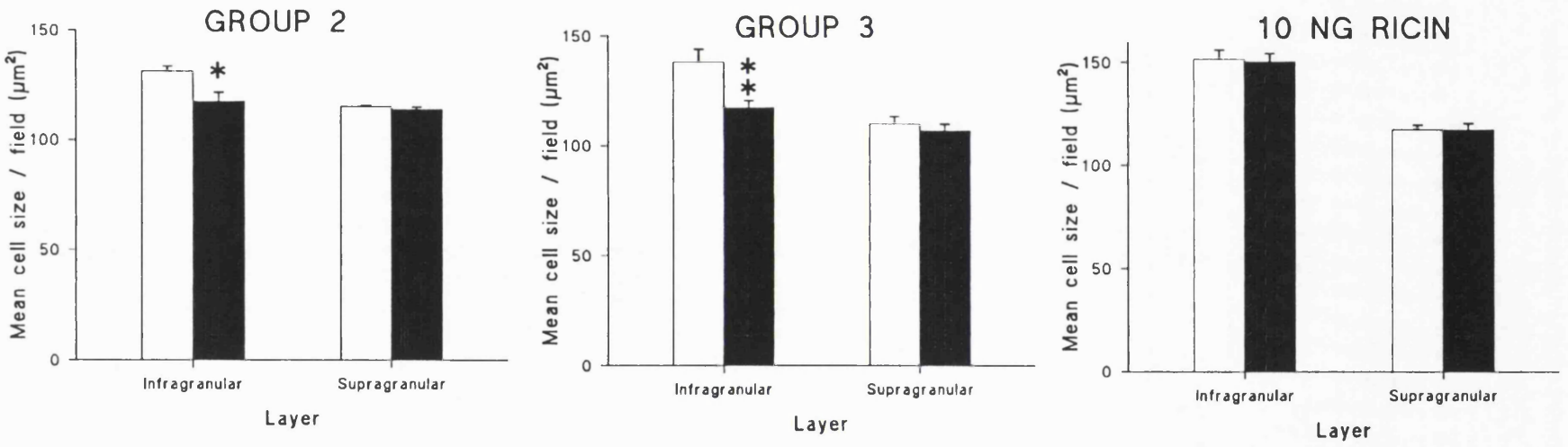

Figure 6.7: CHANGES IN NEOCORTICAL CELL SIZE IN MEDIAL Fr1/Fr2 AREAS FOLLOWING INTRASTRIATAL INJECTION OF TOXIC LECTINS. Histograms show the mean cell size / field > 80 μm^2 (infragranular) or >70 μm^2 (supragranular) in cross sectional area in the neocortex following intrastriatal injection of 2 ng volkensin (groups 2 and 3) or 10 ng ricin. All groups are n=6. Open bars; contralateral side; filled bars- ipsilateral side.
Error bars are SEM; * $p < 0.05$; ** $p < 0.005$, significantly different to corresponding contralateral side (Student's paired *t*-test)

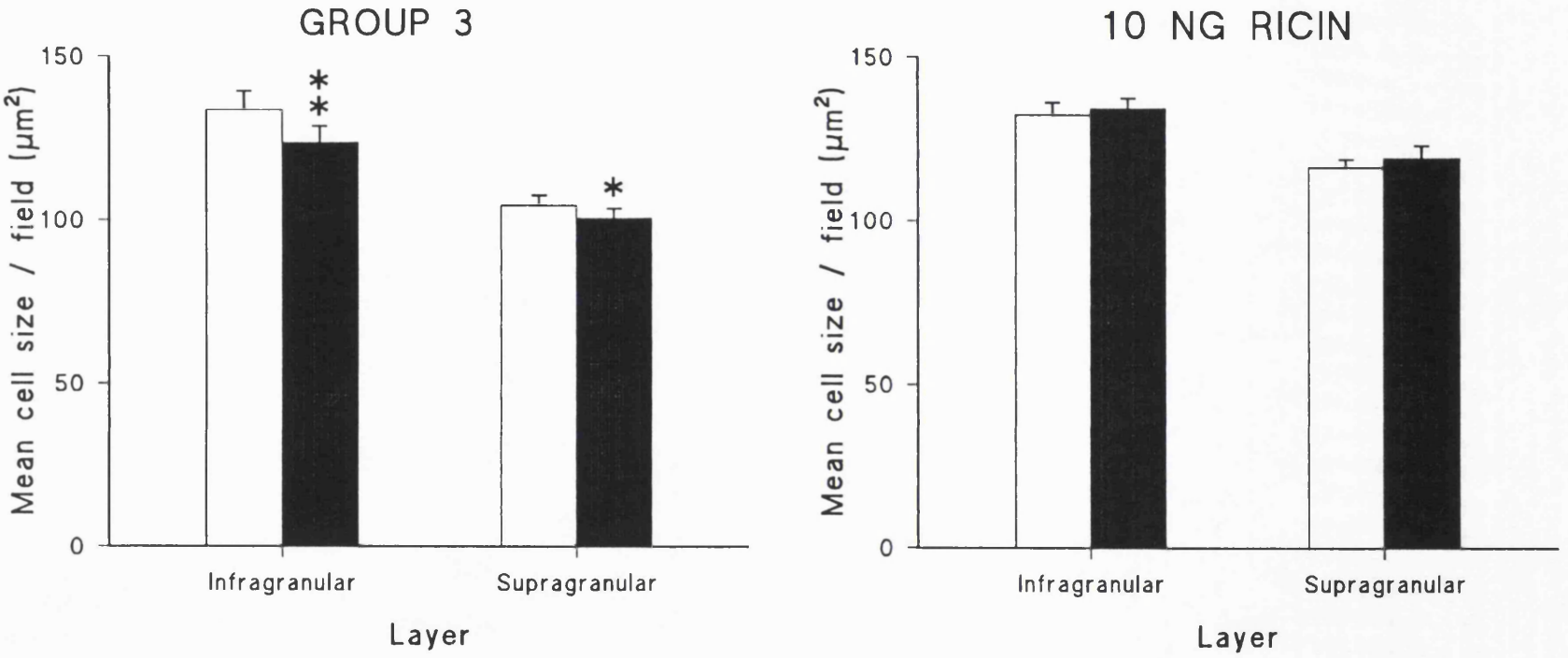

Figure 6.8: CHANGES IN NEOCORTICAL CELL SIZE IN LATERAL Par1/Par2 AREAS FOLLOWING INTRASTRIATAL INJECTION OF TOXIC LECTINS. Histograms show the mean cell size / field > 80 μm^2 (infraganular) or > 70 μm^2 (supragranular) in cross sectional area in the neocortex following intrastriatal injection of 2 ng volkensin (group 3) or 10 ng ricin. All groups are n=6. Open bars; contralateral side; filled bars- ipsilateral side.
Error bars are SEM; * $p < 0.05$, ** $p < 0.001$; significantly different to corresponding contralateral side (Student's paired *t*-test)

In group 3 animals (n=6), in areas Fr1/Fr2, injection of 2 ng volkensin produced a significant reduction in mean cell size on the ipsilateral side to 85 % of the contralateral side in the infragranular layers, 117.6 ± 3.1 (138.1 ± 5.9), (p = 0.004, Student's paired *t*-test). No significant reduction of cell size was observed in supragranular layers ipsilateral to the injection site compared to contralateral in this group of animals, 107.1 ± 2.8 (110.0 ± 3.4). These results are summarised in Figure 6.7. In this group of animals, measurements of mean cell size were also performed for Par1/Par2 areas, in both infragranular and supragranular layers. Injection of 2 ng volkensin produced a significant reduction on the ipsilateral side to 92 % of the contralateral side in infragranular layers, 123.9 ± 4.9 (133.8 ± 5.8), (p = 0.001, Student's paired *t*-test; Figure 6.8). A significant reduction of cell size was also observed in supragranular layers ipsilateral to the injection site to 97 % of the contralateral value in this group of animals, 100.9 ± 2.7 (104.5 ± 3.2), (p= 0.043, Student's paired *t*-test; Figure 6.8). Frequency histograms of the neuronal cell size in the infragranular layers of Par1/Par2 exhibit quite different population distributions on the side ipsilateral to the injection compared with contralateral, suggesting that the decreases in mean cell size on the injected side can be attributed to loss of large cells of greater than 170 μm^2.

In a group of animals injected with 10 ng ricin (n=6), no significant differences were observed in mean cell size measured ipsilateral to the injection compared with contralateral, in Fr1/Fr2 infragranular layers, 150.7 ± 3.9 (151.7 ± 4.5) and supragranular layers, 117.6 ± 3.0 (117.4 ± 2.4); Figure 6.7, or in Par1/Par2 infragranular layers, 134.5 ± 3.0 (132.3 ± 3.9) and supragranular layers, 119.4 ± 3.7 (116.3 ± 2.5); Figure 6.8. These results are summarised in Table 6.2.

6.2.8 Effect of volkensin injections on glial proliferation and GAD-mRNA positive cells.

The effect of intrastriatal volkensin injection on glial proliferation and the preservation of GAD-mRNA positive cells in the area of neuronal loss has been described elsewhere, and was investigated in group 1 animals (Pangalos et al., 1991b; Francis et al., 1992b; Pangalos, 1992). As the histological

appearance, and parameters measured in group 2 and 3 animals were qualitatively and quantitatively similar to those described for group 1 animals, investigation of glial proliferation and GAD-mRNA positive cell number was not performed for the latter animal groups. Measurements of these parameters in group 1 animals revealed that a substantial gliosis occurred as a result of the neuronal damage caused by the transported toxin. The number of GAD-mRNA positive cells were counted from the same areas as those showing loss of cresyl violet stained cells, both in the supragranular and infragranular layers. No significant difference in the number of GAD-mRNA positive cells / field were observed between ipsilateral and contralateral sides, further confirmation that the actions of volkensin were specific to neurones projecting to the injection site.

6.3 Discussion.

6.3.1 Histological interpretations of intrastriatal toxin injections.

The experimental conditions described in this study are similar to those used in a previous study of neuronal loss in infragranular layer of the cortex following volkensin injection (Pangalos et al., 1991b; Francis et al., 1992b; Pangalos, 1992). However, this protocol is different from that used by other workers. Wiley and Stirpe (1988), used volkensin concentrations ranging from 1 - 8 ng and reported animal survival times of 2.5 - 12 days whilst detecting neuronal loss in the substantia nigra, following intrastriatal injection. Injection of 0.5 - 0.8 ng volkensin into the substantia nigra produced loss of excitatory amino acid binding sites in the striatum, reflecting destruction of striatonigral projections (Tallaksen-Greene et al., 1992) with a postoperative survival time of 12 days, whilst in a similar study of D_1 and D_2 binding sites in the striatum, a dose of 2 - 2.5 ng volkensin was used, with two thirds of the total change in binding densities observed within the first 10 days following the lesion (Harrison et al., 1992). High mortality of animals was observed by Contestibile et al. (1990) following hippocampal injection of 1.5 - 3 ng volkensin, while a lower dose of 1.2 ng with a survival time of 10 days produced acceptable loss of septal and contralateral CA3 hippocampal neurones. Injection of 2 ng volkensin into the entorhinal cortex, with a survival time of 14 or 21 days produced loss of ipsilateral CA3 hippocampal pyramidal neurones (this thesis). Additionally, Crino et al. (1990), using the retrogradely transported immunotoxin OX7-saporin, reported limited cell loss in lamina V of the neocortex following striatal injections with a 14 day survival time, and observed extensive cell death in lamina VI following anterior thalamic nuclei injections. However, the recognition site of this agent (OX-7 recognises Thy-1, an abundant surface molecule present on all neurones; saporin is a ribosome inactivating protein) is different to that of volkensin (Wiley, 1992). It is clear from the above studies that differences in the relative toxicity of volkensin may depend on the particular pathway being investigated, with corresponding differences in either or both of axonal transport rate, and vulnerability of neurones to the action of volkensin. Even reciprocal pathways seem to exhibit

different susceptibility to the neurotoxin; cell death in the striatum following injection of volkensin into the substantia nigra takes longer than cell death in the substantia nigra following striatal injection (Harrison et al., 1990). The difference in parameters influencing relative susceptibility in the nigrostriatal pathway may also contribute to the changes observed in the substantia nigra following ricin injection, as injection of quinolinate into the striatum with a survival time of only 7 days had no apparent effect on these neurones, and changes observed in the SN following striatal injection of abrin with survival times of 4 and 13 days were minimal and inconsistent (Wiley and Stirpe, 1988).

The present study confirms that volkensin produces a significant and consistent loss of a subpopulation of neocortical pyramidal neurones, following injection into the striatum. Injection of 2 ng volkensin reduced the number of cells to 59 - 78 % of the control (contralateral) side (Figure 6.5). This compares well with a previous study, where reductions to 71 % and 57 % were observed using 2 and 6 ng of volkensin respectively (Pangalos et al., 1991b). Additionally, the present study has demonstrated the loss of a subpopulation of infragranular pyramidal cells in lateral areas (Par1/Par2) to 72 % of the control value (Figure 6.6). Volkensin produced local necrosis at the injection site, and so it is not possible to exclude that a proportion of the infragranular pyramidal cells destroyed in the neocortex project to other subcortical nuclei, passing through the striatum without synapsing. However, as cell loss was observed in other areas of known afferent projection to the striatum (e.g. from the SN), it is certain that the subpopulation of pyramidal cells destroyed included corticostriatal projection neurones, which are known to project to the striatum (Heimer et al., 1985).

In both groups of volkensin injected animals prepared in this study, it is possible that the infragranular neuronal loss occurs as a result of direct thalamic damage, with subsequent transport of the toxin to neocortical cells projecting to this site. Though a small proportion of layer V infragranular neocortical neurones do project to the thalamus (Wise and Jones, 1977; Faull and Mehler, 1985), the cells of origin of the corticothalamic pathway are mainly confined to the cells of layer VI (Crino et al., 1990), loss of which was not a feature of this study. The lack of change in the number of neocortical

infragranular cells following thalamic injection of ibotenate precludes the possibility of anterograde changes following destruction of thalamic nuclei. However, in the present study, cell loss following retrograde transport of volkensin from thalamic sites cannot be excluded from making a small contribution to the neuronal loss observed in layer V.

The possibility that volkensin may spread directly from the injection site, or from neurones transporting the toxin and subsequently releasing it following cell lysis (from where it may be taken up by adjacent neurones) has been carefully considered, both previously, and in the present study. Several findings support the interpretation that only cells distant from the injection site (in the neocortex) are destroyed only by retrograde transport of volkensin. In previous studies, *in-situ* hybridisation histochemistry for GAD mRNA, a marker of neocortical interneurones, was performed. Since interneurones do not project to the striatum, any reduction in the number GAD mRNA positive cells would suggest that cell loss in the neocortex following volkensin injection was a consequence of either passive diffusion of the toxin from the injection site or secondary spread from neurones destroyed by the toxin which subsequently lysed. No significant differences were observed in the number of positive cells between ipsilateral and contralateral sides (Pangalos et al., 1991b; Pangalos, 1992). Additionally, in all studies, injection of the neurotoxic lectin ricin, similar to volkensin, but only retrogradely transported in the peripheral nervous system (Wiley et al., 1983), produced local lesions around the site of injection, but no cell loss in any area distant to the injection site, including the infragranular layer of the overlying neocortex (Figures 6.5 and 6.6). Though the diffusion properties of the excitotoxin quinolinate may be quite different from those of volkensin, additional evidence against direct spread of volkensin is provided by the lack of damage to cortical areas following intrastriatal injection of quinolinate.

In group 1 animals, injection of 2 ng volkensin produced loss of supragranular neurones in medial Fr1/Fr2 areas, which was not detected in the two groups of animals prepared in this study. However, in group 3 animals, a small reduction on the ipsilateral side in the mean size of supragranular neurones in lateral Par1/Par2 areas (to 97 % of the

contralateral value; Table 6.2) was observed. A previous interpretation of the loss of medial supragranular neurones was that a shrinkage of these neurones had occurred, such that a proportion of the cells fell below the size exclusion criteria set on the image analyser. This hypothesis is supported by the finding of a reduction in mean supragranular cell size in the lateral areas in group 3 animals. It is possible that a number of technical considerations may also contribute to this finding; differences in staining intensity, lesion placement and choice of neocortical region examined should all be considered.

CHAPTER 7: Autoradiographic analysis of ligand binding in the neocortex following intrastriatal and intrathalamic injection of toxins.

7.1 Introduction.

The regional and laminar distribution of receptor subtypes in the neocortex of the rat and human have been extensively studied, though information regarding the localisation of receptors to specific neurones is sparse (see Chapter 5, section 5.1). Previous studies have demonstrated the localisation of 5-HT_{1A} but not 5-HT_{2A} receptors to neocortical layer V pyramidal neurones (Francis et al., 1992b), which reflects cell specific 5-HT receptor subtypes (McCormick and Williamson, 1989). Pangalos and co-workers also reported preliminary findings of the localisation of the kainate sensitive glutamate receptor to these neurones (Pangalos, 1992), while the NMDA receptor was not enriched (Pangalos et al., 1992), again reflecting differential localisation of receptors using the same transmitter. The aim of the present study was to confirm and extend previous work to examine the localisation of receptors using phosphoinositide hydrolysis to generate their second messengers (muscarinic M_1 and α_1 adrenoceptors), as well as several receptors proposed to influence the excitability of pyramidal neurones ($GABA_A$, adenosine A_1, and nicotinic cholinergic), using [^{3}H] pirenzepine, [^{3}H] prazosin, [^{3}H] GABA, [^{3}H] DPCPX and [^{3}H] nicotine respectively. For comparison and confirmation, the localisation of 5-HT_{1A} and kainate sensitive glutamate receptors have also been investigated. It is thought that corticocortical and corticostriatal pyramidal neurones are probably subject to qualitatively similar regulation (McCormick and Williamson, 1989), so the finding of the present study can be contrasted with those producing selective destruction of a subpopulation of hippocampal-entorhinal and corticocortical projecting neurones (See Chapter 9). As described in Chapter 6, three groups of volkensin injected animals were used in the course of these studies, each of six animals. Group 1 had been prepared in a previous study.

7.2 Results.

7.2.1 The binding of [^{3}H] 8-OH-DPAT to 5-HT$_{1A}$ receptors.

Binding of 8-OH-DPAT in the second and third groups of animals was performed as added confirmation of the loss of a subpopulation of infragranular pyramidal neurones, and to further confirm previous findings. The experimental conditions and considerations used for the binding of [^{3}H] 8-OH-DPAT are described in the methods section and in Chapter 5, sections 5.2.4 and 5.3.1, except in group 2 and quinolinate injected animals where a higher concentration of [^{3}H] 8-OH-DPAT was used (2.5 nM instead of 1 nM).

The laminar and regional distribution of [^{3}H] 8-OH-DPAT binding is shown as representative colour coded reconstructions of autoradiograms for volkensin, quinolinate and ibotenate (Figure 7.1) treated animals. Within the neocortex, binding was higher in the deep layers compared to the superficial layers, and higher medially (Fr1/Fr2) compared to that observed in more lateral areas (Par1/Par2). In animals injected with 2 ng volkensin (all groups), the binding of [^{3}H] 8-OH-DPAT on the side ipsilateral to the injection site was noticeably lower than that in the corresponding contralateral side (Figure 7.1).

Quantitative analysis of the binding of [^{3}H] 8-OH-DPAT in group 1 animals (n=6; Table 7.1) revealed that there was no significant reduction in the level of binding medially (Fr1/Fr2) in the superficial layers on the ipsilateral side compared to the contralateral side, while in deep layers, binding on the ipsilateral side was reduced to 77 % ($p < 0.001$, Student's paired *t*-test) of that of the corresponding contralateral area. Laterally, a significant reduction in [^{3}H] 8-OH-DPAT binding on the ipsilateral side to 78 % ($p < 0.01$, Student's paired *t*-test) of that measured in the corresponding area of the contralateral side was observed in the superficial layers. In deep layers, binding was reduced to 67 % ($p < 0.001$, Student's paired *t*-test) of that observed on the contralateral side.

In the second group of animals (n=6; Table 7.1), there was no significant reduction in the level of binding medially (Fr1/Fr2) in the superficial layers on the ipsilateral side compared to the contralateral side, while in deep layers the binding on the ipsilateral side was reduced to 79 % (p

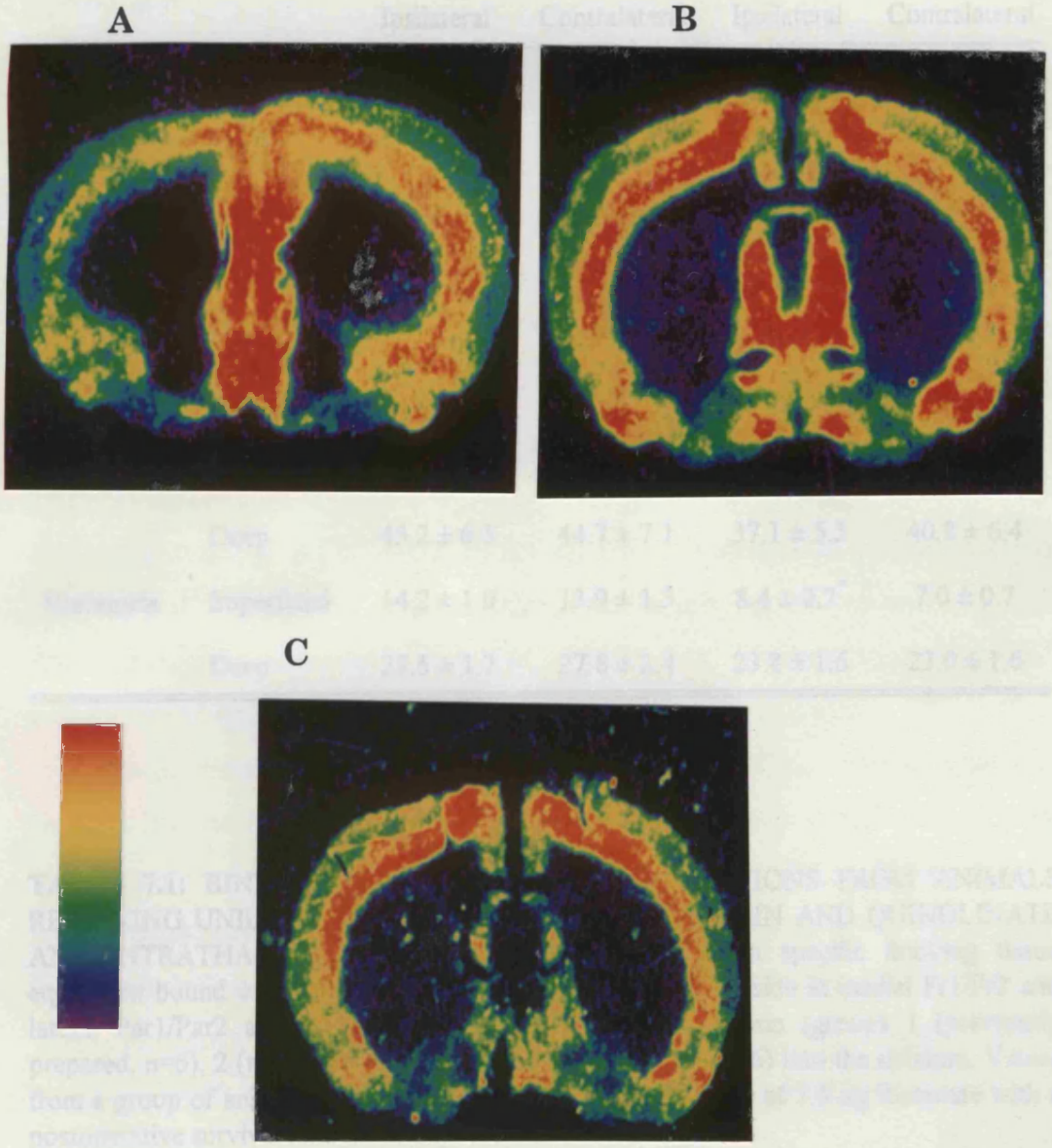

Figure 7.1: REPRESENTATIVE COLOUR-CODED AUTORADIOGRAMS OF [^{3}H] 8-OH-DPAT BINDING IN SECTIONS FROM VOLKENSIN, IBOTENATE AND QUINOLINATE TREATED ANIMALS. Experiments were performed using coronal rat brain sections (12 µm) incubated in 0.17 M Tris-HCl (pH 7.6) containing 4 mM $CaCl_2$, 0.01 % ascorbate and 1 nM [^{3}H] 8-OH-DPAT for 60 min at 25 °C. Non-specific binding was generated using 10 µM 5-HT.
Colour-coded autoradiograms illustrate specific binding in animal receiving (A) 2 ng intrastriatal volkensin, (B) 10 µg intrastriatal quinolinate or (C) 7.5 µg intrathalamic ibotenate, with postoperative survival times of 28, 7 and 12 days, respectively. The scale bar indicates the intensity of autoradiographic signal from purple (lowest) to red (highest). Note the clear loss of binding in the neocortical layers on the side ipsilateral to the injection in (A). Injection site on left.

		Fr1/Fr2		Par1/Par2	
		Ipsilateral	Contralateral	Ipsilateral	Contralateral
Volkensin	Superficial	23.0 ± 7.9	26.2 ± 7.9	**8.9 ± 3.2****	11.4 ± 3.3
(group 1)	Deep	**23.3 ± 7.7**‡	30.5 ± 8.3	**16.5 ± 6.2**‡	24.6 ± 7.1
Volkensin	Superficial	19.9 ±1.0	20.3 ± 1.1	19.1 ± 0.7	21.9 ± 1.9
(group 2)	Deep	**26.2 ± 7.9**‡	41.3 ± 2.0	33.7 ± 0.7	38.5 ± 3.6
Volkensin	Superficial	16.6 ± 4.5	19.3 ± 4.7	**11.3 ± 3.5**†	16.3 ± 1.3
(group 3)	Deep	**25.6 ± 5.6**†	31.7 ± 6.0	**18.7 ± 1.8****	28.5 ± 3.1
Quinolinate	Superficial	28.4 ± 2.7	27.7 ± 3.1	18.6 ± 2.1	20.6 ± 3.1
	Deep	45.2 ± 6.5	44.7 ± 7.1	37.1 ± 5.5	40.8 ± 6.4
Ibotenate	Superficial	14.2 ± 1.0	13.9 ± 1.3	**8.4 ± 0.7***	7.0 ± 0.7
	Deep	27.5 ± 1.7	27.8 ± 2.4	23.8 ± 1.6	23.0 ± 1.6

TABLE 7.1: BINDING OF [^{3}H] 8-OH-DPAT TO SECTIONS FROM ANIMALS RECIEVING UNILATERAL INTRASTRIATAL VOLKENSIN AND QUINOLINATE AND INTRATHALAMIC IBOTENATE. Values are mean specific fmol/mg tissue equivalent bound ± SEM on ipsilateral side and contralateral side in medial Fr1/Fr2 and lateral Par1/Par2 areas, following injection of 2 ng volkensin (groups 1 (previously prepared, n=6), 2 (n=6) and 3 (n=5)), or 10 µg quinolinate (n=6) into the striatum. Values from a group of animals (n=6) receiving intrathalamic injection of 7.5 µg ibotenate with a postoperative survival time of 12 days are also shown.
* $p < 0.05$, ** $p \leq 0.01$, † $p \leq 0.005$, ‡ $p \leq 0.001$, significantly different to contralateral side, Student's paired *t*-test.

= 0.001, Student's paired *t*-test) of that of the corresponding area of the contralateral side. In lateral areas, there was no significant reduction of the binding of [^{3}H] 8-OH-DPAT in either superficial or deep layers.

In the third group of animals (n=5; Table 7.1), there was no significant reduction in binding medially (Fr1/Fr2) in the superficial layers of the ipsilateral side compared to the contralateral side, while in deep layers the binding on the ipsilateral side was reduced to 81 % (p = 0.004, Student's paired *t*-test) of that of the corresponding contralateral area. Laterally, a significant reduction in [^{3}H] 8-OH-DPAT binding on the ipsilateral side to 69 % (p = 0.005, Student's paired *t*-test) of that measured in the corresponding contralateral area was observed in the superficial layers. In deep layers, binding was reduced to 66 % (p = 0.01, Student's paired *t*-test).

The binding of [^{3}H] 8-OH-DPAT on the side ipsilateral to the injection site was not significantly different compared to binding on the contralateral side following intrastriatal injection of 10 μg quinolinate (n=6) in neocortical areas Fr1/Fr2 or Par1/Par2 (Table 7.1).

In animals receiving intrathalamic injection of 7.5 μg ibotenate, with a survival time of 12 days (n=5; Table 7.1), binding on the side ipsilateral to the injection site was not significantly different to binding on the contralateral side in neocortical areas Fr1/Fr2 or more laterally in the deep layers of Par1/Par2. In the superficial layers of Par1/Par2, binding was increased to 120 % (p = 0.045, Student's paired *t*-test) of that observed on the contralateral side. Autoradiography using sections from ibotenate treated animals with a survival time of 6 days was not performed due to paucity of sections.

7.2.2 The binding of [^{3}H] pirenzepine to muscarinic M_1 receptors.

Binding of [^{3}H] pirenzepine in the third groups of animals was performed as added confirmation of the localisation of this receptor to a subpopulation of infragranular pyramidal neurones (Pangalos, 1992). The experimental conditions and considerations for the binding of [^{3}H] pirenzepine are described in the methods section and in Chapter 5, sections 5.2.6 and 5.3.1. Investigations of the localisation of this receptor were also performed in animals injected with 10 ng ricin, 10 μg quinolinate and 7.5 μg ibotenate (6

and 12 day survival time). For binding in the ibotenate groups, a slightly higher concentration of [^{3}H] pirenzepine (3.5 instead of 2.5 nM) was used.

The laminar and regional distribution of [^{3}H] pirenzepine binding is shown as representative colour coded reconstructions of autoradiograms for volkensin and quinolinate treated animals (Figure 7.2). Within the neocortex, binding was higher in the superficial layers compared to the deep layers.

Quantitative analysis of the binding of [^{3}H] pirenzepine in group 1 animals (n=6; Table 7.2) revealed that there was no significant reduction in the level of binding medially (Fr1/Fr2) in the superficial layers of the ipsilateral side compared to the contralateral side, while in deep layers the binding on the ipsilateral side was reduced to 89 % ($p = 0.006$, Student's paired *t*-test) of that of the corresponding contralateral area. Laterally, no significant reduction in [^{3}H] pirenzepine binding was observed in the superficial layers. In deep layers, binding on the ipsilateral side was reduced to 83 % ($p = 0.006$, Student's paired *t*-test) of that observed on the contralateral side.

In the third group of animals (n=5; Table 7.2), there was no significant reduction in the level of binding medially (Fr1/Fr2) in the superficial layers on the ipsilateral side compared to the corresponding contralateral side, while in deep layers the binding on the ipsilateral side was reduced to 84 % ($p = 0.018$, Student's paired *t*-test) of that of the corresponding contralateral area. More laterally, there was no significant reduction of the binding of [^{3}H] pirenzepine in superficial layers. Binding in the deep layers of Par1/Par2 showed a similar trend as that observed in the first group (reduction to 89 % on the ipsilateral side compared to the contralateral side, $p = 0.068$, Student's paired *t*-test).

Following intrastriatal injection of 10 ng ricin (n=5), the binding of [^{3}H] pirenzepine was not significantly affected in either superficial or deep layers of Fr1/Fr2 or Par1/Par2 (Table 7.2).

The binding of [^{3}H] pirenzepine on the side ipsilateral to the injection site was not significantly different compared to binding on the contralateral side following intrastriatal injection of 10 μg quinolinate (n=6) in neocortical areas Fr1/Fr2 or Par1/Par2 (Table 7.2).

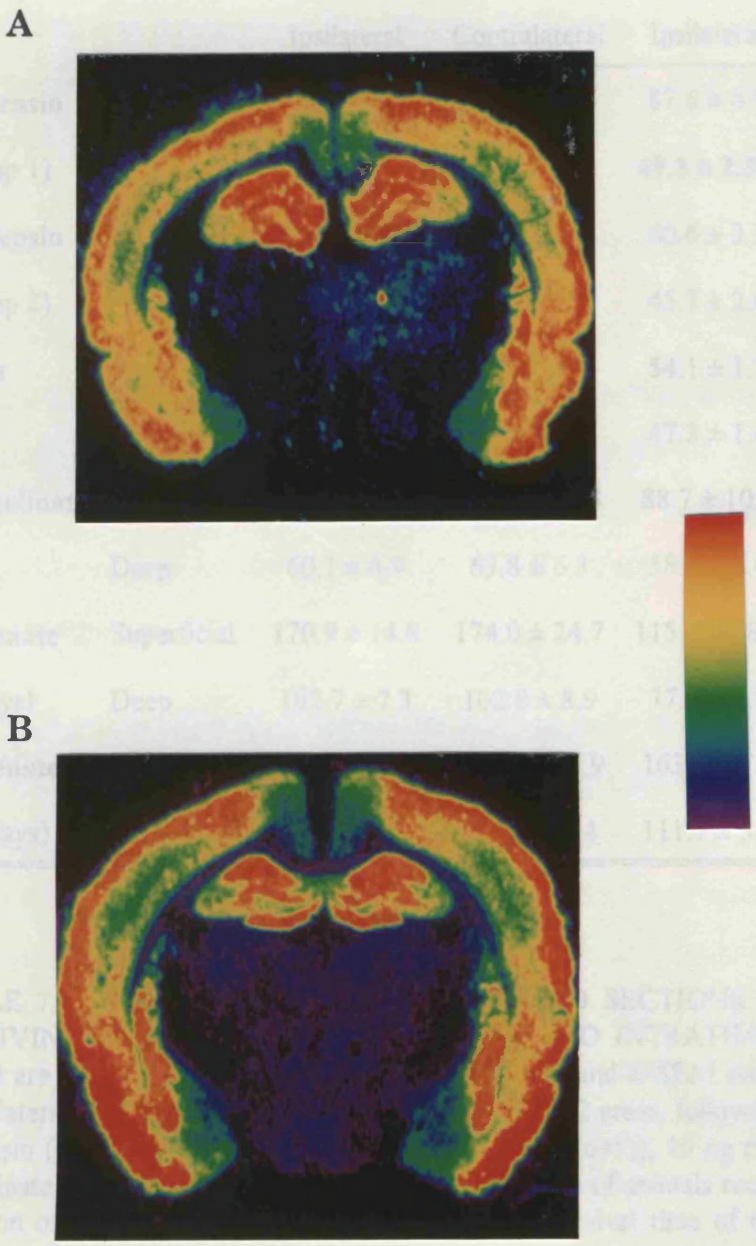

Figure 7.2: REPRESENTATIVE COLOUR-CODED AUTORADIOGRAMS OF [^{3}H] PIRENZEPINE BINDING IN SECTIONS FROM VOLKENSIN AND QUINOLINATE TREATED ANIMALS. Experiments were performed using coronal rat brain sections (12 µm) incubated in PBS (pH 7.4) containing 2.5 nM [^{3}H] pirenzepine for 90 min at 25 °C. Non-specific binding was generated using 10 µM atropine.
Colour-coded autoradiograms illustrate specific binding in animal receiving (A) 2 ng intrastriatal volkensin, or (B) 10 µg intrastriatal quinolinate, with postoperative survival times of 28 and 7 days. The scale bar indicates the intensity of autoradiographic signal from purple (lowest) to red (highest). Injection site on left.

		Fr1/Fr2		Par1/Par2	
		Ipsilateral	Contralateral	Ipsilateral	Contralateral
Volkensin	Superficial	91.1 ± 7.8	92.8 ± 5.3	87.6 ± 6.9	89.8 ± 8.7
(group 1)	Deep	**62.2 ± 3.1****	69.6 ± 2.8	**49.8 ± 2.3****	59.9 ± 3.6
Volkensin	Superficial	68.4 ± 1.7	69.8 ± 1.9	60.6 ± 3.3	60.4 ± 2.1
(group 3)	Deep	**49.1 ± 1.4***	58.7 ± 1.9	45.7 ± 2.6	51.2 ± 2.5
Ricin	Superficial	65.4 ± 1.9	64.8 ± 2.4	54.1 ± 1.7	54.8 ± 1.8
	Deep	51.3 ± 2.5	51.2 ± 2.4	47.3 ± 1.4	46.7 ± 1.8
Quinolinate	Superficial	103.4 ± 14.0	100.3 ± 13.3	88.7 ± 10.4	88.7 ± 10.4
	Deep	60.1 ± 4.9	63.8 ± 6.3	58.5 ± 3.4	55.2 ± 4.5
Ibotenate	Superficial	170.9 ± 14.8	174.0 ± 24.7	115.7 ± 18.9	116.7 ± 15.9
(6 days)	Deep	102.7 ± 7.3	102.8 ± 8.9	77.2 ± 7.7	78.9 ± 6.8
Ibotenate	Superficial	220.5 ± 12.6	209.6 ± 13.9	163.8 ± 7.1	160.0 ± 8.2
(12 days)	Deep	135.4 ± 6.2	138.0 ± 7.4	111.7 ± 5.7	110.1 ± 6.4

TABLE 7.2: BINDING OF [^{3}H] PIRENZEPINE TO SECTIONS FROM ANIMALS RECEIVING UNILATERAL INTRASTRIATAL AND INTRATHALAMIC TOXINS. Values are mean specific fmol/mg tissue equivalent bound ± SEM on ipsilateral side and contralateral side in medial Fr1/Fr2 and lateral Par1/Par2 areas, following injection of 2 ng volkensin (groups 1 (previously prepared, n=6) and 3 (n=5)), 10 ng ricin (n=5) or 10 μg quinolinate (n=6) into the striatum. Values from groups of animals receiving intrathalamic injection of 7.5 μg ibotenate with a postoperative survival time of 6 (n=4) or 12 days (n=6) are also shown.

* $p < 0.02$, ** $p < 0.01$, significantly different to contralateral side, Student's paired *t*-test.

In animals receiving intrathalamic injection of 7.5 μg ibotenate, with a survival time of 6 (n=4) or 12 (n=6) days binding on the side ipsilateral to the injection site was not significantly different to binding on the contralateral side in neocortical areas Fr1/Fr2 or more laterally in Par1/Par2, in either superficial or deep layers.

7.2.3 The binding of [^{3}H] prazosin to α_1 adrenoceptors.

7.2.3.1 Effects of incubation and wash time.

As described in section 2.8.8, after an incubation time of 45 min, the binding of [^{3}H] prazosin was considered to be at equilibrium. A wash time of 2 x 5 min produced approximately 82 % specific binding for total α_1 adrenoceptors, and in the presence of 5-MU, approximately 80 % specific binding to the α_{1b} subtype.

7.2.3.2 Characteristics of [^{3}H] prazosin binding in lesioned rat brain sections.

The binding of [^{3}H] prazosin to total α_1 adrenoceptors, and in the presence of 5-MU, to the α_{1b} subtype was examined in animals injected with 2 ng volkensin (group 2, n=6) and 10 ng ricin (n=3). The regional and laminar distributions of α_{1total} and α_{1b} binding are shown in Figures 7.3 and 7.4 as colour reconstructions of autoradiograms for volkensin and ricin treated animals. Clearly demarcated within the neocortex were superficial, middle and deep layers. Binding to both α_{1total} and α_{1b} receptors was highest in the middle layers, followed by superficial and deep layers.

Quantitative analysis of the binding of [^{3}H] prazosin to α_{1total} receptors in group 2 animals (n=6; Table 7.3) revealed that in the superficial layers there was a significant <u>increase</u> to 108 % ($p = 0.009$, Student's paired *t*-test) compared to the corresponding region of the contralateral cortex. There was also a significant increase to 122 % ($p = 0.016$, Student's paired *t*-test) in the deep layers, but no change in α_{1total} binding in either the middle layer of Fr1/Fr2, or superficial and deep layers of Par1/Par2. In the middle layer of Par1/Par2, there was a significant <u>reduction</u> in binding to 94 % ($p = 0.045$, Student's paired *t*-test) compared to the corresponding region on the side contralateral to the injection site.

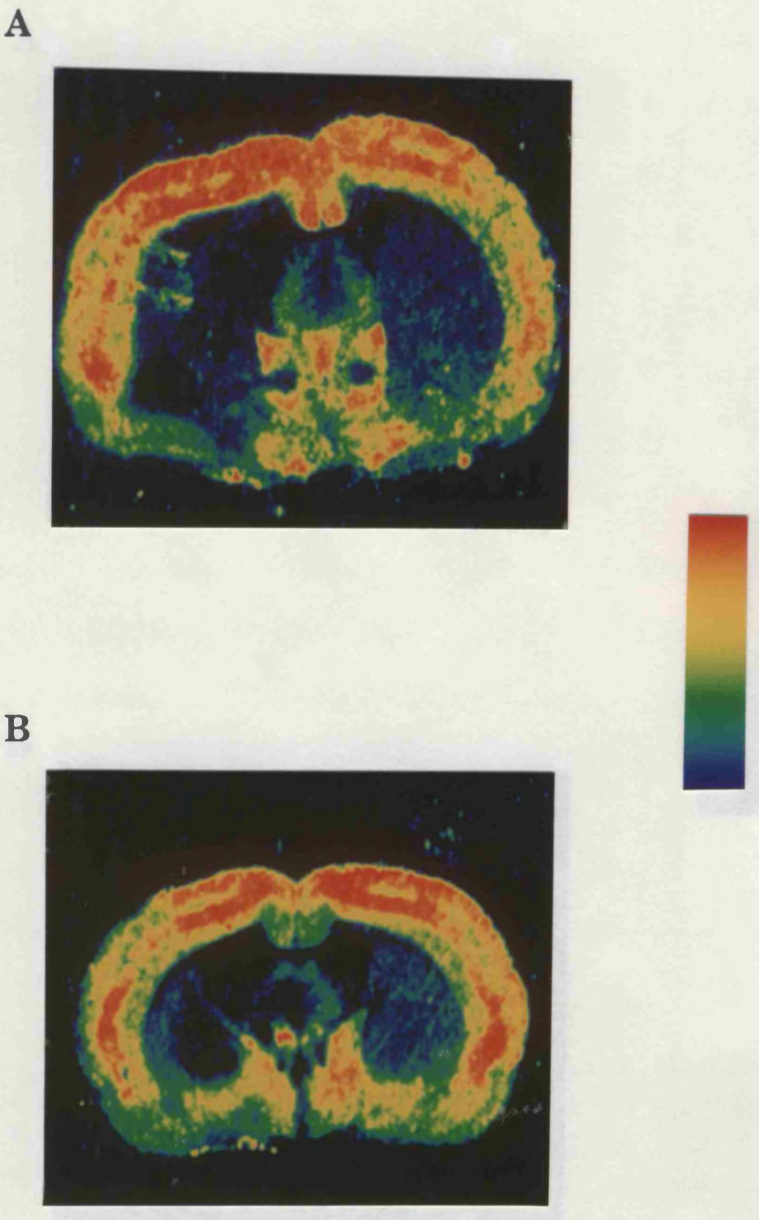

Figure 7.3: REPRESENTATIVE COLOUR-CODED AUTORADIOGRAMS OF [^{3}H] PRAZOSIN BINDING TO TOTAL α_1 ADRENOCEPTORS IN SECTIONS FROM VOLKENSIN AND RICIN TREATED ANIMALS. Experiments were performed using coronal rat brain sections (12 µm) incubated in 50 mM Tris-HCl (pH 7.4) containing 0.4 nM [^{3}H] prazosin for 45 min at 30 °C. Non-specific binding was generated using 10 µM phentolamine.
Colour-coded autoradiograms illustrate specific binding in animal receiving intrastriatal injections of (A) 2 ng volkensin, or (B) 10 ng ricin, with postoperative survival times of 28 days. The scale bar indicates the intensity of autoradiographic signal from blue (lowest) to red (highest). Injection site on left.

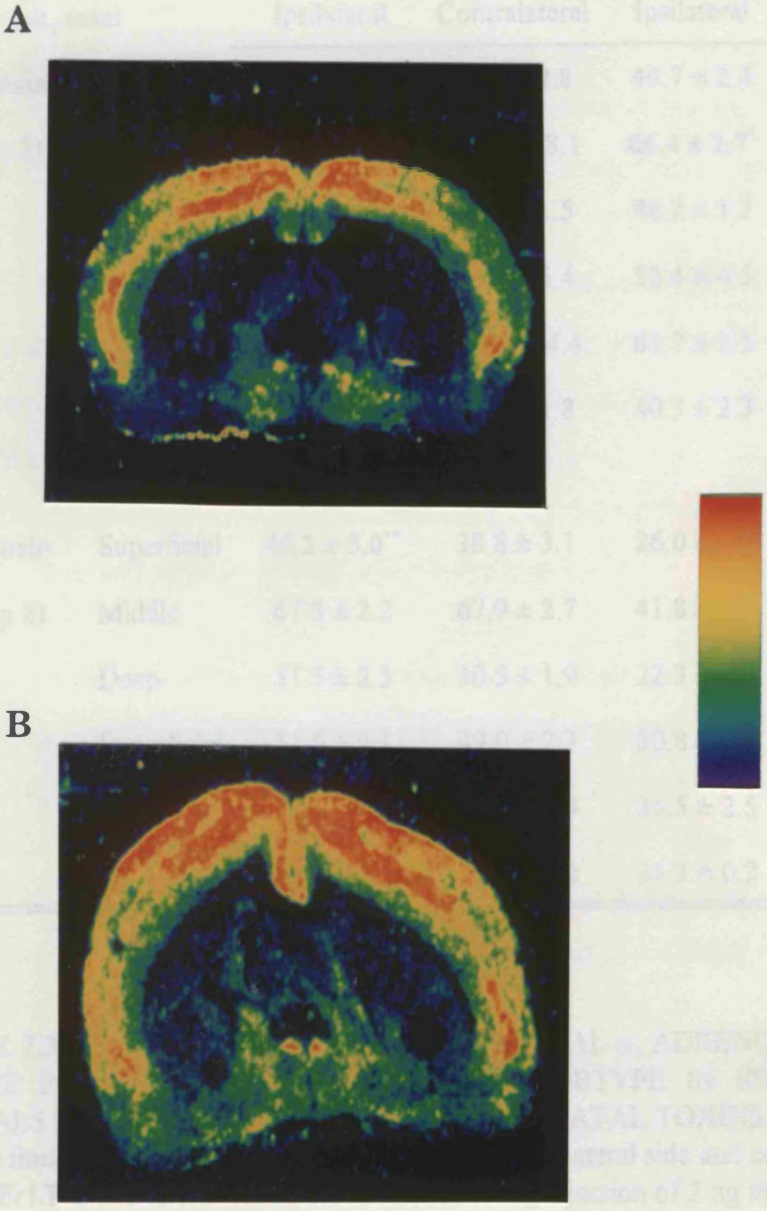

Figure 7.4: REPRESENTATIVE COLOUR-CODED AUTORADIOGRAMS OF [^{3}H] PRAZOSIN BINDING TO α_{1b} ADRENOCEPTORS IN SECTIONS FROM VOLKENSIN AND RICIN TREATED ANIMALS. Experiments were performed using coronal rat brain sections (12 μm) incubated in 50 mM Tris-HCl (pH 7.4) containing 30 nM 5-MU and 0.4 nM [^{3}H] prazosin for 45 min at 30 °C. Non-specific binding was generated using 10 μM phentolamine.
Colour-coded autoradiograms illustrate specific binding in animal receiving intrastriatal injections of (A) 2 ng volkensin, or (B) 10 ng ricin, with postoperative survival times of 28 days. The scale bar indicates the intensity of autoradiographic signal from purple (lowest) to red (highest). Injection site on left.

		Fr1/Fr2		Par1/Par2	
α_1 total		Ipsilateral	Contralateral	Ipsilateral	Contralateral
Volkensin	Superficial	**71.8 ± 3.2**†	66.5 ± 2.8	49.7 ± 2.4	47.6 ± 1.3
(Group 2)	Middle	115.1 ± 6.5	120.4 ± 8.1	**66.4 ± 1.7***	70.5 ± 2.5
	Deep	**59.9 ± 2.5****	49.3 ± 1.5	46.2 ± 1.3	41.9 ± 3.3
Ricin	Superficial	79.9 ± 5.4	75.3 ± 5.4	52.4 ± 4.5	49.4 ± 1.4
	Middle	97.8 ± 5.6	101.1 ± 4.4	61.7 ± 2.5	65.1 ± 1.7
	Deep	49.6 ± 3.5	48.1 ± 1.8	40.3 ± 2.3	50.1 ± 4.3
α_{1b}					
Volkensin	Superficial	**45.2 ± 3.0****	38.8 ± 3.1	26.0 ± 1.8	23.7 ± 1.9
(Group 2)	Middle	67.8 ± 2.2	67.9 ± 2.7	41.8 ± 2.2	40.9 ± 1.8
	Deep	31.5 ± 2.3	30.5 ± 1.9	22.3 ± 1.3	22.0 ± 1.7
Ricin	Superficial	51.5 ± 4.1	49.0 ± 2.3	30.8 ± 2.5	25.3 ± 1.0
	Middle	61.5 ± 8.7	67.8 ± 4.4	36.5 ± 2.5	39.5 ± 2.8
	Deep	29.0 ± 2.0	27.5 ± 1.2	21.3 ± 0.2	21.3 ± 1.2

TABLE 7.3: BINDING OF [^{3}H] PRAZOSIN TO TOTAL α_1 ADRENOCEPTORS AND IN THE PRESENCE OF 5-MU TO THE 1B SUBTYPE IN SECTIONS FROM ANIMALS RECEIVING UNILATERAL INTRASTRIATAL TOXINS. Values are mean specific fmol/mg tissue equivalent bound ± SEM on ipsilateral side and contralateral side in medial Fr1/Fr2 and lateral Par1/Par2 areas, following injection of 2 ng volkensin (group 2, n=6) or 10 ng ricin (n=3).
* $p < 0.05$, ** $p < 0.02$, † $p < 0.01$, significantly different to contralateral side, Student's paired *t*-test.

Quantitative analysis of the binding of [^{3}H] prazosin to the α_{1b} subtype in group 2 animals (n=6; Table 7.3) within areas Fr1/Fr2 also revealed that binding within superficial layers of the neocortex ipsilateral to the injection was significantly increased to 116 % ($p = 0.013$, Student's paired *t*-test) of that measured in the corresponding region of contralateral cortex. There were no significant changes in α_{1b} binding in either middle and deep layers of Fr1/Fr2, or in any layer of Par1/Par2.

Following intrastriatal injection of 10 ng ricin (n=3, Table 7.3), there were no significant changes in the binding of [^{3}H] prazosin to either α_{1total} or α_{1b} receptors in any layer or region between sides ipsilateral and contralateral to the injection site.

Examination of one animal receiving injection of vehicle (PBS) showed no changes in any area examined (data not shown).

7.2.4 The binding of [^{3}H] GABA to $GABA_A$ receptors.

The experimental conditions and considerations for the binding of [^{3}H] GABA are described in the methods section and in Chapter 5, sections 5.2.3 and 5.3.1. All incubations were performed in the presence of 100 μM baclofen to exclude binding to the $GABA_B$ receptor. Investigations of the localisation of this receptor was performed for group 2 volkensin injected animals, and a group of animals injected with 10 ng ricin.

The laminar and regional distribution of [^{3}H] GABA binding is shown as representative colour coded reconstructions of autoradiograms for volkensin and ricin (Figure 7.5) treated animals. Within the neocortex, binding was higher in the superficial layers compared to the deep layers, and higher medially (Fr1/Fr2) compared to that observed in more lateral areas (Par1/Par2).

Quantitative analysis of the binding of [^{3}H] GABA in group 2 animals (n=6; Table 7.4) revealed that there were no significant differences in binding medially (Fr1/Fr2) in the superficial layers or deep layers on the ipsilateral side compared to the contralateral side. Laterally, no significant differences in [^{3}H] GABA binding were observed in the superficial layers or deep layers between sides ipsilateral and contralateral to the injection site.

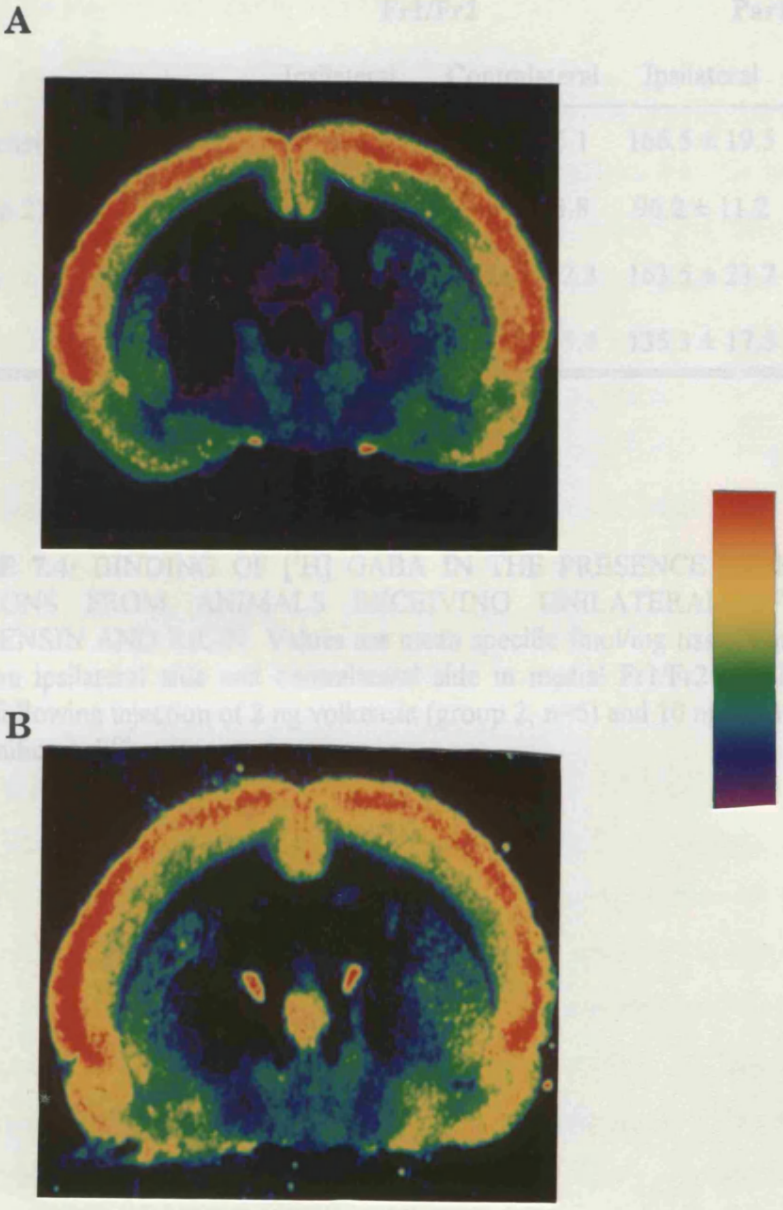

Figure 7.5: REPRESENTATIVE COLOUR-CODED AUTORADIOGRAMS OF [^{3}H] GABA BINDING TO $GABA_A$ RECEPTORS IN SECTIONS FROM VOLKENSIN AND RICIN TREATED ANIMALS. Experiments were performed using coronal rat brain sections (12 µm) incubated in 50 mM Tris-HCl (pH 7.4) containing 100 µM baclofen and 20 nM [^{3}H] prazosin for 45 min at 25 °C. Non-specific binding was generated using 100 µM isoguvacine.
Colour-coded autoradiograms illustrate specific binding in animal receiving intrastriatal injections of (A) 2 ng volkensin, or (B) 10 ng ricin, with postoperative survival times of 28 days. The scale bar indicates the intensity of autoradiographic signal from purple (lowest) to red (highest). Injection site on left.

		Fr1/Fr2		Par1/Par2	
		Ipsilateral	Contralateral	Ipsilateral	Contralateral
Volkensin	Superficial	150.8 ± 8.3	158.3 ± 6.1	166.5 ± 19.5	143.8 ± 7.7
(group 2)	Deep	103.8 ± 12.7	91.7 ± 13.8	96.2 ± 11.2	85.3 ± 7.6
Ricin	Superficial	171.3 ± 23.3	157.5 ± 22.3	163.5 ± 23.7	146.5 ± 13.2
	Deep	132.9 ± 17.7	127.1 ± 15.4	135.3 ± 17.5	131.8 ± 15.7

TABLE 7.4: BINDING OF [^{3}H] GABA IN THE PRESENCE OF BACLOFEN TO SECTIONS FROM ANIMALS RECEIVING UNILATERAL INTRASTRIATAL VOLKENSIN AND RICIN. Values are mean specific fmol/mg tissue equivalent bound ± SEM on ipsilateral side and contralateral side in medial Fr1/Fr2 and lateral Par1/Par2 areas, following injection of 2 ng volkensin (group 2, n=6) and 10 ng ricin (n=4).
No significant differences.

Following intrastriatal injection of 10 ng ricin (n=4), the binding of [^{3}H] GABA was not significantly affected in either superficial or deep layers of Fr1/Fr2 or Par1/Par2 (Table 7.4).

7.2.5 The binding of [^{3}H] DPCPX to adenosine A_1 receptors.

The experimental conditions and considerations for the binding of [^{3}H] DPCPX are described in the methods section 2.8.9. All incubations were performed in the absence of exogenously added magnesium. Investigations of the localisation of this receptor was performed for group 3 volkensin injected animals, and a group of animals injected with 10 ng ricin.

The laminar and regional distribution of [^{3}H] DPCPX binding is shown as representative colour coded reconstructions of autoradiograms (Figure 7.6) for volkensin and ricin treated animals. Clearly demarcated within the neocortex were superficial, middle and deep layers. Within the neocortex, binding was higher in the middle layers compared to superficial and deep layers.

Quantitative analysis of the binding of [^{3}H] DPCPX in group 3 animals (n=6; Table 7.5) revealed that there were no significant differences in binding medially (Fr1/Fr2) in the superficial layers or middle layers on the ipsilateral side compared to the contralateral side, while in deep layers, binding was slightly reduced on the side ipsilateral to the injection to 95 % ($p = 0.023$, Student's paired *t*-test) compared to that measured in the corresponding contralateral area. Laterally, no significant differences in [^{3}H] DPCPX binding were observed in the superficial, middle or deep layers between sides ipsilateral and contralateral to the injection site.

Following intrastriatal injection of 10 ng ricin (n=5), the binding of [^{3}H] DPCPX was not significantly affected in either superficial, middle or deep layers of Fr1/Fr2 or Par1/Par2 (Table 7.5) on the ipsilateral side compared to the contralateral side.

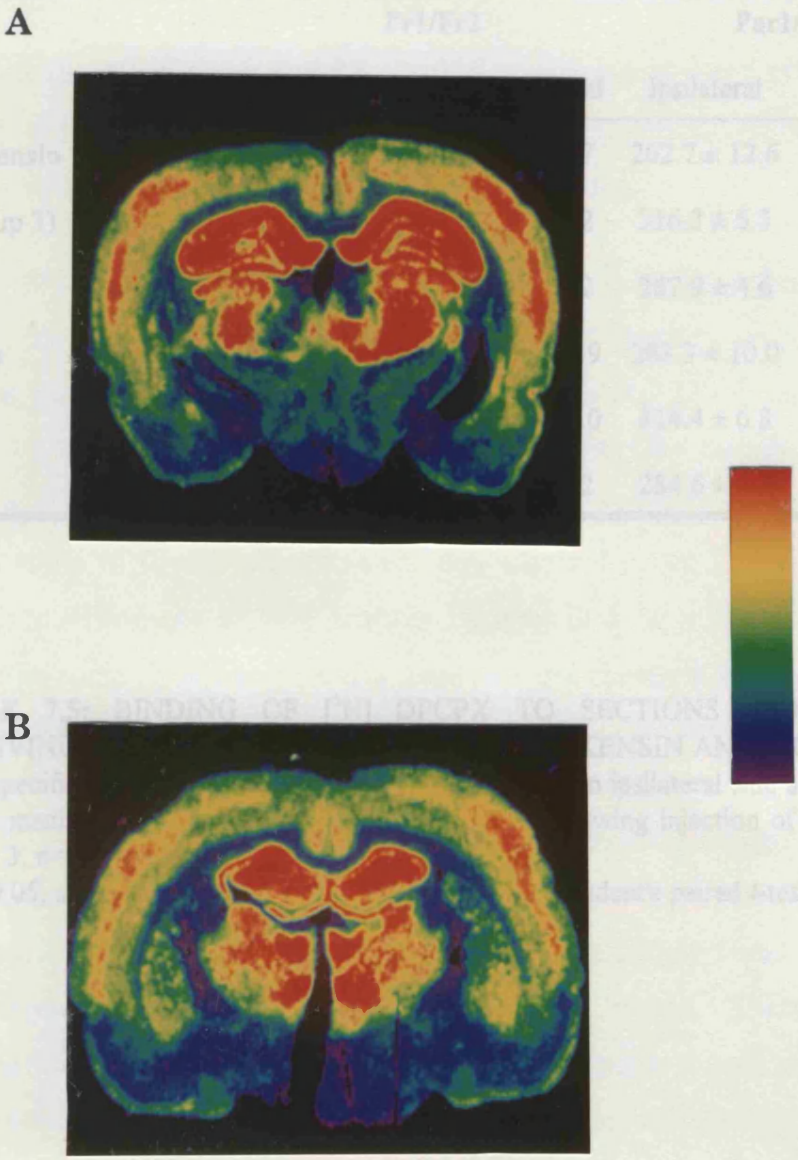

Figure 7.6: REPRESENTATIVE COLOUR-CODED AUTORADIOGRAMS OF [^{3}H] DPCPX BINDING TO ADENOSINE A_1 RECEPTORS IN SECTIONS FROM VOLKENSIN AND RICIN TREATED ANIMALS. Experiments were performed using coronal rat brain sections (12 μm) incubated in 0.17 M Tris-HCl (pH 7.4) containing 1 mM EDTA, 10 μM Gpp(NH)p, and 2 nM [^{3}H] DPCPX for 80 min at 37 °C. Non-specific binding was generated using 10 μM R-PIA.
Colour-coded autoradiograms illustrate specific binding in animal receiving intrastriatal injections of (A) 2 ng volkensin, or (B) 10 ng ricin, with postoperative survival times of 28 days. The scale bar indicates the intensity of autoradiographic signal from purple (lowest) to red (highest). Injection site on left.

		Fr1/Fr2		Par1/Par2	
		Ipsilateral	Contralateral	Ipsilateral	Contralateral
Volkensin	Superficial	233.1 ± 16.8	264.1 ± 5.7	262.7 ± 12.6	285.7 ± 9.2
(Group 3)	Middle	270.6 ± 11.2	296.1 ± 5.2	316.3 ± 6.3	327.3 ± 4.6
	Deep	**281.0 ± 5.1***	296.8 ± 3.2	287.9 ± 4.6	294.3 ± 6.1
Ricin	Superficial	262.1 ± 9.7	269.9 ± 13.9	263.3 ± 10.0	268.2 ± 14.7
	Middle	292.8 ± 9.8	303.8 ± 11.0	314.4 ± 6.8	320.3 ± 9.2
	Deep	278.6 ± 7.8	283.9 ± 9.2	284.6 ± 6.5	290.2 ± 7.4

TABLE 7.5: BINDING OF [^{3}H] DPCPX TO SECTIONS FROM ANIMALS RECEIVING UNILATERAL INTRASTRIATAL VOLKENSIN AND RICIN. Values are mean specific fmol/mg tissue equivalent bound ± SEM on ipsilateral side and contralateral side in medial Fr1/Fr2 and lateral Par1/Par2 areas, following injection of 2 ng volkensin (group 3, n=6) or 10 ng ricin (n=5).
* $p < 0.05$, significantly different to contralateral side, Student's paired *t*-test.

7.2.6 The binding of [^{3}H] nicotine to nicotinic cholinergic receptors.

7.2.6.1 Effects of incubation and wash time.

As described in section 2.8.4, after an incubation time of 90 min, the binding of [^{3}H] nicotine was considered to be at equilibrium. A wash time of 2 x 10 sec produced approximately 75 % specific binding.

7.2.6.2 Characteristics of [^{3}H] nicotine binding in lesioned rat brain sections.

The binding of [^{3}H] nicotine to nicotinic receptors was examined in animals receiving unilateral intrastriatal injections of 2 ng volkensin (group 3, n=6), 10 ng ricin (n=6), and 10 μg quinolinate. The distribution of this receptor was also examined in animals receiving intrathalamic injection of 7.5 μg ibotenate (6 (n=5) and 12 (n=5) day survival times). The regional and laminar distributions of [^{3}H] nicotine binding in 2 ng volkensin and 10 μg quinolinate acid (7 day survival time) animals are shown in Figure 7.7. Clearly demarcated within the neocortex were superficial, middle and deep layers. Binding to nicotinic receptors was highest in the middle layers.

Quantitative analysis of the binding of [^{3}H] nicotine receptors in group 3 animals (n=6; Table 7.6) revealed that in the superficial layers there was a significant reduction to 62 % ($p = 0.015$, Student's paired *t*-test) compared to the corresponding region of the contralateral cortex. There were also significant decreases to 54 % ($p = 0.001$, Student's paired *t*-test) and 67 % ($p = 0.001$, Student's paired *t*-test) in the middle and deep layers respectively on the ipsilateral side. More laterally in Par1/Par2, there were no significant changes in superficial and deep layers, but there was a significant reduction in binding in middle layers to 64 % ($p = 0.022$, Student's paired *t*-test) on the ipsilateral side compared to the corresponding contralateral area.

Following intrastriatal injection of 10 ng ricin (n=6, Table 7.6), there were no significant changes in the binding of [^{3}H] nicotine in any layer (superficial, middle or deep) or region (Fr1/Fr2 or Par1/Par2) between sides ipsilateral and contralateral to the injection site.

The binding of [^{3}H] nicotine on the side ipsilateral to the injection site was not significantly different compared to binding on the contralateral side

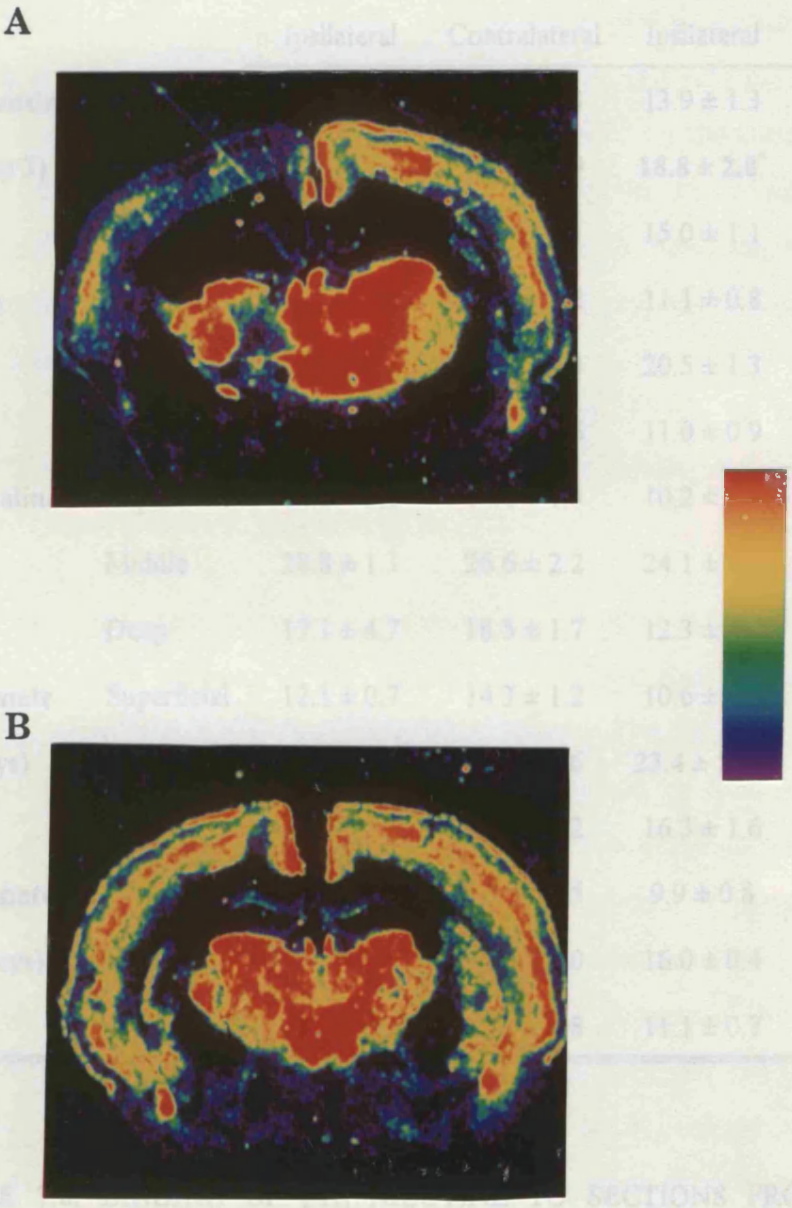

Figure 7.7: REPRESENTATIVE COLOUR-CODED AUTORADIOGRAMS OF [^{3}H] NICOTINE BINDING IN SECTIONS FROM VOLKENSIN AND QUINOLINATE TREATED ANIMALS. Experiments were performed using coronal rat brain sections (12 µm) incubated in 50 mM Tris-HCl (pH 7.4) containing 8 mM $CaCl_2$ and 6 nM [^{3}H] nicotine for 90 min at 25 °C. Non-specific binding was generated using 10 µM carbachol. Colour-coded autoradiograms illustrate specific binding in animal receiving intrastriatal injections of (A) 2 ng volkensin, or (B) 10 µg quinolinate, with postoperative survival times of 28 and 7 days, respectively. The scale bar indicates the intensity of autoradiographic signal from purple (lowest) to red (highest). Note reductions in binding on the ipsilateral side in neocortical areas of (A). Injection site on left.

		Fr1/Fr2		Par1/Par2	
		Ipsilateral	Contralateral	Ipsilateral	Contralateral
Volkensin	Superficial	**14.0 ± 1.0****	22.6 ± 2.3	13.9 ± 1.3	17.4 ± 1.5
(group 3)	Middle	**18.6 ± 1.2‡**	34.3 ± 1.9	**18.8 ± 2.8***	29.0 ± 1.2
	Deep	**17.4 ± 1.1‡**	26.0 ± 1.1	15.0 ± 1.1	17.5 ± 1.0
Ricin	Superficial	12.8 ± 0.8	14.2 ± 1.2	11.1 ± 0.8	12.9 ± 0.7
	Middle	19.0 ± 1.6	23.4 ± 1.4	20.5 ± 1.3	20.4 ± 1.3
	Deep	14.8 ± 1.2	14.7 ± 1.6	11.0 ± 0.9	12.2 ± 1.2
Quinolinate	Superficial	14.6 ± 1.2	14.0 ± 1.3	10.2 ± 1.3	9.7 ± 1.4
	Middle	28.8 ± 1.3	26.6 ± 2.2	24.1 ± 1.4	21.4 ± 1.7
	Deep	17.1 ± 4.7	18.5 ± 1.7	12.3 ± 1.2	11.9 ± 1.3
Ibotenate	Superficial	12.1 ± 0.7	14.3 ± 1.2	10.6 ± 0.9	11.2 ± 1.1
(6 days)	Middle	**21.3 ± 1.6†**	26.4 ± 1.6	**23.4 ± 2.1****	25.9 ± 1.6
	Deep	18.2 ± 1.7	17.6 ± 2.2	16.3 ± 1.6	15.1 ± 2.5
Ibotenate	Superficial	10.3 ± 0.7	11.5 ± 0.5	9.9 ± 0.8	10.1 ± 0.4
(12 days)	Middle	15.5 ± 0.5	16.4 ± 1.0	16.0 ± 0.4	15.2 ± 0.3
	Deep	12.2 ± 0.6	12.8 ± 0.8	11.1 ± 0.7	10.8 ± 0.4

TABLE 7.6: BINDING OF [^{3}H] NICOTINE TO SECTIONS FROM ANIMALS RECEIVING UNILATERAL INTRASTRIATAL AND INTRATHALAMIC TOXINS. Values are mean specific fmol/mg tissue equivalent bound ± SEM on ipsilateral side and contralateral side in medial Fr1/Fr2 and lateral Par1/Par2 areas, following injection of 2 ng volkensin (group 3, n=6), 10 ng ricin (n=6) or 10 µg quinolinate (n=5) into the striatum. Values from groups of animals receiving intrathalamic injection of 7.5 µg ibotenate with a postoperative survival time of 6 (n=5) or 12 days (n=5) are also shown.
* $p < 0.05$, ** $p < 0.02$, † $p < 0.005$, ‡ $p \leq 0.001$, significantly different to contralateral side, Student's paired *t*-test.

following intrastriatal injection of 10 μg quinolinate (n=6) in any layer of neocortical areas Fr1/Fr2 or Par1/Par2 (Table 7.6, Figure 7.7).

In animals receiving intrathalamic injection of 7.5 μg ibotenate, with a survival time of 6 days (n=5; Table 7.6) binding on the side ipsilateral to the injection site was not significantly different to binding on the contralateral side in neocortical areas Fr1/Fr2 or more laterally in Par1/Par2, in either superficial or deep layers. In middle layers, both medially and laterally, binding was significantly reduced to 81 % and 90 % respectively ($p = 0.002$ and 0.014, Student's paired *t*-test).

In ibotenate injected animals with a survival time of 12 days (n=5, Table 7.6), there were no significant differences in binding between ipsilateral and contralateral sides in any area or layer.

7.2.6.3 Saturation analysis of [^{3}H] nicotine in volkensin injected animals.

Saturation analysis of the binding of [^{3}H] nicotine was performed as described in section 2.8.4. Scatchard analysis of [^{3}H] nicotine binding in one volkensin injected animal (Figure 7.8) was performed by "scratch and count" experiments. This gave binding parameters for whole brain sections, with a K_d of 6.6 nM and a B_{max} of 16.3 fmoles/mg tissue equivalent.

Saturation analysis of binding in specific brain areas by autoradiography (Table 7.7) gave results which compared favourably with those obtained in whole brain sections. K_d values obtained ranged from 3.4 - 7.9 nM. There were no significant differences in K_d values between sides ipsilateral and contralateral to the injection site other than in medial middle areas, where there was a significant increase on the lesioned side to 150 % of that observed on the contralateral side ($p = 0.027$, Student's paired *t*-test).

The reduced binding observed using 6 nM [^{3}H] nicotine in medial cortical layers ipsilateral to the injection was accompanied by a reduction in B_{max} in middle and deep layers of Fr1/Fr2 (66 and 61 % of corresponding contralateral value; $p = 0.026$ and $p = 0.005$, Student's paired *t*-test, respectively). A reduction in B_{max} was also observed in the superficial layers of Fr1/Fr2 to 56 % of the contralateral value, though this just failed to reach statistical significance ($p = 0.053$, Student's paired *t*-test). More laterally, reductions in B_{max} were observed in superficial and deep layers of Par1/Par2, to

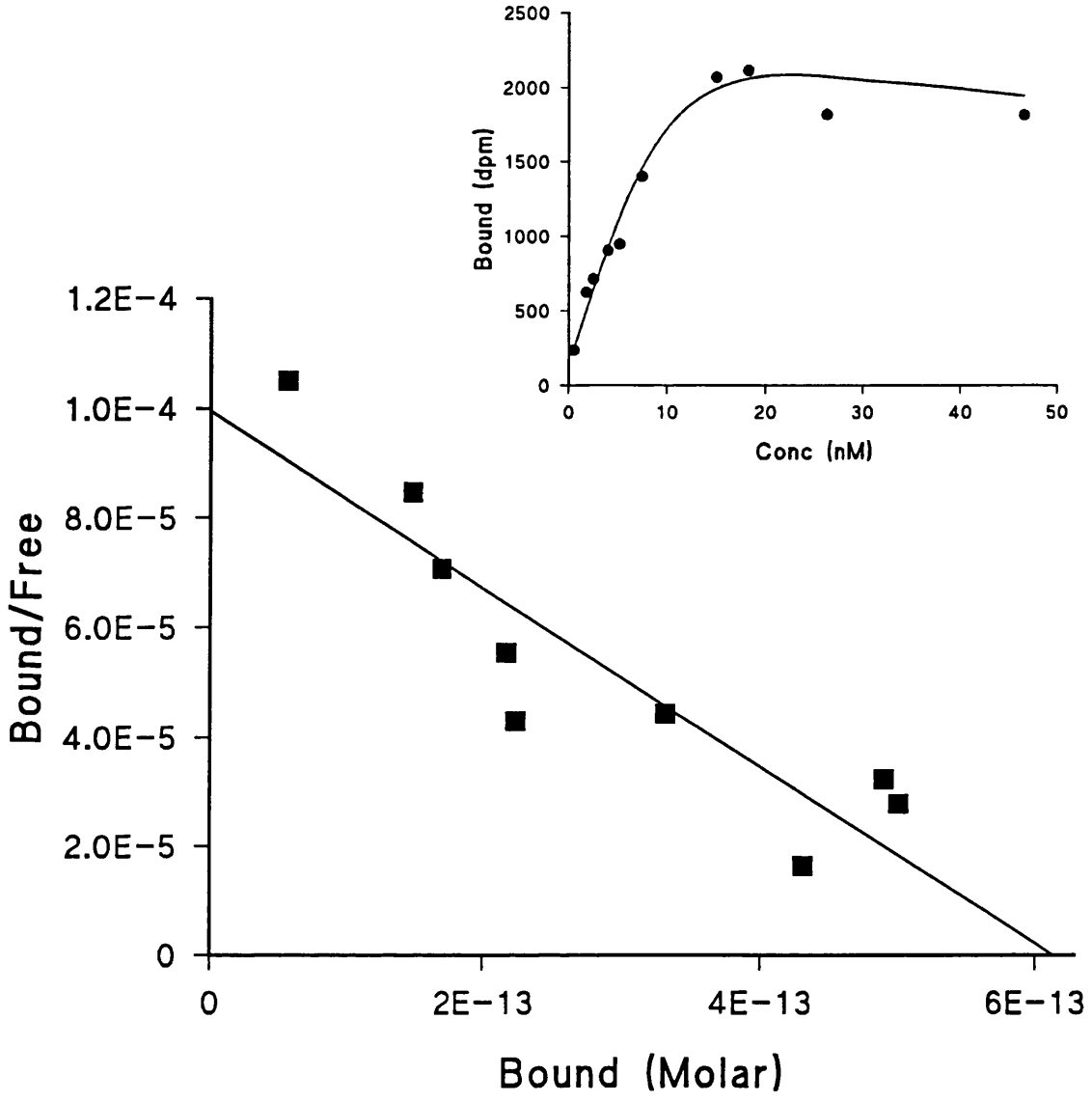

Figure 7.8: SATURATION ANALYSIS OF [^{3}H] NICOTINE BINDING IN WHOLE BRAIN SECTIONS FROM A VOLKENSIN INJECTED ANIMAL. Experiments were performed using coronal rat brain sections from a group 3, volkensin injected animal, which were incubated in 50 mM Tris-HCl (pH 7.4) containing 8 mM $CaCl_2$ and 0.5 - 50 nM [^{3}H] nicotine for 90 min at 25 °C. Non-specific binding was generated using 100 μM carbachol.
Data points represent mean specific binding from 4 sections determined by scratch and count from a single rat. The main plot shows a representative Scatchard analysis, replotted from the EBDA program (McPherson, 1985), with a least squares regression line. Inset shows the saturation curve for the analysis. Parameters determined from this experiment were: K_d = 6.6 nM, B_{max} = 16.3 fmol/mg tissue equivelent.

		Fr1/Fr2		Par1/Par2	
		Ipsilateral	Contralateral	Ipsilateral	Contralateral
K_d (nM)	Superficial	5.5 ± 1.6	6.8 ± 1.3	4.7 ± 0.5	4.9 ± 0.3
	Middle	**5.1 ± 0.6***	3.4 ± 0.3	7.9 ± 2.6	4.3 ± 0.8
	Deep	3.7 ± 0.5	4.2 ± 0.5	5.0 ± 0.7	5.0 ± 0.8
B_{max}	Superficial	18.2 ± 2.2	32.4 ± 3.1	**17.4 ± 1.3***	25.3 ± 1.2
(fmol/mg	Middle	**29.4 ± 1.1***	44.3 ± 3.1	37.8 ± 3.8	49.2 ± 3.2
tissue equiv)	Deep	**20.6 ± 2.6****	33.5 ± 0.9	**19.4 ± 2.1***	28.5 ± 0.7
Hill	Superficial	0.95 ± 0.02	0.95 ± 0.03	0.91 ± 0.07	0.99 ± 0.04
Coefficient	Middle	1.07 ± 0.05	0.91 ± 0.04	0.97 ± 0.09	0.98 ± 0.06
	Deep	0.94 ± 0.05	0.96 ± 0.03	0.92 ± 0.08	0.99 ± 0.04

TABLE 7.7: PARAMETERS OF SCATCHARD ANALYSES OF THE BINDING OF [^{3}H] NICOTINE TO SECTIONS FROM ANIMALS RECEIVING UNILATERAL INTRASTRIATAL VOLKENSIN DETERMINED BY AUTORADIOGRAPHY. K_d values are mean nM ± SEM on ipsilateral side and contralateral side in medial Fr1/Fr2 and lateral Par1/Par2 areas. B_{max} values are fmol/mg tissue equivelent on ipsilateral side and contralateral side in medial Fr1/Fr2 and lateral Par1/Par2 areas. Single site binding kinetics are indicated by Hill coefficients close to unity. Values are from 4 group 3 volkensin injected animals.* $p < 0.05$, ** $p < 0.01$, significantly different to contralateral side, Student's paired *t*-test.

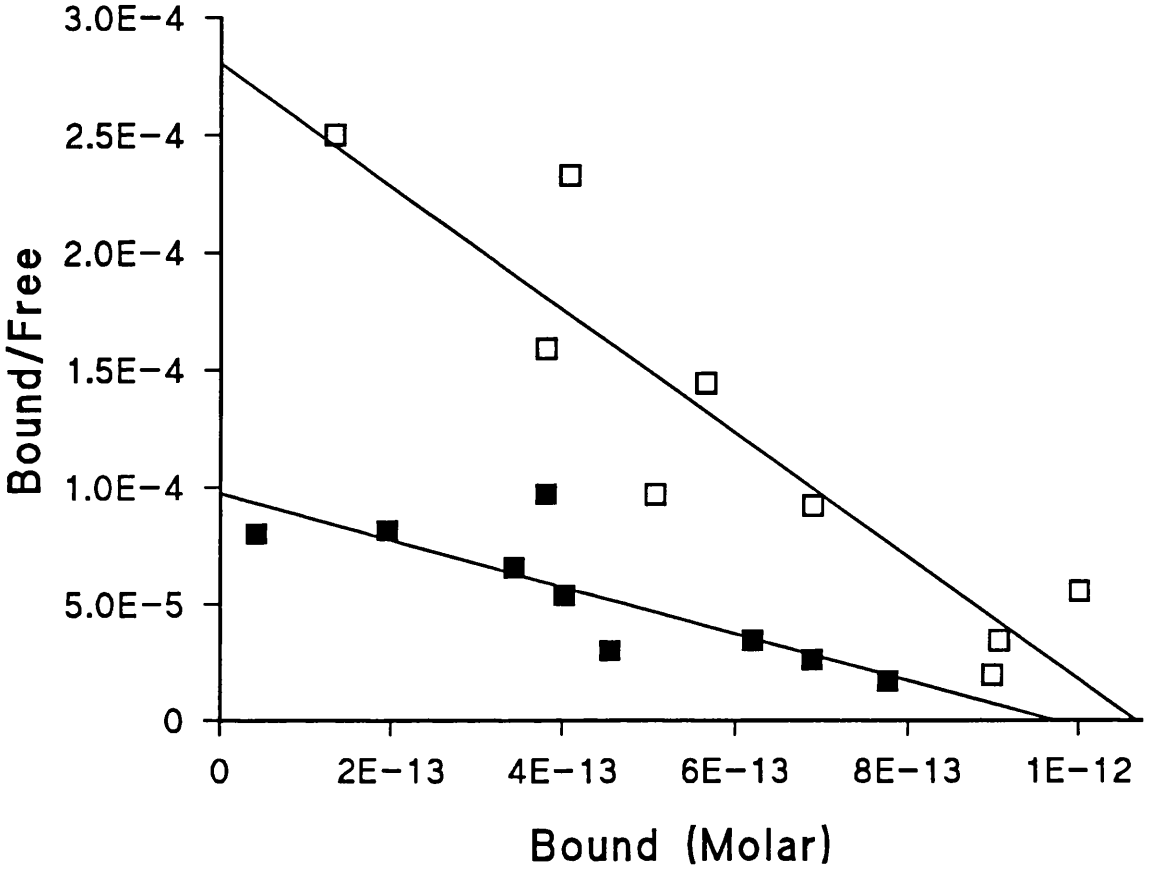

Figure 7.9: REPRESENTATIVE SCATCHARD ANALYSIS OF [^{3}H] NICOTINE BINDING IN SUPERFICIAL CORTICAL LAYERS OF A VOLKENSIN INJECTED ANIMAL. Experimental conditions were as described in Figure 7.8. Data points represent mean specific binding for 4 sections determined autoradiographically from a single rat. Binding is to the superficial cortical layers of Fr1/Fr2, contralateral (■) and ipsilateral (□) to an intrastriatal injection of 2 ng volkensin. Data replotted from the EBDA program (McPherson, 1985), with a least squares regression line.
The binding parameters from the complete group of animals are given in Table 7.7.

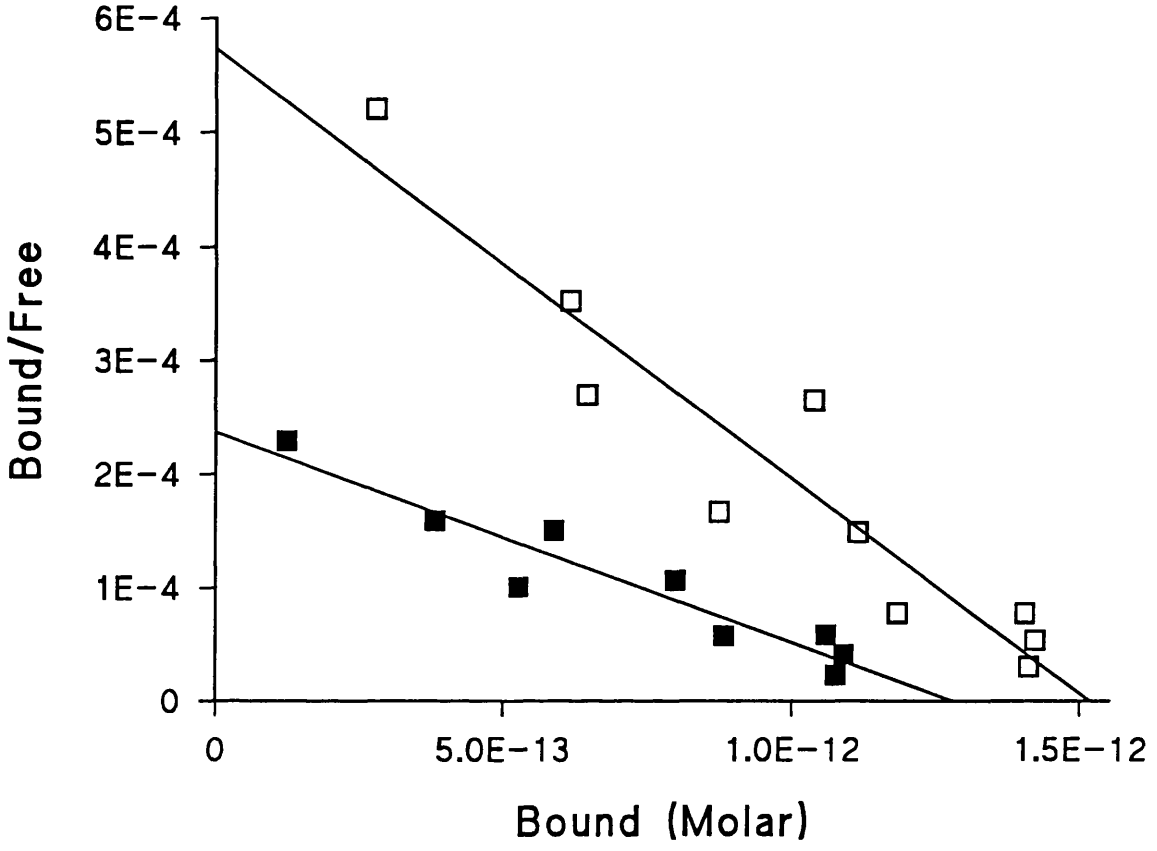

Figure 7.10: REPRESENTATIVE SCATCHARD ANALYSIS OF [^{3}H] NICOTINE BINDING IN MIDDLE CORTICAL LAYERS OF A VOLKENSIN INJECTED ANIMAL. Experimental conditions were as described in Figure 7.8. Data points represent mean specific binding for 4 sections determined autoradiographically from a single rat. Binding is to the middle cortical layers of Fr1/Fr2, contralateral (■) and ipsilateral (□) to an intrastriatal injection of 2 ng volkensin. Data replotted from the EBDA program (McPherson, 1985), with a least squares regression line.
The binding parameters from the complete group of animals are given in Table 7.7.

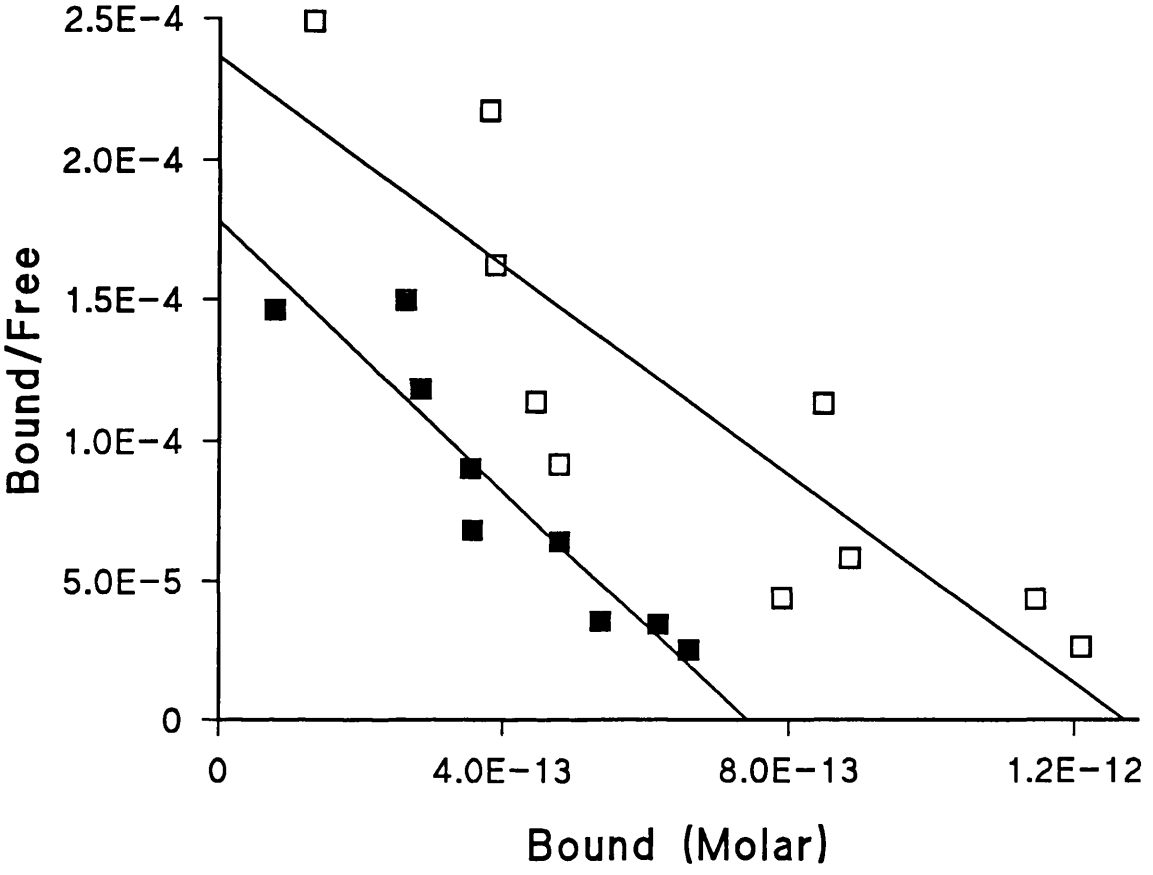

Figure 7.11: REPRESENTATIVE SCATCHARD ANALYSIS OF [^{3}H] NICOTINE BINDING IN DEEP CORTICAL LAYERS OF A VOLKENSIN INJECTED ANIMAL. Experimental conditions were as described in Figure 7.8. Data points represent mean specific binding for 4 sections determined autoradiographically from a single rat. Binding is to the deep cortical layers of Fr1/Fr2, contralateral (■) and ipsilateral (□) to an intrastriatal injection of 2 ng volkensin. Data replotted from the EBDA program (McPherson, 1985), with a least squares regression line.
The binding parameters from the complete group of animals are given in Table 7.7.

69 (p = 0.040, Student's paired *t*-test) and 68 (p = 0.031, Student's paired *t*-test) % of the corresponding contralateral value respectively. Although a reduction in B_{max} was also observed in the middle layers of Par1/Par2, this did not attain statistical significance. Representative Scatchard plots are shown in Figures 7.9 - 7.11 for Fr1/Fr2 superficial, middle and deep layers respectively.

In all cases, Hill coefficients were close to 1 (Table 7.7), indicating that binding conformed to single site kinetics. Correlation coefficients for Scatchard and Hill plots were also close to unity (0.79 - 0.93 and 0.89 - 0.96 respectively).

7.2.7 Binding of [^{3}H] kainate to kainate sensitive glutamate receptors.

The experimental conditions and considerations for the binding of [^{3}H] kainate are described in the methods section and in Chapter 5, sections 5.2.2 and 5.3. Investigations of the localisation of this receptor was performed for groups 1 and 2 volkensin injected animals, 2 groups of animals injected with 10 ng ricin, and animals receiving 10 μg quinolinate and 7.5 μg ibotenate (6 and 12 day survival times).

The laminar and regional distribution of [^{3}H] kainate binding is shown as representative colour coded reconstructions of autoradiograms for volkensin and ricin treated animals (Figure 7.12). Within the neocortex, binding was higher in the deep layers compared to the superficial layers, and higher in lateral areas (Par1/Par2) compared to that observed more medially (Fr1/Fr2).

Quantitative analysis of the binding of [^{3}H] kainate in group 1 animals (n=6; Table 7.8) revealed that there was no significant reduction in binding medially (Fr1/Fr2) in the superficial layers on the ipsilateral side compared to the contralateral side, while in deep layers the binding on the ipsilateral side was reduced to 89 % (p = 0.013, Student's paired *t*-test) of that of the corresponding contralateral area. Laterally, no significant reduction in [^{3}H] kainate binding was observed in the superficial or deep layers on the ipsilateral side compared to that observed on the contralateral side. Quantitative analysis was also performed in a group of animals injected with 6 ng volkensin, which also produced a significant loss of infragranular neurones in medial Fr1/Fr2 areas (Pangalos, 1992). In this group, no significant reductions in the binding

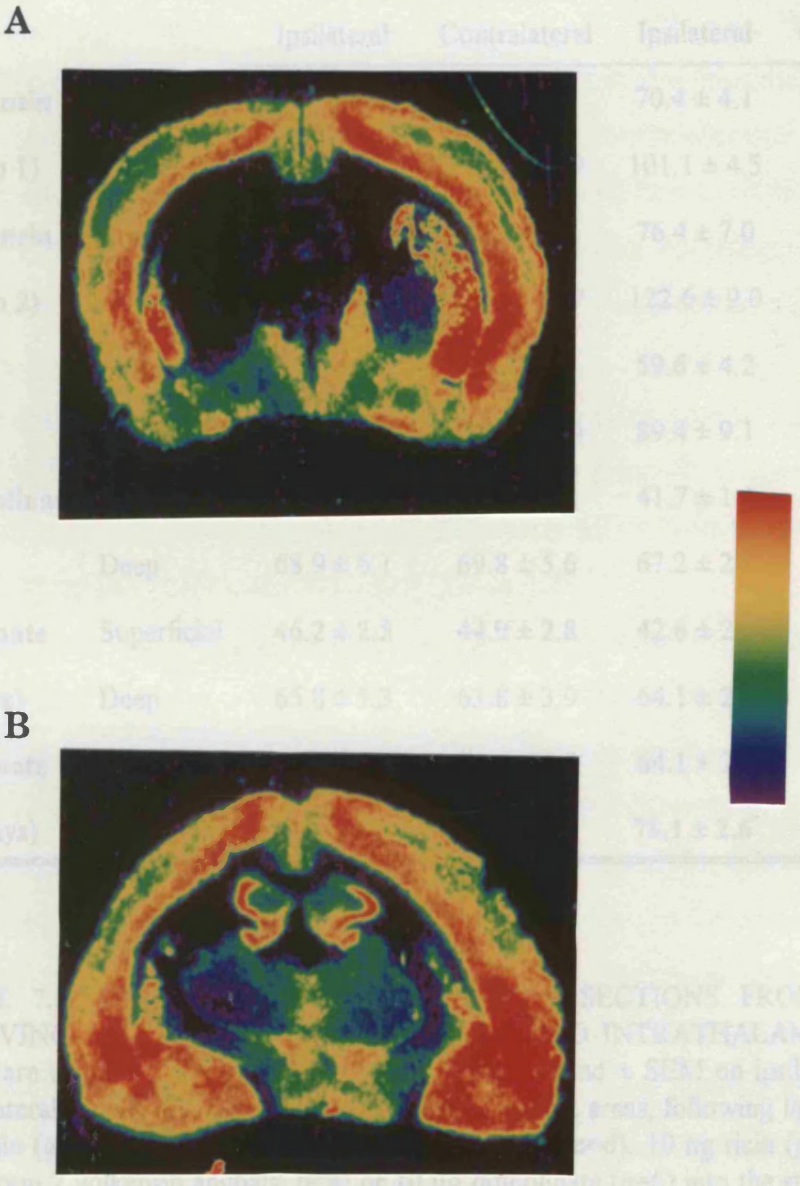

Figure 7.12: REPRESENTATIVE COLOUR-CODED AUTORADIOGRAMS OF [^{3}H] KAINATE BINDING IN SECTIONS FROM VOLKENSIN AND RICIN TREATED ANIMALS. Experiments were performed using coronal rat brain sections (12 µm) incubated in 50 mM Tris-citrate (pH 7.0) containing 30 nM [^{3}H] kainate for 45 min at 2 °C. Non-specific binding was generated using 10 µM kainate.
Colour-coded autoradiograms illustrate specific binding in animal receiving intrastriatal injections of (A) 2 ng volkensin, or (B) 10 ng ricin, with postoperative survival times of 28 days. The scale bar indicates the intensity of autoradiographic signal from purple (lowest) to red (highest). Injection site on left.

		Fr1/Fr2		Par1/Par2	
		Ipsilateral	Contralateral	Ipsilateral	Contralateral
Volkensin	Superficial	65.7 ± 2.3	74.9 ± 5.3	70.4 ± 4.1	69.7 ± 3.4
(group 1)	Deep	**90.8 ± 4.6****	101.8 ± 6.9	101.1 ± 4.5	102.1 ± 6.0
Volkensin	Superficial	72.9 ± 3.1	74.9 ± 3.9	76.4 ± 7.0	79.9 ± 1.6
(group 2)	Deep	**94.1 ± 3.9**†	114.2 ± 6.7	122.6 ± 9.0	121.6 ± 5.1
Ricin	Superficial	72.2 ± 8.1	72.3 ± 8.4	59.6 ± 4.2	61.0 ± 5.8
	Deep	91.6 ± 11.7	91.6 ± 11.4	89.4 ± 9.1	83.3 ± 10.4
Quinolinate	Superficial	**52.7 ± 4.3***	57.3 ± 4.8	41.7 ± 1.4	43.2 ± 3.4
	Deep	68.9 ± 6.1	69.8 ± 5.6	67.2 ± 2.1	67.9 ± 6.3
Ibotenate	Superficial	46.2 ± 2.5	44.9 ± 2.8	42.8 ± 2.2	42.3 ± 2.4
(6 days)	Deep	65.8 ± 3.3	63.8 ± 3.9	64.1 ± 2.1	62.4 ± 4.6
Ibotenate	Superficial	71.7 ± 2.0	66.4 ± 4.5	64.1 ± 2.2	67.9 ± 4.2
(12 days)	Deep	77.3 ± 4.2	73.8 ± 3.8	**78.1 ± 2.6***	72.3 ± 4.0

TABLE 7.8: BINDING OF [^{3}H] KAINATE TO SECTIONS FROM ANIMALS RECEIVING UNILATERAL INTRASTRIATAL AND INTRATHALAMIC TOXINS. Values are mean specific fmol/mg tissue equivalent bound ± SEM on ipsilateral side and contralateral side in medial Fr1/Fr2 and lateral Par1/Par2 areas, following injection of 2 ng volkensin (groups 1 (previously prepared, n=6) and 2 (n=6), 10 ng ricin (group analysed with group 2 volkensin animals; n=4) or 10 µg quinolinate (n=6) into the striatum. Values from groups of animals receiving intrathalamic injection of 7.5 µg ibotenate with a postoperative survival time of 6 (n=5) or 12 (n=6) days are also shown.
* $p < 0.05$, ** $p < 0.01$, † $p < 0.005$, significantly different to contralateral side, Student's paired *t*-test.

of [^{3}H] kainate were found in any area or layer on the ipsilateral side compared to that measured in the corresponding contralateral areas.

In group 2 volkensin injected animals (n=6; Table 7.8), there was no significant reduction in binding medially (Fr1/Fr2) in the superficial layers of the ipsilateral side compared to the corresponding contralateral area, while in deep layers the binding on the ipsilateral side was reduced to 82 % ($p = 0.002$, Student's paired *t*-test) of that of the corresponding contralateral area. In lateral areas, there was no significant reduction of the binding of [^{3}H] kainate in either superficial or deep layers.

Following intrastriatal injection of 10 ng ricin (n=3; analysed with group 1 volkensin animals and n=4; analysed with group 2 volkensin animals), the binding of [^{3}H] kainate was not significantly affected in either superficial or deep layers of Fr1/Fr2 or Par1/Par2 (Table 7.8).

A small but significant decrease in the binding of [^{3}H] kainate was found in the ipsilateral superficial layers of animals injected with 10 μg quinolinate (n=6; Table 7.8) to 92 % of that observed on the contralateral side ($p = 0.039$, Student's paired *t*-test). No significant differences were found in the deep layers of Fr1/Fr2 or superficial or deep layers of Par1/Par2.

Analysis of the binding if [^{3}H] kainate in animals receiving intrathalamic injection of 7.5 μg ibotenate, with a survival time of 6 (n=5; Table 7.8) or 12 (n=6; Table 7.8) days revealed that binding was reduced to 93 % ($p = 0.038$, Student's paired *t*-test) in the deep layers of ipsilateral Par1/Par2 compared to that observed in the corresponding contralateral area. In all other medial and lateral layers, no significant differences were found in binding between ipsilateral and contralateral areas.

7.3 Discussion.

7.3.1 Experimental considerations.

Quantitative comparisons of binding data between different experiments by various investigators are difficult to make, since autoradiographic procedures vary between different laboratories. For example, different incubation conditions may be used for a particular [^{3}H] ligand, or different types of [^{3}H] standard may be used (e.g. brain paste or synthetic polymer tissue equivalent standards). Furthermore, few autoradiographic studies have examined the binding of [^{3}H] ligands quantitatively in the rat neocortex.

Notwithstanding these considerations, the regional and laminar distributions and binding values for [^{3}H] 8-OH-DPAT in the present study compare well with those reported by other investigators. Hensler et al. (1991) and Pangalos (1992) reported binding of 12-20 and 10-30 fmol/mg tissue at a concentration of 1 nM [^{3}H] 8-OH-DPAT respectively.

The regional localisation of [^{3}H] pirenzepine binding reported in this thesis is in excellent agreement with that described by Atack et al. (1989). Additionally, *in-situ* hybridisation histochemistry revealed a laminar distribution of m_1 mRNA in the neocortex, where higher levels were observed in superficial cortical layers compared to deep layers (Buckley et al., 1988). The precise relationship between muscarinic receptor subtypes and the affinity of pirenzepine for the M_1 receptor has been determined from genetically defined subtypes (Hulme et al., 1990), and in the present study only a small proportion of the binding observed using [^{3}H] pirenzepine can be attributed to the M_4 receptor (see Chapter 5, section 5.3.1). Additionally *in-situ* hybridisation histochemistry for the M_4 receptor revealed very low levels of m_4 mRNA within the neocortex (Buckley et al., 1988; Brann et al., 1988). Specific binding values obtained in the present study (45 - 103 fmol/mg tissue compare) favourably with values obtained by Atack et al. (1989) (52 fmol/mg tissue) at concentrations of 2.5 nM [^{3}H] pirenzepine.

The regional and laminar distribution of α_{1total} and α_{1b} receptors is in good agreement with that described by other workers (Grimm et al., 1992). Specific binding values obtained also compare favourably with those described

by other workers. It is probable that the binding values described in the present study are close to B_{max}, as binding kinetics of [^{3}H] prazosin to α_{1total} exhibit low K_d values (< 0.5 nM, Blendy et al., 1991) and similar binding values were reported by Grimm et al. (1992), using a higher concentration of [^{3}H] prazosin to label α_{1total} receptors.

The regional and laminar distribution of [^{3}H] GABA to the $GABA_A$ receptor is in excellent agreement with that described by other workers (Bowery et al., 1987; Chu et al., 1990). The specific binding values obtained in the present study (85 - 170 fmol/mg tissue), using a concentration of [^{3}H] GABA of 20 nM were (after correction of tissue to protein equivalence of 10 %) similar to those described (61 - 95 fmol/mg tissue equivalent (Chu et al., 1990), and 64 pmol/g (Bowery et al., 1987)).

The distribution of adenosine A_1 receptor visualised using [^{3}H] DPCPX is in good agreement to that described by other workers (Van der Ploeg et al., 1992), and similar to that described for the binding of [^{3}H] CHA, another ligand for the A_1 receptor. [^{3}H] DPCPX binding was significantly reduced by inclusion of magnesium in the incubation medium. Subsequent incubations were performed in the absence of exogenously added Mg^{2+}. Values for specific binding of [^{3}H] DPCPX in the rat neocortex are sparse, though the results from the present study are in the same order of magnitude for those described for the receptor B_{max} in membrane binding studies (Lohse et al., 1987). This is not unexpected, as the affinity for DPCPX for the A_1 receptor is high (K_d < 1 nM, Lohse et al., 1987), and thus binding values at the concentration of [^{3}H] DPCPX used in this study are likely to be close to B_{max}.

The regional and laminar distribution of [^{3}H] nicotine binding is in excellent agreement with that described by other workers by autoradiography (Clarke et al., 1985). *In-situ* hybridisation histochemistry also demonstrated the presence of ligand binding subunits, particularly α2, α3, and α4-2 subunits in the neocortex (Wada et al., 1989). Saturation analysis by "scratch and count" methods produced a K_d value of 6.6 nM, and a B_{max} of 16.6 fmol/mg tissue, which compare very well with reported values (6 nM and 14.3 fmol/mg tissue, K_d and B_{max} respectively). Saturation analysis from autoradiograms gave

similar K_d (3.4 - 7.9 nM) and B_{max} (18.2 - 49.2 fmol/mg tissue equivalent) values, with Hill coefficients indicative of single site binding kinetics.

The distribution of kainate sensitive glutamate receptors visualised by [^{3}H] kainate binding compares favourably with that observed by other workers (Monaghan and Cotman, 1982; Greenamyre and Young, 1989b). Values for specific binding in this study (42 - 121 fmol/mg tissue) are also comparable with those previously reported (88 - 125 fmol/mg tissue) (Okazaki et al., 1990). As described in Chapter 5, section 5.3.1, incubations were performed in the absence of exogenously added Ca^{2+}.

7.3.2 Receptor distribution and localisation in lesioned animals.

The present study confirms reductions in the binding of [^{3}H] 8-OH-DPAT, [^{3}H] pirenzepine and [^{3}H] kainate to 5-HT_{1A}, M_1, and kainate sensitive glutamate receptors on the ipsilateral side in animals receiving 2 ng of intrastriatal volkensin. In addition, reductions in binding following volkensin injection were also observed using [^{3}H] nicotine and [^{3}H] DPCPX binding to nicotinic cholinergic and adenosine A_1 receptors, with sparing of the binding of [^{3}H] GABA to $GABA_A$ and [^{3}H] prazosin to α_1 receptors. By contrast, no reductions in binding were observed for any ligand in animals injected with 10 ng ricin, and only limited changes were observed with some ligands in animals receiving intrastriatal or intrathalamic injections of quinolinate or ibotenate. Few lesioning paradigms have focused on the localisation of receptor types in the rat neocortex, though Crino et al. (1990) used intracaudate and intrathalamic injection of a different suicide transport agent, OX7-saporin, and a shorter, 14 day survival period to ascribe changes in 5-HT_{1A} receptors in the cortex. Following intracaudate injection, neither pyramidal cell number nor 5-HT_{1A} receptors were altered in layer V of the neocortex, though intrathalamic injection successfully destroyed cells of origin of the corticothalamic pathway and reduced 5-HT_{1A} receptors in the cingulate cortex. Furthermore, Sahin et al (1992), used excitotoxin injections into the cortex and thalamus to study the localisation of nicotinic and muscarinic receptors in the cortex (see below).

The most likely interpretation of the observed reduction in [^{3}H] 8-OH-DPAT, [^{3}H] nicotine, [^{3}H] pirenzepine, [^{3}H] kainate and [^{3}H] DPCPX binding is that the respective receptors are present postsynaptically on infragranular pyramidal cells, which project to the volkensin injected area. Reductions in binding to 5-HT_{1A} and nicotinic receptors were greater than the concurrent reductions observed in cell numbers, indicating that these receptors are present in disproportionately high numbers on the affected neurones, and can be described as being "enriched" on the cells which were destroyed. Smaller reductions in the binding of [^{3}H] pirenzepine, [^{3}H] kainate and [^{3}H] DPCPX indicate a more homogeneous distribution of the receptors between the affected neurones and the remaining cells. Where reductions were observed in deep layers of the neocortex, it is likely that the receptors and localised to the cell bodies of the affected neurones, while changes which extend throughout the depth of the neocortex may be indicative of localisation to dendrites or terminals of the axon collaterals of the affected neurones, since local axon collaterals originating from pyramidal cells are one of the most consistently demonstrated features of neocortical circuitry (Lund and Boothe, 1975; Feldman, 1984; Kisvarday et al., 1986; Peters, 1987).

The possibility that the receptors which exhibit significant reductions on the side ipsilateral to the lesion are located on interneurones destroyed by the re-uptake of toxin following corticostriatal projecting cell death is unlikely. Previous studies (Pangalos et al., 1991a; Pangalos et al., 1991b; Pangalos, 1992) have demonstrated the preservation of GAD-mRNA positive neurones in the areas where neocortical cell loss occurred, and the present study employed an identical paradigm. Thus it is improbable that trans-synaptic degeneration or diffusion occurred. Additionally, this data, as well as the fact that intrastriatal injection of ricin, similar in nature to volkensin, but only effective as a suicide transport agent in the peripheral nervous system, did not produce any reduction in binding of any ligand studied makes it unlikely that receptors were lost following diffusion of the toxin to the cortex.

Another interpretation for the localisation of 5-HT_{1A} receptors is that these sites are located presynaptically either as autoreceptors or as heteroreceptors. Autoreceptor localisation is unlikely, as no reduction in [^{3}H]

8-OH-DPAT binding was observed following medial forebrain bundle lesioning with 5,7 dihydroxytryptamine in animals with a postoperative survival time of 21 days, yet presynaptic markers (5-HT, 5-HIAA and binding of a 5-HT uptake inhibitor) were markedly reduced (Hall et al., 1985; Verge et al., 1986). Moreover, dorsal raphe neurones projecting to the striatum do not also form corticopetal fibres (Tork, 1985). The possibility that the 5-HT_{1A} sites are localised to terminals of non serotonergic projections from the injection site is also unlikely, as the striatal area affected does not project to the neocortex (Heimer et al., 1985) and injection of 10 ng ricin, which caused similar striatal necrosis, did not result in a reduction in [^{3}H] 8-OH-DPAT binding. Similarly, no reductions in the binding of [^{3}H] 8-OH-DPAT were observed following intrastriatal injection of quinolinate. Though the thalamic nuclei groups do form projections to the cortex, and some volkensin injected animals exhibited limited thalamic damage, these projections are primarily to retrosplenial, cingulate, temporal and occipital cortices, with only a sparse innervation to Fr1/Fr2 (Faull and Mehler, 1985). Furthermore, intrathalamic injection of ibotenate produced a small but significant increase in [^{3}H] 8-OH-DPAT binding in superficial layers of Par1/Par2, with no significant changes in other neocortical areas, and thus it is unlikely that the changes observed in volkensin injected animals can be attributed to loss of thalamocortical projecting neurones. It is possible that this increase may be attributable to denervation supersensitivity following the loss of thalamocortical projections, and if this is the case it is probable that the reductions in [^{3}H] 8-OH-DPAT binding in volkensin injected animals is somewhat masked by this phenomenon. Additionally, 5-HT_{1A} receptors have been reported to be found on astrocytes (Whitaker-Azmitia and Azmitia, 1989; Whitaker-Azmitia et al., 1990), and in the present study, marked gliosis occurs in areas of neocortical cell loss, and thus this may also mask the loss of 5-HT_{1A} sites. The 5-HT_{1A} receptors that are affected in Fr1/Fr2 appear to be primarily confined to the immediate vicinity of the cell body, since there was no significant reduction in binding in these neocortical superficial layers. By contrast, in groups 1 and 3 volkensin injected animals, significant reductions were also observed on the

ipsilateral side in the superficial layers of Par1/Par2, indicating that the 5-HT_{1A} sites are distributed over the apical dendrites as well as the cell bodies.

This study has also confirmed that small, but consistent reductions in the binding of [^{3}H] pirenzepine to the muscarinic M_1 receptor are observed in areas where neocortical cell loss occurred. Again, there is the possibility that these receptors are autoreceptors or heteroreceptors. However, M_1 receptors are considered to be localised primarily on postsynaptic neurones, on the basis of the work of Sahin et al (1992), where cortical excitotoxin injection which spared extrinsic fibres reduced muscarinic receptors. Similarly, electrophysiological studies suggest that muscarinic agonists increase the firing rate of cortical pyramidal neurones (McCormick and Williamson, 1989). Furthermore, Atack et al. (1989) and Wenk and Rokaeus (1988) observed no change in [^{3}H] pirenzepine binding following lesioning of the nucleus basalis of Meynert, though there are contradictory data from Bogdanovic et al. (1993) and Dawson et al. (1991), where reduced M_1 binding occurred in lower and all cortical layers respectively following nucleus basalis lesioning. M_1 heteroreceptors on the terminals of neurones which project from the injection site are also unlikely to be involved. As described in the preceding paragraph, the striatal area lesioned does not project to the neocortex, and no changes in [^{3}H] pirenzepine binding were observed in animals injected with intrastriatal ricin or quinolinate. Although the innervation of the thalamocortical pathway may contribute to the changes observed, no alteration in cortical [^{3}H] pirenzepine binding was observed following thalamic lesioning in the present study, or that of Vogt and Burns (1988). It is likely that M_1 receptors are localised on the cell bodies of the affected neurones, as significant reductions in binding were only observed in lower cortical layers of volkensin injected animals. However, reductions in [^{3}H] pirenzepine binding were less marked than those observed for 5-HT_{1A} sites, and thus it is probable that a greater proportion of 5-HT_{1A} than M_1 sites are concentrated on layer V pyramidal neurones forming the corticostriatal pathway. It is unlikely that the binding of [^{3}H] pirenzepine to the M_4 receptor contributed significantly to the results obtained in the present study, as *in-situ* hybridisation histochemistry for m_4

mRNA revealed very low levels within the neocortex (Buckley et al., 1988; Brann et al., 1988).

Although it is possible that structural changes caused by volkensin injection resulted in secondary alterations in neuronal and non-neuronal interactions, the most straightforward interpretation for the slight increases in α_{1total} and α_{1b} receptors is that these additional binding sites are located on glial cells, and the marked gliosis that occurs in the area of cell loss (Pangalos et al., 1992) accounts for these observations. It has previously been reported that α_1 receptors are present on glial cells in culture (Wilson et al., 1990). This may have obscured reductions in binding effected by neocortical cell loss, except perhaps in the middle layer of Par1/Par2. An alternative explanation for the increase in α_1 binding could be denervation supersensitivity, i.e., a postsynaptic increase in receptor number following loss of afferent projection, previously reported for these receptors (Grimm et al., 1992). The neocortex receives noradrenergic innervation from the locus coeruleus, though the majority of the striatum is not innervated from this nucleus (Loughlin et al., 1982). However, it is possible that some bifurcating axons project to both the striatum and the cortex from the locus coeruleus, and destruction of these cell bodies results in noradrenergic denervation and consequent upregulation of postsynaptic receptor populations. There also remains the possibility that there was an increase in the density of small neurones, below the exclusion threshold set during cell counting, and this receptor type may be localised on these cells.

The binding of [^{3}H] GABA to $GABA_A$ receptors was not reduced in animals injected with volkensin, and it may be concluded that pyramidal neurones forming the corticostriatal pathway are not enriched with $GABA_A$ receptors. However, electrophysiological studies demonstrate the inhibitory action of GABA on pyramidal neurones. The lack of change may be therefore be attributable to other explanations. First, that the inhibitory regulation of pyramidal neurones is by $GABA_B$ receptors. Second, that the remaining neurones may upregulate the number of $GABA_A$ receptors which they bear. Third, $GABA_A$ receptors are found on glial cells (Von Blankenfeld and Kettenmann, 1992), and given the marked gliosis that occurs in the affected area, the loss of $GABA_A$ receptors effected by loss of neurones may be masked.

Finally, the affected cells may contribute only a small number of sites to total $GABA_A$ binding in the neocortex, and hence, any small reduction consequent upon the loss of these cells may not be detectable overall. Thus, in the present study it is not possible to exclude the possibility that $GABA_A$ receptors are present to a limited extent on the affected neurones.

Adenosine is thought to be co-released with noradrenaline from noradrenergic varicosities (Ossward and Azevedo, 1991), and most reports suggest that the action of the A_1 receptor is to inhibit terminal release of transmitter (Fredholm et al., 1983; Fredholm and Dunwiddie, 1988). However, most studies of the localisation of adenosine receptors focus on the hippocampal formation, where, in CA1, pre- and postsynaptic localisation of the receptor has been demonstrated (Deckert and Jorgenson, 1988). The present study demonstrates a small but significant decrease in the deep layers of the ipsilateral side in volkensin injected animals, suggesting that these receptors are present on the affected neurones. A larger change may be obscured by increases in the number of glial cells, which have been demonstrated to bear A_1 receptors (Rudolphi et al., 1992).

Substantial reductions were observed in the binding of [^{3}H] nicotine to nicotinic cholinergic receptors in superficial, middle and deep layers of Fr1/Fr2 and middle layers of Par1/Par2. These reductions were accompanied by decreased B_{max} values in middle and deep layers of Fr1/Fr2 and superficial and deep layers of Par1/Par2. K_d values were unchanged between ipsilateral and contralateral sides with the exception of a small increase ipsilaterally in the middle layers of Fr1/Fr2. Though the most straightforward interpretation of this data is that nicotinic receptors are localised to the cell bodies and dendrites of the affected neurones, several other possibilities should be explored. Autoreceptor localisation of nicotinic sites is unlikely, as lesioning of the nucleus basalis of Meynert did not reduce the binding of [^{3}H] nicotine in cortical layers (Wenk and Rokaeus, 1988; Miyai et al., 1990). However, a proportion of nicotinic sites seem to be present as heteroreceptors on the terminals of thalamocortical projecting neurones. Following thalamic lesions using kainate or electrolytic techniques, Sahin et al. (1992) observed up to 50 % reduction in [^{3}H] nicotine binding in the cortex; however, cortical excitotoxin

injection produced a 40 % loss of [^{3}H] nicotine binding, which is consistent with the order of change observed in the present study where cortical pyramidal neurones have been destroyed. A postsynaptic localisation of a proportion of nicotine sites is also supported by studies by Hill et al. (1993), who localised the beta2 subunit of the receptor to the cell bodies and dendrites of pyramidal neurones and by Bravo and Karten (1992) who used monoclonal antibodies to the nicotinic receptor, and described localisation on the cell bodies of layer III and V pyramidal neurones. Double labelling (immunohistochemistry and fluorescent retrograde tracer) was employed to demonstrate the projection of these neurones to subcortical targets. Thus it is clear that there exists a heterogeneous distribution of nicotinic receptors to both pre- and postsynaptic sites, and it is probable that the presynaptic receptors are heteroreceptors of non-cholinergic (thalamic) projections to the cortex, which is supported by the present study where intrathalamic injection of ibotenate reduced the binding of [^{3}H] nicotine in the ipsilateral middle layers of Fr1/Fr2 in 6 day survival time animals. It is therefore possible that between 40 - 50 % of the reduction observed in [^{3}H] nicotine binding in the middle layers of volkensin injected animals could be attributable to the loss of thalamocortical fibres, though the slight increase in K_d value in this area should also be considered as a confounding factor.

Small but consistent reductions in the binding of [^{3}H] kainate were observed in the deep layers of Fr1/Fr2 on the ipsilateral side of volkensin injected animals. While no changes were observed in animals injected with ricin, a small but significant reduction in binding was observed in the superficial layers of Fr1/Fr2 in animals receiving intrastriatal quinolinate. Kainate heteroreceptors on terminals of neurones which project from the injection site to the cortex are unlikely to be involved, as the striatal area lesioned does not project to the neocortex (Heimer et al., 1985), so the only possible corticopetal fibres that might bear such receptors are those of the thalamocortical pathway. However intrathalamic injection of ibotenate did not cause reductions in [^{3}H] kainate binding in the neocortical areas examined. Moreover, a small increase in the binding of [^{3}H] kainate was observed in the deep layers of Par1/Par2 following intrathalamic ibotenate injection, but only

at a survival time of 12 days. This suggests, that in this area, the kainate receptor may be subject to denervation supersensitivity, supported by findings following entorhinal lesions, where upregulation of the receptor was observed in the DG, but only at survival times of 21 days or more (Ulas et al., 1990). It should be noted that in the present study, the binding of both [^{3}H] kainate and [^{3}H] nicotine was higher in the contralateral cortical layers of volkensin injected animals than that observed in ricin injected animals, though binding in volkensin injected animals was comparable with that observed in control animals (data not shown). It is likely that this is attributable to experimental variation, however, future studies should address the possibility of complex adaptive bilateral changes following volkensin injection, using matched samples with identical experimental conditions.

The present study provides compelling evidence for the specific enrichment of 5-HT_{1A} and nicotinic receptors to layer V neocortical pyramidal neurones, though further studies are required to differentiate between pre- and postsynaptic nicotinic sites. Muscarinic M_1 receptors are also present on these cells, though they bear a smaller proportion of the population of M_1 receptors than that of 5-HT_{1A} and nicotinic receptors. Smaller reductions in the binding of [^{3}H] kainate to the kainate sensitive glutamate receptor are consistent with a more uniform distribution. Since glutamate and aspartate are considered to be neurotransmitters at the majority of neocortical synapses, it is likely that the kainate receptor is present on a number of neuronal types throughout the cortex. Indeed, the abundance of the receptor on the cell bodies and dendrites of other neocortical neurones may obscure a clear reduction in the markers for this receptor on the affected neurones. Though these neurones may be subject to regulation by adenosine A_1, $GABA_A$ and alpha adrenoceptors, the present study provides less compelling evidence for the specific localisation of these receptors to the affected neurones.

CHAPTER 8: Histological investigations of a subpopulation of neocortical pyramidal neurones following unilateral intracortical injections of neurotoxic agents.

8.1 Introduction.

As described in Chapter 6, the major cell type of the neocortex is the pyramidal neurone. This thesis has described selective destruction of two types of pyramidal neurone; hippocampal CA3 neurones and corticofugal projecting layer V pyramidal neurones. The biochemical sequelae of such a loss has been described for each of these lesioning paradigms. It has been proposed that the loss of corticocortical projecting glutamatergic neurones which form the association pathways (Neary et al., 1986; DeKosky and Scheff, 1990) contribute to the cognitive deficit observed in AD, a view supported by the finding of prominent cell loss and tangle formation in layer III in *post-mortem* samples of association cortex but not primary sensory areas (Braak and Braak, 1985; Pearson et al., 1985). The cells that are lost, together with those subject to tangle formation, form the majority of cortical efferents (Jones, 1984), and thus this final lesioning paradigm has focused on the selective destruction of layer III and V pyramidal neurones which project trans-callosally to contralateral neocortex. Biochemical sequelae of the loss of these pyramidal neurones are compared with those consequent on a loss of CA3 and layer V pyramidal neurones to examine the heterogeneity of receptor populations of these cells with the aim of pharmacological targeting and manipulation of the activity of these cells in the context of treating the symptoms and progression of AD. The initial objective, therefore, was to prepare groups of animals and to investigate the consistency of volkensin induced selective loss of pyramidal neurones of origin of the corticocortical pathway.

8.2 Results.

8.2.1 Determination of volkensin and ricin dosage and survival time.

All surgical procedures and above investigations were performed by Prof. R.C.A. Pearson (University of Sheffield). Initial experiments were performed using small (typically n=3) groups of animals. Injection placement

was as described in the Chapter 2, section 2.6.3, and was consistent throughout the study. Initial volkensin and ricin doses were based on previous studies (Pangalos et al., 1991b); however, initial ricin doses of 25 ng caused animal death before the appropriate postoperative survival delay had elapsed, and subsequent ricin doses of 12.5 ng were used. Groups of volkensin injected animals were prepared with postoperative survival times of 7, 14, 21 and 28 days. No apparent qualitative changes were observed in contralateral cortex in groups of animals with 7 or 14 day survival times. Examination of Gallyas stained sections from a 21 day postoperative delay animal revealed significant degeneration of contralateral projecting axons from supragranular and infragranular neurones, although substantial neuronal loss in these layers was not apparent, confirmed by quantitative evaluation. These findings justify the 28 day survival period used subsequently, in which there was a clear columnar loss of supragranular and infragranular pyramidal neurones.

8.2.2 Retrograde labelling of neocortical pyramidal neurones following intracortical HRP injection.

Injection placement of 1 μl HRP (see methods, section 2.6.3) in 3 animals was as above. Following a 24 hr survival period, brain sectioning and chromogen development, labelled cells were counted in contralateral cortex corresponding to the injection site in 4 contiguous fields through the depth of the neocortex. Cells of both supragranular and infragranular layers were labelled, with an equal distribution (Figure 8.1). Surgical procedures and labelled cell counts were performed by Prof. R.C.A. Pearson (University of Sheffield).

8.2.3 Cell loss as a result of spread of toxins directly from the injection site.

Volkensin and ricin injections were centred in the dorsal neocortex underlying the removed bone flap. Stereotaxic co-ordinates were not used to guide the placement of injections, and thus some variation in placement occurred between animals.

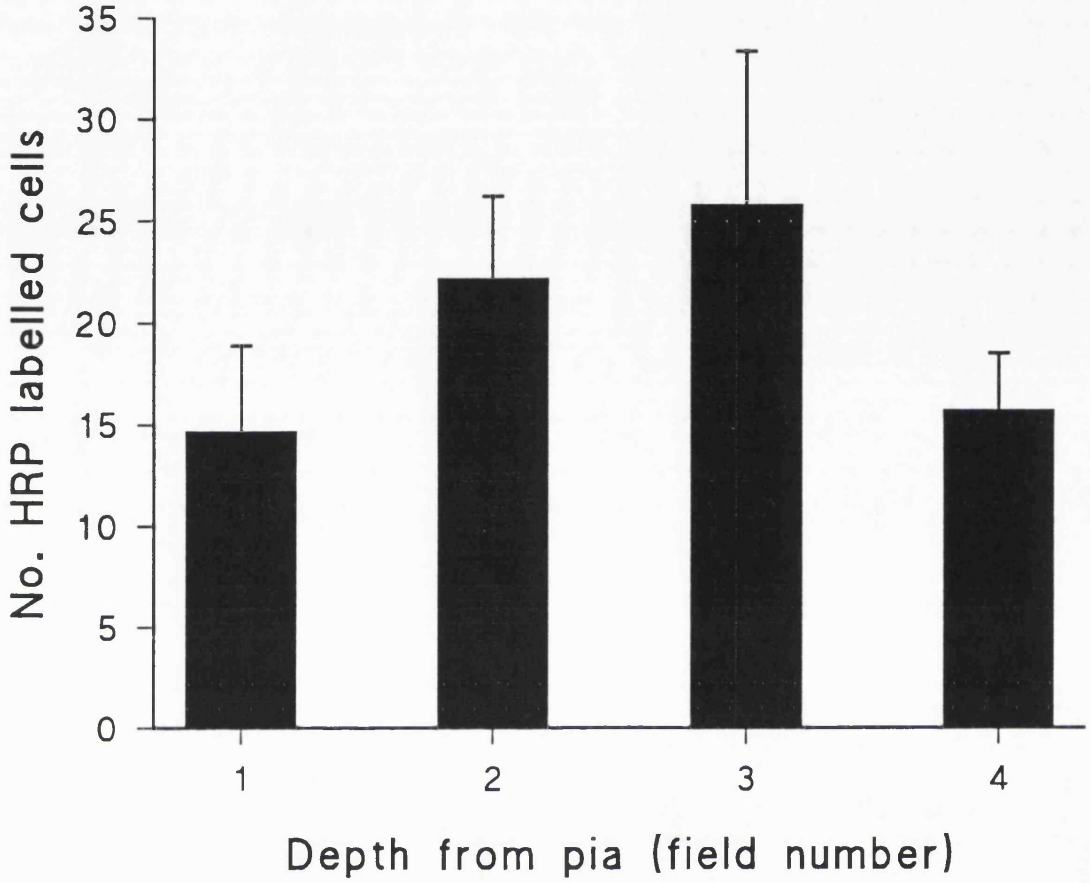

Figure 8.1: NUMBER OF HRP LABELLED CELLS IN THE NEOCORTEX CONTRALATERAL TO CORTICAL INJECTION OF HRP. Injection of deionised water containing 1 μl 20 % HRP type VI, 2 % Triticum Vulgaris and 1% DMSO was made into the left neocortex. After a 24 hr survival period, animals (n=3) were perfused transcardially with phosphate buffer containing 2 % paraformaldehyde and 1.5 % glutaraldehyde. Following sectioning (50 μm), sections were washed in 6 changes of deionised H_2O, pre-soaked in 97.5 parts 0.02 % ammonium heptomolybdate in phosphate buffer / 2.5 parts tetramethylbenzedine (TMB) in absolute alcohol, and chromogen developed by addition of 1 ml 0.3 % H_2O_2. Following satisfactory colour development, sections were rinsed again in 6 changes of dH_2O, and counterstained with 0.5 % neutral red.
Data is mean number of labelled cells $\pm$ SEM in four contiguous fields through the depth of the neocortex contralateral to the injection site.

In all volkensin injected animals, lesions were extensive, with considerable disruption of the cortical structure and hemisphere conformation (Figure 8.2). Cortical lesions extended from bregma - 2.30 mm to bregma - 7.8 mm. All animals displayed destruction of a substantial proportion of cortical areas Fr1/Fr2, HL and Par1 (Paxinos and Watson, 1982; Zilles, 1985) rostrally, extending caudally into occipital cortex areas 2 (medial and lateral) and 1 (medial and binocular). In 5 of the 7 animals, there was also involvement of the retrosplenial agranular area (close to the midline) and in 4 animals temporal cortex area 1 was disrupted. In all cases, there was direct damage of adjacent subcortical structures, with destruction of anterior corpus callosum, fimbria hippocampus, cingulum and anterior hippocampal CA1, with substantial enlargement of the lateral ventricles on both ipsilateral and contralateral sides. Moving caudally, less hippocampal involvement was apparent, with sparing of CA3. In 3 of the 7 animals, the dorsal blade of the DG was also involved. In 1 animal, there was also disruption of caudal subcortical structures, including anterodorsal presubiculum and adjacent subiculum, and superior colliculus to the level of the intermediate grey area. In the same animal, there was lateral spread in the cortex into temporal area 2. There was no evidence of involvement of contralateral cortical or subcortical areas in any animal examined due to direct spread of the toxin.

Injection of 12.5 ng ricin caused necrosis of the cortex (Figure 8.2), though structural disruption of the hemisphere was much less marked, with a smaller level of ventricular enlargement. Again, the corpus callosum, fimbria hippocampus and cingulum were involved. Most animals displayed limited involvement of the hippocampal areas, with disruption limited to dorsal CA1. In all cases, the DG was spared, and spread in the cortex was limited to Fr1/Fr2, HL and Par1 (rostral) to occipital cortex areas 2 (medial) and 1 (medial and binocular). In 2 of the 6 ricin injected animals, there was also involvement of the retrosplenial agranular area. There was no evidence of damage to contralateral cortical or subcortical areas in any animal examined.

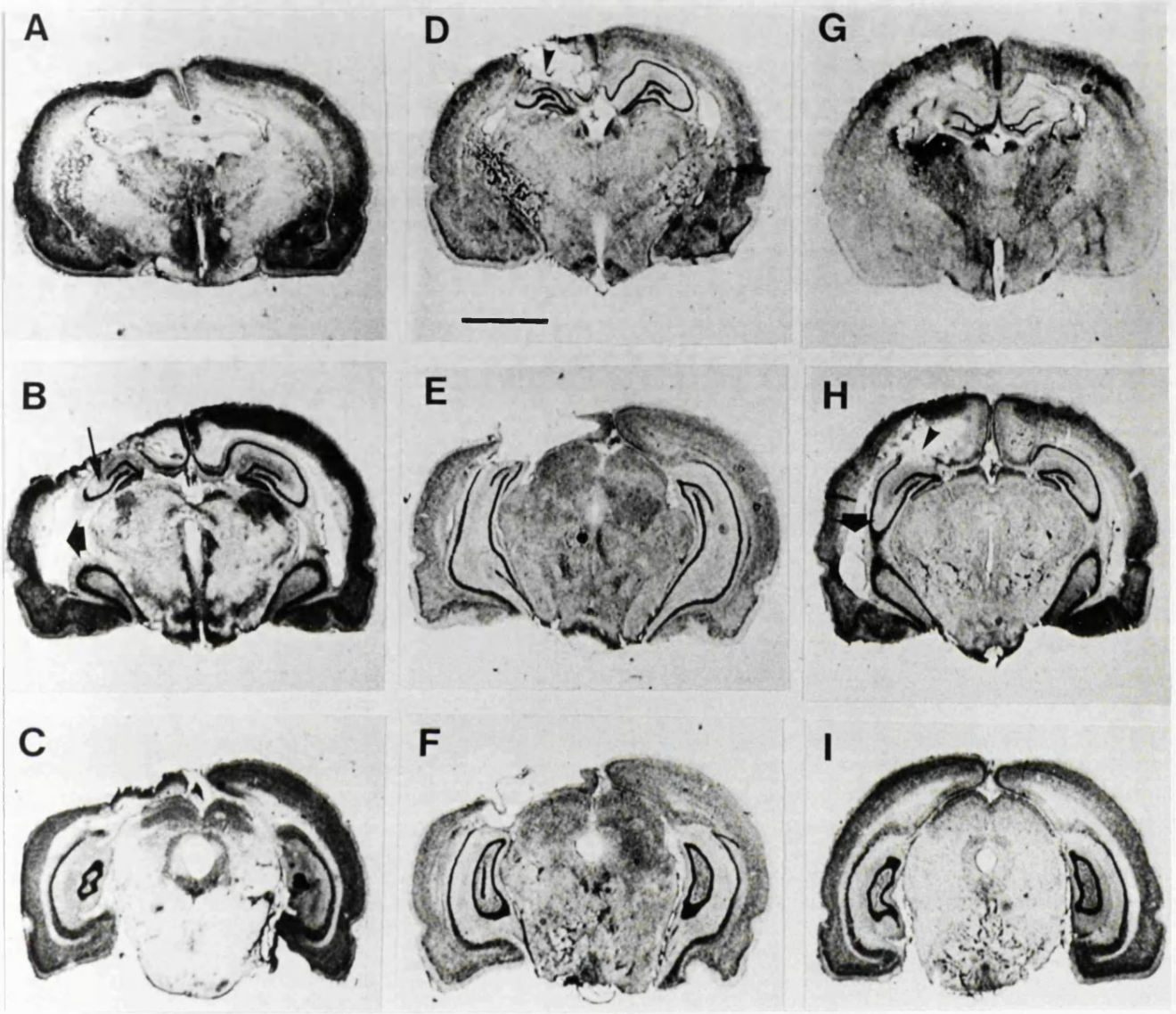

Figure 8.2: PHOTOMICROGRAPHS OF CORONAL SECTIONS OF THE BRAIN AT DIFFERENT ROSTRO-CAUDAL LEVELS FOLLOWING UNILATERAL INTRACORTICAL TOXIN INJECTION. A - C: Rat 1 following injection of 2.5 ng volkensin. Note the severe cortical damage (B and C) and preservation of hippocampal structures CA3 and DG (small arrow in B), as well as more ventral structures, and the marked ventricular enlargement on the ipsilateral (large arrow in B) and contralateral side. D - F: Rat 2 following injection of 2.5 ng volkensin. Note severe cortical damage (D - F) and involvement of hippocampal CA1 regions (arrowhead in D). G - I: Rat 3 following injection of 12.5 ng ricin. Cortical damage is not as severe as the two volkensin cases, but note marked necrosis in G and H, and ventricular enlargement on the ipsilateral (large arrow in H) and contralateral sides.
Injection on left side. All photographs taken at the same magnification. All sections counterstained with cresyl violet. Scale bar (D) 3 mm.

8.2.4 Cell counts in the neocortex in control and toxin injected animals.

Qualitative examination of the neocortex contralateral to the injection site revealed a clear, columnar loss of both supragranular and infragranular pyramidal neurones in animals injected with 2.5 ng volkensin. This loss was most marked in more medial areas. Measurements of cell numbers and size were performed as described in section 2.7.6.3, in areas contralateral to the injection site (neocortical areas Fr1 and HL, occipital cortex area 2 (mediomedial, mediolateral and lateral) and area 1 (medial and binocular) (Zilles, 1985)). Constraints were set on the image analysis system of 50 (supragranular layers) and 70 (infragranular layers) μm^2, which excluded most glia and smaller (non-pyramidal) neurones, on the basis of examination of neurones which had an obvious pyramidal morphology. Due to the nature of the lesion, comparisons between sides ipsilateral and contralateral to the injection site could not be made as before, and thus statistical comparisons were performed between volkensin, ricin and control groups.

Following injection of 2.5 ng volkensin, the number of supragranular pyramidal neurones was significantly reduced to 52 and 51 % of that observed in ricin and control groups respectively (Table 8.1, Figure 8.3). There were no significant differences between the number of infragranular pyramidal neurones in ricin and control groups. In animals receiving cortical ablation (n=2), the number of supragranular pyramidal neurones contralateral to the ablation was similar to that observed in ricin and control groups, although no statistics could be performed (Table 8.1).

Quantitative analysis of the number of infragranular pyramidal neurones contralateral to the injection site revealed a significant reduction in volkensin injected animals to 55 and 59 % of that observed in ricin and control animals respectively (Table 8.1, Figure 8.3). There were no significant differences in the number of infragranular neurones counted in ricin and control groups. In animals receiving cortical ablation, the number of infragranular pyramidal neurones was similar to that observed in ricin and control groups (Table 8.1).

	Supragranular		Infragranular	
	Number/field	Size (μm^2)	Number/field	Size (μm^2)
Volkensin (n=6)	**145.0±15.8***	**75.4±1.5†**	**87.9±8.5***	**99.5±0.9†**
Ricin (n=6)	279.9±21.5	89.3±3.7	160.7±15.9	122.3±6.5
Control (n=5)	285.0±11.4	88.6±7.5	148.5±12.1	118.4±11.3
Ablation (n=2)	242.7	81.4	145.5	92.3

Table 8.1: NEOCORTICAL CELL LOSS AND CHANGES IN MEAN CELL SIZE IN CONTRALATERAL NEOCORTEX OF VOLKENSIN, RICIN AND CONTROL ANIMALS. Values are mean ± SEM of number of cells counted/field above 50 (supragranular) and 70 (infragranular) μm^2 in cross sectional area, and mean ± SEM of mean cell profile area (μm^2), following intracortical injection of 2.5 ng volkensin or 12.5 ng ricin. Data is also shown for unoperated control animals, and animals receiving cortical ablation in the same area as the injection site in toxin injected animal. Data is from quantitation in neocortical areas corresponding, but contralateral to the injection site, in volkensin and ricin injected animals, and similar areas in control and ablation groups.
* significantly different from values obtained from ricin and control groups, $p < 0.05$, ANOVA followed by LSD tests.
† significantly different from ricin injected group, Kruskal-Wallis ANOVA followed by Mann-Whitney U tests.
Cortically ablated animals were not included in statistical analysis.

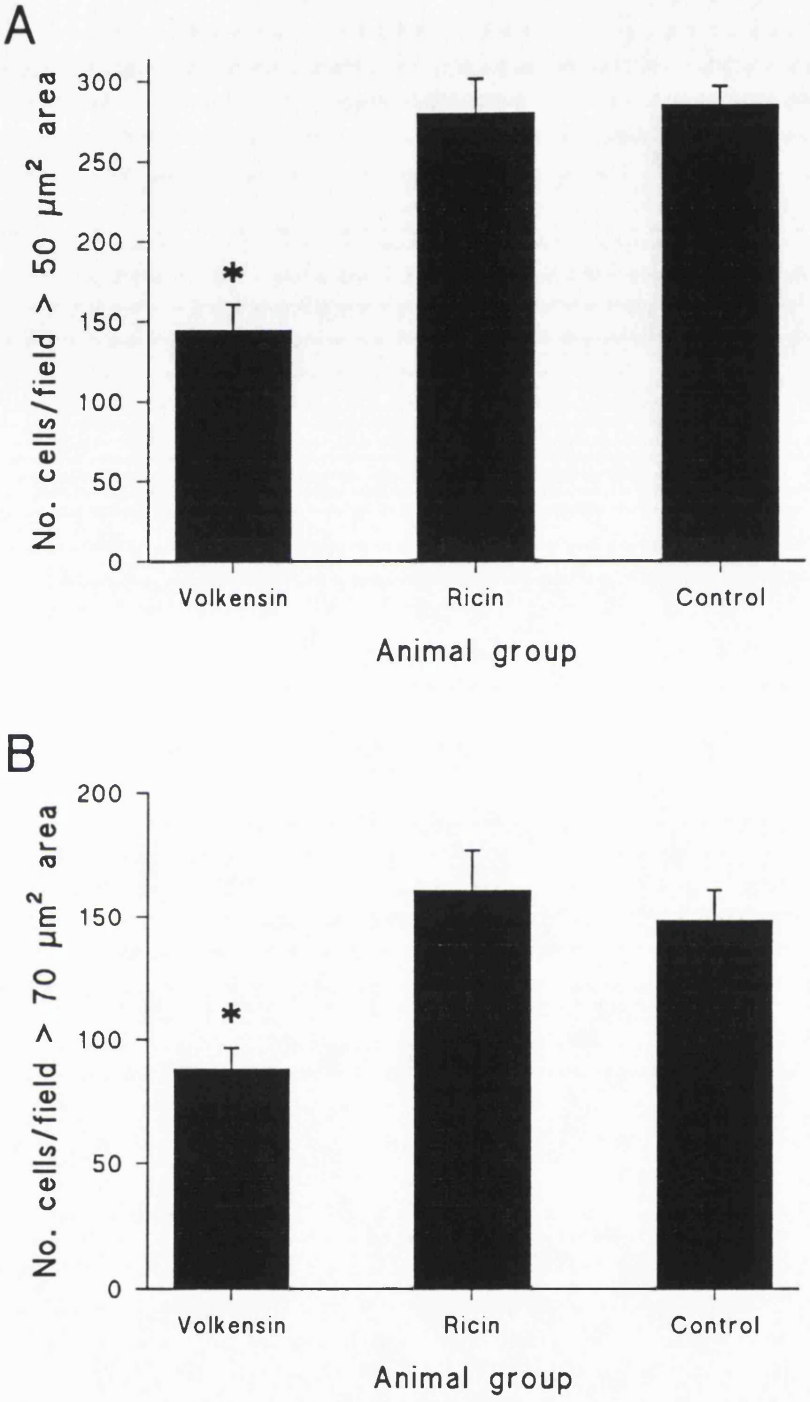

Figure 8.3: NEOCORTICAL CELL NUMBERS IN ANIMALS RECEIVING INTRACORTICAL INJECTION OF VOLKENSIN AND RICIN, AND UN-OPERATED CONTROLS. Histograms show the mean number of cell profiles (no. cells/field) in the neocortex of control animals (n=5) and those receiving 2.5 ng intracortical volkensin (n=6) or 12.5 ng intracortical ricin (n=6) with 28 day survival periods in areas corresponding, but contralateral to the injection site, in superficial (histogram A) and deep (histogram B) layers. Exclusion criteria of > 50 μm^2 and > 70 μm^2 were set for superficial and deep layer counts respectively.
Error bars are SEM; * $p < 0.05$ (ANOVA followed by LSD test), significantly different to cell numbers in ricin and control groups.

8.2.5 Quantification of cell size in the neocortex in control and toxin injected animals.

The infragranular and supragranular neurone loss described in the previous section was accompanied by reductions in cell size in both layers when assessed qualitatively. Quantitative analysis of the cell size of supragranular neurones in volkensin injected animals revealed a reduction to 84 and 85 % of that observed in ricin and control animals respectively (Table 8.1, Figure 8.4). However, data did not conform to a single population model, and thus non-parametric statistics were employed. Kruskal-Wallis ANOVA followed by Mann-Whitney U tests revealed a significant difference between the size of supragranular neurones in volkensin injected animals compared to those injected with ricin ($p=0.02$); the difference between volkensin and control animal groups just failed to reach statistical significance ($p=0.07$). No significant differences between ricin and control groups were found. The mean supragranular layer cell size in cortically ablated animals was similar to that observed in ricin and control groups (Table 8.1).

Quantitative analysis of cell size in infragranular layers revealed similar findings (Table 8.1, Figure 8.4), with reductions in volkensin injected animals to 81 and 84 % of that observed in ricin and control injected animals. Non-parametric analysis (Kruskal-Wallis followed by Mann-Whitney U) revealed that these differences were significant between volkensin and ricin injected animals ($p=0.004$), but not between volkensin and control groups. No significant differences were observed in cell size between ricin and control groups. The mean infragranular layer cell size in animals receiving cortical ablation was similar to that observed in volkensin groups, though no statistical analysis was performed (Table 8.1).

8.2.6 Quantification of glutamic acid decarboxylase (GAD) mRNA positive cells in volkensin, ricin and control groups.

To confirm further that the actions of volkensin were specific to neurones projecting to the injection site, *in-situ* hybridisation histochemistry for GAD mRNA was performed. As described in chapter 4, section 4.2.5, this enzyme is a well established marker of interneurones. GAD-mRNA positive

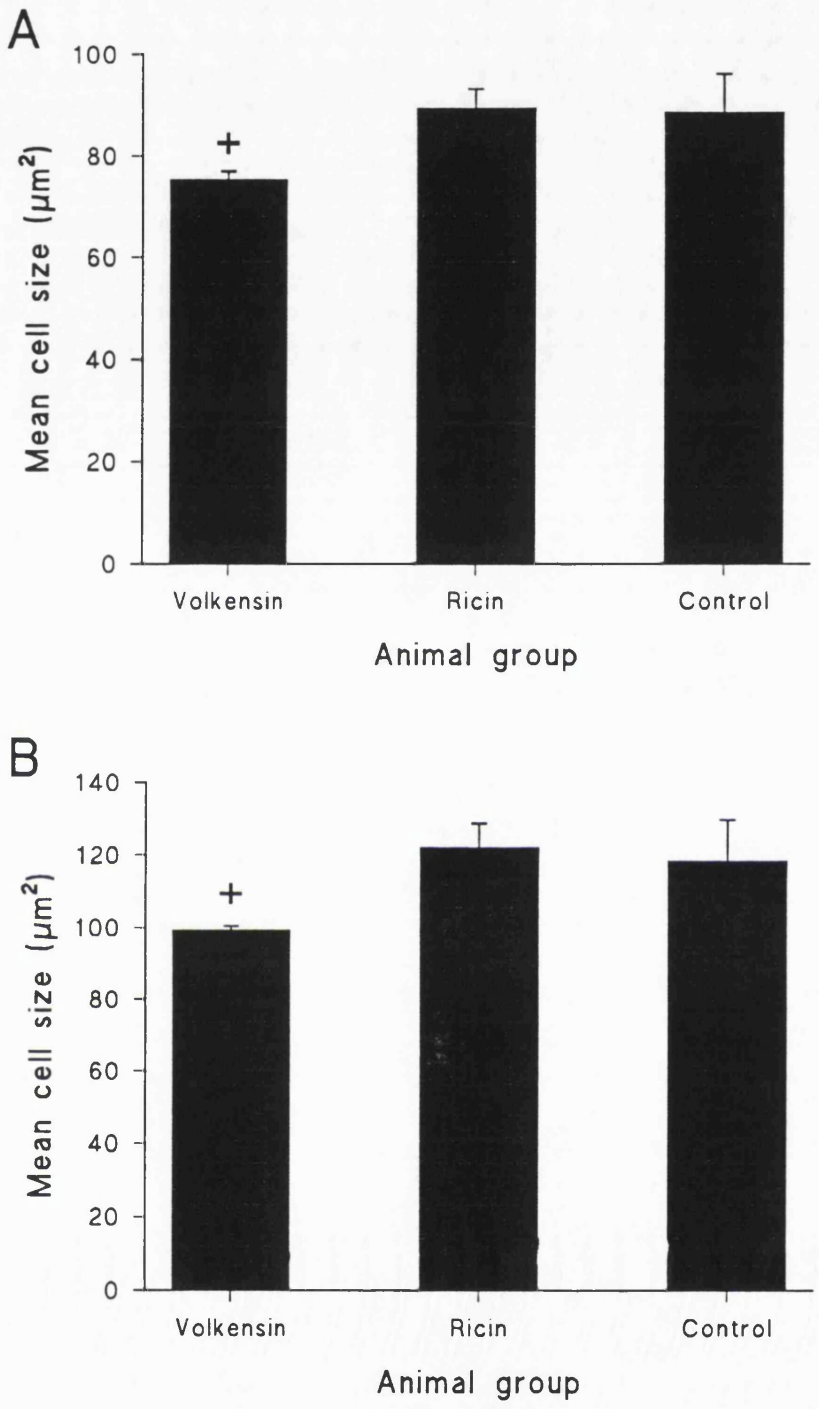

Figure 8.4: CHANGES IN MEAN NEOCORTICAL CELL SIZE IN ANIMALS RECEIVING INTRACORTICAL INJECTION OF VOLKENSIN AND RICIN, AND UN-OPERATED CONTROLS. Histograms show the mean cell profiles area (μm^2) / field > 50 μm^2 (superficial layers; histogram A) or > 70 μm^2 (deep layers; histogram B) in the neocortex of control animals (n=5) and those receiving 2.5 ng intracortical volkensin (n=6) or 12.5 ng intracortical ricin (n=6) with 28 day survival periods in areas corresponding, but contralateral to the injection site.
Error bars are SEM; * $p < 0.05$ (Kruskal-Wallis ANOVA followed by Mann-Whitney U test), significantly different to mean cell size in ricin group.

cells (Figure 8.5) were counted from the same areas as those showing loss of Nissl stained cells, in one frame throughout the depth of the neocortex. No significant difference in the number of GAD-mRNA positive cells/field or their mean profile area were observed between volkensin, ricin, control and cortical ablation groups (Table 8.2).

8.2.7 Effect of volkensin injections on glial proliferation within the neocortex.

Extensive glial proliferation in the neocortex was reported on the ipsilateral side of animals receiving intrastriatal injection of volkensin (Pangalos, 1992). Examination of sections processed for immunocytochemical detection of GFAP in the present study revealed less marked gliosis on the side contralateral to the injection site in volkensin injected animals. However, qualitatively, gliosis in contralateral cortex of volkensin injected animals was greater than that observed in corresponding areas in sections from ricin and control animals (Figure 8.6).

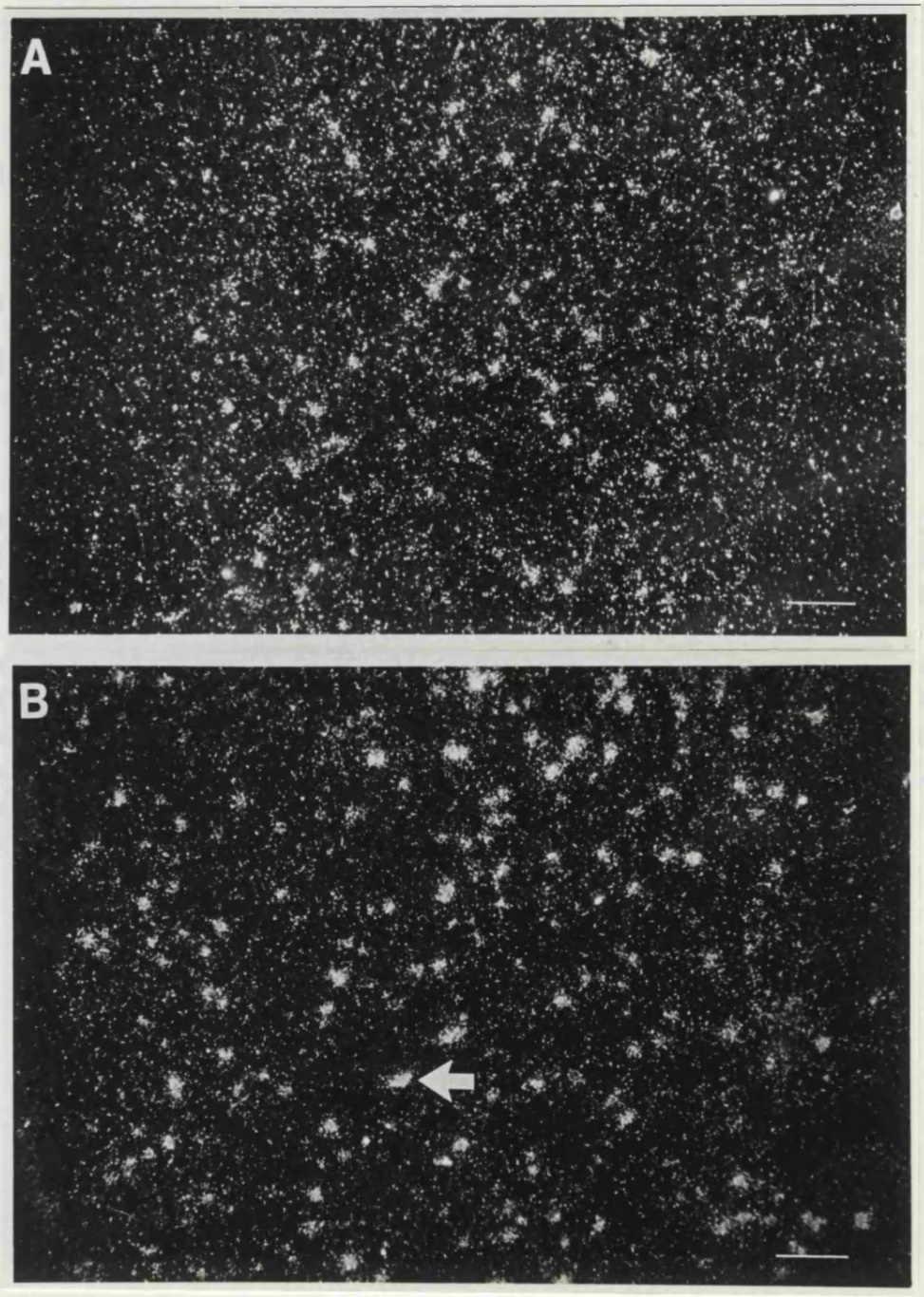

Figure 8.5: PHOTOMICROGRAPH OF CONTRALATERAL RAT NEOCORTEX IN A VOLKENSIN ANIMAL AND EQUIVALENT AREA IN A CONTROL ANIMAL SHOWING *IN-SITU* HYBRIDISATION WITH GAD mRNA. Top panel (A) shows emulsion dipped section of rat neocortex, on the side contralateral to intracortical injections of 2.5 ng volkensin. Lower panel (B) shows equivalent area in a control animal. GAD mRNA-positive cells are heavily labelled with silver grains (example arrowed in B). Note higher background in (A), but equivalent numbers of labelled cells in (A) and (B). Both micrographs taken at the same magnification. Scale bars 100 μm.

	No. labelled cells / field	Mean cell profile area (μm^2)
Volkensin (n=6)	38.1 ± 10.5	167.2 ± 13.3
Ricin (n=4)	54.8 ± 11.8	153.7 ± 4.8
Control (n=4)	49.1 ± 18.9	162.5 ± 34.1
Ablation (n=5)	30.2 ± 4.7	192.8 ± 17.4

Table 8.2: NUMBER OF GAD mRNA POSITIVE CELLS/FIELD AND MEAN CELL PROFILE AREA IN VOLKENSIN AND RICIN INJECTED ANIMALS AND CONTROL AND ABLATION GROUPS. Experiments were performed using coronal rat brain sections incubated with a previously prepared ^{35}S labelled probe specific for GAD mRNA for 16 hr at 24 °C. After development of emulsion, sections were counterstained with cresyl violet. The number and size of GAD mRNA positive cells was determined in neocortex corresponding, but contralateral to the lesion (volkensin, ricin and ablation), and in equivalent areas in control animals.
Data is mean ± SEM. No significant differences between any group.

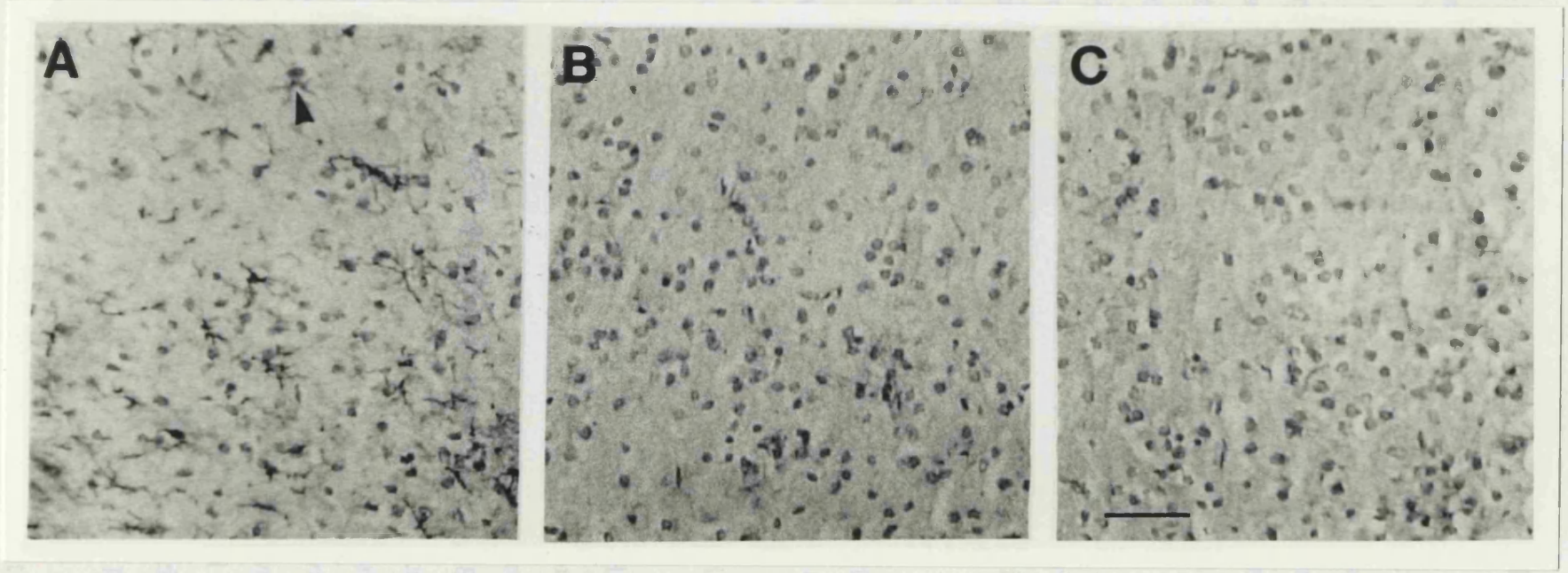

Figure 8.6: PHOTOMICROGRAPHS OF RAT NEOCORTEX STAINED USING AN ANTI-GFAP ANTIBODY. Photomicrographs show GFAP positive cells in contralateral cortex of animals receiving intracortical injection of 2.5 ng volkensin (A) or 12.5 ng ricin (B). Panel C shows the typical appearance of the neocortex of a control animal.
Note the increased number of GFAP positive cells in the volkensin injected animal (example arrowed) compared to ricin and control animal sections.
Sections counterstained with cresyl violet. All photomicrographs taken at the same magnification. Scale bar (C) 200μm.

8.3 Discussion.

8.3.1 Interpretations of the histological findings following intracortical toxin injections.

The dose of volkensin (2.5 ng) and postoperative survival time (28 days) used in the present study are similar to those used in the two preceding lesioning paradigms described in this thesis (chapters 4 and 6), although these doses and survival times are different from those used by other workers (see chapter 4, section 4.3.1, and chapter 6, section 6.3.1). It appears that cortical pyramidal neurones which project subcortically and trans-callosally are similarly susceptible to the toxicity of volkensin. By contrast, destruction of a subpopulation of CA3 hippocampal pyramidal neurones was apparent after a postoperative survival time of 14 days, suggesting increased susceptibility of these neurones to the toxic effects of volkensin, or a more rapid axonal transport rate.

The present study demonstrates that intracortical injection of volkensin produces a significant loss of a subpopulation of neocortical pyramidal neurones, with cell numbers in supragranular layers reduced to 52 and 51 % of those observed in ricin and control groups, and in infragranular layers to 55 and 59 % of those observed in ricin and control groups. The most likely explanation is that the pyramidal neurones affected project contralaterally to the injection site, which conforms to known contralateral projections of reciprocal innervation of neocortical areas (see Introduction, section 1.3.1 and MacLean, 1985; Zilles and Wree, 1985; Jones, 1984), forming commissural fibres which connect the hemispheres. Intracortical injection of HRP also labelled contralateral neocortical pyramidal neurones of supragranular and infragranular laminae, and examination of Gallyas stained sections from animals with a postoperative survival time of 21 days revealed degeneration of axon processes of contralateral infragranular and supragranular neurones, which provides additional support for the specific retrograde action of volkensin. However, in the present study it is not possible to exclude loss of pyramidal neurones in the neocortex which send their axons <u>through</u> the injection site to other cortical targets. It is likely that this is the case for a

proportion of the affected neurones, as there was substantial involvement of the corpus callosum in volkensin injected animals, and thus contralaterally projecting pyramidal cells with a variety of targets would be affected. It is unlikely that hippocampal involvement contributed significantly to the neuronal loss, as most contralateral hippocampal projections to both the CA fields and the DG originate from non-neocortical structures (Bayer, 1985).

In this study, the possibility that volkensin may spread from the injection site directly, or from neurones initially transporting the toxin and then re-releasing it into the surrounding neuropil upon cell lysis (from where it may be taken up by adjacent neurones) has been carefully considered. This is unlikely; *in-situ* hybridisation histochemistry did not reveal any reduction in GAD mRNA positive cells in contralateral neocortex following volkensin injection; direct spread from the injection site, or re-release of volkensin from neurones destroyed would also destroy interneurones. Also, injection of ricin did not cause any contralateral neocortical neuronal loss, though necrosis (albeit more limited than that observed using volkensin) was observed at the injection site. Finally, histological analysis revealed that the cell loss distant to the injection site conformed to known afferent projections to the contralateral cortex, and was not seen in areas closer to the injection site but without afferent axons to the neocortex.

Traditionally, "association fibres" refer to fibres that interconnect homolateral (primarily supragranular) cortical layers. Additionally, trans-callosal connections between homotopic (same cell type and area) and heterotopic neurones which project to areas connected ipsilaterally by traditional association fibres have been described (Hedreen and Yin, 1981; Jones, 1984; MacLean, 1985). It is likely that a proportion of trans-callosal projecting neurones have branched axons, which also form association fibres. Thus, of the lesioning paradigms described in this thesis, neurones destroyed in the present study most closely represent corticocortical projecting association fibres which are degenerate in AD.

CHAPTER 9: Autoradiographic analysis of ligand binding in the neocortex following intracortical toxin injections.

9.1 Introduction.

Autoradiographic investigations of the receptor populations of corticofugal projecting neocortical pyramidal neurones is described in chapter 7. This subpopulation of pyramidal neurones were found to be enriched with 5-HT_{1A}, nicotinic, and to a lesser extent, muscarinic receptors. Degeneration of glutamatergic corticocortical projecting neurones is consistent feature of AD, and appears to contribute to the cognitive deficit (as reviewed, Francis et al., 1993). As pyramidal neurones may be subject to qualitatively similar regulation, this final autoradiographic study, combined with those described in chapters 5 and 7 should provide further information in the context of discovering a consistent marker for pyramidal neurones, as well as possible sites for therapeutic intervention for the treatment of the symptoms and progression of the disease.

The aim of the present study was to examine the localisation of receptors proposed to influence the excitability of corticocortical projecting pyramidal neurones, using [^{3}H] 8-OH-DPAT, [^{3}H] ketanserin, [^{3}H] pirenzepine, [^{3}H] nicotine and [^{3}H] DPCPX to study the regional and laminar distribution of 5-HT_{1A}, 5-HT_{2A}, muscarinic M_1, nicotinic and adenosine A_1 receptors respectively in animals receiving intracortical injection of neurotoxic lectins. The results obtained in this study may be compared and contrasted with findings described for hippocampal pyramidal neurones (chapter 5) and corticofugal projecting pyramidal neurones (chapter 7).

9.2 Results.

9.2.1 The binding of [^{3}H] 8-OH-DPAT to 5-HT_{1A} receptors.

The experimental conditions and considerations for the binding of [^{3}H] 8-OH-DPAT are described in the methods section, and in Chapter 5, sections 5.2.4 and 5.3.1. Quantitative evaluations of the binding of [^{3}H] 8-OH-DPAT was made as described in Chapter 2, section 2.8.11.1 in medial areas corresponding, but contralateral to the lesion in volkensin (n = 7), and ricin (n

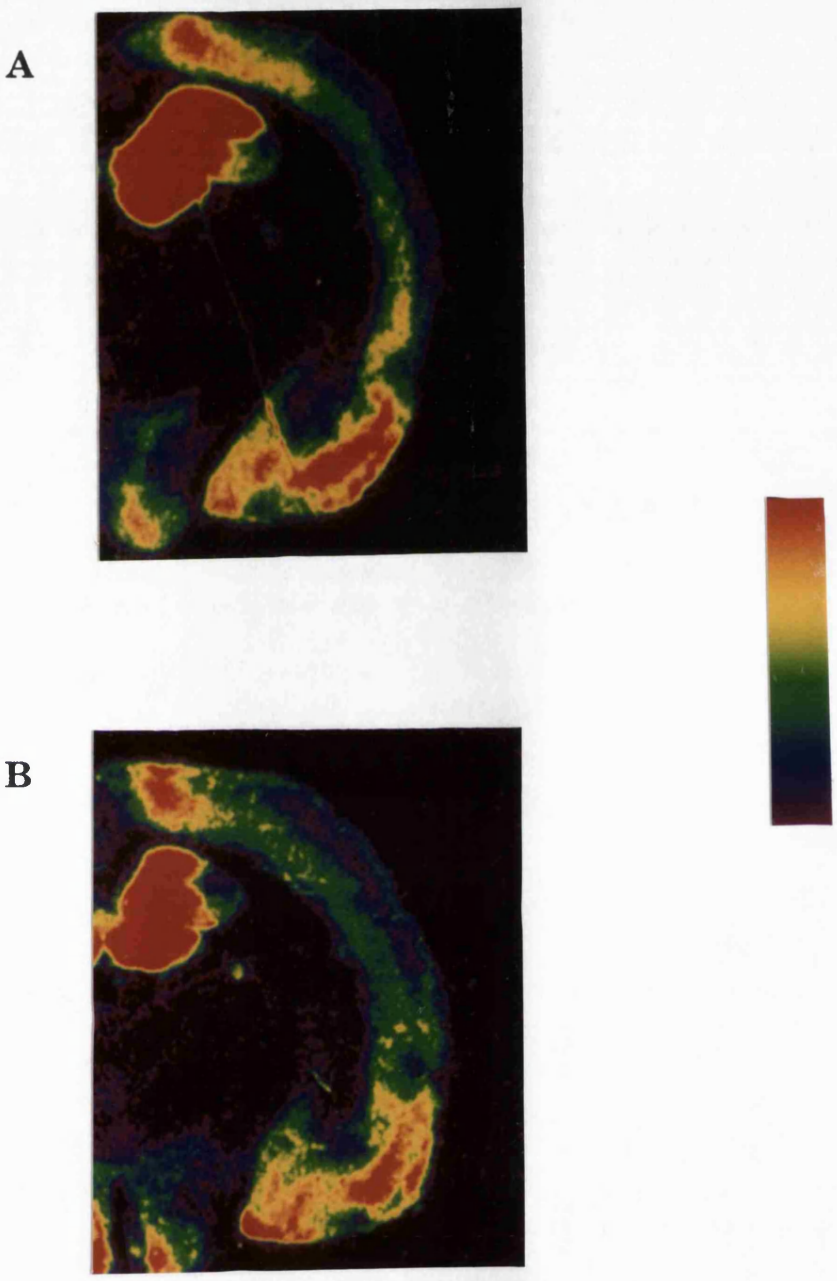

Figure 9.1: REPRESENTATIVE COLOUR-CODED RECONSTRUCTIONS OF AUTORADIOGRAMS OF [^{3}H] 8-OH-DPAT BINDING IN SECTIONS FROM VOLKENSIN AND RICIN TREATED ANIMALS. Experiments were performed using coronal sections incubated in 170 mM Tris-HCl (pH 7.6) containing 4 mM $CaCl_2$, 0.01 % ascorbate and 1 nM [^{3}H] 8-OH-DPAT for 60 min at 25 °C. Non-specific binding was generated using 10 μM 5-HT.
Colour coded autoradiograms illustrate the side contralateral to the lesion for an animal receiving intracortical injection of 2.5 ng volkensin (A) or 12.5 ng ricin (B). The scale bar indicated the intensity of the autoradiographic signal from purple (lowest) to red (highest).

= 5) injected animals. Data from control animals was augmented with data from equivalent areas of contralateral cortex of animals receiving intrastriatal ricin injection, under identical experimental conditions to increase the number of cases for statistical analysis (n=9).

The regional and laminar distribution of [^{3}H] 8-OH-DPAT binding in contralateral cortex is shown as colour coded reconstructions of autoradiograms for volkensin and ricin treated animals (Figure 9.1). Within the neocortex, binding was higher in the deep layers compared to the superficial layers.

Quantitative analysis of the binding of [^{3}H] 8-OH-DPAT in superficial layers (Table 9.1) revealed no significant differences in binding between volkensin (17.4 ± 1.4 fmol/mg tissue equivalent), ricin (16.2 ± 1.3 fmol/mg tissue equivalent) or control groups (18.9 ± 2.5 fmol/mg tissue equivalent).

Quantitative analysis of the binding of [^{3}H] 8-OH-DPAT in deep layers (Table 9.1) revealed no significant differences in binding between volkensin (25.6 ± 2.0 fmol/mg tissue equivalent), ricin (23.8 ± 1.2 fmol/mg tissue equivalent) or control groups (30.2 ± 3.3 fmol/mg tissue).

9.2.2 The binding of [^{3}H] ketanserin to 5-HT$_{2A}$ receptors.

The experimental conditions and considerations for the binding of [^{3}H] ketanserin are described in the methods section and in Chapter 5, section 5.2.5. Quantitation of the binding of [^{3}H] ketanserin was made as described in Chapter 2, section 2.8.11.1 in medial areas corresponding, but contralateral to the lesion in volkensin (n = 7) and ricin (n = 5) injected animals. Data from control animals was pooled with data from equivalent areas of contralateral cortex of animals receiving intrastriatal ricin injection, under identical experimental conditions to increase the number of cases for statistical analysis (n = 10).

The regional and laminar distribution of [^{3}H] ketanserin binding in contralateral cortex is shown as colour coded reconstructions of autoradiograms for volkensin and ricin treated animals (Figure 9.2). Clearly demarcated within the neocortex were superficial, middle and deep layers.

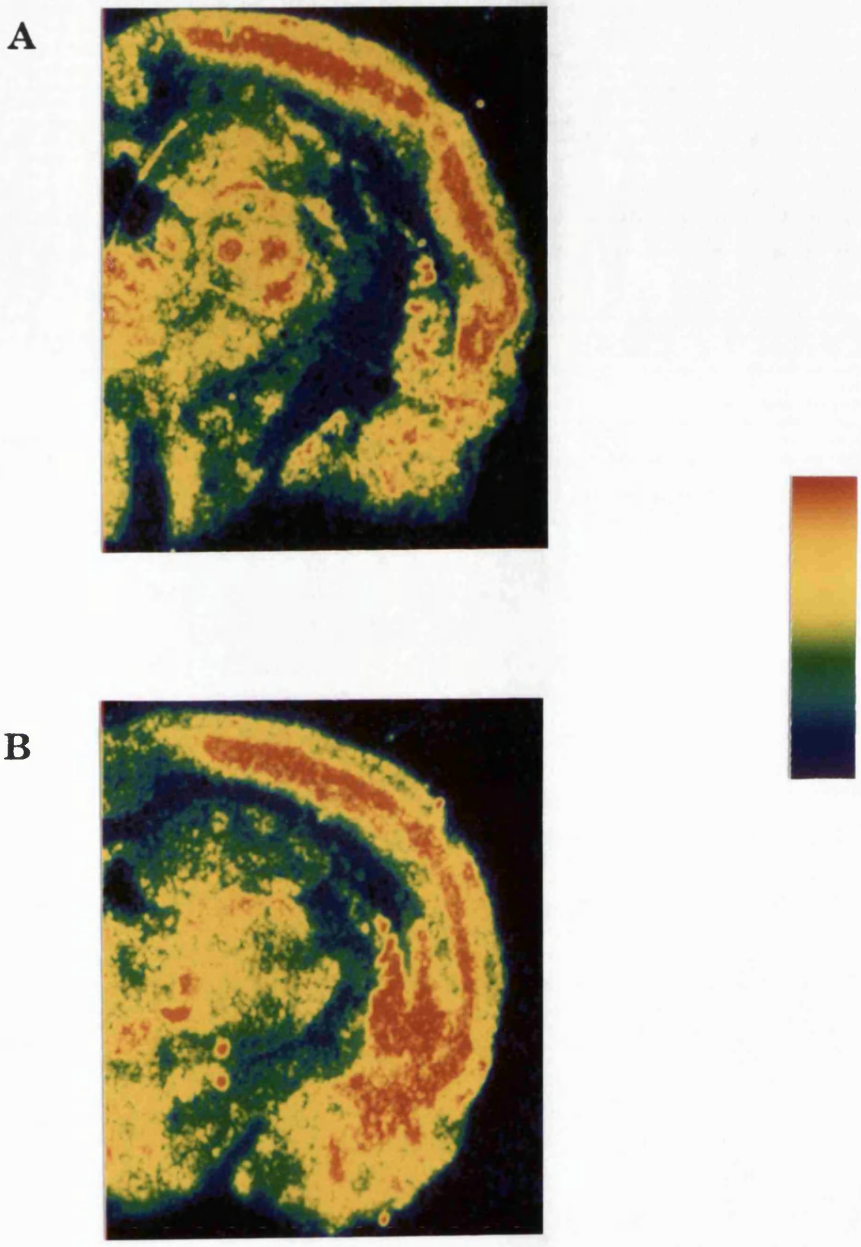

Figure 9.2: REPRESENTATIVE COLOUR-CODED RECONSTRUCTIONS OF AUTORADIOGRAMS OF [^{3}H] KETANSERIN BINDING IN SECTIONS FROM VOLKENSIN AND RICIN TREATED ANIMALS. Experiments were performed using coronal sections incubated in 170 mM Tris-HCl (pH 7.7) containing 2 nM [^{3}H] ketanserin for 120 min at 25 °C. Non-specific binding was generated using 10 μM mianserin.
Colour coded autoradiograms illustrate the side contralateral to the lesion for an animal receiving intracortical injection of 2.5 ng volkensin (A) or 12.5 ng ricin (B). The scale bar indicates the intensity of the autoradiographic signal from purple (lowest) to red (highest).

Binding was higher in the middle layers compared to superficial and deep layers.

Quantitative analysis of binding in superficial layers (Table 9.1) revealed no significant differences between volkensin (26.2 ± 2.8 fmol/mg tissue equivalent), ricin (27.4 ± 0.6 fmol/mg tissue equivalent) or control groups (31.7 ± 2.9 fmol/mg tissue equivalent). No significant differences in binding in middle layers between volkensin (50.7 ± 7.2 fmol/mg tissue equivalent), ricin (54.8 ± 1.9 fmol/mg tissue equivalent) or control groups (55.4 ± 6.0 fmol/mg tissue equivalent) were found, or in deep layers between volkensin (30.3 ± 3.6 fmol/mg tissue equivalent), ricin (30.8 ± 1.9 fmol/mg tissue equivalent) or control groups (30.7 ± 1.6 fmol/mg tissue equivalent).

9.2.3 The binding of [^{3}H] pirenzepine to muscarinic M_1 receptors.

The experimental conditions and considerations for the binding of [^{3}H] pirenzepine are described in the methods section, and in Chapter 5, sections 5.2.6 and 5.3.1. Quantitation of the binding of [^{3}H] pirenzepine was made as described in Chapter 2, section 2.8.11.1 in medial areas corresponding, but contralateral to the lesion in volkensin (n = 7) and ricin (n = 5) injected animals. Data from control animals was pooled with data from equivalent areas of contralateral cortex of animals receiving intrastriatal volkensin and ricin injections, but with identical experimental conditions to increase the number of cases for statistical analysis (n = 13).

The regional and laminar distribution of [^{3}H] pirenzepine binding in contralateral cortex is shown as colour coded reconstructions of autoradiograms for volkensin and ricin treated animals (Figure 9.3). Binding was higher in the superficial layers compared to deep layers.

Quantitative analysis of the binding of [^{3}H] pirenzepine in superficial neocortical areas (Table 9.1) revealed a significant reduction in binding in volkensin treated animals to 78 and 75 % of the binding observed in ricin and control groups respectively (42.8 ± 2.9, 55.1 ± 2.7 and 56.9 ± 2.0 fmol/mg tissue equivalent in volkensin, ricin and control groups; $p < 0.05$, ANOVA followed by LSD test). There were no significant differences in the binding of [^{3}H] pirenzepine in superficial layers between ricin and control groups.

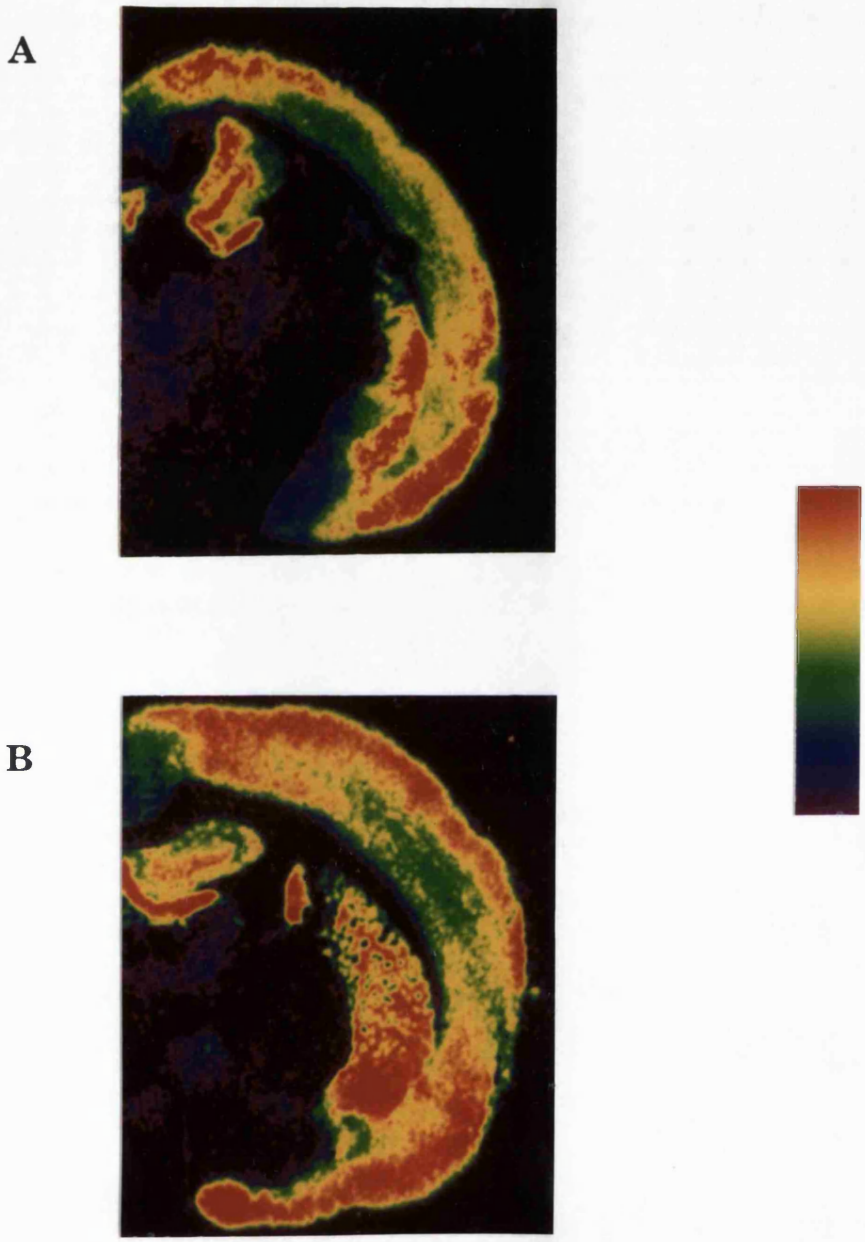

Figure 9.3: REPRESENTATIVE COLOUR-CODED RECONSTRUCTIONS OF AUTORADIOGRAMS OF [^{3}H] PIRENZEPINE BINDING IN SECTIONS FROM VOLKENSIN AND RICIN TREATED ANIMALS. Experiments were performed using coronal sections incubated in PBS (pH 7.4) containing 2.5 nM [^{3}H] pirenzepine for 90 min at 25 °C. Non-specific binding was generated using 10 μM atropine.
Colour coded autoradiograms illustrate the side contralateral to the lesion for an animal receiving intracortical injection of 2.5 ng volkensin (A) or 12.5 ng ricin (B). The scale bar indicates the intensity of the autoradiographic signal from purple (lowest) to red (highest). Note reduction of binding in medial areas in (A) compared to (B).

Significant reductions in the binding of [^{3}H] pirenzepine were also observed in the deep layers of volkensin injected animals, to 80 and 68 % of that observed in ricin and control groups (30.1 ± 4.4, 37.8 ± 5.4 and 44.0 ± 2.3 fmol/mg tissue equivalent in volkensin, ricin and control groups, respectively; $p < 0.05$, ANOVA followed by LSD tests). There were no significant differences in the binding of [^{3}H] pirenzepine in deep layers between ricin and control groups (Table 9.1).

9.2.4 The binding of [^{3}H] nicotine to nicotinic cholinergic receptors.

The experimental conditions and considerations for the binding of [^{3}H] nicotine are described in the methods section, and in Chapter 7, sections 7.2.6.1 and 7.3.1. Quantitation of the binding of [^{3}H] nicotine was made as described in Chapter 2, section 2.8.11.1 in medial areas corresponding, but contralateral to the lesion in volkensin (n = 7) and ricin (n = 5) injected animals, and in equivalent areas in control animals (n = 4).

The regional and laminar distribution of [^{3}H] nicotine binding in contralateral cortex is shown as colour coded reconstructions of autoradiograms for volkensin and control animals (Figure 9.4). Clearly demarcated within the neocortex were superficial, middle and deep layers. Binding was higher in the middle layers compared to superficial and deep layers.

Quantitative analysis revealed no significant differences in binding of [^{3}H] nicotine to superficial layers (Table 9.1) of volkensin treated animals (19.8 ± 0.7 fmol/mg tissue equivalent) compared to ricin (21.4 ± 1.6 fmol/mg tissue equivalent) and control groups (22.1 ± 1.0 fmol/mg tissue equivalent).

No significant differences in binding were found in middle layers (Table 9.1) between volkensin (26.6 ± 1.8 fmol/mg tissue equivalent), ricin (30.1 ± 2.6 fmol/mg tissue equivalent) or control groups (28.1 ± 1.4 fmol/mg tissue equivalent.

Quantitative analysis of the binding of [^{3}H] nicotine in deep neocortical areas (Table 9.1) revealed a significant reduction in binding in volkensin treated animals to 64 % of the binding observed control animals (15.2 ± 1.1 and 23.6 ± 1.3 fmol/mg tissue equivalent in volkensin and control groups; $p <$

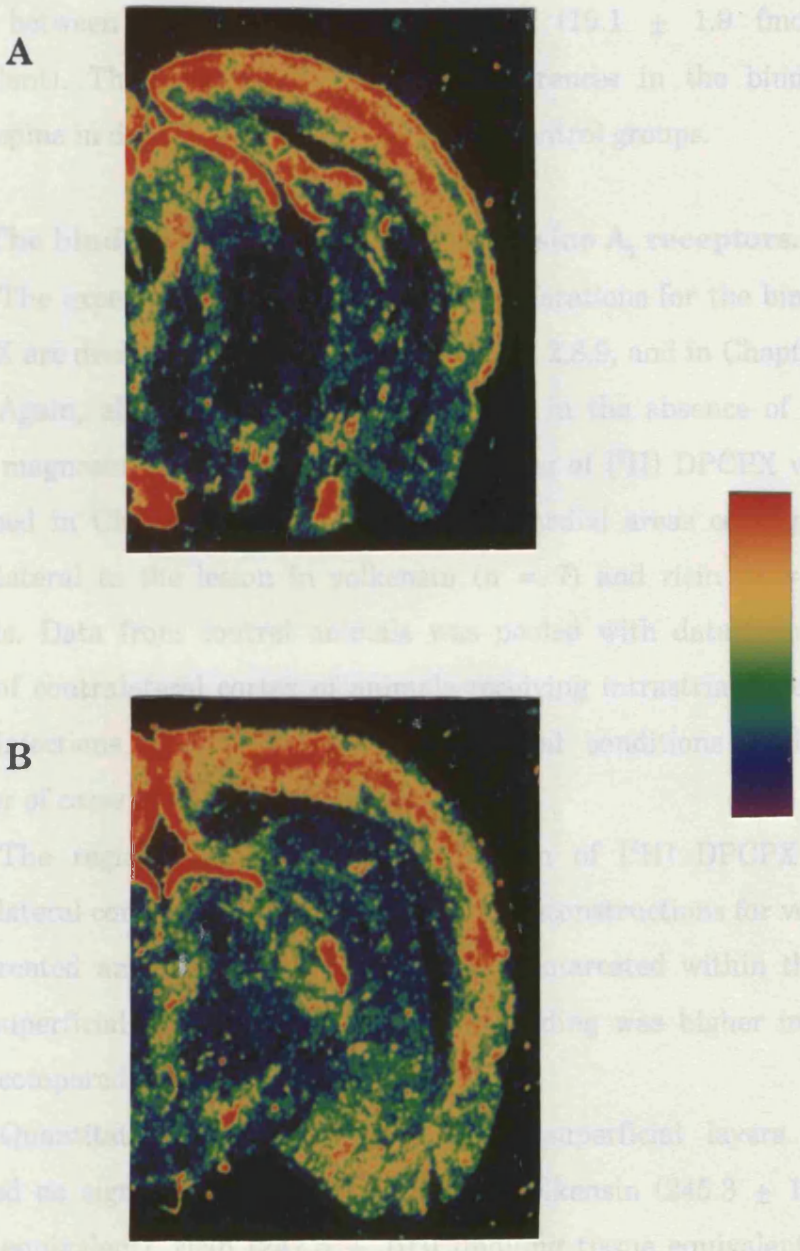

Figure 9.4: REPRESENTATIVE COLOUR-CODED RECONSTRUCTIONS OF AUTORADIOGRAMS OF [^{3}H] NICOTINE BINDING IN SECTIONS FROM VOLKENSIN TREATED AND CONTROL ANIMALS. Experiments were performed using coronal sections incubated in 50 mM Tris-HCl (pH 7.4) containing 8 mM $CaCl_2$ and 6 nM [^{3}H] nicotine for 90 min at 25 °C. Non-specific binding was generated using 10 μM carbachol.
Colour coded autoradiograms illustrate the side contralateral to the lesion for (A) an animal receiving intracortical injection of 2.5 ng volkensin or (B) a control animal. The scale bar indicates the intensity of the autoradiographic signal from purple (lowest) to red (highest). Note reduction of binding in deep layers of medial cortex in (A) compared to (B).

0.05, ANOVA followed by LSD test). However, no significant differences were found between volkensin and ricin groups (19.1 ± 1.9 fmol/mg tissue equivalent). There were no significant differences in the binding of [^{3}H] pirenzepine in deep layers between ricin and control groups.

9.2.5 The binding of [^{3}H] DPCPX to adenosine A_1 receptors.

The experimental conditions and considerations for the binding of [^{3}H] DPCPX are described in the Chapter 2, section 2.8.9, and in Chapter 7, section 7.3.1. Again, all incubations were performed in the absence of exogenously added magnesium. Quantitation of the binding of [^{3}H] DPCPX was made as described in Chapter 2, section 2.8.11.1 in medial areas corresponding, but contralateral to the lesion in volkensin (n = 7) and ricin (n = 5) injected animals. Data from control animals was pooled with data from equivalent areas of contralateral cortex of animals receiving intrastriatal volkensin and ricin injections, under identical experimental conditions to increase the number of cases for statistical analysis (n = 8).

The regional and laminar distribution of [^{3}H] DPCPX binding in contralateral cortex is shown as colour coded reconstructions for volkensin and ricin treated animals (Figure 9.5). Clearly demarcated within the neocortex were superficial, middle and deep layers. Binding was higher in the middle layers compared to superficial and deep layers.

Quantitative analysis of binding in superficial layers (Table 9.1) revealed no significant differences between volkensin (245.3 ± 10.5 fmol/mg tissue equivalent), ricin (242.5 ± 10.0 fmol/mg tissue equivalent) or control groups (246.7 ± 7.0 fmol/mg tissue equivalent).

Quantitative analysis of binding in middle layers (Table 9.1) revealed no significant differences between volkensin (278.2 ± 5.6 fmol/mg tissue equivalent), ricin (271.6 ± 8.3 fmol/mg tissue equivalent) or control groups (276.6 ± 7.4 fmol/mg tissue equivalent).

No significant differences in binding were found in deep layers (Table 9.1) between volkensin (263.4 ± 5.54 fmol/mg tissue equivalent), ricin (258.9 ± 6.2 fmol/mg tissue equivalent) or control groups (259.4 ± 4.9 fmol/mg tissue equivalent).

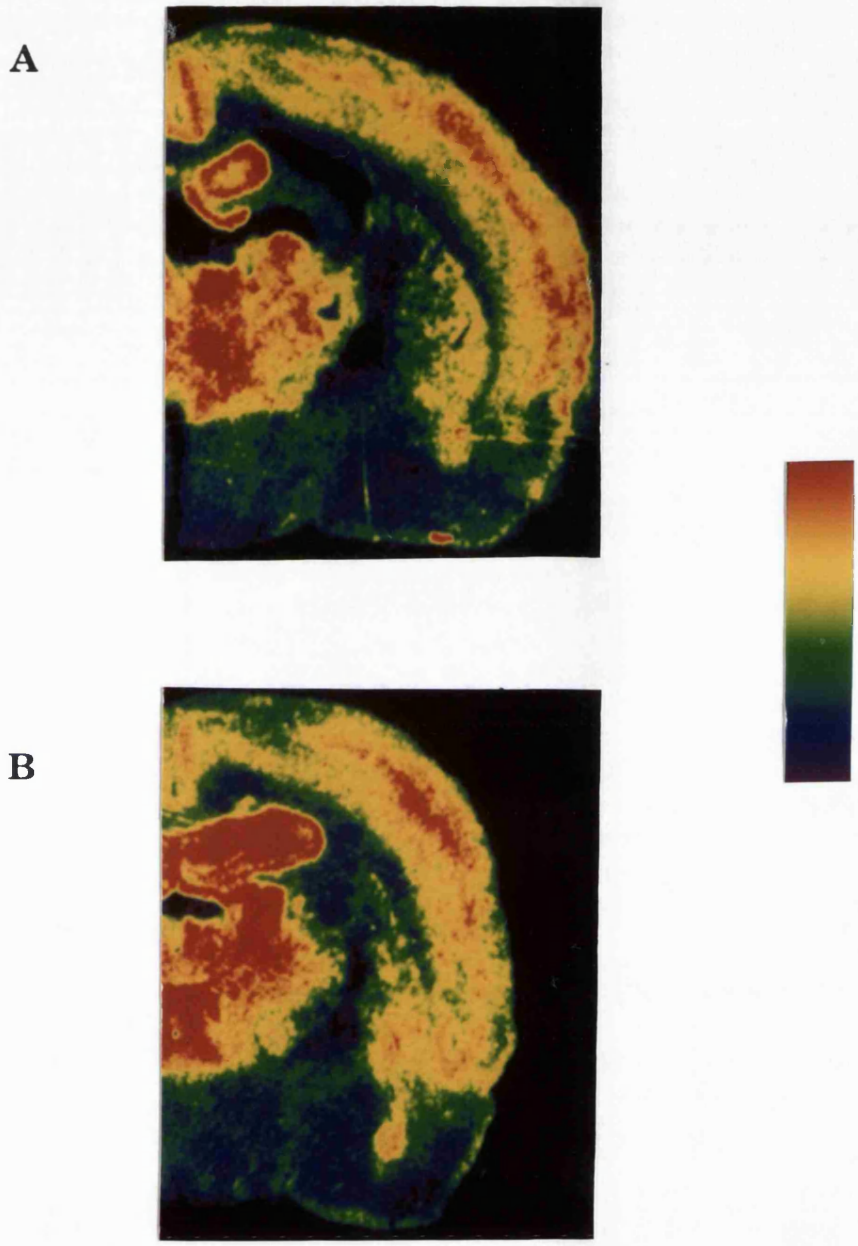

Figure 9.5: REPRESENTATIVE COLOUR-CODED RECONSTRUCTIONS OF AUTORADIOGRAMS OF [^{3}H] DPCPX BINDING IN SECTIONS FROM VOLKENSIN AND RICIN TREATED ANIMALS. Experiments were performed using coronal sections incubated in 170 mM Tris-HCl (pH 7.4) containing 1 mM EDTA, 10 μM Gpp(NH)p, and 2 nM [^{3}H] DPCPX for 80 min at 37 °C. Non-specific binding was generated using 10 μM R-PIA.
Colour coded autoradiograms illustrate the side contralateral to the lesion for an animal receiving intracortical injection of 2.5 ng volkensin (A) or 12.5 ng ricin (B). The scale bar indicates the intensity of the autoradiographic signal from purple (lowest) to red (highest).

Ligand (receptor)	Layer	Volkensin	Ricin	Control
[^{3}H] 8-OH-DPAT	superficial	17.4±1.4	16.2±1.3	18.9±2.5 (9)
(5-HT_{1A})	deep	25.6±2.0	23.8±1.2	30.2±3.3 (9)
[^{3}H] ketanserin	superficial	26.2±2.8	27.4±0.6	31.7±2.9 (10)
(5-HT_2)	middle	50.7±7.2	54.8±1.9	55.4±6.0 (10)
	deep	30.3±3.6	30.8±1.9	30.7±1.6 (10)
[^{3}H] pirenzepine	superficial	**42.8±2.9***	55.1±2.7	56.9±2.0 (13)
(muscarinic M_1)	deep	**30.1±1.7***	37.3±2.4	44.0±2.3 (13)
[^{3}H] nicotine	superficial	19.8±0.7	21.4±1.6	22.1±1.0 (4)
(nicotinic)	middle	26.6±1.8	30.1±2.6	28.1±1.4 (4)
	deep	**15.2±1.1†**	19.1±1.9	23.6±1.3 (4)
[^{3}H] DPCPX	superficial	245.3±10.5	242.5±10.0	246.7±7.0 (8)
(adenosine A_1)	middle	278.2±5.6	271.6±8.3	276.6±7.4 (8)
	deep	263.4±5.5	258.9±6.2	259.4±4.9 (8)

Table 9.1: SUMMARY OF AUTORADIOGRAPHIC BINDING DATA IN VOLKENSIN, RICIN AND CONTROL GROUPS. Data is mean specific binding ± SEM (fmol/mg tissue equivalent), in volkensin (n=7), ricin (n=5) or control groups (n in parentheses) in neocortical layers corresponding, but contralateral to the lesion, and in equivalent areas in control (unoperated) animals.

* $p < 0.05$, ANOVA followed by LSD test, significantly different from ricin and control groups, and † $p < 0.05$, significantly different from control group.

9.3 Discussion.

9.3.1 Experimental considerations.

The regional and laminar distribution of [^{3}H] 8-OH-DPAT, [^{3}H] pirenzepine, [^{3}H] nicotine and [^{3}H] DPCPX binding to 5-HT_{1A}, muscarinic M_1, nicotinic and adenosine A_1 receptors was in good agreement with that described by other workers (Chapter 7, section 7.3.1).

The binding of [^{3}H] ketanserin to the 5-HT_{2A} receptor also produced a similar pattern and density as that described by other workers (Pazos and Palacios, 1985; Radja et al., 1991). Pazos et al. (1985) reported binding values of 10 - 60 fmol/mg tissue in rat brain which compares favourably with the present study (26 - 55 fmol/mg tissue). [^{3}H] ketanserin has been reported to bind to a site other than the 5-HT_{2A} receptor (probably an amine transporter) in both the rat striatum and the rabbit neocortex (Leysen et al., 1988; Dewar et al., 1990b). However, addition of the monoamine depleting agent, tetrabenazine, was found to have no effect on [^{3}H] ketanserin binding within the rat neocortex, whilst binding in the striatum was reduced (Pazos et al., 1985; Pangalos, 1992) and suggests that in the rat neocortex, [^{3}H] ketanserin binding is to the 5-HT_{2A} site.

9.3.2 Receptor distribution and localisation in lesioned animals.

The present study demonstrates significant reductions in the binding of [^{3}H] pirenzepine and [^{3}H] nicotine to muscarinic M_1 and nicotinic acetylcholine receptors, in both superficial and deep layers ([^{3}H] pirenzepine) and deep layers ([^{3}H] nicotine) respectively, on the side contralateral to the lesion in volkensin injected animals. Differences in binding were observed compared to that determined in ricin and control animals for [^{3}H] pirenzepine binding and compared to control groups for [^{3}H] nicotine binding. As described in Chapter 7, section 7.3.2, few lesioning paradigms have focused on receptor distribution on pyramidal neurones of the neocortex, and thus the present study, together with the other two lesioning paradigms described in this thesis provide important information regarding the receptor repertoires of three different subpopulation of cortical pyramidal neurones.

The most likely interpretation of the observed reduction in the binding of [^{3}H] pirenzepine and [^{3}H] nicotine is that the respective receptors are present postsynaptically on the pyramidal neurones which project contralaterally to the injection site, and are destroyed following intracortical volkensin injection. The reduction in binding to M_1 receptors was less than the concurrent reductions observed in cell numbers, which supports the findings described for corticofugal projecting neurones, where the receptor, though present but not highly enriched on the affected cells. The reduction in binding to the nicotinic receptor was of the same order of magnitude as the observed cell loss, though reductions were observed only in deep (probably reflecting layer V pyramidal neurones) layers, which again is consistent with the localisation described in Chapter 7.

The possibility that the receptors which are significantly reduced in number in contralateral cortex are located on interneurones or neurones destroyed by passive diffusion of the toxin or by the re-uptake of the toxin following corticocortical cell death is unlikely. The preservation of GAD mRNA positive cells indicates that interneurones were not affected, which would not occur had passive diffusion or re-uptake had occurred. Additionally, several receptors investigated in the present study were unaffected by volkensin injection, and intracortical ricin injection did not produce any reduction in the binding of any ligand studied, making it unlikely that the affected receptors were lost following diffusion of the toxin into the areas studied.

Another interpretation for the localisation of the M_1 receptor is that these sites are located presynaptically either as autoreceptors or as heteroreceptors. However, other studies indicate that a proportion of M_1 receptors are certainly localised to postsynaptic sites; cortical excitotoxin injection, which spared extrinsic fibres, reduced muscarinic sites (Sahin et al., 1992), and electrophysiological studies demonstrate that muscarinic agonists increased the firing rate of cortical pyramidal neurones (McCormick and Williamson, 1989). Autoreceptor localisation is unlikely, as projections from the cholinergic nuclei are unlikely to project through the injection site to contralateral areas; no reduction in [^{3}H] pirenzepine binding was observed in animals receiving intracortical ricin injection, and ChAT positive

interneurones project only to ipsilateral areas (Sofroniew et al., 1983; Sofroniew et al., 1985). Furthermore, Atack et al. (1989) and Wenk and Rokaeus (1988) observed no cortical changes in [^{3}H] pirenzepine binding following lesioning of the NBM, although comparisons were made between sides ipsilateral and contralateral to the lesion. Degeneration of branched axons which project both to the injection site and to the area investigated on the contralateral side is also unlikely to explain the reduction observed in [^{3}H] pirenzepine binding, as projections from the NBM to the cortex form mainly topographic ipsilateral projections (Saper, 1984). M_1 heteroreceptors on the terminals of neurones projecting from the injection site are also unlikely to be involved. Though the area lesioned does project contralaterally to the area investigated, no changes in [^{3}H] pirenzepine binding were observed following intracortical injection of 12.5 ng ricin, which would destroy contralaterally projecting axons and their terminals. It is probable that M_1 receptors are present on the cell bodies of the affected neurones, as the pattern of binding loss matched the pattern of neuronal loss. However, it is possible that the loss in [^{3}H] pirenzepine binding observed in superficial layers reflects localisation to the apical dendrites of layer V neocortical pyramidal neurones, although this was not a feature of corticofugal projecting neurones (see Chapter 7). Moreover, *in-situ* hybridisation histochemistry demonstrated the presence of m_1 mRNA in cells localised to neocortical supragranular layers (Brann et al., 1988; Buckley et al., 1988).

A substantial reduction in the binding of [^{3}H] nicotine was observed in deep cortical layers contralateral to the injection site in volkensin injected animals compared to that observed in control animals. Differences in binding between volkensin and ricin injected animals did not reach statistical significance. Because of this disparity, only results from control group animals from the same experiment were included in the statistical analysis, rather than augmenting the numbers of control animals with data from other experiments. No differences in binding were observed between ricin and control groups. Though the most likely explanation of this data is that nicotinic receptors are localised to the cell bodies of layer V contralaterally projecting neurones, several other possibilities should be explored. Autoreceptor localisation of

nicotinic sites is unlikely, as lesioning of the NBM did not reduce cortical [^{3}H] nicotine binding (Wenk and Rokaeus, 1988; Miyai et al., 1990), and projections from the NBM to the cortex form mainly topographic ipsilateral projections (Saper, 1984). However, a proportion of nicotinic sites may be heteroreceptors of projections from the injection site. Heteroreceptor localisation of nicotinic sites has been demonstrated for some projections (Sahin et al., 1992), though the same study also showed reductions in cortical [^{3}H] nicotine binding following intracortical excitotoxin injection, but only at longer survival times, which may reflect changes in terminal organisation following loss of innervation targets. In the present study, the lack of significance bewteen ricin and volkensin groups may indicate that a small proportion of nicotinic sites are localised presynaptically; cortical ricin injection would affect such receptors. However, no significant differences were found between ricin and control groups; subsequent investigations should pursue this possibility in larger animal groups. Evidence for a postsynaptic localisation of nicotinic sites is provided by the study of Bravo and Karten (1992), where immunohistochemistry using a monoclonal antibody for the nicotinic receptor demonstrated clear labelling of the cell bodies of layer V pyramidal neurones. Moreover, *in-situ* hybridisation histochemistry for alpha and beta subunits of the nicotinic receptor reveal the presence of mRNA in layer III and layer V cell pyramidal cell bodies (Heinemann et al., 1991b; Hill et al., 1993), although the presence of mRNA does not preclude the possibility of subsequent transport of the receptor to distant sites. Certainly, a proportion of nicotinic sites are localised to corticofugal projecting layer V pyramidal neurones (see Chapter 7), and this is also likely to be the case for corticocortical projecting neurones.

The most probable explanation for the lack of change of the binding of [^{3}H] 8-OH-DPAT, [^{3}H] ketanserin and [^{3}H] DPCPX is that the respective receptors are not enriched on the affected neurones. Changes in these receptors may be masked by gliosis, though this is unlikely, as more extensive gliosis was observed in the neocortex of animals injected with 2 ng intrastriatal volkensin (see Chapter 7), which was not sufficient to mask changes in binding to 5-HT_{1A} and adenosine A_1 sites. It is more likely that the affected cells may only contribute a small number of sites to total 5-HT_{1A} and adenosine A_1 sites,

and hence any small reduction consequent upon the loss of these cells may not be detectable overall. Therefore the present study cannot exclude the possibility that a small number of these receptors are present on the affected neurones. It is interesting to note that the 5-HT_{1A} receptor, which is amongst the most enriched on corticofugal projecting neurones does not appear to be enriched upon this subpopulation of corticocortical projecting neurones.

The present study provides compelling evidence for the specific localisation of muscarinic M_1 and nicotinic sites to corticocortical projecting neurones which are destroyed by contralateral intracortical volkensin injection. M_1 receptors appear to be localised to both infragranular and supragranular projection neurones, while nicotinic receptors are limited to the pyramidal neurones of infragranular layers. The muscarinic M_1 receptor has also been shown to be localised to corticofugal neurones of layer V and hippocampal CA3 pyramidal neurones. This receptor therefore represents a consistent marker for the subpopulations of pyramidal neurones examined in this thesis, and may be present on all pyramidal neurones. By contrast, the 5-HT_{1A} receptor, which was found to be highly enriched on infragranular corticofugal projecting neurones shows distinct regional heterogeneity between different pyramidal neurone types. The situation for the nicotinic receptor is somewhat more complicated; although this site appear to be enriched on both corticofugal and corticocortical neurones, the possibility remains that a proportion of the binding observed is attributable to presynaptic sites. Nevertheless, this receptor represents a promising candidate for investigation in future studies.

CHAPTER 10: General Discussion.

10.1 Introduction.

Cerebral atrophy is common in the dementias which occur in the presenile and elderly. Alzheimer's disease (AD) is considered to be the commonest cause of cerebral atrophy, and is characterised clinically by progressive loss of memory and other cognitive functions, resulting in a profound dementia. This decline is accompanied by the progressive loss of cortical pyramidal neurones, and is hallmarked by accumulation in the brain of insoluble fibrous material, both extracellularly and within the perikarya of pyramidal neurones. Extracellular deposits are composed of beta-amyloid protein, ßA4, which forms the core of senile or neuritic plaques. Neurofibrillary lesions constitute the intraneuronal deposits, and are found in cell bodies and apical dendrites as neurofibrillary tangles (NFT), in distal dendrites as neuropil threads, and in the abnormal neurites which are associated with some plaques. Neurofibrillary lesions develop in the cells which are considered to undergo degeneration in AD.

The study of cortical pyramidal cells provides important information concerning the progression of the disease, and aspects which may contribute to the primary cognitive deficit observed in AD. The progression of neurofibrillary formation with regard to cell types, layers and brain regions is the subject of a comprehensive study of Braak and Braak (1991). The first neurofibrillary lesions observed in AD are found within the pre-alpha layer of the transentorhinal region, with progression into the entorhinal cortex. Subsequent extensive entorhinal cell loss, with spread of neurofibrillary lesions to pyramidal cells of CA1 of the hippocampus, and involvement of basal forebrain structures precede massive development of neurofibrillary lesions in neocortical association areas. The above study also attempted to address neuropathological staging of amyloid based pathology. However, the method of visualisation used was inconsistently described, although a distinction between amyloid deposits and neuritic or senile plaques was made. The progressive appearance of amyloid deposits (which may lead to formation of neuritic plaques) begins in frontal, temporal and parietal isocortex, increasing in density with disease development. At later stages in the disease, virtually all

isocortical areas reveal densely packed deposits, with gradually increasing involvement of subcortical areas. The hippocampal formation harbours relatively few deposits. At this final stage of the disease, criteria for the neuropathological diagnosis of AD are met. It is tempting to assume that these sequences of involvement also reflects- in a still unknown manner- the clinical course of AD. Though this proposal is likely, lack of a clear diagnosis in early disease stages precludes a definitive test of this hypothesis. However, significant correlations have been described between tangle count in certain areas and dementia (Terry et al., 1991), a relationship not observed in studies of plaques (Terry et al., 1994). In the stages of the disease where significant neocortical pathology is observed, the pyramidal neurone is primarily affected, including those of the archicortical CA1 region, and neocortical cells which project corticocortically, forming association fibres (Hof and Morrison, 1994). Other studies of pyramidal neurone pathology support these findings. Samples obtained from neurosurgical craniotomy were examined for pyramidal cell density (Neary et al., 1986) and synaptic integrity (DeKosky and Scheff, 1990) in the temporal and frontal cortex, respectively. In both studies there were significant differences between AD and control tissue, though it should be emphasised that it is difficult to assess the suitability of the controls. In the former study, the nature of the control tissue is not described at all, whilst in the other report AD biopsy samples are compared only with autopsy controls. However, in a comprehensive study of autopsy tissue, with adequate controls, Terry et al. (1991) found significant correlations between psychological test performance, neocortical synapses and tangle count. This supports data from the biopsy studies, where significant correlations between cell and synaptic counts and the rating of dementia were found in both studies.

Among the neurochemical measures studied, those of acetylcholine seem to be most severely and consistently affected. Presynaptic cholinergic deficits, measured in biopsy tissue from young AD patients by measurement ACh synthesis by incorporation of radiolabelled glucose, revealed significant (inverse) correlations between synthesis in cortex from the medial temporal gyrus and the rating of cognitive impairment (Francis et al., 1985). Presynaptic 5-HT markers (5-HT release and uptake, 5-HT and 5-HIAA tissue

content), and to a lesser extent NA are also reduced, although postsynaptic indices and VCSF concentrations of these compounds are unaltered. 5-HIAA concentration in temporal cortex inversly correlated with the tangle count of histologically verified AD patients (Palmer et al., 1987a). However, studies of [^{3}H] paroxetine binding, a marker for presynaptic 5-HT terminals was altered in *post-mortem* tissue only in BA21, an area significantly affected by the diseases, although a significant loss of serotonergic cell bodies in the dorsal raphe nucleus was observed (Chen et al., 1994). The previous studies have shown that cholinergic markers are consistently reduced regardless of the area studied, whereas deficiency of 5-HT activity is probably never widespread. Furthermore, serotonergic pathology did not relate to psychological test scores (Palmer et al., 1987a). These data suggest that even at the end stages of the disease, serotonergic synapses are not as severely affected as those of the cholinergic system.

Evidence of presynaptic glutamatergic pathology is more difficult to assess, because of the high concentration (10 mM) and metabolic role of glutamate (see Introduction, section 1.5.4). However, the glutamate concentration of temporal lobe biopsy samples from AD patients was reduced by 14 %, and the value for individual subjects related to the density of pyramidal neurones in layer III (Lowe et al., 1990), and probably reflects the loss of corticocortical association fibres, although K^+-evoked release of aspartate and glutamate was not reduced in AD. Tritiated D-aspartate may be reliably assayed in prompt autopsy samples. Uptake was found to be reduced by 50 % in temporal cortex of AD patients (Procter et al., 1988c), which is likely to reflect loss of synapses of corticocortical fibres. Loss of glutaminase positive neurones has also been noted in the cortex of AD patients (Akiyama et al., 1989; Kowall and Beal, 1991). Moreover, loss of glutamatergic neurones would reduce excitatory input into the remaining neurones, resulting in cortical hypoactivity, and this may be reflected by glucose hypometabolism (Mata et al., 1980), apparent in PET imaging studies of AD sufferers (Foster et al., 1983; Duara et al., 1986; Rapoport et al., 1991), although these techniques are sensitive to atrophy.

There is no direct evidence relating glutamatergic transmission to dementia, although indirect evidence suggests the importance of this transmitter system to memory and behaviour (see Introduction, section 1.6.5.6). In AD, cortical pyramidal neurone hypoactivity (exacerbated by the cholinergic deficit), is central to the cognitive deficit observed, and the majority of these neurones probably use glutamate as their transmitter. Many neurofibrillary tangle bearing neurones in the cortex and hippocampus are also glutamate immunoreactive (Kowall and Beal, 1991), and degeneration of hippocampal glutamatergic neurones appears to be prominent, based on autopsy studies (Hyman et al., 1984; Kowall and Beal, 1991). Thus studies described in this thesis are relevant to AD in the context of improving glutamatergic pyramidal cell activity, and such treatments may serendipitously slow the progression of the disease (see section 10.4.2).

10.2 On the findings in human samples.

The present study (Chapter 3) has demonstrated that the glycine site of the NMDA receptor is viable in AD, although previous reports (Procter et al., 1989) found significantly reduced glycine stimulation of [^{3}H] MK-801 binding in AD compared to control tissue. While the pharmacological profile of the NMDA receptor to glutamate matched that described for rat, there appeared to be incomplete coupling of the glycine site and the receptor in AD compared to control tissue. Moreover, comparison of B_{max} values for [^{3}H] MK-801 binding revealed a reduction in AD, though it is unclear whether this reduction was indicative of fewer NMDA complexes, or reduced neuronal density. Reduced glycine stimulation of [^{3}H] MK-801 binding was also observed in the present study, though a small number of controls precluded statistical analysis. Nevertheless, glycine had a significant stimulatory effect on the binding of [^{3}H] MK-801, as did DCS in the absence of exogenously added glycine. DCS was observed to have a pharmacological profile consistent with that of a partial agonist in AD tissue.

Due to the well documented role in excitotoxicity (see Introduction, section 1.6.5.5), the potential utility of an agonist at the NMDA receptor complex has been viewed cautiously. Manipulation of the glycine site of the

NMDA receptor complex may therefore be a more suitable method of partially correcting pyramidal cell dysfunction in AD and normalising neuronal activity (Bowen, 1990). The success of such an approach depends on a number of other factors, such as the extent of neuronal loss, and the effects of endogenous ligands. Compounds most suitable for such a treatment strategy would be partial agonists, such as DCS, which may be expected to avoid the problems associated with over stimulation. Studies in living rats suggest that the glycine site of the NMDA receptor complex is not saturated (Thiels et al., 1992), and it is likely that the situation is similar in human brain. Additionally, DCS has been shown to improve aspects of learning and memory in several paradigms. Schuster and Schmidt (1992) and Sirvio et al. (1992) demonstrated that DCS improved spatial learning tasks in hippocampal lesioned and muscarinic antagonist treated rats, respectively, while Wesnes et al. (1991) showed a similar improvement in scopolamine induced memory impairment in young humans.

10.3 On the findings in the rat.

In the rat brain lesioning paradigms described in this thesis, subpopulations of cortical pyramidal neurones were destroyed following volkensin injection; unilateral entorhinal cortex injection of 2 ng volkensin destroyed hippocampal CA3 pyramidal neurones; unilateral intrastriatal injection of 2 ng volkensin destroyed corticofugal infragranular neocortical pyramidal neurones; and unilateral intracortical injection of 2.5 ng volkensin destroyed trans-callosal projecting neocortical pyramidal neurones. In all cases, appropriate control animals were included to confirm the specificity of the retrograde action of volkensin. Sections from animals were processed for autoradiographic studies using [^{3}H] ligands for various receptors, depending on the lesion type (see Chapter 2, Table 2.2). From these studies, it was apparent that not all receptors were associated to the same extent with the affected pyramidal neurones, and that different pyramidal neurones may bear different qualitative and quantitative receptor populations. Interpretations of these data are summarised in Table 10.1.

Studies of hippocampal CA3 pyramidal neurones revealed differences in the apparent degree of localisation for different receptors to the affected

	CA3	Corticofugal		Cortico-cortical	
		Medial	Lateral	Superficial	Deep
5-HT_{1A}	+	+++	++	-	-
5-HT_2	NP	NA	NA	-	-
Muscarinic M_1	++	++	+	++	++
Nicotinic	NA	+++	++	-	++
NMDA	+	NA	NA	NA	NA
Kainate	+	++	-	NA	NA
Adenosine A_1	NA	+	-	-	-
$Alpha_{1total}$	NA	-	-	NA	NA
$Alpha_{1b}$	NA	-	-	NA	NA
$GABA_A$	-	-	-	NA	NA

Table 10.1: SUMMARY OF RECEPTOR LOCALISATION TO CORTICAL PYRAMIDAL NEURONES DESTROYED IN THREE LESIONING PARADIGMS. CA3; subpopulation of hippocampal CA3 pyramidal neurones destroyed following entorhinal cortex injection of volkensin. Corticofugal; subpopulation of subcortically projecting layer V neocortical pyramidal neurones destroyed following intrastriatal volkensin injection, in medial (Fr1/Fr2) and lateral (Par1/Par2) areas. Cortico-cortical; subpopulation of neocortical pyramidal neurones projecting trans-callosally from both superficial (layer III) and deep (layer V) cortical laminae destroyed following intracortical volkensin injection.
+ + +; receptor investigated is present is disproportionately high numbers on the affected neurones (highly enriched) compared to the remaining neurones. + +; enriched, but with a more homogeneous distribution between the affected and remaining neurones. +; present, but not enriched on the affected neurones. -; no evidence of specific localisation to affected neurones. NA; not assessed. NP; not present in area investigated. Note the high levels of enrichment of the 5-HT_{1A} and nicotinic receptors to corticofugal neurones, and the consistent localisation of the mucarinic M_1 receptor to all neuronal groups studied.

neurones, though all the receptors investigated in the present study, with the exception of $GABA_A$ (which may, nevertheless be present on these neurones; see Chapter 5, section 5.3.3) were found to be present on these neurones. Only one receptor, muscarinic M_1, was found to be significantly enriched (i.e. the receptor is present in disproportionately high numbers on the affected neurones compared to those remaining). As described in Chapter 5, section 5.3.1, the presence of this receptor on hippocampal pyramidal neurones is supported by other studies using ligand binding (Perry et al., 1984; Tonnaer et al., 1988; Messer et al., 1989; Frey and Howland, 1992), *in-situ* hybridisation histochemistry (Buckley et al., 1988) and electrophysiology (Dutar and Nicoll, 1988). The EAA receptors, NMDA and kainate, were also found to be associated with CA3 pyramidal neurones, although enrichment was not as marked as for the M_1 receptor. The 5-HT_{1A} receptor, previously reported to be selectively enriched on corticofugal layer V neurones, was also found to be associated with CA3 pyramidal neurones which is in agreement with electrophysiological studies (Andrade, 1992), though again, enrichment was less than that observed for M_1 receptors. The muscarinic M_1 receptor therefore represents the best marker for hippocampal CA3 pyramidal neurones.

Corticofugal projecting infragranular pyramidal neurones also exhibit heterogeneous receptor populations. It has previously been demonstrated that the 5-HT_{1A} receptor is selectively enriched upon these neurones (Francis et al., 1992b), a finding supported by the present study. Additionally, significant reductions were found in [^{3}H] nicotine, [^{3}H] pirenzepine, [^{3}H] kainate and [^{3}H] DPCPX binding to nicotinic and muscarinic M_1 cholinoceptors, kainate glutamate and adenosine A_1 receptors respectively. The reductions in [^{3}H] nicotine binding were of the same order of magnitude as those observed for [^{3}H] 8-OH-DPAT binding to the 5-HT_{1A} receptor, whilst smaller, but consistent reductions in [^{3}H] pirenzepine binding were observed in all volkensin injected animal groups studied. With the exception of [^{3}H] nicotine, binding of all these [^{3}H] ligands was significantly reduced medially (Fr1/Fr2) in the deep but not superficial layers. This suggests that the receptors are associated predominately with pyramidal cell bodies. In more lateral areas (Par1/Par2), [^{3}H] 8-OH-DPAT, and [^{3}H] nicotine were reduced throughout the depth of the

neocortex, while reductions in deep layers only were observed for [^{3}H] pirenzepine. No reductions were observed in the binding of the other ligands to lateral areas. These data suggest cell body localisation of M_1 receptors; 5-HT_{1A} and nicotinic sites may be present on both the cell bodies and dendrites of the affected neurones. However, interpretations of non-cell body localisation of nicotinic sites is confounded by a possible presynaptic distribution. From this work, the most selective markers of corticofugal projecting pyramidal neurones are 5-HT_{1A} and nicotinic receptors; M_1 receptors, though less enriched, are also consistently localised to these cells. Binding of [^{3}H] kainate was reduced by approximately the same amount as that observed for [^{3}H] pirenzepine; however, therapeutic manipulation of this site by agonists should be viewed with caution due to the risk of excitotoxicity.

The final lesioning paradigm described in this thesis destroyed a subpopulation of corticocortical projecting neocortical pyramidal neurones. The affected neurones in superficial layers of neocortex are considered to be most closely related to the corticocortical association neurones which are degenerate in AD. Neurones in deeper layers of the neocortex were also destroyed by volkensin injection, and these neurones are also degenerate in the disease. Autoradiographic studies of receptor localisation to these neurones also revealed a degree of heterogeneity. [^{3}H] Pirenzepine binding was significantly reduced in both superficial (corresponding to layer III) and deep (corresponding to layer V) laminae of the neocortex in volkensin injected animals, while [^{3}H] nicotine binding was significantly reduced only in deep layers. No reductions in the binding of the other ligands used in this study ([^{3}H] 8-OH-DPAT, [^{3}H] ketanserin and [^{3}H] DPCPX) were observed. Infragranular pyramidal neurones were destroyed in the present and previous lesioning paradigms: it is interesting to note the differential localisation of the 5-HT_{1A} receptor on these neurones, suggesting the existence of quite distinct subpopulations of infragranular cells, which have characteristic receptor populations depending on their innervation target. The M_1 receptor was shown to be a good marker for CA3 and corticofugal pyramidal neurones (see above) and the present study provides additional evidence for the localisation of this receptor to the cell bodies of layer V neocortical pyramidal neurones.

Additionally, the receptor appears to be enriched on layer III pyramidal neurones destroyed by contralateral intracortical volkensin injection. Nicotinic receptors, shown in the previous study (see above) to be localised to layer V corticofugal neurones, also appear to be enriched on layer V corticocortical neurones, and may represent a specific marker for neocortical infragranular pyramidal neurones irrespective of their innervation target.

It is clear from these studies that different neuronal populations may be specifically enriched with different receptors. One of the aims of these studies was to determined whether there is a common receptor marker for all pyramidal neurones, and more specifically to those neurones affected in AD. While the 5-HT_{1A} receptor is a good marker for corticofugal neurones, specific enrichment was not demonstrated on rat corticocortical neurones (although the situation in human brain may be different- see section 10.4.1). The muscarinic M_1 receptor was found to be enriched on all of the subpopulations of pyramidal neurone investigated, and may represent the sought-after common marker. The distribution of the nicotinic receptor also suggests that this may be a suitable marker and pharmacological target for neocortical pyramidal neurones. The result of pharmacological manipulation of these receptors, as well as the possible therapeutic advantages in the treatment of the cognitive symptoms and progression of AD and suitability for *in-vivo* imaging is discussed below.

10.4 Implications for the treatment of Alzheimer's Disease.

It is proposed that treatment for both the symptoms and the progression of AD should focus on increasing the activity of the remaining cortical pyramidal neurones, which should correct cortical hypoactivity (Francis et al., 1993). Therefore a plausible approach would be to target a neurotransmitter receptor which is present upon these cells, whose manipulation may affect neuronal excitability. Results from this study suggest three possible therapeutic targets: the glycine site of the NMDA receptor; the 5-HT_{1A} receptor, and postsynaptic cholinergic receptors (M_1 and nicotinic).

10.4.1 Cognitive symptoms.

The NMDA receptor- ionophore complex mediates at least part of excitatory glutamatergic transmission (see Introduction, section 1.6.5.1). The NMDA recognition site of the receptor is coupled to an ion channel, which is gated by magnesium in a voltage dependent manner. The co-agonist glycine is required for activation of the complex, and increasing concentrations of glycine stimulate receptor activity. The NMDA receptor appears to play an important part in long term potentiation (LTP) (Collingridge, 1987), particularly in the hippocampal formation (Collingridge et al., 1983), and LTP induction, implicated in memory formation, also requires glycine to be present (Bashir et al., 1990). It therefore appears that the NMDA receptor- ionophore complex is a suitable target for manipulation in AD in the context of cognitive enhancement. The use of partial agonists at the glycine modulatory site, such as DCS, militates against excitotoxicity. The present study therefore supports the use of DCS for the treatment of AD, with the proviso that the effective doses probably lie within a narrow range (see Chapter 3, section 3.2.2.2). The resultant improvement of glutamatergic transmission and improved pyramidal neurone activity (Figure 10.1) not only are proposed to improve the cognitive deficit observed in AD, but may also slow the progression of the disease (see section 10.4.2). Reduced sensitivity of the NMDA receptor- ionophore complex to glycine has been described in AD (Procter et al., 1991), and if this should prove to be a characteristic of the disease itself, there would be even greater rationale for this proposed treatment.

The pharmacological approach for enhancing glutamatergic transmission using specific 5-HT_{1A} antagonists has been previously proposed (Pangalos, 1992; Francis et al., 1993; Bowen et al., 1994). Activation of the 5-HT_{1A} receptor, negatively coupled to adenylyl cyclase, has an inhibitory action, in both hippocampal and cortical preparations of rat tissue (Beck and Choi, 1991; Andrade, 1992), effected by increased K^+ conductance. Moreover, electrophysiological studies in fresh human neurosurgical samples demonstrated an 8-OH-DPAT induced hyperpolarisation and increased membrane conductance in temporal and hippocampal pyramidal neurones (McCormick and Williamson, 1989). Present and previous (Francis et al.,

1992b) studies demonstrate the selective enrichment of 5-HT_{1A} receptors on corticofugal pyramidal neurones. Support for the proposal of enhanced glutamatergic activity by 5-HT_{1A} antagonists is supported by the studies of Dijk et al. (1994a), who demonstrated by *in vivo* microdialysis increased NMDA induced glutamate release in the striatum by cortical application of a 5-HT_{1A} antagonist. The present study did not demonstrate enrichment of these receptors on corticocortical projecting pyramidal neurones. However, an important species difference should be emphasised. In the rodent, neocortical 5-HT_{1A} receptors are predominately found in deep layers. In the primate, the B_{max} value in lower layers is comparable with that observed in the rat; however, there is an additional high density of sites in superficial layers (Cross and Slater, 1989; Waeber et al., 1989). This observation suggests that in humans, the receptor may be present on ipsilateral projecting corticocortical pyramidal neurones (DeFelipe and Jones, 1988), consistent with the hypothesis that these receptors may be important in the regulation of the activity of these cells.

The viability and preservation of the 5-HT_{1A} receptor is difficult to assess in AD. Although Bowen et al (1989) describe loss of [^{3}H] 8-OH-DPAT binding in temporal and parietal areas (when results are expressed relative to protein content), in *post-mortem* tissue, and propose loss of this site as an index of affected cortical pyramidal neurones, other reports describe more limited changes (Middlemiss et al., 1986b; Procter et al., 1988b). However, the influence of differences in mean age of the cases (Bowen et al., 1989) (more widespread losses of 5-HT_{1A} receptors were reported in an older group of patients compared to control than in other reports where younger cases were investigated) and inadvertent selection of cases because of non-cognitive symptoms cannot be excluded as an alternative explanation of some of these discrepant findings. Moreover, it appears that the coupling of the remaining receptors with their G-proteins is preserved in AD (O'Neill et al., 1991). Therefore treatment of AD patients with a 5-HT_{1A} antagonist should facilitate the effects of the remaining proportion of transmitter glutamate by inhibiting the tonic hyperpolarising action of 5-HT on pyramidal neurones (see Figure 10.1), thereby compensating for the reduced excitatory input caused by the

degenerative process. The involvement of the serotonergic system on learning and memory has been studied elsewhere: decreased 5-HT availability can enhance learning and memory (Ogren, 1982), while procedures designed to enhance 5-HT activity have been reported to impair avoidance responses (Essman, 1973; Ogren and Johansson, 1985) and discrimination learning (Wetzel et al., 1980). Administration of 8-OH-DPAT impairs spatial learning in a water maze, probably by a postsynaptic agonist effect (Carli and Samanin, 1992). It should be noted that both presynaptic (localised to dorsal raphe neurones, and innervated by axon collaterals of serotonergic neurones) and postsynaptic 5-HT_{1A} sites have been demonstrated (De Montigny and Aghajanian, 1977; Blier et al., 1993). Moreover, some selective agents at the 5-HT_{1A} receptor show different activity profiles at these sites (Andrade and Nicoll, 1987b; Sprouse and Aghajanian, 1987; Radja et al., 1992), although this may be attributable to the receptor reserve for agonists. Antagonists at both sites would block postsynaptic 5-HT_{1A} actions, but increase terminal 5-HT release which may affect non-5-HT_{1A} receptors; available evidence suggests that any resulting behavioural effects may be positive. At present, few selective 5-HT_{1A} antagonists are available, although several novel compounds are under investigation (e.g. WAY-100135, Fletcher et al., 1991).

A corollary of the present study is that 5-HT_{1A} agonists may be useful in the development of neuroprotective agents in cerebral ischaemia. The hyperpolarising effects that these compounds may have on pyramidal neurones would decrease glutamatergic activation, and therefore the likelihood of calcium influx, and associated excitotoxic damage. Again, careful consideration should be given to the pre- and postsynaptic effects of such compounds.

The pharmacological approach for enhancing glutamatergic transmission by manipulation of the cholinergic system is the subject of extensive literature (as reveiwed, Becker, 1991; McKinney and Coyle, 1991). Both the muscarinic M_1 and nicotinic cholinoceptors are excitatory, though the mechanisms of action differ. The M_1 receptor is linked via a G-protein to the phospholipase C (PLC) signal transduction system (Figure 10.1), which yields IP_3 and DAG from hydrolysis of phosphotidylinositol bisphosphate (PIP_2). These second messengers mobilise calcium from intracellular stores, and

activate protein kinase C, respectively (Figure 10.1). The final effect of receptor activation is reduction of potassium conductance via "M" channels (I_M), effecting slow excitation. The nicotinic receptor is a classical cation channel-linked receptor; activation causes sodium influx and subsequent depolarisation. Both excitatory mechanisms have been extensively studied, and M_1 receptor activation produces a prolonged facilitation of cortical and hippocampal neurones (McCormick and Prince, 1985; Dutar and Nicoll, 1988; McCormick and Prince, 1986; Cole and Nicoll, 1984) rendering them more likely to depolarise following excitatory glutamatergic inputs (Metherate et al., 1988). Moreover, in fresh human brain biopsies, muscarinic agonists reduced I_M, causing slow excitation of pyramidal neurones (McCormick and Williamson, 1989). This facilitation of excitability has also been shown to play a role in LTP induction in rat cerebral cortex (Lin and Phillis, 1991). Most electrophysiological studies of the effects of nicotine have focused on EEG effects following systemic administration, however, presynaptic nicotinic receptors may increase transmitter glutamate release. Bath application of nicotine to mouse hippocampal slices resulted in an increase in the amplitude of spikes, and appearance of multiple population spikes in the CA1 pyramidal cell layer (Freund et al., 1988). In rat cortical slice preparations, iontophoretic application of nicotine and analogues increased excitability of pyramidal neurones in the prefrontal cortex (Vidal and Changeux, 1989). These observations suggest that both muscarinic M_1 and nicotinic cholinoceptors mediate excitatory effects on cortical pyramidal neurones.

The density of the total muscarinic receptor population in the brains of patients with AD has been reported as increased, decreased, or unchanged (Hardy et al., 1985; Whitehouse, 1987; Giacobini, 1990; Perry et al., 1990). Such variations may be attributed to differing degrees of degeneration of intrinsic or extrinsic neuronal elements, inadequate characterisation, or incomplete allowance for epiphenomena (i.e. *post-mortem* delay, duration of terminal coma) of the brain tissue examined. Alternatively, the degree of regulatory responses to the denervation (i.e. postsynaptic receptor upregulation) or other aspects of the cortical pathological conditions may vary. Several studies have used selective ligands to study the distributions of

muscarinic receptor subtypes in the disease, with similarly disparate results. Again, investigators have reported increased, decreased or unchanged levels of both postsynaptic M_1 receptors, and presynaptic (thought to reflect cholinergic neurone density) M_2 receptors (Mash et al., 1985; Flynn et al., 1991 ;Svensson et al., 1992; Nordberg et al., 1992a), although M_2 receptors are reported to be decreased more consistently. *In-situ* hybridisation histochemistry studies also report increased (Harrison et al., 1991) and decreased (Wang et al., 1992) levels of m_1 mRNA in Alzheimer brain. In considering the suitability of the M_1 receptor as a therapeutic site, the possibility of impaired coupling of the receptor and G-protein or effector mechanisms should also be assessed. The activity of PLC in AD appears to be unchanged (Shimohama et al., 1992), and Pearce and Potter (1991) report no loss of receptor- G-protein coupling. Jope et al. (1994) reported impaired G-protein- PLC coupling, though G-protein levels and PLC activity were unchanged between AD and control cases. However, the validity of this study is questionable- though the AD and control cases were age and *post-mortem* delay matched, no information regarding duration of terminal coma was given. Moreover, experiments were performed at a single calcium concentration, and PLC activity is highly sensitive to this ion. Different Ca^{2+} concentrations in AD and control cases brain would give rise to the interpretation of impaired coupling. Flynn and Mash (1985) report loss of high affinity agonist binding sites in AD brain, although this may reflect alterations in receptor regulatory mechanisms (i.e. protein kinase C levels (Cole et al., 1988)). The activity and coupling of the M_1 receptor to it G-protein and effector is now the subject of a current study (see Appendix).

Several studies have examined the nicotinic receptor in AD brain. Out of 8 autopsy studies (1981-1988), six show decreases in nicotinic receptors in AD of 44 - 65 % of normal, and two show no change (as reveiwed, Giacobini, 1990). Moreover, most studies conclude that the observed reduction in [^{3}H] nicotine corresponds to loss of high affinity nicotinic site (Giacobini, 1990; Nordberg et al., 1992a), and it is likely that a proportion of this reduction reflects loss of presynaptic sites.

There is a wealth of data on the cognitive effects of manipulation of the cholinergic system, both pre- and postsynaptically, in animal and human

models. Many studies have been reported documenting lesion- induced cortical cholinergic marker deficits in animals (for review, see Olton and Wenk, 1987), which are consistent regardless of the agent or technique used to affect the NBM. These lesions are commonly associated with cognitive decline (impairments of: passive avoidance conditioned response, discrete trial alternation, choice accuracy in match-to-sample and radial arm maze, and initial learning with increased latency and errors in the water maze; for review, see Pepeu et al., 1990). A number of these studies also demonstrated that these cognitive deficits can be reversed using cholinomimetic drugs (see Introduction, section 1.10.1), such as the cholinesterase inhibitor, physostigmine, or receptor agonists such as pilocarpine and oxtremorine (Haroutanian et al., 1986). Although specific behavioural paradigms vary between laboratories, the general findings have been similar. Irrespective of the cholinomimetic used, recovery from NBM lesion-induced cognitive deficits can be induced by a wide variety of cholinomimetic agents. Similarly, administration of cholinergic antagonists (e.g. scopolamine) has also been shown to impair cognitive function in both rodent and primate models, and is often used as a paradigm to test putative "cognitive enhancers" (Wesnes and Warburton, 1984; Aigner and Mishkin, 1986; Aigner and Mishkin, 1993). Nicotinic receptors have also been found to be important for maintaining optimal performance in a variety of cognitive tasks. In humans, nicotine-induced improvement of rapid information processing is particularly well documented (for review, see Levin, 1992). In experimental animals, nicotine has been found to improve learning and memory in a variety of tasks (Battig, 1970; Haroutanian et al., 1985), while the nicotinic antagonist mecamylamine was found to impair memory performance (Levin et al., 1987).

It is therefore clear that there is ample rationale for cholinergic based therapy for the treatment of the cognitive symptoms observed in AD, and the current study provides evidence for M_1 and nicotinic receptors as suitable targets for modulating the function of neocortical pyramidal neurones. M_1 receptor localisation to hippocampal pyramidal neurones may also ameliorate the hippocampal dysfunction observed in AD, though localisation of these, and nicotinic receptors, to CA1 hippocampal pyramidal neurones has not yet been

established using the present paradigms. Enhancing cholinergic function may be achieved by two main methods: administration of anticholinesterase drugs, or administration of cholinergic agonists. Both of these approaches would increase pyramidal neurone excitability, and should reverse the effect of glutamatergic hypoactivity of these neurones. However, only the former would affect both muscarinic and nicotinic receptors; agonists at both sites may produce a greater incidence of central and peripheral side effects. One anticholinesterase, tetrahydroaminoacridine (THA, Tacrine, "Cognex"), has passed the Food and Drug Administration's stringent licensing procedures for use in treating "mild to moderate" Alzheimer's disease. However, since first claims of its efficacy in AD in a controlled trial in 1986, further studies have been almost equally divided between those reporting benefit for some AD patients, and those reporting no benefit (Byrne and Arie, 1994). The dose of Tacrine varies considerably between studies, and most report high levels of hepatotoxicity and cholinergic side effects. Also, most studies used too few patients to provide the power to prove or disprove the hypothesis. Well designed trials with adequate numbers of subjects showed that Tacrine benefits some patients, and the benefits are expressed either as improvement in the core deficits of AD, or as a reduced rate of deterioration (Davis et al., 1992). However, only very few patients benefit greatly. This may be due to many reasons: the dose may be inadequate; larger doses are commonly associated with more side effects and incidence of toxicity, with resulting withdrawal of the subject from the study; also, positive diagnosis of AD cannot be absolute in life: it is likely that a number of patients included in a trial may be suffering from other forms of dementia. While it is clear that Tacrine is not an ideal anticholinesterase inhibitor, with high incidence of toxicity and short duration of action, the results of some trials are encouraging. It is hoped that the next "generation" of anticholinesterase inhibitors will address these problems (Giacobini et al., 1991). There are a number of M_1 selective agonists under development (e.g. AF102B, Fisher et al., 1992), whose action on central postsynaptic receptors is also proposed to enhance pyramidal cell activity, by facilitating the action of other, excitatory transmitters. It may transpire that the most effective treatments for AD may require polypharmacy, with a 5-HT_{1A}

antagonist given in conjunction with an anticholinesterase inhibitor, for example. Full investigation of these proposals await development of selective, non-toxic and long-lasting agents.

10.4.2 Progression of the disease.

As described previously, AD is characterised by two histopathological features, amyloid plaques and neurofibrillary tangles (NFT). While the aetiology of the disease is unknown, a common consequence proposed by current hypotheses is neuronal cell death. The precise relationship between amyloid precursor protein processing, formation of ßA4 and its deposition as insoluble material in neuritic plaques has not yet been established (see Introduction, section 1.8.2.1), although the role of amyloid in the development and progression of the disease forms a central theme in many hypotheses of aetiology. Similar depositions are observed in Down syndrome patients, usually over 40 years of age, and to a lesser extent in normal ageing. Hyperphosphorylation of tau may account for its abnormal transformation into paired helical filament (PHF) tau, a key constituent of NFTs, which are closely associated with neuronal death. It is proposed that transmitter based interference with mechanisms of ßA4 production and hyperphosphorylation of tau may impair disease progression. Moreover, it may be speculated that such therapy may also affect apolipoprotein E4 (apo-E4; see Introduction, section 1.8.4.2) expression or secretion from astrocytes (Pitas et al., 1987; Diedrich et al., 1991) in homozygous individuals for this allele, considered to be a major risk factor for AD (Saunders et al., 1993). Production of apo-E4 may be a link between abnormal ßA4 deposition and tangle formation, as this variant has been demonstrated to bind with high avidity to soluble ßA4. Moreover, the E3 (absent in homozygous E3 individuals) allele may stabilise tau, preventing hyperphosphorylation and self assembly into PHF (Bowen et al., 1994).

Some *in vivo* and *in vitro* studies suggest that ßA4 places neurones at risk for degeneration (see Introduction, section 1.8.2.1), although ßA4 deposits do not appear to be degenerative foci (as reviewed, Cotman and Pike, 1994). Early studies of APP metabolism elucidated what is now known as the α-secretase pathway, activity of which precludes formation of intact ßA4, and

yields a truncated N terminal secreted fragment designated APP_S. Subsequently, additional routes of APP processing have been discovered. In the endosomal/lysosomal pathway, APP is processed into a series of 8 -12 kD fragments that include the intact ßA4 region (Golde et al., 1992). A possibly separate pathway involves normal cellular secretion of soluble ßA4 (Seubert et al., 1992; Haass et al., 1992b). A substantial portion of APP secretion by human mixed brain cell cultures, as well as present in CSF, is a form of APP precisely cleaved at the amino terminus of ßA4 by ß-secretase (Seubert et al., 1993). Subsequent processing by alternative, possibly lysosomal, pathways may be involved in the production of intact, secreted ßA4. This recent discovery of apparently normal ßA4 production has led some to question the hypothesis that ßA4 production, overproduction or aberrant compartmentalisation or processing of APP leads or contributes to the pathology of the disease. However, putative abnormal processing, or overproduction of ßA4 may preclude a normal, essential extracellular function of alternatively processed, secreted APP_S. APP proccessing may be affected by protein phosphorylation: increased production of APP_S has been associated with PKC activation (i.e. via M_1 receptor activation) (Caporaso et al., 1992; Nitsch et al., 1992; Webster et al., 1993), or inhibition of production of second messengers of the PLC signal transduction mechanism (Clarke et al., 1993b) which concurrently decreases ßA4 secretion (Buxbaum et al., 1993; Gabuzda et al., 1993; Fukushima et al., 1993). Increased neuronal activity is also associated with increased APP secretion (Nitsch et al., 1993; Dijk et al., 1994b), and it is proposed that these effects are mediated by enhanced α-secretase activity. These data suggest that correction of glutamatergic hypoactivity, with resultant increases in pyramidal neurone activity, using the methods described in the preceding section, would not only improve the cognitive symptoms of AD, but would also be expected to decrease secretion of potentially amyloidogenic APP fragments (Figure 10.1). If ßA4 production is central to the disease progression, this would retard development of further pathology and symptoms.

Mechanisms regulating the hyperphosphorylation of tau, leading to formation of PHF tau and NFTs are less well described (see Introduction, section 1.8.3.2). It may be pessimistically speculated that agents which

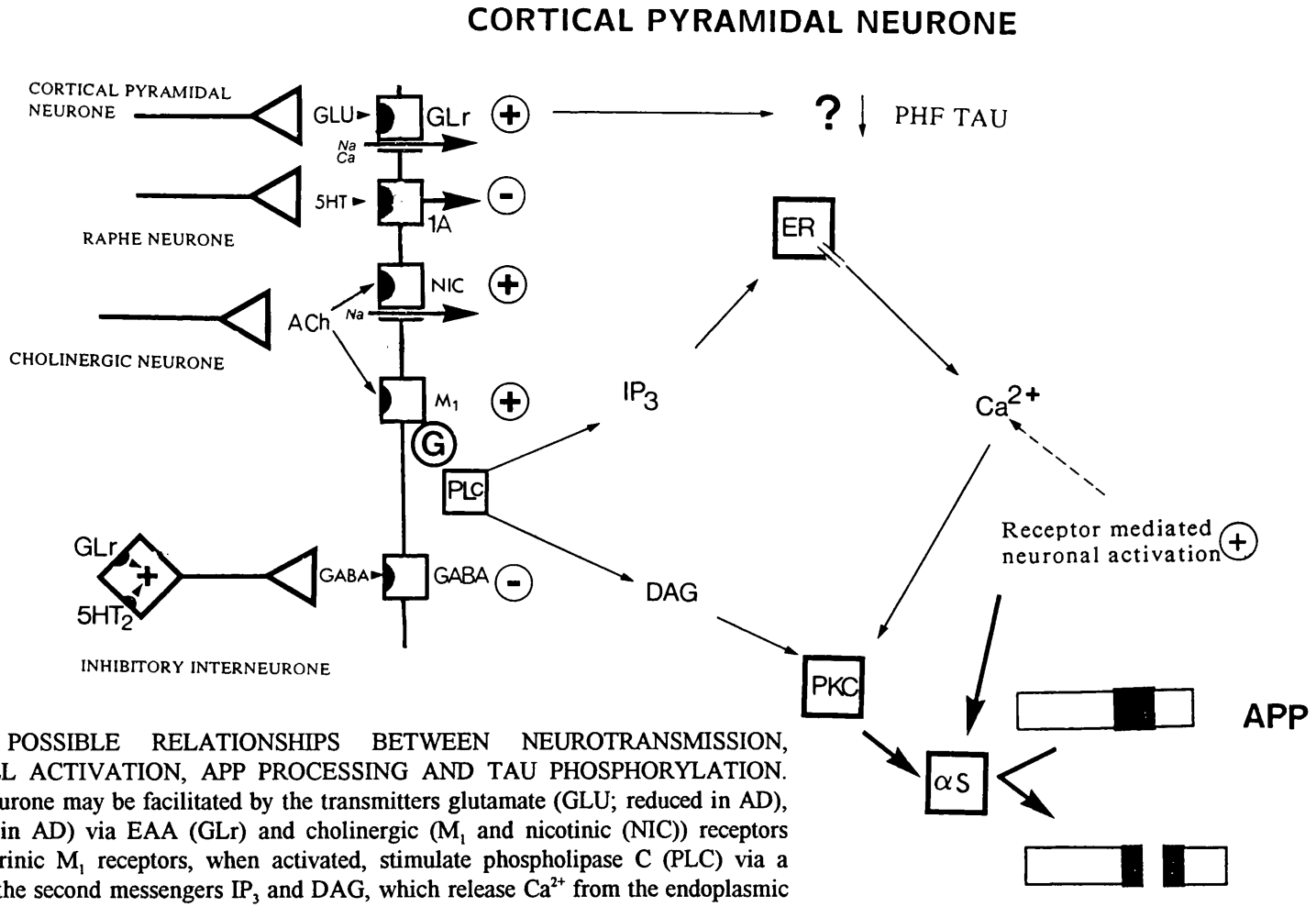

FIGURE 10.1: POSSIBLE RELATIONSHIPS BETWEEN NEUROTRANSMISSION, PYRAMIDAL CELL ACTIVATION, APP PROCESSING AND TAU PHOSPHORYLATION. Excitation of the neurone may be facilitated by the transmitters glutamate (GLU; reduced in AD), and ACh (reduced in AD) via EAA (GLr) and cholinergic (M_1 and nicotinic (NIC)) receptors respectively. Muscarinic M_1 receptors, when activated, stimulate phospholipase C (PLC) via a G-protein, yielding the second messengers IP_3 and DAG, which release Ca^{2+} from the endoplasmic reticulum (ER) and stimulate protein kinase C (PKC), respectively. Increased α-secretase (αS) activity, precluding formation of ßA4, may be mediated by PKC activation and/or neuronal activity, possibly by a Ca^{2+} dependent mechanism. Stimulation of glutamate receptors (and thus increased neuronal activity) may also decrease tau hyperphosphorylation (PHF TAU). 5-HT and GABA, less affected by the disease, mediate inhibition via $5\text{-}HT_{1A}$ and GABA receptors, respectively.

stimulate PKC activity (i.e. via the M_1 receptor) may lead to PHF formation. However, there is little evidence that this is the case: PKC has been demonstrated to phosphorylate tau, but this does not lead to the characteristic shift in mobility associated with PHF tau. Moreover, one kinase implicated in the formation of PHF tau, glycogen synthase kinase (GSK) (Brion et al., 1993), may be downregulated and inactivated by PKC activation (Goode et al., 1992). Additionally, findings of a recent study suggest that hypoactivity of glutamatergic neurones may be implicated in aberrant mechanisms of tau hyperphosphorylation, a proposal based on observations that when treated with a high (1 mM) concentration of glutamate, primary cultures of foetal rat cortical neurones contained much lower amounts of hyperphosphorylated tau (Davis et al., 1994) (Figure 10.1), identified with antibody AT8 (Brion et al., 1993).

This data provides further evidence for the rationale of transmitter based therapy directed at improving the state of pyramidal neurone activation. Treatment with cholinomimetics, 5-HT_{1A} antagonists, or agents which act at excitatory amino acid receptors would be expected to ameliorate the glutamatergic hypoactivity associated with loss of excitatory input to cortical pyramidal neurones, and consequentially treat the symptoms of the cognitive deficit observed in AD, while influencing mechanisms of possible aberrant APP processing and tau hyperphosphorylation, with resultant slowing of the disease process.

10.5 Implications for in vivo imaging.

Functional brain imaging techniques of positron emission tomography (PET) and the lower resolution single-photon emission computed tomography (SPECT) of subjects with AD have been reported to correlate with cognitive deficit (Cutler et al., 1985; Miller et al., 1987). The former technique, which showed selective glucose hypometabolism in the parietotemporal lobes was sensitive to atrophy (Chawluk et al., 1987). AD neuropathology is most prominent in these areas (see Introduction, section 1.8.1), and hypometabolism was not reported *in vitro* when assessed in neocortical biopsies (Sims et al., 1983b), so the scans probably provide evidence of early neuronal degeneration in parietotemporal areas, also revealed by blood flow imaging (Gustafson et al.,

1987; Neary et al., 1987). This proposal is supported by observations of unchanged glucose metabolic rates in normal ageing (Foster, 1994), and the focal parietotemporal hypometabolism in suspected AD cases. It is now becoming clear that while PET does not provide unequivocal diagnosis of AD, characteristic patterns of hypometabolism in both cortical and subcortical structures may provide evidence in addition to behavioural data which aids correct diagnosis (Foster, 1994). Present and previous (Bowen et al., 1993b) studies suggest that the 5-HT_{1A} receptor is a selective marker for pyramidal neurones, and loss of these sites may index losses of subpopulations of pyramidal neurones from the neocortex. However, the present study also suggests that M_1 and nicotinic receptors appear to be selective markers of a wider diversity of pyramidal neurones, and development of PET ligands specific for these receptors may therefore provide a specific method for determining the extent of pyramidal cell pathology, aiding early diagnosis of the disorder.

Despite its potential, labelling drugs for study with PET is severely limited, as most drugs do not posses the necessary properties. Several characteristics must be favourable for a drug to be successfully labelled for use with PET. First, a rapid synthesis must be devised that adds the positron emitting isotope to the parent compound. This reaction must have a high yield, and be free of significant contaminating side products, so purification may be easily completed before the decay of the positron-emitting compound. Since the half life of positron-emitting isotopes is measured in minutes, this is obviously a challenge. Second, to be able to interpret results, the radioactivity measured in the brain must be attributable to a known species. This is unlikely if, in addition to the parent compound, labelled metabolites also enter the brain. Obviously, the ligand should also be capable of crossing the blood brain barrier effectively. Third, the drug must possess a slow dissociation rate from the receptor at physiological temperature, and fourth, the drug must be safe at the doses required, and not accumulate excessively in any organ system (Hartig and Lever, 1990; Foster, 1994).

Little progress has been made in the development of selective PET ligands for the 5-HT receptor subtypes, with the possible exception of the

5-HT_2 receptor. A specific ligand, [^{11}C] methyl-bromo-LSD is now available for use in humans, though the ligand may also cross react with α_1 and D_2 receptors in certain areas such as the basal ganglia (Wong et al., 1987; Maziere and Maziere, 1990; Hartig and Lever, 1990). An iodinated derivative of 8-OH-DPAT has been developed for study of the 5-HT_{1A} receptor, with visualisation by SPECT. However, in common with 8-OH-DPAT (Dr. S. Hume, personal communication), exceptionally high non-specific binding is a significant drawback (Kung et al., 1986). However, advances are being made, and new compounds for this site are under current investigation and development (Bjork et al., 1991; Liau et al., 1991). A very recent report proposes the use of S14506, a piperazine derivative, as a possible selective 5-HT_{1A} receptor ligand for use *in vivo*, and it appears that this drug possesses a suitable pharmacological and pharmacokinetic profile (Lima et al., 1994). The 5-HT_{1A} antagonist WAY-100135 (Fletcher et al., 1991) may also possess a suitable profile.

A number of studies have described muscarinic agents which may be used in PET and SPECT studies. Original studies used QNB, which labels total muscarinic receptors, a feature in common with many current PET ligands for these receptors (Maziere and Maziere, 1990; Mulholland et al., 1992; Suhara et al., 1993). Few attempts have been made to visualise muscarinic receptors in the brains of AD patients, and these ligands are unsuitable to distinguish different receptor subtypes. Recent attempts to distinguish subtypes using [^{11}C] methyl-benztropine have been more successful (Dewey et al., 1990), although this agent is unable to distinguish between M_1 and M_2 receptors. [^{11}C] tropanyl benzilate (TRB) has also been used to study muscarinic receptors in an AD brain, though again, this ligand is not subtype selective. The AD patient demonstrated a typical pattern of temporoparietal glucose metabolism. Receptor distribution did not reflect regional blood flow or metabolism, with observation of high signals in basal ganglia and less in the cortex. There was no difference between the AD patient and the normal control in either the distribution or the number of muscarinic sites measured by TRB.

The use of nicotinic receptor ligands to visualise pyramidal neurone loss in AD should be carefully assessed, given the possible presynaptic localisation of a proportion of nicotinic receptors. Although it may be possible to distinguish pre- and postsynaptic nicotinic sites by careful correlation with loss of binding in subcortical structures, studies to date have not attempted to do this, instead proposing that nicotinic receptors are exclusively presynaptic markers. Most studies describe reduced [^{3}H] nicotine binding in *post-mortem* AD brain samples. This is also reflected by PET studies using [^{11}C] nicotine, where distribution of this ligand agreed with the distribution of nicotinic receptors in autopsy brain (Adem et al., 1989). Reduced binding of [^{11}C] nicotine enantiomers was observed in AD, particularly in temporal cortex, although there was significant variation in the AD brain signal. Frontal cortical [^{11}C] nicotine binding was also reduced in AD patients compared to controls, and patients with the lowest cortical binding also had the lowest Mini-Mental-State-Evaluation values (Nordberg et al., 1990). Subsequent studies report that Tacrine restores cholinergic nicotinic receptors and glucose hypometabolism in mild- to moderately demented patients with suspected AD (Nordberg et al., 1992b). NGF infusion, proposed to "rescue" degenerating cholinergic neurones, also increased uptake and binding of [^{11}C] nicotine in frontal and temporal cortex, with a persistent increase in cerebral blood flow (Olson et al., 1992). These two studies support post- and presynaptic localisation of nicotine binding sites, respectively, and suggest that use of such a ligand may be important for detection of AD; effects of drugs designed to restore cholinergic function and thus improve glutamatergic hypoactivity may also be studied using the technique of PET.

Given the lack of clear alteration of the numbers of M_1 receptors in AD brain, it is likely that PET ligands aimed at allowing visualisation of 5-HT_{1A} or nicotinic cholinergic receptors may be more appropriate for studying pyramidal neurone pathology *in vivo*. Development of further ligands, with subsequent study of subjects with a wide diversity of dementia severity, following by *post-mortem* evaluation of the disease state is vital to ascertain the suitability of PET as a diagnostic tool for examining disease progression and pyramidal neurone pathology.

10.6 Future studies.

Suicide transport lesioning to destroy selective subpopulations of neurones in the brain is clearly a powerful technique for examination of the biology of these cells, and allows biochemical markers to be ascribed for use as pharmacological targets for treatment and study of the disease progression. Future studies are planned to investigate the receptor populations of entorhinal pyramidal neurones, affected early in the disease (Pearson et al., 1985; Braak and Braak, 1991), by injection of volkensin into the dentate gyrus. Other applications of the volkensin lesioning paradigm include study of pyramidal neurones of the neocortex which connect homolaterally, and would most closely mimic cortical association fibres of the human brain.

Autoradiographic studies are limited by resolution; future studies should aim to combine results from autoradiography, *in-situ* hybridisation histochemistry, and electrophysiology to describe more precise receptor localisation.

Findings which describe receptor enrichment to neocortical pyramidal neurones should be extended to examine the integrity of signal transduction pathways in diseased brain. Indeed, work is now proceeding to investigate the coupling of the M_1 receptor to its effector, PLC, as adequate physiological receptor function is vital to any treatment strategies (see Appendix). Moreover, the effects of receptor activation or inhibition on the processing of APP and tau hyperphosphorylation should be investigated in primary tissue culture.

It remains to be established what effect the degree of neuronal deactivation has on APP processing, though a plausible explanation for the presence of senile plaques in AD is the loss of cholinergic modulation (Bowen et al., 1994). Likewise it is important to discover any effect of transmitter based therapy on the understudied aberrant mechanism of tau phosphorylation or de-phosphorylation, and effects on the novel non-amyloidogenic homologue of APP ($APLP_2$ or APPH) (Bowen et al., 1993a). Investigations should also include studies of any interaction between these mechanisms and apolipoprotein E3 (Bowen et al., 1994), which may inhibit tau self assembly into PHF.

The underlying cause of the pathological changes observed in AD are as yet undiscovered. While a genetic basis may account for a small percentage of incidence, it is likely that the cause of sporadic AD is multifactorial. The exact contribution of amyloidosis to the aetiology of the disease is also uncertain, as is the role of tau protein, though neurofibrillary tangles seem to be associated with the disease progression. Nevertheless, there are millions of AD sufferers, for whom symptomatic treatment of the cognitive deficit by transmitter based therapy would drastically improve quality of life. Therefore it is vital that work based on transmitter abnormalities of the disease be continued, which may also help in the early and accurate diagnosis of the disease. Moreover, there is mounting evidence that neurotransmitter dysfunction plays a pivotal role in the amyloidogenesis and tau hyperphosphorylation of AD, and these recent developments in this rapidly changing field suggest that transmitter based treatment, using drugs designed to improve the state of pyramidal neurone activation, will address symptomatic and progressive aspects of the disease.

REFERENCES

Adem, A., Nordberg, A., Singh Jossan, S., Sara, V., and Gillberg, P.G. (1989). Quantitative autoradiography of nicotinic receptors in large cryosection of human brain hemispheres. Neurosci. Lett. *101*, 247-252.

Adrendt, T., Bigl, V., Tennstedt, A., and Arendt, A. (1985). Neuronal loss in different parts of the nuleus basalis is related to neuritic plaque formation in cortical target areas in Alzheimer's disease. Neuroscience *14*, 1-14.

Aigner, T.G. and Mishkin, M. (1986). The effects of physostigmine and scopolamine on recognition in monkeys. Behav. Neurol. Biol. *45*, 81-87.

Aigner, T.G. and Mishkin, M. (1993). Scopolamine impairs recall of one-trial stimulus-reward association in monkeys. Behav. Brain Res. *54*, 133-136.

Akiyama, H., McGeer, P.L., Itagaki, S., McGeer, E.G., and Kaneko, T. (1989). Loss of glutaminase-positive cortical neurons in Alzheimer's disease. Neurochem. Res. *14*, 353-358.

Alkon, D.L., Amaral, D.G., Bear, M.F., Black, J., Carew, T.J., Cohen, N.J., Disterhoft, J.F., Eichenbaum, H., Golski, S., Gorman, L.K., Lynch, G., McNaugton, B.L., Mishkin, M., Moyer, J.R., Olds, J.L., Olton, D,S., Otto, T., Squire, L.R., Staubli, U., Thompson, L.T., and Wible, C. (1991). Learning and memory. Br. Res. Rev. *16*, 193-220.

Alzheimer, A. (1907). Über eine eigenartige Erkrankung der Hirnrinde. Allgemeine Zeitschrift für Psychiatrie und Psychisch-Gerichtlich Medicin *64*, 146-148.

Amaral, D.G. and Insausti, R. (1990). Hippocampal formation. In The human nervous system. G. Paxinos, ed. (London: Academic Press), pp. 711-755.

Anden, N.E., Dahlstrom, A., Fuxe, K., Larson, K., Olson, L., and Ungerstedt, U. (1966). Ascending monoamine neurones to the telencephalon and diencephalon. Acta Physiol. Scand. *67*, 313-326.

Andrade, R., Malenka, R.C., and Nicoll, R.A. (1986). A G protein couples serotonin and $GABA_B$ receptors to the same channels in hippocampus. Science *234*, 1261-1265.

Andrade, R. and Nicoll, R.A. (1987a). Pharmacologically distinct actions of serotonin on single pyramidal neurones of the rat hippocampus recorded in vitro. J. Physiol. *394*, 99-124.

Andrade, R. and Nicoll, R.A. (1987b). Novel anxiolytics discriminate between postsynaptic and presynaptic mediating different physiological responses on single neurones of the rat hippocampus. Naunyn-Schmiedeberg's Arch. Pharmacol. Exp. Pathol. *336*, 5-10.

Andrade, R. (1992). Electrophysiology of 5-HT_{1A} receptors in the rat hippocampus and cortex. Drug Dev. Res. *26*, 275-286.

Andreasen, M. and Lambert, J.D.C. (1991). Noradrenaline receptors participate in the regulation of GABAergic inhibition in area CA1 of the rat hippocampus. J. Physiol. *439*, 649-669.

Arai, H., Kobayashi, K., Ichimiya, Y., Kosaka, K., and Iizuka, R. (1985). Free-amino acids in postmortem cerbral cortices from patients with Alzheimer-type dementia. Neurosci. Res. *2*, 486-490.

Aramori, I. and Nakanishi, S. (1992). Signal transduction and pharmacological characteristics of a metabatropic receptor mGluR1 in transfected CHO cells. Neuron *8*, 757-765.

Armstrong, D.E., Saper, C.B., Levey, A.I., Wainer, B.H., and Terry, R. (1983). Distribution of cholinergic neurones in rat brain: demonstrated by immunocytochemical localisation of choline acetyltransferase. J. Comp. Neurol. *216*, 53-68.

Atack, J.R., Wenk, G.L., Wagster, M.V., Kellar, K.J., Whitehouse, P.J., and Rapoport, S.I. (1989). Bilateral changes in neocortical 3H pirenzepine and 3H oxotremorine-M binding following unilateral lesions of the rat nucleus basalis magnocellularis: An autoradiographic study. Brain Res. *483*, 367-372.

Barbieri, L., Falasca, A.I., and Stirpe, F. (1984). Volkensin, the toxic lectin of Adenia volkensii (kilyambiti plant). FEBS Lett. *171*, 277-279.

Baron, B.M., Harrison, B.L., Miller, F.P., Mcdonald, I.A., Salituro, F.G., Schmidt, C.J., Sorensen, S.M., White, H.S., and Palfreyman, M.G. (1990). Activity of 5,7-dichlorokynurenic acid, a potent antagonist at the N-methyl-D-aspartate receptor-associated glycine binding site. Mol. Pharmacol. *38*, 554-561.

Barr, M.L. (1974). The human nervous system: An anatomical viewpoint (Maryland: Harper International).

Bashir, Z.I., Tam, B., and Collingridge, G.L. (1990). Activation of the glycine site in the NMDA receptor is necessary for the induction of LTP. Neurosci. Lett. *108*, 261-266.

Battig, K. (1970). The effect of pre- and post-trial application of nicotine on the 12 problems of Hebb-Williams test in the rat. Psychopharmacology *18*, 68-76.

Baughman, R.W. and Gilbert, C.D. (1981). Aspartate and glutamate as possible neurotransmitters in the visual cortex. J. Neurosci. *1*, 427-439.

Baumgarten, H.G. and Lachenmayer, L. (1972). 5,7-dihydroxytryptamine: Improvement in chemical lesioning of indoleamine neurones in mammalian brain. Z. Zellforsch. Mikrosk. *135*, 399-414.

Baumgold, J. (1992). Muscarinic receptor-mediated stimulation of adenylyl cyclase. Trends Pharmacol. Sci. *13*, 339-340.

Bayer, S.A. (1985). Hippocampal region. In The rat nervous system. Volume 1 Forebrain and midbrain. G. Paxinos, ed. (London: Academic press),

Beck, S.G. and Choi, K.C. (1991). 5-hydroxytryptamine hyperpolarizes CA3 hippocampal pyramidal cells through an increase in potassium conductance. Neurosci. Lett. *133*, 93-96.

Becker, R.E. (1991). Therapy of the cognitive deficit in Alzheimer's disease. In Cholinergic basis for Alzheimer therapy. R.E. Becker and E. Giacobini, eds. (Boston: Birkhauser), pp. 1-22.

Beckstead, R.M. (1978). Afferent connections of the entorhinal area in the rat as demonstrated by retrograde labelling with horseradish peroxidase. Brain Res. *152*, 249-264.

Beckstead, R.M. (1979). An autoradiographic examination of cortical and subcortical projections of the mediodorsal-projection (prefrontal) cortex in the rat. J. Comp. Neurol. *184*, 43-62.

Beer, M.S., Middlemiss, D.N., and McAllister, G. (1993). 5-HT_1-like receptors: six down and still counting. Trends Pharmacol. Sci. *14*, 228-231.

Bekenstein, J.W., Bennet, J.P., Wooten, G.F., and Lothman, E.W. (1990). Autoradiographic evidence that NMDA receptor-coupled channels are located postsynaptically in the perforant path-dentate granule cell system of the rat hippocampal formation. Brain Res. *514*, 334-342.

Berlan, M., Montastruc, J-L., and Lafontan, M. (1992). Pharmacological prospects for α_2 adrenoceptor antagonist therapy. Trends Pharmacol. Sci. *13*, 277-286.

Bigl, V., Woolf, N.J., and Butcher, L.L. (1982). Cholinergic projections from the basal forebrain to frontal parietal, temporal, occipital and cingulate cortices: A combined fluorescent tracer and acetylcholinesterase analysis. Brain Res. Bull. *8*, 727-749.

Bjork, L., Cornfield, L.J., Nelson, D.L., Hillver, S.E., Anden, N.E., Lewander, T., and Hacksell, U. (1991). Pharmacology of the novel 5-hydroxytryptamine 1A receptor antagonist (S)-5-fluoro-8-hydroxy-2-(dipropylamino)tetralin: inhibition of (R)-8-hydroxy-2-(dipropylamino)tetralin-induced effects. J. Pharmacol. Exp. Ther. *258*, 58-65.

Blackstad, T.W. and Kjaerheim, A. (1961). Special axo-dendritic synapses in the hippocampal cortex. Electron and light microscopic studies on the layer of mossy fibres. J. Comp. Neurol. *117*, 133-159.

Blendy, J.A., Perry, D.C., Pabreza, L.A., and Kellar, K.J. (1991). Electroconvulsive shock increases alpha 1b but not alpha 1a binding sites in rat cerebral cortex. J. Neurochem. *57*, 1548-1555.

Blessed, G., Tomlinson, B.E., and Roth, M. (1968). The association between quantitative measures of dementia and senile changes in the cerebral grey matter of elderly subjects. Br. J. Psychiat. *144*, 797-811.

Blier, P., Lista, A., and De Montigny, C. (1993). Differential properties of pre- and postsynaptic 5-HT_{1A} receptors in the dorsal raphe and hippocampus: I. Effect of spiperone. J. Pharmacol. Exp. Ther. *265*, 7-15.

Bockaert, J., Fozard, J.R., Dumuis, A., and Clarke, D.E. (1992). The 5-HT_4 receptor: a place in the sun. Trends Pharmacol. Sci. *13*, 141-144.

Bogdanovic, N., Islam, A., Nilsson, L., Bergstrom, L., Winblad, B., and Adem, A. (1993). Effects of nucleus basalis lesion on muscarinic receptor subtypes. Exp. Brain Res. *97*, 225-232.

Bondareff, W., Mountjoy, C.Q., and Roth, M. (1981). Selective loss of neurones of origin of adrenergic projection to cerebral cortex (nucleus locus coeruleus) in senile dementia. Lancet *i*, 783-784.

Bonner, T.I., Buckley, N.J., Young, A.C., and Brann, M.R. (1987). Identification of a family of muscarinic acetylcholine receptors genes. Science *237*, 527-532.

Bonner, T.I., Young, A.C., Brann, M.R., and Buckley, N.J. (1988). Cloning and expression of the human and rat M5 muscarinic acetylcholine receptor gene. Neuron *1*, 403-410.

Bowen, D.M., Goodhardt, M.J., Strong, A.J., Smith, C.B., White, P., Branston, N.M., Symon, L., and Davison, A.N. (1976a). Biochemical indices of brain structure, function and "hypoxia" in cortex from baboons with middle cerebral artery occlusion. Brain Res. *117*, 503-507.

Bowen, D.M., Smith, C.B., White, P., and Davison, A.N. (1976b). Neurotransmitter-related enzymes and indices of hypoxia in senile dementia and other abiotrophies. Brain *99*, 459-496.

Bowen, D.M., Benton, J.S., Spillane, J.A., Smith, C.C.T., and Allen, S.J. (1982a). Choline acetyltransferase activity and histopathology of frontal neocortex from biopsies of demented patients. J. Neurol. Sci. *57*, 191-202.

Bowen, D.M., Sims, N.R., Lee, K.A., and Marek, K.L. (1982b). Acetylcholine synthesis and glucose oxidation are preserved in human brain obtained shortly after death. Neurosci. Lett. *31*, 195-199.

Bowen, D.M., Allen, S.J., Benton, J.S., Goodhardt, M.J., Haan, E.A., Palmer, A.M., Sims, N.R., Smith, C.C.T., Spillane, J.A., Esiri, M.M., Neary, D., Snowden, J.S., Wilcock, G.K., and Davison, A.N. (1983). Biochemical assessment of serotonergic and cholinergic dysfunction and cerebral atrophy in Alzheimer's disease. J. Neurochem. *41*, 266-272.

Bowen, D.M., Najlerahim, A., Procter, A.W., Francis, P.T., and Murphy, E. (1989). Circumscribed changes of the cerebral cortex in neuropsychiatric disorders of later life. Proc. Natl. Acad. Sci. USA. *86*, 9504-9508.

Bowen, D.M. (1990). Treatment of Alzheimer's disease: Molecular pathology versus neurotransmitter-based therapy. Br. J. Psychiat. *157*, 327-330.

Bowen, D.M., Francis, P.T., Chessell, I.P., Webster, M-T., Procter, A.W., Chen, C., Qume, M., Neary, D., Cross, A.J., and Green, A.R. (1993a). Alzheimer's Disease: Is the improvement of cholinergic transmission the correct strategy? In Alzheimer's Disease: Clinical and treatment aspects. N. Cutler, C.G. Gottfries, and K. Siegfried, eds. (Chichester: John Wiley),

Bowen, D.M., Francis, P.T., Pangalos, M.N., and Chessell, I.P. (1993b). Neurotransmitter receptors of rat cortical pyramidal neurones: implications for in vivo imaging and therapy. J. Reprod. Fert. *46 (Suppl)*, 131-143.

Bowen, D.M., Francis, P.T., Chessell, I.P., and Webster, M-T. (1994). Neurotransmission - the link integrating Alzheimer research? Trends. Neurosci. *17*, 149-150.

Bowery, N.G., Hill, D.R., Hudson, A.L., Doble, A., Middlemiss, D.N., Shaw, J., and Turnbull, M.J. (1980). (-) Baclofen decreases neurotransmitter release in the mammalian CNS by an action at a novel GABA receptor. Nature *283*, 92-94.

Bowery, N.G., Hudson, A.L., and Price, G.W. (1987). $GABA_A$ and $GABA_B$ receptor site distribution in the rat central nervous system. Neuroscience *20*, 365-383.

Braak, H. and Braak, E. (1985). On areas of transition between entorhinal allocortex and temporal isocortex in the human brain. Normal morphology and lamina-specific pathology in Alzheimer's disease. Acta Neuropathol. *68*, 325-332.

Braak, H. and Braak, E. (1991). Neuropathological stageing of Alzheimer-related changes. Acta Neuropathol. *82*, 239-259.

Bradley, P.B., Engel, G., Fenuik, W., Fozard, J.R., Humphrey, P.P.A., Middlemiss, D.N., Mylecharane, E.J., Richardson, B.P., and Saxena, P.R.

(1986). Proposals for the classification and nomenclature of functional receptors for 5-hydroxytryptamine. Neuropharmacology *25*, 563-576.

Branchek, T., Adham, N., Macchi, M., Kao, H.T., and Hartig, P.R. (1990). [^{3}H] DOB and [^{3}H] ketanserin label two affinity sites of the cloned human 5-hydroxytryptamine2 receptor. Mol. Pharmacol. *38*, 604-609.

Brann, M.R., Buckley, N.J., and Bonner, T.I. (1988). The striatum and cerebral cortex express different muscarinic receptor mRNAa. FEBS Lett. *230*, 90-94.

Bravo, H. and Karten, H.J. (1992). Pyramidal neurons of the rat cerebral cortex, immunoreactive to nicotinic acetylcholine receptors, project mainly to subcortical targets. J. Comp. Neurol. *320*, 62-68.

Brion, J-P., Smith, C., Couck, A-M., Gallo, J-M., and Anderton, B.H. (1993). Developmental changes in tau phosphorylation- fetal tau is transiently phosphorylated in a manner similar to paired helical filament tau characteristic of Alzheimer's disease. J. Neurochem. *61*, 2071-2080.

Brun, A. (1983). An overview of light and electron microscopic changes. In Alzheimer's disease: the standard reference. B. Reisberg, ed. (New York: Free Press), pp. 37-47.

Buckley, N.J. and Burnstock, G. (1986). Autoradiographic localisation of peripheral M1 muscarinic receptors using 3H pirenzepine. Brain Res. *375*, 83-91.

Buckley, N.J., Bonner, T.I., and Brann, M.R. (1988). Localization of a family of muscarinic receptor mRNAs in rat brain. J. Neurosci. *8*, 4646-4652.

Buckley, N.J., Bonner, T.I., Buckley, C.M., and Brann, M.R. (1989). Antagonist binding properties of five cloned muscarinic receptors expressed in CHO-K1 cells. Mol. Pharmacol. *35*, 469-476.

Butcher, L.L. (1978). Recent advances in histochemical techniques for the study of central cholinergic mechanisms. In Cholinergic mechanisms and psychopharmacology. J. Jenden, ed. (New York: Plenum), pp. 93-124.

Buxbaum, J.D., Koo, E.H., and Greengard, P. (1993). Protein phosphorylation inhibits production of Alzheimer amyloid ß/A4 peptide. Proc. Natl. Acad. Sci. USA. *90*, 9195-9198.

Bylund, D.B. (1988). Subtypes of alpha2-adrenoceptors: pharmacological and molecular biological evidence converge. Trends Pharmacol. Sci. *9*, 356-361.

Byrne, E.J. and Arie, T. (1994). Tetrahydroaminoacridine and Alzheimer's diease. Br. Med. J. *308*, 868-869.

Cai, N. and Erdo, S.L. (1992). The effects of kainate and the glutamate agonist, AMPA, are not separable in rat neocortical cultures. Neurosci. Lett. *141*, 57-60.

Cajal, S.R (1909). Histologie du systeme nerveux de l'homme et des vertebres (Paris: Maloine).

Cameron, D.L. and Williams, J.T. (1993). Dopamine D1 receptors facilitate transmitter release. Nature *366*, 344-347.

Caporaso, G.L., Gandy, S.E., Buxbaum, J.D., Ramabhadran, T.V., and Greengard, P. (1992). Protein phosphorylation regulates secretion of Alzheimer ß/A4 amyloid precursor protein. Proc. Natl. Acad. Sci. USA. *89*, 3055-3059.

Carli, M. and Samanin, R. (1992). 8-hydroxy-2-(di-n-propylamino)tetralin impairs spatial learning in a water maze: role of postsynaptic 5-HT_{1A} receptors. Br. J. Pharmacol. *105*, 720-726.

Carpenter, M.B. and Sutin, J. (1983). Human neuroanatomy (Baltimore: Williams & Wilkins).

Chalmers, D.T., Dewar, D., Graham, D.I., Brooks, D.N., and McCulloch, J. (1990). Differential alterations of cortical glutamatergic binding sites in senile dementia of the Alzheimer type. Proc. Natl. Acad. Sci. USA. *87*, 1352-1356.

Chalmers, D.T. and Watson, S.J. (1991). Comparative distribution of 5-HT1A receptor mRNA and 5-HT1A binding in rat brain - a combined in situ hybridisation / in vitro autroradiographic study. Brain Res. *561*, 51-60.

Chang, H.C. and Gaddum, J.H. (1933). Choline esters in tissue extracts. J. Physiol. *79*, 255-285.

Chang, H.T., Wilson, C.J., and Kitai, S.T. (1981). Single neostriatal efferent axons in the globus pallidus: A light and electron microscopic study. Science *213*, 915-918.

Chang, H.T., Wilson, C.J., and Kitai, S.T. (1982). A Golgi study of rat neostriatal neurones: Light microscopic analysis. J. Comp. Neurol. *208*, 107-126.

Chawluk, J.B., Alavi, A., Dann, R., Hurtig, H.I., Bais, S., Kushner, M.J., Zimmerman, R.A., and Reivich, M.J. (1987). Positron emission tomography in aging and dementias: effect of cerebral atrophy. J. Nucl. Med. *28*, 431-437.

Chen, C.P.L-H., Alder, J.T., Hope, R.A., Francis, P.T., McDonald, B., Esiri, M.M., and Bowen, D.M. (1994). The 5-hydroxytryptaminergic system in Alzheimer's Disease exhibits plasticity and is affected by neuroleptic medication. Br. J. Pharmacol. (in press)

Cheng, A.V.T., Ferrier, I.N., Morris, C.M., Jabeen, S., Sahgal, A., McKeith, I.G., Edwardson, J.A., Perry, R.H., and Perry, E.K. (1991). Cortical serotonin-S2 receptor binding in Lewy body dementia, Alzheimer's and Parkinson's disease. J. Neurol. Sci. *106*, 50-55.

Choi, D.W. (1991). Excitotoxicity. In Excitatory amino acid antagonists. B.S. Meldrum, ed. (Oxford: Blackwell Scientific Publications), pp. 216-236.

Chu, D.C.M., Penney, J.B., and Young, A.B. (1987). Cortical $GABA_B$ and $GABA_A$ receptors in Alzheimer's disease: A quantitative autoradiographic study. Neurology *37*, 1454-1459.

Chu, D.C.M., Albin, R.L., Young, A.B., and Penney, J.B. (1990). Distribution and kinetics of $GABA_B$ binding sites in rat central nervous system: A quantitative autoradiographic study. Neuroscience *34*, 341-357.

Cimino, M., Marini, P., Colombo, S., Cattabeni, F., and Meldolesi, J. (1992). [^{3}H]-CGP 39653 mapping of glutamatergic N-methyl-D-aspartate receptors in the brain of aged rats. Neurosci. Res. Com. *12*, 31-39.

Clarke, N.A., Procter, A.W., Webster, M-T., Francis, P.T., Hodgkiss, A.D., and Bowen, D.M. (1993a). Effect of Li^+ therapy and site of origin on the cerebrospinal fluid ß-amyloid precursor protein derivatives. Biochem. Soc. Trans. *21*, 241S.

Clarke, N.A., Webster, M-T., Francis, P.T., Procter, A.W., Hodgkiss, A.D., and Bowen, D.M. (1993b). ß-Amyloid precursor protein-like immunoreactivity can be altered in humans by drugs affecting neurotransmitter function. Neurodegeneration *2*, 243-248.

Clarke, P.B.S., Schwartz, R.D., Paul, S.M., Pert, C.B., and Pert, A. (1985). Nicotinic binding in rat brain: Autoradiographic comparison of [^{3}H] acetylcholine, [^{3}H] nicotine, and [^{125}I]-alpha-bungarotoxin. J. Neurosci. *5*, 1307-1315.

Claro, E., Garcia, E., and Picotose, F. (1989). Carbachol and histamine stimulation of guanine-nucleotide dependent phosphoinositide hydrolysis in rat brain cortical membranes. Biochem. J. *261*, 29-35.

Cleveland, D.W., Hwo, S.Y., Kirschner, M.W. (1977). Purification of tau, a microtubule associated protein that induces assembly of microtubules from purified tubulin. J. Mol. Biol. *116*, 207-225.

Cole, A.E. and Nicoll, R.A. (1984). The pharmacology of cholinergic excitatory responses in hippocampal pyramidal cells. Brain Res. *305*, 283-290.

Cole, G., Dobkins, K.R., and Hansen, L.A. (1988). Decreased levels of protein kinase C in Alzheimer brain. Brain Res. *452*, 165-174.

Collerton, D. (1986). Cholinergic function and intelectual decline in Alzheimer's disease. Neuroscience *19*, 1-28.

Collingridge, G.L., Kehl, S.J., and McLennan, H. (1983). Excitatory amino acids in synaptic transmission in the Schaffer collateral-commissural pathway of the rat hippocampus. J. Physiol. -London *334*, 33-46.

Collingridge, G.L. (1987). NMDA receptors - their role in long-term potentiation. Trends. Neurosci. *10*, 288-293.

Collingridge, G.L. and Singer, W. (1990). Excitatory amino acid receptors and synaptic plasticity. In TIPS Special Report: Pharamacology of excitatory amino acids. G. Collingridge and D. Lodge, eds. (Cambridge: Elsevier), pp. 42-53.

Collis, M.G. and Hourani, S.M.O. (1993). Adenosine receptor subtypes. Trends Pharmacol. Sci. *14*, 360-366.

Contestabile, A., Fasolo, A., Virgli, M., Migani, P., Villani, L., and Stirpe, F. (1990). Anatomical and neurochemical evidence for suicide transport of a toxic lectin, volkensin, injected in the rat dorsal hippocampus. Brain Res. *537*, 279-286.

Contestabile, A. and Stirpe, F. (1993). Ribosome-inactivating proteins from plants as agents for suicide transport and immunolesioning in the nervous system. Eur. J. Neurosci. *5*, 1292-1301.

Conti, F., Fabri, M., and Manzoni, T. (1988). Glutamate-positive corticocortical neurons in the somatic sensory areas I and II of cats. J. Neurosci. *8*, 2948-2960.

Corder, E.H., Saunder, A.M., Strittmatter, W.J., Schmechel, D.E., Gaskell, P.C., Small, G.W., Roses, A.D., Haines, J.L., and Pericak-Vance, M.A. (1993). Gene dose of apolipoprotein E type 4 allele and the risk of Alzheimer disease in late onset families. Science *261*, 921-923.

Cotman, C.W. and Pike, C.J. (1994). Beta amyloid and its contributions to neurodegeneration in Alzheimer disease. In Alzheimer Disease. R.D. Terry, R. Katzman, and K.L. Bick, eds. (New York: Raven Press), pp. 305-315.

Cowburn, R.F., Hardy, J.A., Roberts, P.J., and Briggs, R. (1988). Regional distribution of pre- and postsynaptic glutamatergic function in Alzheimer's disease. Brain Res. *452*, 403-407.

Cowburn, R.F., Hardy, J.A., and Roberts, P.J. (1989). Neurotransmitter deficits in Alzheimer's disease. In In Alzheimer's disease towards an understanding of the aetiology and pathogenesis. D.C. Davies, ed. (London: Libby), pp. 9-32.

Cox, J.A., Lysko, P.G., and Henneberry, R.C. (1989). Excitatory amino acid neurotoxicity at the *N*-methyl-D-aspartate receptor in cultured neurons: role of the voltage-dependent magnesium block. Brain Res. *499*, 267-272.

Crino, P.B., Vogt, B.A., Volicer, L., and Wiley, R.G. (1990). Cellular localization of serotonin 1A, 1B and uptake sites in cingulate cortex in the rat. J. Pharmacol. Exp. Ther. *252*, 651-657.

Cross, A.J., Crow, T.J., Perry, E.K., Perry, R.H., Blessed, G., and Tomlinson, B.E. (1981). Reduced dopamine-beta hydroxylase activity in Alzheimer's disease. Br. Med. J. *282*, 93-94.

Cross, A.J., Crow, T.J., Johnson, J.A., Joseph, M.H., Perry, E.K., Perry, R.H., Blessed, G., and Tomlinson, B.E. (1983). Monoamine metabolism in senile dementia of Alzheimer type. J. Neurol. Sci. *60*, 383-392.

Cross, A.J., Crow, T.J., Ferrier, I.N., Johnson, J.A., Bloom, S.R., and Corsellis, J.A.N. (1984a). Serotonin receptor changes in dementia of the Alzheimer's type. J. Neurochem. *43*, 1574-1581.

Cross, A.J., Crow, T.J., Johnson, J.A., Perry, E.K., Perry, R.H., Blessed, G., and Tomlinson, B.E. (1984b). Studies on neurotransmitter receptor systems in neocortex and hippocampus in senile dementia of the Alzheimer-type. J. Neurol. Sci. *64*, 109-117.

Cross, A.J., Skan, W.J., Slater, P., Mitchell, I.J., and Crossman, A.R. (1987). Autoradiographic analysis of [^{3}H] kainic acid binding in primate brain. J. Rec. Res. *7*, 775-797.

Cross, A.J., Slater, P., Perry, E.K., and Perry, R.H. (1988). An autoradiographic analysis of serotonin receptors in human temporal cortex: Changes in Alzheimer-type dementia. Neurochem. Int. *13*, 89-96.

Cross, A.J. and Slater, P. (1989). High affinity serotonin binding sites in human brain: a comparison of cerebral cortex and basal ganglia. J. Neural Transm. *76*, 211-219.

Curet, O. and De Montigny, C. (1988). Electrophysiological characterization of adrenoceptors in the rat dorsal hippocampus. I. Receptors mediating the effect of microiontophoretically applied norepinephrine. Brain Res. *475*, 35-46.

Curtis, D.R. and Watkins, J.C. (1961). The chemical excitation of spinal neurones by certain amino acids. J. Physiol. *166*, 94-188.

Cutler, N.R., Haxby, J.V., Duara, R., Grady, C.L., Kay, A.D., Kessler, R.M., Sundram, M., and Rapoport, S. (1985). Clinical history, brain metabolism and neuropsychological function in Alzheimer's disease. Ann. Neurol. *18*, 298-309.

Dale, H.H. (1938). Acetylcholine as a neurotransmitter. J. Mt. Sinai Hosp. *4*, 401-429.

Daly, J.W., Buttslamb, P., and Padgett, W. (1983). Subclasses of adenosine receptors in the central nervous system-interaction with caffeine and related methylxanthines. Cell Mol. Neurobiol. *3*, 69-80.

Davies, P. and Maloney, A.J.F. (1976). Selective loss of central cholinergic neurones in Alzheimer's disease. Lancet *ii*, 1403.

Davies, P. (1979). Neurotransmitter-related enzymes in senile dementia of the Alzheimer type. Brain Res. *171*, 319-327.

Davis, D.R., Brion, J-P., Couck, A-M., Gallo, J-M., Hanger, D.P., Ladhani, K., Lewis, C., Miller, C.C.J., Rupniak, T., Smith, C., and Anderton, B.H. (1994). Glutamate and cochicine cause dephosphorylation of the microtubule associated protein tau and a change in perikaryal tau-immunoreactivity in rat cortical neurones in primary culture. Brain Res. Assoc. *11*, 38.(Abstract)

Davis, G.C., Williams, A.C., Markey, S.P., Ebert, M.H., Caine, E.D., Reichert, C.M., and Kopin, I.J. (1979). Chronic parkinsonism secondary to intravenous injection of meperidine analogues. Psychiatr. Res. *1*, 249-254.

Davis, K.L., Thal, L.J., Gamzu, E.R, Davis, C.S., Woolson, R.F., Gracon, S.I., Drachman, D.A., Schneider, L.S., Whitehouse, P.J., Hoover, T.M., Morris, J.C., Kawas, C.H., Knopman, D.S., Earl, N.L., Kumar, V., and Doody, R.S. (1992). A doule-blind, placebo-controlled multicenter study of tacrine for Alzheimer's disease. N. Engl. J. Med. *327*, 1253-1259.

Dawson, G.R., Heyes, C.M., and Iversen, S.D. (1992). Pharmacological mechanisms and animal models of cognition. Behav. Pharamacol. *3*, 285-297.

Dawson, V.L., Hunt, M.E., and Wamsley, J.K. (1991). Alterations in cortical muscarinic receptors following cholinotoxin (AF64A) lesion of the rat nucleus basalis magnocellularis. Neurobiol. Aging *13*, 25-32.

De Montigny, C. and Aghajanian, G.K. (1977). Preferential action of 5-methoxytryptamine and 5-methoxydimethytryptamine on presynpatic serotonin receptor: A comparitive iontophoretic study with LSD and serotonin. Neuropharmacology *16*, 811-818.

Deckert, J. and Jorgenson, M.B. (1988). Evidence for pre- and post-synaptic localisation of adenosine A_1 receptors in the CA1 region of rat hippocampus: a quantitative autoradiographic study. Brain Res. *446*, 161-164.

DeFelipe, J. and Jones, E.G. (1988). Cajal on the cerebral cortex: An annotated translation of the complete writings (Oxford: Oxford University Press).

Dekker, A.J.A.M., Connor, D.J., and Thal, L.J. (1990). The role of cholinergic projections from the nucleus basalis in memory. Neurosci. Biobehav. Rev. *15*, 299-317.

DeKosky, S. and Scheff, S.W. (1990). Synapse loss in frontal cortex biopsies in Alzheimer's disease: correlation with cognitive severity. Ann. Neurol. *27*, 457-464.

Derkach, V., Suprenant, A., and North, R.A. (1989). 5-HT3 receptors are membrane ion channels. Nature *339*, 706-709.

Desmond, N.L. and Levy, W.B. (1982). A quantitative anatomical study of the granule cell dendritic fields of the rat dentate gyrus using a novel probabalistic model. J. Comp. Neurol. *212*, 131-145.

Dewar, D., Graham, D.I., and McCulloch, J. (1990a). 5-HT2 receptors in dementia of Alzheimer type: a quantitative autoradiographic study of frontal cortex and hippocampus. J. Neural Transm. P-D Sect. *2*, 129-137.

Dewar, D., Lima, L., and Reader, T.A. (1990b). 3H ketanserin binds to non-5-HT2 sites in rabbit cerebral cortex and neostriatum. Neurochem. Res. *15*, 507-514.

Dewar, D., Chalmers, D.T., Graham, D.I., and McCulloch, J. (1991). Glutamate metabotropic and AMPA binding sites are reduced in Alzheimer's disease: an autoradiographic study of the hippocampus. Brain Res. *553*, 58-64.

Dewey, S.L., Volkow, N.D., Logan, J., MacGregor, R.R., Fowler, J.S., Schlyer, D.J., and Bendriem, B. (1990). Age related decreases in muscarinic cholinergic receptor binding in the human brain measured with positron emission tomography (PET). J. Neurosci. Res. *27*, 569-575.

Dickenson, A.H. (1989). 5-Hydroxytryptamine. In Neurotransmitters, drugs and disease. R.A. Webster and C.C. Jordan, eds. (Oxford: Blackwell), pp. 143-155.

Diedrich, J.F., Minnigan, H., Carp, R.I., Whitaker, J.N., Race, R., Frey, W., and Haase, A.T. (1991). Neuropathological changes in scrapie and Alzheimer's disease are associated with increased with increased apolipoprotein E and cathepsin D in astrocytes. J. Virol. *65*, 4759-4768.

Dijk, S., Francis, P.T., and Bowen, D.M. (1994a). NMDA-induced glutamate release from rat cortical pyramidal neurones is potentiated by a 5-HT_{1A} antagonist. Br. J. Pharmacol. (in press)

Dijk, S., Francis, P.T., Stratmann, G.C., Smith, M.A., and Bowen, D.M. (1994b). An in vivo study on factors affecting amino acid and APP release from corticostriatal neurones, using push-pull and microdialysis technology. Soc. Neurosci. Abs. (in press)

Donoghue, J.P., Kerman, K.L., and Ebner, F.F. (1979). Evidence for two organisational plans within the somatic sensory-motor cortex of the rat. J. Comp. Neurol. *183*, 647-664.

Donoghue, J.P., Wenthold, R.J., and Altschuler, R.A. (1985). Localisation of glutaminase-like and aspartate aminotransferase-like immunoreactivity in neurons of cerebral neocortex. J. Neurosci. *5*, 2597-2608.

Donoghue, J.P. and Kitai, S.T. (1981). A collateral pathway to the neostriatum from corticofugal neurones of the rat sensory-motor cortex. An intracellular study. J. Comp. Neurol. *201*, 1-13.

Donoghue, J.P. and Wise, S.P. (1982). The motor cortex of the rat: Cytoarchitecture and microstimulation mapping. J. Comp. Neurol. *212*, 76-88.

Drachman, D.A. and Leavitt, J. (1974). Human memory and the cholinergic system. Arch. Neurol. *30*, 113-121.

Drejer, J., Benveniste, H., Diemer, N.H., and Schousboe, A. (1985). Cellular origin of ischaemia-induced glutamate release from brain tissue *in vivo* and *in vitro*. J. Neurochem. *45*, 145-151.

Drewes, G., Lichtenburg-Kraag, B., and Doring, F. (1992). Mitogen activated (MAP) kinase transforms tau protein into an Alzheimer-like state. EMBO J. *6*, 2131-2138.

Duara, R., Grady, C.L., Haxby, J., Sundaram, M., Cutler, N.R., Heston, L., Moore, A., Schlageter, N.L., Larson, S., and Rapoport, S.I. (1986). Positron emission tomography in Alzheimer's disease. Neurology *36*, 879-887.

Dudai, Y. (1989). The Neurobiology of Memory (Oxford: Oxford University Press).

Dunnett, S.B., Everitt, B.J., and Robbins, T.W. (1991). The basal forebrain-cortical cholinergic system: Interpreting the functional consequences of excitotoxic lesions. Trends. Neurosci. *14 (11)*, 494-501.

Dutar, P. and Nicoll, R.A. (1988). Classification of muscarinic responses in hippocampus in terms of receptor subtypes and second messenger systems: electrophysiological studies in vitro. J. Neurosci. *8*, 4214-4224.

Eckenstein, F. and Baughman, R.W. (1984). Two types of cholinergic innervation in cortex, one co-localised with vasoactive intestinal polypeptide. Nature *309*, 153-155.

Eckenstein, F. and Sofroniew, M.V. (1983). Identification of central cholinergic neurones containing both choline acetyltransferase and acetylcholinesterase and of central neurones containing only acetylcholinesterase. J. Neurosci. *3*, 2286-2291.

Egebjerg, J., Bettler, B., Hermans-Borgmeyer, I., and Heinemann, S. (1991). Cloning of a cDNA for a glutamate receptor activated by kainate but not AMPA. Nature *351*, 745-748.

Ellison, D.W., Beal, M.F., Mazurek, M.F., Bird, E.D., and Martin, J.B. (1986). A postmortem study of amino acid neurotransmitters in Alzheimer's disease. Ann. Neurol. *20*, 616-621.

Esch, F.S., Keim, P.S., Beattie, E.C., Blacher, R.W., Culwell, A.R., Oltersdorf, T., McClure, D., and Ward, P.J. (1990). Cleavage of amyloid ß peptide during constitutive processing of its precursor. Science *248*, 1122-1124.

Esiri, M.M., Pearson, R.C.A., and Powell, T.P.S. (1986). The cortex of the primary auditory area in Alzheimer's disease. Brain Res. *366*, 385-387.

Esiri, M.M., Pearson, R.C.A., Steele, J.E., Bowen, D.M., and Powell, T.P.S. (1990). A quantitative study of the neurofibrillary tangles and the choline acetyltransferase activity in the cerebral cortex and the amygdala in Alzheimer's disease. J. Neurol. Neurosurg. Psychiatry *53*, 161-165.

Esquirol, J.E.D. (1838). Des maladies mentales (Paris: Balliere).

Essman, W.B. (1973). Age dependent effects of 5-hydroxytryptamine upon memory consolidation and cerebral protein synthesis. Pharmacol. Biochem. Behav. *1*, 7-14.

Fagg, G.E. (1987). Phencyclidine and related drugs bind to the activated N-methyl-D-aspartate receptor- channel complex in rat brain membranes. Neurosci. Lett. *76*, 221-227.

Fagg, G.E. and Foster, A.C. (1983). Amino acid neurotransmitters and their pathways in the mammalian central nervous system. Neuroscience *9*, 701-719.

Fagg, G.E. and Massieu, L. (1991). Excitatory amino acids receptor sub-types. In Excitatory amino acid antagonists. B. Meldrum, ed. (Oxford: Blackwell Scientific), pp. 39-63.

Fallon, J.H. and Moore, R.Y. (1979). Raphe nuclei in the rat: Efferent projections to forebrain studied using the HRP-retrograde transport method. Soc. Neurosci. Abs. *4*, 272.

Fastbom, J. and Fredholm, B.B. (1990). Regional differences in the effect of guanine nucleotides on agonist and antagonist binding to adenosine A_1 receptors in rat brain, as revealed by autoradiography. Neuroscience *34*, 759-769.

Faull, R.L.M. and Mehler, W.R. (1985). Thalamus. In The rat nervous system. G. Paxinos, ed. (London: Academic Press), pp. 129-168.

Felder, C.C., Ma, A.L., Briley, E.M., and Axelrod, J. (1993). Muscarinic acetylcholine receptor subtypes associated with release of Alzheimer amyloid precursor derivatives activate multiple signal transduction pathways. In Alzheimer's disease. R.M. Nitsch, J.H. Growdon, S. Corkin, and R.J. Wurtman, eds. (New York: New York Academy of Sciences), pp. 15-18.

Feldman, M.L. (1984). Morphology of the pyramidal neuron. In Cerebral cortex: Volume 1, Cellular components of the cerebral cortex. A. Peters and E.G. Jones, eds. (New York: Plenum Press), pp. 123-200.

Fischer, B.O., Ottersen, O.P., and Storm-Mathisen, J. (1991). Axonal transport of D-[^{3}H]-aspartate in the claustrocortical projection. Neuroscience *7 (Suppl)*, S69.

Fisher, A., Gurwitz, D., Barak, D., Haring, R., Karton, I., Brandeis, R., Pittel, Z., Marciano, D., Meshulam, H., Vogel, Z., and Heldman, E. (1992). Rigid analogues of acetylcholine can be M1 selective agonist: implications for a rational treatment strategy in Alzheimer's disease. Bioorg. Med. Chem. Lett. *2*, 839-844.

Fisher, R.S., Buchwald, N.A., Hull, C.D., and Levine, M.S. (1988). GABA-ergic basal forbrain neurones project to the neocortex: The localization of glutamic acid decarboxylase and choline acetyl transferase in feline corticopetal neurones. J. Comp. Neurol. *272*, 489-502.

Fisher, S.K. and Agranoff, B.W. (1987). Receptor activation and inositol lipid hydrolysis in neuronal tissues. J. Neurochem. *48*, 999-1017.

Fletcher, A., Bill, D.J., Brammer, N.T., Cliffe, I.A., Forster, Y., and Lloyd, G.K. (1991). WAY100135: A novel and highly selective 5-HT_{1A} receptor antagonist. Soc. Neurosci. Abs. *17*, 92.(Abstract)

Flynn, D.D., Weinstein, D.A., and Mash, D.C. (1991). Loss of high-affinity agonist binding to M1 muscarinic receptors in Alzheimer's disease: implications for the failure of cholinergic replacement therapies. Ann. Neurol. *29*, 256-262.

Fonnum, F. (1970). Topographical and sub-cellular localisation of choline acetyltransferase in the rat hippocampal region. J. Neurochem. *17*, 1029-1037.

Fonnum, F. (1984). Glutamate: A neurotransmitter in mammalian brain. J. Neurochem. *42*, 1-11.

Fonnum, F. and Walaas, I. (1978). The effect of intrahippocampal kainic acid injections and surgical lesions on neurotransmitter in hippocampus and septum. J. Neurochem. *31*, 1173-1181.

Fosse, V.M. and Fonnum, F. (1987). Biochemical evidence for glutamate and/or aspartate as neurotransmitters in fibres from the visual cortex to the lateral posterior thalamic nucleus (Pulvinar) in rats. Brain Res. *400*, 219-224.

Foster, A.C. (1991). Channel blocking drugs for the NMDA receptor. In Excitatory amino acid antagonists. B. Meldrum, ed. (Oxford: Blackwell Scientific), pp. 164-179.

Foster, A.C. and Wong, E.H.F. (1987). The novel anticonvulsant MK-801 binds to the activated state of the N-methyl-D-aspartate receptor in rat brain. Br. J. Pharmacol. *91*, 403-409.

Foster, N.L., Chase, T.N., Fedio, P., Patronas, N.J., Brooks, R.A., and DiChiro, G. (1983). Alzheimer's Disease: focal cortical changes shown in positron emission tomography. Neurology *33*, 961-965.

Foster, N.L. (1994). PET imaging. In Alzheimer Disease. R.D. Terry, R. Katzman, and K.L. Bick, eds. (New York: Raven Press), pp. 87-103.

Fowler, C.J., Cowburn, R.F., and O'Neill, C. (1992a). Brain signal transduction disturbances in neurodegenerative disorders. Cell. Sig. *4*, 1-9.

Fowler, C.J., O'Neill, C., Winblad, B., and Cowburn, R.F. (1992b). Neurotransmitter, receptor and signal transduction disturbances in Alzheimer's disease. Acta Neurol. Scand. Suppl. *139*, 59-62.

Francis, P.T., Palmer, A.M., Sims, N.R., Bowen, D.M., Davison, A.N., Esiri, M.M., Neary, D., Snowden, J.S., and Wilcock, G.K. (1985). Neurochemical studies of early-onset Alzheimer's disease. Possible influence on treatment. N. Engl. J. Med. *313*, 7-11.

Francis, P.T., Pangalos, M.N., and Bowen, D.M. (1992a). Animal and drug modelling for Alzheimer synaptic pathology. Prog. Neurobiol. *39*, 517-545.

Francis, P.T., Pangalos, M.N., Pearson, R.C.A., Middlemiss, D.N., Stratmann, G.C., and Bowen, D.M. (1992b). 5-HT_{1A} but not 5-HT_2 receptors are enriched on neocortical pyramidal neurones destroyed by intrastriatal volkensin. J. Pharmacol. Exp. Ther. *261*, 1273-1281.

Francis, P.T., Sims, N.R., Procter, A.W., and Bowen, D.M. (1993). Cortical pyramidal neurone loss may cause glutamatergic hypoactivity and cognitive impairment in Alzheimer's disease: investigative and therapeutic perspectives. J. Neurochem. *60*, 1589-1604.

Francis, P.T. and Bowen, D.M. (1989). Tacrine, a drug with therapeutic potential for dementia: post-mortem biochemical evidence. Can. J. Neurol. Sci. *16*, 504-510.

Fredholm, B.B., Jonzon, B., and Lindgren, E. (1983). Inhibition of noradrenaline release from hippocampal slices by a stable adenosine analogue. Acta Physiol. Scand. (suppl) *515*, 7-10.

Fredholm, B.B. and Dunwiddie, T.T. (1988). How does adenosine inhibit neurotransmitter release? Trends Pharmacol. Sci. *9*, 130-134.

Freund, R.K., Jungschaffer, D.A., Collins, A.C., and Wehner, J.M. (1988). Evidence for modulation of GABAergic transmission by nicotine. Brain Res. *453*, 215-220.

Frey, K.A. and Howland, M.M. (1992). Quantitative autoradiography of muscarinic cholinergic receptor binding in the rat brain: Distinction of receptor subtypes in antagonist competition assays. J. Pharmacol. Exp. Ther. *263*, 1391-1400.

Fukushima, D., Konishi, M., Maruyama, K., Miyamoto, T., Ishiura, S., and Suzuki, K. (1993). Activation of the secretory pathway leads to a decrease in the intracellular amyloidogenic fragments generated from the amyloid precursor protein. Biochem. Biophys. Res. Comm. *194*, 202-207.

Fulton, R.J., Blakey, D.C., Knowles, P.P., Uhr, J.W., Thorpe, P.E., and Vitetta, E.S. (1986). Purification of ricin A1, A2 and B chains and characterisation of their toxicity. J. Biol. Chem. *261*, 5314-5319.

Fuxe, K. (1965). Evidence for the existence of monoamine neurones in the central nervous system, IV Distribution of monoamine terminals in the central nervous system. Acta Physiol. Scand. (suppl) *64*, 37-85.

Fuxe, K., Roberts, P., and Schwarcz, R. (1984). Excitotoxins (London: MacMillan).

Gabuzda, D.H., Busciglio, J., and Yankner, B.A. (1993). Inhibition of beta-amyloid production by activation of protein kinase C. J. Neurochem. *61*, 2326-2329.

Gaddum, J.H. and Picarelli, Z.P. (1957). Two kinds of tryptamine receptor. Br. J. Pharmacol. *12*, 323-328.

Gahwiler, B.H. and Brown, D.A. (1985). $GABA_B$ receptor activated K^+ current in voltage clamped CA3 pyramidal cells in hippocampal cultures. Proc. Natl. Acad. Sci. USA. *82*, 1558-1562.

Garland, B.J. and Cross, P.S. (1982). Epidemiology and psychopathology in old age: Some implications for clinical studies. Psychiat. Clin. *5*, 11-26.

Garthwaite, G. and Garthwaite, J. (1988). Electron microscopic autoradiography of 3H D-aspartate uptake sites in mouse cerebellar slices shows poor labelling of mossy fibre terminals. Brain Res. *440*, 162-166.

Geary, W.A. and Wooten, G.F. (1983). Quantitative film autoradiography of opiate agonist and antagonist binding in rat brain. J. Pharmacol. Exp. Ther. *225*, 234-240.

Geddes, J.W. and Cotman, C.W. (1986). Plasticity in hippocampal excitatory amino acid receptors in Alzheimer's disease. Neurosci. Res. *3*, 672-678.

Geddes, J.W.., Chang-Chui, H., Cooper, S.M., Lott, I.T., and Cotman, C.W. (1986). Density and distribution of NMDA receptors in the human hippocampus in Alzheimer's disease. Brain Res. *399*, 156-161.

Giacobini, E. (1990). The cholinergic system in Alzheimer disease. Prog. Brain Res. *84*, 321-332.

Giacobini, E., Linville, D., Messamore, E., and Ogane, N. (1991). Toward a third generation of cholinesterase inhibitors. In Cholinergic basis for Alzheimer's therapy. R.E. Becker and E. Giacobini, eds. (Boston: Birkhauser), pp. 477-490.

Gibb, A.J. and Colquhoun, D. (1991). Glutamate activation of a single NMDA receptor channel produces a cluster of channel openings. Proc. R. Soc. Lond. (B) *243*, 39-45.

Girault, J.A., Barbeito, L., Spampinato, U., Gozlan, H., Glowinski, J., and Besson, M-J. (1986). *In vivo* release of endogenous amino acids from the rat striatum: further evidence for a role of glutamate and aspartate in corticostriatal neurotransmission. J. Neurochem. *47*, 98-106.

Glenner, G.G. (1979). Congophilic microangiopathy in the pathogenesis of Alzheimer's syndrome. Med. Hypotheses *5*, 1231-1236.

Glenner, G.G. and Wong, C.W. (1984). Initial report of the purification and characterization of a novel cerebrovascular amyloid protein. Biochem. Biophys. Res. Comm. *120*, 885-890.

Goate, A., Chartier-Harlin, M.C., Mullan, M., Brown, J., Crawford, F., Fidani, L., Giuffra, L., Haynes, A., Irving, N., James, L., Mant, R., Newton, P., Rooke, K., Roques, P., Talbot, C., Pericak-Vance, M., Roses, A., Williamson, R., Rossor, M., Owen, M., and Hardy, J. (1991). Segregation of a missense mutation in the amyloid precursor protein gene with familial Alzheimer's disease. Nature *349*, 704-706.

Goedert, M., Spillantini, M.G., Cairns, N.J., and Crowther, R.A. (1992). Tau proteins of Alzheimer paried helical filaments: Abnormal phosphorylation of all six brain isoforms. Neuron *8*, 159-168.

Goedert, M. (1993). Tau protein and the neurofibrillary pathology of Alzheimer's Disease. Trends. Neurosci. *16*, 460-465.

Golde, T.E., Estus, S., Younkin, L.H., Selkoe, D.J., and Younkin, S.G. (1992). Processing of the amyloid protein precursor to potentially amyloidogenic derivatives. Science *255*, 728-730.

Goldgaber, D., Lerman, M.I., McBridge, O.W., Saffiot, U., and Gajdusek, D.C. (1987). Characterization and chromosomal localisation of a cDNA encoding brain amyloid of Alzheimer's disease. Science *235*, 877-880.

Goldman, P.S. and Nauta, W.J.H. (1977). An intricately patterned prefronto-caudate projection in the rhesus monkey. J. Comp. Neurol. *171*, 369-386.

Goode, N., Hughes, K., Woodgett, J.R., and Parker, P.J. (1992). Differential regulation of glycogen synthase kinase-3 beta by protein kinase C isotypes. J. Biol. Chem. *267*, 16878-16882.

Goodman, R.R., Cooper, M.J., Gavish, M., and Snyder, S.H. (1982). Guanine nucleotide and cation regulation of the binding of [^{3}H]-cyclohexyladenosine and [^{3}H]-diethylphenylxantine to adenosine A_1 receptors in brain membranes. Mol. Pharmacol. *21*, 329-335.

Gottfries, C.G., Adolfsson, R., Aquilonius, S.M., Carlsson, A., Eckernas, S.-A., Nordberg, A., Oreland, L., Svennerholm, L., Wiberg, A., and Winblad, B. (1983). Biochemical changes in dementia disorders of Alzheimer type (AD/SDAT). Neurobiol. Aging *4*, 261-271.

Gottleib, D.I. and Cowan, W.M. (1973). Autoradiographic studies of the commisural and ipsilateral association connections of the hippocampus and dentate gyrus. I. The commisural connections. J. Comp. Neurol. *149*, 393-422.

Green, J.R., Halpern, L.M., and Van Niel, S. (1970). Choline acetylase and acetylcholinesterase changes in chronic isolated cerebral cortex of the cat. Life Sci. *9*, 481-488.

Greenamyre, J.T., Olson, J.M.M., Penney, J.B., and Young, A.B. (1985a). Autoradiographic characterisation of N-methyl-D-aspartate-, quisqualate- and kainate-sensitive glutamate binding sites. J. Pharmacol. Exp. Ther. *233*, 254-263.

Greenamyre, J.T., Penney, J.B., Damato, C.J., and Young, A.B. (1985b). Alterations in L-glutamate binding in Alzheimer's and Huntingdon's diseases. Science *227*, 1496-1499.

Greenamyre, J.T., Penney, J.B., D'Amato, C.J., and Young, A.B. (1987). Dementia of the Alzheimer's type: changes in hippocampal L-[^{3}H]glutamate binding. J. Neurochem. *48*, 543-551.

Greenamyre, J.T., Maragos, W.F., Albin, R.L., Penney, J.B., and Young, A.B. (1988). Glutamate transmission and excitotoxicity in Alzheimer's disease. Prog. Neuro-Psychopharmacol. *12*, 421-430.

Greenamyre, J.T., Higgins, D.S., and Young, A.B. (1990). Sodium-dependent D-aspartate 'binding' is not a measure of presynaptic neuronal uptake sites in an autoradiographic assay. Brain Res. *19; 511*, 310-318.

Greenamyre, J.T. and Young, A.B. (1989a). Excitatory amino acids in Alzheimer's disease. Neurobiol. Aging *10*, 593-602.

Greenamyre, J.T. and Young, A.B. (1989b). Synaptic localisation of striatal NMDA, quisqualate and kainate receptors. Neurosci. Lett. *101*, 133-137.

Greenberg, S.G. and Davies, P. (1990). A preparation of Alzheimer paired helical filaments that displays distinct tau proteins by polyacrylamide gel electrophoresis. Proc. Natl. Acad. Sci. USA. *87*, 5827-5831.

Grimm, L.J., Blendy, J.A., Kellar, K.J., and Perry, D.C. (1992). Chronic reserpine administration selectively up-regulates $ß_1$ and α_{1b}-adrenergic receptors in rat brain: An autoradiographic study. Neuroscience *47*, 77-86.

Grimwood, S., Moseley, A.M., Carling, R.W., Leeson, P.D., and Foster, A.C. (1992). Characterization of the binding of [^{3}H]L-689,560, an antagonist for the glycine site on the NMDA receptor, to rat brain membranes. Mol. Pharmacol. *41*, 923-930.

Gustafson, L., Edvinsson, L., Dahlgren, N., Hagberg, B., Risberg, J., Rosen, I., and Ferno, H. (1987). Intravenous physostigmine treatment of Alzheimer's disease evaluated by psychometric testing, regional cerebral blood flow (rCBF) measurement, and EEG. Psychopharmacology *93*, 31-35.

Haass, C., Koo, E.H., and Mellon, A. (1992a). Targetting of cell-surface ß-amyloid precursor protein to lysosomes: alternative processing into amyloid bearing fragments. Nature *357*, 500-503.

Haass, C., Schlossmacher, M.G., Hung, A.Y., Vigo-Pelfrey, C., Mellon, A., Ostaszewski, B.L., Lieberburg, I., Koo, B.H., Schenk, D., Teplow, D.B., and Selkoe, D.J. (1992b). Amyloid ß-peptide is produced by cultured cells during normal metabolism. Nature *359*, 322325.

Hagan, J.J., Salamone, J.D., Simpson, J., Iversen, S.D., and Morris, R.G.M. (1988). Place navigation in rats is impaired by lesions of medial septum and diagonal band but not nucleus basalis magnocellularis. Behav. Brain Res. *27*, 9-20.

Hagan, J.J. and Morris, R.G.M. (1988). The cholinergic hypothesis of memory; a review of animal experiments. In Handbook of Psychopharmacology. L.L. Iversen, S.D. Iversen, and S.H. Snyder, eds. (Plenum Press), pp. 237-323.

Halasy, K., Miettinen, R., Szabat, E., and Freund, T.F. (1992). GABAergic interneurones are the major postsynaptic targets of median raphe afferents in the rat dentate gyrus. Eur. J. Neurosci. *4*, 144-153.

Hall, M.D., EI Mestikawy, S., Emerit, M.B., Pichat, L., Hamon, M., and Gozlan, H. (1985). [^{3}H]8-Hydroxy-2-(di-n-propylamino)tetralin binding to pre- and postsynaptic 5-hydroxytryptamine sites in various regions of the rat brain. J. Neurochem. *44*, 1685-1696.

Hammer, R., Berrie, C., Birdsall, N.J.M., Burgen, A.S.V., and Hulme, E.C. (1980). Pirenzepine distinguishes between different subclasses of muscarinic receptors. Nature *283*, 90-92.

Han, C., Abel, P.W., and Minneman, K.P. (1987). Alpha-1 adrenoceptor subtypes linked to different mechanisms for increasing intracellular Ca^{2+} in smooth muscle. Nature *329*, 333-335.

Handelmann, G.E., Nevins, M.E., Mueller, L.L., Arnolde, S.M., and Cordi, A.A. (1989). Milacemide, a glycine prodrug, enhances performance of learning tasks in normal and amnesic rodents. Pharmacol. Biochem. Behav. *34*, 823-828.

Hardy, J.A., Adolfsson, R., Alafuzoff, I., Bucht, G., Marcusson, J., Nyberg, P., Perdahl, E., Wester, P., and Winblad, B. (1985). Transmitter deficits in Alzheimer's disease. Neurochem. Int. *4*, 545-563.

Hardy, J.A., Cowburn, R., Barton, A.J.L., Reynolds, G.P., Loftdahl, E., O'Carrol, A., Wester, P., and Winblad, B. (1987). Region specific loss of glutamate innervation in Alzheimer's disease. Neurosci. Lett. *73*, 77-80.

Hardy, J.A. and Higgins, G.A. (1992). Alzheimer's disease: The amyloid cascade hypothesis. Science *256*, 184-185.

Haroutanian, V., Barnes, E., and Davis, K.L. (1985). Cholinergic modulation of memory in rats. Psychopharmacology *87*, 266-271.

Haroutanian, V., Kanof, P.D., Tsuboyama, G.K., Campbell, G.A., and Davis, K.L. (1986). Animal models of Alzheimer's disease: Behaviour, pharmacology, transplants. Can. J. Neurol. Sci. *13*, 385-393.

Harrison, M.B., Wiley, R.G., and Wooten, G.F. (1990). Selective localisation of striatal D1 receptors to striatonigral neurones. Brain Res. *528*, 317-322.

Harrison, M.B., Wiley, R.G., and Wooten, G.F. (1992). The time course of changes in D_1 and D_2 receptor binding in the striatum following a selective lesion of striatonigral neurons. Brain Res. *596*, 330-336.

Harrison, P.J., Barton, A.J.L., Najlerahim, A., and Pearson, R.C.A. (1990). Distribution of a kainate/AMPA receptor mRNA in normal and Alzheimer brain. NeuroReport *1*, 149-152.

Harrison, P.J., Barton, A.J., Najlerahim, A., McDonald, B., and Pearson, R.C.A. (1991). Increased muscarinic receptor messenger RNA in Alzheimer's disease temporal cortex demonstrated by in situ hybridization histochemistry. Mol. Brain Res. *9*, 15-21.

Hartig, P.R. and Lever, J.R. (1990). Serotonin receptors. In Quantitative imaging: Neurotransmitters and enzymes. J.J. Frost and H.N. Wagner, eds. (New York: Raven), pp. 153-164.

Hasselmo, M.E. and Bower, J.M. (1993). Acetylcholine and memory. Trends. Neurosci. *16*, 218-222.

Hedreen, J.C. and Yin, T.C.T. (1981). Homotropic and heterotropic callosal afferents of caudal inferior parietal lobule in macaca mulatta. J. Comp. Neurol. *197*, 605-621.

Heimer, L., Alheid, G.F., and Zaborszky, L. (1985). Basal ganglia. In The rat nervous system. G. Paxinos, ed. (Sydney: Academic Press), pp. 37-86.

Heinemann, S., Bettler, B., Boulter, J., Deneris, E., Gasic, G., Hartley, M., Hollman, M., Hughes, T.E., O'Shea-Greenfield, A., and Rogers, S. (1991a). The glutamate receptors: genes, structure, and expression. In Glutamate, cell death and memory. P. Ascher, D.W. Choi, and Y. Christen, eds. (Berlin: Springer-Verlag), pp. 12-29.

Heinemann, S., Boulter, J., Connolly, J., Deneris, E., Duvoisin, R., Hartley, M., Hermans-Borgmeyer, I., Hollmann, M., O'Shea-Greenfield, A., Papke, R., Rogers, S., and Patrick, J. (1991b). The nicotinic receptor genes. Clin. Neuropharmacol. (Suppl.) *14 S1*, S45-S61.

Henderson, G., Johnson, J.W., and Ascher, P. (1990). Competitive antagonists and partial agonists at the glycine modulatory site of the mouse N-methyl-D-aspartate receptor. J. Physiol. -London *430*, 189-212.

Hendry, S.H.C. and Jones, E.G. (1986). Reduction in number of immunostained GABA neurones in deprived-eye dominance columns of monkey area 17. Nature *320*, 750-753.

Hensler, J.G., Kovachich, G.B., and Frazer, A. (1991). A quantitative autoradiographic study of serotonin1A receptor regulation: Effect of 5,7-dihydroxytryptamine and antidepressant treatments. Neuropsychopharmacology *4*, 131-144.

Herrling, P.L. (1985). Pharmacology of the corticocaudate excitatory postsynaptic potential in the cat: evidence for its mediation by quisqualate-and kainate-receptors. Neuroscience *14*, 417-426.

Hertz, L., Yu, A., Potter, R.L., Fisher, T.E., and Schousboe, A. (1983). Metabolic fluxes from glutamate and towards glutamate in neurones and astrocytes in primary cultures. In Glutamine, glutamate and GABA in the central nervous system. L. Hertz, E. Kvamme, E.G. McGeer, and A. Schousboe, eds. (New York: Liss), pp. 327-342.

Hill, J.A., Zoli, M., Bourgeois, J-P., and Changeux, J-P. (1993). Immunocytochemical localisation of a neuronal nicotinic receptor: the beta2 subunit. J. Neurosci. *13*, 1551-1568.

Hjorth-Simonsen, A. (1971). Hippocampal efferents to the ipsilateral entorhinal area: An experimental study in the rat. J. Comp. Neurol. *142*, 417-438.

Hof, P.R. and Morrison, J.H. (1994). The cellular basis of cortical disconnection in Alzheimer's disease and related dementing conditions. In Alzheimer Disease. R.D. Terry, R. Katzman, and K.L. Bick, eds. (New York: Raven Press), pp. 197-229.

Hollman, M. and Heinemann, S. (1994). Cloned glutamate receptors. Ann. Rev. Neurosci. *17*, 31-108.

Hood, W.F., Compton, R.P., and Monahan, J.B. (1989). D-Cycloserine: a ligand for the N-methyl-D-aspartate coupled glycine receptor has partial agonist characteristics. Neurosci. Lett. *98*, 91-95.

Hoover, D.B., Muth, E.A., and Jacobowitz, D.M. (1978). A mapping of the distribution of acetylcholine, choline acetyltransferase and acetylcholinesterase in discrete areas of rat brain. Brain Res. *153*, 295-306.

Horton, R.W. (1989). Amino acid transmitters. In Neurotransmitters, drugs and disease. R.A. Webster and C.C. Jordan, eds. (Oxford: Blackwell), pp. 165-181.

Houser, C.R., Crawford, G.D., Barber, R.P., Salvaterra, P.M., and Vaughn, J.E. (1983). Organisation and morphological characteristics of cholinergic neurones: An immunocytochemical study with a monoclonal antibody to choline acetyltransferase. Brain Res. *266*, 97-119.

Hoyer, D., Pazos, A., Probst, A., and Palacios, J.M. (1986). Serotonin receptors in the Human brain. II. Characterisation and autoradiographic localisation of 5-HT_{1c} and 5-HT_2 recognition sites. Brain Res. *376*, 97-107.

Hubbard, C.M., Redpath, G.T., Macdonald, T.L., and VandenBerg, S.R. (1989). Modulatory effects of aluminum, calcium, lithium, magnesium, and zinc ions on [^{3}H]MK-801 binding in human cerebral cortex. Brain Res. *486*, 170-174.

Hubel, D.H. and Wiesel, T.N. (1965). Receptive fields and functional architecture in two nonstriate visual areas (18 and 19) of the cat. J. Neurophysiol. *28*, 229-289.

Hubel, D.H. and Wiesel, T.N. (1974). Sequence regularity and geometry of orientation columns in the monkey striate cortex. J. Comp. Neurol. *158*, 267-294.

Huettner, J.E. and Bean, B.P. (1988). Blockade of the *N*-methyl-D-aspartate-activated current by the anticonvulsant MK-801: selective binding to open channels. Proc. Natl. Acad. Sci. USA. *85*, 1307-1311.

Hulme, E.C., Birdsall, N.J.M., and Buckley, N.J. (1990). Muscarinic receptor subtypes. Ann. Rev. Pharmacol. Toxicol. *30*, 633-673.

Hung, A., Munsat, T., and Selkoe, D. (1994). Regulation of ß amyloid precursor protein processing into non-amyloidogenic and amyloidogenic derivations by protein kinase C. Soc. Neurosci. Abs. (in press)

Hyman, B.T., Van Hoesen, G.W., Damasio, A.R., and Barnes, C.L. (1984). Alzheimer's disease: Cell specific pathology isolates the hippocampal formation. Science *225*, 1168-1170.

Hyman, B.T., Van Hoesen, G.W., and Damasio, A.R. (1987). Alzheimer's disease: Glutamate depletion in the hippocampal perforant pathway zone. Ann. Neurol. *22*, 37-40.

Iishi, T. (1966). Distribution of Alzheimer's neurofibrillary changes in the brain stem and hypothalamus of senile dementia. Acta Neuropathol. *6*, 181-187.

Jaarsma, D., Sebens, J.B., and Korf, J. (1991). Reduction of adenosine A_1 receptors in the perforant pathway terminal zone in Alzheimer hippocampus. Neurosci. Lett. *121*, 111-114.

Jaim-Etcheverry, G. and Zieher, L.M. (1980). DSP-4: A novel compound with neurotoxic effects on noradrenergic neurones of adult and developing rats. Brain Res. *188*, 513-523.

Jansen, K.L.R., Faull, R.L.M., Dragunow, M., and Synek, B.L. (1990). Alzheimer's disease: changes in hippocampal N-methyl-D-aspartate, quisqualate, neurotensin, adenosine, benzodiazepine, serotonin and opioid rceptors - an autoradiographic study. Neuroscience *32*, 613-627.

Jarrard, L.E. (1986). Selective hippocampal lesions and behaviour: Implications for current research and theorising. In The Hippocampus. R.L. Isaacson and K.H. Pibram, eds. (New York: Plenum), pp. 93-126.

Johnson, J.W. and Ascher, P. (1987). Glycine potentiates the NMDA response in cultured mouse brain neurones. Nature *325*, 529-531.

Jonas, P. and Sakmann, B. (1992). Glutamate receptor channels in isolated patches from CA1 and CA3 pyramidal cells of rat hippocampal slices. J. Physiol. *455*, 143-171.

Jones, C.R., Hoyer, D., and Palacios, J.M. (1990). Adrenoceptor autoradiography. In The pharmacology of noradrenaline in the central nervous system. D.J. Heal and C.A. Marsden, eds. (London: Oxford University Press), pp. 41-75.

Jones, E.G. (1975). Varieties and distributions of non-pyramidal cells in the somatic sensory cortex of the squirrel monkey. J. Comp. Neurol. *160*, 205-268.

Jones, E.G., Coulter, J.D., Burton, H., and Porter, R. (1977). Cells of origin and terminal distribution of corticostriatal fibres arising in the sensory-motor cortex of monkeys. J. Comp. Neurol. *173*, 53-80.

Jones, E.G. (1984). Laminar distribution of cortical efferent cells. In Cerebral cortex: Volume 1, Cellular components of the cerebral cortex. A. Peters and E.G. Jones, eds. (New York: Plenum Press), pp. 521-553.

Jones, E.G., Hendry, S.H.C., and DeFelipe, J. (1984). GABA-peptide neurones in the primate cerebral cortex: A limited cell class. In Cerebral cortex, Vol 4: Further aspects of cortical function, including hippocampus. E.G. Jones and A. Peters, eds. (New Yok: Plenum), pp. 237-266.

Jones, E.G. (1986). Cerebral cortical neurotransmitters. J. Neurosurg. *65*, 135-153.

Jonsson, G. (1980). Chemical neurotoxins as denervation tools in neurobiology. Ann. Rev. Neurosci. *3*, 169-187.

Jope, R.S., Song, L., Li, X., and Powers, R. (1994). Impaired phosphoinositide hydrolysis in Alzheimer's disease brain. Neurobiol. Aging (in press)

Kaneko, T. and Mizuno, N. (1988). Immunohistochemical study of glutaminase-containing neurons in the cerebral cortex and thalamus of the rat. J. Comp. Neurol. *267*, 590-602.

Kang, J., Lemaire, J.G., Unterbeck, A., Salbaum, J.M., Masters, C.L., Grzeschik, K.H., Multhaup, G., Beyreuther, K., and Muller-Hill, B. (1987). The precursor of Alzheimer's disease amyloid A4 protein resembles a cell surface receptor. Nature *325*, 733-736.

Kato, K. and Zorumski, C.F. (1993). Nitric oxide inhibitors facilitate the induction of hippocampal long-term potentiation by modulating NMDA responses. J. Neurophysiol. *70*, 1260-1263.

Katzman, R. (1976). The prelevance and malignancy of Alzheimer's disease. Arch. Neurol. *33*, 217-218.

Katzman, R. (1994). Apolipoprotein E4 as the major genetic susceptibility factor for Alzheimer disease. In Alzheimer Diease. R.D. Terry, R. Katzman, and K.L. Bick, eds. (New York: Raven Press), pp. 455-457.

Kemp, J.M. and Powell, T.P.S. (1970). The cortico-striate projection in the monkey. Brain *93*, 525-546.

Kesslak, J.P., Korotzer, A., Song, A., Kamali, K., and Cotman, C.W. (1991). Effects of tetrahydroaminoacridine (THA) on functional recovery after sequential lesion of the entorhinal cortex. Brain Res. *557*, 57-63.

Kilpatrick, G.L., Jones, B.J., and Tyers, M.B. (1987). Identification and distribution of 5-HT_3 receptors in rat brain using radioligand binding. Nature *330*, 746-748.

Kisvarday, Z.F., Martin, K.A.C., Freund, T.F., Magloczky, Z., Whitteridge, D., and Somogyi, P. (1986). Synaptic targets of HRP-filled layer III pyramidal cells in the cat striate cortex. Exp. Brain Res. *64*, 541-552.

Koh, J-Y., Yang, L.L., and Cotman, C.W. (1990). ß - Amyloid protein increases the vulnerability of cultured cortical neurons to excitotoxic damage. Brain Res. *533*, 315-320.

Kohler, C., Chan-Palay, V., Haglund, L., and Steinbusch, H. (1980). Immunohistochemical localisation of serotonin nerve terminals in the lateral entorhinal cortex of the rat. Demonstration of two separate patterns of innervation from the midbrain raphe. Anat. Embryol. *160*, 121-129.

Kohler, C. (1986). Cytochemical architecture of the entorhinal area. In Excitatory amino acids and epilepsy. R. Schwarcz and Y. Ben-Ari, eds. (New York: Plenum Press), pp. 83-98.

Kohler, C. and Steinbusch, H.W.M. (1982). Identification of serotonin and non-serotonin containing neurones of the midbrain raphe projecting to the entorhinal area and the hippocampal formation. A combined immunohistochemical and flourescent retrograde tracing study in the rat brain. Neuroscience *7*, 951-975.

Kornhuber, J., Retz, W., Riederer, P., Heinsen, H., and Fritze, J. (1988). Effect of antemortem and postmortem factors on [^{3}H]glutamate binding in the human brain. Neurosci. Lett. *93*, 312-317.

Kornhuber, J.K., Burkhardt-Mack, F., Kornhuber, M.E., and Riederer, P. (1989). [^{3}H]-MK-801 binding sites in post-mortem human frontal cortex. Eur. J. Pharmacol. *162*, 483-490.

Kosik, K.S. and Greenberg, S.M. (1994). Tau protein and Alzheimer disease. In Alzheimer disease. R.D. Terry, R. Katzman, and K.L. Bick, eds. (New York: Raven Press), pp. 335-344.

Kowall, N.W. and Beal, M.F. (1991). Glutamate-, glutaminase-, and taurine-immunoreactive neurones develop neurofibrillary tangles in Alzheimer's disease. Ann. Neurol. *29*, 162-167.

Krieg, W.J.S. (1946). Connections of the cerebral cortex. 1.The albino rat B.Structure of the cortical areas. J. Comp. Neurol. *84*, 277-323.

Krieg, W.J.S. (1947). Connections of the cerebral cortex. I. The albino rat, C. Extrinsic connections. J. Comp. Neurol. *86*, 267-394.

Kristiansen, U., Lambert, J.D.C., Falch, E., and Krogsgaard-Larsen, P. (1991). Electrophysiological studies of the $GABA_A$ receptor ligand, 4-PIOL, on cultured hippocampal neurones. Br. J. Pharmacol. *104*, 85-90.

Kuhar, M.J. (1985). Receptor localisation with the microscope. In Neurotransmitter receptor binding. H.I. Yamamura, S.J. Enna, and M.J. Kuhar, eds. (New York: Raven), pp. 153-176.

Kung, H.F., Guo, Y-Z., and Billings, J.B. (1986). New serotonin receptor site specific brain imaging agent: Radioactive iodinated 8-OH-DPAT. J. Nucl. Med. *27*, 972.

Kwak, S., Aizawa, H., Ishida, M., and Shinozaki, H. (1992). New, potent kainate derivatives: comparison of their affinity for [^{3}H] kainate and [^{3}H] AMPA binding sites. Neurosci. Lett. *139*, 114-117.

Levey, A.I., Kitt, C.A., Simonds, W.F., Price, D.L., and Brann, M.R. (1991). Identification and localisation of muscarinic acetylcholine receptor proteins in brain with subtype specific antibodies. J. Neurosci. *11*, 3218-3226.

Levin, E.D., Castonguay, M., and Ellison, G.D. (1987). Effects of the nicotinic receptor blocker, mecamylamine, on radial arm maze performance in rats. Behav. Neurol. Biol. *48*, 206-212.

Levin, E.D. (1992). Nicotinic systems and cognitive function. Psychopharmacology *108*, 417-431.

Lewis, D.A., Campbell, M.J., Terry, R.D., and Morrison, J.H. (1987). Laminar and regional distributions of neurofibrillary tangles and neuritic plaques in Alzheimer's disease a quantitative study of visual and auditory cortices. J. Neurosci. *7*, 1799-1809.

Leysen, J.E., Eens, A., Gommeren, W., Van Gompel, P., Wynants, J., and Jansen, P.A. (1988). Identification of nonserotonergic 3H ketanserin binding sites associated with nerve terminals in rat brain and with platelets; Relation with release of biogenic amine metabolites induced by ketanserin- and tetrabenzine-like drugs. J. Pharmacol. Exp. Ther. *244*, 310-321.

Liau, L.M., Sleight, A.J., Pitha, J., and Peroutka, S.J. (1991). Characterization of a novel and potent 5-hydroxytryptamine$_{1A}$ receptor antagonist. Pharmacol. Biochem. Behav. *38*, 555-559.

Lidov, H.G.W., Grzanna, R., and Molliver, M.E. (1980). The serotonin innervation of the cerebral cortex in the rat: An immunohistochemical analysis. Neuroscience *5*, 207-227.

Lima, L., Laporte, A.M., Gaymard, C., Lanfumey, L., Mocaer, E., and Hamon, M. (1994). In vitro and in vivo labelling of central 5-HT_{1A} receptors with a new selective agonist radioligand [^{3}H] S 14506. Br. J. Pharmacol. (in press)

Lin, Y. and Phillis, J.W. (1991). Muscarinic agonist mediated induction of long term potentiation in rat cerebral cortex. Brain Res. *551*, 342-345.

Linden, J., Tucker, A.L., and Lynch, K.R. (1991). Molecular cloning of adenosine A_1 and A_2 receptors. Trends Pharmacol. Sci. *12*, 326-329.

Lloyd, G.K., Lowenthal, A., Javoyagid, F., and Constantidinis, J. (1991). GABA-A receptor complex function in frontal cortex membranes from control and neurological patients. Eur. J. Pharmacol. *197*, 33-39.

Lodge, D. and Collingridge, G.L. (1991). TIPS Special report: The pharmacology of excitatory amino acids (Cambridge: Elsevier).

Lodge, D. and Johnson, K.M. (1991). Noncompetative excitatory amino acid receptor antagonists. In TIPS special report: The Pharmacology of excitatory amino acids. D. Lodge and G. Collingridge, eds. (Amsterdam: Elsevier), pp. 13-18.

Lohse, M.J., Klotz, K-N., Lindenborn-Fotinos, J., Reddington, M., Schwabe, U., and Olsson, R.A. (1987). 8-Cyclopentyl-1,3-dipropylxanthine (DPCPX)- a selective high affinity antagonist radioligand for A_1 adenosine receptors. N-S Arch. Pharmacol. *336*, 204-210.

Lorente de No, R. (1933). Studies on the structure of the cerebral cortex: I. the area entorhinalis. J. Psychol. Neur. *45*, 381-438.

Lorente de No, R. (1934). Studies of the structure of the cerebral cortex: II continuation of the study of the ammonical system. J. Psychol. Neur. *46*, 113-177.

Loring, R.H. and Zigmond, R.E. (1988). Characterization of neuronal nicotinic receptors by snake venom neurotoxins. Trends. Neurosci. *11*, 73-78.

Loughlin, S.E., Foote, S.L., and Fallon, J.H. (1982). Locus coeruleus projections to cortex: Topography, morphology and collateralization. Brain Res. Bull. *9*, 287-294.

Lowe, S.L., Francis, P.T., Procter, A.W., Palmer, A.M., Davison, A.N., and Bowen, D.M. (1988). Gamma-aminobutyric acid concentration in brain tissue at two stages of Alzheimer's disease. Brain *111*, 785-799.

Lowe, S.L., Bowen, D.M., Francis, P.T., and Neary, D. (1990). Ante mortem cerebral amino acid concentrations indicate selective degeneration of glutamate-enriched neurons in Alzheimer's disease. Neuroscience *38*, 571-577.

Lowe, S.L. and Bowen, D.M. (1990). Glutamic acid concentration in brains of patients with Alzheimer's disease. Biochem. Soc. Trans. *18*, 443-444.

Lowry, O.H., Rosebrough, N.J., Farr, S.L., and Randall, R.J. (1951). Protein measurement with the Folin phenol reagent. J. Biol. Chem. *193*, 265-275.

Loy, R., Koziell, D., Lindsey, J., and Moore, R.Y. (1980). Noradrenergic innervation of the adult rat hippocampal formation. J. Comp. Neurol. *189*, 699-710.

Lund, J.S. and Boothe, R.G. (1975). Interlaminar connections and pyramidal neuron organisation in the visual cortex. J. Comp. Neurol. *159*, 305-334.

Lynch, G., Bahr, B.A., and Vanderklish, P.W. (1991). Induction and stabilisation of long-term potentiation. In Glutamate, cell death and memory. P. Ascher, D.W. Choi, and Y. Christen, eds. (Berlin: Springer-Verlag), pp. 45-60.

MacLean, P.D. (1985). Fiber systems of the forebrain. In The rat nervous system. G. Paxinos, ed. (London: Academic Press), pp. 417-440.

Madison, D.V. and Nicoll, R.A. (1986). Actions of noradrenaline recorded intracellularly in rat hippocampal CA1 pyramidal neurones in vitro. J. Physiol. *372*, 221-244.

Magistretti, P.J. and Morrison, J.H. (1988). Noradrenaline and vasoactive intestinal peptide containing neuronal systems in neocortex: Functional convergence with contrasting morphology. Neuroscience *24*, 367-378.

Manallack, D.T., Wong, M.G., O'Shea, R.D., and Beart, P.M. (1990). Topography of the glycine site of the NMDA receptor. Molecular Neuropharmacology *1*, 7-15.

Mann, D.M., Lincoln, J., Yates, P.O., Stamp, J.E., and Toper, S. (1980). Changes in monoamine containing neurones of the human CNS in senile dementia. Br. J. Psychiat. *136*, 533-541.

Mann, D.M.A. and Yates, P.O. (1983). Serotonergic nerve cells in Alzheimer's disease. J. Neurol. Neurosurg. Psychiatry *46*, 96.

Maragos, W.F., Chu, D.C.M., Young, A.B., Damato, C.J., and Penney, J.B. (1987a). Loss of hippocampal 3H TCP binding in Alzheimer's disease. Neurosci. Lett. *74*, 371-376.

Maragos, W.F., Greenamyre, J.T., Penney, J.B., and Young, A.B. (1987b). Glutamate dysfunction in Alzheimer's disease: an hypothesis. Trends. Neurosci. *10*, 65-68.

Maragos, W.F., Greenamyre, J.T., Chu, D.C.M., Penney, J.B., and Young, A.B. (1991). A study of cortical and hippocampal NMDA and PCP receptors following selective cortical and subcortical lesions. Brain Res. *538*, 36-45.

Marsden, C.D. and Harrison, M.J.G. (1972). Outcome of investigations of patients with presenile dementia. Br. Med. J. *2*, 249-254.

Mash, D.C., Flynn, D.D., and Potter, L.T. (1985). Loss of M2 muscarinic receptors in the cerebral cortex in Alzheimer's disease and experimental cholinergic denervation. Science *228*, 1115-1117.

Mason, S.T. and Fibiger, H.C. (1979). Regional topography within noradrenergic locus coerulus as revealed by retrograde transport of horseradish peroxidase. J. Comp. Neurol. *187*, 703-724.

Masters, C.L., Simms, G., Weinmann, N.A., Multhaup, C., McDonald, B.L., and Beyreuther, K. (1985). Amyloid plaque core protein in Alzheimer's disease and down syndrome. Proc. Natl. Acad. Sci. USA. *82*, 4245-4249.

Mata, M., Fink, D.J., and Gainer, H. (1980). Activity dependent energy metabolism in rat posterior pituitary primarily reflects sodium pump activity. J. Neurochem. *34*, 213-215.

Mathers, D.A. (1987). The $GABA_A$ receptor: new insights from single-channel recording. Synapse *1*, 96-101.

Mattson, M.P. (1988). Neurotransmitters in the regulation of neuronal cytoarchitecture. Br. Res. Rev. *13*, 179-212.

Mattson, M.P., Dou, P., and Kater, S.B. (1988). Outgrowth regulating actions of glutamate in isolated hippocampal pyramidal neurones. J. Neurosci. *8*, 2087-2100.

Mattson, M.P., Cheng, B., Davis, D., Bryant, K., Lieberburg, I., and Rydel, R.E. (1992). ß-amyloid peptides destabilize calcium homeostasis and render human cortical neurons vulnerable to excitotoxicity. J. Neurosci. *12*, 376-389.

Mattson, M.P., Culwell, A.R., and Esch, F.S. (1993). Evidence for neuroprotective and intraneuronal calcium regulating roles for secreted forms of ß-amyloid precursor protein. Neuron *10*, 243-254.

Mayer, M.L. (1991). Physiology and biophysics of the NMDA receptor channel complex. In Excitatory amino acid antagonists. B.S. Meldrum, ed. (Oxford: Blackwell Scientific Publications), pp. 64-83.

Maziere, B. and Maziere, M. (1990). Where have we got to with neuroreceptor mapping of the human brain. Eur. J. Nuclear Med. *16*, 817-835.

McAlonan, G.M., Robbins, T.W., and Everitt, B.J. (1993). Effects of medial dorsal thalamic and ventral pallidal lesions on the aquisition of a conditioned place preference: Further evidence for the involvement of the ventral striatopallidal system in reward-related processes. Neuroscience *52*, 605-620.

McCormick, D.A. (1990). Cellular mechanisms of cholinergic control of neocortical and thalamic neuronal excitability. In Brain cholinergic systems. M. Steriade and D. Biesold, eds. (Oxford: Oxford University Press), pp. 236-264.

McCormick, D.A. and Prince, D.A. (1985). Two types of muscarinic responses to acetycholine in mammalian cortical neurones. Proc. Natl. Acad. Sci. USA. *82*, 6344-6348.

McCormick, D.A. and Prince, D.A. (1986). Mechanisms of action of acetylcholine in the guinea-pig cerebral cortex in vitro. J. Physiol. *375*, 169-194.

McCormick, D.A. and Williamson, A. (1989). Convergence and divergence of neurotransmitter action in human cerebral cortex. Proc. Natl. Acad. Sci. USA. *86*, 8098-8102.

McGeer, E.G., McGeer, P.L., Akiyama, H., and Harrop, R. (1990). Cortical glutaminase, beta-glucuronidase and glucose utilisation in Alzheimer's disease. Can. J. Neurol. Sci. *16*, 511-515.

McKinney, M. and Coyle, J.T. (1991). The potential for muscarinic receptor subtype specific pharmacotherapy for Alzheimer's disease. Mayo Clin. Proc. *66*, 1225-1237.

McMahon, H.T. and Nicholls, D.G. (1990). Glutamine and aspartate loading into synaptosomes; a reevaluation of effects on calcium dependent excitatory amino acids release. J. Neurochem. *54*, 373-380.

McNamara, D. and Dingledine, R. (1990). Dual effect of glycine on NMDA-induced neurotoxicity in rat cortical cultures. J. Neurosci. *10*, 3970-3976.

Meldrum, B.S. and Garthwaite, J. (1990). Excitatory amino acid neurotoxicity and neurodegenerative disease. Trends Pharmacol. Sci. *11*, 993-996.

Messer, W.S., Ellerbrock, B., Price, M., and Hoss, W. (1989). Autoradiographic analyses of agonist binding to muscarinic receptor subtypes. Biochem. Pharmacol. *38*, 837-850.

Metherate, R., Tremblay, N., and Dykes, R.W. (1988). Transient and prolonged effects of acetylcholine on responsiveness of cat somatosensory cortical neurones. J. Neurophysiol. *59*, 1253-1276.

Middlemiss, D.N., Bowen, D.M., and Palmer, A.M. (1986a). Serotonin neurones and receptors in Alzheimer's disease. In New concepts in Alzheimer's disease. M. Briley, A. Kato, and M. Weber, eds. (London: MacMillan press), pp. 89-102.

Middlemiss, D.N., Palmer, A.M., Edel, N., and Bowen, D.M. (1986b). Binding of the novel serotonin agonist 8-hydroxy-2-(di-n-propylamino) tetralin in normal and Alzheimer brain. J. Neurochem. *46*, 993-996.

Miller, J.D., De Leon, M.J., Ferris, S.H., Kluger, A., George, A.E., Reisberg, B., Sachs, H.J., and Wolf, A.R. (1987). Abnormal temporal lobe response in Alzheimer's disease during cognitive processing as measured by ^{11}C-2-deoxy-D-glucose and PET. J. Cereb. Blood Flow Metab. *7*, 248-251.

Miller, R.J. (1991). The revenge of the kainate receptor. Trends. Neurosci. *14*, 477-479.

Miyai, I., Ueno, S., Yorifuji, S., Fujimura, H., and Tarui, S. (1990). Alterations in neocortical expression of nicotinic acetylcholine receptor mRNAs following unilateral lesions of the rat nucleus basalis magnocellularis. J. Neural Transm. *82*, 79-91.

Monaghan, D.T., Mena, E.E., and Cotman, C.W. (1982). The effect of entorhinal cortical ablation on the distribution of muscarinic cholinergic receptors in the rat hippocampus. Brain Res. *234*, 480-485.

Monaghan, D.T., Yao, D., and Cotman, C.W. (1985). L-3H-glutamate binds to kainate-,NMDA- and AMPA-sensitive binding sites: An autoradiographic analysis. Brain Res. *340*, 378-383.

Monaghan, D.T., Geddes, J.W., Yao, J.K., Chung, C., and Cotman, C.W. (1987). [^{3}H]TCP binding sites in Alzheimer's disease. Neurosci. Lett. *73*, 197-200.

Monaghan, D.T. and Cotman, C.W. (1982). The distribution of [^{3}H] kainic acid binding sites in rat CNS as determined by autoradiography. Brain Res. *252*, 91-100.

Monahan, J.B., Handelmann, G.E., Hood, W.F., and Cordi, A.A. (1989). D-Cycloserine, a positive modulator of the N-methyl-D-aspartate receptor, enhances performance of learning task in rats. Pharmacol. Biochem. Behav. *34*, 649-653.

Moriyoshi, K., Masu, M., Ishii, T., Shigemoto, R., Mizuno, N., and Nakanishi, S. (1991). Molecular cloning and characterization of the rat NMDA receptor. Nature *354*, 31-37.

Mountcastle, V.B. (1957). Modality and topographic properties of single neurones of cat's somatic sensory cortex. J. Neurophysiol. *20*, 408-434.

Mountjoy, C.Q., Rossor, M.N., Iversen, L.L., and Roth, M. (1984). Correlation of cortical cholinergic and GABA deficits with quantitative neuropathological findings in senile dementia. Brain *107*, 507-518.

Mouradian, M.M., Contreras, P.C., Monahan, J.B., and Chase, T.N. (1988). [^{3}H]MK-801 binding in Alzheimer's disease. Neurosci. Lett. *93*, 225-230.

Mulholland, G.K., Otto, C.A., Jewett, D.M., Kilbourn, M.R., Koeppe, R.A., Sherman, P.S., Petry, N.A., Carey, J.E., Atkinson, E.R., and Archer, S. (1992).

Synthesis, rodent biodistribution, dosimetry, metabolism and monkey images of carbon-11-labeled (+)-2 alpha-tropanyl benzilate: a central muscarinic imaging agent. J. Nucl. Med. *33*, 423-430.

Mullan, M. and Crawford, F. (1993). Genetic and molecular advances in Alzheimer's disease. Trends. Neurosci. *16*, 398-409.

Mynlieff, M. and Dunwiddie, T.V. (1988). Noradrenergic depression of synaptic responses in hippocampus of rat: evidence for mediation by alpha-1 receptors. Neuropharmacology *27*, 391-398.

Nagai, R., McGeer, P.L., Peng, J.H., McGeer, E.G., and Dolman, C.E. (1983). Choline acetyltransferase immunohistochemistry in brains of Alzheimer's disease patients and controls. Neurosci. Lett. *36*, 195-199.

Najlerahim, A., Harrison, P.J., Barton, A.J.L., Heffernan, J., and Pearson, R.C.A. (1990). Distribution of messenger RNAs encoding the enzymes glutaminase, aspartate aminotransferase and glutamic acid decarboxylase in rat brain. Mol. Brain Res. *7*, 317-333.

Najlerahim, A. and Bowen, D.M. (1988). Biochemical measurements in Alzheimer's disease reveal a necessity for improved neuroimaging techniques to study metabolism. Biochem. J. *251*, 305-308.

Nakamura, S., Suenaga, T., Akiguchi, I., Kimura, J., Tokushima, Y., Kitaguchi, N., Takahashi, Y., and Shiojiri, S. (1992). Immunohistochemical localization of the proteinase inhibitor region of amyloid precursor proteins in the neocortex of Alzheimer's disease and aged controls. Acta Neuropathol. *84*, 244-249.

Neary, D., Snowden, J.S., Mann, D.M., Bowen, D.M., Sims, N.R., Northen, B., Yates, P.O., and Davison, A.N. (1986). Alzheimer's disease: a correlative study. J. Neurol. Neurosurg. Psychiatry *49*, 229-237.

Neary, D., Snowden, J.S., Shields, R.A., Burjan, A.W., Northern, B., Macdermott, N., Prescott, M.C., and Testa, H.J. (1987). Single photon emission tomography using [99m]Tc-HM-PAO in the investigation of dementia. J. Neurol. Neurosurg. Psychiatry *50*, 1101-1109.

Newcombe, J., Woodroofe, M.N., and Cuzner, M.L. (1986). Distribution of glial fibrillary acidic protein in gliosed human white matter. J. Neurochem. *47*, 1713-1719.

Nicholls, D.G., Sihra, T.S., and Sanchez-Prieto, J. (1987). Calcium dependent and independent release of glutamate from synaptosomes monitored by continuous fluorometry. J. Neurochem. *49*, 50-57.

Nicholls, D.G. and Sihra, T.S. (1986). Synaptosomes possess an exocytotic pool of glutamate. Nature *321*, 772.

Nilsson, O.G., Leanza, G., Rosenblad, C., Lappi, D.A., Wiley, R.G., and Bjorklund, A. (1992). Spatial learning impairment in rats with selective immunolesion of the forebrain cholinergic system. NeuroReport *3*, 1005-1008.

Ninomyia, H., Fukunaga, T., Taniguchi, T., Fujiwara, M., Shimohama, S., and Kameyama, M. (1990). 3H TCP binding in human frontal cortex: Decreases in Alzheimer-type dementia. J. Neurochem. *54*, 526-532.

Nitsch, R.M., Slack, B.E., Wurtman, R.J., and Growdon, J.H. (1992). Release of Alzheimer amyloid precursor stimulated by activation of muscarinic acetylcholine receptors. Science *258*, 304-307.

Nitsch, R.M., Farber, S.A., Growdon, J.H., and Wurtman, R.J. (1993). Release of amyloid ß-protein precursor derivatives by electrical depolarization of rat hippocampal slices. Proc. Natl. Acad. Sci. USA. *90*, 5191-5193.

Nordberg, A., Hartvig, P., Lilja, A., Viitanen, M., Amberla, K., Lundqvist, H., Andersson, Y., Ulin, J., Winblad, B., and Langstrom, B. (1990). Decreased uptake and binding of ^{11}C nicotine in brain of Alzheimer patients as visualised by positron emission tomography. J. Neural Transm. *2*, 215-224.

Nordberg, A., Alafuzoff, I., and Winblad, B. (1992a). Nicotinic and muscarinic subtypes in the human brain: Changes with aging and dementia. J. Neurosci. Res. *31*, 103-111.

Nordberg, A., Lilja, A., Lundqvist, H., Hartvig, P., Amberla, K., Viitanen, M., Warpman, U., and Johansson, M. (1992b). Tacrine restores cholinergic nicotinic receptors and glucose metabolism in Alzheimer patients as visualised by positron emission tomography. Neurobiol. Aging *13*, 747-758.

Normile, H.J., Jenden, D.J., Kuhn, D.M., Wolf, W.A., and Altman, H.J. (1990). Effects of combined serotonergic depletion and lesions of the nucleus basalis magnocellularis on acquisition of a complex spatial discrimination task in the rat. Brain Res. *536*, 245-250.

O'Neill, C., Cowburn, R.F., Wiehager, B., Alafuzoff, I., Winblad, B., and Fowler, C.J. (1991). Preservation of 5-hydroxytryptamine$_{1A}$ receptor-G protein interactions in the cerebral cortex of patients with Alzheimer's disease. Neurosci. Lett. *133*, 15-19.

Ogren, S. (1982). Central serotonin neurones and learning in the rat. In Biology of serotonergic transmission. N.N. Osborne, ed. (London: Wiley), pp. 751-763.

Ogren, S. and Johansson, C. (1985). Separation of the associative and non-associative effects of brain serotonin released by p-chloroamphetamine: Dissociable serotonergic involvement in avoidance learning, pain and motor function. Psychopharmacology *86*, 12-26.

Okazaki, M.M., McNamara, J.O., and Nadler, J.V. (1990). Kainate and quisqualate receptor autoradiography in rat brain after angular bundle kindling. Neuroscience *37*, 135-142.

Olney, J.W., Ho, O.L., and Rhea, V. (1971). Cytotoxic effects of acidic and sulphur containing amino acids on the infant mouse nervous system. Exp. Brain Res. *14*, 61-76.

Olson, L., Nordberg, A., Von Holst, H., Backman, L., Ebendal, T., Alafuzoff, I., Amberla, K., Hartving, A., Herlitz, A., Lilja, A., Lundqvist, H., Langstrom, B., Meyerson, B., Persson, A., Vitanen, M., Winblad, B., and Seiger, A. (1992). Nerve growth factor affects ^{11}C-nicotine binding, blood flow, EEG, and verbal episodic memory in an Alzheimer patient (Case Report). J. Neural Transm. *4*, 79-95.

Olton, D.S. and Wenk, G.L. (1987). Dementia: animal models of the cognitive impairments produced by degeneration of the basal forebrain cholinergic system. In Psychopharmacology: The third generation of progress. H.Y. Meltzer, ed. (New York: Raven Press), pp. 941-954.

Olucha, F., Martinez-Garcia, F., and Lopez-Garcia, C. (1985). A new stabilising agent for the tetramethylbenzedine (TMB) reaction product in the histochemical detection of horseradish peroxidase (HRP). J. Neurosci. Meth. *13*, 131-138.

Ossward, W. and Azevedo, I. (1991). Role of adenosine in the trophic effects of sympathetic innervation. Trends Pharmacol. Sci. *12*, 442-444.

Ottersen, O.P. (1991). Excitatory amino acid neurotransmitters: anatomical systems. In Excitatory amino acid antagonists. B.S. Meldrum, ed. (Oxford: Blackwell Scientific Publications), pp. 14-38.

Palfreyman, M.G. and Baron, B.M. (1991). Non-competitive NMDA antagonists, acting on the glycine site. In Excitatory amino acid antagonists. B. Meldrum, ed. (Oxford: Blackwell Scientific), pp. 101-129.

Palmer, A.M. (1987). Central monoamine neurones in Alzheimer's disease (University of London, PhD).

Palmer, A.M., Francis, P.T., Benton, J.S., Sims, N.R., Mann, D.M., Neary, D., Snowden, J.S., and Bowen, D.M. (1987a). Presynaptic serotonergic dysfunction in patients with Alzheimer's disease. J. Neurochem. *48*, 8-15.

Palmer, A.M., Francis, P.T., Bowen, D.M., Benton, J.S., Neary, D., Mann, D.M., and Snowden, J.S. (1987b). Catecholaminergic neurones assessed ante-mortem in Alzheimer's disease. Brain Res. *414*, 365-375.

Pangalos, M.N., Francis, P.T., Foster, A.C., Pearson, R.C.A., Middlemiss, D.N., and Bowen, D.M. (1991a). 5-HT_{1A} and NMDA but not 5-HT_2 receptors are

enriched on rat neocortical pyramidal neurones selectively destroyed by intrastriatal volkensin. Br. J. Pharmacol. *104*, 66p.

Pangalos, M.N., Francis, P.T., Middlemiss, D.N., Pearson, R.C.A., and Bowen, D.M. (1991b). Selective destruction of a sub-population of cortical neurones by suicide transport of volkensin, a lectin from Adenia volkensii. J. Neurosci. Meth. *40*, 17-29.

Pangalos, M.N. (1992). Biochemical approaches to investigate neocortical pyramidal neurones. PhD Thesis (University of London).

Pangalos, M.N., Francis, P.T., Foster, A.C., Pearson, R.C.A., Middlemiss, D.N., and Bowen, D.M. (1992). NMDA receptors assessed by autoradiography with [^{3}H] L-689,560 are present but not enriched on corticofugal-projecting pyramidal neurones. Brain Res. *596*, 223-230.

Parent, A., Dea, D., Quirion, R., and Poirier, J. (1993). [^{3}H] Phorbol ester binding sites and neuronal plasticity in the hippocampus following entorhinal cortex lesions. Brain Res. *607*, 23-32.

Parkinson, F.E. and Fredholm, B.B. (1992). Magnesium-dependent enhancement of endogenous agonist binding to A_1 adnosine receptors: A complicating factor in quantitative autoradiography. J. Neurochem. *58*, 941-950.

Parnavelas, J.G., Burne, R.A., and Lin, C.S. (1983). Distribution and morphology of functionally identified neurones in the visual cortex of the rat. Brain Res. *261*, 21-29.

Pascual, J., Grijalba, B., Garcia-Sevilla, J.A., Zarranz, J.J., and Pazos, A. (1992). Loss of high affinity a_2 adrenoceptors in Alzheimer's disease: an autoradiographic study in frontal cortex and hippocampus. Neurosci. Lett. *142*, 36-40.

Patneau, D.K. and Mayer, M.L. (1991). Kinetic analysis of interactions between kainate and AMPA: Evidence for activation of a single receptor in mouse hippocampal neurons. Neuron *6*, 785-798.

Paudel, H.K., Lew, J., Ali, Z., and Wang, J.H. (1993). Brain proline directed protein kinase phosphorylates tau on sites that are abnormally phosphorylated in tau associated with Alzheimer's paired helical filaments. J. Biol. Chem. *268*, 23512-23518.

Paxinos, G. and Watson, C.R.R. (1982). The rat brain in stereotaxic coordinates (London: Academic Press).

Pazos, A., Cortes, R., and Palacios, J.M. (1985). Quantitative autoradiographic mapping of serotonin receptors in the rat brain. II. Serotonin-2 receptors. Brain Res. *346*, 231-249.

Pazos, A. and Palacios, J.M. (1985). Quantitative Autoradiographic mapping of serotonin receptors in the rat brain. I.Serotonin-1 Receptors. Brain Res. *346*, 205-230.

Pearce, B.D. and Potter, L.T. (1991). Coupling of m1 muscarinic receptors to G protein in Alzheimer disease. Alzheimer. Dis. Assoc. Disord. *5*, 163-172.

Pearson, R.C.A., Sofroniew, M.V., Cuello, A.C., Powell, T.P.S., Eckenstein, F., Esiri, M.M., and Wilcock, G.K. (1983). Persistence of cholinergic neurones in the basal nucleus in a brain with senile dementia of the Alzheimer type demonstrated by immunohistochemical staining for choline acetyltransferase. Brain Res. *289*, 375-379.

Pearson, R.C.A., Esiri, M.M., Hiorns, R.W., Wilcock, G.K., and Powell, T.P.S. (1985). Anatomical correlates of the distribution of the pathological changes in the neocortex in Alzheimer's disease. Proc. Natl. Acad. Sci. USA. *82*, 4531-4534.

Peinado, J.M. and Mora, F. (1986). Glutamic acid as putative transmitter of the interhemispheric corticocortical connections in the rat. J. Neurochem. *47*, 1598-1603.

Pellerin, L. and Wolfe, L.S. (1991). Release of arachidonic acid by NMDA receptor activation in the rat hippocampus. Neurochem. Res. *16*, 983-989.

Penney, J.B., Maragos, W.F., Greenamyre, J.T., Debowey, D.L., Hollingsworth, Z., and Young, A.B. (1990). Excitatory amino acid binding sites in the hippocampal region of Alzheimer's disease and other dementias. J. Neurol. Neurosurg. Psychiatry *53*, 314-320.

Pepeu, G., DiPatre, P.L., and Casamenti, F. (1990). Spontaneous and drug-stimulated recovery of cortical cholinergic function after lesion of the nucleus basalis. In Brain cholinergic systems. M. Steriade and D. Biesold, eds. (Oxford: Oxford Science Publications), pp. 357-363.

Pericak-Vance, M.A., Bebout, J.L., and Gaskell, P. (1991). Linkage studies in familial Alzheimer disease: evidense for chromosome 19 linkage. Am. J. Hum. Genet. *48*, 1034-1050.

Peroutka, S.J. and Snyder, S.H. (1979). Multiple serotonin receptors: differential binding of ^{3}H-5-HT, ^{3}H-LSD, and ^{3}H-spiroperidol. Mol. Pharmacol. *16*, 687-695.

Perry, E.K., Gibson, P.H., Blessed, G., Perry, R.H., and Tomlinson, B.E. (1977a). Neurotransmitter abnormalities in senile dementia. J. Neurol. Sci. *34*, 247-265.

Perry, E.K., Perry, R.H., Blessed, G., and Tomlinson, B.E. (1977b). Necropsy evidence of central cholinergic deficits in senile dementia. Lancet *i*, 189.

Perry, E.K., Atack, J.R., Perry, R.H., Hardy, J.A., Dodd, P.R., Edwardson, J.A., Blessed, G., Tomlinson, B.E., and Fairbairn, A.F. (1984). Intralaminar neurochemical distribution in human midtemporal cortex: Comparison between Alzheimer's disease and the normal. J. Neurochem. *42*, 1402-1410.

Perry, E.K., Smith, C.J., Court, J.A., and Perry, R.H. (1990). Cholinergic nicotinic and muscarinic receptors in dementia of Alzheimer, Parkinson and Lewy body types. J. Neural Transm. P-D Sect. *2*, 149-158.

Perry, E.K., Court, J.A., Johnson, M., Piggott, M.A., and Perry, R.H. (1992). Autoradiographic distribution of [^{3}H] nicotine binding in human cortex: Relative abundance in subicular complex. J. Chem. Neuroanat. *5*, 399-405.

Perry, R.H., Candy, J.M., Perry, E.K., Irving, D., Blessed, G., Fairbairn, A.F., and Tomlinson, B.E. (1982). Extensive loss of choline acetyltransferase activity is not reflected by neuronal loss in the nucleus of Meynert in Alzheimer's Disease. Neurosci. Lett. *33*, 311-315.

Peters, A. (1987). Number of neurones and synapses in primary visual cortex. In Cerebral cortex, Vol 6:Further aspects of cortical function, including hippocampus. A. Peters and E.G. Jones, eds. (New York: Plenum), pp. 267-294.

Pitas, R.E., Boyles, J.K., Lee, S.H., Foss, D., and Mahey, R.W. (1987). Astrocytes synthesize apolipoprotein E and metabolize apolipoprotein E-containing lipoproteins. Biochim. Biophys. Acta *917*, 148-161.

Plum, F. (1979). Dementia: An approaching epidemic. Nature *279*, 372-373.

Pompeiano, M., Palacios, J.M., and Mengod, G. (1992). Distribution and cellular localization of mRNA coding for 5-HT_{1A} receptor in the rat brain: correlation with receptor binding. J. Neurosci. *12*, 440-453.

Preston, R.J., Bishop, G.A., and Kitai, S.T. (1980). Medium spiny neurone projections from the rat striatum: An intracellular horseradish peroxidase study. Brain Res. *183*, 253-263.

Price, R.H., Hollingsworth, Z., Young, A.B., and Penney, J.B. (1993). Excitatory amino acid receptor regulation after subthalamic nucleus lesions in the rat. Brain Res. *602*, 157-160.

Procter, A.W., Lowe, S.L., Palmer, A.M., Francis, P.T., Esiri, M.M., Stratmann, G.C., Najlerahim, A., Patel, A.J., Hunt, A., and Bowen, D.M. (1988a). Topographical distribution of neurochemical changes in Alzheimer's disease. J. Neurol. Sci. *84*, 125-140.

Procter, A.W., Middlemiss, D.N., and Bowen, D.M. (1988b). Selective loss of serotonin recognition sites in the parietal cortex in Alzheimer's disease. Int. J. Geriat. Psychiatry *3*, 37-44.

Procter, A.W., Palmer, A.M., Francis, P.T., Lowe, S.L., Neary, D., Murphy, E., Doshi, R., and Bowen, D.M. (1988c). Evidence of glutamatergic denervation and possible abnormal metabolism in Alzheimer's disease. J. Neurochem. *50*, 790-802.

Procter, A.W., Wong, E.H., Stratmann, G.C., Lowe, S.L., and Bowen, D.M. (1989). Reduced glycine stimulation of [^{3}H]MK-801 binding in Alzheimer's disease. J. Neurochem. *53*, 698-704.

Procter, A.W., Stratmann, G.C., Francis, P.T., Lowe, S.L., Bertolucci, P.H.F., and Bowen, D.M. (1991). Characterisation of the glycine modulatory site of the N-methyl-D-aspartate receptor-ionophore complex in human brain. J. Neurochem. *56*, 299-310.

Pulsinelli, W.A., Brierley, J., and Plum, F. (1982). Temporal profile of neuronal damage in models of transient forebrain ischaemia. Ann. Neurol. *11*, 491-498.

Radja, F., Laporte, A-M., Daval, G., Gozlan, H., and Hamon, M. (1991). Autoradiography of serotonin receptor subtypes in the central nervous system. Neurochem. Int. *18*, 1-15.

Radja, F., Daval, G., Hamon, M., and Verge, D. (1992). Pharmacological and physicochemical properties of pre- versus postsynaptic 5-HT_{1A} receptor binding sites in the rat brain: A quantitative autoradiographic study. J. Neurochem. *58*, 1338-1346.

Ransom, R.W. and Stec, N.L. (1988). Cooperative modulation of [^{3}H]MK-801 binding to the *N*-methyl-D-aspartate receptor-ion channel complex by L-glutamate, glycine, and polyamines. J. Neurochem. *51*, 830-836.

Rapoport, S.I., Horowitz, B., Grady, C.L., Haxby, J.V., DeCarli, C., and Schapiro, M.B. (1991). Abmormal brain glucose metabolism in Alzheimer's disease, as measured by positron emission tomography. Adv. Exp. Med. Biol. *291*, 231-248.

Reynolds, G.P., Arnold, L., Rossor, M.N., Iversen, L.L., Mountjoy, C.Q., and Roth, M. (1984). Reduced binding of [3H] ketanserin to cortical 5-HT2 receptors in senile dementia of the Alzheimer type. Neurosci. Lett. *44*, 47-51.

Robakis, N.K., Ramakrishna, N., Wolfe, G., and Wisniewski, H.M. (1987). Molecular cloning and characterization of a cDNA encoding the cerebrovascular and the neuritic plaque amyloid peptides. Proc. Natl. Acad. Sci. USA. *84*, 4190-4194.

Robertson, J., Loviny, T.L.F., Goedert, M., Jakes, R., Murray, K.J., Anderton, B.H., and Hanger, D.P. (1993). Phosphorylation of tau by cyclic-AMP-dependent protein kinase. Dementia *4*, 256-263.

Rockel, A.J., Hiorns, R.W., and Powell, T.P.S. (1980). The basic uniformity in structure of the neocortex. Brain *103*, 221-244.

Room, P., Postema, F., and Korf, J. (1981). Divergent axon collaterals of rat coeruleus neurones: Demonstration by fluorescent double labelling technique. Brain Res. *221*, 219-230.

Rose, A.M., Hattori, T., and Fibiger, H.C. (1976). Analysis of the septo-hippocampal pathway by light and electron microscopic autoradiography. Brain Res. *108*, 170-174.

Rose, M. (1927). Die sog. Riechrinde beim Menschem und beim Affen. II. Teil des "Allocortex bei Tier und Mensch". J. Psychol. Neur. *34*, 261-401.

Rossor, M.N., Garrett, N.J., Johnson, A.L., Mountjoy, C.Q., Roth, M., and Iversen, L.L. (1982). A postmortem study of the cholinergic and GABA systems in senile dementia. Brain *105*, 313-330.

Rothman, S.M. and Olney, J.W. (1986). Glutamate and the pathophysiology of hypoxic-ischemic brain damage. Ann. Neurol. *19*, 105-111.

Rothman, S.M. and Olney, J.W. (1987). Excitotoxicity and the NMDA receptor. Trends. Neurosci. *10*, 299-302.

Royce, G.J. (1982). Laminar origin of cortical neurones which project upon the caudate nucleus. A horseradish peroxidase study investigation in the cat. J. Comp. Neurol. *205*, 8-29.

Ruat, M., Traiffort, E., Arrang, J.M., Tardivel-Lacombe, J., Diaz, J., Leurs, R., and Schwartz, J.C. (1993a). A novel rat serotonin (5-HT6) receptor: molecular cloning, localisation and stimulation of cAMP accumulation. Biochem. Biophys. Res. Comm. *193*, 268-276.

Ruat, M., Traiffort, E., Leurs, R., Tardivel-Lacombe, J., Diaz, J., Arrang, J.M., and Schwartz, J.C. (1993b). Molecular cloning, characterisation and localisation of a high affinity serotonin receptor (5-HT7) activating cAMP formation. Proc. Natl. Acad. Sci. USA. *90*, 8547-8551.

Rudolphi, K.A., Schubert, P., Parkinson, F.E., and Fredholm, B.B. (1992). Neuroprotective role of adenosine in cerebral ischaemia. Trends Pharmacol. Sci. *13*, 439-445.

Ruutiainen, J., Newcombe, J., Salmi, A., Dahl, D., and Frey, H. (1981). Measurement of glial fibrillary acidic protein (GFAP) and anti-GFAP antibodies by solid phase radioimmunoassays. Acta Neurol. Scand. *63*, 297-305.

Sahin, M., Bowen, W.D., and Donoghue, J.P (1992). Location of nicotinic and muscarinic cholinergic and μ-opiate receptors in rat cerebral neocortex: evidence from thalamic and cortical lesions. Brain Res. *579*, 135-147.

Saper, C.B. (1984). Organisation of cerebral cortical afferent systems in rat, I. Magnocellular basal nucleus. J. Comp. Neurol. *222*, 313-342.

Sasaki, H., Muramoto, O., Kanazawa, I., Arai, H., Kosaka, K., and Iizuka, R. (1986). Regional distribution of amino acid transmitters in postmortem brains of presenile and senile dementia of Alzheimer type. Ann. Neurol. *19*, 1865-1870.

Saunders, A.M., Strittmatter, W.J., Schmechel, D., St.George-Hyslop, P.H., Pericak-Vance, M.A., Joo, S.H., Rosi, B.L., Gusella, J.F., Crapper-McLachlan, D.R., Alberts, M.J., Hulette, C., Crain, B., Goldgaber, D., and Roses, A.D. (1993). Association of apolipoprotein E allele E4 with late onset familial and sporadic Alzheimer's disease. Neurology *43*, 1467-1472.

Schmechel, D.E., Saunders, A.M., Strittmatter, W.J., Crain, B.J., Hulette, C.M., Joo, S.H., Pericak-Vance, M.A., Goldgaber, D., and Roses, A.D. (1993). Increased amyloid peptise deposition in cerebral cortex as a consequence of apolipoprotein E genotype in late-onset Alzheimer disease. Proc. Natl. Acad. Sci. USA. *90*, 9649-9653.

Schmuck, K., Ullmer, C., Engels, P., and Lubbert, H. (1994). Cloning and functional characterization of the human 5-HT_{2B} serotonin receptor. FEBS Lett. *342*, 85-90.

Schubert, D., Jin, L.W., and Saitoh, T. (1989). The regulation of amyloid ß protein precursor secretion and its modulatory role in cell adhesion. Neuron *3*, 689-694.

Schuster, G.M. and Schmidt, W.J. (1992). D-cycloserine reverses the working memory impairment of hippocampal-lesioned rats in a spatial learning task. Eur. J. Pharmacol. *224*, 97-98.

Schwarcz, R. (1980). Effects of tissue storage and freezing on brain glutamate uptake. Life Sci. *28*, 1147-1154.

Seeburg, P.H. (1993). The molecular biology of mammalian glutamate receptor channels. Trends. Neurosci. *9*, 359-365.

Selkoe, D.J. (1994). Normal and abnormal biology of the ß-amyloid precursor protein. Ann. Rev. Neurosci. *17*, 489-517.

Seubert, P., Vigo-Pelfrey, C., Esch, F., Lee, M., Dovey, H., Davis, D., Sinha, S., Schlossmacher, M., Whaley, J., Swindlehurst, C., McCormack, R., Wolfert, R., Selkoe, D., Lieberburg, I., and Schenk, D. (1992). Isolation and quantification of soluble Alzheimer's ß-peptide from biological fluids. Nature *359*, 325-327.

Seubert, P., Oltersdorf, T., Lee, M.G., Barbour, R., Blomquist, C., Davis, D.L., Bryant, K., Fritz, L.C., Galasko, D., Thal, L.J., Lieberburg, I., and Schenk,

D.B. (1993). Secretion of ß-amyloid precursor protein cleaved at the amino terminus of the ß-amyloid peptide. Nature *361*, 260-263.

Sheldon, P.W. and Aghajanian, G.K. (1990). Serotonin (5-HT) induces IPSPs in pyramidal layer cells of the rat piriform cortex: Evidence for the involvement of a 5-HT2 activated interneurone. Brain Res. *506*, 62-69.

Shimohama, S., Fujimoto, S., Taniguchi, T., and Kimura, J. (1992). Phosphotidylinositol-specific phospholipase C activity in the postmortem human brain: no alteration in Alzheimer's disease. Brain Res. *579*, 347-349.

Shoji, M., Golde, T.E., and Ghiso, J. (1992). Production of the Alzheimer amyloid ß protein by normal proteolytic processing. Science *258*, 126-129.

Silverstein, F.S., Buchanan, K., and Johnston, M.V. (1986). Perinatal hypoxia-ischemia disrupts striatal high-affinity [^{3}H]glutamate uptake into synaptosomes. J. Neurochem. *47*, 1614-1619.

Simpson, M.D., Royston, M.C., Deakin, J.F., Cross, A.J., Mann, D.M., and Slater, P. (1988). Regional changes in [^{3}H]D-aspartate and [^{3}H]TCP binding sites in Alzheimer's disease brains. Brain Res. *462*, 76-82.

Sims, N.R., Bowen, D.M., Allen, S.J., Smith, C.C.T., Neary, D., Thomas, D.J., and Davison, A.N. (1983a). Presynaptic cholinergic dysfunction in patients with dementia. J. Neurochem. *40*, 503-509.

Sims, N.R., Bowen, D.M., Neary, D., and Davison, A.N. (1983b). Metabolic processes in Alzheimer's disease: adenine nucleotide content and production of $^{14}CO_2$ from [U-^{14}C]glucose in vitro in human neocortex. J. Neurochem. *41*, 1329-1334.

Sirvio, J., Ekonsalo, T., Riekkinen, P., Lahtinen, H., and Reikkinen, P. (1992). D-cycloserine, a modulator of the N-methyl-D-aspartate receptor, improves spatial learning in rats treated with muscarinic antagonist. Neurosci. Lett. *146*, 215-218.

Sisodia, S.S., Koo, E.H., Beyreuther, K., Unterbeck, A., and Price, S.L. (1990). Evidence that ß-amyloid protein in Alzheimer's disease is not derived by normal processing. Science *248*, 492-495.

Sladek, J.R. and Bjorklund, A. (1982). Monoamine transmitter histochemistry: A twenty year commemoratum. Brain Res. Bull. *9*,

Sloper, J.J., Hiorns, R.W., and Powell, T.P.S. (1979). A qualitative and quantitative electron microscopic study of the neurones in the primate motor and somatic sensory cortices. Phil. Trans. Royal Soc. (London) *285*, 141-171.

Sofroniew, M.V., Eckenstein, F., and Cuello, A.C. (1983). Immunohistochemistry of cholinergic neurones in the rat brain and spinal cord. Neurosci. Lett. *14*, S348.

Sofroniew, M.V., Campbell, P.E., Cuello, A.C., and Eckenstein, F. (1985). Central cholinergic neurons visualized by immunohistochemical detection of choline acetyltransferase. In The rat nervous system. G. Paxinos, ed. (London: Academic Press), pp. 471-485.

Sofroniew, M.V. and Pearson, R.C.A. (1985). Degeneration of cholinergic neurons in the basal nucleus following kainic or N-methyl-D-aspartic acid application to the cerebral cortex in the rat. Brain Res. *339*, 186-190.

Spencer, D.G., Horvath, E., and Traber, J. (1986). Direct autoradiographic determination of M1 and M2 muscarinic acetylcholine receptor distribution in the rat brain: Relation to cholinergic nuclei projections. Brain Res. *380*, 59-68.

Sprouse, J.S. and Aghajanian, G.K. (1987). Electrophysiological responses of serotonergic dorsal raphe neurons to 5-HT_{1A} and 5-HT_{1B} agonists. Synapse *1*, 3-9.

St.George-Hyslop, P.H., Crapper-McLachlan, D.R., Tuda, T., and Rogaev, E. (1994). Alzheimer's disease and possible gene interaction. Science *263*, 537.

Staubli, U., Rogers, G., and Lynch, G. (1994). Facilitation of glutamate receptors enhances memory. Proc. Natl. Acad. Sci. USA. *91*, 777-781.

Staubli, U. and Lynch, G. (1992). NMDA receptors and memory: Evidence from pharmacological and correlational studies. In Neurobiology of the NMDA receptor from chemistry to the clinic. A.P. Kozikowski, ed. (New York: VCH),

Steele, J.E., Palmer, A.M., Stratmann, G.C., and Bowen, D.M. (1989). The N-methyl-D-aspartate receptor complex in Alzheimer's disease: reduced regulation by glycine but not zinc. Brain Res. *500*, 369-373.

Steele, J.E., Robinson, T.N., Cross, A.J., Bowen, D.M., and Green, A.R. (1991). A comparison of 3H MK-801 and N-[1-(2-thienyl)cyclohexyl]-3-4-[3H]piperidine binding to the N-methyl-D-aspartate receptor complex in human brain. J. Neurochem. *56*, 1248-1254.

Steele, J.E., Cross, A.J., and Bowen, D.M. (1992). N-methyl-D-aspartate receptor-associated ionophores determined in Alzheimer's disease by [^{3}H]MK-801 and N-[1-(2-thienyl)cyclohexyl]-3,4-[^{3}H]piperidine binding. Neurodegeneration *1*, 225-230.

Stephenson, F.A. and Olson, R.W. (1983). Biochemical pharmacology of the GABA receptor-ionophore protein complex. In CNS receptors- From molecular pharmacology to behaviour. P. Mandel and F.V. DeFeudis, eds. (New York: Raven Press), pp. 71-80.

Steward, O. and Scoville, S.A. (1976). Cells of origin of the entorhinal cortical afferents to the hippocampus and fascia dentate of the rat. J. Comp. Neurol. *169*, 347-370.

Stirling, J.M., Cross, A.J., and Green, A.R. (1989). The binding of [^{3}H]-thienyl cyclohexylpiperidine ([^{3}H]-TCP) to the NMDA-phencyclidine receptor complex. Neuropharmacology *28*, 1-7.

Stirpe, F., Barbieri, L., Abbondanza, A., Falasca, A.I., Brown, A.N.F., Sandvig, K., Olsnes, S., and Pihl, A. (1985). Properties of volkensin, a toxic lectin from Adenia Volkinsii. J. Biol. Chem. *260*, 14589-14595.

Storm-Mathisen, J. and Ottersen, O.P. (1983). Immunohistochemistry of glutamate and GABA. In Glutamine, glutamate and GABA in the central nervous system. L. Hertz, E. Kvamme, E.G. McGeer, and A. Schousboe, eds. (New York: Liss), pp. 185-201.

Strasser, R.H., Ihl-Vahl, R., and Marquetant, R. (1992). Molecular biology of adrenergic receptors. J. Hypertension *10*, 501-506.

Streit, P. (1980). Selective retrograde labelling indicating the transmitter of neuronal pathways. J. Comp. Neurol. *191*, 429-463.

Strittmatter, W.J., Saunders, A.M., Schmechel, D., Pericak-Vance, M., Enghild, J., and Salvesen, G.S. (1993). Apolipoprotein E: high avidity binding to b-amyloid and increased frequency of type 4 allele in late onset familial Alzheimer disease. Proc. Natl. Acad. Sci. USA. *90*, 1977-1981.

Subramanium, S. and Mcgonigle, P. (1990). Quantitative autoradiographic characterisation of the binding of (+)-5-methyl-10,11-dihydro-5H-dibenzo[a,d]cyclohepten-5,10-imine ([^{3}H]MK-801) in rat brain: regional effects of polyamines. J. Pharmacol. Exp. Ther. *256*, 811-819.

Suhara, T., Inoue, O., Kobayashi, K., Suzuki, K., and Tateno, Y. (1993). Age related changes in human muscarinic acetylcholine receptors measured by positron emission tomography. Neurosci. Lett. *149*, 225-228.

Sulkava, R., Haltia, M., Paetau, A., Wikstrom, J., and Palo, J. (1983). Accuracy of clinical diagnosis in primary degenerative dementia: Correlation with neuropathological findings. J. Neurol. Neurosurg. Psychiatry *46*, 9-13.

Summers, R.J. and McMartin, L.R. (1993). Adrenoceptors and their second messenger systems. J. Neurochem. *60*, 10-23.

Suzuki, T., Nairn, A.C., Gandy, S.E., and Greengard, P. (1992). Phosphorylation of Alzheimer amyloid precursor protein by protein kinase C. Neuroscience *48*, 755-761.

Svennby, G., Roberg, B., Hogstadt, S., Torgner, I.A., and Kvamme, E. (1986). Phosphate activated glutaminase in the crude mitochondrial fraction (P2 fraction) from human brain cortex. J. Neurochem. *47*, 1351-1355.

Svensson, A-L., Alafuzoff, I., and Nordberg, A. (1992). Characterisation of muscarinic receptor subtypes in Alzheimer and control brain cortices by selective muscarinic antagonists. Brain Res. *596*, 142-148.

Swanson, L.W. (1976). The locus coerulus: A cytoarchitectonic, Golgi and immunhistochemical study in the albino rat. Brain Res. *110*, 39-56.

Swanson, L.W., Wyss, J.M., and Cowan, W.M. (1978). An autoradiographic study of the organisation of the intrahippocampal association pathways in the rat. J. Comp. Neurol. *181*, 681-716.

Swanson, L.W. (1981). A direct projection from Ammon's horn to prefrontal cortex in the rat. Brain Res. *217*, 150-154.

Swanson, L.W., Sawchenko, P.E., and Cowan, W.M. (1981). Evidence for collateral projections by neurons in Ammon's horn, the dentate gyrus and subiculum: a multiple retrograde study in the rat. J. Neurosci. *1*, 548-559.

Tallaksen-Greene, S.J., Wiley, R.G., and Albin, R.L. (1992). Localisation of striatal excitatory amino acid binding site subtypes to striatonigral projection neurons. Brain Res. *594*, 165-170.

Tanabe, Y., Masu, M., and Isii, T. (1992). A family of metabotropic receptors. Neuron *8*, 169-179.

Tanaka, H., Shimizu, H., Kumasaka, Y., Hirose, A., Tatsuno, T., and Nakamura, M. (1991). Autoradiographic localization and pharmacological characterization of [^{3}H] tandospirone binding sites in the rat brain. Brain Res. *546*, 181-189.

Tanzi, R.E., Gusella, J.F., and Watkins, P.C. (1987). Amyloid ß-protein gene: cDNA, mRNA, distribution and genetic linkage near the Alzheimer locus. Science *235*, 880-884.

Terry, R.D., Masliah, E., Salmon, D.P., Butters, N., DeTeresa, R., Hill, R., Hansen, L.A., and Katzman, R. (1991). Physical basis of cognitive alterations in Alzheimer's disease: synapse loss is the major correlate of cognitive impairment. Ann. Neurol. *30*, 572-580.

Terry, R.D., Masliah, E., and Hansen, L.A. (1994). Structural basis of the cognitive alterations in Alzheimer diease. In Alzheimer Disease. R.D. Terry, R. Katzman, and K.L. Bick, eds. (New York: Raven Press), pp. 179-196.

Terry, R.D. and Wisniewski, H.M. (1970). The ultrastructure of the neurofibrillary tangle and the senile plaques. In CIBA foundation symposium on Alzheimer's disease and related condition. G.E.W. Wolstenholme and M. O'Conner, eds. (London: J & A Churchill), pp. 145-168.

Thiels, E., Weisz, D.J., and Berger, T.W. (1992). In vivo modulation of N-methyl-D-aspartate receptor-dependent long-term potentiation by the glycine modulatory site. Neuroscience *46*, 501-509.

Thompson, L.T., Moskal, J.R., and Disterhoft, J.F. (1992). Hippocampus-dependent learning facilitated by a monoclonal antibody or D-cycloserine. Nature *359*, 638-641.

Tomlinson, B.E. (1977). Morphological changes and dementia in old age. In Ageing and dementia. W.L. Smith and M. Kinsbourne, eds. (New York: Spectrum), pp. 25-56.

Tomlinson, B.E. and Corsellis, J.A.N. (1984). Ageing and the dementias. In Greenfield's Neuropathology. J.H. Adams, J.A.N. Corsellis, and L.W. Duchen, eds. (London: Edward Arnold), pp. 951-1025.

Tonnaer, J.A., Ernste, B.H., Wester, J., and Kelder, K. (1988). Cholinergic innervation and topographical organization of muscarinic binding sites in rat brain: a comparative autoradiographic study. J. Chem. Neuroanat. *1*, 95-110.

Tork, I. (1985). Raphe nuclei and serotonin containing systems. In The rat nervous system. G. Paxinos, ed. (London: Academic Press), pp. 43-78.

Tranzer, J.P. and Thoenen, H. (1967). Ultramorphologische Veranderungen der sympatischen Nervenendigungen der Katzenach Vorbehandling mit 5- and 6-Hydroxy-Dopamin. Naunyn-Schmiedeberg's Arch. Pharmacol. Exp. Pathol. *257*, 343.

Ulas, J., Monaghan, D.T., and Cotman, C.W. (1990). Kainate receptors in the rat hippocampus: A distribution and time course of changes in response to unilateral lesions of the entorhinal cortex. J. Neurol. Sci. *10*, 2352-2362.

Ungerstedt, U. (1971). Stereotaxic mapping of the monoamine pathways in the rat brain. Acta Physiol. Scand. (suppl) *367*, 1-48.

Van Calker, D., Muller, M., and Hamprecht, B. (1979). Adenosine regulates via two different receptors, the accumulation of cAMP in cultured brain cells. J. Neurochem. *33*, 999-1005.

Van der Ploeg, I., Parkinson, F.E., and Fredholm, B.B. (1992). Effect of pertussis toxin on radioligand binding to rat brain adenosine A_1 receptors. J. Neurochem. *58*, 1221-1229.

Verge, D., Daval, G., Marcinkiewicz, M., Patey, A., EI Mestikawy, S., Gozlan, H., and Hamon, M. (1986). Quantitative autoradiography of Multiple 5-HT, receptor subtypes in the brain of control or 5,7-Dihydroxytryptamine-treated rats. J. Neurosci. *6*, 3474-3482.

Vidal, C. and Changeux, J.P. (1989). Pharmacological profile of nicotinic acetylcholine receptors in the rat prefrontal cortex: an electrophysiological study in a slice preparation. Neuroscience *29*, 261-270.

Vincent, S.R. and McGeer, E.G. (1980). A comparison of sodium dependent glutamate binding with high affinity glutamate uptake in rat striatum. Brain Res. *184*, 99-108.

Vogt, B.A., Plager, M.D., Crino, P.B., and Bird, E.D. (1990). Laminar distributions of muscarinic acetylcholine, serotonin, GABA and opioid receptors in human posterior cingulate cortex. Neuroscience *36*, 165-174.

Vogt, B.A., Crino, P.B., and Volicer, L. (1991). Laminar alterations in gamma-aminobutyric $acid_A$, muscarinic, and ß adrenoceptors and neuron degeneration in cingulate cortex in Alzheimer's disease. J. Neurochem. *57*, 282-290.

Vogt, B.A. and Burns, D.L. (1988). Experimental localisation of muscarinic subtypes to cingulate cortical afferents and neurons. J. Neurosci. *8*, 643-652.

Vogt, B.A. and Miller, M.W. (1983). Cortical connections between rat cingulate cortex and visual, motor and postsubicular cortices. J. Comp. Neurol. *216*, 192-210.

Von Blankenfeld, G. and Kettenmann, H. (1992). Glutamate and GABA receptors in vertebrate glial cells. Mol. Neurobiol. *5*, 31-43.

Vulliet, R., Halloran, S.M., Braun, R.B., Smith, A.J., and Lee, G. (1992). Proline-directed phosphorylation of human tau protein. J. Biol. Chem. *267*, 22570-22574.

Wada, E., Wada, K., Boulter, J., Deneris, E., Heinemann, S., Patrick, J., and Swanson, L.W. (1989). Distribution of Alpha2, Alpha3, Alpha4 and Beta2 neuronal nicotinic receptor subunit mRNAs in the central nervous system: A hybridization histochemical study in the rat. J. Comp. Neurol. *284*, 314-335.

Waeber, C., Dietl, M.M., Hoyer, D., and Palacios, J.M. (1989). 5.HT_1 receptors in the vertebrate brain. Regional distribution examined by autoradiography. N-S Arch. Pharmacol. *340*, 486-494.

Wallace, M.A. and Claro, E. (1990). Comparison of serotonergic to muscarinic cholinergic stimulation of phosphoinositide-specific phospholipase C in rat brain cortical membranes. J. Pharmacol. Exp. Ther. *255*, 1296-1300.

Wang, S-Z., Zhu, S-Z., Mash, D.C., and El-Fakahany, E.E. (1992). Comparison of the concentration of messenger RNA encoding four muscarinic receptor subtypes in control and Alzheimer brains. Mol. Brain Res. *16*, 64-70.

Warwick, R. and Williams, P.L. (1973). Gray's Anatomy (Edinburgh: Longman).

Wasco, W., Bupp, K., Magendantz, M., Gusella, J.F., and Tanzi, R.E. (1992). Identification of a mouse brain cDNA that encodes a protein related to the Alzheimer disease-associated amyloid ß protein precursor. Proc. Natl. Acad. Sci. USA. *89*, 10758-10762.

Wasco, W., Gurubhagavatula, S., Paradis, M.D., Romario, D.M., Sisodia, S.S., Hyman, B.T., Neve, R.L., and Tanzi, R.E. (1993). Isolation and characterization of the human APLP2 gene encoding a homologue of the Alzheimer's associated amyloid ß protein precursor. Nature genetics *5*, 95-100.

Watson, G.B., Bolanowski, M.A., Baganoff, M.P., Deppeler, C.L., and Lanthorn, T.H. (1990). D-Cycloserine acts as partial agonist in the glycine modulatory site of the NMDA receptor expressed in xenopus oocytes. Brain Res. *510*, 158-160.

Webster, K.E. (1961). Cortico-striate interrelations in the albino rat. J. Anat. *95*, 532-544.

Webster, M-T., Vekrellis, K., Francis, P.T., Pearce, B.R., and Bowen, D.M. (1993). Factors affecting the ß-amyloid precursor in PC12 cells. Biochem. Soc. Trans. *21*, 239S.

Weidemann, A., Konig, G., Bunke, D., Fischer, P., Salbaum, J.M., and Masters, C.L. (1989). Identification, biogenesis, and localization of precursors of Alzheimer's disease A4 amyloid protein. Cell *57*, 115-126.

Welker, C. and Sinha, M. (1972). Somatotopic organization of SmII cerebral neocortex in albino rat. Brain Res. *37*, 132-136.

Wenk, G.L. and Rokaeus, A. (1988). Basal forebrain lesions differentially alter galanin levels and acetylcholinergic receptors in the hippocampus and neocortex. Brain Res. *460*, 17-21.

Wenk, H., Meyer, U., and Bigl, V. (1977). Centrofugal cholinergic connections in the olfactory system of rats. Neuroscience *2*, 797-800.

Wenk, H., Bigl, V., and Meyer, U. (1980). Cholinergic projections from magnocellular nuclei of the basal forebrain to cortical areas in rats. Brain Res. Rev. *2*, 295-316.

Wenthold, R.J. and Altschuler, R.A. (1983). Immunocytochemistry of aspartate aminotransferase and glutaminase. In Glutamine, glutamate and GABA in the central nervous system. L. Hertz, E. Kvamme, E.G. McGeer, and A. Schousboe, eds. (New York: Liss), pp. 33-50.

Werner, P., Voigt, M., Keinanen, K., Wisden, W., and Seeburg, P.H. (1991). Cloning of a putative high affinity kainate receptor expressed predominantly in hippocampal CA3 cells. Nature *351*, 742-744.

Wesnes, K., Jones, R.W., and Kirby, J. (1991). The effects of D-cycloserine, a glycine agonist, in a human model of the cognitive deficits associated with ageing and dementia. Br. J. Clin. Pharmacol. *31*, 577p-578p.

Wesnes, K.A. and Warburton, D.M. (1984). Effects of scopolamine and nicotine on human rapid information processing performance. Psychopharmacology *82*, 147-150.

Westbrook, G.L. (1993). Glutamate receptors and excitotoxicity. In Molecular and cellular approaches to the treatment of neurological disease. S.G. Waxman, ed. (New York: Raven Press), pp. 35-50.

Westbrook, G.L. and Mayer, M.L. (1987). Micromolar concentrations of Zn^{2+} antagonise NMDA and GABA responses of hippocampal neurones. Nature *328*, 640-643.

Wetzel, W., Getsova, V.M., Jork, R., and Matthies, H. (1980). Effect of serotonin on Y-maze retention and hippocampal protein synthesis in rats. Pharmacol. Biochem. Behav. *12*, 319-322.

Whitaker-Azmitia, P.M., Murphy, R., and Azmitia, E.C. (1990). Stimulation of astroglial 5-HT1A receptors releases the serotonergic growth factor, protein S-100, and alters astroglial morphology. Brain Res. *528*, 155-158.

Whitaker-Azmitia, P.M. and Azmitia, E.C. (1989). Stimulation of astroglial serotonin receptors produces media which regulates development of serotonergic neurones. Brain Res. *497*, 80-85.

White, P., Bowen, D.M., and Davison, A.N. (1978). Alzheimer's disease: distribution of protein on sucrose density gradient centrifugation. Acta Neuropathol. *41*, 253-256.

Whitehouse, P.J., Price, D.L., Struble, R.G., Clark, A.W., Coyle, J.T., and DeLong, M.R. (1982). Alzheimer's disease and senile dementia: loss of neurones in basal forebrain. Science *215*, 1237-1239.

Whitehouse, P.J. (1987). Neurotransmitter receptor alterations in Alzheimer disease: a review. Alzheimer. Dis. Assoc. Disord. *1*, 9-18.

Wiley, R.G., Blessing, W.W., and Reis, D.J. (1982). Suicide transport: destruction of neurons by retrograde transport of ricin, abrin and modeccin. Science *216*, 889-890.

Wiley, R.G., Talman, W.T., and Reis, D.J. (1983). Ricin transport distinguishes between central and peripheral neurones. Brain Res. *269*, 357-360.

Wiley, R.G. (1992). Neural lesioning with ribosome-inactivating proteins: suicide transport and immunolesioning. Trends. Neurosci. *15*, 285-290.

Wiley, R.G. and Stirpe, F. (1988). Modeccin and volkensin but not abrin are effective suicide transport agents in rat CNS. Brain Res. *438*, 145-154.

Williams, K., Romano, C., Dichter, M.A., and Molinoff, P.B. (1991). Modulation of the NMDA receptor by polyamines. Life Sci. *48*, 469-498.

Wilson, K.M., Gilchrist, S., and Minneman, K.P. (1990). Comparison of α_1-adrenergic receptor-stimulated inositol phosphate formation in primary neuronal and glial cultures. J. Neurochem. *55*, 691-697.

Winfield, D.A., Gatter, K.C., and Powell, T.P.S. (1980). An electron microscopic study of the types and proportions of neurons in the cortex of motor and visual areas of the cat and rat. Brain Res. *103*, 245-258.

Winfield, D.A., Brooke, R.N.L., Sloper, J.J., and Powell, T.P.S. (1981). A combined Golgi-electron microscopic study of the synapses made by the proximal axon and recurrent collaterals of a pyramidal cell in the somatic sensory cortex of the monkey. Neuroscience *6*, 1217-1230.

Wischik, C.M., Novak, M., Thogersen, H.C., Edwards, P.C., Runswick, M.J., Jakes, R., Walker, J.E., Milstein, C., Roth, M., and Klug, A. (1988). Isolation of a fragment of tau derived from the core of the paired helical filament of Alzheimer disease. Proc. Natl. Acad. Sci. USA. *85*, 4506-4510.

Wisden, W., Laurie, D.J., Monyer, H., and Seeburg, P.H. (1992). The distribution of 13 $GABA_A$ receptor subunit mRNAs in the rat brain. I. Telencephalon, diencephalon, mesencephalon. J. Neurosci. *12*, 1040-1062.

Wise, S.P. and Jones, E.G. (1977). Cells of origin and terminal distribution of descending projections of the rat somatic sensory cortex. J. Comp. Neurol. *175*, 129-158.

Wisniewski, H.M., Wegiel, J., and Wang, K.C. (1989). Ultrastructural studies of the cells forming amyloid fibres in classical plaques. Can. J. Neurol. Sci. *16*, 535-542.

Wong, D.F., Lever, J.R., Hartig, P.R., Dannals, R.F., Villemagne, V., Hoffman, B.J., Wilson, A.A., Ravert, H.T., Links, J.M., Scheffel, U., and Wagner, H.N. (1987). Localisation of serotonin 5-HT2 receptros in living human brain by positron emission tomography using N1-(11C-methyl)-2-Br-LSD. Synapse *1*, 393-398.

Wong, E.H.F., Kemp, J.A., Priestley, T., Knight, A.R., Woodruff, G.N., and Iversen, L.L. (1986). The anticonvulsant MK-801 is a potent *N*-methyl-D-aspartate antagonist. Proc. Natl. Acad. Sci. USA. *83*, 7104-7108.

Wong, E.H.F., Knight, A.R., and Ransom, R.W. (1987). Glycine modulates [^{3}H] MK-801 binding to the NMDA receptor in rat brain. Eur. J. Pharmacol. *142*, 487-488.

Yamamoto, T., Iwasaki, Y., Konno, H., and Kudo, H. (1985). Primary degeneration of motor neurones by toxic lectins conveyed from the peripheral nerve. J. Neurol. Sci. *70*, 327-337.

Yamamoto, T. and Hirano, A. (1985). Nucleus raphe dorsalis in Alzheimer's disease: Neurofibrillary tangles and loss of large neurones. Ann. Neurol. *17*, 573-577.

Yamamura, H.I., Kuhar, M.J., Greenberg, D., and Snyder, S.H. (1974). Muscarinic cholinergic receptor binding: Regional distribution in monkey brain. Brain Res. *66*, 541-546.

Yamamura, H.I. and Snyder, S.H. (1974). Muscarinic cholinergic binding in rat brain. Proc. Natl. Acad. Sci. USA. *71*, 1725-1729.

Yankner, B.A., Dawes, L.R., Fisher, S., Villa-Komaroff, L., Oster-Granite, M.L., and Neve, R.L. (1990). Neurotoxicity of a fragment of the amyloid precursor associated with Alzheimer's Disease. Science *245*, 417-420.

Yeterian, E.H. and Van Hoesen, G.W. (1978). Cortico-striate projections in the rhesus monkey: The organisation of certain cortico-caudate connections. Brain Res. *139*, 43-63.

Young, A.B. and Penney, J.B. (1994). Neurotransmitter receptors in Alzheimer disease. In Alzheimer Disease. R.D. Terry, R. Katzman, and K.L. Bick, eds. (New York: Raven Press), pp. 293-303.

Young, A.M.J. and Bradford, H.F. (1986). Excitatory amino acid neurotransmitters in the corticostriate pathway: Studies using intracerebral microdialysis in vivo. J. Neurochem. *47*, 1399-1404.

Zilles, K. (1985). The cortex of the rat (Berlin: Springer-Verlag).

Zilles, K. and Wree, A. (1985). Cortex: Areal and laminar structure. In The rat nervous system. G. Paxinos, ed. (London: Academic Press), pp. 375-415.

Zilles, K. (1990). Cortex. In The Human nervous system. G. Paxinos, ed. (London: Academic Press), pp. 757-802.

Zilles, K., Gross, G., Schleicher, A., Schildgen, S., Bauer, A., Bahro, M., Schwendemann, G., Zech, K., and Kolassa, N. (1991). Regional and laminar distributions of α_1-adrenoceptors and their subtypes in human and rat hippocampus. Neuroscience *40*, 307-320.

APPENDIX: Preliminary investigations of receptor mediated phospholipase C (PLC) stimulation in AD and control brain

A1.1 Introduction.

If cholinomimetic therapy is to succeed in the treatment of the cognitive and progressive aspects of AD, it is important to ascertain whether the coupling of muscarinic (particularly M_1) receptors to their signal transduction and effector pathways is preserved in the remaining pyramidal neurones of AD brain (see Chapter 10, section 10.4.1).

Experimental procedures used to measure the activity of the phosphoinositide system predominately use intact cells with pre-labelled substrate lipids, prior to activation of the intact system with appropriate agonists. These methods preclude the use of human brain membranes, as effective incorporation of precursors into phosphoinositides in responsive compartments does not occur (Fowler et al., 1992a). However, a method developed by Claro and collegues (Claro et al., 1989; Wallace and Claro, 1990) allows measurement of phosphoinositide hydrolysis in brain membranes using exogenous labelled phosphoinositides. Using a modification of this method, Jope et al. (1994) described impaired phosphoinositide hydrolysis in AD brain. In the same study, the authors reported preservation of Ca^{2+} stimulated PLC activity and the amount of the G-protein thought to be responsible for the coupling of muscarinic receptors to PLC ($G_{q/11}$). The authors therefore concluded that in AD, functional responses of muscarinic cholinergic receptors are impaired as a result of decreased function of the receptor-G-protein complex. However, agonist stimulation of PLC activity was studied only at one Ca^{2+} concentration, and given the sensitivity of PLC to Ca^{2+}, this is considered a possible confounding factor. The present, preliminary, investigations address this shortcoming by studying agonist stimulation of PLC at a range of added Ca^{2+} concentrations in control and AD brain samples.

A1.2 Materials and methods.

A1.2.1 Human brain samples.

Four, rapid *post-mortem* time AD brain samples were removed from frontal cortical areas. *Post-mortem* examinations were made within 3 hr of death, of patients who had clinical diagnoses fulfilling DSM-III criteria for dementia. Brains were treated as described in Chapter 2, section 2.2. The age range of these patients was 64 - 83 yr, with coma times ranging from 0 - 12 hr. One rapid *post-mortem* sample (age 72, *post-mortem* delay 1 hr, terminal coma 0 hr) with a clinical diagnosis of depression, free from histopathological signs of AD was used as one of four control cases.

Three neurosurgical samples, removed from frontal areas from patients to gain access to deep-seated tumours were used as the remaining control cases. The age range of these patients was 33 - 50 yr. All were free of dementia in life.

A1.2.2 Membrane preparation.

A 500 mg aliquot of grey matter was weighed and homogenised in 10 vols of ice-cold 20 mM Tris-HCl (pH 7.0) containing 1 mM EGTA using a glass-teflon homogeniser (model Tri-R; Stir-R Instruments, U.S.A.) with 9 up and down strokes. The homogenate was divided into two aliquots, and spun in centrifuge tubes at 30,000 *g* (20,000 rpm) for 15 min. The supernatant was carefully removed and the pellets re-suspended in buffer using an Ultra-Turax T25 homogeniser (IKA laboratories, Hamburg, Germany) set at 13,500 rpm and spun again for 15 min at the same speed. This step was repeated one further time, and pellets were re-suspended in 10 vol buffer, aliquoted into 500 μl samples, spun and frozen at -40 °C.

On the day of the assay, membrane pellets were thawed on ice, and re-suspended in 3 ml buffer (100 mM Tris-maleate (pH 6.8) containing 6 mM $MgCl_2$, 8 mM LiCl, 3 mM EGTA and 1 μM GTP-γ-S), to give an approximate protein content of 1 mg/ml.

A1.2.3 PLC assay.

PLC activity was assayed using a final concentration of 100 μM phosphotidylinositol (0.05 μCi [^{3}H] PI (Amersham International, Bucks, UK) + 90 μM cold PI (Sigma Chemicals Co, Poole, Dorset, UK)) as substrate. The substrate mixture was dried under a stream of helium, before suspension in 10 mM sodium deoxycholate in DIW (final concentration in assay tube 1 mM). Following a 10 min equilibration of membranes with Ca^{2+} additions (five concentrations added; 0.1, 0.3, 1 ,3 and 10 mM) and 1 mM carbachol (where applicable) at room temperature, 10 μl of the substrate was added to each tube, to give a final volume, including all additions, of 100 μl per tube. Samples were incubated for 25 min at 37 °C in a shaking water bath.

Reactions were stopped by the addition of 1.2 ml of chloroform/methanol (1:2 v/v). Chloroform (0.5 ml) and 0.25 M HCl (0.5 ml) were added and the reaction mixtures were thoroughly vortexed. The phases were allowed to separate (2 hr at 4 °C), and a 0.75 ml sample of the aqueous (upper) phase was mixed with 2 ml Emulsifier-Safe (Packard) and the radioactivity determined by liquid scintillation spectrometry.

A1.3 Results.

A1.3.1 Ca^{2+} mediated PLC stimulation.

Increasing concentrations of added Ca^{2+} resulted in increased PLC activity, reflected by increased radioactivity detected in the upper phase. Maximal stimulation was observed at 10 mM added Ca^{2+}. No significant differences between Ca^{2+}-stimulated PLC activity in control (n=4) and AD (n=4) samples were observed (Figure A1.1A).

A1.3.2 Carbachol-stimulated PLC activity

The cholinergic agonist, carbachol, in the presence of GTP-γ-S, stimulated PLC activity at a range of Ca^{2+} concentrations. No significant differences were observed between maximal carbachol-stimulated PLC activity in AD (n=4) and control (n=4) cases (114.5 $\pm$ 10.3 and 117.5 $\pm$ 5.3 % stimulation over that observed in the absence of carbachol, AD and control,

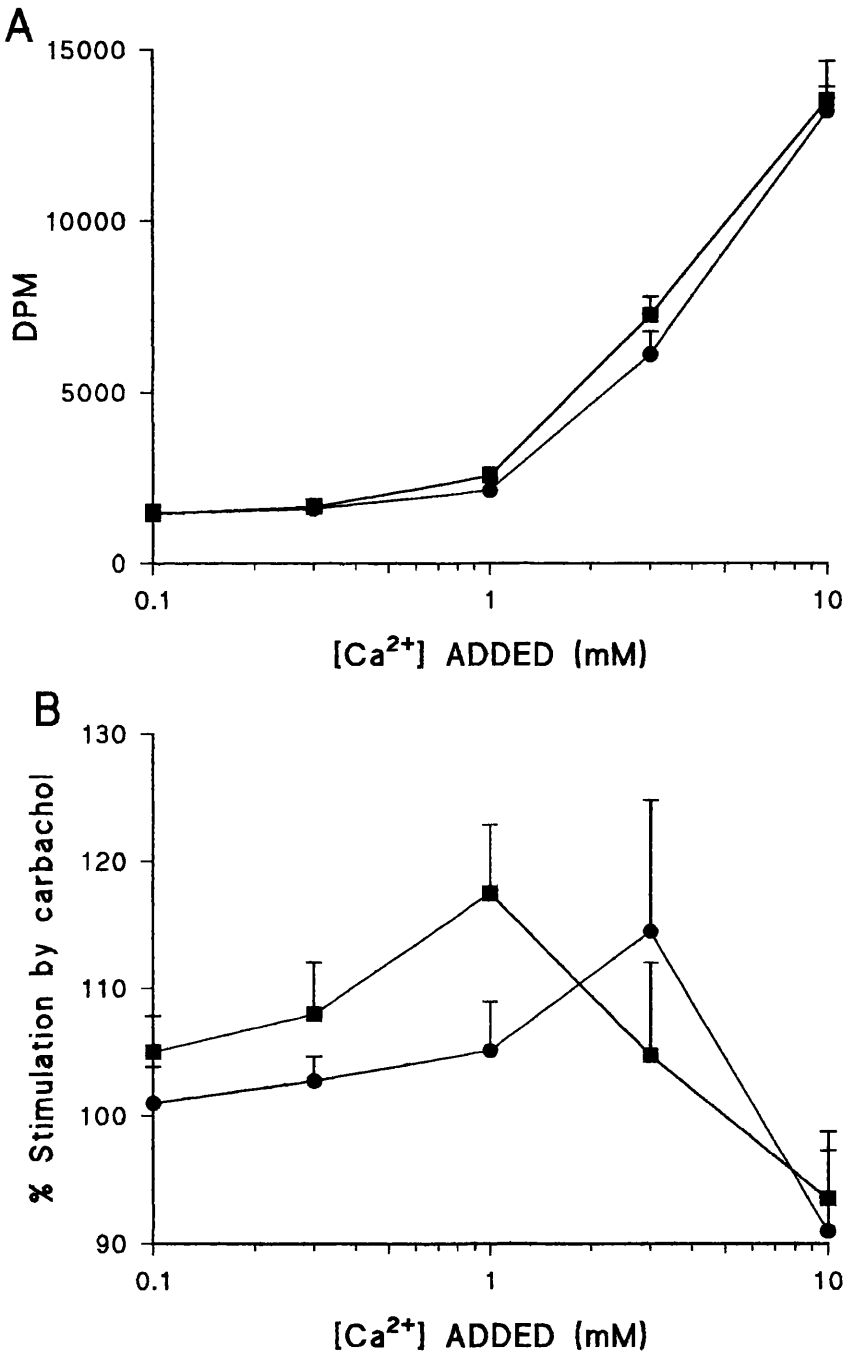

Figure A1.1: PLC STIMULATION BY Ca^{2+} AND CARBACHOL IN AD AND CONTROL TISSUE. (A) shows Ca^{2+} stimulation of PLC; increasing added Ca^{2+} concentrations dose-dependently increased PLC activity in AD (●, n=4) and control (■, n=4). No significant differences were observed between AD and control PLC stimulation by Ca^{2+}. (B) shows carbachol stimulation of PLC. At 1 mM added Ca^{2+} , there was a significant difference between AD (●, n=4) and control (■, n=4) stimulation ($p < 0.05$, Student's *t*-test), but no difference between maximal AD and control stimulation at added Ca^{2+} concentrations of 3 and 1 mM, respectively.
Data is mean ± SEM.

respectively; Figure A1.1B). However, the maximal stimulation in AD and control cases was observed at different added Ca^{2+} concentrations (3 mM and 1 mM, respectively; Figure A1.1B), suggesting the significant difference between AD and control tissue described by Jope et al. (1994) is wholly attributable to experiments being performed at a single Ca^{2+} concentration (corresponding to 0.66 mM added Ca^{2+} in the present study). At the closest Ca^{2+} concentration in the present study (1 mM), there was a significant difference between AD and control carbachol-stimulated PLC activity (105.0 ± 3.8 and 117.5 ± 5.3 % stimulation over that observed in the absence of carbachol, AD and control (both n=4), respectively, $p < 0.05$, Student's *t*-test).

A1.4 Discussion.

Previous studies have proposed that the receptor-G-protein-signal transduction pathway of muscarinic M_1 receptors is in some way impaired in AD (Flynn et al., 1991; Jope et al., 1994 but see also Pearce and Potter, 1991), although most authors report unchanged activity of PLC (Shimohama et al., 1992; Jope et al., 1994). The suitability of the M_1 receptor as a site for therapy in AD is dependent upon such coupling, with at least some activity being essential for effective treatment (see Chapter 10, section 10.4.1).

The preliminary results of the present study suggest that there is no impairment of receptor mediated PLC stimulation in AD brain, and that the previous study (Jope et al., 1994), where such a deficit was described, failed to allow for differences in the agonist-stimulated Ca^{2+}-dependence of this receptor system. It is possible that the shift in Ca^{2+}-dependence of agonist stimulation observed is attributable to a *post-mortem* effect- control tissue was obtained by neurosurgery, while AD tissue was obtained *post-mortem*. However, one control sample, from a depressive patient, was also obtained *post-mortem*, and maximal carbachol-stimulated PLC activity was observed at an added Ca^{2+} concentration of 1 mM, in common with that observed in the neurosurgical samples.

While it is clear that further investigation of the relationship between *post-mortem* delay and agonist-stimulated PLC activity is required, as well as a more comprehensive comparison between AD and control tissue, this

preliminary study provides encouraging evidence of the preservation of muscarinic receptor-effector systems in AD, and thus supports the use of cholinomimetics for the treatment of the cognitive (see Chapter 10, section 10.4.1) and progressive (see Chapter 10, section 10.4.2) aspects of AD.

ACKNOWLEDGEMENTS.

The studies described in this thesis were carried out at the Department of Neurochemistry of the Institute of Neurology, 1 Wakefield St., London WC1N 1PJ. I am grateful to a number of members of the laboratory who have assisted in experimental techniques, particularly Dion Davis, a sandwich student from the Polytechnic of East London. I would also like to thank Gary Stratmann for his help in locating many elusive brain samples.

I also thank Dr. Andrew Procter for his help in analysis of the results of the D-cycloserine study, Prof. Carl Pearson and Paul Heath for their contributions to the lesioning studies, and Dr. Brian Pearce for advise and help with some data interpretations. My thanks are also extended to Drs. Nicola Woodroofe and Jia Newcombe for help and advice with the immunocytochemical techniques, and also to Dr. Derek Middlemiss for reading and checking this manuscript.

I am deeply indebted to Dr. Paul Francis, who has given day to day guidance of the studies, invaluable technical input and advise with interpretations, as well as reading and checking large portions of this manuscript.

I am also very grateful to my supervisor, Prof. David Bowen, for energy, enthusiasm, support and suggestions throughout my years at the Institute.

Finally, I should like to thank my parents and brother, for their support and encouragement throughout this study.